CHEMICAL PROBES FOR HISTONE LYSINE DEMETHYLASES

Philip A. Gerken

A dissertation presented in fulfilment of the requirements for the award of the degree of

Doctor of Philosophy

of the

University of Oxford

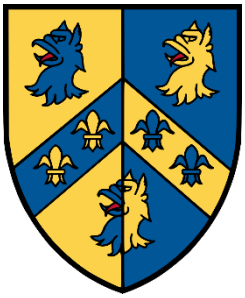

Chemistry Research Laboratory
12 Mansfield Road
OX1 3TA

Trinity College
Broad Street
OX1 3BH

December 2016

This thesis is dedicated to my father, Dr Heiko Gerken. Thank you for your encouragement, your sense of humor, and for providing me with the best possible opportunities in life.

DECLARATION

This dissertation describes work carried out in the Chemistry Research Laboratory and the Target Discovery Institute (Nuffield Department of Medicine) at the University of Oxford between October 2013 and December 2016. The dissertation is the product of my own work. It includes results that were obtained through collaboration, which are specifically indicated in the text.

Philip A. Gerken

ACKNOWLEDGEMENTS

In the words of perhaps the most eminent Austro-American philosopher of all time:

Life is continuously being hungry. The meaning of life is not simply to exist, to survive, but to go ahead, to go up, to achieve, to conquer.[*]

I feel incredibly privileged to have spent the last three years under the supervision of Prof. Martin D. Smith, who has continuously encouraged me to be "hungry" and strive towards ambitious goals. I am tremendously grateful for his advice, insights, and for all the knowledge and skills that I have acquired during the time I have spent working in his research group.

In addition, this work would not have been possible without the vision and guidance of my industrial supervisor, Dr Paul E. Brennan. His energy and optimism motivated me to develop a broader understanding of chemical biology and continually strive to become a well-rounded scientist. In this regard, I am also thankful to the SABS-IDC doctoral training program for everything I learned during my first year as a postgraduate student and for providing generous funding through an EPSRC scholarship.

As is commonly the case with collaborative scientific projects, I am hugely indebted to a number of individuals for their important contributions to this work. Within the TDI, I would like to acknowledge and thank Dr Anthony Tumber for expertly evaluating compound activity using the AlphaScreen and RapidFire assays, Dr Stephanie Hatch for evaluating cellular activity using the immunofluorescence assay, Barbara Mair and Dr Thomasz Konopka for their work on quantitative transcriptomics, Dr Georgina Berridge for help and advice regarding all things related to mass spectrometry, and Dr Rebecca Konietzny and Marie Laetitia-Thezenas for MS/MS data collection. Within the SGC, I would like thank whoever expressed and purified the

[*] Arnold Schwarzenegger on the meaning of life.

proteins required for this project (I am sorry I still have no idea who you are) and the mass spectrometry staff for maintaining the protein MS equipment. Within the CRL, I am grateful to the NMR and MS support staff for their analytical assistance and to Dr Barbara Odell in particular for running so many variable-temperature NMR experiments.

I must of course acknowledge the many wonderful members of the MDS and PEB research groups (past and present), who have made the last three years so memorable. Postdocs are undoubtedly the unsung heroes of any research group, and I am grateful to Drs Jamie Wolstenhulme, Craig Johnston, Craig Campbell, Katherine England, Bryony Elbert, and Niels Münster for their patient advice and support. I also consider myself incredibly lucky to have worked alongside so many talented undergraduate and graduate chemists. To all the illustrious occupants of CRL labs F4 and F5: Roly Armstrong, Emily Kiss, Alex Cavell, Ben Rahemtulla, Krishna Sharma, Aubert Ribaucourt, Antti Lahdenpera, Younes Hassanpour, Hasanain Almohseni, Yifei Li, Pascal Delany, John Joliffe, Alison Fugard, Katrina Badiola, Arseni Borissov, Minh Tran, Shuyu Chu, Tudor Balan, and Nick Parker – thank you for all the fun times. It's been an absolute pleasure working with and learning from you.

My family has always been incredibly supportive and keen to glean some information from me regarding the nature of my work. I hope you will find this thesis enlightening! Mom, whatever it is, please don't worry. Dad, it's never too late to learn how to use an iphone. Laura and Mona, you definitely deserve better birthday and Christmas presents from me.

My final acknowledgement goes to my girlfriend Rebecca. Thank you for putting up with my constant tardiness, my lack of social grace, and my appalling taste in music. You are wonderful, and I look forward to our many adventures together.

ABBREVIATIONS

°C	degrees Celsius
2-OG	2-oxoglutarate
3-D	three-dimensional
Å	Ångstöms
Ac	acetyl
aq.	aqueous
Ar	*denotes aromatic system*
Asp	aspartic acid
Bn	benzyl
Boc	*tert*-butoxycarbonyl
Bu	*n*-butyl
c	centi-
cat.	catalyst
COSY	correlation spectroscopy
cyc	cyclohexyl
d	deci-
d.r.	diastereomeric ratio
dba	dibenzylideneacetone
DIPEA	diisopropylethylamine
DMAP	4-dimethylaminopyridine
DMF	dimethylformamide
DMSO	dimethylsulfoxide
EIC	extracted ion chromatogram
e.r.	enantiomeric ratio
eq.	equivalents
ESI	electrospray ionization
Et	ethyl
f	frequency
FT	Fourier transform
g	grams

Glu	glutamic acid
h	hours
h	Planck's constant
H	histone
HMBC	heteronuclear multiple-bond correlation spectroscopy
HMDS	hexamethyldisilazide
HPLC	high-performance liquid chromatography
HRMS	high-resolution mass spectrometry
HSQC	heteronuclear single-quantum correlation spectroscopy
Hz	hertz
i	iso
IC_{50}	inhibitor concentration corresponding to 50% of the maximal response
IR	infra-red
IUPAC	International Union of Pure and Applied Chemistry
JmjC	Jumanji-C
k	kilo-
K	Kelvin
K	lysine
KDM	histone lysine demethylase
K_M	Michaelis-Menten constant
L	liters
LDA	lithium diisopropylamide
LRMS	low-resolution mass spectrometry
Lys	lysine
m	milli-
M	moles per liter
m	*meta*-
m	meters
Me	methyl
min	minutes
mol	moles
MP	melting point
MS	mass spectrometry

MS/MS	tandem mass spectrometry
n	*denotes generic integer*
n	nano-
NBS	*N*-bromosuccinimide
NMP	1-methyl-2-pyrrolidinone
NMR	nuclear magnetic resonance
nOe	nuclear Overhauser effect
o	*ortho-*
p	*para-*
Ph	phenyl
ppm	parts per million
Pr	*n*-propyl
PTC	phase-transfer catalysis
Py	pyridyl
quant.	quantitative
R	*denotes generic substituent*
rt	room temperature
s.	solid
S_NAr	nucleophilic aromatic substitution
t	*tertiary*
THF	tetrahydrofuran
TMS	trimethylsilyl
UV	ultraviolet
λ	wavelength
μ	micro-
ν	rate
ν_{max}	maximum rate

ABSTRACT

The primary objective of this DPhil research project was to develop selective and cell-active inhibitors of the histone lysine demethylase KDM2A, which could potentially lead to the discovery of a novel chemical probe. Chapter one of this thesis introduces the role of histone lysine demethylases (KDMs) in the epigenetic regulation of gene expression and discusses the value of chemical probes as tools to study these enzymes. Chapter two describes the synthesis of a library of indoline-based KDM2A inhibitors using a modular synthetic approach to explore key structure-activity relationships and a chiral counterion-mediated strategy to synthesize lead candidates enantioselectively (Figure 1).

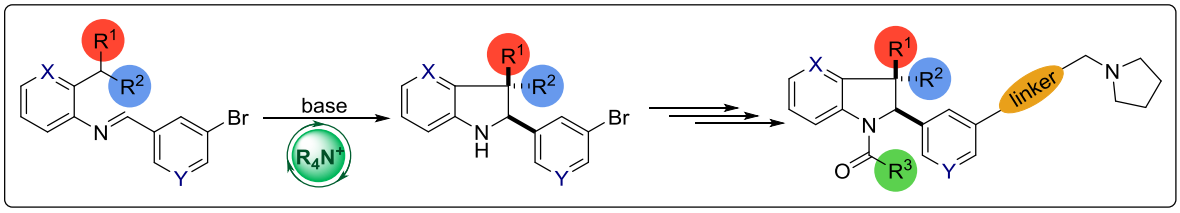

Figure 1 – Modular synthetic strategy towards library of indoline-based KDM2A inhibitors.

Chapter three discusses investigations into the cellular activity of lead compounds and explores strategies to address limitations associated with cytotoxicity and promiscuity. Chapter four describes the application of a variety of experimental techniques to identify the mode of target inhibition. Finally, chapter five focuses on the development of an enantioselective *C*-acylation reaction to access spirocyclic fragments asymmetrically (Figure 2).

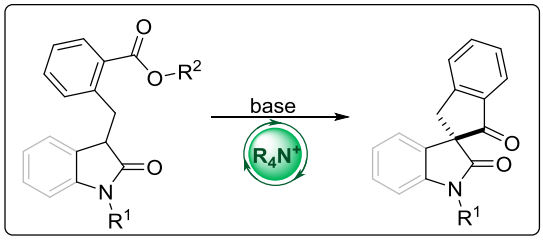

Figure 2 – Enantioselective synthesis of spirocyclic scaffolds using chiral phase-transfer catalysis.

TABLE OF CONTENTS

1. INTRODUCTION

1.1 Epigenetics

1.1.1 Chromatin and Gene Expression

In 1974, Roger Kornberg proposed that the structure of chromatin is based on a repeating unit of histone oligomers closely associated with DNA.[1, 2] This discovery revealed the molecular framework for the packaging of genetic information in eukaryotic cells. Over the following decades, advances in experimental techniques helped identify the broad spectrum of chemical modifications of both histones and DNA and thus provided an insight into the mechanisms by which gene expression is regulated.[3] Together, the structural organization of chromatin and the dynamic nature of its chemical transformation constitute the foundation of epigenetics.

The complete human genome contains approximately 3 billion base pairs.[4] Crucially, this genetic code is broadly conserved within all cells of an individual. Therefore, the differentiation of cells, their ability to perform specialized functions, and their requirement to respond to environmental stimuli relies on the precise regulation of gene expression. The modulation of chromatin structure is an essential aspect of this. The basic repeating unit of chromatin is the nucleosome, which consists of 146 DNA base pairs wrapped around an octameric histone protein core (Figure 1.1).[5, 6] An additional linker histone (H1) stabilizes the nucleosome complex and is crucial for the packaging of chromatin.[7] The amino-terminal regions of the histones (frequently referred to as *N*-terminal “tails”) extend beyond the nucleosome core. This makes them accessible to a

variety of enzymes, which catalyze a range of chemical modifications including phosphorylation, ubiquitination, acetylation, and methylation.[8] The precise combination of chemical groups decorating the histone *N*-terminal tails influences the compactness of chromatin either directly or indirectly *via* the recruitment of proteins that control chromatin structure.[9] This, in turn, affects the accessibility of genes to the transcription apparatus and hence the extent to which they are transcribed.

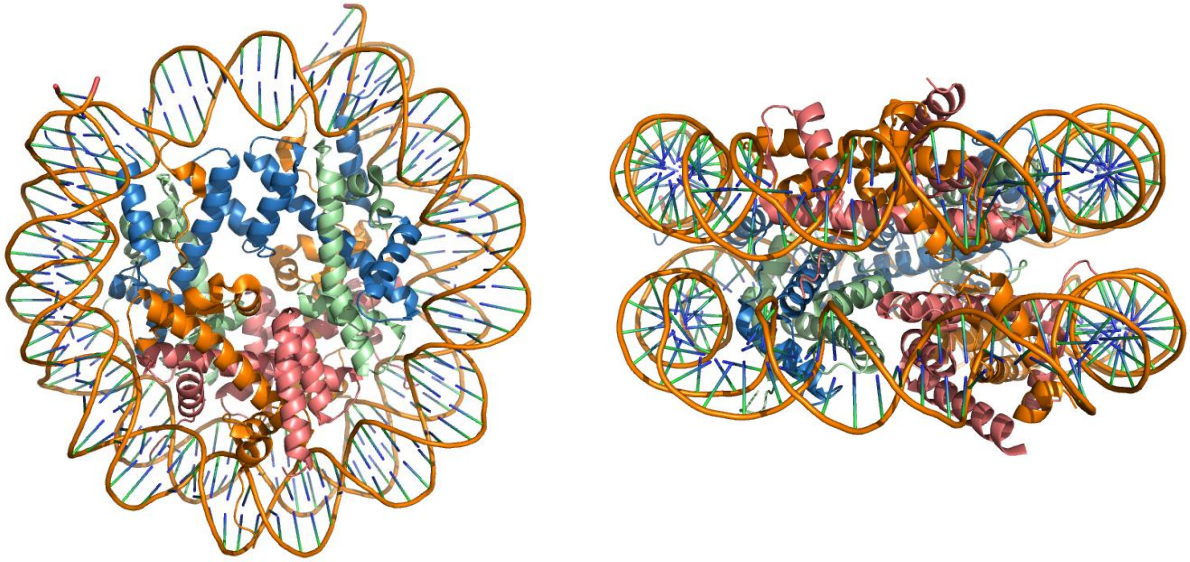

Figure 1.1 – X-ray crystal structure of the human nucleosome complex (PDB ID: 2CV5).[10] DNA wraps around a core of histone proteins consisting of 2 copies of 4 histones: H2A, H2B, H3, and H4. The histone *N*-terminal regions (tails) protrude beyond the nucleosome core and may be subjected to a variety of post-translational modifications.

1.1.2 Writers, Readers, and Erasers

The proteins involved in the epigenetic regulation of gene expression can be broadly divided into 3 categories: writers, readers, and erasers.[11] Writers are enzymes that catalyze the addition of chemical groups to the histone *N*-terminal tails. The most widely-studied writers are histone acetyltransferases (HATs) and histone methyltransferases (HMTs),

which catalyze the acetylation of lysine residues and the methylation of either lysine or arginine residues respectively. Histone acetylation is broadly associated with activation of gene expression, as acetyl groups neutralize the positive charge on lysine residues. This reduces the affinity of histones for DNA, which contains a negatively-charged phosphate backbone, causing chromatin to adopt a more open, unfolded structure.[12] Histone methylation is arguably the most complex form of post-translational histone modification, as multiple methylation states are possible for both lysine and arginine residues. Methyl marks are recognized by a variety of regulatory proteins that either increase or decrease the extent of transcription, so that histone methylation may be associated with both activation and repression of gene expression.[13] The observation that particular combinations of acetylation and methylation states often collaborate to bring about a particular change of gene expression has given rise to the "histone code hypothesis".[14]

Readers are domains that selectively bind to epigenetic marks on the histone *N*-terminal tails and typically exist within complexes of other domains or proteins that influence chromatin structure and transcription. Bromodomains, for example, recognize acetylated lysine residues and are often found in proteins that also contain enzymatic domains that add or remove epigenetic marks.[15] Methylated lysine residues, in turn, are recognized by a variety of readers including plant homeodomains (PHDs), tudor domains, and malignant brain tumor (MBT) domains. A common feature of all of these domains is the presence of an "aromatic cage", which forms a binding pocket for the methylated lysine residues. The resulting complex is stabilized by cation-π interactions involving the charged methyl amino-group of methylated lysine and the aromatic residues of the reader domain.[16]

Finally, erasers catalyze the removal of the chemical groups from the histone *N*-terminal tails and are therefore a counterbalance to the writers. Histone deacetylases (HDACs) and histone lysine demethylases (KDMs) remove the post-translational modifications introduced by HATs and HMTs respectively. The reversibility of both histone acetylation and methylation is an essential requirement for the dynamic nature of the epigenetic regulation of gene expression.[17]

1.1.3 Chemical Probes for Epigenetics

Regulation of gene expression *via* the chemical transformation of chromatin and DNA has a profound impact on a number of fundamental biological processes, including cellular differentiation,[18] embryonic development,[19] and ageing.[20] However, the complex and interwoven character of epigenetics often makes elucidating the precise downstream effects of individual epigenetic components difficult to determine. Traditional approaches relying on gene knockdown using siRNA[21] can provide some insight, but such strategies frequently give rise to ambiguous results. It is reasoned that the partial or complete subdual of expression of a specific writer, reader, or eraser not only removes *it* from the cellular system, but also perturbs the activities of other epigenetic proteins and domains that usually interact with it. For example, the histone lysine demethylases KDM2A has been shown to associate with the HP1 family of heterochromatin-stabilizing proteins, which are essential for the maintenance of the heterochromatin-rich regions around the centromeres and telomeres of chromosomes.[22, 23] Knocking down the entire KDM2A gene would therefore not only attenuate the level of histone lysine demethylation, but also influence the HP1-mediated regulation of chromatin structure. Consequently, a more subtle approach that enables researchers to selectively target the individual functional roles of

specific epigenetic proteins and domains is required. The use of selective chemical probes represents one such strategy.

In general, the term *chemical probe* refers to a small molecule that facilitates the study of the mechanistic roles and phenotypic impacts of a protein or domain.[24] Although chemical probes can interact with their targets in a variety of ways, including inhibition, activation, and fluorescent binding, this thesis will largely focus on chemical probes that act as inhibitors. A particular challenge associated with the development of chemical probes for epigenetics is achieving selectivity between the structurally similar members of each protein family, which is essential if a chemical probe is to be a useful tool for elucidating the downstream effects of the individual writers, readers, and erasers of epigenetics.[25] In addition, targeting epigenetics represents a pivotal approach to addressing disease at the transcription level, and well-characterized, readily available chemical probes have the potential to accelerate the development of novel pharmaceuticals. In particular, epigenetic chemical probes may be used to validate and invalidate potential targets for drug discovery research programs. This is perhaps best illustrated by the discovery of the BET-bromodomain inhibitor JQ1 (Figure 1.2).[26] Within the first 4 years of the initial disclosure of its biological activity, five clinical trials for unique BET bromodomain inhibitors were initiated.[27]

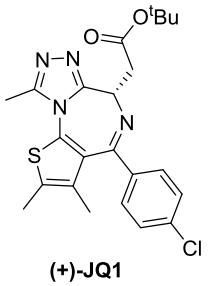

(+)-JQ1

K_D BRD2 128 nM
K_D BRD3 60 nM
K_D BRD4 49 nM
K_D BRDT 190 nM

Figure 1.2 – The BET bromodomain chemical probe JQ1 and its measured dissociation constants with respect to the four (full length) members of the BET bromodomain family.

1.2 Histone Lysine Demethylases

1.2.1 Phylogeny and Mechanisms of Catalysis

Histone lysine demethylases (KDMs) are divided into 2 subfamilies based on their sequence homologies and catalytic mechanisms: The flavin-dependent lysine-specific demethylases (LSD or KDM1 subfamily) and the Jumanji-C (JmjC) domain containing 2-oxoglutarate dependent lysine demethylases.[28] KDMs belonging to the KDM1 subfamily are structurally closely related to the monoamine oxidases (MOAs) and require a flavin adenine dinucleotide (FAD) cofactor for demethylation. A possible mechanism of catalysis involving a single electron transfer from the methylated lysine sidechain to the flavin cofactor is illustrated in Figure 1.3, although alternative mechanistic pathways involving hydrogen atom transfer, nucleophilic attack, and hydride transfer have also been proposed.[29] The chemical requirements of all of these mechanisms dictate the substrate scope of FAD-dependent demethylases, and the 3 members of this subfamily (KDM1A, KDM1B-1, and KDM1B-2) do not display activity towards trimethylated lysine residues, which would be unable to form the required iminium ion intermediate.

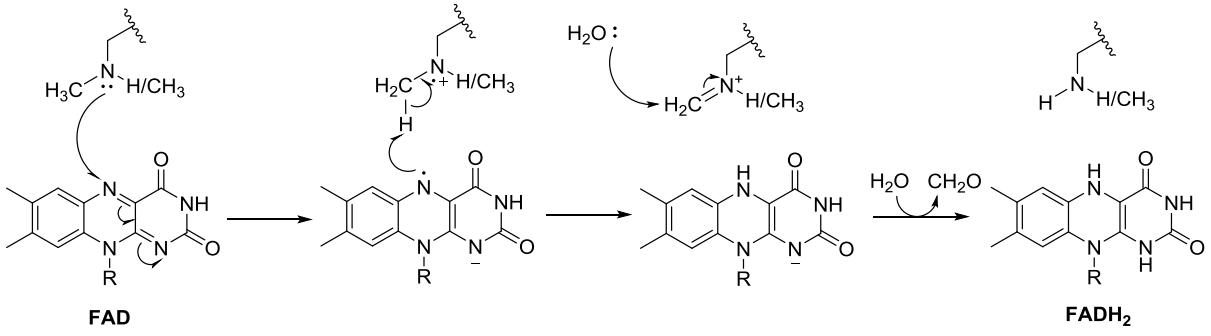

Figure 1.3 – A possible catalytic mechanism of demethylation by KDMs belonging to the KDM1 subfamily: SET from the methylated lysine sidechain to the FAD cofactor produces an intermediate iminium ion, which reacts with water to release formaldehyde as a byproduct.

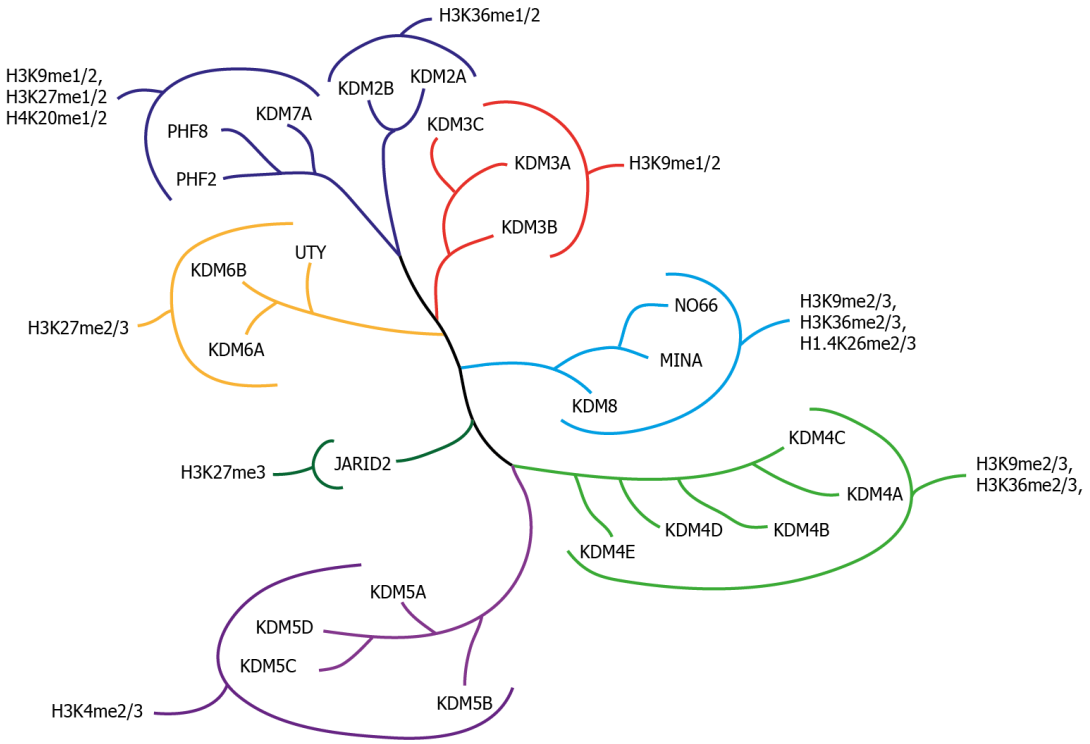

Figure 1.4 – Phylogenetic tree of the JmjC subfamily of histone lysine demethylases, showing reported substrate selectivities.

The JmjC subfamily of KDMs is significantly larger and comprises around 20 enzymes, which can be grouped broadly into 7 further subfamilies based on sequence homology and substrate specificity (Figure 1.4).[11, 30] They belong to the 2-oxoglutarate (2-OG) dependent oxygenase family of enzymes, which contain a catalytically-active Fe^{II} ion and oxidize their substrates *via* a radical mechanism that involves the concomitant oxidative decarboxylation of 2-OG to succinate. The mechanistic details of this reaction have been probed extensively and are summarized in Figure 1.5. In the majority of enzymes, the Fe^{II} ion is coordinated by 2 histidines and 1 acidic residue.[31, 32] 2-OG coordinates in a bidentate manner, and its *C*5 carboxylate group interacts electrostatically with a basic residue such as lysine or arginine.[33] Oxygen binds and initiates the oxidative decarboxylation of 2-OG to generate succinate, CO_2, and an intermediate Fe^{IV}-oxo species, for which there is spectroscopic evidence.[34, 35] This reactive Fe^{IV}-oxo intermediate

effectively inserts an oxygen atom into the C-H bond of one of the methyl groups of the methylated lysine substrate, presumably *via* a radical rebound mechanism.[33, 36] As with the FAD-dependent demethylases, the initial reaction product collapses to release the demethylated lysine residue and formaldehyde as a byproduct. However, unlike enzymes in the KDM1 subfamily, many of the JmjC demethylases show activity towards trimethylated lysine residues, and in several cases arginine demethylation has been observed as well.[37] This enhanced substrate scope is enabled by their distinct mechanism of catalysis.

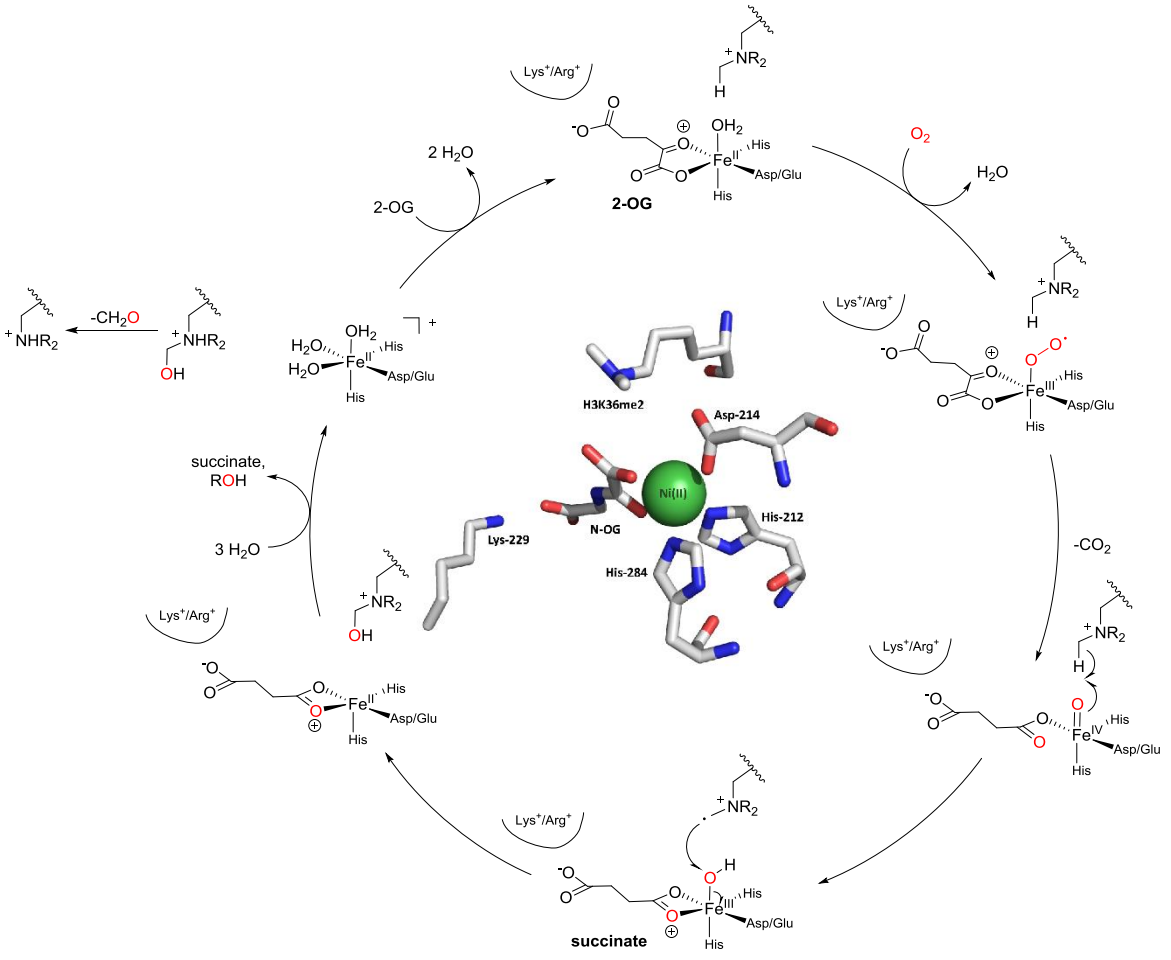

Figure 1.5 – Catalytic cycle of JmjC KDMs: Oxidative decarboxylation of bound 2-OG generates succinate and a Fe(IV)-oxo intermediate, which reacts with one of the methyl groups of the methyl-lysine substrate. The X-ray crystal structure of the KDM2A active site (Ni^{II} instead of Fe^{II} and *N*-OG instead of 2-OG) is depicted at the center of the cycle (PDB ID: 4QXC).[38]

1.2.2 Inhibitors of KDMs

The fundamental importance of KDMs in maintaining the dynamic equilibrium of histone methylation and their connection to a variety of diseases[13, 30, 39] has led to the development of a range of selective inhibitors. Molecules based on the scaffold of the known monoamine oxidase inhibitor tranylcypromine (**1**) form the largest class of KDM1 inhibitors (Figure 1.6).[40] Structural studies have shown that these compounds are irreversible inhibitors that form covalent adducts with the FAD cofactor and that the substituents on the phenyl ring of the tranylcypromine core occupy the substrate binding site.[41, 42] Recently, A. Mai and co-workers developed the bifunctional pan-KDM inhibitors **4** and **5** by linking the KDM1-selective tranylcypromine motif with JmjC-KDM inhibitory motifs based on bipyridine and 8-hydroxyquinoline respectively.[43]

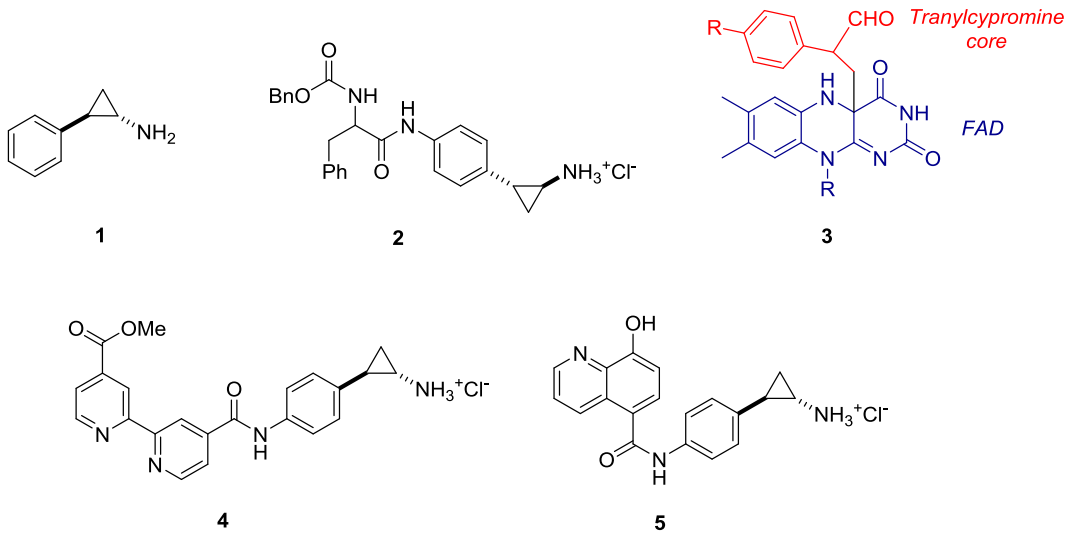

Figure 1.6 – Inhibitors of the KDM1 subfamily of lysine demethylases: tranylcypromine (**1**) is a known monoamine oxidase (MOA) inhibitor and its scaffold forms the basis of many selective KDM1 inhibitors such as **2**. These compounds are irreversible inhibitors and react with the FAD cofactor in the enzyme active site (**3**).

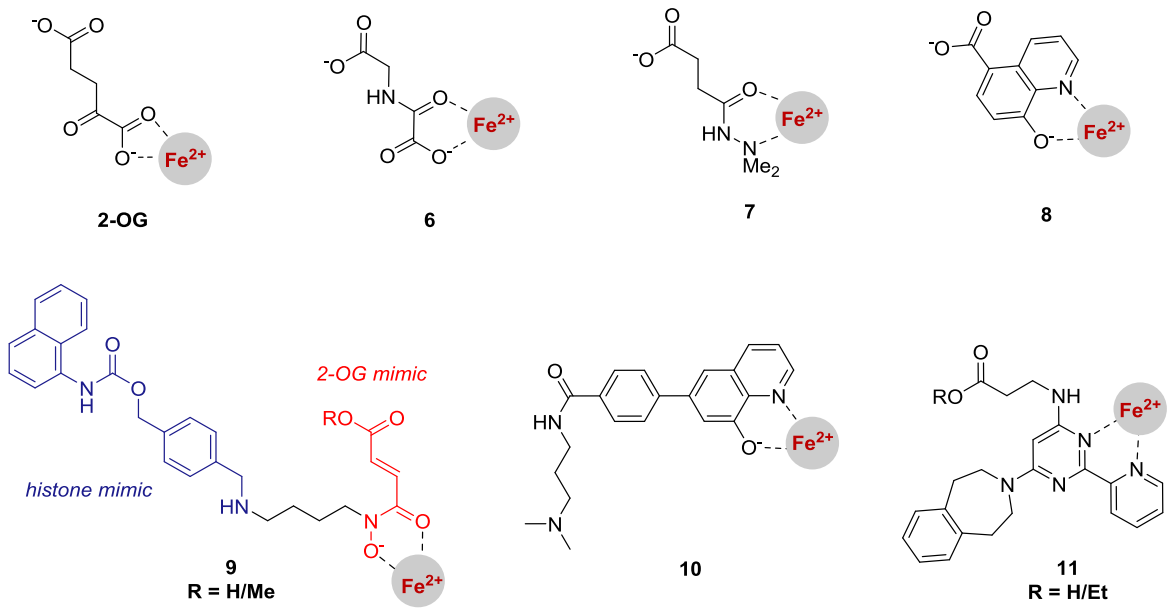

Figure 1.7 – Inhibitors of the JmjC subfamily of KDMs based on iron-chelating 2-OG mimics: These inhibitors tend to be small, polar acidic compounds with variable degrees of selectivity. GSK-J1 (**11**) is a widely distributed chemical probe for the KDM5 and KDM6 demethylases.

The majority of inhibitors of the JmjC lysine demethylases are iron-chelating 2-OG mimics and include a variety of small, polar molecules such as *N*-oxalylglycine (*N*-OG **6**),[44] daminozide (**7**),[45] and IOX1 (**8**),[46] a well-studied broad spectrum 2-OG oxygenase inhibitor (Figure 1.7). One strategy for improving the potency and selectivity of such scaffolds is based on combining iron-chelating motifs with fragments that extend into the histone binding pocket. This approach led to the discovery of the potent yet non-selective inhibitor methylstat (**9**), in which a hydroxamic acid "head group" is linked to a methyllysine mimic. The methyl ester prodrug version of **9** was found to inhibit KDM4C-catalyzed demethylation of H3K9me3 in HeLa cells.[47] Similarly, the bifunctional KDM4 inhibitor **10** combines a 2-OG-competitive 8-hydroxyquinoline unit with a fragment resembling the dimethyllysine sidechain.[48] In 2012, GSK-J1 (**11**) was reported as a potent and selective inhibitor of members of the KDM6 subfamily. Structural studies revealed that the pyridyl-pyrimidine core chelates Fe^{II} in a bidentate fashion, with the acidic sidechain occupying the 2-OG

binding pocket. The ethyl ester prodrug version of **11** was shown to inhibit proinflammatory gene activation in human macrophages, demonstrating the potential of KDM inhibitors in drug discovery.[49] Since this initial report, however, further investigations revealed that **11** is also a potent inhibitor of the KDM5 demethylases.[50] This illustrates the importance of extensively characterizing the selectivity profile of a chemical probe candidate before it should be used as a tool to elucidate connections between a subfamily of epigenetic proteins and a specific biological process. Finally, recent examples of highly potent 2-OG-competitive KDM inhibitors include a series of KDM4/5-selective pyridopyrimidinones[51] and a series of KDM5 inhibitors based on a cyanopyrazole scaffold.[52]

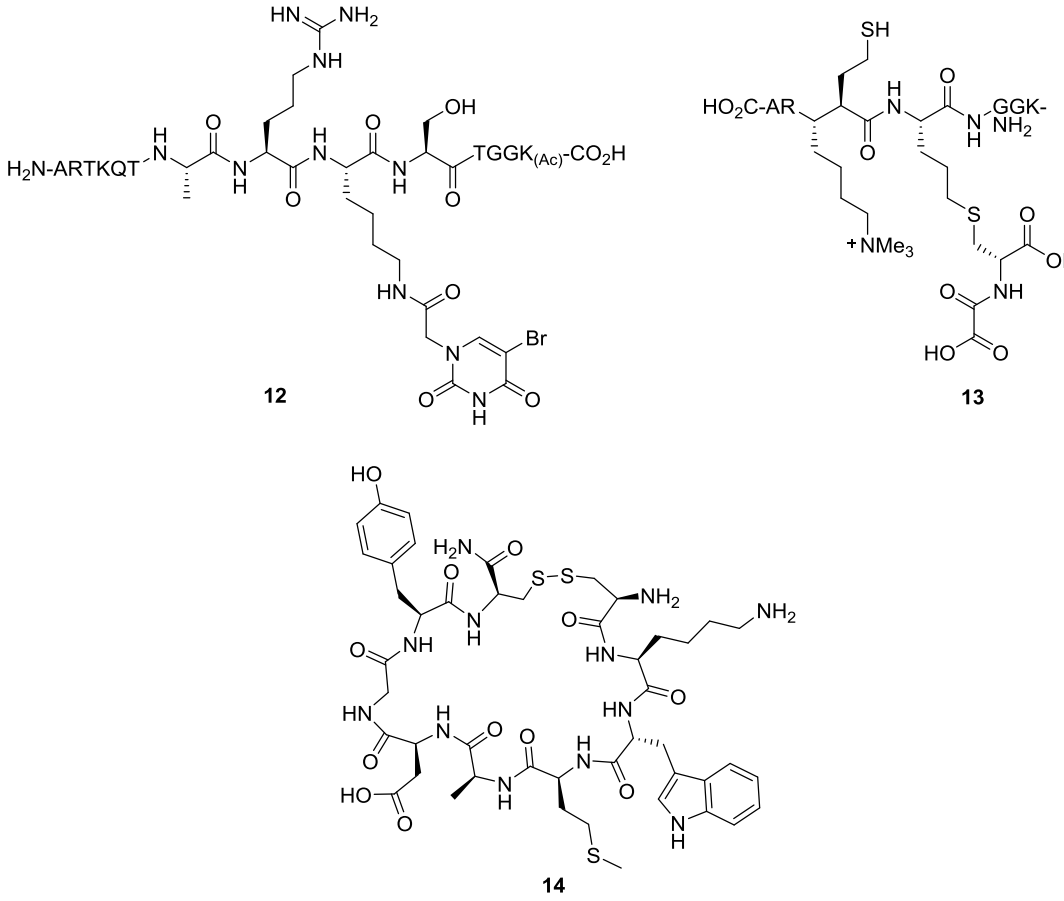

Figure 1.8 – Peptide inhibitors of JmjC KDMs: Modified linear peptides based on the relevant H3 tail sequence such as **12** and **13** occupy the histone binding site. The cyclic peptide inhibitor **14** was found to interact with several allosteric sites on KDM4C.

An alternative approach to inhibiting the JmjC lysine demethylases relies on linear and cyclic peptides as mimics of the histone substrate or as allosteric binders (Figure 1.8). In 2011, R. P. Clausen and J. L. Kristensen described a strategy for discovering peptides that selectively inhibit PHF8, KDM4A, and KDM4C based on truncating and modifying the relevant histone 3 (H3) tail sequence (**12**).[53] Shortly afterwards, C. J. Schofield and co-workers used a rational design approach relying on non-denaturing mass spectrometry and x-ray crystallography to identify a reasonably potent and selective inhibitor of KDM4A and KDM4E. In this study, modified peptides were covalently linked to *N*-oxalyl-cysteine to generate adducts that occupy both the 2-OG and substrate binding sites (**13**).[54] The discovery of cyclic peptide inhibitors such as **14** was facilitated by the creation of a phage display library. Hydrogen/deuterium exchange mass spectrometry suggests an allosteric mode of inhibition with respect to KDM4C.[55]

Although the strategies described above have led to the discovery of a variety of reasonably potent and in some cases even selective inhibitors of the JmjC KDMs, the majority of these 2-OG competitors and peptides are generally not suitable as chemical probes. In particular, the molecules derived from either approach are usually characterized by poor cellular permeability and can therefore not be used to explore the impact of KDM inhibition in a cellular context. The research described in this thesis attempts to address the need for novel classes of inhibitors of the JmjC KDMs. Specifically, it focuses on the development and characterization of a highly selective, cell-active inhibitor and potential chemical probe for the histone lysine demethylase KDM2A.

1.3 KDM2A

1.3.1 Structural Features and Substrate Selectivity

KDM2A selectively catalyzes the demethylation of both mono- and di-methylated lysine 36 on histone 3 (H3K36).[56] Like most of the JmjC KDMs, it has several aliases, notably FBXL11 (F-box and leucine-rich repeat protein 11) and JHDM1A (JmjC domain containing histone demethylase 1A). In its entirety, KDM2A consists of 1161 amino acid residues and contains 9 domains (Figure 1.9-A). A truncated version of KDM2A without the CXXC, PHD, Fbox, and LRR repeat domains retains the full enzyme's catalytic activity, although loss of the PHD domain in particular reduces turnover.[56] The CXXC domain recognizes and binds to non-methylated CpG DNA islands, thereby directing demethylation to segments of chromatin in the vicinity of these genetic markers.[57, 58] The PHD domain is atypical in that it does not contain an aromatic cage for recognizing methylated lysine residues and does not appear to bind to any known epigenetic marks.[58] Similarly, the precise functional roles of the JmjN, Fbox, and LRR repeat domains are still under investigation.

A detailed study exploring the structural origins of the enzyme's substrate selectivity using a 13-residue peptide to replicate the H3 tail was reported by the D. J. Patel and O. Gozani.[38] It revealed that molecular recognition of the peptide by KDM2A involves the JmjC, hairpin, mixed, and C-terminal domains. The peptide's G33, G34, and P38 residues enable the necessary U-shaped conformation in the active complex, and the aromatic sidechain of Y41 occupies a pocket outside the active site (Figure 1.9-B). These residues and their relative locations are unique to the H3K36 sequence. The lack of activity of KDM2A towards trimethylated H3K36 may be explained by a potential steric clash between the lysine sidechain's additional CH_3 group and 2-OG.

A

B

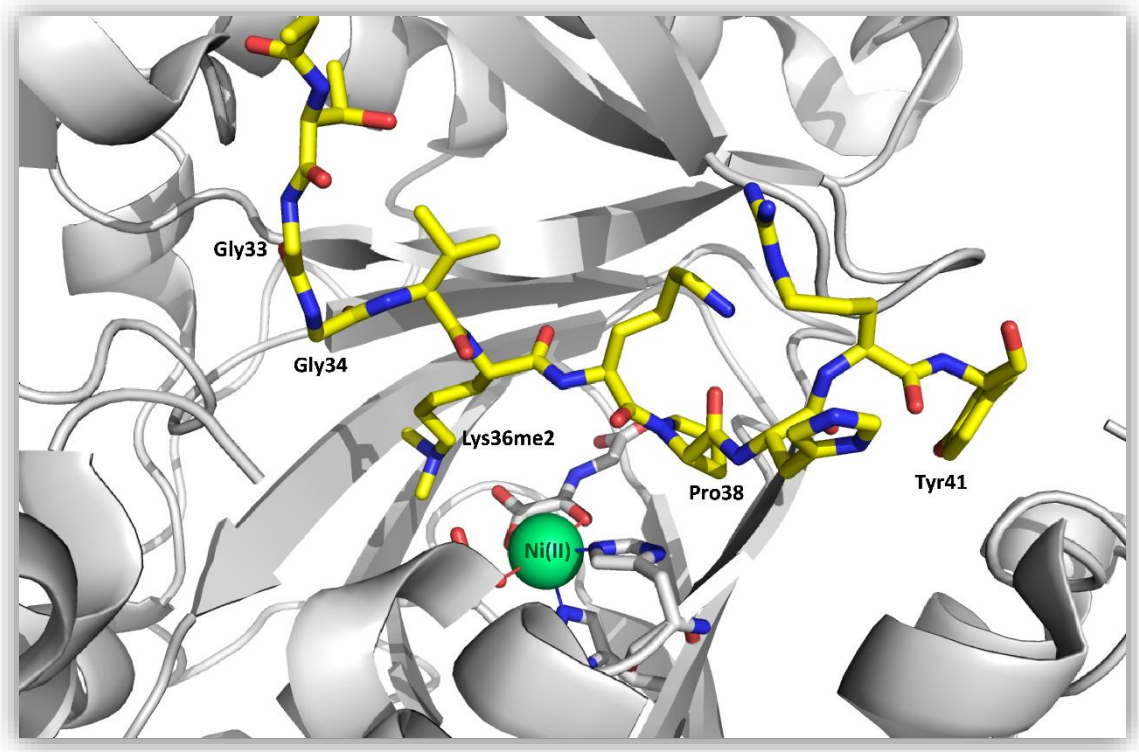

Figure 1.9 – A. Complete domain architecture of KDM2A: The CXXC, PHD, FBox, and LRR repeat domains are not essential for catalytic activity. B. An x-ray crystal structure (PDB ID: 4QXC)[38] showing the peptide substrate (yellow) inside KDM2A's JmjC domain active site (grey): Important peptide residues for substrate recognition are highlighted.

1.3.2 Biological Importance and Implications in Disease

Due to its role in regulating the methylation dynamics of H3K36, which impact gene expression patterns across the entire genome, KDM2A has been implicated in a variety of fundamental biological processes and diseases. For example, it has been shown to be involved in the regulation of NF-κB, which coordinates cytokine production and the immune response.[59] Both KDM2A and the closely related demethylase KDM2B are involved

in the vitamin-C-dependent reprogramming of somatic cells to induced pluripotent stem cells.[60] In addition, gene knockdown experiments suggest that KDM2A may play a crucial role in embryonic development.[61] Studies have shown that the methylation state of H3K36 may be connected to specific oncogenic consequences.[62-64] As a result, KDM2A has been linked to various cancers. Notably, the enzyme is found to be overexpressed in gastric cancer cells,[65] and its knockdown reduces the proliferation of non-small cell lung cancer (NSCLC) cells.[66] Together, these findings suggest that inhibiting KDM2A may represent a strategy for targeting certain cancers at the transcription level. However, in the absence of a selective, cell-permeable chemical probe for KDM2A, target validation remains a challenge.

1.3.3 Inhibitors of KDM2A

Several of the relatively broad spectrum 2-OG competitors described in subsection 1.2.2 show inhibitory activity towards KDM2A. For example, the plant growth regulator daminozide (**7**) appears to be remarkably selective for the KDM2/7 subfamily relative to representative members of most of the other KDM subfamilies as well as other 2-OG dependent oxygenases.[45] In addition, initial studies suggest that both methylstat (**9**) and the fluorescent analogue methylstat^{fluor} (**15**) are potent (sub-μM) inhibitors of KDM2A.[47, 67] However, to our knowledge, the only highly-selective KDM2A inhibitor disclosed in the literature to date is the triazolopyridine-based compound (**16**) reported by C. J. Schofield and P. E. Brennan in 2014, which is also thought to occupy the 2-OG binding site (Figure 10).[68] As a single enantiomer, **16** has an IC_{50} of 63 nM towards KDM2A (using the RapidFire assay – see subsection 2.1.2) and greater than 30-fold selectivity over representative members of most of the other KDM subfamilies. Unfortunately, **16** does not inhibit

demethylation of H3K36me2 in a cells, and development of a cell-active pro-drug has proven to be challenging.[69] A similar imidazole-pyridine scaffold has recently been developed by Quanticel Pharmaceuticals (**17**). Derivatives display inhibitory activity towards KDM2A, KDM2B, and PHF8.[70]

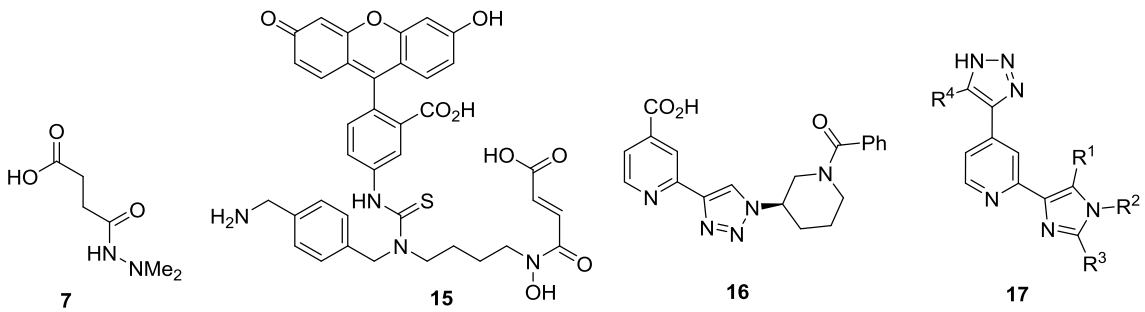

Figure 1.10 – Inhibitors of KDM2A: Methylstat^{fluor} (**15**) is a fluorescent analogue of methylstat (**9**). The triazolopyridine-based inhibitor **16** displays greater than 30-fold selectivity towards KDM2A but is unable to penetrate cells. Imidazole-pyrimidines (**17**) may be a potent new class of KDM2 inhibitors.

1.4 Project Background

1.4.1 Rationale and Hit Identification

Due to the limitations of both 2-OG mimics and peptides as KDM inhibitors, we envisaged an alternative approach towards the development of a novel selective inhibitor and chemical probe candidate for KDM2A. Specifically, we aimed to develop a small, non-peptidic molecule that would compete with the enzyme's histone substrate and therefore be more likely to possess the physicochemical properties required for cellular permeability. In order to identify a starting point, a library of known binders to methyl-lysine reading domains and HMTs was screened for inhibitory activity against a select panel of KDMs using

an AlphaScreen (see subsection 2.1.1).[*] We reasoned that such a specialized library would be more likely to contain molecules that also interact with demethylases. Samples of many of the tested compounds were generously provided by Prof. Stephen Frye, University of North Carolina. From this initial screen, indole **18** was identified as a promising hit for further optimization, due to its reasonably low IC_{50} and apparent selectivity for KDM2A (Table 1.1). The *N*-alkyl pyrrolidine group is a common motif in inhibitors of methyl-lysine reading domains and HMTs, as it has been shown to mimic the dimethylated lysine sidechain.[71, 72] It was therefore initially proposed that **18** might be acting as a peptide/histone competitor.

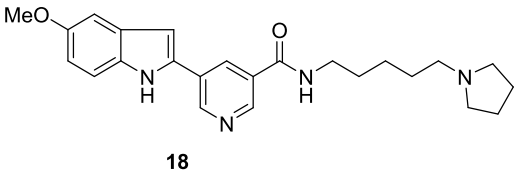

18

Enzyme	% Inhibition ([18] = 20 μM)
KDM2A	93
KDM3A	37
JMJD4C	0
KDM5B	36
KDM6B	0

Table 1.1 – Inhibitory activity of initial hit **17** against a panel of demethylases.

After confirming its potency using the orthogonal RapidFire activity assay (see subsection 2.1.2), a small library of close analogues of **18** was synthesized and tested to explore structure-activity relationships (SARs) around the indole core.[†] Key results of this preliminary investigation are illustrated in Figure 1.11. Replacing the methoxy substituent at the *C*5 position with a trifluoromethoxy group led to a drop in inhibitory activity (**18** vs. **19** and **20** vs. **21**). Functionalization at the indole *N*H position to generate a *tert*-butyl carbamate (**20**) and a *S*-phenylsulfonamide (**22**) resulted in an increase in potency, while the other sulfonamide (**23**) and cyclohexyl amide (**24**) examples were found to be less active than the original hit.

[*] This work was done by Dr Anthony Tumber, Target Discovery Institute.
[†] This work was done by Dr Tamas Szommer, Target Discovery Institute.

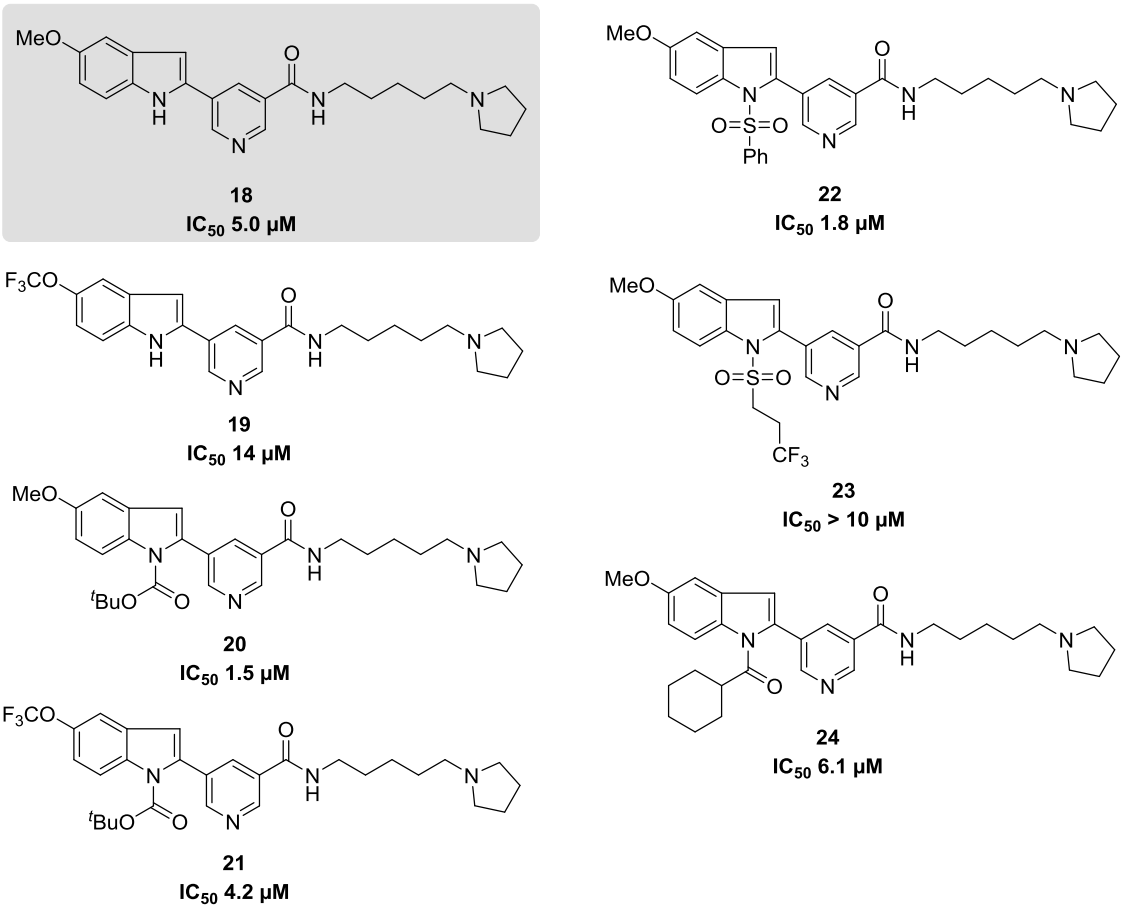

Figure 1.11 – Initial SAR studies around the indole core of **18**, including IC_{50} values for KDM2A inhibition (determined by RapidFire activity assay*).

1.4.2 Pharmacophore Design and Synthetic Approach

We hypothesized that both the inhibitory activity and selectivity of **18** might be further improved by replacing the original indole scaffold with an indoline ring system, which would potentially enable a more efficient exploration of chemical space. Therefore, pharmacophore **25** was proposed, and we aimed to generate a library of potential KDM2A inhibitors based on this structure (Figure 1.12). A modular synthetic approach would be

* IC_{50}-determination experiments were performed in duplicate by Dr Anthony Tumber. The values presented here correspond to the arithmetic mean of the 2 obtained measurements displayed to 2 significant figures. This approach for presenting inhibitory activities will be adopted throughout this thesis. For a more statistically-rigorous summary of all RapidFire results, see section 8.1 in the appendix.

employed to expedite SAR studies, and we anticipated being able to apply recently-developed methodology to synthesize lead compounds asymmetrically.

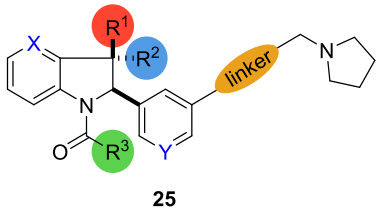

25

Figure 1.12 – Indoline-containing pharmacophore.

Previous research in the Smith group has focused on the development of cation-directed enantioselective cyclization reactions to generate various heterocyclic scaffolds, including indolines[73, 74] and aza-indolines,[75] indolenines,[76] pyrroloindolines,[77] and indanes[78] (Figure 1.13). These reactions rely on the formation of a tight-ion pair involving a chiral quaternary ammonium catalyst and the deprotonated substrate. The stereocontrolled 5-*endo*-trig cyclization of aldimines under basic conditions and in the presence of a cinchona-alkaloid catalyst (**26** to **27**) is most relevant to this project.

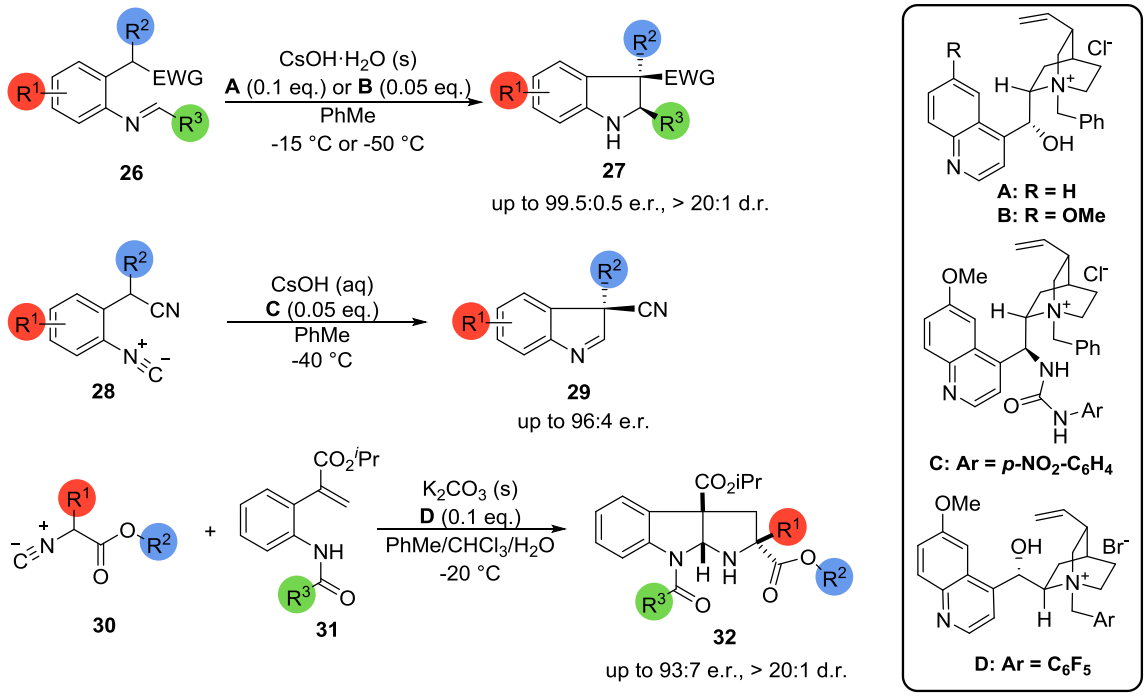

Figure 1.13 – Examples of cation-directed cyclization reactions developed in the Smith group.

Our general synthetic strategy towards the generation of a diverse library of functionalized indolines is illustrated in Scheme 1.1. We anticipated that the modular nature of this synthetic approach would provide access to a variety of compounds containing different substituents at the indoline *C*2 and *C*3 positions. In addition, we envisaged making use of enantioselective phase-transfer catalysis to control both the relative and the absolute stereochemistry of the indoline core (**34** to **35**). *N*-acylation would stabilize this core towards oxidation and provide an additional handle for functionalization. Finally, metal-catalyzed cross coupling reactions would be used to link the indoline ring system to the *N*-alkyl pyrrolidine "head-group" *via* a choice of linkers.

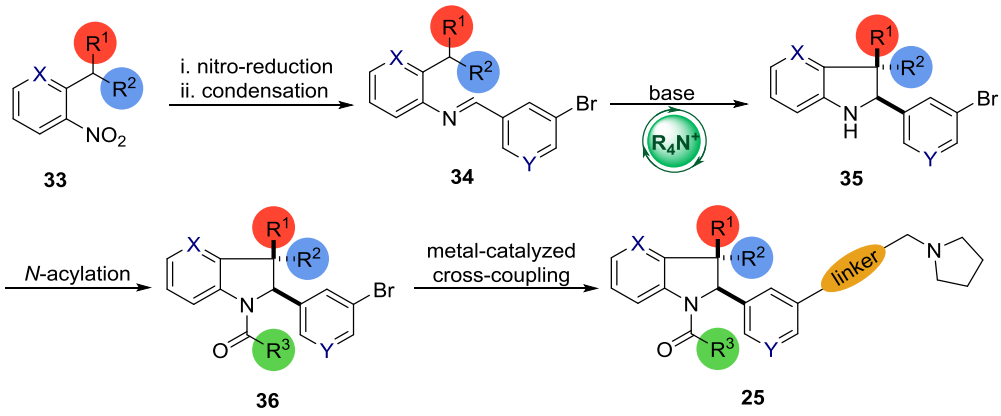

Scheme 1.1 – General synthetic approach to the creation of a library of potential KDM2A inhibitors based on the structure of pharmacophore **25**.

This thesis will explore the details, scope, and limitations of this synthetic approach in the context of developing novel KDM2A inhibitors and chemical probe candidates. Subsequently, it will describe investigations into the mode of inhibition of lead compounds, drawing on a variety of experimental techniques. The insights attained in the course of these studies demonstrate the successful application and further development of asymmetric organocatalysis to a topical challenge in chemical biology.

2. SYNTHESIS OF A LIBRARY OF KDM2A INHIBITORS

2.1 Biochemical Activity Assays

2.1.1 AlphaScreen™

The availability of robust biological assays is essential for investigating structure-activity relationships effectively. At the outset of this project, two biochemical activity assays, the AlphaScreen™ and the RapidFire assay, could be relied upon to provide reproducible results for KDM inhibition. These assays have been applied widely within the Structural Genomics Consortium (SGC). Unless otherwise stated, all of the IC_{50} values presented in this thesis were obtained by Dr Anthony Tumber at the Target Discovery Institute (TDI).

The application of **A**mplified **L**uminescence **P**roximity **H**omogenous **A**ssay (ALPHA) technology to the study of JmjC-KDMs was first reported by A. Kawamura and C. J. Schofield in 2010.[79] The principle features of this assay are illustrated in Figure 2.1. Biotinylated peptide oligomers containing a specific mono-, di-, or trimethyl-lysine residue are immobilized on streptavidin-coated "donor" beads, which contain a covalently-attached photosensitizer such as phthalocyanine. Antibodies that selectively recognize a particular methylation state of the peptide are immobilized on streptavidin-coated "acceptor" beads, which contain covalently-attached thioxene and one or multiple fluorophores. Upon illumination of this system with a 680 nm laser, the photosensitizer on the donor beads is

electronically excited and causes the excitation of ambient oxygen to its more reactive singlet state *via* collision-mediated energy transfer.[80] Provided that the antibody is bound to the peptide and the donor and acceptor beads are therefore in close proximity (within approx. 200 nm), this singlet oxygen has a distinct likelihood of reacting with the thioxene on the acceptor beads. The reactive intermediates that are formed can undergo chemiluminescence and thereby excite the fluorophores on the acceptor beads.[81] This generates a measurable fluorescence signal.

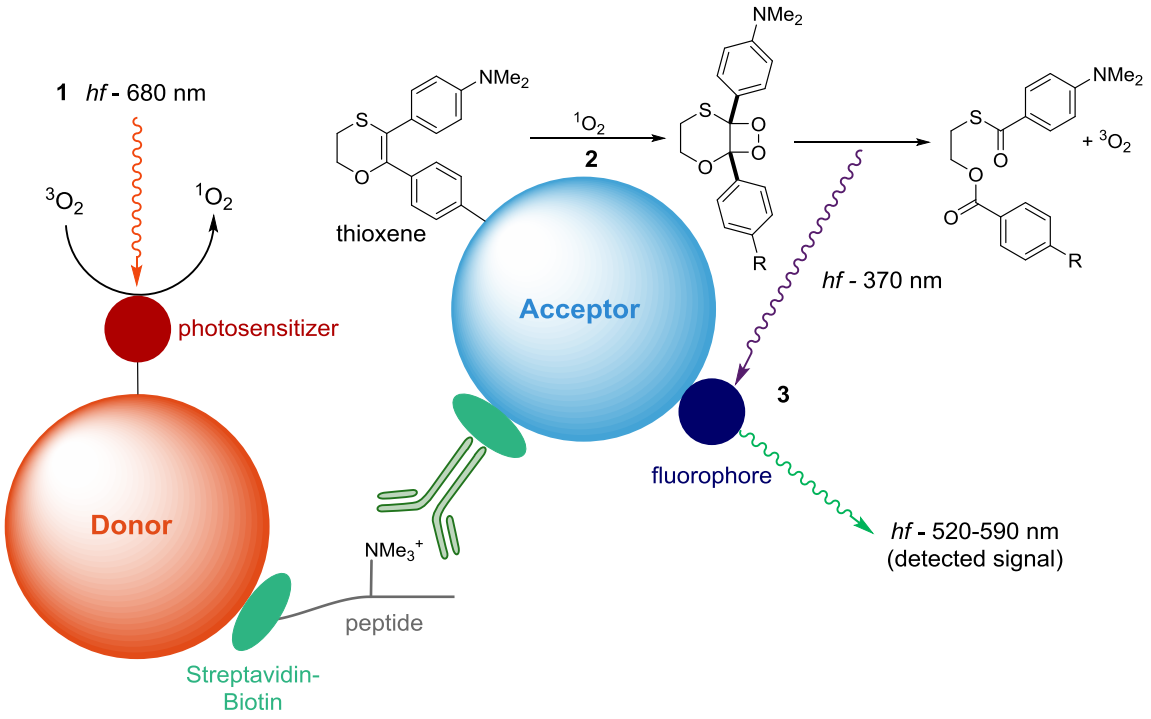

Figure 2.1 – General principle of the AlphaScreen™: 1) A 680 nm laser excites photosensitizers immobilized on the surface of the donor beads, resulting in the formation of singlet oxygen. 2) Singlet oxygen reacts with thioxene immobilized on the surface of the acceptor beads. The decomposition of the resulting intermediates generates chemiluminescence, which excites immobilized fluorophores. 3) Fluorescence is only detected if the beads are in sufficient proximity to enable the efficient transfer of energy between them.

In the presence of the relevant catalytically-active KDM, the methyl-lysine residues on the peptide will be demethylated, and consequently the antibody will not bind. As a result, the donor and acceptor beads are likely to be too far apart to enable the efficient transfer of energy from the photosensitizer to thioxene *via* singlet oxygen. Instead, the singlet oxygen that is generated is more likely to be consumed by various quenching processes.[82] This ultimately results in a reduction of the fluorescence signal. The extent of this signal reduction can be attenuated by adding a KDM inhibitor.

The principle strength of the AlphaScreen™ is its high degree of signal amplification, as each donor bead is able to emit up to 60,000 molecules of singlet oxygen per second.[83] Therefore, only small quantities of peptide and protein are required, making it an ideal platform for high-throughput screening (HTS). Principle drawbacks of the AlphaScreen™ include potential fluorescence and fluorescence-quenching by compounds containing aromatic functional groups as well as quenching of singlet oxygen by inhibitors. Both of these events distort the measured signal and may generate either false-positive or false-negative results. Therefore, it is essential to have an independent, non-luminescence-based assay to verify inhibitory activities.

2.1.2 RapidFire Activity Assay

The RapidFire activity assay provides a relatively direct insight into the catalytic activity of KDMs. It relies on a high-throughput mass spectrometer to monitor the progress of demethylation of an approximately 20-meric peptide substrate.* The peaks corresponding to peptides in different methylation states may be integrated, and the ratio of the integration areas reveals the conversion of the reaction.[84] The addition of an

* Peptide sequence: SAPATGGVK(Me2)KPHRYRPGTVAL

enzymatic inhibitor reduces the conversion at a given time point in a concentration-dependent manner. Typical spectra generated by this assay and a time-course activity plot are illustrated in Figure 2.2.

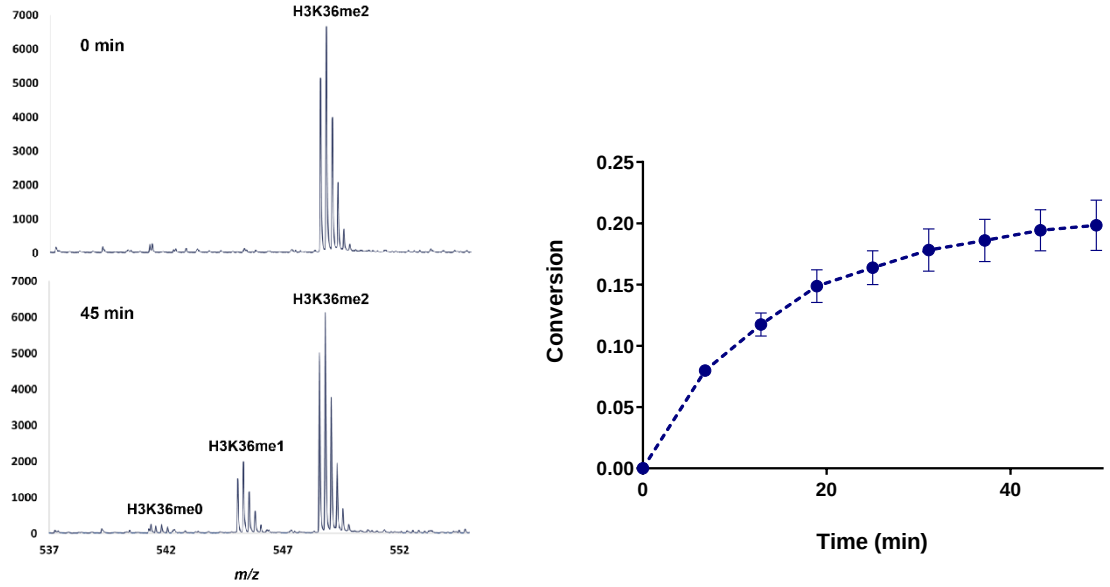

Figure 2.2 – A) The KDM2A-catalyzed conversion of the H3K36me2 peptide to H3K36me1 and H3K36me0 peptides may be monitored over time using the RapidFire MS assay. B) Time-course activity plot of KDM2A-catalyzed demethylation of H3K36me2 peptide.

Thanks to its simplicity, the RapidFire assay is generally regarded as a robust and reliable approach to determining inhibitory activities. Its principle drawbacks are the requirement for a costly and elaborate mass-spectrometry platform, a relatively low level of sensitivity so that larger quantities of peptide and enzyme are required, and a long sample run-time. These factors make the RapidFire assay less suitable for HTS or selectivity screening, and it is generally applied to lead optimization instead.

2.2 SAR Studies with Racemic Indolines

2.2.1 Criteria for Chemical Probe Development

In order to devise a clear project goal, we decided to adopt the SGC guidelines for

chemical probe development, which outline the criteria that an inhibitor needs to satisfy before being considered a true chemical probe:[85]

1) *In vitro* potency (i.e. IC_{50}, K_i, or K_D) ≤ 100 nM.
2) > 30-fold selectivity relative to other proteins in the same family (i.e. members of the KDM3, KDM4, KDM5, KDM6, and KDM7 subfamilies in our case).
3) Significant on-target cellular activity at 1 µM.

We envisaged using both the AlphaScreen™ and RapidFire activity assays to assess *in vitro* potency of synthesized compounds and provide guidance for SAR investigations. For lead compounds, we would also obtain AlphaScreen™ IC_{50}-values with respect to representative members of the various KDM subfamilies in order to evaluate selectivity. It is important to note that all KDM assays of the same type (i.e. AlphaScreen™ or RapidFire) contain analogous components at identical concentrations, measure the same output, and operate according to the same principles, and we therefore reasoned that comparing IC_{50} values would provide a reliable insight into selectivity. Finally, cellular activities of lead compounds would be determined using an immunofluorescence-based assay to monitor histone demethylation in a cellular context (subsection 3.1.1).

2.2.2 Substituents at the Indoline C3 Position

We began our methodical exploration of SARs around the indoline core of pharmacophore **25** by investigating the effect of various substituents at the indoline *C*3-position. To a certain extent, the scope of potential functional group combinations was limited by our chosen synthetic approach, which required the *C*3-substituents to be sufficiently electron-withdrawing to enable deprotonation and subsequent cyclization of

imine **42** to generate the desired indoline core (Scheme 2.1). In most cases, we envisaged introducing these groups *via* a nucleophilic aromatic substitution on 1-fluoro-2-nitrobenzene **37**. Reduction of the nitro group, followed by condensation with 5-bromo-3-pyridinecarboxaldehyde would afford imine **42**. Under racemic reaction conditions, we anticipated that imine **42** would cyclize to afford a mixture of separable diastereomers. Acylation with a simple acetyl group in the first instance would stabilize the indoline core towards oxidation, and a Stille-Migita cross-coupling would introduce the *N*-alkyl pyrrolidine function connected to the indoline core by a *trans*-alkene linker.

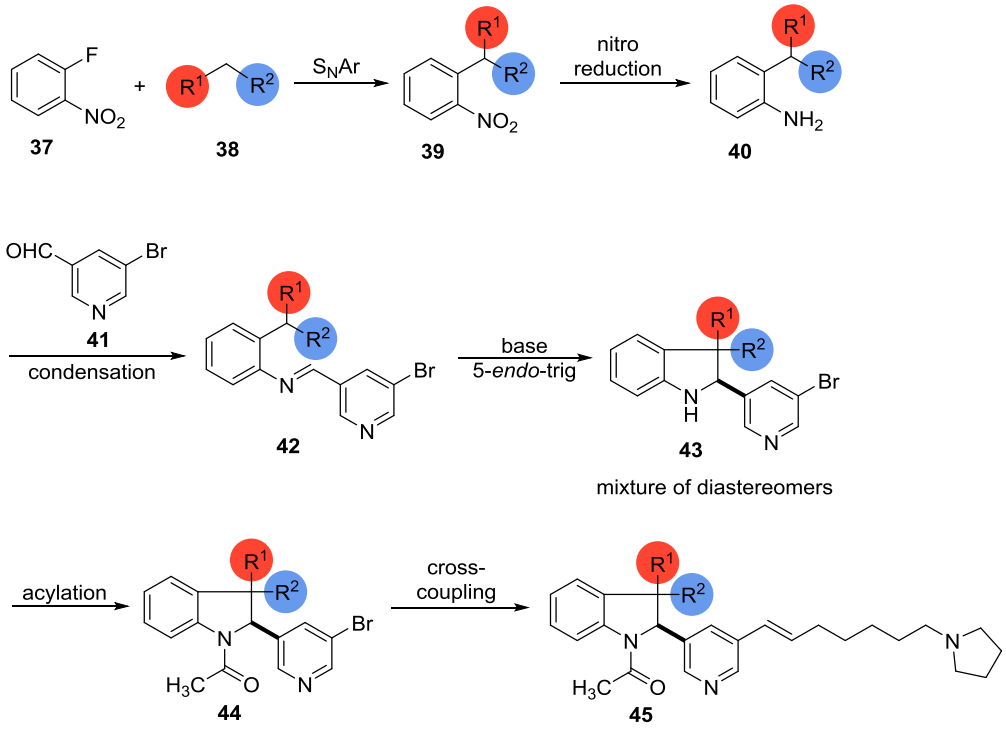

Scheme 2.1 – Synthetic approach towards the exploration of SARs around the indoline *C*3 position.

To begin with, nitrile **46** (R^1,R^2 = *Ph*,*CN*) was synthesized using a S_NAr reaction, involving treatment of a mixture of 1-fluoro-2-nitrobenzene and benzyl cyanide with aqueous NaOH in the presence of stoichiometric tetrabutylammonium bisulfate. The use of tetrabutylammonium salts in reactions of this type and the significance of their stoichiometry has been discussed previously by M. Mąkosza.[86] The reaction could be

performed on a multi-gram scale and reproducibly afforded nitrile **46** in moderate yield. Reduction of the nitro group to generate aniline **47** was accomplished using zinc powder in the presence of NH_4Cl.[87] No reduction of the nitrile function under these conditions was observed. Aniline **47** was subsequently condensed with 5-bromo-3-pyridinecarboxaldehyde **41** using excess $MgSO_4$ as a desiccant to afford imine **48** as a single geometrical isomer (Scheme 2.2).

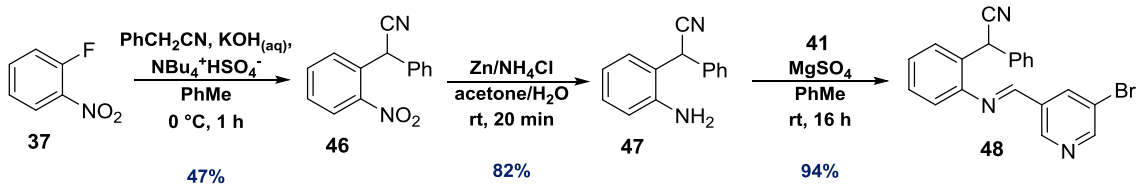

Scheme 2.2 – Synthesis of imine **48** *via* S_NAr, followed by nitro-group reduction and condensation.

To form the indoline core, imine **48** was treated with 2 equivalents of sublimed KO^{t}Bu. At room temperature and after a reaction time of 1 h, imine **48** was consumed completely to afford a 1:1.3 mixture of indoline diastereomers **49** and **50**. Lowering the temperature to 0 °C and reducing the reaction time to 20 minutes increased this ratio to 1:1.7, while maintaining complete conversion (Scheme 2.3). In order to determine whether the KO^{t}Bu-induced cyclization of imine **48** is reversible, both diastereomers were re-subjected to the reaction conditions. Indeed, **49** and **50** were found to interconvert under these conditions.

Indolines have a propensity to undergo oxidation to indolenines (3H-indoles) on standing, and *N*-protection of the indoline core was therefore necessary to minimize this complication. Both diastereomers were found to be moderately unreactive to a variety of acetylating reagents including acetic anhydride and di-*tert*-butyl dicarbonate. However, the use of acetyl chloride and pyridine gave an excellent yield of both desired protected products **52** and **53** in a rapid manner (Scheme 2.4).

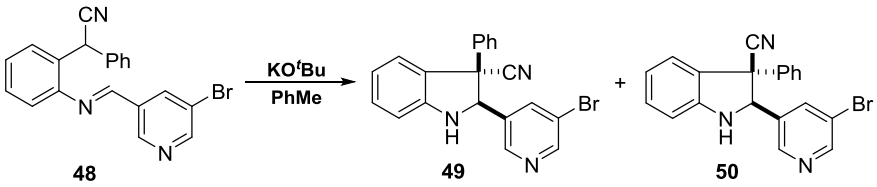

Conditions	49:50	Isolated yield
60 min, rt	1:1.3	75%
20 min, 0 °C	1:1.7	84%

Scheme 2.3 – Cyclization of imine **48** to afford a diastereomeric mixture of indolines **49** and **50**. The relative stereochemistries of both products were determined by nOe spectroscopy.

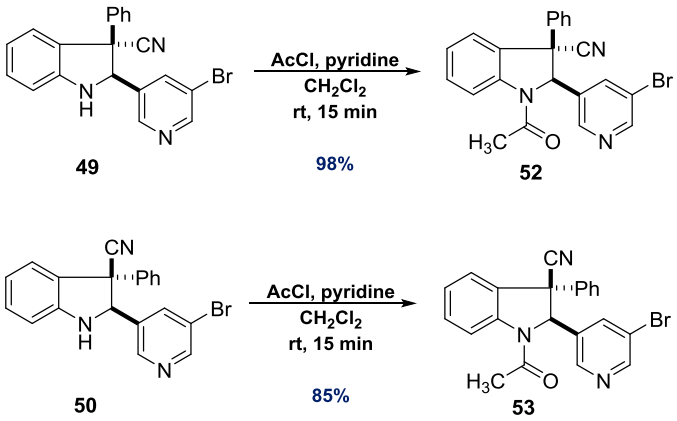

Scheme 2.4 – *N*-Acetylation of the indoline core.

We envisaged using the bromopyridine moiety on the indoline *C*2 position as a functional handle for coupling to the indoline core *via* metal-catalyzed cross-coupling methodologies. Scheme 2.5 illustrates the synthesis of *E*-7-tributylstannyl-hept-6-en-1-pyrrolidine **57**, which we anticipated could be utilized as a cross-coupling partner *via* a Stille-Migita reaction.[88, 89] J. M. Chong and co-workers had previously demonstrated the impact of different Pd(0) catalysts and phosphine ligands on the regioselectivity of hydrostannylation reactions involving terminal alkynes.[90] In the course of their investigations, bulkier phosphine ligands were generally found to improve regioselectivity, and, for most substrates, the combination of $Pd_2(dba)_3$ with $Cyc_3PH^+BF_4^-$ in $(^iPr)_2NEt$ maximized the yield of the desired *E*-vinylstannane product (Figure 2.3). Application of

these reaction conditions to the hydrostannylation of 7-hetyn-1-ol **54** with tributyltin hydride afforded vinylstannane **55** in good yield and as a single regio- and stereoisomer. Furthermore, this reaction could be performed reliably on a gram-scale. The primary alcohol group of **55** was converted to an alkyl bromide using an Appel reaction,[91] and substitution with pyrrolidine generated vinylstannane **57** in moderate yield.

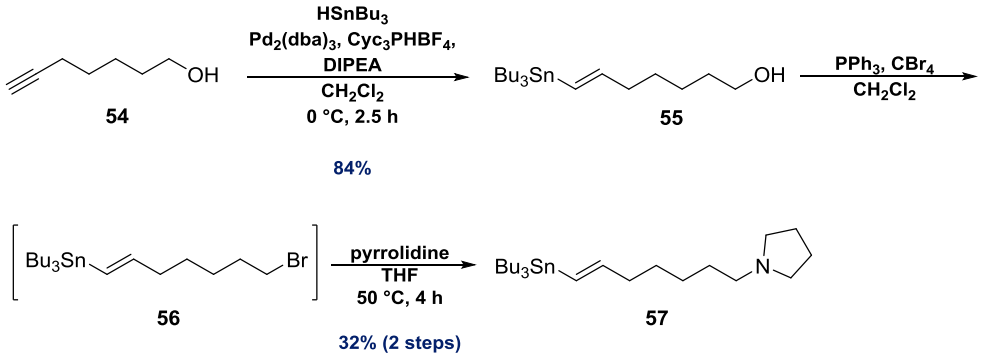

Scheme 2.5 – Synthesis of vinylstannane **57**.

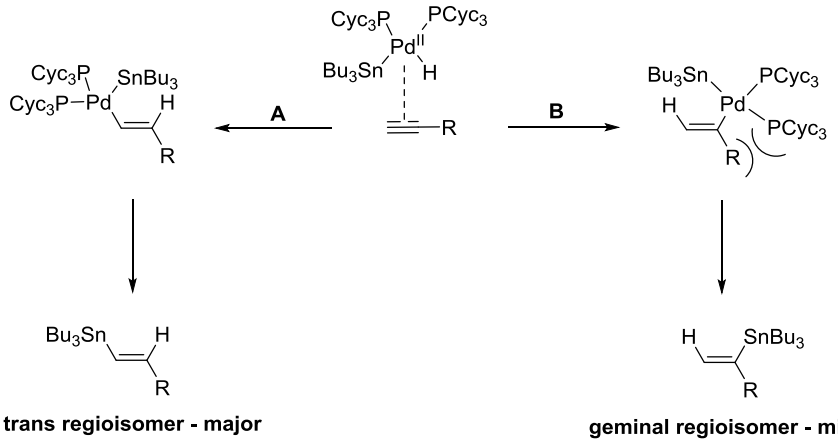

Figure 2.3 – Mechanistic rational for the observed regioselectivity of hydrostannylation of terminal alkynes, as proposed by J. M. Chong. The reaction is suggested to proceed *via* initial hydropalladation rather than stannylpalladation. Pathway **A** is preferred over pathway **B**, as it avoids steric clash involving the bulky phosphine ligands.

A variety of catalysts and reaction conditions for the Pd(0)-catalyzed cross-coupling of aryl halides and vinylstannanes have been reported.[92] Fortunately, we were able to draw

on the extensive experience of Smith group member Dr Craig Johnston to decide which of these conditions would be most applicable to our combination of coupling partners. The Stille-Migita cross-coupling of indolines **52** and **53** with vinylstannane **57** was ultimately carried out in the presence of catalytic $Pd(PPh_3)_4$ in NMP, according to a procedure previously described by D. M. Berger.[93] Under these conditions, indolines **58** and **59** were obtained in moderate yield with complete retention of the *E*-alkene geometry (Scheme 2.6).

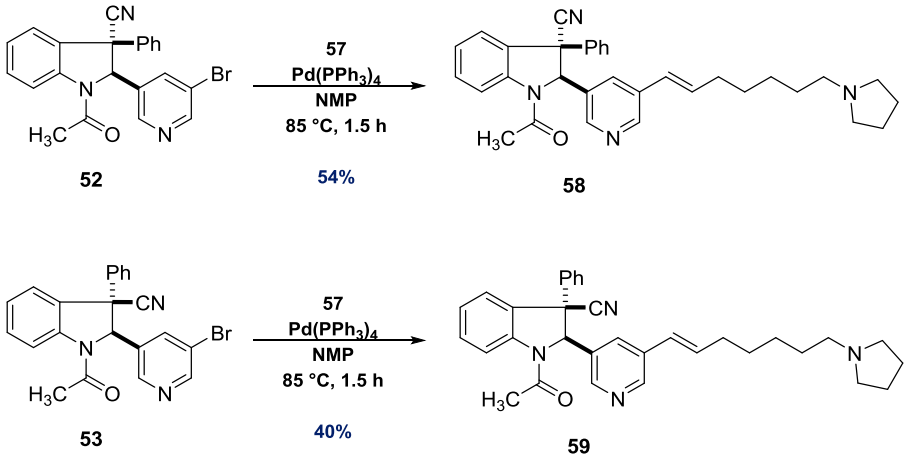

Scheme 2.6 – Stille-Migita cross coupling to afford indolines **58** and **59**. The *E*-geometry of the alkene linker was confirmed by analysis of the alkene-proton coupling constants.

We decided to apply this six-step synthetic route to the synthesis of analogues of **58** and **59**, bearing different functional groups on the indoline *C*3 position. Scheme 2.7 illustrates the synthesis of indolines **69** and **70**, in which the nitrile group of **58** and **59** is replaced by a methyl ester. Different reagents and reaction conditions to those discussed previously were used to effect the S_NAr reaction between 1-fluoro-2-nitrobenzene **37** and methyl phenylacetate **61**. This transformation proved to be substantially less reliable than the analogous reaction with benzyl cyanide due to the formation of a variety of unidentified side products. The nitro group of ester **62** was reduced by hydrogenation over a palladium on charcoal catalyst, as reduction using Zn powder and NH_4Cl resulted in *in situ* cyclization

of the initial aniline product to form a lactam. Aniline **63** was also found to undergo lactamization during silica-gel column chromatography, and it was therefore necessary to use unpurified material in the condensation with 5-bromo-3-carboxaldehyde **41** to generate imine **64**. Imine **64** was cyclized under identical reaction conditions to those applied to imine **48** to afford the diastereomeric indolines **65** and **66** in essentially equal proportions. Indolines **65** and **66** were acetylated using acetyl chloride and pyridine, and the resulting products underwent cross-coupling with vinylstannane **57** to afford **69** and **70** in moderate yield.

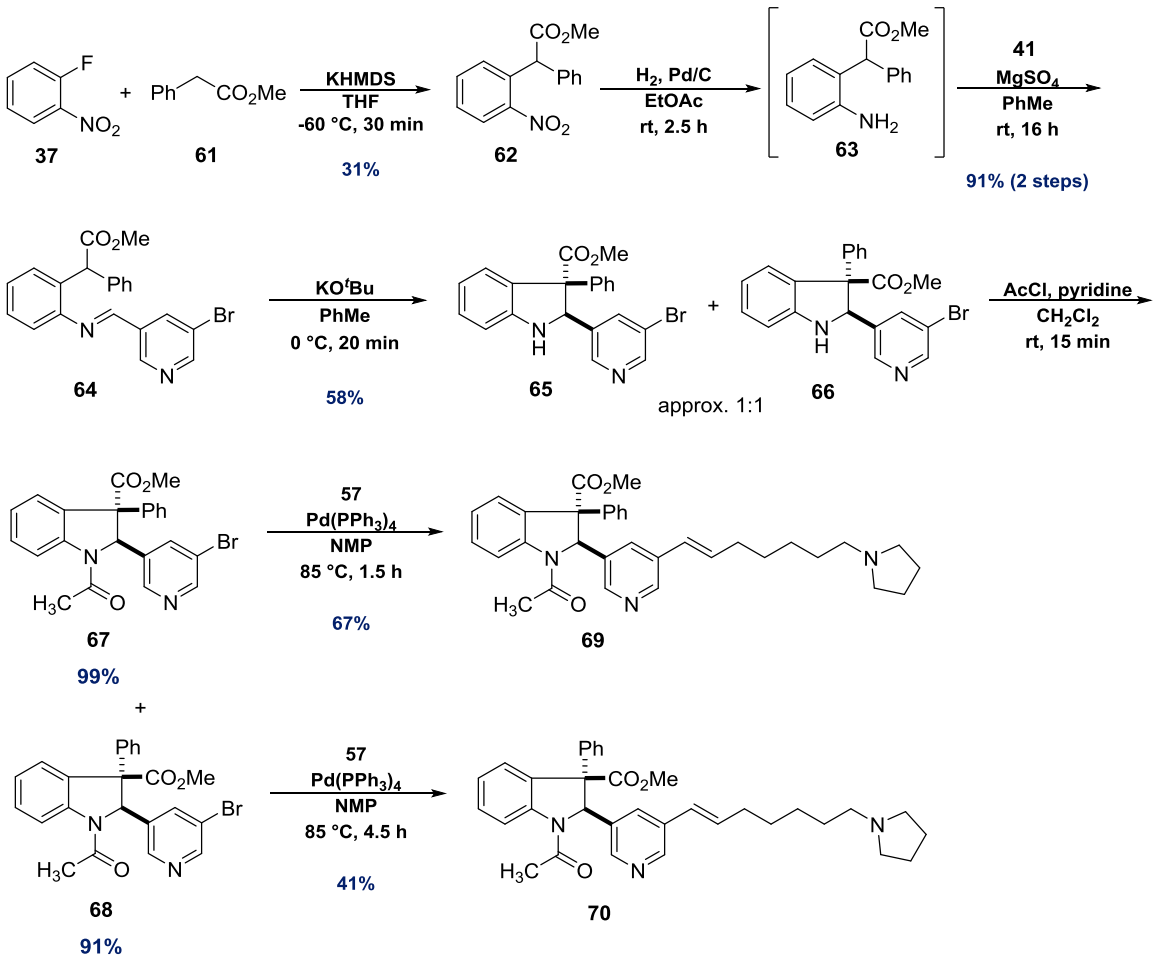

Scheme 2.7 – Synthesis of indolines **69** and **70**: The relative stereochemistries of indolines **65** and **66** were assigned by nOe spectroscopy.

In order to have an example that did not contain a phenyl substituent on the indoline *C*3 position, we investigated the possibility of a nitrile-ester combination of functional groups on this site. Ethyl cyanoacetate **72** and 1-fluoro-2-nitrobenzene **37** underwent a S_NAr reaction to afford ester **73**. As had been observed with the conversion of nitro-ester **62** to aniline **63**, aniline **74** was susceptible to *in situ* lactamization when Zn-powder and NH_4Cl were used for reduction of the nitro group. A hydrogenation reaction was therefore performed instead. We anticipated that treatment of the unpurified aniline **74** with 5-bromo-3-carboxaldehyde **41** in the presence of excess $MgSO_4$ as a desiccant would afford imine **75**. However, we identified the isolated product of this reaction as indoline **77**, obtained as a 97:3 mixture of diastereomers. The relative stereochemistry of the major product was determined by X-ray crystallography (Figure 2.4). We postulate that the spontaneous cyclization of imine **75** is a result of the facile formation of a reactive zwitterionic form (**76**). Acetylation of indoline **77** and Stille-Migita cross-coupling with vinylstannane **57** afforded indoline **79** (Scheme 2.8).

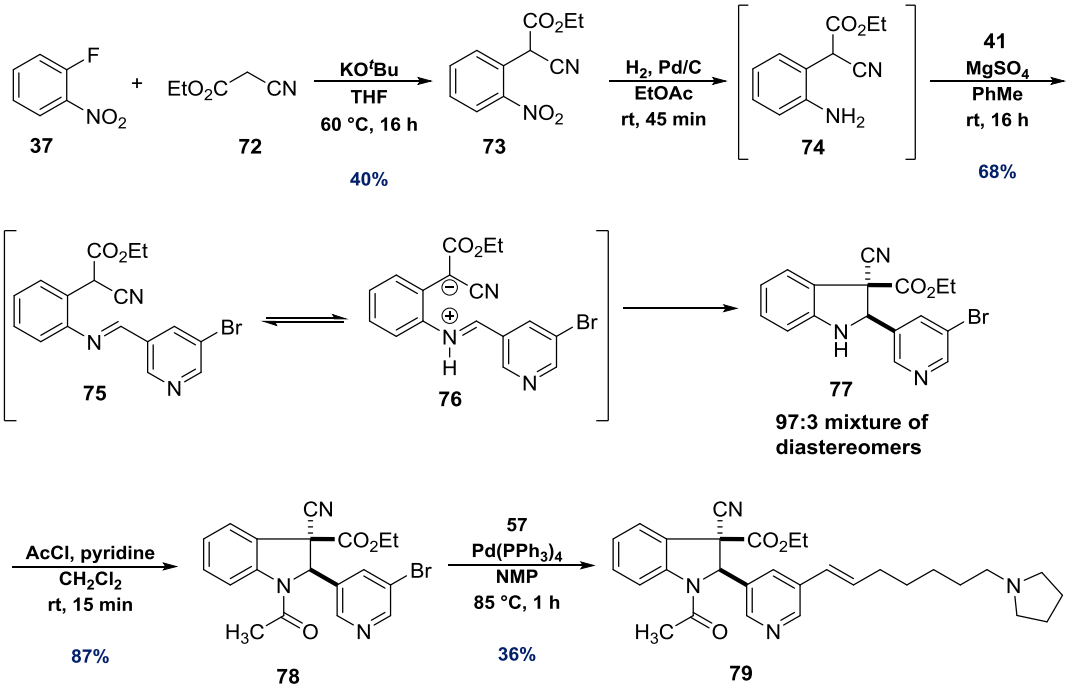

Scheme 2.8 – Synthesis of indoline **79**. Imine **75** could not be isolated, and underwent spontaneous cyclization to indoline **77**.

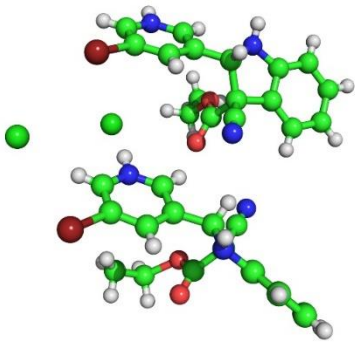

Figure 2.4 – X-ray crystal structure of the major diastereomer of indoline **77**.*

As a final example, we investigated the possibility of an ester-alkyl combination of substituents on the indoline *C*3 position. Condensation of methyl-2-nitrophenylacetic acid **82** with paraformaldehyde afforded ester **83** in excellent yield. Conveniently, both the alkene and the nitro group could be reduced by hydrogenation over a palladium on charcoal catalyst to give aniline **84**, which was condensed without further purification with 5-bromo-3-pyridinecarboxaldehyde **41**, yielding imine **85** (Scheme 2.9).

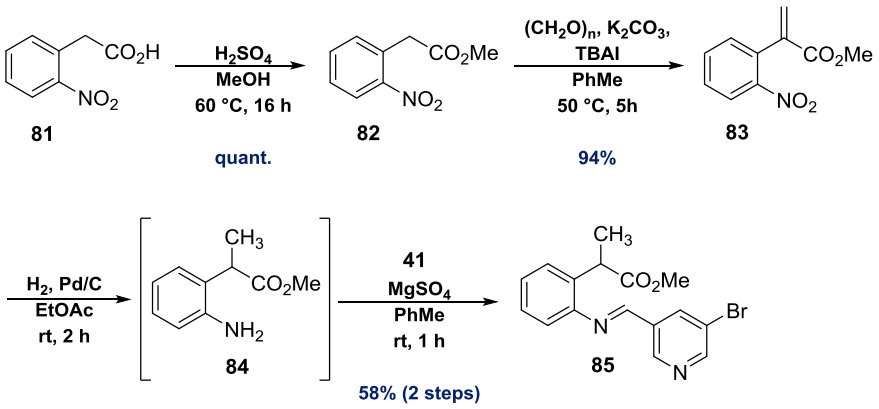

Scheme 2.9 – Synthesis of imine **85**.

Attempts to induce the cyclization of imine **85** with a variety of bases including KO^{t}Bu, NaH, and KHMDS in either toluene or THF proved unfruitful. Given the stark colour change of the reaction mixture upon addition of these bases, we considered it likely that

* X-ray diffraction data was collected and the structure solved by John Joliffe.

deprotonation to generate a delocalized anionic intermediate was occurring. The absence of reactivity was therefore attributed to a higher activation energy barrier of cyclization. Unfortunately, heating the reaction mixture to address this potential issue also failed to induce the desired reaction, suggesting than an alternative synthetic approach would be needed to obtain this particular substitution pattern on the indoline ring system (Scheme 2.10).

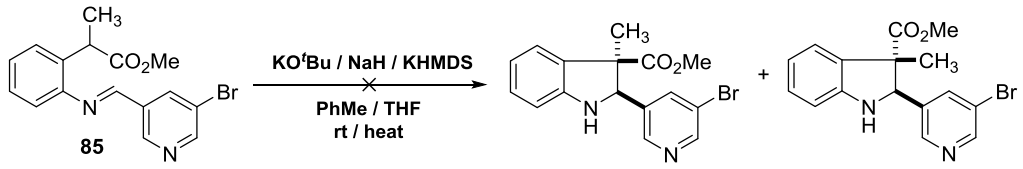

Scheme 2.10 – Unsuccessful cyclization of imine **85**.

Aware of the potential assay interference issues associated with organotin or palladium contaminants, we eluted all final KDM2A inhibitor candidates through a short column of K_2CO_3-silica, previously reported as a highly effective method for removing organotin impurities,[94] and filtered the eluent through a pad of Celite™ as a means of removing any remaining palladium salts. The compounds were subsequently tested for inhibitory activity using the RapidFire activity assay (Figure 2.5).

Excitingly, indolines **58** and **59** showed substantially improved potency relative to the original indole hit **18**. Indolines **69** and **70** appeared to be marginally more potent, and indoline **79** was similarly effective to **18**. For both of the investigated diastereomeric pairs (**58**, **59** and **69**, **70**), the *syn* diastereomers (**59** and **70**) were found to be more potent than their respective *anti* analogues (**58** and **69**). Given these promising results, we decided to focus on indoline scaffolds containing the Ph,CN substitution pattern on the *C*3 position for the remainder of our SAR investigations.

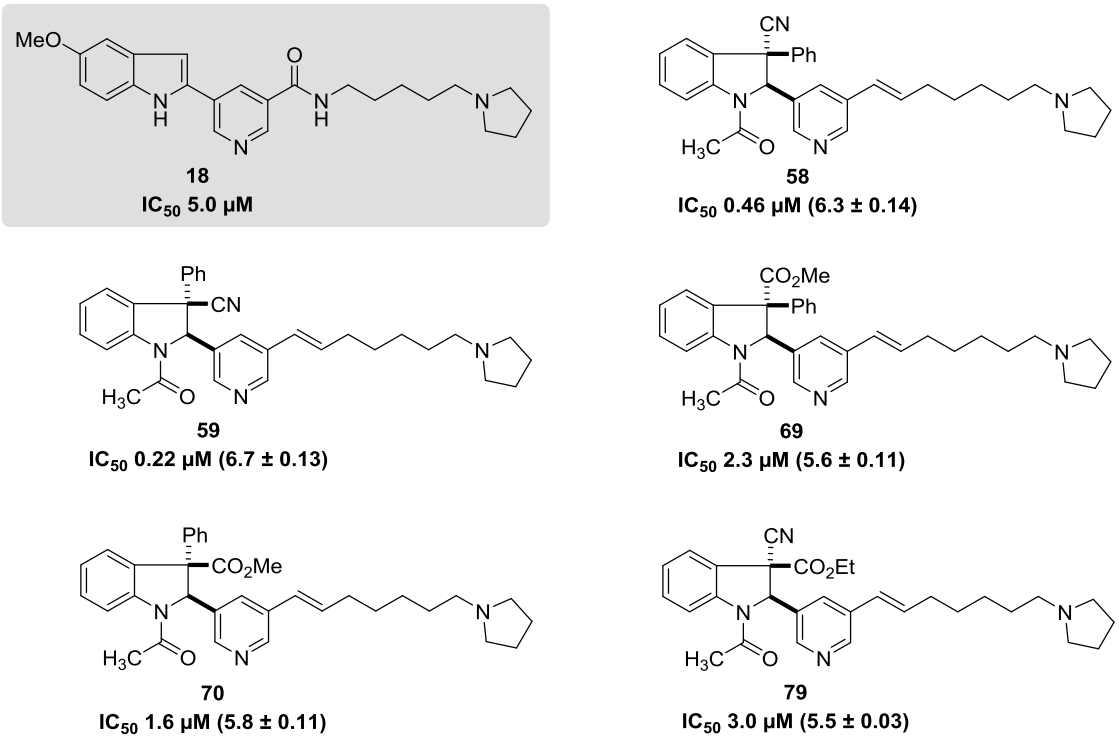

Figure 2.5 – Effect of *C*3 substituents on inhibitory activity. IC_{50} values were determined by RapidFire activity assay. pIC_{50} values and errors are shown in parentheses.*

2.2.3 Head Group and Linker

We had initially hypothesized that the *N*-alkyl pyrrolidine motif in the original hit **18** was acting as a dimethyllysine mimic and that **18** and its derivatives might therefore occupy the histone binding site. To explore the significance of the pyrrolidine "head-group" with respect to inhibition, a series of indoline analogues was synthesized by Dr Jamie Wolstenhulme and tested for inhibitory activity using the AlphaScreen™ (Figure 2.6). For practical synthetic reasons, this series is based on a slightly different indoline core to the one described in the previous subsection. The pyridyl ring at the indoline *C*2 position is replaced by a phenyl ring, and an ether linker is used instead of an *E*-alkene. In general, the combination of these 2 modifications yielded weaker KDM2A inhibitors (Figure 2.6).

* For a statistical error analysis of inhibitory activities, see section 8.1 in the appendix.

Replacing the pyrrolidine head-group with piperidine did not have a significant effect on potency (**86** vs. **87**), while using a morpholine head-group was found to diminish inhibitory activity (**88**). Substituting pyrrolidine with diethylamine (**89**) or cyclopentane (**90**) resulted in a dramatic decrease in KDM2A inhibition, suggesting that a cyclic tertiary amine "head-group" is critical for achieving a high level of potency.

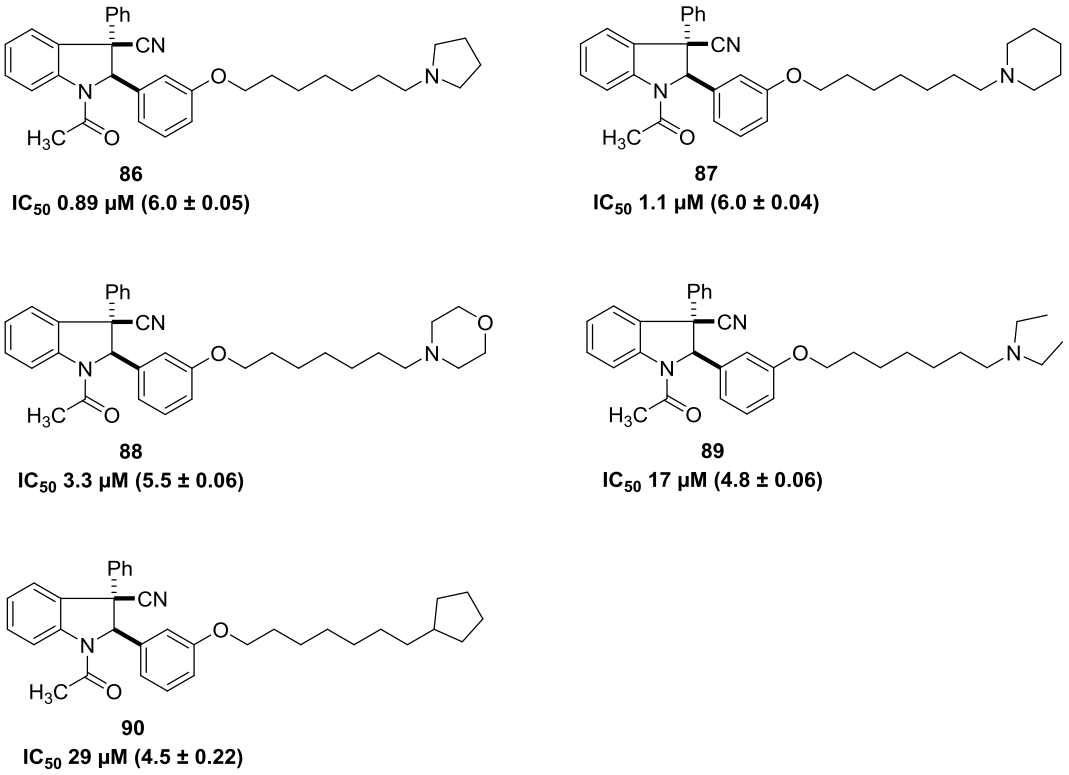

Figure 2.6 – Effect of "head-group" on inhibitory activity.* IC_{50} values were determined by RapidFire activity assay. pIC_{50} values and errors are shown in parentheses.

Next, we decided to explore the effect of varying the length of the alkyl chain on inhibitory activity. A series of indolines with alkyl chains of different lengths was synthesized by Dr Jamie Wolstenhulme and evaluated using the AlphaScreen™ (Table 2.1). A chain length of seven or eight atoms (including oxygen) was found to be optimal,

* Compounds synthesized by Dr Jamie Wolstenhulme.

although we were surprised that there was not a more substantial drop in inhibitory activity for compounds with much shorter or longer alkyl chains.

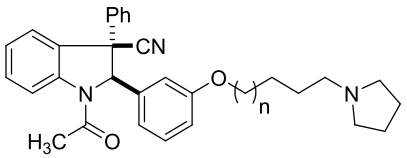

n	IC_{50} (μM)
1	2.0 (5.7 ± 0.12)
2	1.3 (5.9 ± 0.13)
3	1.0 (6.0 ± 0.06)
4	0.89 (6.0 ± 0.05)
5	1.4 (5.9 ± 0.07)
6	1.5 (5.8 ± 0.17)

Table 2.1 – Effect of alkyl chain length on inhibitory activity.* IC_{50} values were determined by RapidFire activity assay. pIC_{50} values and errors are shown in parentheses.

Having identified the optimal chain length and head-group, we wanted to investigate a range of linkers between the indoline core and the *N*-alkyl pyrrolidine motif. Synthesis of the diastereomeric pyridyl analogues of ether-linked indoline **86** is illustrated in Scheme 2.11. Condensation of aniline **47** with 5-(benzyloxy)nicotinaldehyde **91*** afforded imine **92** in good yield, and KO^{t}Bu-induced cyclization of this substrate afforded an inseparable mixture of diastereomers. Fortunately, the acetylated indolines **94** and **95** *were* separable by silica-gel column chromatography. In both cases, the benzyl group was removed by hydrogenation over a palladium on charcoal catalyst, and *O*-alkylation of the resulting products with 1,7-dibromoheptane **97**, followed by substitution with pyrrolidine, afforded the final KDM2A inhibitor candidates **99** and **102**.

We rationalized that using more configurationally-constrained linkers might improve potency, as this would reduce conformational flexibility overall and consequently lower the entropic "cost" of binding to KDM2A. Alkyne **105** was synthesized in two steps from heptyn-1-ol **103** and was used as a substrate for Sonogashira coupling[95] to indolines **52** and **53**, generating the alkyne-linked products **106** and **107** (Scheme 2.12).

* Compounds synthesized by Dr Jamie Wolstenhulme.

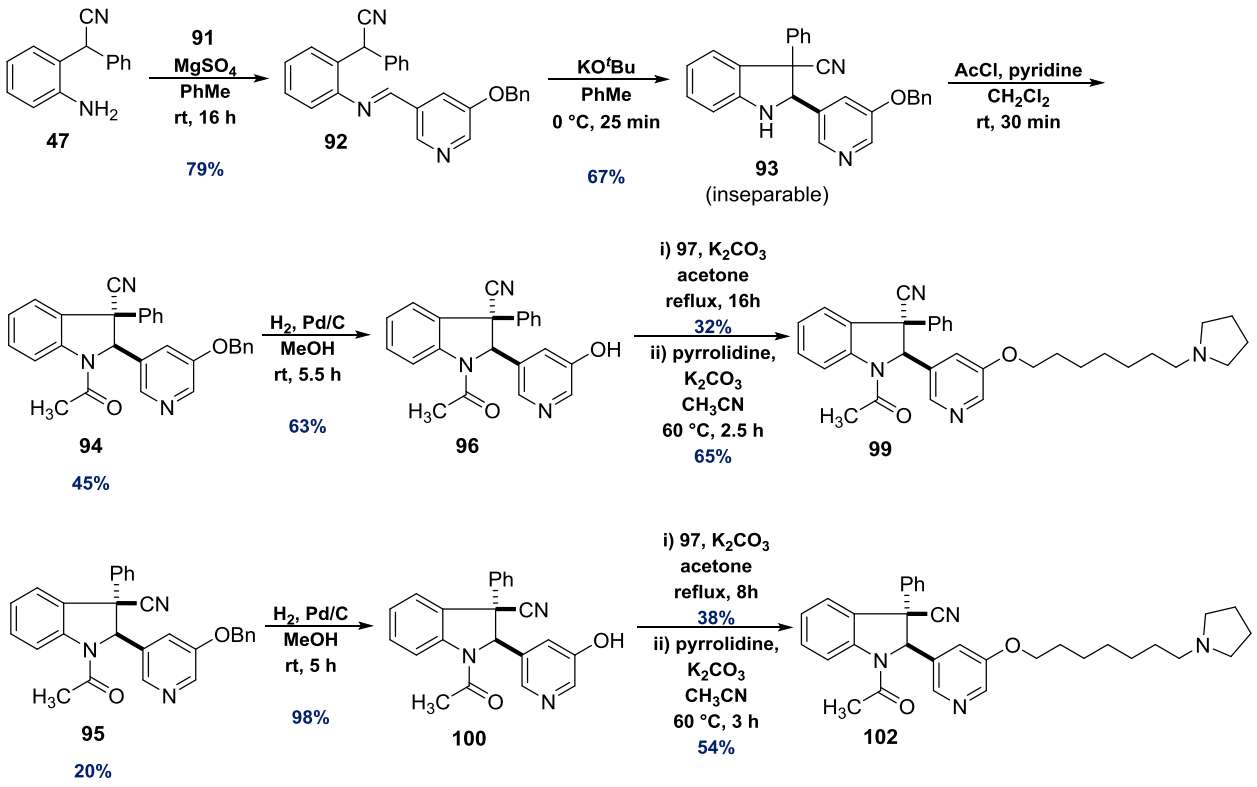

Scheme 2.11 – Synthesis of ether-linked indolines **99** and **102**. Indoline **93** was obtained as an inseparable mixture of diastereomers.

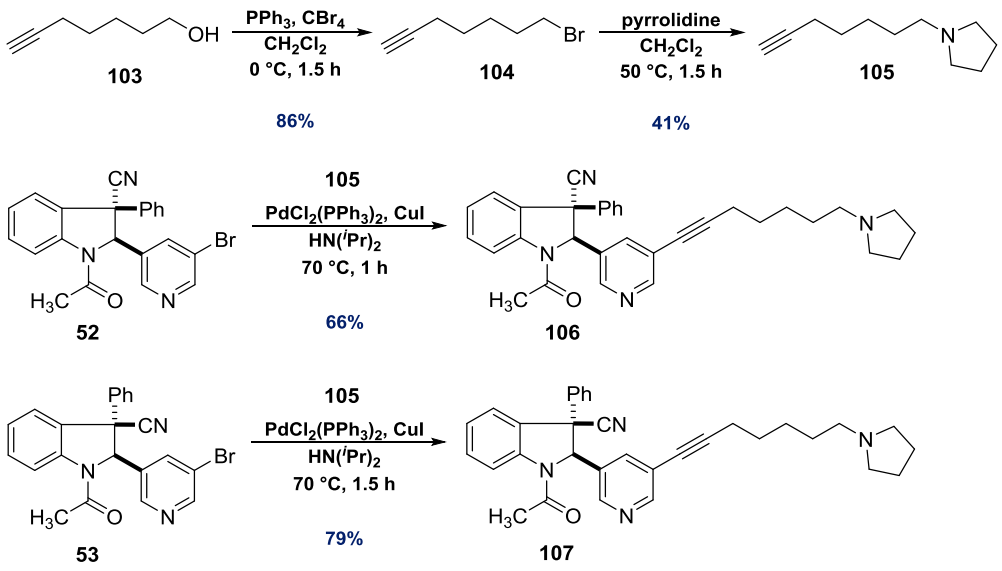

Scheme 2.12 – Synthesis of alkyne **105** and indolines **106** and **107**.

In order to be able to make a direct comparison to a more conformationally-flexible analogue, the *syn*-diastereomer **107** was subsequently converted to the fully-saturated

alkane-linked compound **108** by hydrogenation over a palladium on charcoal catalyst (Scheme 2.13).

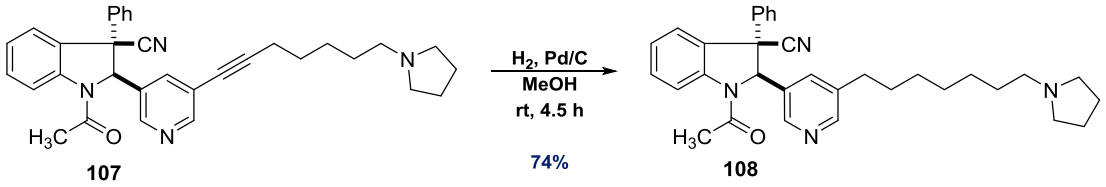

Scheme 2.13 – Hydrogenation of alkyne-linked indoline **107**.

Synthesis of a *Z*-alkene-linked analogue posed an interesting challenge. Partial hydrogenation of the alkyne linker of **107** in a *syn*-selective manner using Lindlar's catalyst[96] was considered as a possible option. However, given the challenges frequently associated with over-reduction in this reaction, we envisaged using a stereoselective coupling instead. Fortunately, K. Oshima and co-workers had reported a hydroindation-coupling sequence to access functionalized *Z*-alkenes (Scheme 2.14),[97] and within the Smith group, this reaction was applied to the total synthesis of the polycyclic alkaloid gephyrotoxin by fellow group member Shuyu Chu.[98] Mechanistically, this transformation is based on the *in situ* generation of $HInCl_2$ from $InCl_3$ and DIBAL-H, which is thought to undergo radical *trans*-hydrometallation to the alkyne substrate in the presence of a radical initiator such as BEt_3 (Figure 2.7). The resulting *Z*-vinylindane can subsequently undergo Pd(0)-catalyzed Suzuki-type coupling to aryl iodides.

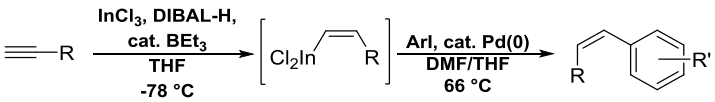

Scheme 2.14 – *Trans*-hydroindation of terminal alkynes, followed by Suzuki-type coupling to generate *Z*-alkenes as reported by K. Oshima.

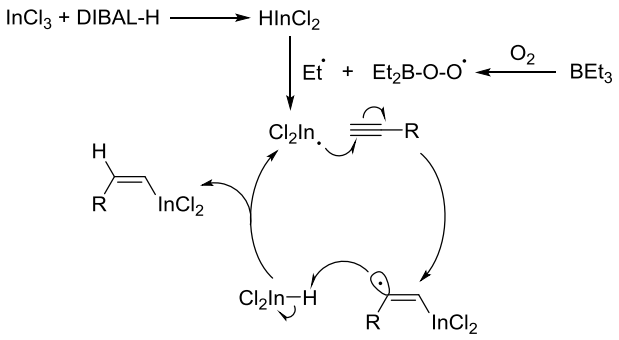

Figure 2.7 – Radical mechanism of *trans*-hydroindation.

Initially, we attempted to perform hydroindation using alkyne **105**, followed by coupling to indoline **53**. However, a complex mixture of products containing only a trace of the desired coupling adduct was obtained. We postulated that the presence of the basic pyrrolidine group was responsible for inducing a variety of side reactions, and alkyne **105** was therefore protonated with 1 equivalent of acetic acid before addition to the hydroindation reaction mixture (Scheme 2.15). Unfortunately, this failed to improve the outcome, and we therefore sought an alternative route to indoline **109**.

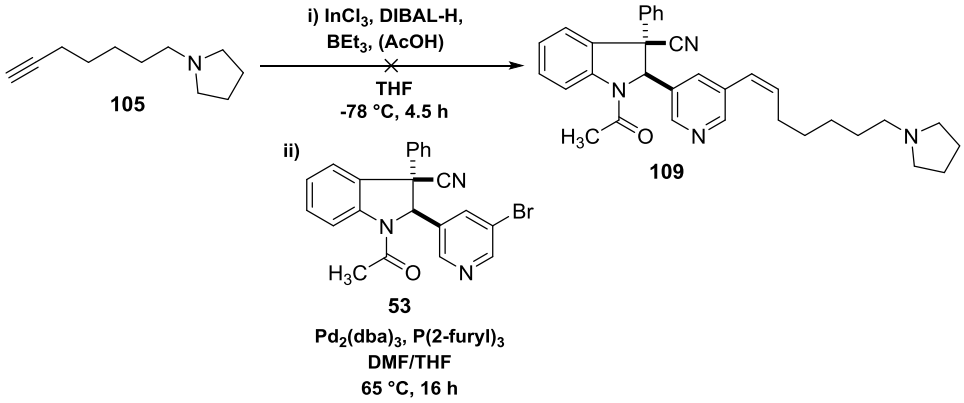

Scheme 2.15 – Attempted hydroindation and coupling with alkyne **105** and indoline **53**.

Given the apparent incompatibility of alkyne **105** with this methodology, we decided to attempt the same hydroindation-coupling sequence using 6-heptyn-1-ol **103** as the alkyne component. Pleasingly, we were able to isolate the *Z*-alkene-linked indoline **110** as the major reaction product. The yield of this transformation could be improved by using

$Pd(PPh_3)_4$ as the catalyst instead of $Pd_2(dba)_3$/P(2-furyl)$_3$ (Scheme 2.16). The primary alcohol of indoline **110** was subsequently converted to a tosylate leaving group, which was displaced by pyrrolidine to afford indoline **109** (Scheme 2.17).

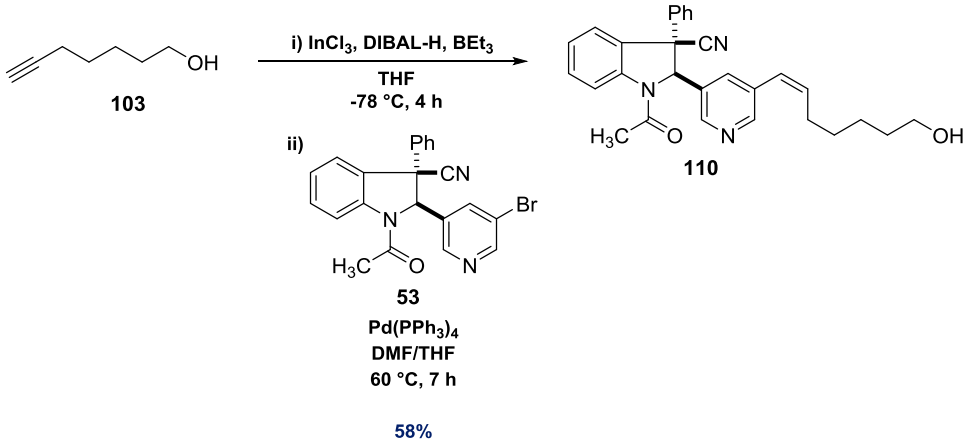

Scheme 2.16 – Hydroindation of 6-heptyn-1-ol **103**, followed by coupling to indoline **53**. The *Z*-geometry of the alkene linker was confirmed by analysis of the alkene-proton coupling constants.

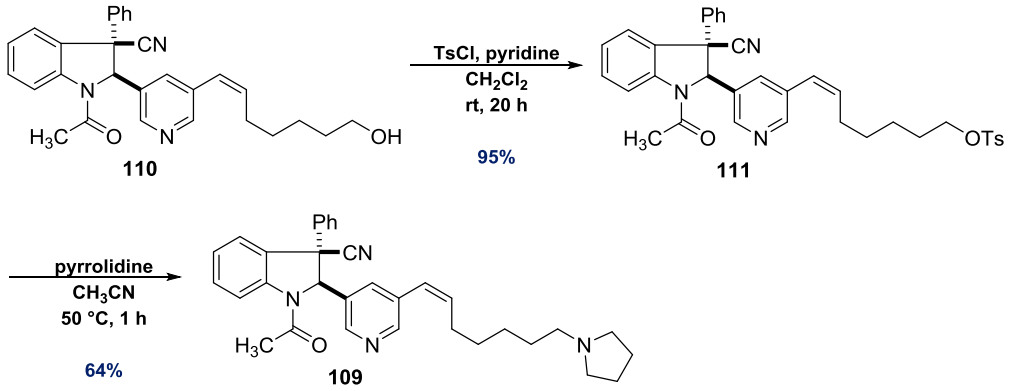

Scheme 2.17 – Tosylation of indoline **110**, followed by displacement of tosylate by pyrrolidine.

In order to have a final example of a configurationally-constrained linker, we envisaged using a copper-catalyzed click reaction to connect the indoline core and *N*-alkyl pyrrolidine motif through a triazole ring. The azide component of this reaction (**114**) was synthesized in two steps from 1,5-dibromopentane **112**, and the alkyne components (**118** and **119**) were synthesized by Sonogashira coupling of indolines **52** and **53** with trimethylsilyl-acetylene **115**, followed by TMS-deprotection with TBAF.

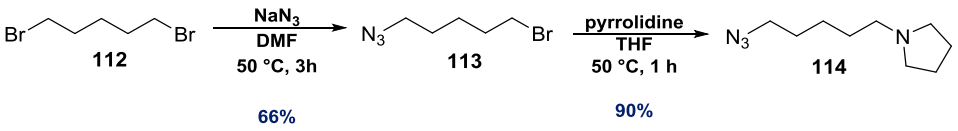

Scheme 2.18 – Synthesis of the azide component of the triazole-click reactions.

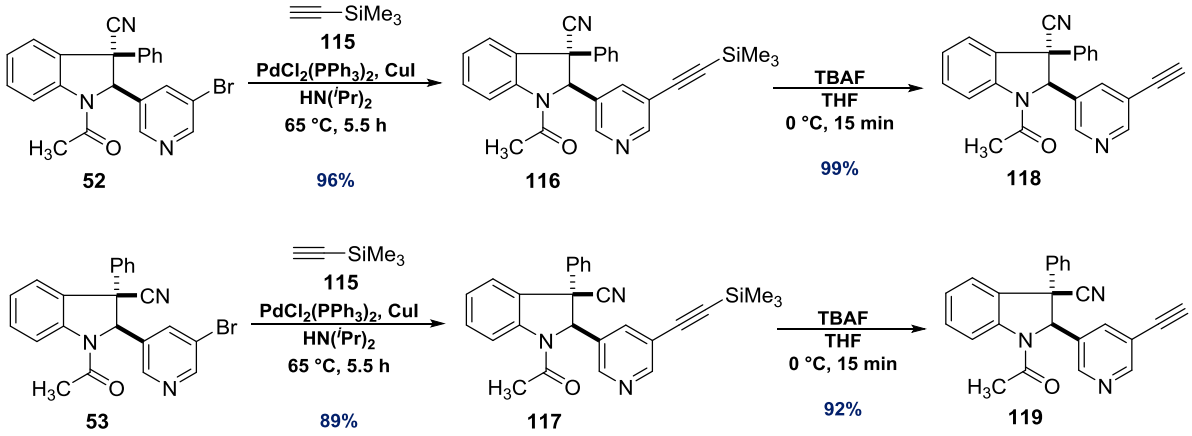

Scheme 2.19 – Synthesis of the alkyne components of the triazole-click reactions.

The combination of $CuSO_4$ and sodium-L-ascorbate has been used extensively as a reliable method of generating Cu^I *in situ*.[99] We therefore adopted a procedure that uses this combination of reagents to carry out click reactions of indolines **118** and **119** with azide **114** (Scheme 2.20). In spite of the relatively modest yields of these transformations, we obtained sufficient material for an evaluation of biological activity.

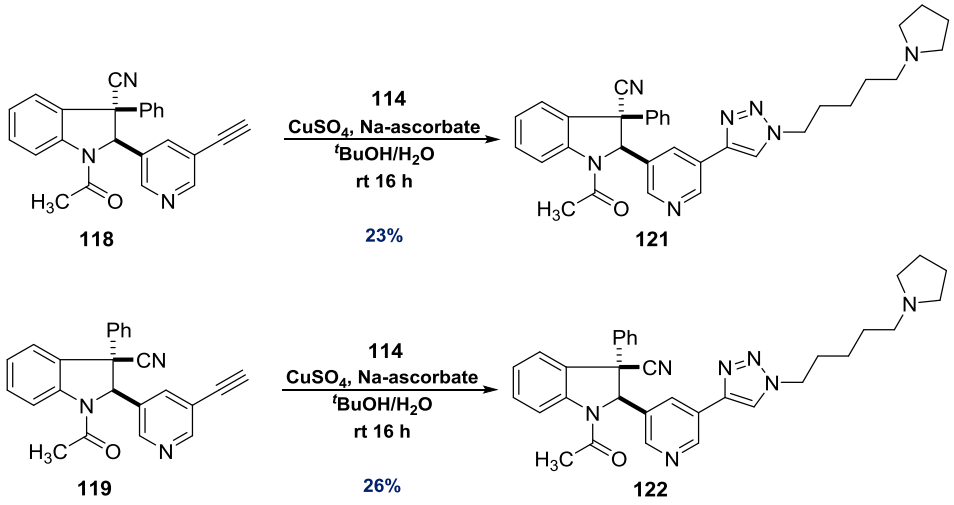

Scheme 2.20 – Cu-catalyzed click reactions of azide **114** with indolines **118** and **119**.

The impact of varying the linker on KDM2A inhibitory activity was assessed using the AlphaScreen™ and RapidFire activity assay (Figure 2.8). As for the *E*-alkene-linked indolines **58** and **59**, the *syn*-diastereomers (**102**, **107**, and **122**) were all found to be more potent than their respective *anti*-analogues (**99**, **106**, and **121**). The observation that the ether-linked compounds (**99** and **102**) and the saturated alkane compound **108** displayed higher inhibitory activities than analogues with more conformationally-rigid linkers such as alkynes **106** and **107** and triazoles **121** and **122** suggests that a reasonably high degree of linker flexibility is desirable. Finally, the observed IC_{50} value of the *Z*-alkene-linked indoline **109** was found to be greater than that of its *E*-alkene equivalent **59**.

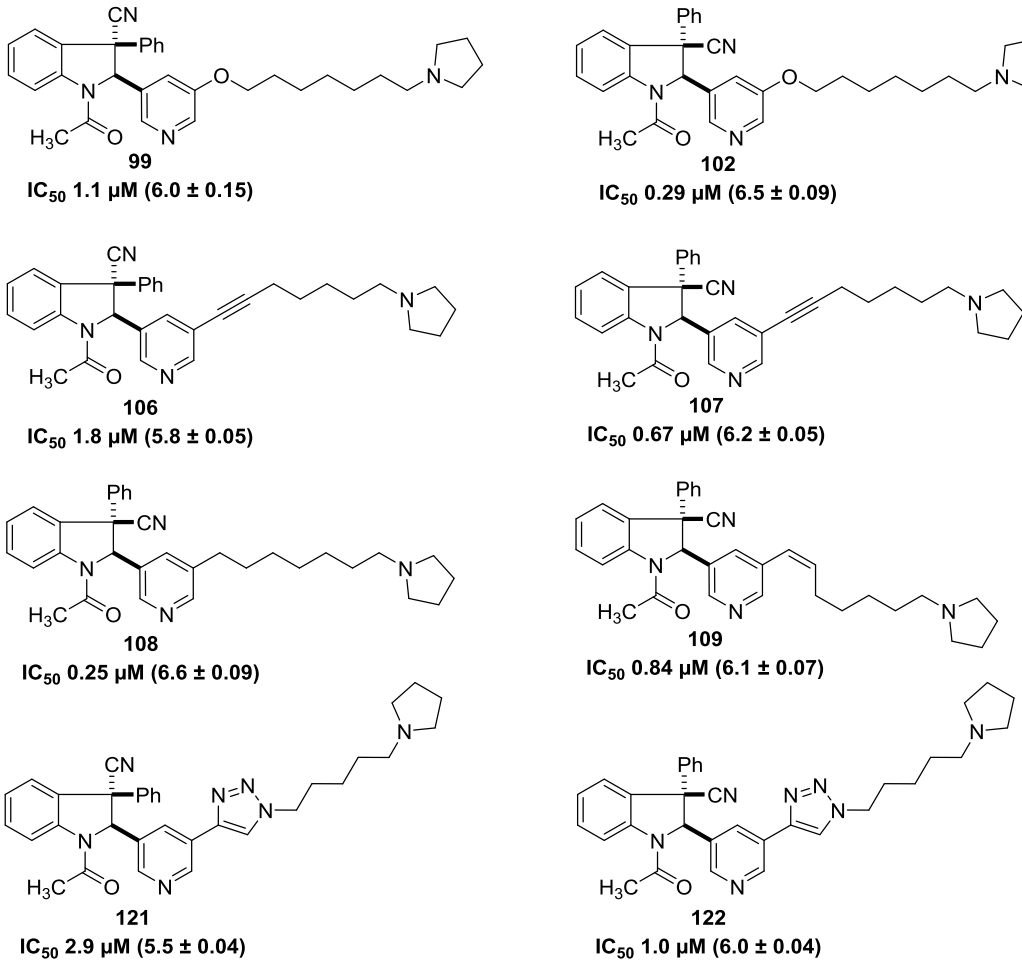

Figure 2.8 – Effect of linker on inhibitory activity. IC_{50} values were determined by RapidFire activity assay. pIC_{50} values and errors are shown in parentheses.

2.2.4 Aromatic Rings at the Indoline C2 Position

Having explored the substituents at the indoline *C*3 position, linker, alkyl chain, and head-group, we wanted to investigate the significance of the aryl ring at the indoline *C*2 position. The majority of examples described so far contain a pyridyl ring at this site. In order to gauge the contribution of the pyridyl-nitrogen to inhibition, examples containing an analagously-substituted phenyl ring were synthesized. Cyclization of imine **123** afforded indolines **124** and **125** in an approximately 1:2 ratio. Both products were acetylated and underwent Stille-Migita cross-coupling with vinylstannane **57** (Scheme 2.21).

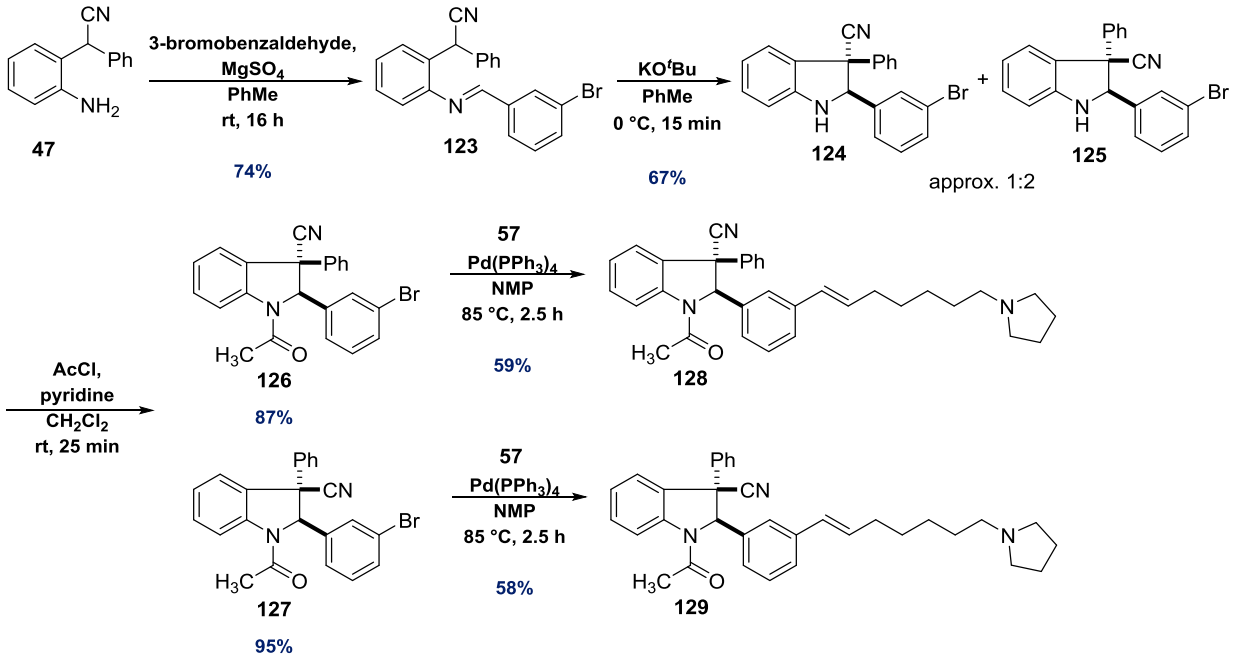

Scheme 2.21 – Synthesis of *C*2-phenyl examples **128** and **129**. The relative stereochemistries of indolines **124** and **125** was assigned by analogy to previously-reported similar compounds.[74]

We anticipated that a wide range of aldehydes could be condensed with aniline **47**, providing access to a diverse library of indolines with different *C*2 substituents. However, we were limited by the low commercial availability of halogenated aromatic aldehydes and their precursors, and we therefore focused on the synthesis of indolines containing regioisomeric furyl rings at the indoline *C*2 position.

Condensation of aniline **47** with 4-bromo-2-furaldehyde **131** was found to proceed very slowly, even when pyrrolidine was used as a nucleophilic catalyst.[100] Curiously, cyclization of imine **132** afforded indoline **133** as a single diastereomer, while cyclization of imine **138** gave an inseparable mixture of diastereomers. The acetylated indolines **139** and **140** could be separated by silica-gel column chromatography, and Sonogashira coupling of all acetylated products with alkyne **105**, followed by hydrogenation, afforded indolines **136**, **142**, and **144** (Scheme 2.22).

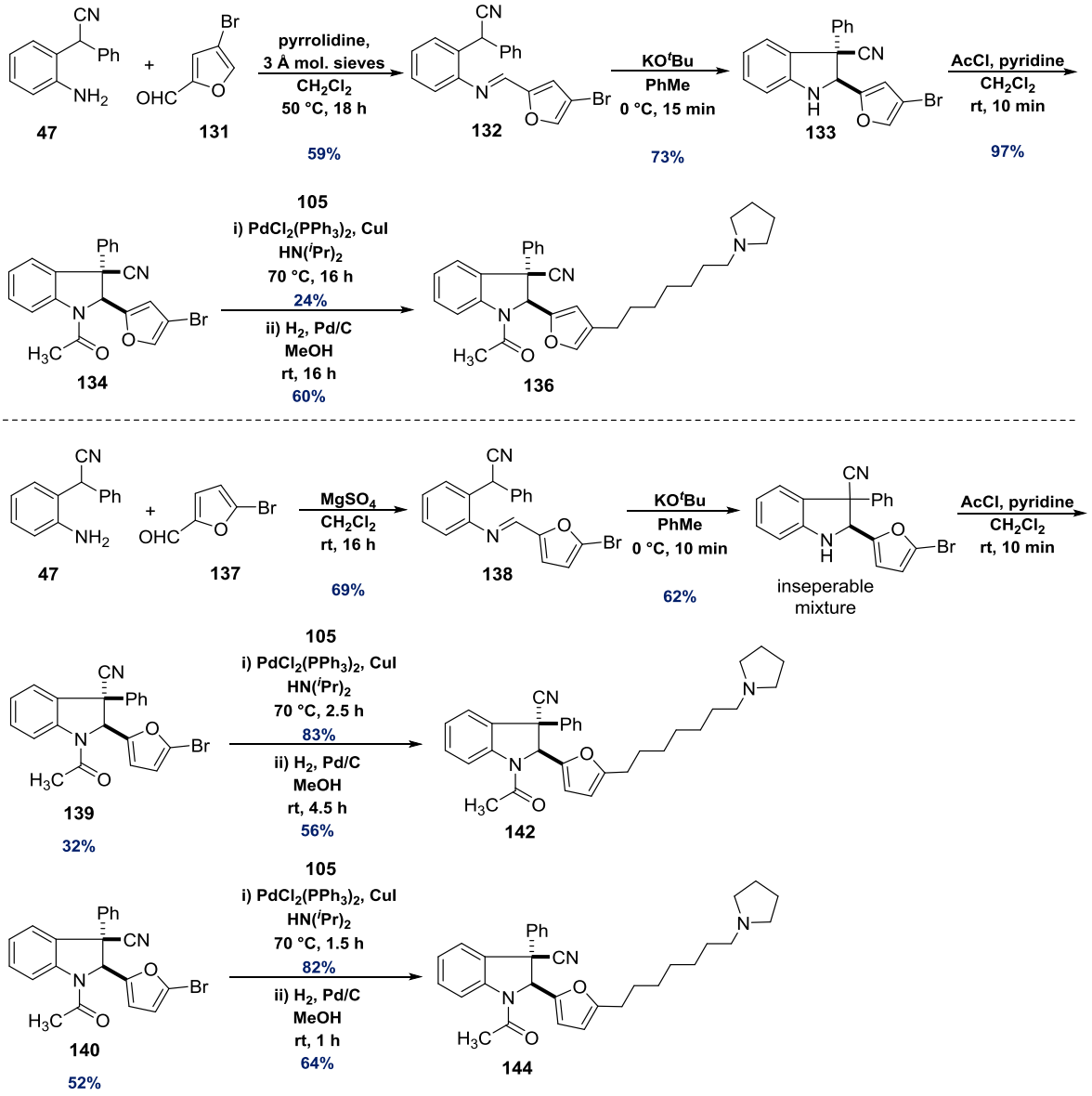

Scheme 2.22 – Synthesis of furyl-containing indolines with both alkyne and alkane linkers.

The impact of varying the *C*2 aryl ring on inhibitory activity was assessed using the RapidFire assay. The diastereomeric phenyl indolines **128** and **129** had very similar IC_{50} values, and both were found to be substantially weaker inhibitors than their pyridyl equivalents, implying that the pyridyl nitrogen plays an important role in the inhibitor-KDM2A interaction. Of the furyl analogues, the *syn* 5´-alkane-linked diastereomer **144** was more potent than both the *anti* 5´-alkane-linked diastereomer **142** and the *syn* 4´-alkane-linked diastereomer **136**. Finally, the alkyne-linked indolines **135** and **143** were found to be weaker than their fully saturated linker equivalents **136** and **144**, confirming the importance of linker flexibility for inhibitory activity (Figure 2.9).

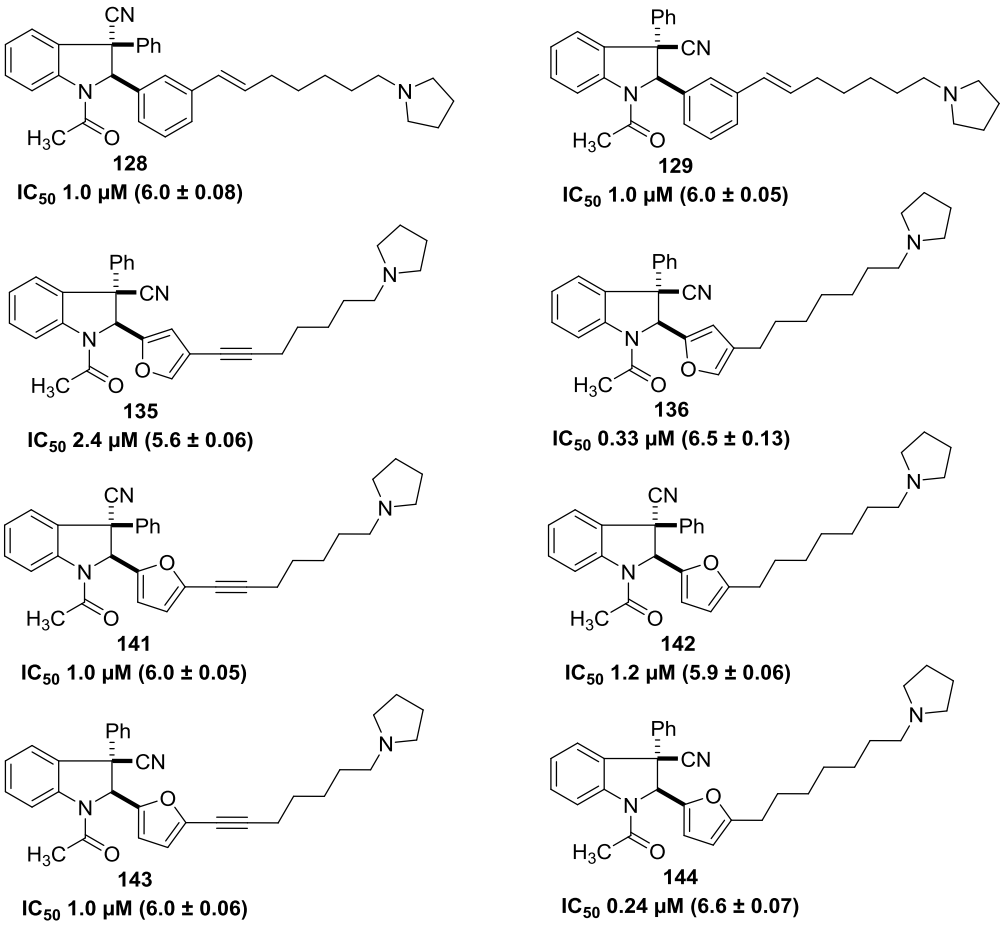

Figure 2.9 – Effect of *C*2 aryl ring on inhibitory activity. IC_{50} values were determined by RapidFire activity assay. pIC_{50} values and errors are shown in parantheses.

2.2.5 Selectivity

In order to determine their selectivity towards KDM2A, several indolines were tested for inhibitory activity against a representative panel of KDMs belonging to different subfamilies.* Excitingly, all compounds displayed exceptionally high selectivity towards KDM2A based on AlphaScreen™ IC_{50} values obtained under identical conditions (Table 2.2). The high potency and selectivity displayed by indoline **59** in particular led us to pursue this compound as a promising lead for chemical probe development.

Compound	KDM2A	KDM3A	KDM4A	KDM4C	KDM5B	KDM5C	KDM6B
59	0.25	115		>1000		219	>100
144	0.24[a]	11	17	36	14	9.9	14
58	0.28	>1000		112		242	>100
122	0.82			39		36	247
121	1.8	>1000		72		>1000	>1000

Table 2.2 – AlphaScreen™ IC_{50} values (μM) under identical conditions for a panel of KDMs. [a] IC_{50} determined by RapidFrire activity assay.

2.3 Enantioselective Synthesis

2.3.1 A Resolution Approach

So far, all indoline-based KDM2A inhibitors had been synthesized and tested as racemic mixtures. In order to obtain optically-pure samples of both enantiomers, we wanted to carry out a chemical resolution of the indoline core. Chloroformate **147** was synthesized in 2 steps from L-(+)-mandelic acid,[101] and *N*-acylation of indoline **50** using this chiral resolving agent afforded a mixture of diastereomers that were (just about) separable by silica-gel column chromatography (Scheme 2.23).

* Selectivity profiling was conducted by Dr Anthony Tumber. For a statistical analysis of these results, see section 8.1 in the appendix.

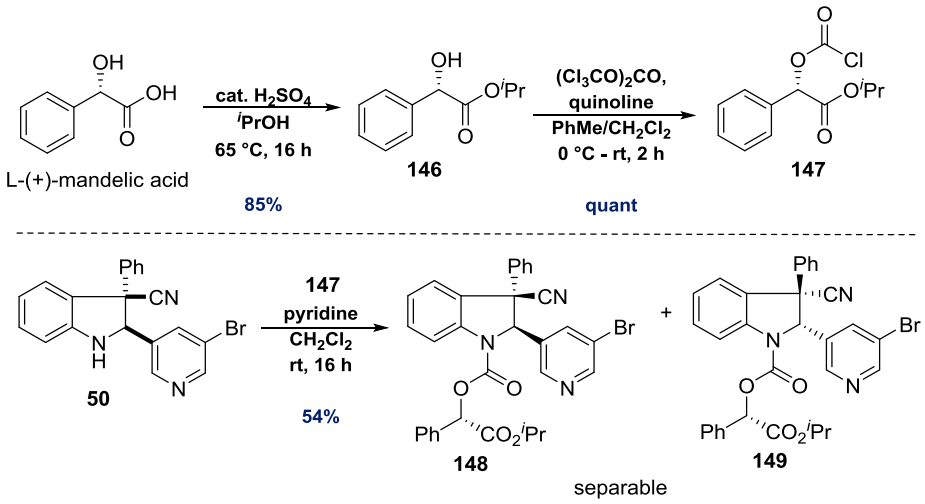

Scheme 2.23 – Synthesis and application of chloroformate **147** as a chiral resolving agent.

We initially attempted to remove the carbamate resolving group with SmI_2 as a single electron source. The group of D. Proctor has demonstrated the application of SmI_2 as a selective reducing agent for a range of functional groups including isopropyl esters,[102] and we anticipated that the alcohol product of this reduction would rapidly collapse to afford the deprotected, optically-pure indoline cores. Unfortunately, in spite of numerous attempts using both commercial and freshly-prepared SmI_2, the desired transformation was not accomplished (Scheme 2.24).

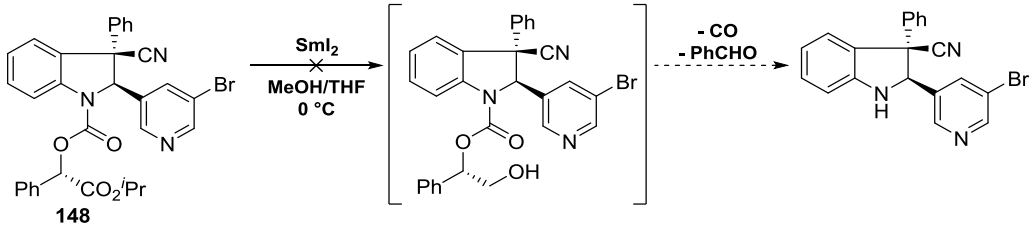

Scheme 2.24 – Unsuccessful deprotection of carbamate resolving group using SmI_2.

We reasoned that hydrogenolysis of the chiral resolving groups might be a possible alternative to SmI_2-deprotection. Indeed, Sonogashira coupling of indolines **148** and **149** with alkyne **105**, followed by hydrogenolysis, concomitant reduction of the alkyne linker, and *N*-acetylation afforded sufficient amounts of the optically pure indolines **(*R*,*R*)-108** and

(*S*,*S*)-108 for biological testing. The intermediates of this sequence were used without purification in order to expedite synthesis of the final products (Scheme 2.25). Ultimately, both indoline enantiomers were obtained with e.r. > 99:1 and were tested for inhibitory activity using the RapidFire activity assay (Table 2.3). Although there is a significant difference in potency between the enantiomers, the magnitude of this difference is smaller than what is commonly observed for many chiral chemical probes (e.g. JQ1 – 49-190 nM vs. inactive,[26] LP99 – 99 nM vs. inactive,[103] SGC-CBP30 – 79 nM vs. 501 nM[104]).

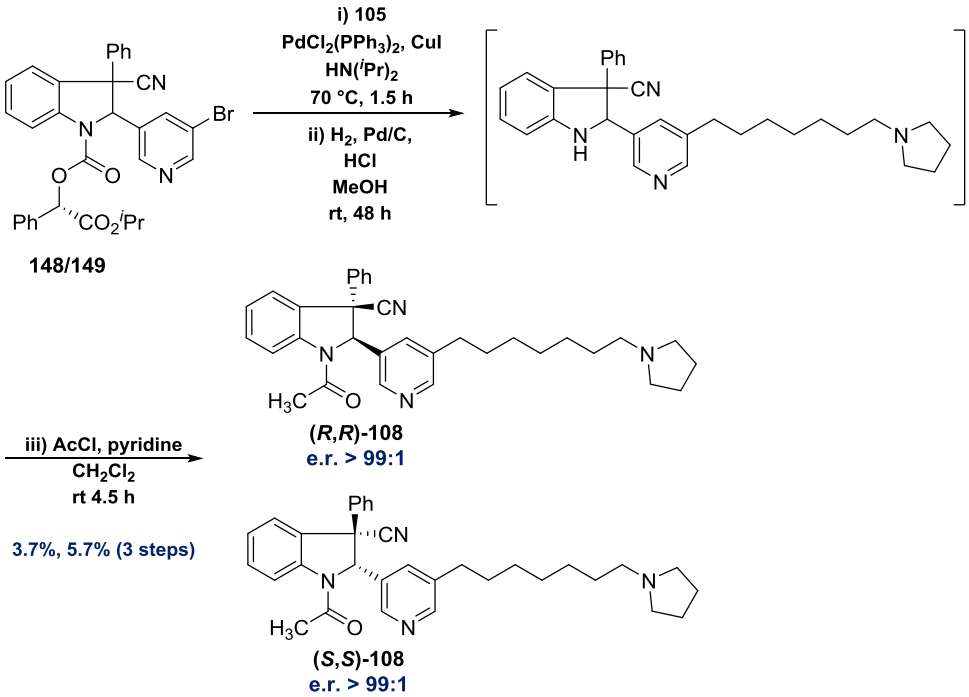

Scheme 2.25 – Telescoped synthesis of resolved, optically pure indolines **(*R*,*R*)-108** and **(*S*,*S*)-108**.

Compound	IC_{50} (μM)
108	0.25 (6.6 ± 0.09)
(*R*,*R*)-108	0.39 (6.4 ± 0.04)
(*S*,*S*)-108	0.16 (6.8 ± 0.03)

Table 2.3 – Inhibitory activities of enantiomers of indoline **108**. Absolute stereochemistry is assigned retrospectively (see subsection 2.3.3). pIC_{50} values and errors are shown in parentheses.

2.3.2 Enantioselective PTC – Effect of Substrate Structure

Given the limitations of chiral resolution, we envisaged an alternative approach to the enantioselective synthesis of lead compounds that would be based on asymmetric catalysis. As described previously, a particular area of interest within the Smith group is the use of chiral, cationic phase-transfer catalysts to influence the stereochemical outcome of cyclization reactions (see Subsection 1.4.2). At the outset of this project, a substantial amount of research into the enantioselective cyclization of imines based on 2-phenylacetonitrile-anilines had already been carried out (Scheme 2.26).

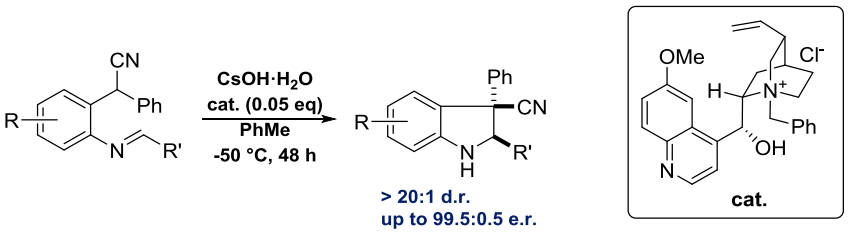

Scheme 2.26 – Chiral cation controlled enantioselective cyclization of imines to form indolines. Use of the pseudoenantiomeric phase-transfer catalyst affords the opposite enantiomer.[74]

A detailed analysis of the kinetics of this reaction by group members Krishna Sharma and Dr Jamie Wolstenhulme revealed a complex catalytic mechanism. It was proposed that the quininium phase-transfer catalyst both initiates and participates in an autocatalytic reaction cycle (Figure 2.10). Initially, deprotonation of the imine substrate occurs at the interfacial boundary and the resulting anion is extracted into the organic phase by the catalyst, where it undergoes enantioselective cyclization to form an indolinyl anion. This indolinyl anion can deprotonate the catalyst to generate a zwitterionic species in a rapid and irreversible manner. As a zwitterion, the catalyst can deprotonate another molecule of substrate in the organic phase and thereby continue the reaction cycle. Finally, regarding the imine cyclization itself, quantum calculations based on density functional theory (DFT)

suggest that the transformation proceeds *via* a formally-disfavored 5-*endo*-trig[105] ring-closure as opposed to a 6π-electrocyclization.

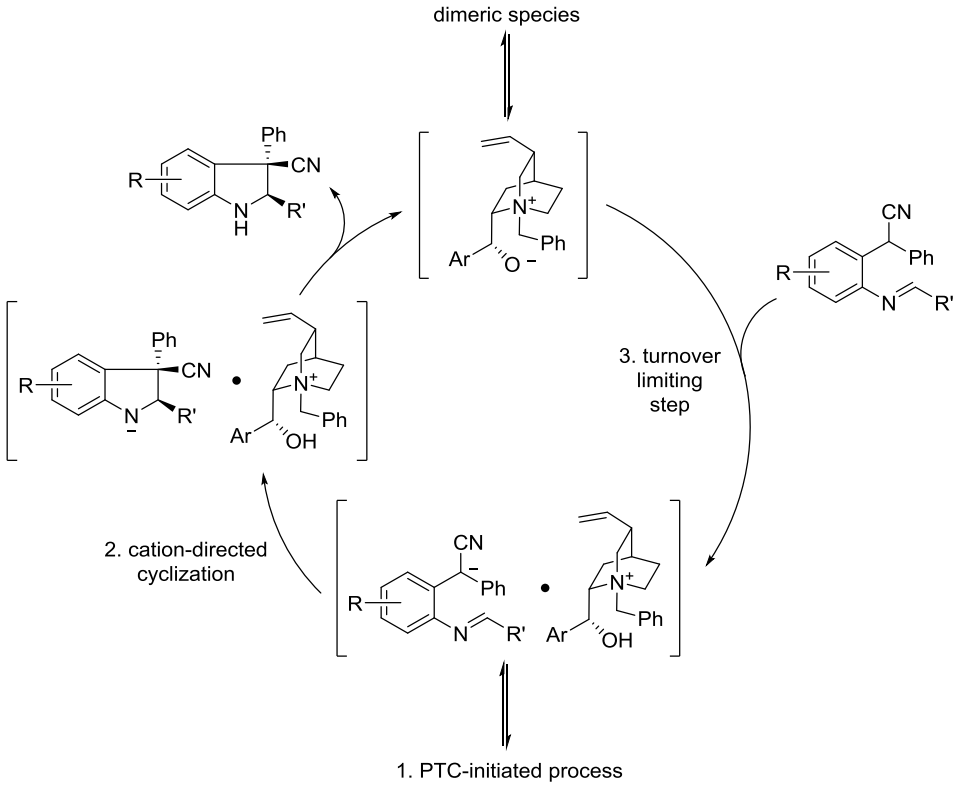

Figure 2.10 – Proposed catalytic cycle of imine cyclization, based on reaction kinetics. This figure is conceptually reproduced from M. D. Smith *et al*. JACS. **2015**, 137 (41).

We initially attempted to apply the optimized reaction conditions for these 2-phenylacetonitrile-aniline-derived aldimines to the cyclization of imine **48**. Unfortunately, only a very modest e.r. was attained with this substrate (Scheme 2.27). A limited screen of bases, reaction conditions, and catalysts failed to improve the outcome.

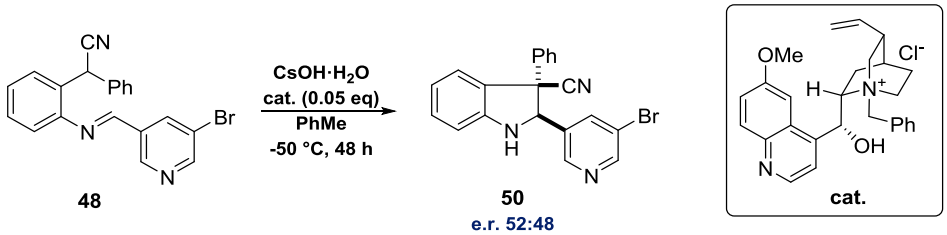

Scheme 2.27 – Application of previously discovered optimized conditions to the cyclization of imine **48** resulted in only a minor enantiomeric excess.

In order to investigate the extent to which pyridyl substituents and regiochemistry might affect enantioselectivity, we attempted the cyclization of imines **153** and **155** under similar reaction conditions. In both cases, a marginal improvement in enantioselectivity was observed (Scheme 2.28 – A,B). Although these encouraging results did not address the fundamental synthetic issue at hand, we concluded that modifying the pyridyl ring would be the most promising approach to achieving higher levels of asymmetric induction. This hypothesis was ultimately confirmed by the cyclization of the *OBn*-pyridyl imine **92** to afford indoline **93** with a very promising e.r. (Scheme 2.28 – C). We anticipated that indoline **93** would be a useful precursor to lead compounds, and we therefore concentrated efforts on improving the enantioselectivity of this reaction by exploring conditions and catalysts.

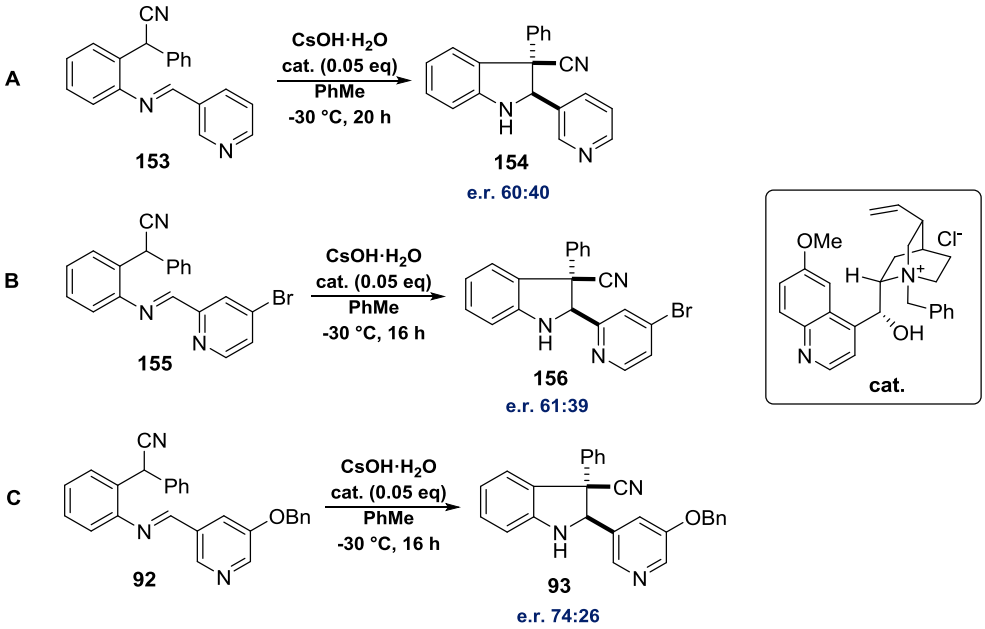

Scheme 2.28 – Effect of pyridyl substitution on enantioselectivity of imine cyclization.

2.3.3 Enantioselective PTC – Screening and Synthesis[*]

To begin with, we attempted to improve the enantioselectivity of the cyclization of imine **92** to indoline **93** by investigating the catalyst component of this reaction. The most

[*] These investigations were carried out together with Dr Jamie Wolstenhulme.

common core scaffold of chiral phase transfer catalysts is based on the cinchona alkaloid structure, although several alternative scaffolds based on axially-chiral BINOL derivatives and other motifs have also been developed over the years.[106] In order to expedite screening, reactions were performed on a relatively small scale (40 mg imine **92**), and only the enantioselectivity of each reaction was initially evaluated (Figure 2.11). In general, catalysts based on the quinine scaffold performed better than catalysts based on quinidine, and the Maruoka[107] and Lygo[108] catalysts (**I** and **J**) were largely ineffective at controlling product stereochemistry. The highest level of enantioselectivity was attained with the quininium salt **F**.

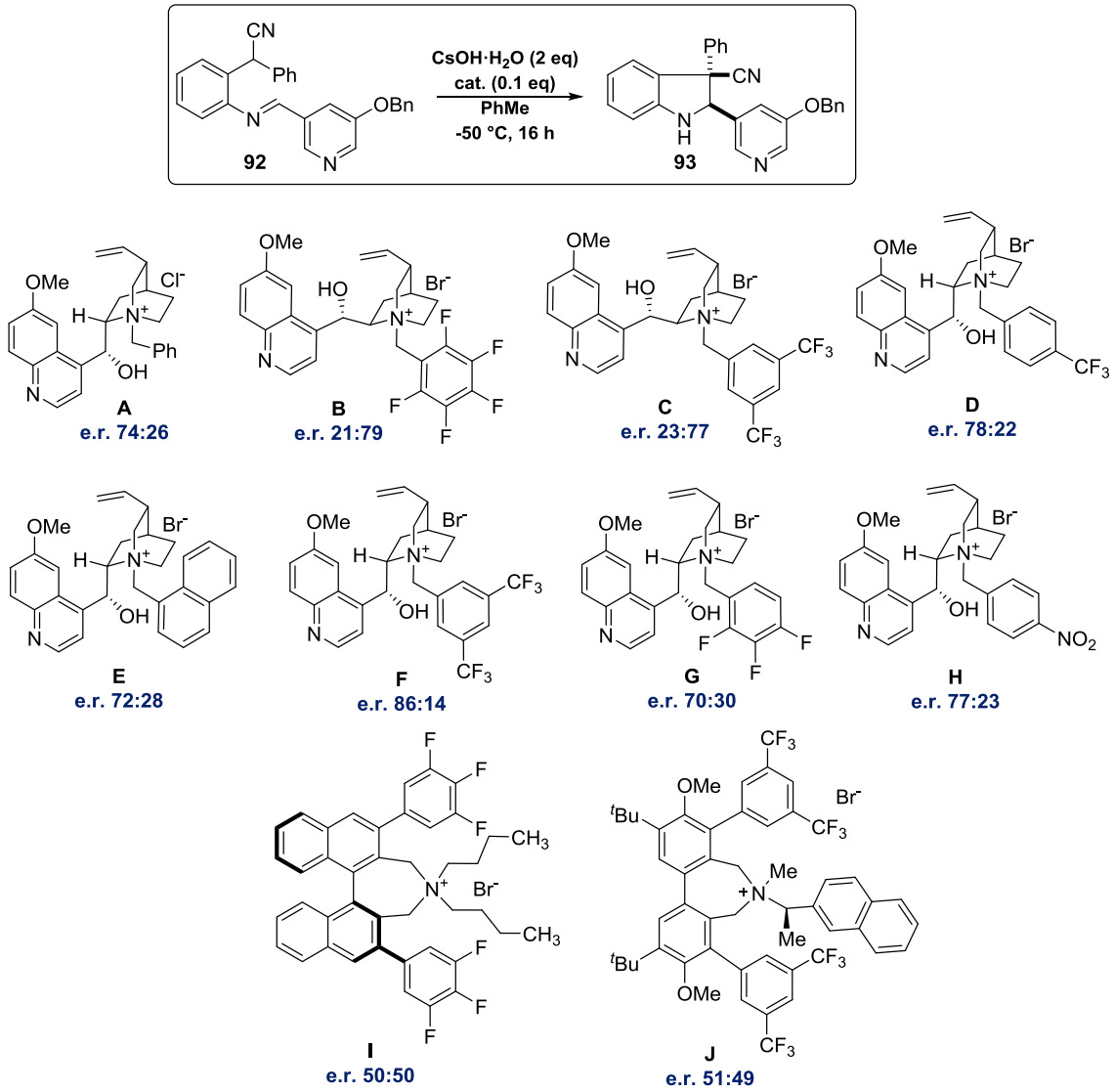

Figure 2.11 – Screen of phase-transfer catalysts for the cyclization of imine **92** to indoline **93**.

Having identified the best catalyst, we conducted a screen of solvents, catalyst concentrations, and temperatures. Key findings are summarized here and in Table 2.4:

1. Of all the investigated solvents, toluene afforded the most favorable balance of reactivity and selectivity.

2. Lowering the catalyst loading to 5 mol % caused a complete loss of conversion at -50 °C, but led to improved enantioselectivity at -30 °C. Raising the catalyst loading to 20 mol % resulted in a loss of enantioselectivity at -30 °C.

3. Addition of CH_2Cl_2 to the reaction mixture (10% v/v) largely recovered reactivity at -50 °C, but led to a dramatic drop in enantioselectivity.

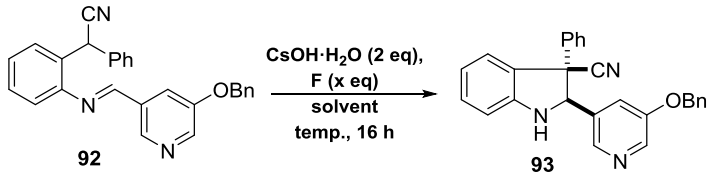

Solvent	Catalyst loading (eq)	Temperature (°C)	e.r. (93)
PhMe	0.1	-50	86:14
$O(^iPr)_2$	0.1	-50	No reaction
PhF	0.1	-35	53:47
9:1 PhMe/^{i}PrOH	0.1	-50	51:49
PhMe	0.05	-50	No reaction
PhMe	0.05	-30	89:11
PhMe	0.2	-30	84:16
9:1 PhMe/CH_2Cl_2	0.05	-50	64:36

Table 2.4 – Screen of solvents, catalyst loadings, and temperatures.

We applied the optimized reaction conditions to the cyclization of imine **92** in the presence of catalyst **F** and its pseudoenatiomer **C**. On a relatively small reaction scale (50 mg imine **92**), enantiomeric ratios of 89:11 and 15:85 were obtained, and the diastereomeric ratio exceeded 20:1 for both catalysts. Augmenting the scale of these reactions to 1 gram of imine **92** led to a slight drop in both e.r. and d.r. (Scheme 2.29). Nevertheless, we were satisfied that the enantioenrichment would be sufficient in both

cases to enable an effective resolution either by recrystallization or semi-preparatory chiral HPLC.

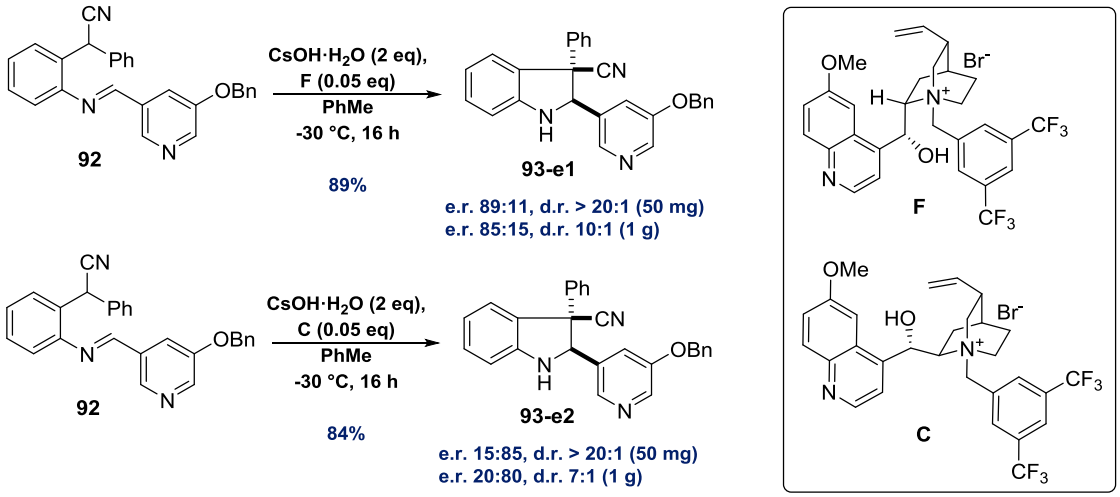

Scheme 2.29 – Optimized reaction conditions for the enantioselective cyclization of imine **92**.

Attempts to improve the enantiomeric excess by recrystallization proved unsuccessful. However, we succeeded in identifying conditions that enable the separation of both enantiomers of **93** on a YMC amylose-SA semi-preparatory HPLC column. This allowed us to obtain the two enantiomeric forms of indoline **93** in e.r. > 99:1. *N*-Acetylation of both enantiomers and hydrogenolysis of the *O*-linked benzyl groups afforded the common intermediates **(*R*,*R*)-100** and **(*S*,*S*)-100**, which would serve as precursors to optically-pure KDM2A inhibitor candidates. (Scheme 2.30). The absolute stereochemistry of these common intermediates was assigned by X-ray crystallography (Figure 2.12).

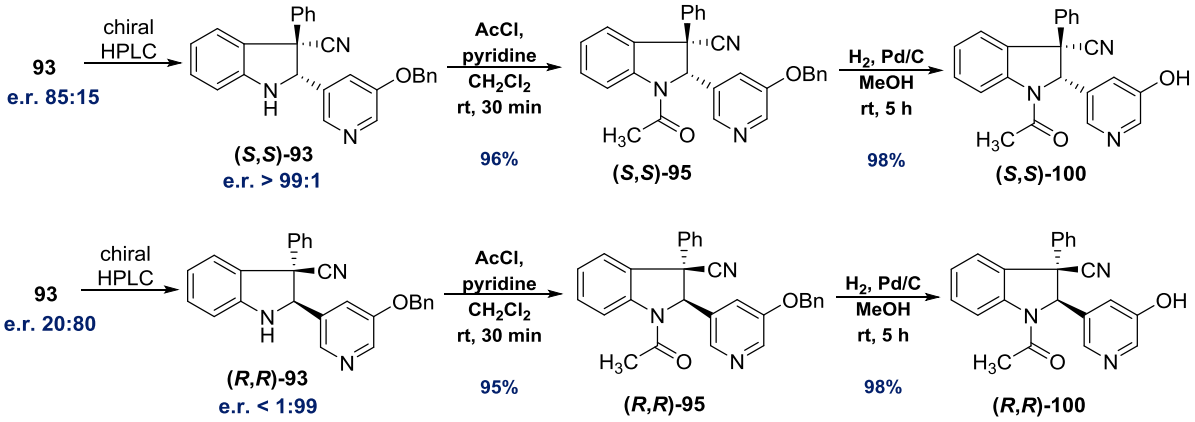

Scheme 2.30 – Synthesis of optically-pure intermediates **(*S*,*S*)-100** and **(*R*,*R*)-100**.

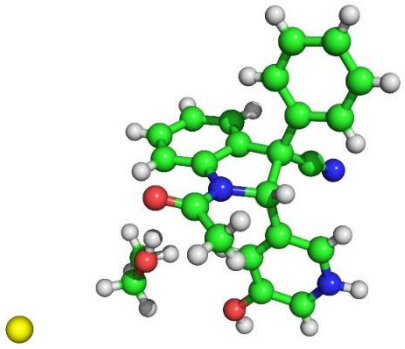

Figure 2.12 – X-ray crystal structure of HCl salt of indoline **(*S*,*S*)-100**.*

The two enantiomeric forms of indoline **102** could be obtained in e.r. > 99:1 by *O*-alkylation of **(*S*,*S*)-100** and **(*R*,*R*)-100** with 1,7-dibromoheptane, followed by substitution with pyrrolidine (Scheme 2.31). An evaluation of KDM2A inhibition using the RapidFire activity assay revealed that the (2*S*,3*S*)-indoline core (derived from imine cyclization catalyzed by **F**) is more potent than the (2*R*,3*R*)-indoline core (derived from imine cyclization catalyzed by **C**) (Table 2.5).

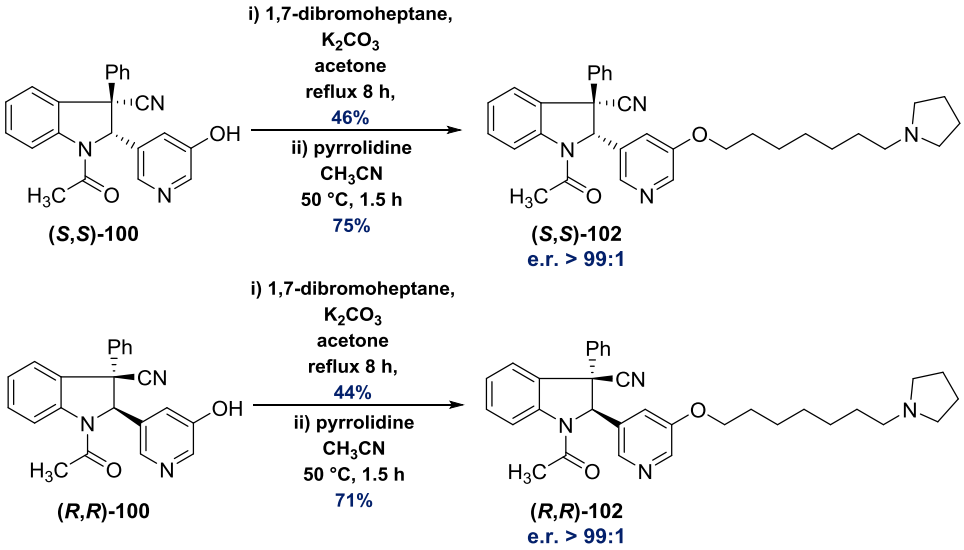

Scheme 2.31 – Synthesis of optically-pure KDM2A inhibitors **(*S*,*S*)-102** and **(*R*,*R*)-102**.

Compound	IC_{50} (μM)
(*S*,*S*)-102	0.39 (6.4 ± 0.06)
(*R*,*R*)-102	0.84 (6.1 ± 0.07)

Table 2.5 – Inhibitory activities of enantiomeric indolines **(*S*,*S*)-102** and **(*R*,*R*)-102**.

* X-ray diffraction data was collected and the structure solved by John Joliffe.

Finally, the optically-pure indoline **(*S*,*S*)-108**, previously obtained *via* a chiral resolution of the indoline core (subsection 2.3.1), could be synthesized from intermediate **(*S*,*S*)-100**. The hydroxyl substituent of the pyridyl ring was converted to a triflate group in good yield, and Sonogashira coupling with alkyne **105**, followed by hydrogenation, afforded indoline **(*S*,*S*)-108** in e.r. > 99:1 (Scheme 2.32). The identity of this compound could be confirmed by comparison of the HPLC retention time with that of the more potent enantiomer obtained *via* chiral resolution (IC_{50} = 0.16 μM). An extensive activity screen using a panel of representative KDMs confirmed that **(*S*,*S*)-108** is a highly selective inhibitor of KDM2A (Table 2.6). In addition, **(*S*,*S*)-108** was found to be inactive towards a representative panel of methyl-lysine binding domains.*

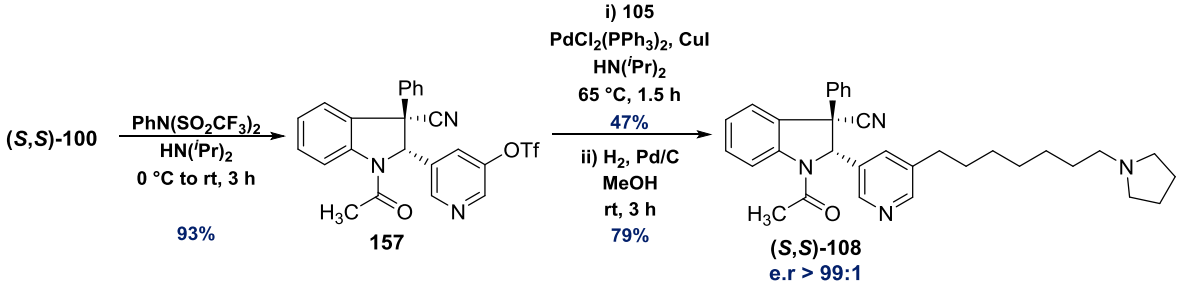

Scheme 2.32 – Synthesis of optically-pure **(*S*,*S*)-108** from intermediate **(*S*,*S*)-100**.

KDM2A	KDM3A	KDM4A	KDM4C	KDM4D	KDM5B	KDM5C	KDM6B
0.16	39	639	430	321	17	16	20

Table 2.6 – AlphaScreen™ IC_{50} values (μM) of **(*S*,*S*)-108** against a panel of KDMs.†

With a robust asymmetric synthetic strategy towards a promising lead compound in hand, we turned our attention to the evaluation of the potential biological activity of these KDM2A inhibitors within cells. The next chapter of this thesis will focus on attempts to modulate both on-target and off-target cellular activity by altering key molecular features in a rational manner.

* MBD screening was conducted at the SGC-Toronto by Guillermo Senistera and Dr Masoud Vedadi.
† For a statistical analysis of the data, see section 8.1 in the appendix.

3. LEAD OPTIMIZATION

3.1 Cellular Activity

3.1.1 Inhibition of Histone Demethylation[*]

Cellular inhibitory activity was measured using an immunofluorescence (IF) assay to quantify H3K36me2 in HeLa cells. Experiments were performed with two cell lines: wild-type (WT) cells containing catalytically-active KDM2A, and mutant (MUT) cells containing constitutively-inactive KDM2A. Excitingly, when indolines **(*S*,*S*)-102** (IC_{50} 0.39 μM) and **(*S*,*S*)-108** (IC_{50} 0.16 μM) were tested in this assay, both compounds demonstrated a dose-dependent effect on cellular H3K36me2 levels in WT cells (Figure 3.1). Indoline **(*S*,*S*)-108** was particularly promising, as it induced a significant increase in the intracellular concentration of H3K36me2 at relatively low compound concentrations (39 ± 11 % increase at approx. 1 μM). As a control, the pan-2-OG dependent deoxygenase inhibitor IOX1[46] was tested in the same assay and was found to inhibit demethylation of $H3K36me_2$ at considerably higher concentrations (> 15 μM). However, it is uncertain whether this is a consequence of KDM2A inhibition or the effect of general cytotoxicity.

Cytotoxicity towards HeLa cells was measured by monitoring overall cell numbers over a range of compound concentrations. Indolines **(*S*,*S*)-102** and **(*S*,*S*)-108** were found to be cytotoxic when dosed above 10 μM, so that their effects on cellular H3K36me2 levels at higher concentrations (> 5 μM) should be viewed with caution, as these may not entirely reflect on-target activity. In order to better understand the nature of both on-target and

[*] These experiments were done by Dr Stephanie Hatch, Target Discovery Institute.

off-target contributions to cellular activity, we decided to take advantage of recent advances in the field of quantitative transcriptomics.

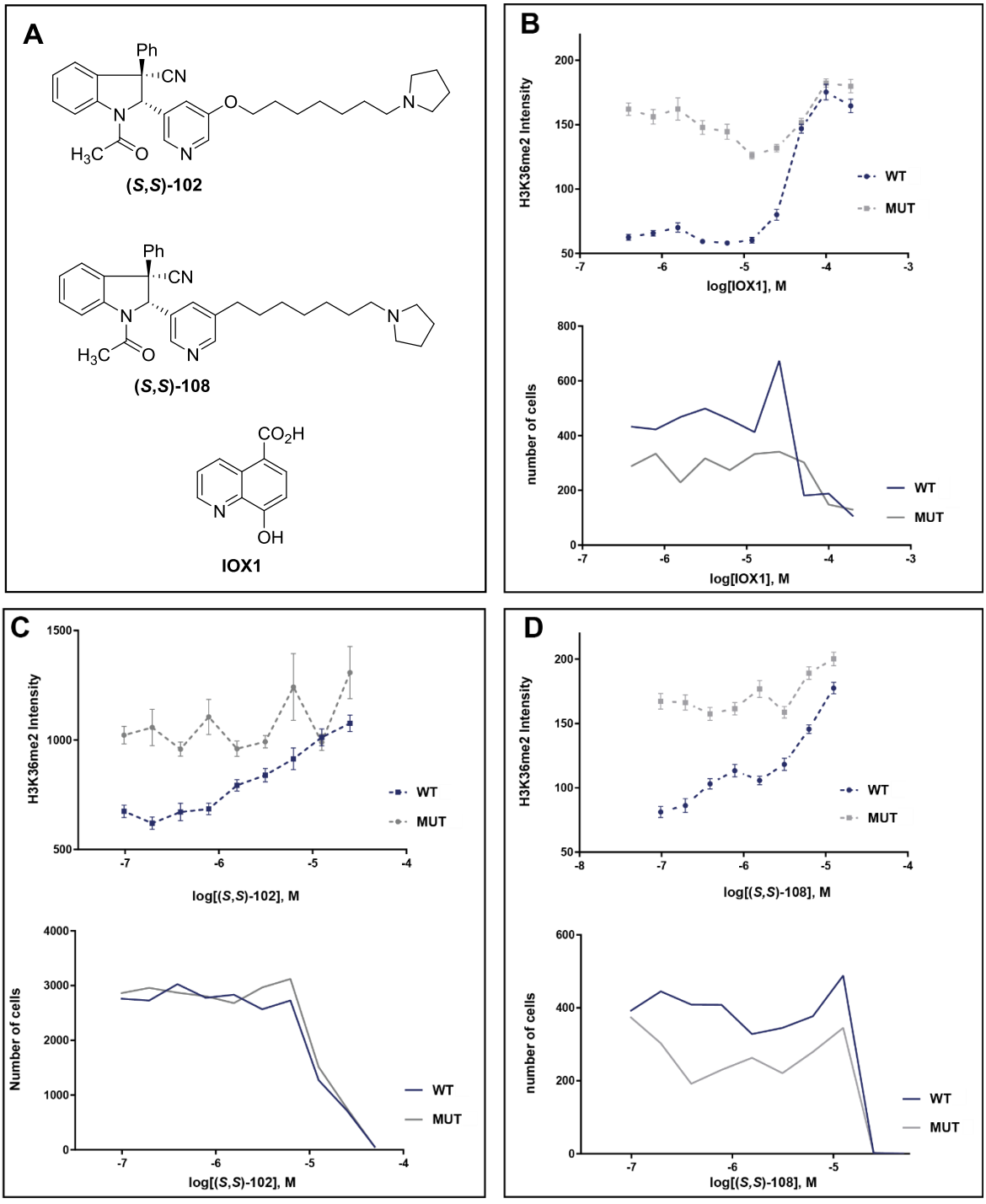

Figure 3.1 – Inhibition of H3K36me2 demethylation in HeLa cells: A) Structures of KDM2A inhibitors **(*S*,*S*)-102** and **(*S*,*S*)-108**, and pan 2-OG deoxygenase inhibitor **IOX1**. B) IF assay and cytotoxicity of IOX1. C) IF assay and cytotoxicity of **(*S*,*S*)-102**. D) IF assay and cytotoxicity of **(*S*,*S*)-108**.

3.1.2 Transcriptomics[*]

Effects on gene expression levels were explored using a highly multiplexed 3' mRNA sequencing method as previously described by Gapp and co-workers.[109] Within a diverse panel of in-house compounds, our series of indoline-containing KDM2A inhibitors was represented by **(*S*,*S*)-108** and **89**, which we considered to be a suitable structurally-analogous "inactive" control (IC_{50} 17 µM). When dosed at a concentration of 10 µM, both molecules influenced expression levels of more than 200 genes in HAP1 cells. However, at a concentration of 1 µM, only the active analogue **(*S*,*S*)-108** had a significant effect on expression levels (Figure 3.2-A). We postulate that this concentration dependence may be a consequence of predominantly off-target effects at high concentrations, as opposed to a more specific effect resulting from KDM2A inhibition at low concentrations. The overlap of the gene expression signatures of **(*S*,*S*)-108** and **89** is depicted in Figure 3.2-B.

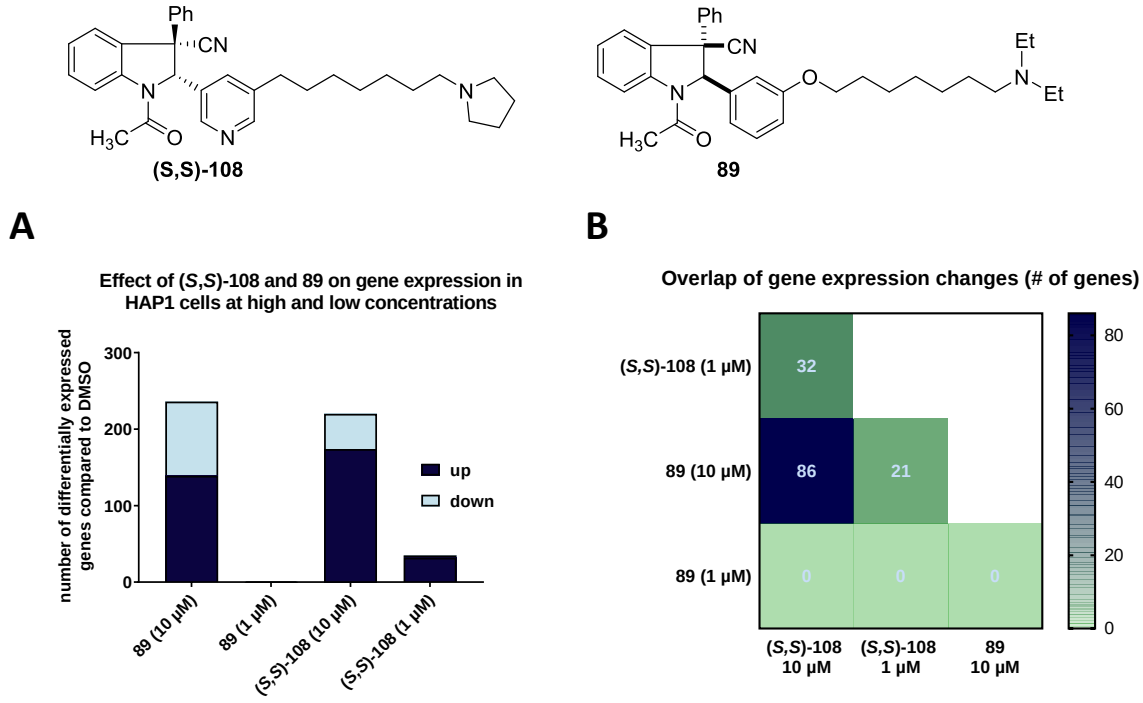

Figure 3.2 – Quantitative transcriptomics analysis of gene expression changes caused by **(*S*,*S*)-108** and **89**: A) Total number of genes with altered expression levels. B) Overlap of gene expression changes.

[*] Experiments and data analysis were done by Barbara Mair and Dr Thomasz Konopka respectively.

We concluded that, while our lead compound **(*S*,*S*)-108** is clearly able to penetrate into cells and influence H3K36me2 demethylation, it is not suitable for use as a chemical probe due to the magnitude of off-target activity at higher compound concentrations, which we felt would interfere with studies investigating the roles of KDM2A in biology. We therefore sought to develop an inhibitor with a wider *on-target activity window*[*] by modifying the structure of **(*S*,*S*)-108** so as to reduce the number and magnitude of non-specific interactions within cells.

3.2 Addressing Off-Target Activity and Cytotoxicity

3.2.1 Linker Modifications

In 1997, C. A. Lipinski published a review article analyzing various physical and chemical properties of drug candidates that had successfully advanced to phase II clinical trials.[110] The insights provided by this landmark publication continue to impact common practices in medicinal chemistry today by influencing library design and guiding strategies for lead optimization. Specifically, Lipinski proposed a set of guidelines (commonly known as the "rule-of-5") to help identify hits and lead compounds that would be more likely to progress through the drug discovery pipeline as a result of favorable physicochemical and pharmacokinetic properties:

1) Fewer than 5 H-bond donors (i.e. O-H and N-H bonds)
2) Molecular weight < 500 g mol^{-1}.
3) Log*P* ≤ 5.
4) < 10 H-bond acceptors (i.e. O and N atoms).

[*] Range of compound concentrations over which cellular effects are predominantly due to KDM2A inhibition (i.e. on-target) as opposed to non-specific interactions (i.e. off-target).

Although it was never our intention to develop a molecule that could potentially form the basis of a drug discovery program, we reasoned that the insights gained from Lipinski's analysis could also be applied to the development of chemical probes. In particular, we recognized that most of our indoline-based KDM2A inhibitors were characterized by both a higher molecular weight and *C*log*P* than recommended by the "rule-of-5" guidelines (Figure 3.3). This particular combination of traits did not appear to limit compound solubility; however, we attributed the observed off-target activity and cytotoxicity of indoline **(*S*,*S*)-108** to its relatively high lipophilicity (*C*log*P* = 5.88)[*111]. Our reasoning was largely based on the work of J. D. Hughes and co-workers, who observed a strong correlation between log*P* and *in vivo* toxicity and identified compound promiscuity as a key contributor to this trend.[112] We therefore focused our efforts on identifying chemical modifications to **(*S*,*S*)-108**, which would increase polarity and thereby improve the ratio of on-target to off-target activity.

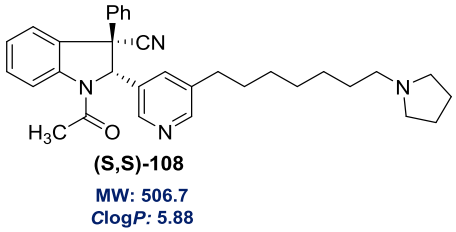

Figure 3.3 – The molecular weight and *C*log*P* of indoline **(*S*,*S*)-108** are both higher than recommended according to Lipinski's guidelines.

We considered the saturated hydrocarbon chain of indoline **(*S*,*S*)-108** and its analogues to be the most obvious molecular feature that we could modify in order to reduce lipophilicity. Initially, we hoped that replacing the alkyl chain of **108** with a more polar polyethylene-glycol (PEG) linker would be a viable solution. Indoline **159**

[*] Calculated using the Molinspiration™ cheminformatics web-based tool (www.molinspiration.com).

(*C*log*P* = 3.30) was therefore synthesized from racemic **100** and tested for inhibitory activity against KDM2A (Scheme 3.1). Unfortunately, a dramatic loss of potency was observed, suggesting that simply incorporating multiple heteroatoms into the linear alkyl chain was unlikely to represent a viable strategy for reducing lipophilicity. Attempts were also made to introduce an amide linker *via* Pd-catalyzed carbonylative coupling[113] of indoline **53** and carboxylation using Knochel's "turbo Grignard" reagent.[114] However, neither of these methods yielded the desired products in our hands (Scheme 3.2). In order to accelerate the discovery of modifications that would increase polarity while maintaining potency, we turned to a rational-design approach based on computational docking.

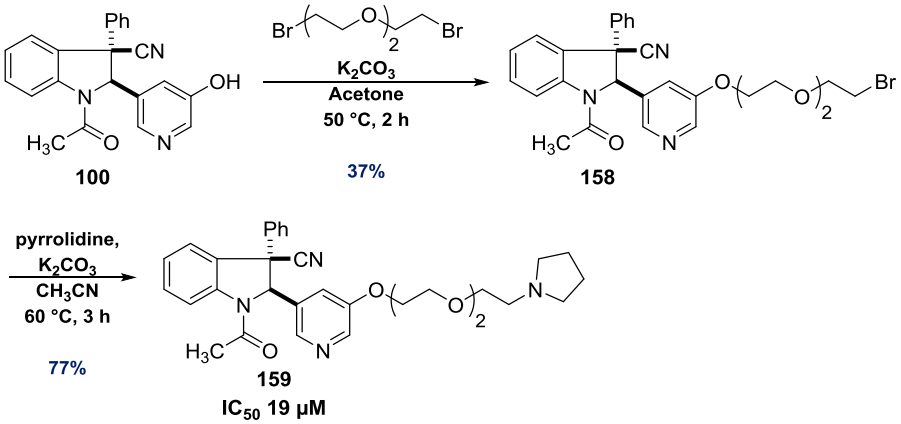

Scheme 3.1 – Synthesis of racemic PEG-linked indoline **159**.

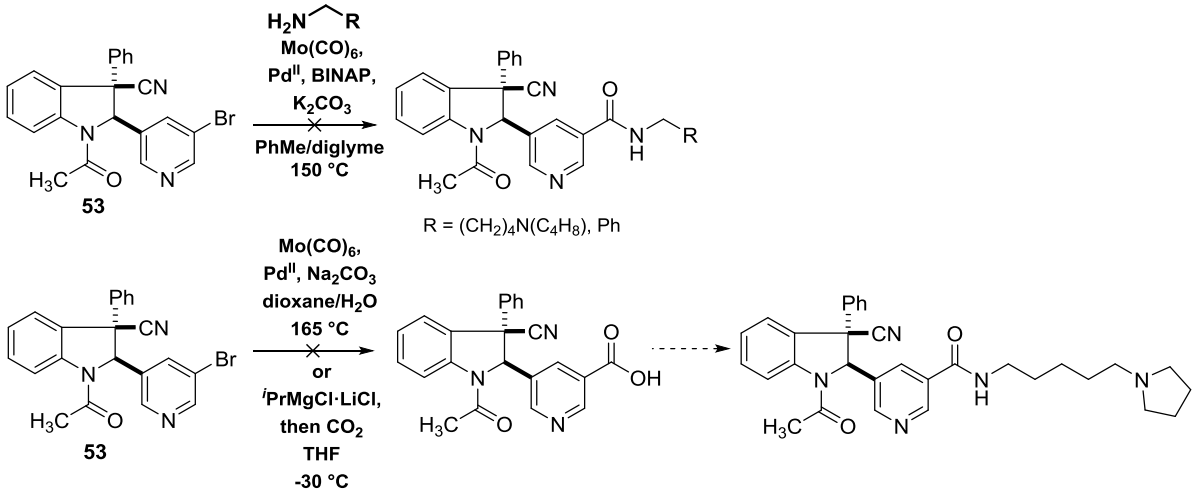

Scheme 3.2 – Attempted synthesis of amide linkers *via* carbonylative coupling or carboxylation of indoline **53**.

3.2.2 Computational Docking

Computational docking has become an increasingly important tool in drug discovery, as it enables the prediction of ligand binding conformations and important ligand-protein interactions. When combined with structural insights from X-ray crystallography, it represents a powerful strategy for both hit identification and lead optimization. This is perhaps best illustrated by the computer-aided discovery of a highly potent series of non-nucleoside HIV reverse transcriptase inhibitors by K. S. Anderson and W. L. Jorgensen using a combination of virtual screening and computational docking of inhibitor candidates.[115]

In spite of numerous attempts, the acquisition of an X-ray co-crystal structure of indoline **(*S*,*S*)-108** bound to KDM2A was not accomplished.[*] In order to obtain a structural insight into the inhibitor-protein interaction, we therefore relied on computational docking using X-ray crystal structures of KDM2A in both apo[116] and peptide-bound[38] states available through the protein data bank (PDB).[117] We made the assumption that **(*S*,*S*)-108** would bind within the active site of the enzyme's JmjC domain, and we initially used the open-source program *AutoDock Vina*[118] to predict the most likely binding conformation within this area. *AutoDock Vina* is a grid-based docking program, which samples all possible ligand positions and conformations within a predefined region of the protein target and allocates a "score" based on steric repulsion, coulombic forces, and van der Waals interactions. In these scoring calculations, the protein structure is represented as a static grid, so that conformational changes of the protein upon ligand binding are not considered. Similarly, the solvent is approximated as a continuous medium, and solvent contributions to both the

[*] X-ray crystallography trials with KDM2A were carried out by researchers at the SGC.

enthalpy and entropy of binding consequently do not feature in the overall scoring algorithm.

Figures 3.4 illustrates the highest-scoring docking solution using indoline **(*S*,*S*)-108** and the peptide-bound structure of KDM2A (PDB code: 4QXC). In this proposed complex, the protonated *N*-alkyl pyrrolidine group extends into the peptide binding pocket, mimicking the dimethyl-lysine sidechain of the peptide substrate. The indoline core adopts a conformation that overlaps with the remainder of the peptide (Figure 3.5). Although we did not identify any specific interactions that would be consistent with our SAR studies (e.g. significance of the *C*3 substituents and pyridyl ring), the need for a conformationally-flexible chain linking the indoline core and the pyrrolidine head group could potentially be explained by the presence of a narrow channel through which the dimethyl-lysine sidechain is threaded to access the enzyme's catalytic site.

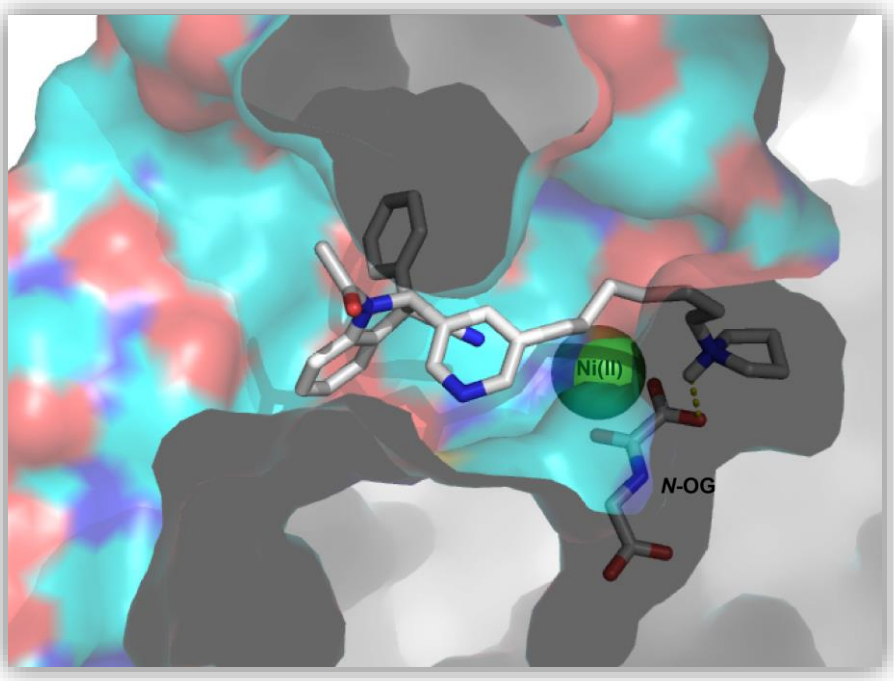

Figure 3.4 – Docking solution of indoline **(*S*,*S*)-108** in KDM2A active site using *AutoDock Vina*.

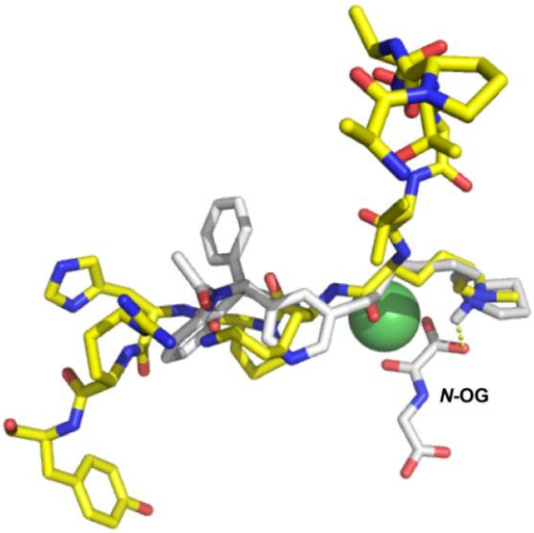

Figure 3.5 – Overlap of indoline **(*S*,*S*)-108** docking solution (white) with dimethylated peptide substrate (yellow), using *AutoDock Vina*.

While we recognized the limitations of computational docking as a method of obtaining accurate structural information, we envisaged using it as a tool to identify potential modifications to the inhibitor's alkyl chain. A virtual screen of analogues of **(*S*,*S*)-108** derived from commercially-available or easily accessible poised linker synthons was conducted using the docking program *Molsoft-ICM*.[119*] In general, modifications that constrained linker flexibility resulted in poor docking scores, and identifying synthetically-tractable alterations that would increase polarity proved challenging. Eventually, exploring possible changes in the vicinity of the pyrrolidine head-group revealed that a β-hydroxyl motif could potentially undergo a number of favorable H-bonding interactions with key residues in the KDM2A active site (Figure 3.6). We therefore identified indoline **160** as a promising synthetic target. The presence of an additional stereogenic center on the alkyl chain posed a challenge, and we decided it would be important to consider a number of possible stereoisomers of **160** in order to maximize the likelihood of discovering an improved KDM2A inhibitor.

[*] Work done in collaboration with Helene Pierson, under the supervision of Dr Brian Marsden, SGC.

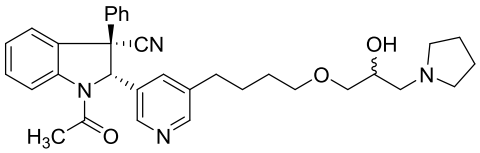

160

***C*Log*P*: 3.70**

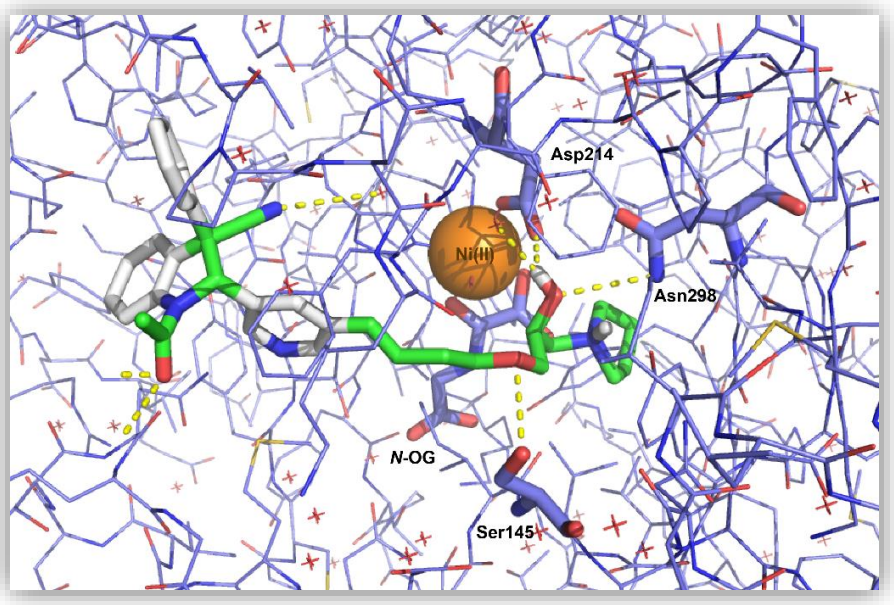

Figure 3.6 – Docking solution of indoline **160** in KDM2A active site using *Molsoft-ICM*.

Scheme 3.3 illustrates the synthesis of the enantiomeric alkyne fragments **163** and **164** from the chiral pool reagents (*R*)- and (*S*)-epichlorohydrin. The chemoselectivity of reactions involving various nucleophiles and epichlorohydrin has been studied extensively, as it dictates the absolute stereochemistry of the reaction product.[120] Direct displacement of chloride results in overall retention of configuration, whereas epoxide-opening followed by intramolecular substitution results in inversion of configuration. K. Urata demonstrated that complete inversion of configuration could be achieved with oxygen-based nucleophiles under phase-transfer catalysis,[121] and this methodology was later applied to the synthesis of analogues of the fatty-acid derived acetogenin class of natural products by R. L. Grée.[122] Our choice of reagents and reaction conditions draws on the insights provided by these investigations.

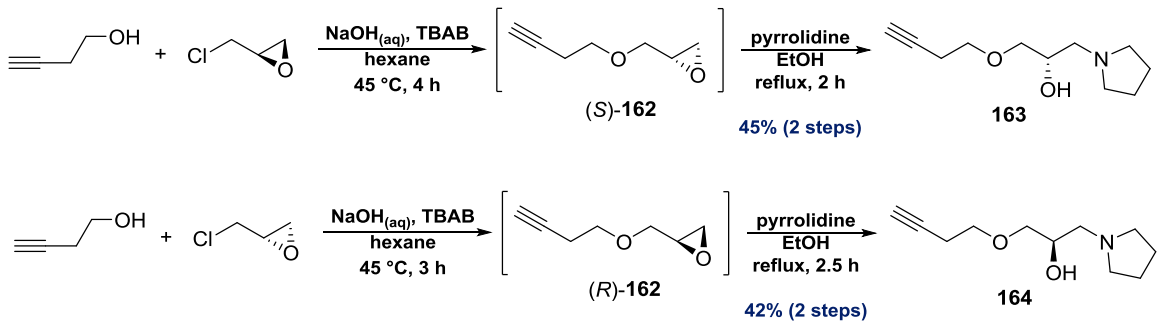

Scheme 3.3 – Synthesis of enantiomeric alkynes **163** and **164** from *R*-(-)-epichlorohydrin and *S*-(+)-epichlorohydrin respectively.

Alkynes **163** and **164** subsequently underwent Sonogashira coupling with optically-pure indolines **(*R*,*R*)-157** and **(*S*,*S*)-157**, to afford all possible stereoisomeric products featuring a *syn*-arrangement of functional groups at the indoline *C*2 and *C*3 positions. Reduction of the alkyne linker of each product by hydrogenation over a palladium on charcoal catalyst afforded the stereoisomeric alkane-linked compounds **166**, **168**, **170**, and **172** (Scheme 3.4).

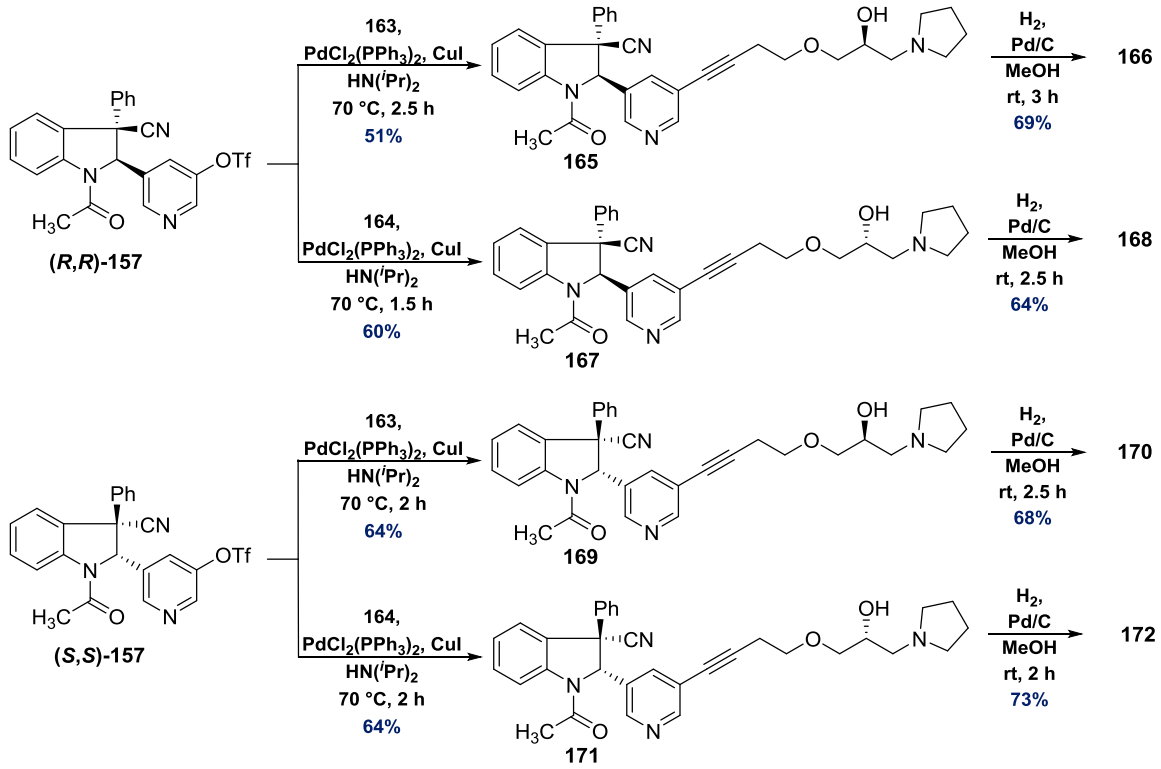

Scheme 3.4 – Synthesis of stereoisomeric alkyne- and alkane-linked KDM2A inhibitor candidates, containing linker modifications suggested by computational docking.

Unfortunately, biological testing revealed that all isomers were substantially weaker inhibitors of KDM2A than analogues with unfunctionalized hydrocarbon chains (Figure 3.7). This setback highlights the limitations of using computational docking to assist inhibitor discovery. In our case, the conclusions derived from *in silico* screening and docking were ultimately based on flawed assumptions and approximations. In particular, our hypothesis that the inhibitors occupy the peptide binding site would eventually be invalidated using a variety of experimental techniques (see Chapter 4).

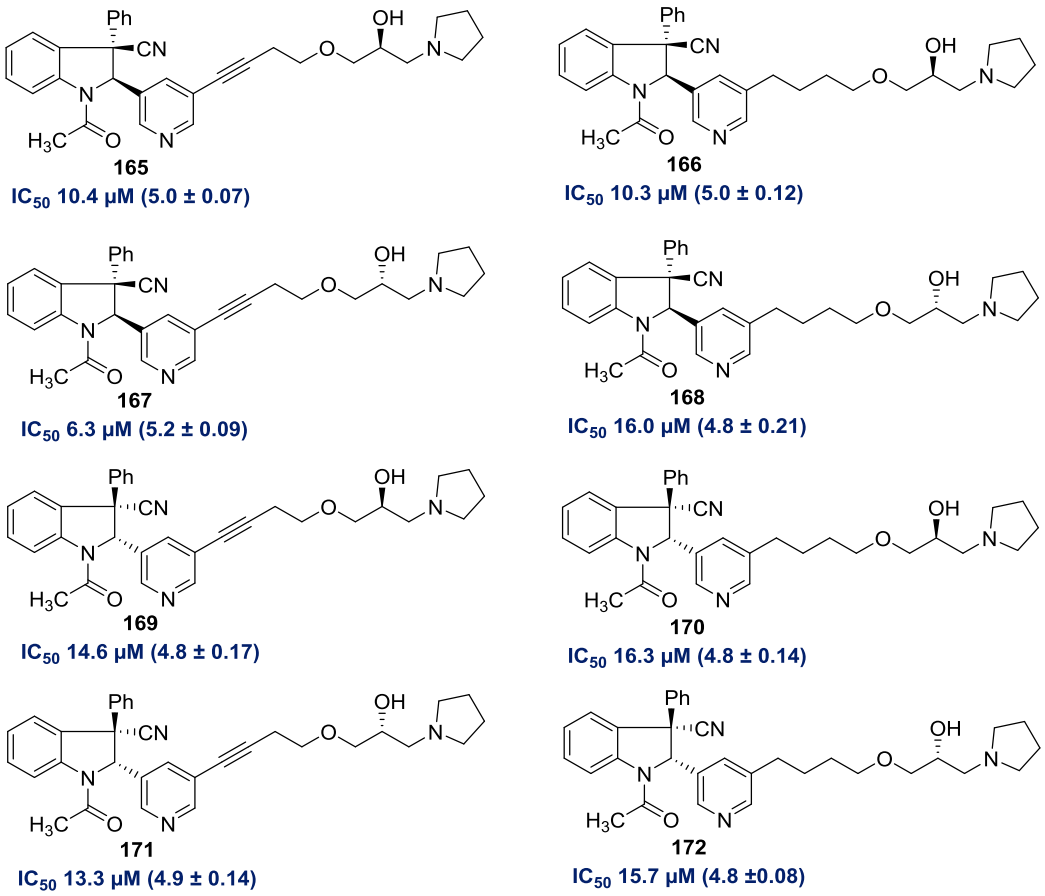

Figure 3.7 – RapidFire IC_{50} values for isomeric inhibitor candidates incorporating linker modifications suggested by computational docking. pIC_{50} values and errors are shown in parentheses.

3.2.3 Indoline Core Modifications

Given the apparent challenge of introducing polar modifications to the linker and alkyl chain without compromising inhibitory activity, we decided to focus our efforts on incorporating more heteroatoms in the indoline core itself. Previous work in the Smith group by Dr Alan Lamb explored enantioselective synthetic approaches to 4- and 6-*aza*-indolines,[75] and we therefore envisaged synthesizing potential KDM2A inhibitors based on these scaffolds.

To begin with, regioisomeric aminopyridines **175** and **177** were synthesized in two steps from the relevant chloropyridine starting reagents. Benzyl cyanide and stoichiometric TDA-1 were used in both S_NAr reactions, and the resulting products were reduced to the desired anilines using zinc powder and NH_4Cl (Scheme 3.5). TDA-1 is a "trident" phase-transfer catalyst initially reported by G. Soula[123] and first applied to substitution reactions of chloropyridines by P. Ballesteros.[124]

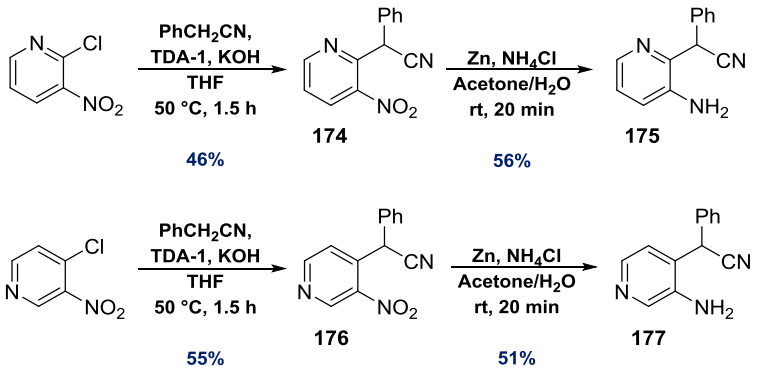

Scheme 3.5 – Synthesis of aminopyridines **175** and **177**.

Condensation of aminopyridine **175** with 5-bromo-3-pyridinecarboxaldehyde afforded the desired imine product **178**, albeit after a longer reaction time than required for the equivalent aniline **47**. Conversely, condensation of aminopyridine **177** with 5-bromo-3-pyridinecarboxaldehyde was *not* achieved under a variety of reaction conditions.

The lack of reactivity of 4-substituted aminopyridines with aromatic aldehydes had also been encountered by Dr Alan Lamb in the course of his investigations,[125] and we therefore decided to focus our synthetic efforts on generating *aza*-indolines from imine **178**. Cyclization of **178** under racemic reaction conditions afforded an inseparable mixture of diastereomers, which were subsequently acetylated using acetyl chloride and pyridine. The major *syn* diastereomer was isolated and subjected to a Stille-Migita cross-coupling reaction with vinylstannane **57** to afford *aza*-indoline **181** (*C*log*P* = 4.95) in moderate yield (Scheme 3.6).

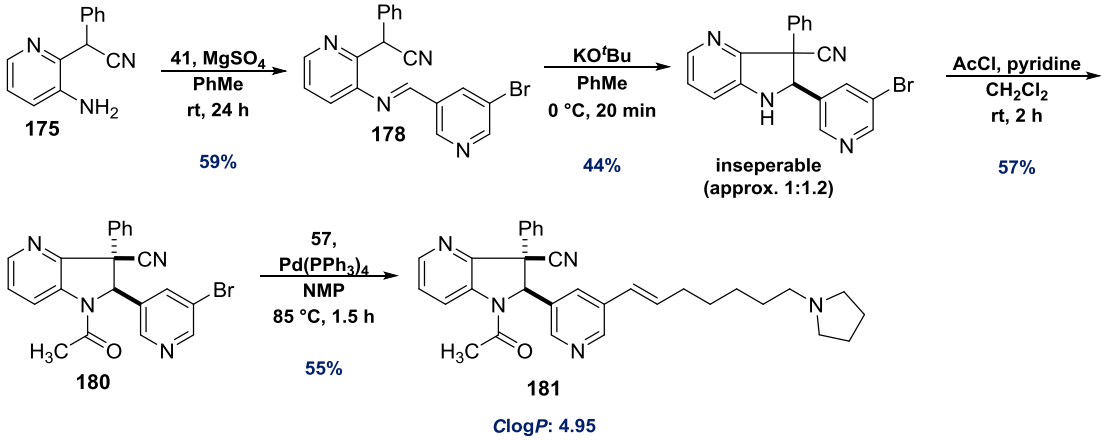

Scheme 3.6 – Synthesis of *aza*-indoline **181**. The relative stereochemistry of intermediate **180** was assigned by analogy to indolines **52** and **53**.

As an alternative approach to increasing the polarity of the indoline ring system, we envisaged incorporating a polar aromatic heterocycle as one of the substituents on the *C*3 position. To this end, synthesis of the thiazole-containing indoline **189** was accomplished (Scheme 3.7). Nucleophilic aromatic substitution of 2-chlorothiazole **182** by 2-nitrophenylacetonitrile **183** proved challenging, and the low yield of this transformation is attributed to a number of side reactions involving the initial product **184**. Reduction of **184** by hydrogenation over a palladium on charcoal catalyst did afford the desired aniline,

but partial decomposition of this product in the course of silica gel column chromatography made complete purification of **185** difficult. Condensation of the impure aniline with 5-bromo-3-pyridinecarboxaldehyde was found to proceed very slowly (approx. 15% conversion after 48 h), and instead of the expected imine **186**, indoline **189** was obtained as a single diastereomer. This suggests that imine **186** undergoes spontaneous cyclization once formed, possibly *via* a zwitterionic intermediate (**187** and **188**) as previously proposed for imine **75** (Subsection 2.2.2). A trace of aminal **190** was also observed, although the amount of isolated material was insufficient to enable complete characterization. To complete the synthesis of the final KDM2A inhibitor candidate **193** (*C*log*P* = 4.39), **189** was acetylated to afford indoline **192**, which underwent Stille-Migita cross-coupling with vinylstannane **57** (Scheme 3.8).

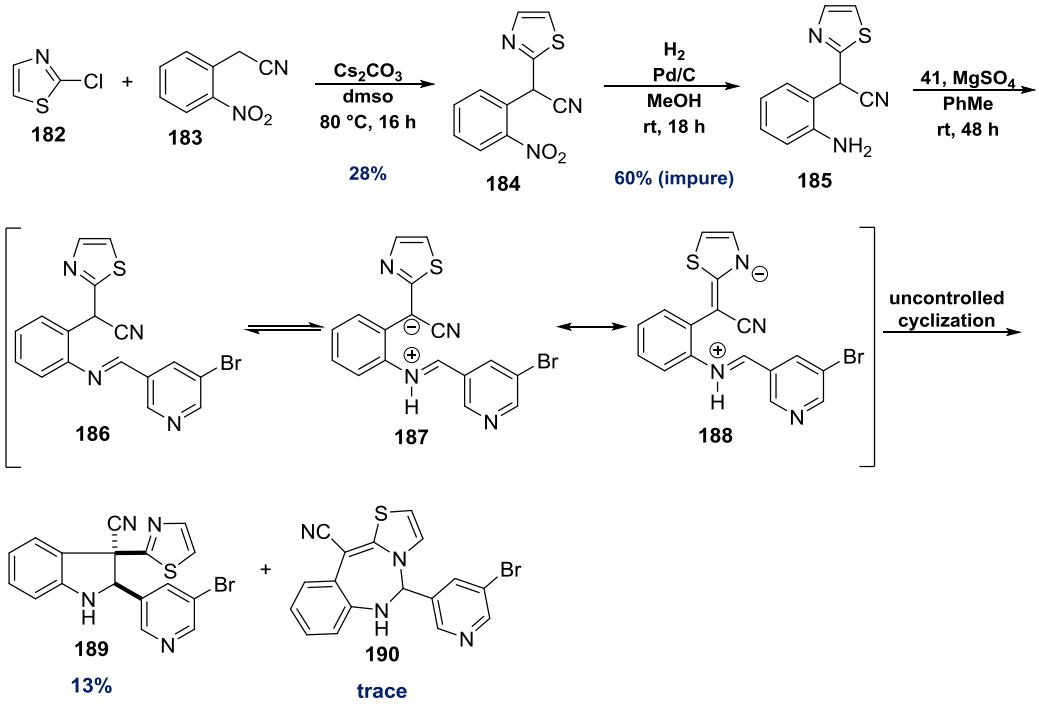

Scheme 3.7 – Synthesis of thiazole-containing indoline **189**. Imine **186** was not isolated, as it underwent spontaneous cyclization to indoline **189** and aminal **190**. The stereochemistry of indoline **189** was tentatively assigned by analogy to indolines **49** and **50**.

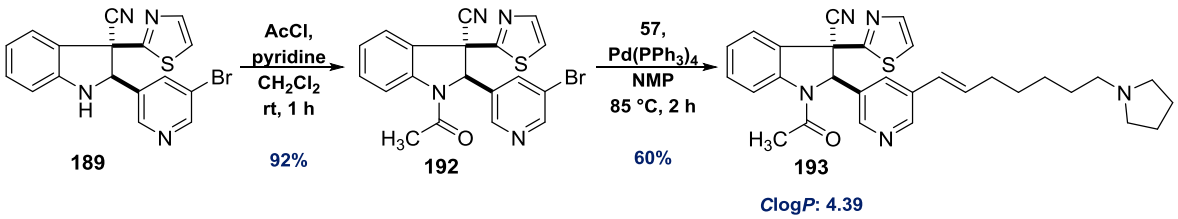

Scheme 3.8 – Synthesis of thiazole-containing KDM2A inhibitor candidate **193**.

Aza-indoline **181** and thiazole **193** were tested for inhibition of KDM2A using the RapiFdire assay. Unfortunately, both compounds were found to be substantially weaker inhibitors than their more lipophilic analogues (Figure 3.8). We concluded that a more methodical approach would be required to identify a successful strategy for incorporating polar functionality while maintaining inhibitory activity.

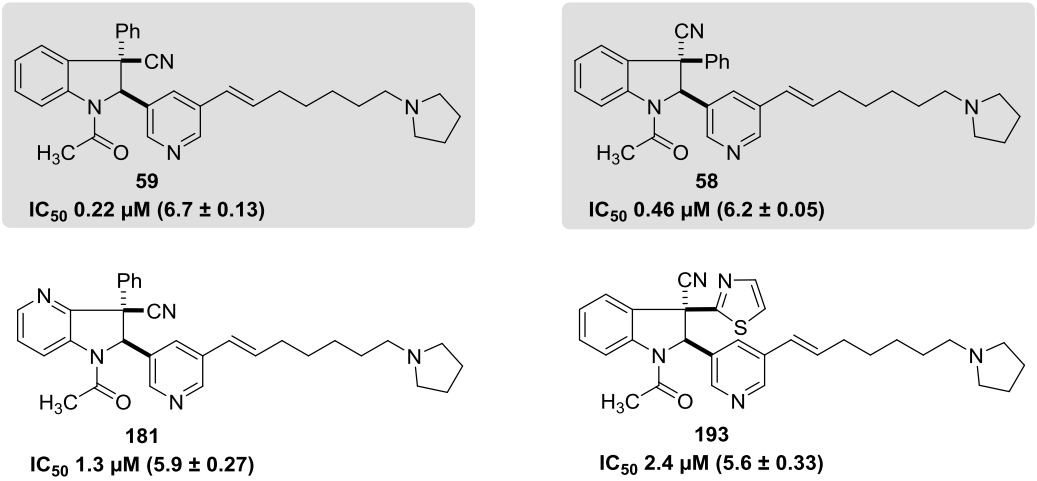

Figure 3.8 – RapidFire IC_{50} values of *aza*-indoline **181** and thiazole **193**, along with pIC_{50} values and errors. Activities of the previously-discussed indolines **58** and **59** are shown for comparison.

3.2.4 N-Acyl Group Modifications

Since Lipinski's seminal analysis highlighting the relationships between certain physical and chemical properties of pharmaceutical candidates and their likelihood of success in the drug discovery pipeline, lipophilic efficiency (LiPE) has emerged as a particularly insightful parameter with respect to lead optimization.[126] It was first defined

by P. D. Leeson and B. Springthorpe according to the equation: LiPE = pIC_{50}* – Log*P*.[127] It is important to recognize that on-target biological activity depends on the precise interplay of both enthalpic and entropic contributions to the relevant ligand-protein interaction.[128] That said, due to the importance of the *hydrophobic effect* in ligand binding, increasing compound lipophilicity generally results in enhanced biological activity. As discussed previously, this enhanced activity often arises at the expense of greater promiscuity and hence toxicity. LiPE is therefore a measure of how efficiently a molecule is able to balance the desirable traits of high biological activity and moderate lipophilicity.

Figure 3.9 shows a LiPE plot of our indoline-based KDM2A inhibitors divided into 2 compound series. Series A corresponds to molecules featuring different indoline *C*2/*C*3 substituents and linker motifs, while molecules in series B contain different indoline *N*-acyl groups.† For the compounds in series A, we observed a general correlation between biological activity and lipophilicity: Reducing *C*log*P* led to a loss of inhibitory activity. In contrast, altering the identity of the *N*-acyl group appeared to have a much less pronounced effect on inhibition. We therefore concluded that the *N*-acyl group would offer the most promising handle for introducing polarity without compromising inhibitory activity, and we envisaged incorporating a selection of polar functional groups at the carbonyl α-position (Scheme 3.9).

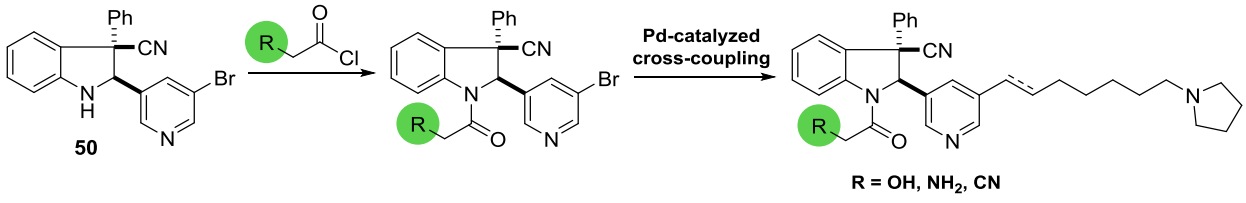

Scheme 3.9 – Modular synthetic approach towards incorporating polar functionalilty in the indoline *N*-acyl motif.

* pIC_{50} = – log[IC_{50} (μM)].
† Series B compounds were synthesized by Dr Jamie Wolstenhulme.

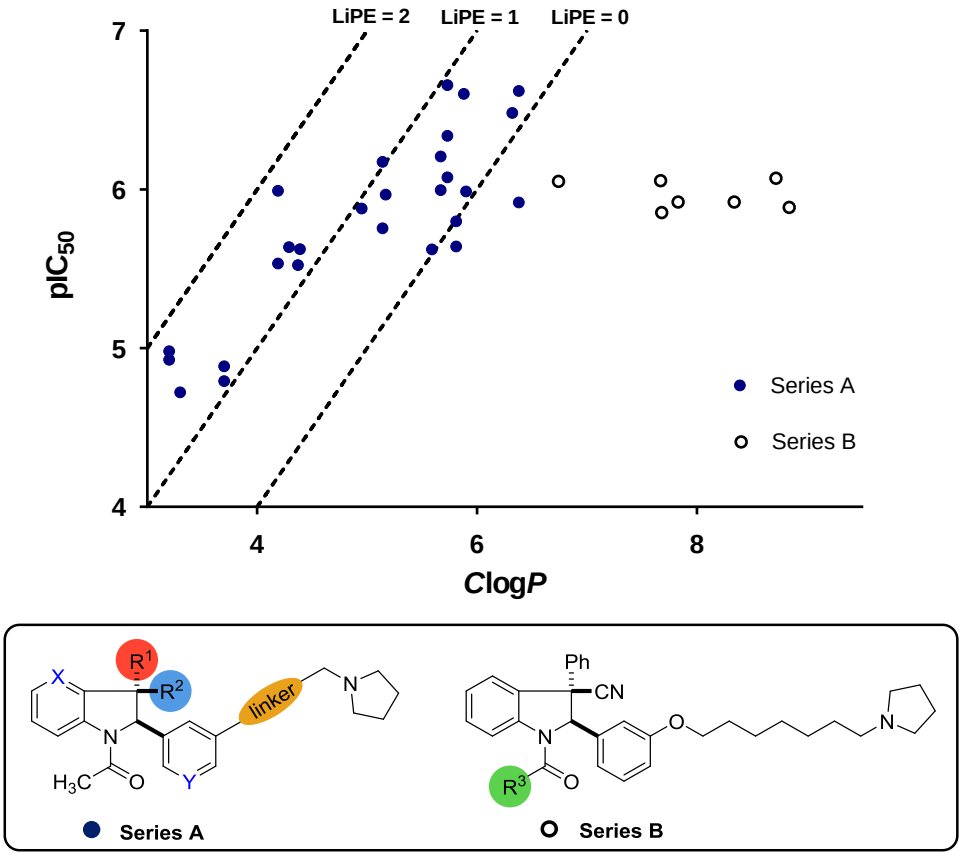

Figure 3.9 – LiPE plot of indoline-based KDM2A inhibitors corresponding to series A and B.

The previously-established limited reactivity of the indoline nitrogen necessitated the synthesis of α-functionalized acetyl chlorides as acylating reagents. Thus, incorporation of a cyano group was accomplished by *in situ* formation of 2-cyanoacetyl chloride from its carboxylic acid precursor, followed by reaction with the indoline core **50**. Sonogashira coupling with alkyne **105** and hydrogenation over a palladium on charcoal catalyst afforded the saturated alkyl-linked indoline **196** (Scheme 3.10).

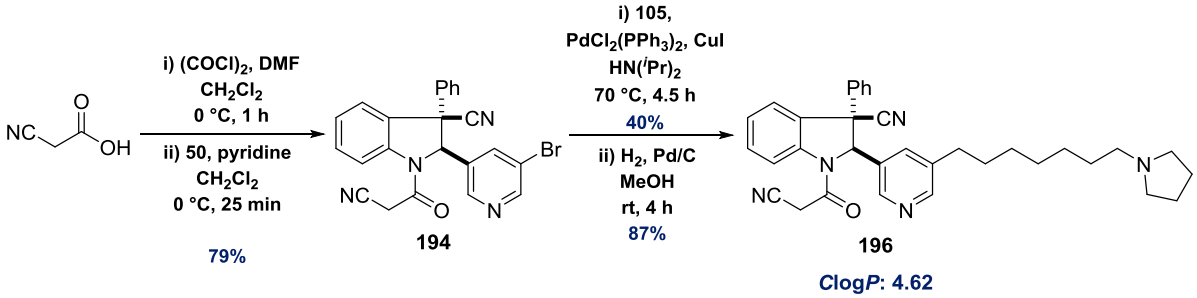

Scheme 3.10 – Synthesis of α-cyano-acetyl indoline **196**.

We envisioned the preparation of a hydroxylated analogue through *N*-acylation of indoline **50** with benzyloxyacetyl chloride **197**, followed by Sonogashira coupling, alkyne reduction, and deprotection. We chose to employ a benzyl protecting group, as we anticipated that this would enable simultaneous reduction and deprotection in a single step. Initial acylation and Sonogashira coupling afforded indoline intermediate **199**, albeit in modest yield. Treatment of this intermediate with hydrogen under Pd/Rh catalysis was successful in effecting alkyne double reduction; however *O*-debenzylation was not observed. Attempts to deprotect the hydroxyl group *via* high-pressure hydrogenolysis over a variety of catalysts and subsequently with BF_3/NaI[129] proved unsuccessful (Scheme 3.11).

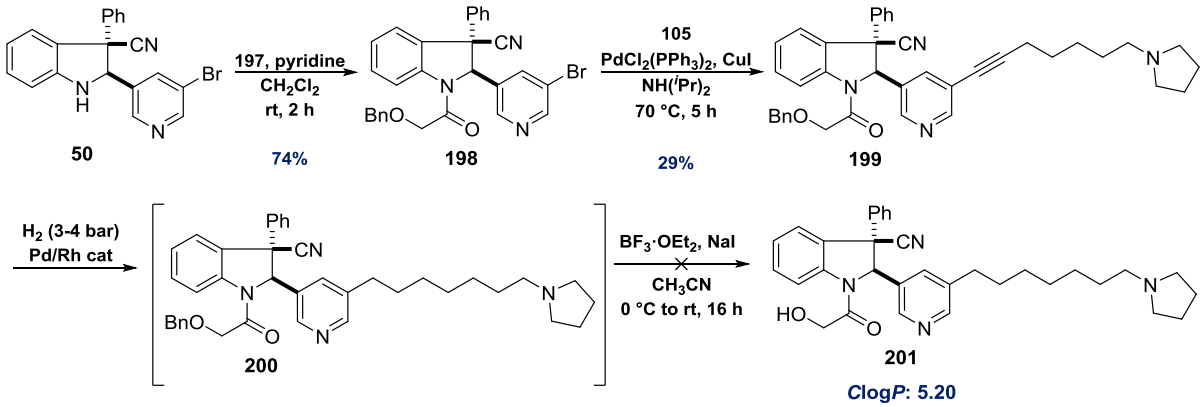

Scheme 3.11 – Synthesis of alkyne-linked indoline **199** and unsuccessful benzyl-ether deprotection.

We therefore decided to adopt an alternative protecting group strategy and synthesized the TBS-protected indoline **203** from glycolic acid. Sonogashira coupling of **203** with alkyne **105** afforded indoline **205** in moderate yield. However, deprotection of the silyl ether with TBAF gave rise to a mixture of inseparable products **206** and **207** (Scheme 3.12). Moreover, the amide bond of the desired indoline **206** was found to be highly susceptible to cleavage even under relatively mild conditions, such as those encountered in the course of aqueous work-up with $NaHCO_3$ and purification by silica gel column chromatography. This suggests that even if the alkyne linker of **207** could be reduced cleanly, the lack of

stability of the alkyl-linked product means that it is unlikely to be a suitable KDM2A chemical probe candidate.

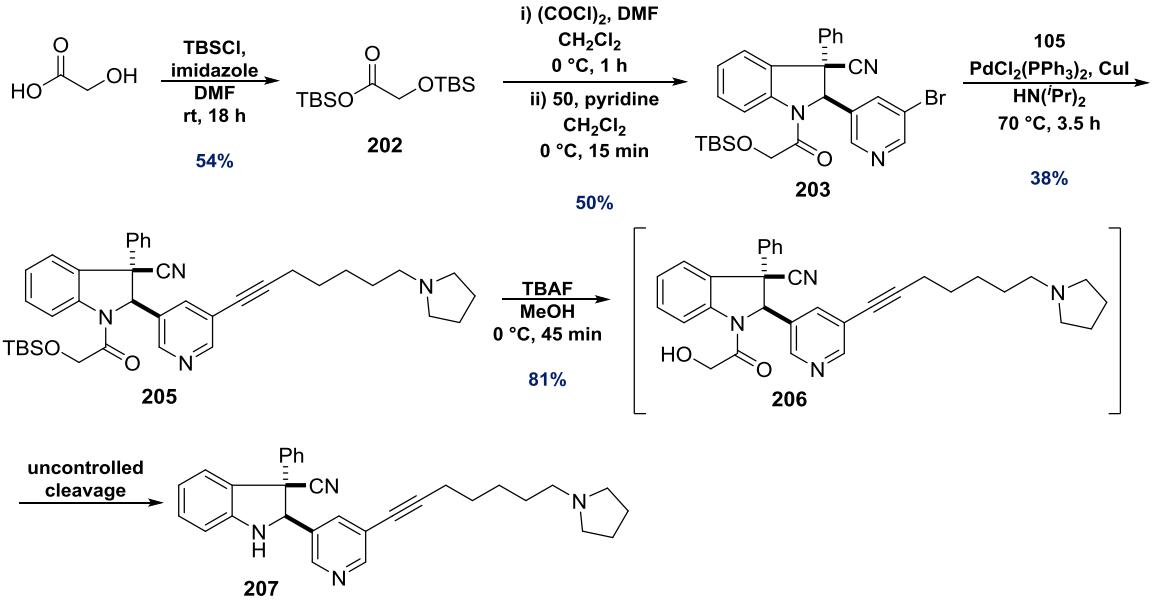

Scheme 3.12 – Synthesis of alkyne-linked indoline **205**. TBS-deprotection by TBAF afforded the desired product **206**, which was susceptible to uncontrolled cleavage of the amide bond.

We reasoned that replacing the hydroxyl group in **206** with a less electron-withdrawing primary amine would improve stability towards uncontrolled cleavage of the amide bond. The amine would be masked in the form of a comparatively unreactive phthalimide group, which we anticipated could be removed with N_2H_4 at the end of the synthetic sequence. Thus, indoline **50** was acylated with α-(*N*-phthalimido)-acetyl chloride **209** to afford indoline **210**, which underwent Sonogashira coupling followed by hydrogenation of the alkyne linker. The resulting product **212** was cautiously treated with aqueous N_2H_4 to afford the indoline **213** (*C*log*P* = 4.64) in reasonably good yield (Scheme 3.13). At first glance, **213** appeared to be substantially more stable than its hydroxyl-containing analogue would likely have been, although some cleavage of the amide bond was observed after prolonged exposure to N_2H_4.

Finally, the acetyl-free indolines **207** and **214** were synthesized to provide further insight into the importance of the *N*-acyl group with respect to inhibition (Scheme 3.14). These compounds are predicted to be more lipophilic than their acetylated analogues and were found to undergo gradual oxidation to indolenines and other products upon exposure to air. Nonetheless, we anticipated that an evaluation of their biological activities would be instructive.

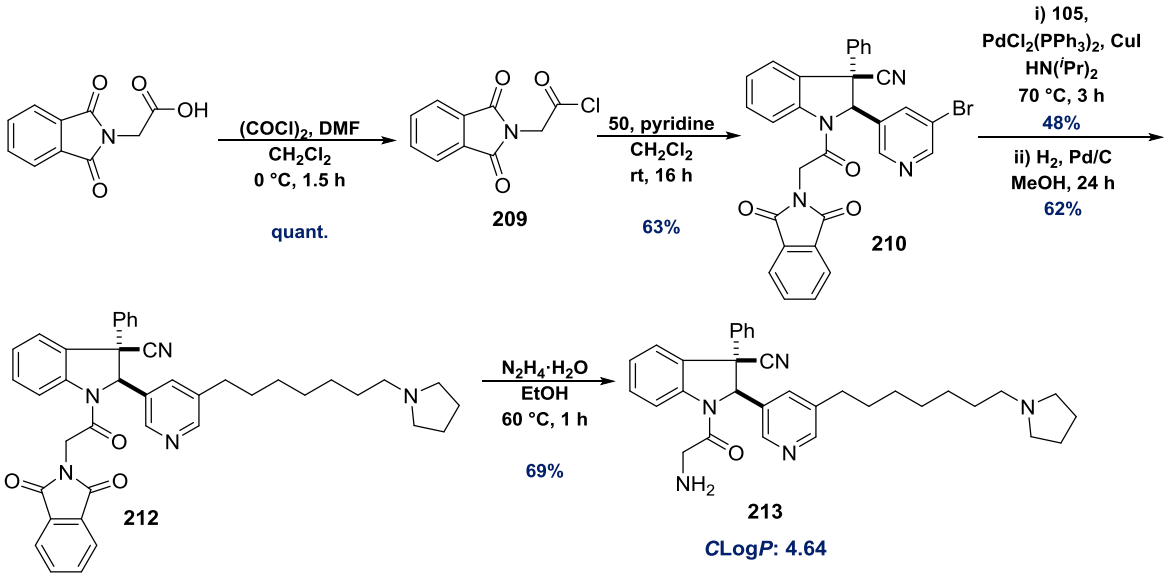

Scheme 3.13 – Synthesis of α-aminoacetyl-containing indoline **213**.

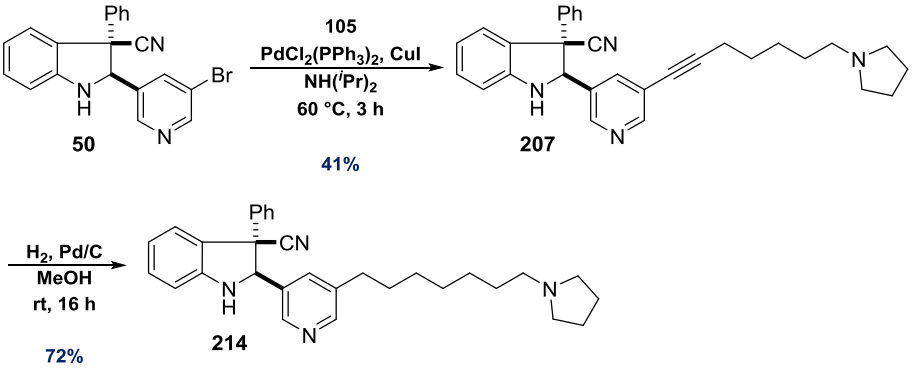

Scheme 3.14 – Synthesis of acetyl-free indolines **207** and **214**.

The effect of varying the indoline *N*-acyl group on inhibitory activities was evaluated using the RapidFire assay (Figure 3.10). Excitingly, α-aminoacetyl-indoline **213** was found

to be a substantially more potent inhibitor than acetyl-indoline **108** (**213:** IC_{50} 0.12 µM; LiPE 2.3 vs. **108:** IC_{50} 0.25 µM; LiPE 0.7). We postulate that the greater inhibitory activity of **213** is a consequence of electrostatic or H-bonding interactions between the primary amine and either residues in the enzyme binding site or ambient solvent molecules. Replacing the acetyl group of **108** with an α-cyanoacetyl motif led to a drop in potency. However, the magnitude of this change was relatively small when compared to the observed losses of potency as a result of increasing the polarity of the indoline core or linker (subsections 3.2.1, 3.2.3). Finally, removing the acetyl group completely led to a marginal improvement in inhibitory activity at the expense of increased lipophilicity (**214**: IC_{50} 0.20 µM, LiPE 0.4). Together, these observations appear to confirm our hypothesis that the indoline *N*-acyl group provides a promising handle for modulating polarity without compromising inhibition of KDM2A.

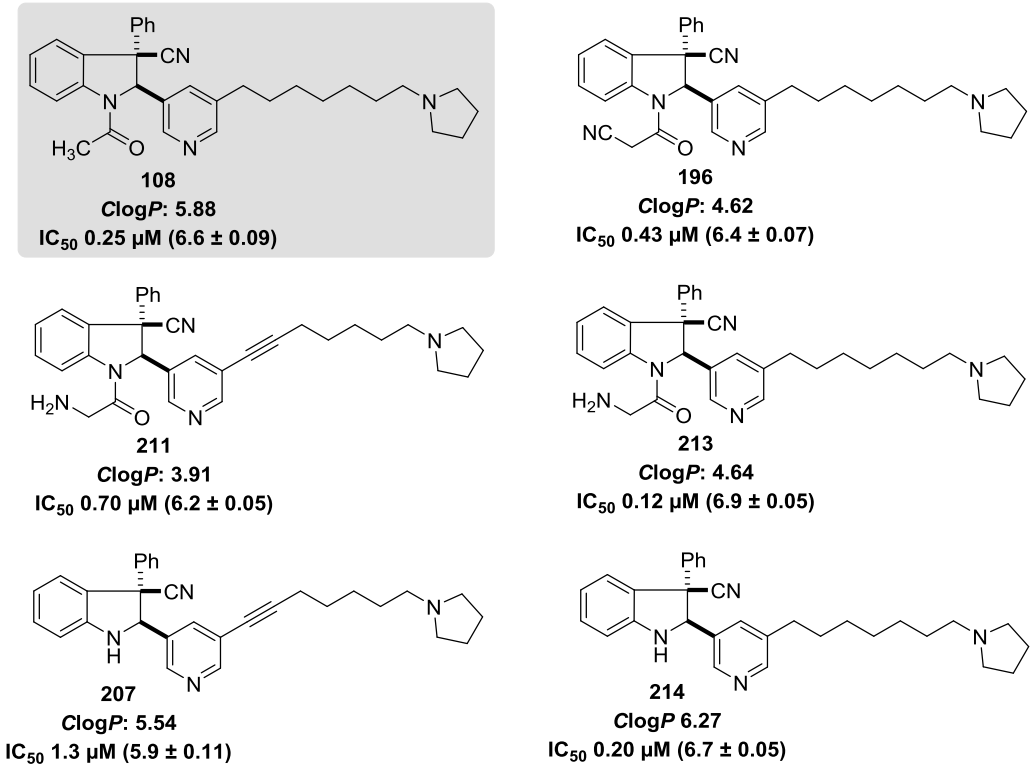

Figure 3.10 – RapidFire IC_{50} and *C*log*P* values of KDM2A inhibitors with different indoline *N*-acyl groups. pIC_{50} values and errors are shown in parentheses.

Given the susceptibility of the α-hydroxyacetyl amide bond to hydrolysis under relatively mild conditions, we were concerned that a similar effect would occur with indoline **213**. We therefore monitored a 20 mM aqueous solution of **213** at rt by LCMS. Unfortunately, even after a period of 1 hour, hydrolysis of the amide bond to afford indoline **214** was observed. **214**, in turn, undergoes gradual oxidation to the corresponding indolenine and other products. This decomposition led to a marked drop in inhibitory activity, and retesting the aqueous stock solution of **213** gave rise to IC_{50} values of 0.36 µM and 2.0 µM after one and two freeze-thaw cycles respectively. A possible explanation for the lability of the amide bond in **213** is the occurrence of intramolecular general base catalysis involving the terminal amino group (Scheme 3.11).

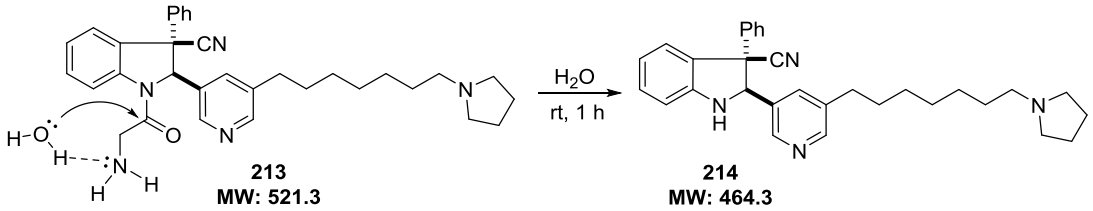

Scheme 3.11 – Facile hydrolysis of the amide bond of **213**, possibly as a result of general base catalysis.

The requirement for chemical probes to demonstrate unambiguous, on-target cellular activity presented a particularly difficult challenge in this project. While we were ultimately unable to provide a convincing solution to this problem, we identified a promising strategy for modulating key physical properties of lead compounds while maintaining inhibitory activity towards KDM2A. We anticipate that future work based on this approach could eventually yield a unique KDM2A chemical probe candidate (subsection 4.3.4). The next chapter of this thesis will primarily focus on exploring the mechanism of KDM2A inhibition using a broad range of experimental techniques.

4. MECHANISM OF INHIBITION

4.1 Identifying the Inhibitor Class

4.1.1 Inhibitor Demethylation

Computational docking of **(*S*,*S*)-108** in the KDM2A active site suggests that the inhibitor's pyrrolidine head-group mimics the dimethyl-lysine sidechain of the histone substrate (Subsection 3.2.2). We therefore reasoned that a dimethylamine head-group might be susceptible to catalytic demethylation. To test this hypothesis, dimethylamine-capped indoline **216** was synthesized from alkyl bromide **101** (Scheme 4.1). As expected, indoline **216** was found to be a weaker inhibitor of KDM2A than its pyrrolidine-capped analogue (**100:** IC_{50} 0.29 µM).

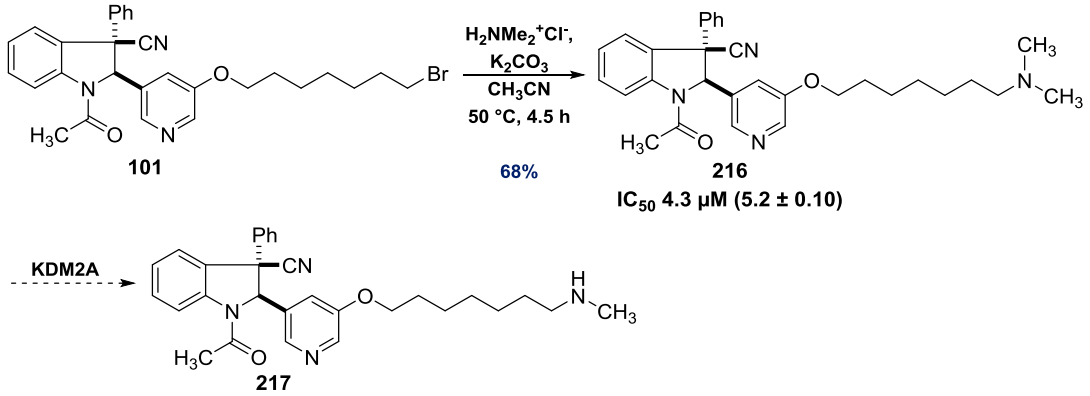

Scheme 4.1 – Synthesis of dimethylamine-capped indoline **216** and possible demethylation by KDM2A.

216 was incubated with up to one equivalent of KDM2A in the presence of excess 2-OG and Fe^{II} and monitored by mass spectrometry for enzyme-catalyzed demethylation; however, no conversion of **216** to **217** was observed. While we realized that this absence

of reactivity did not necessarily invalidate our hypothesis regarding inhibitor occupancy of the peptide binding site, it highlighted the need for further considerations of the potential modes of enzyme inhibition. ·

4.1.2 Kinetics of Enzyme Inhibition

The demethylation of H3K36me2 and its peptidic analogue by KDM2A most likely proceeds *via* an ordered, sequential mechanism. Crystallographic and spectroscopic investigations on closely related 2-OG deoxygenases are consistent with initial coordination of 2-OG to Fe^{II} in the active site, followed by consecutive binding of the peptide substrate and O_2.[130, 131] Figure 4.1 summarizes the possible modes of inhibition based on this catalytic mechanism. In addition, work by W. W. Cleland[132] and J. S. Blanchard[133] on the theory of multi-substrate enzyme catalysis provides the basis for the derivation of a steady state rate law accounting for all possible KDM2A-inhibitor interactions.

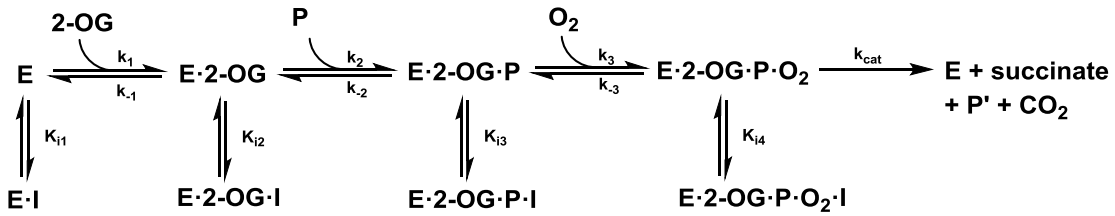

$$v = \frac{v_{max}[2OG][P][O_2]}{\left(\frac{k_{-1}}{k_1} * \frac{k_{-2}}{k_2} * \frac{k_{-3}}{k_3} + \frac{k_{-1}}{k_1} * K_P[O_2] + K_{2OG}[P][O_2]\right)\left(1 + \frac{[I]}{K_{i1}}\right) + \left(\frac{k_{-2}}{k_2} * K_{O_2}[2OG] + K_P[2OG][O_2]\right)\left(1 + \frac{[I]}{K_{i2}}\right) + K_{O_2}[2OG][P]\left(1 + \frac{[I]}{K_{i3}}\right) + [2OG][P][O_2]\left(1 + \frac{[I]}{K_{i4}}\right)}$$

Figure 4.1 – Ordered, sequential mechanism of KDM2A-catalyzed demethylation of the peptide substrate (P) and possible modes of dead-end inhibition, giving rise to a theoretical steady-state rate law. v_{max} is the maximum rate of reaction and $K_X = \frac{[E][X]}{[E \cdot X]}$.

We envisaged using the RapidFire mass spectrometry platform to measure the initial rate of KDM2A-catalyzed peptide-demethylation over a range of 2-OG and inhibitor concentrations and hence establish whether our inhibitor binds the enzyme competitively with respect to 2-OG (i.e. K_{i2}, K_{i3}, K_{i4} >> 0). This approach has previously been used to confirm the mode of inhibition of a variety of 2-OG mimics.[45, 49, 134] To begin, the effect of varying the concentration of 2-OG on the consumption of the dimethylated peptide substrate was measured with the aim of determining a practical 2-OG concentration range for analysis (Figure 4.2). Intriguingly, the conversion of substrate to product appeared to reach a maximum when [2-OG] = 5 µM before diminishing at higher cofactor concentrations, indicating a degree of substrate inhibition. To our knowledge, inhibition of KDM2A by 2-OG has not been reported in the literature. However, L. M. Mirica noted that KDM4C is subject to substrate inhibition and proposed that this is a consequence of competition between 2-OG and O_2.[135] In order to ensure that oxygen would not be the rate-limiting substrate, we focused on a range of 2-OG concentrations corresponding to the "regular", positive relationship between substrate concentration and reaction rate – in this case, [2-OG] ≤ 3 µM.

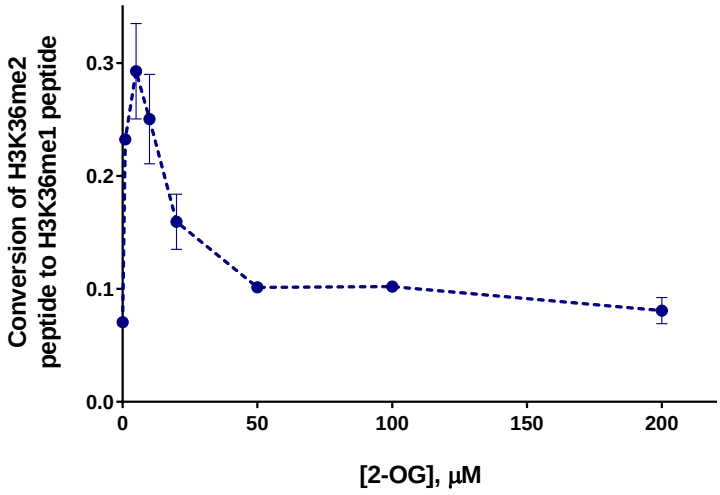

Figure 4.2 – Substrate inhibition of KDM2A by 2-OG. Concentrations are: 0, 1, 5, 10, 20, 50, 100, and 200 µM.

The relationship between [2-OG] and the initial rate of enzyme-catalyzed demethylation at different concentrations of the optically-pure inhibitor **(*S*,*S*)-108** (IC_{50} 0.16 μM) is depicted in Figure 4.3, along with the corresponding Lineweaver-Burk plot.[136] The observation that v_{max} decreases with increasing inhibitor concentration allows us to rule out a mode of inhibition that is purely competitive with respect to 2-OG.

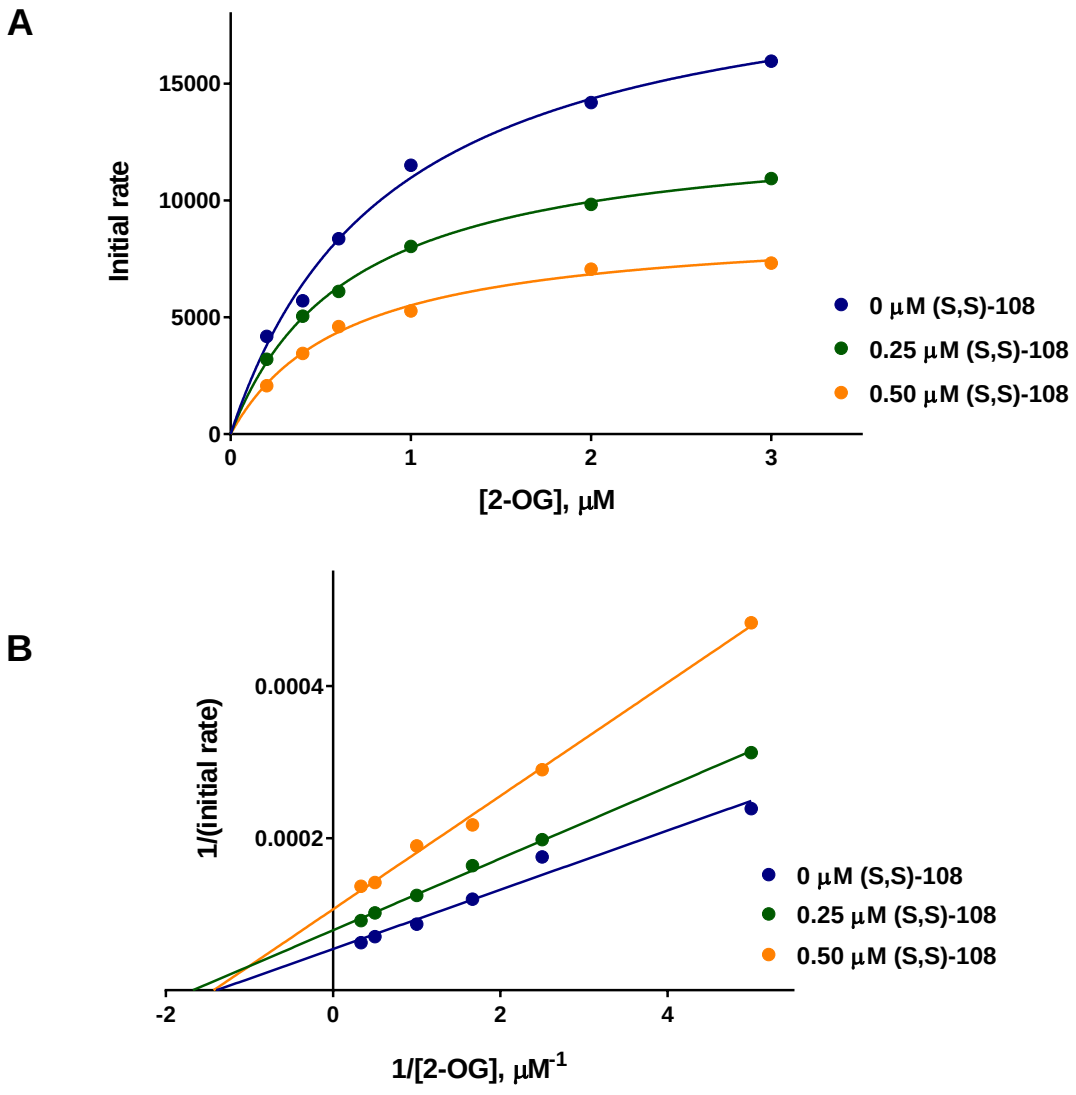

Figure 4.3 – A) Plot of [2-OG] vs. initial rate of peptide demethylation. The concentration of the peptide substrate is 10 μM. B) Lineweaver-Burke plot, illustrating non-competitive inhibition wrt 2-OG.*

* For a complete regression analysis of these results, see subsection 8.2.2 in the appendix.

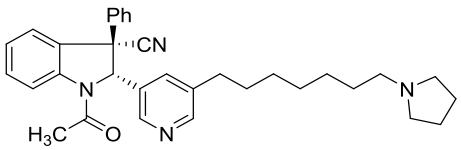

(S,S)-108

We envisaged using an analogous approach to explore the mode of KDM2A inhibition with respect to the peptide substrate. As this would entail measuring the initial rate of demethylation over a range of peptide concentrations, it was important to ensure that the peptide would not saturate the mass spectrometer's detector, thus obscuring the obtained results. No signal saturation at peptide concentrations up to 50 µM was observed (Figure 4.4).

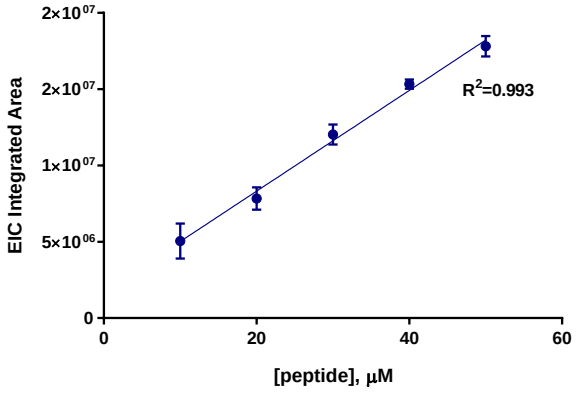

Figure 4.4 – MS extracted ion chromatogram (EIC) integrated areas as a function of [peptide].

The relationship between [peptide] and the initial rate of enzyme-catalyzed demethylation at different concentrations of **(*S*,*S*)-108** is depicted in Figure 4.5, along with the corresponding Lineweaver-Burk plot.[136] As before, the observation that v_{max} decreases with increasing inhibitor concentration suggests a mode of inhibition that is not purely competitive with respect to the peptide substrate.

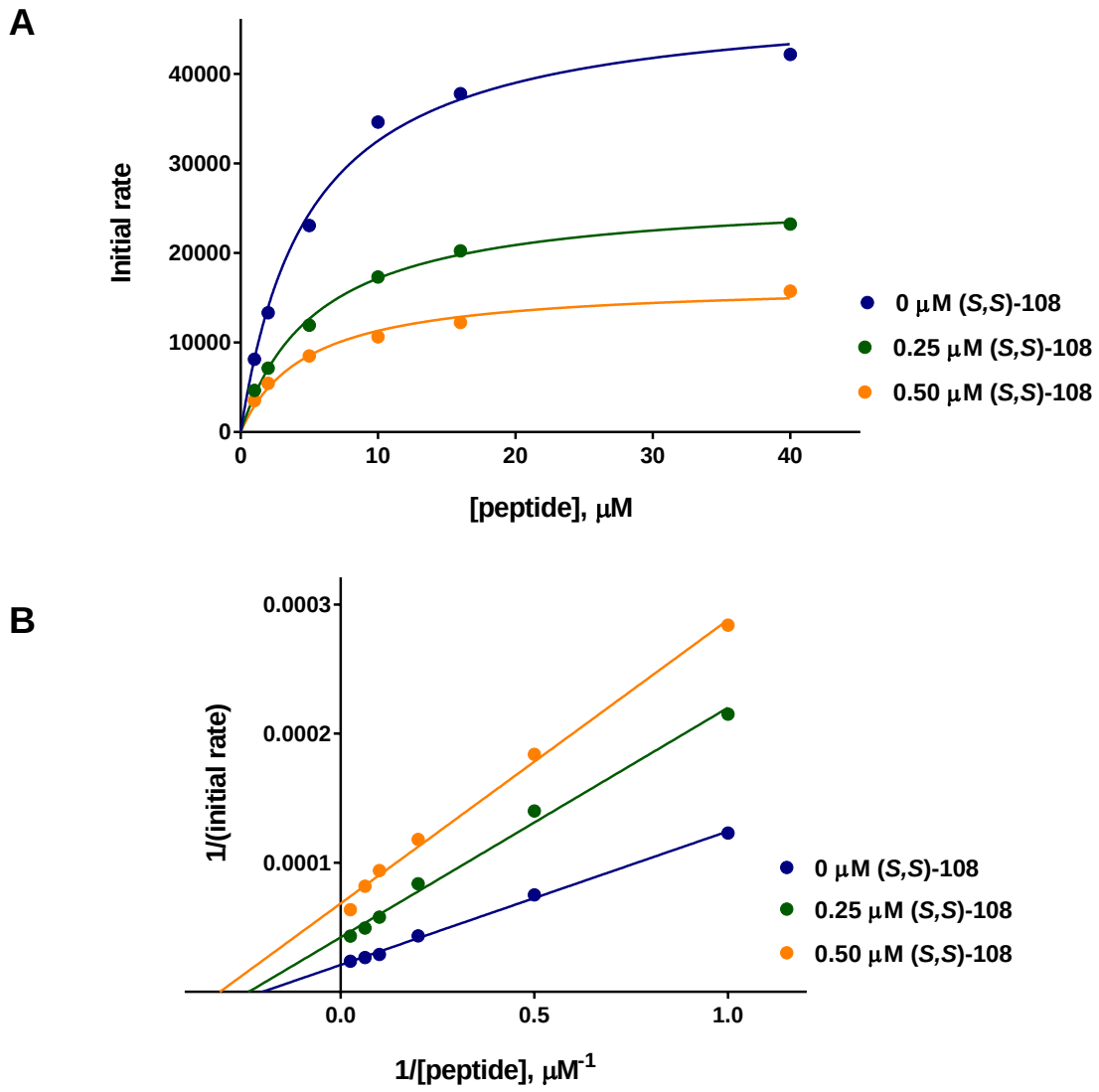

Figure 4.5 – A) Plot of [peptide] vs. initial rate of peptide demethylation. The concentration of the 2-OG cosubstrate is 10 μM. B) Lineweaver-Burke plot, illustrating non-competitive inhibition kinetics of **(*S*,*S*)-108** wrt the peptide.*

4.2 Confirmation of Binding

4.2.1 Biolayer Interferometry

Having explored the kinetics of enzyme inhibition, we sought to obtain more information about the stoichiometry and thermodynamic parameters of the enzyme-

* For a regression analysis of both graphs, see section 8.2 in the appendix.

inhibitor interaction. We initially envisaged employing isothermal titration calorimetry (ITC) to achieve this. In an ITC experiment, heat exchange between a sample cell and a reference cell within an adiabatic container is measured. The sample cell contains a solution of protein or ligand, and the exothermic or endothermic ligand-protein interaction is monitored during the course of titration. This provides information about the stoichiometry as well as the enthalpic and entropic contributions to binding.[137] Unfortunately, we were unable to find precedent for the application of ITC to KDM-ligand interactions, and attempts to identify conditions that provided an adequate signal-to-noise ratio for our system proved unsuccessful. Moreover, the low sensitivity of ITC necessitates the commitment of a relatively large quantity of protein, which precluded optimization of an ITC-based assay for KDM2A binding.

To gain an insight into the strength of the inhibitor-KDM2A binding interaction and determine the corresponding K_D, we therefore turned to a more sensitive technique: bio-layer interferometry (BLI). In a BLI experiment, a protein or ligand is immobilized on the tip of a fiber-optic biosensor, usually by incorporating a biotin-tag on either species and exploiting the effectively irreversible biotin-streptavidin binding interaction. Immersion of the tip in a solution of the corresponding ligand or protein results in ligand-protein association, which increases the optical thickness of the biosensor. This change in optical thickness alters the interference pattern of white light that is reflected from the tip of the fiber-optic biosensor, and the consequential wavelength shift may be measured in real time (Figure 4.7).[138]

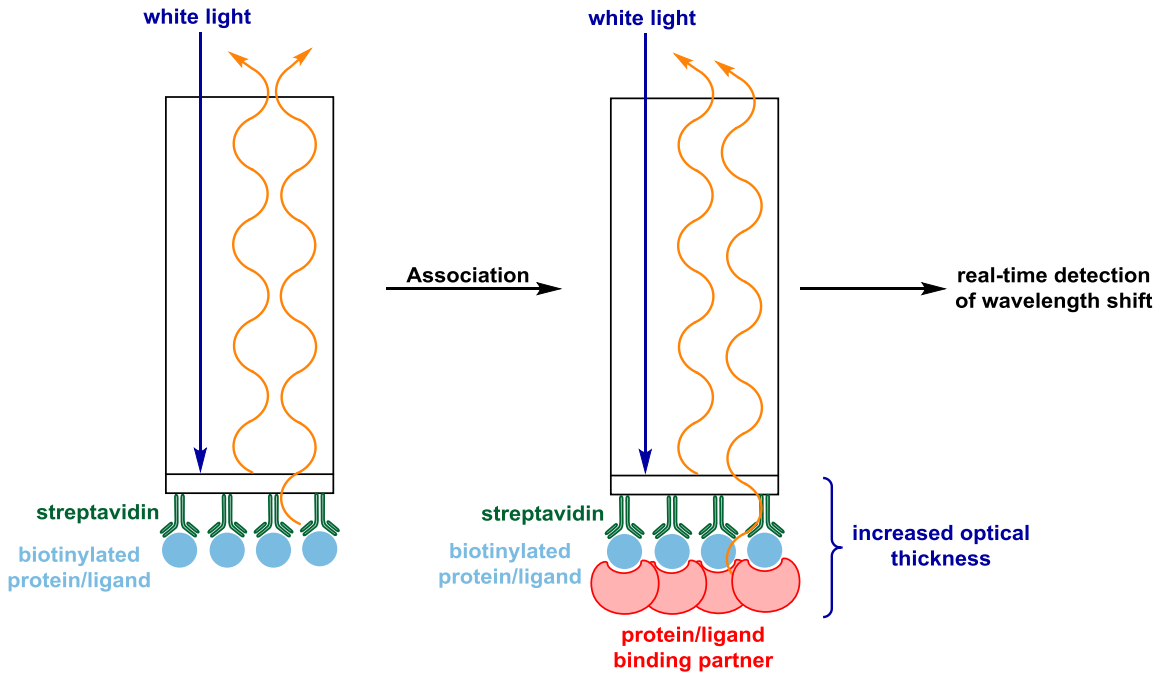

Figure 4.7 – Principles of bio-layer interferometry (BLI): The association of immobilized protein/ligand with its binding partner increases the optical thickness of the bio-layer at the tip of a fiber-optic biosensor. The resulting wavelength shift of reflected white light may be measured in real time.

Initial work carried out within the SGC focused on engineering a biotinylated version of KDM2A to be used in BLI assays. However, the incorporation of a biotin tag at various locations in the protein sequence led to a dramatic loss of catalytic activity. It was therefore necessary to synthesize a biotinylated inhibitor instead. Previous research by Dr Katherine England in the C. Schofield research group revealed that a long linker connecting biotin and the inhibitor scaffold (ideally 23 PEG units) is essential for minimizing non-specific interactions between streptavidin and KDM2A.[69] With this in mind, we synthesized the biotin-tagged indoline **224** (Scheme 4.2).

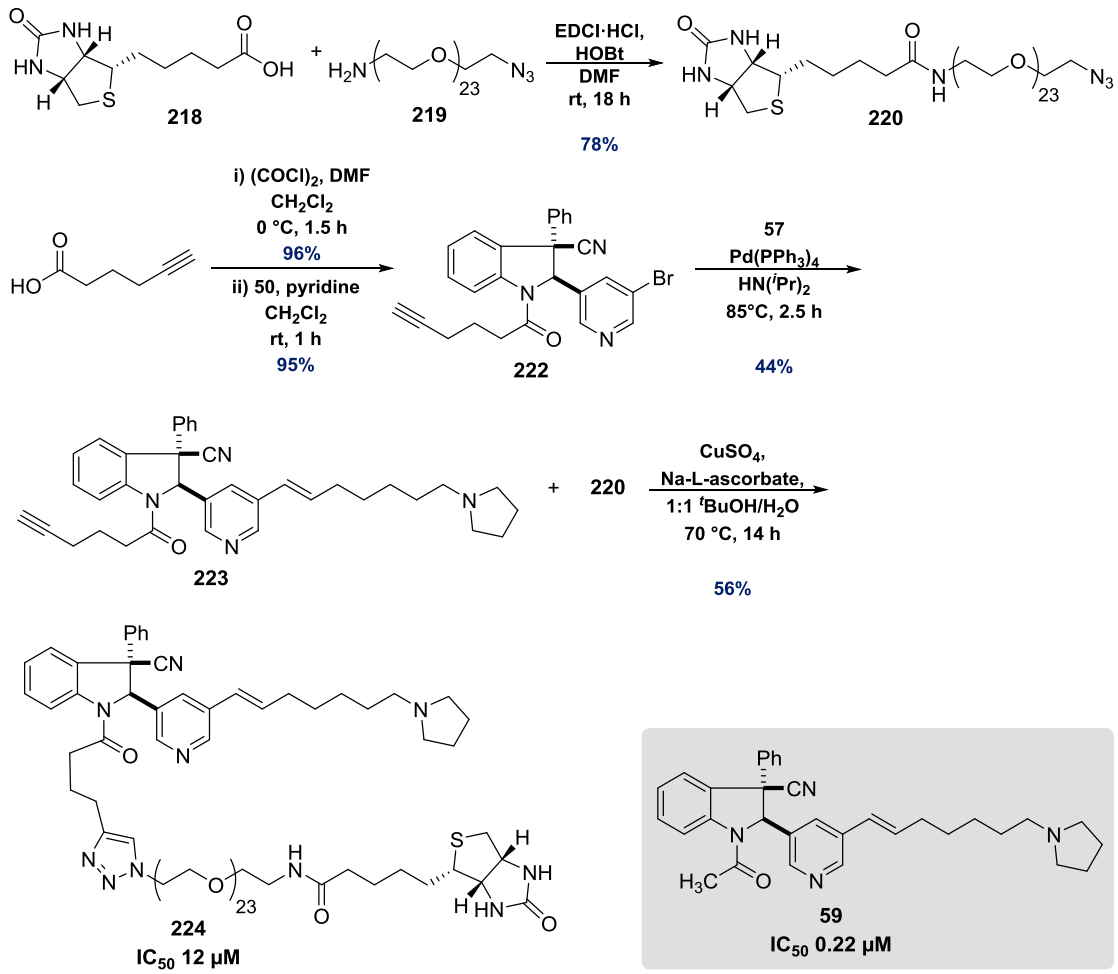

Scheme 4.2 – Synthesis of the biotinylated indoline **224** for BLI investigations.

A Cu-catalyzed click reaction was employed to connect the biotin tag **220** to the indoline inhibitor scaffold **223**. We reasoned that functionalization at the indoline *N*-acyl position would be most likely to afford a compound that largely retains inhibitory activity towards KDM2A (subsection 3.2.4). However, a substantial loss of potency relative to the acetylated analogue **59** was observed (12 µM vs. 0.22 µM), and we considered that the residual, weak inhibitory activity of **224** could be primarily a consequence of non-specific interactions between the long PEG chain and KDM2A. This was supported by the observation that, while **224** bound effectively to the streptavidin-coated biosensor tips (Figure 4.8-A), there was no significant difference between binding of immobilized **224** to KDM2A and binding of the PEG-biotin control to KDM2A (Figure 4.8-B). An alternative

experimental approach was therefore required to confirm and measure the strength of inhibitor-KDM2A association.

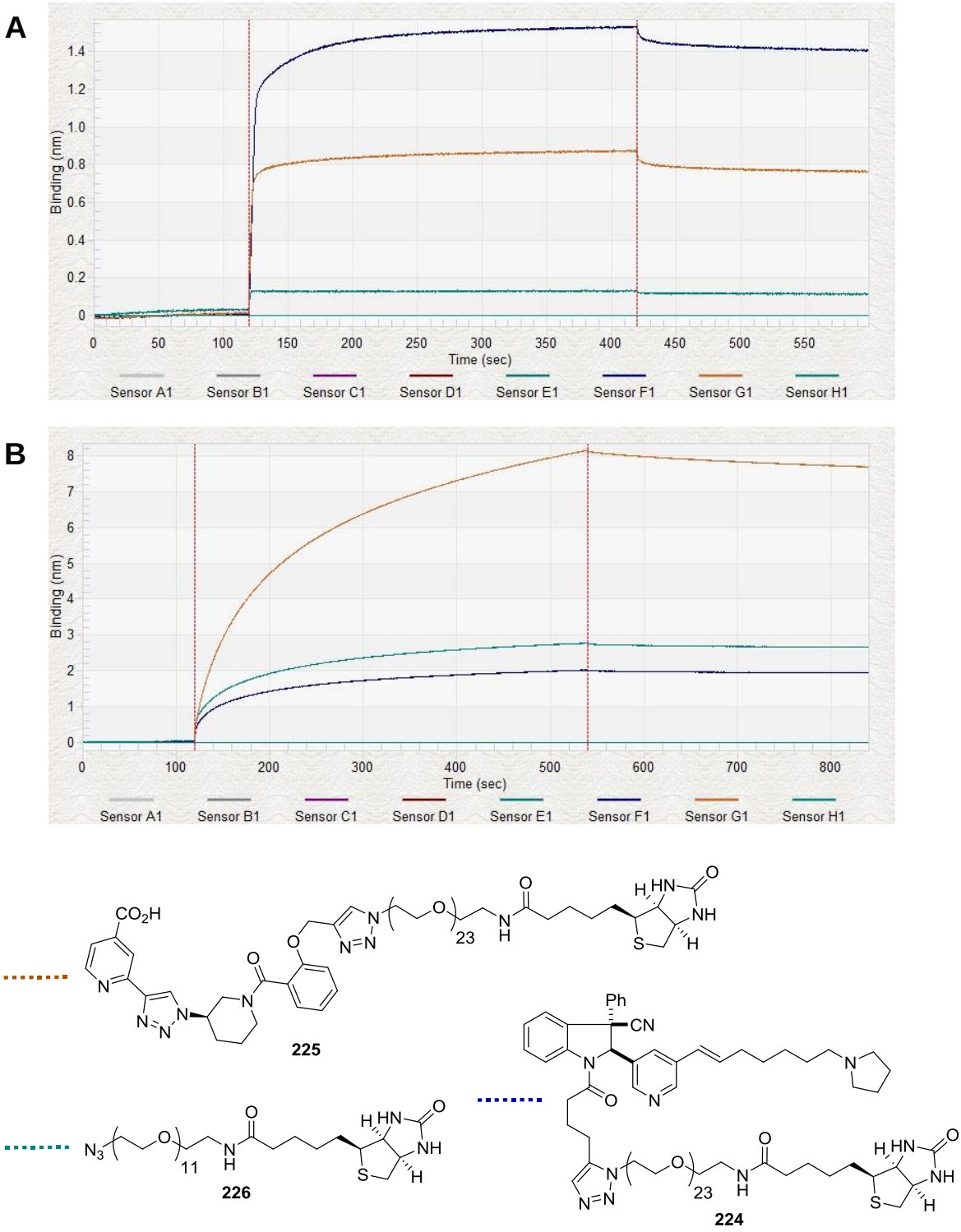

Figure 4.8 – BLI binding curves: A) Immobilization of biotinylated compounds on streptavidin-coated biosensor tips. B) Association with KDM2A. **225** and **226** were used as positive and negative controls respectively.

4.2.2 Native Mass Spectrometry[*]

Native (i.e. non-denaturing) mass spectrometry has become an increasingly important method for studying biomolecular interactions,[139] and we therefore envisaged its application to studying the association of **(*S*,*S*)-108** and KDM2A. Encouragingly, we observed a clear complex of the enzyme and **(*S*,*S*)-108**, corresponding to a 1:1 binding stoichiometry (Figure 4.9). However, the strength of this interaction was insufficient to accurately determine the corresponding dissociation constant (K_D) using this method. It is possible that the 2-OG cofactor and/or peptide substrate (which had been omitted for this experiment) are required for stronger association, and studies exploring the potential cooperativity of these binding interactions by native MS are underway.

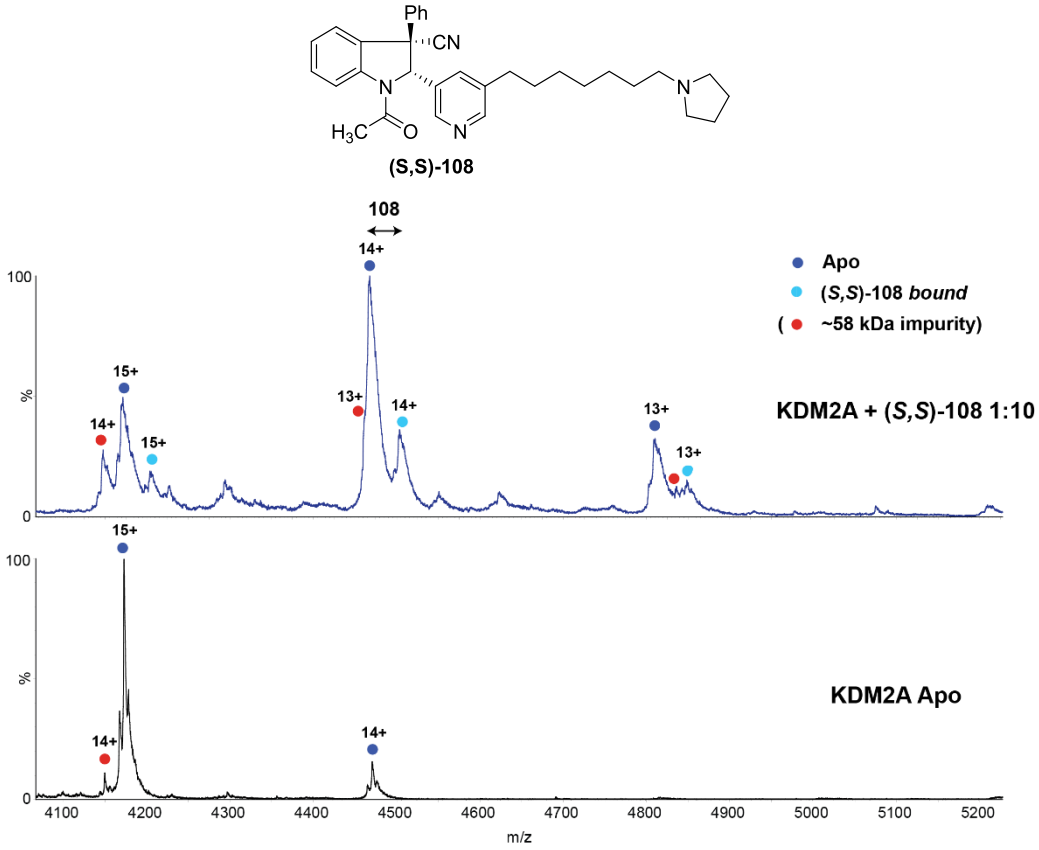

Figure 4.9 – Native MS spectra of apo-KDM2A (bottom) and a 1:10 mixture of KDM2A and **(*S*,*S*)-108**. The +13, +14, and +15 charge states are depicted.

[*] This work was carried out by Shane Chandler, under the supervision of Prof Justin Benesch, CRL.

4.3 Covalent Labelling of KDM2A

4.3.1 Synthesis of a Photoaffinity Inhibitor

Due to the difficulty of obtaining an X-ray co-crystal structure of our lead compound bound to KDM2A, an alternative approach was required to identify the inhibitor binding site. The use of photoaffinity probes in combination with modern experimental techniques in proteomics to characterize protein-ligand interactions forms the basis of a continually-growing area of research.[140-142] Within the field of KDMs, C. Schofield and co-workers recently demonstrated the application of the 4-component Ugi reaction[143] to the synthesis of a series of photoaffinity probes based on the 2-OG deoxygenase inhibitor IOX1.[144] We therefore sought to synthesize a photoreactive indoline inhibitor of KDM2A to study the inhibitor-enzyme binding interaction.

A variety of photoreactive functional groups have been employed in the development of photoaffinity probes, including aryl azides, benzophenones, and diazirines. We anticipated that installing an aliphatic diazirine motif through *N*-acylation of the indoline core would be most likely to afford an inhibitor that is both potent and as structurally similar as possible to previously synthesized lead compounds. An examination of the recent literature in this area revealed that aliphatic diazirines have been used successfully in a number of photo-crosslinking studies. For example, Krom and Meijler incorporated an aliphatic diazirine into the alkyl chain of the fatty acid-derived signaling molecule 3-oxo-C_{12}-HSL and demonstrated selective covalent labelling of the bacterial transcriptional activator LasR.[145] Similarly, J. W. Keillor and co-workers synthesized a diazirine-containing cinnamic acid derivative, which helped reveal conformational changes of the pig liver transglutaminase binding site upon ligand association.[146]

Scheme 4.3 illustrates the synthesis of the racemic diazirine-containing KDM2A inhibitor **230**. The preparation of diazirine **228** from levulinic acid has been described J. C. Jewett and co-workers.[147] We subsequently converted this intermediate to the corresponding acyl chloride, which was used to effect *N*-acylation of indoline **50**. Stille-Migita cross-coupling of the diazirine-containing product **229** with vinylstannane **57** under slightly milder reaction conditions than previously employed (60 °C vs. 85 °C) afforded the target photoreactive indoline **230** in moderate yield.

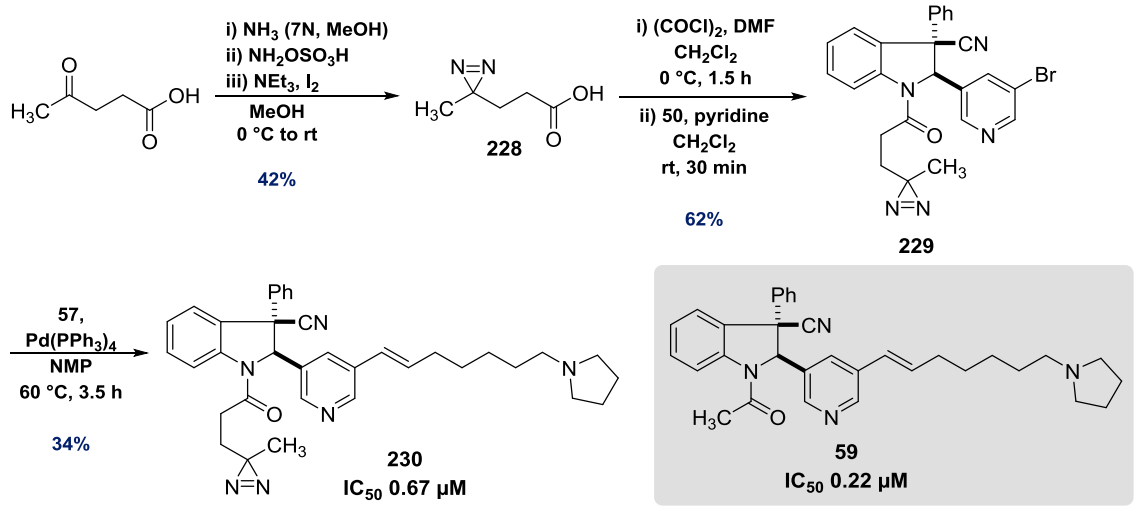

Scheme 4.3 – Synthesis of the photoreactive KDM2A inhibitor **230**.

Encouragingly, **230** was found to be a reasonable potent inhibitor of KDM2A, and we therefore proceeded with our envisaged photo-crosslinking trials. To ensure homogenous and reproducible sample irradiation and minimize the impact of radiation-induced protein denaturation, solutions of KDM2A and **230** were maintained at 4 °C and exposed to light at a wavelength of 350 nm using a CaproBox (Caprotec, Berlin). Furthermore, we included an excess of $NiCl_2$ in the photo-crosslinking solution, guided by the observation of X. Wang and co-workers that KDM2A is stabilized towards aggregation by Ni^{II}.[67] Finally, we ensured that KDM2A and **230** were incubated at 4 °C for 45 min prior

to irradiation to guarantee that a thermodynamic equilibrium of protein-ligand association would be reached before covalent labelling.

Photo-crosslinking of KDM2A and **230** was monitored using a Q-TOF mass spectrometer. Excitingly, the formation of the covalently-modified protein was found to progress as expected with increasing duration of sample irradiation, and after an irradiation time of 15 min, the proportion of labelled protein appeared to reach a maximum value of approximately 18%. A small amount of doubly-labelled KDM2A was also detected after longer irradiation times (Figure 4.10).

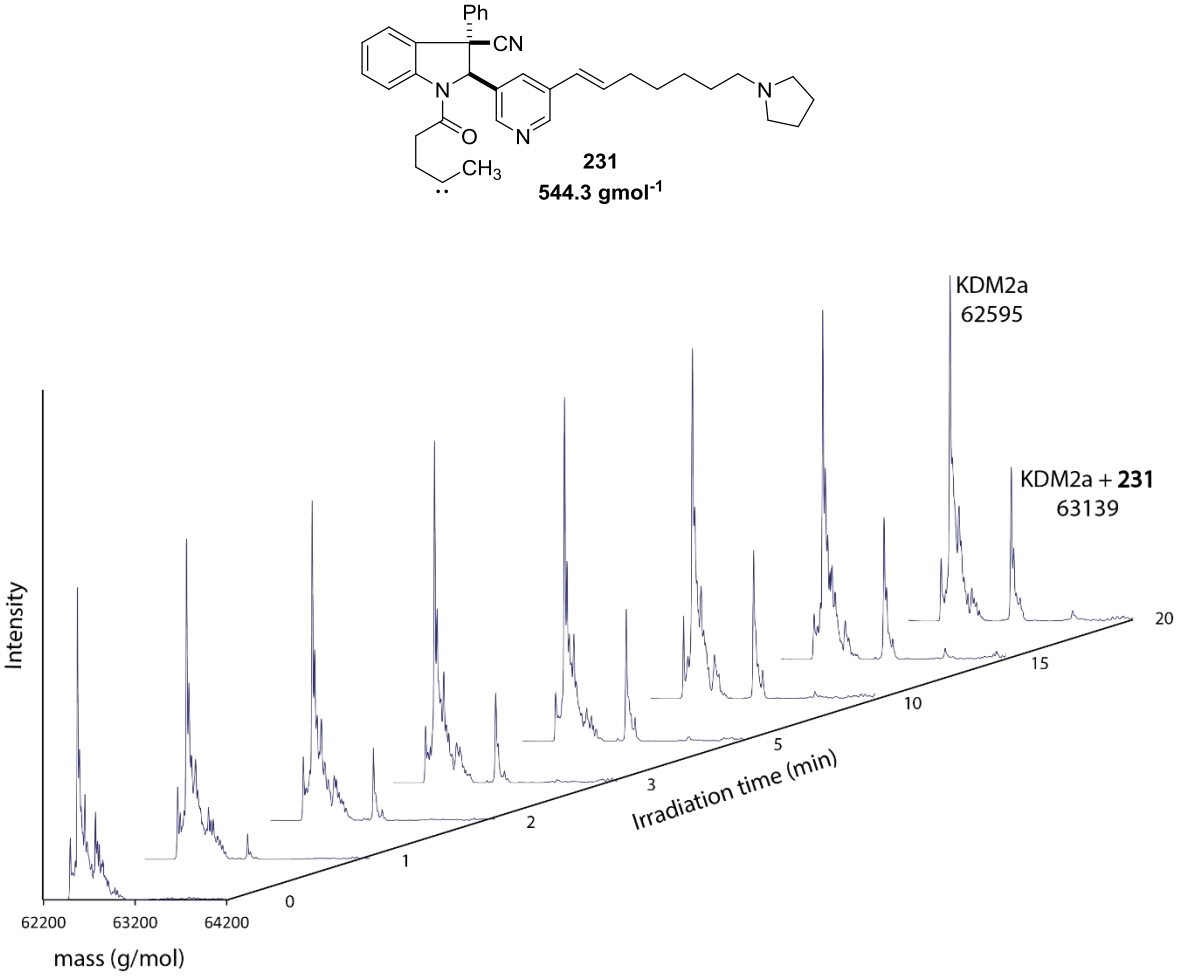

Figure 4.10 – Progress of KDM2A photo-crosslinking as a function of irradiation time – KDM2A (1 µM), **230** (4 µM), 2-OG (10 µM), and $NiCl_2$ (50 µM) in MES buffer (pH 7.0).

4.3.2 Synthesis of a Bifunctional Photoaffinity Probe Candidate

Photoaffinity probes frequently contain functional motifs such as biotin tags or fluorescent markers, which make them useful tools for studying their protein targets in a cellular context. In particular, such functionalized photoaffinity probes may be used to validate target engagement and explore off-target activity. We therefore decided to synthesize a modified photoaffinity probe for KDM2A, containing a terminal alkyne "handle", which would be poised to react *via* a Cu-catalyzed click reaction with the azide group of modified biotin after photo-crosslinking. In theory, cellular pulldown studies could subsequently be used to confirm binding to KDM2A within cells, thus complementing our previously-described approach based on transcriptomics (subsection 3.1.2).

Scheme 4.4 illustrates an efficient, two-step synthesis of the bifunctional diazirine **233**. Terminal alkyne **232** could be synthesized in moderate yield from 2,3-dihydrofuran, employing synthetic methodology previously discovered within the group of D. M. Hodgson.[148] To obtain the desired diazirine product, use of neat, condensed NH_3 instead of a concentrated NH_3/MeOH solution was found to be essential.

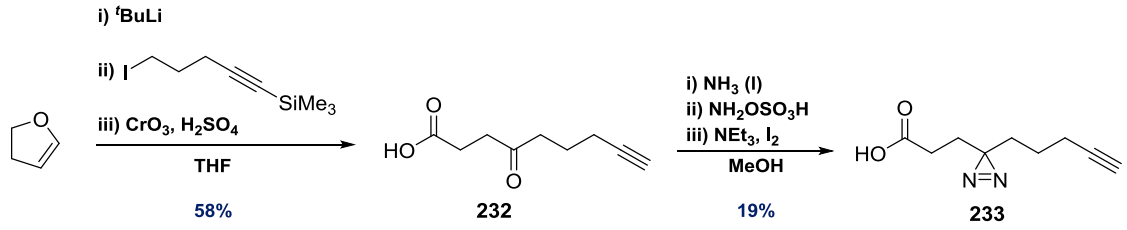

Scheme 4.4 – Synthesis of bifunctional diazirine **233**.

Unfortunately, all attempts to acylate indoline **50** using **233** *via* direct amide coupling proved unsuccessful. We postulate that this is a consequence of the relatively low reactivity of the indoline nitrogen. In addition, we were unable to convert **233** into the corresponding acyl chloride **235**, which appeared to be unstable, even at low temperatures (Scheme 4.5).

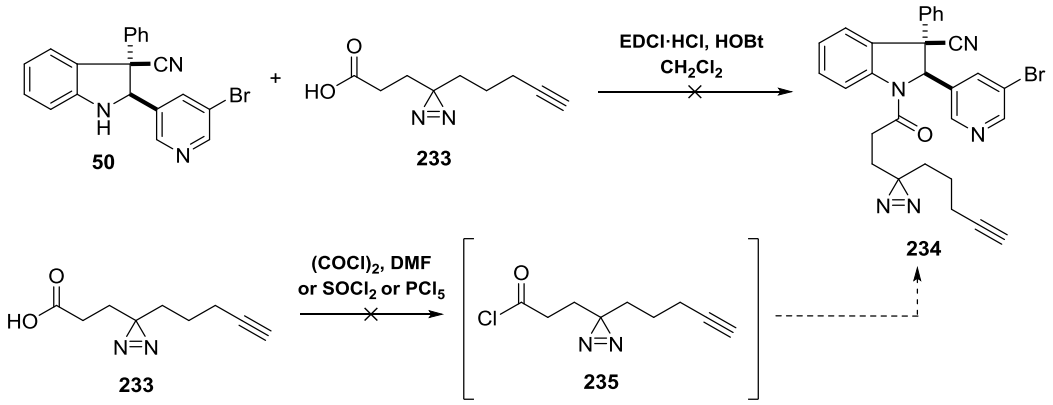

Scheme 4.5 – Unsuccessful direct coupling of diazirine **233** to the indoline core.

We reasoned that direct coupling of **233** to a primary amino group appended to the indoline core would potentially offer a solution to this problem. To investigate this hypothesis, we synthesized indoline **239** *via* acylation of **50** with phthalimide **236**, followed by Stille-Migita cross-coupling and amine deprotection using N_2H_4. Encouragingly, the additional methylene unit between the terminal amino group and the amide carbonyl bond in **239** appeared to confer stability towards hydrolysis. We therefore anticipate that indoline **239** (*c*log*P* = 4.09) might prove to be a suitable alternative to the previously-discussed hydrolytically-labile inhibitor **213** (subsection 3.2.4). Finally, amide coupling of **239** with diazirine **233** afforded the desired bifunctional photoreactive indoline **240** in good yield (Scheme 4.6).

Encouragingly, **240** was found to undergo efficient photo-crosslinking with KDM2A, although a small amount of double-labelling was also observed (Figure 4.11). Before proceeding with any cellular pulldown studies using **240**, we turned our attention to identifying the inhibitor binding site. This would involve degradation of the covalently-modified protein into a series of peptide fragments, followed by peptide sequencing using state-of-the art LC-MS/MS analysis.

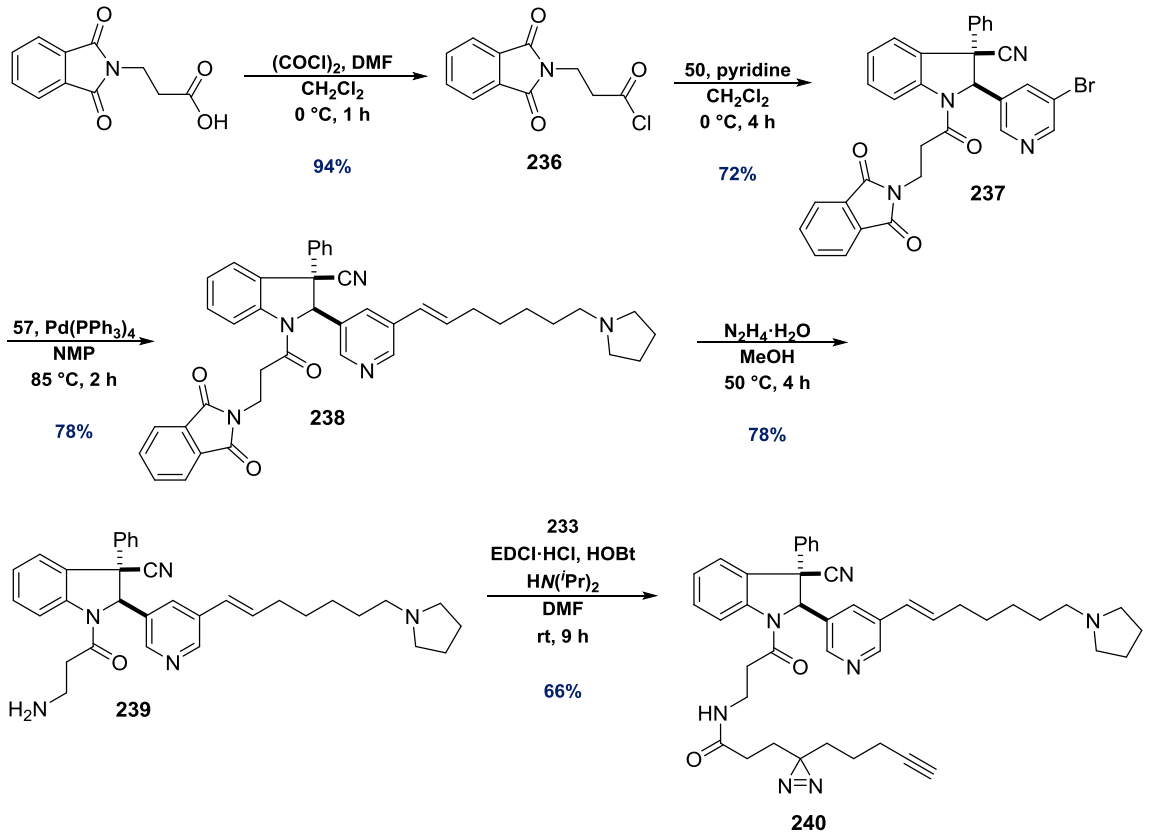

Scheme 4.6 – Synthesis of **240**, a potential photoaffinity probe for cellular target engagement studies.

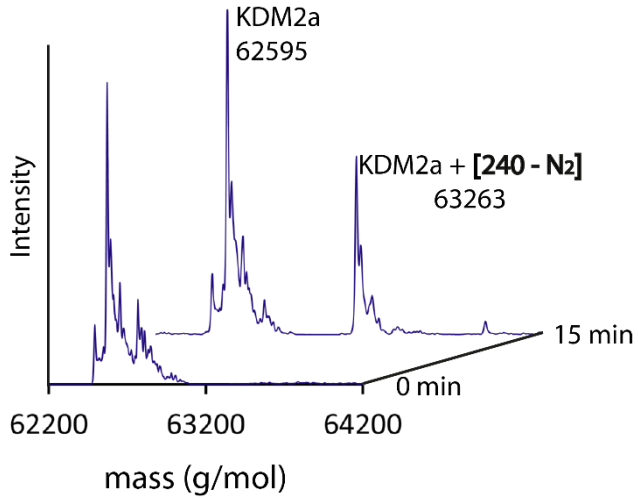

Figure 4.11 – Photo-crosslinking of **240** and KDM2A – KDM2A (1 µM), **240** (4 µM), $NiCl_2$ (50 µM), and 2-OG (10 µM) in MES buffer (pH 7.0).

4.3.3 KDM2A digest and MS/MS

To obtain a solution of peptide fragments, which would be amenable to sequencing by LC-MS/MS, a sample containing a mixture of **230**-labelled and unlabelled KDM2A was first subjected to an elastase digest. Elastase is a serine protease, and the isoform that was employed for our analysis (elastase II) is selective for peptide bonds with hydrophobic sidechains in the P1 position (*N*-terminal side of amide).[149] We anticipated that the use of a protease with such broad substrate selectivity would lead to a series of overlapping KDM2A peptide fragments and therefore provide a clear indication of the principle binding site of **230**.

Following chromatographic separation of the peptide fragments, the identity and position of covalently-modified amino acid residues was determined by MS/MS fragmentation analysis.* In total, 29 amino acids were identified as being susceptible to photo-crosslinking. An examination of the distribution of photo-crosslinked residues revealed that the highest proportion of labelled peptides corresponded to the protein's *N*-terminal region, and residues located within the sequence $_{21}$RYEDDGISDDEIEGKRTFDL$_{40}$ were by far the most susceptible to photo-crosslinking – 52% of all labelled peptides contained residues in this region. The next highest frequency region ($_{121}$MTMAQWTRYYETPEEEREKL$_{140}$) encompassed residues present in 12% of all labelled peptides. The distribution of labelled peptides across the protein sequence is illustrated in Figure 4.12, and Figure 4.13 shows a typical peptide fragmentation spectrum used to identify the locations of modified residues.

* Data was collected and processed by Dr Rebecca Konietzy in the research group of Prof. Benedikt Kessler, TDI. An illustration of the entire KDM2A sequence labelling distribution is shown in subsection 8.3.2 of the appendix.

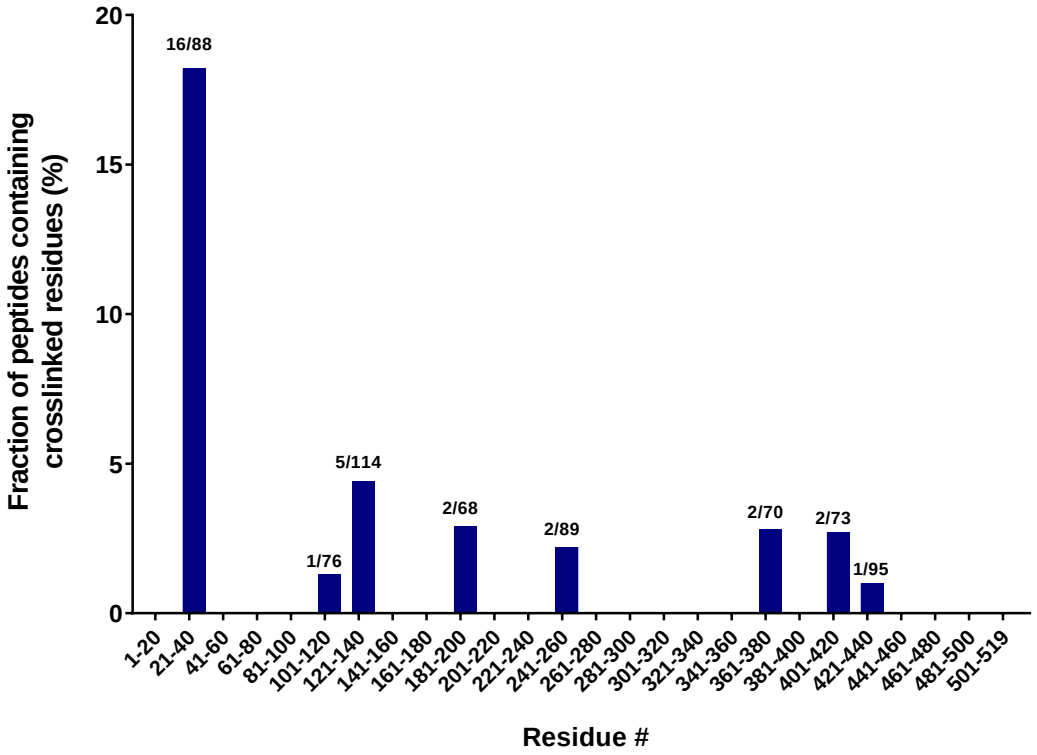

Figure 4.12 – Distribution of labelled peptides, showing apparent preference for photo-crosslinking of residues near the protein *N*-terminus. Observed ratios of labelled to unlabelled peptides are displayed above each bar.

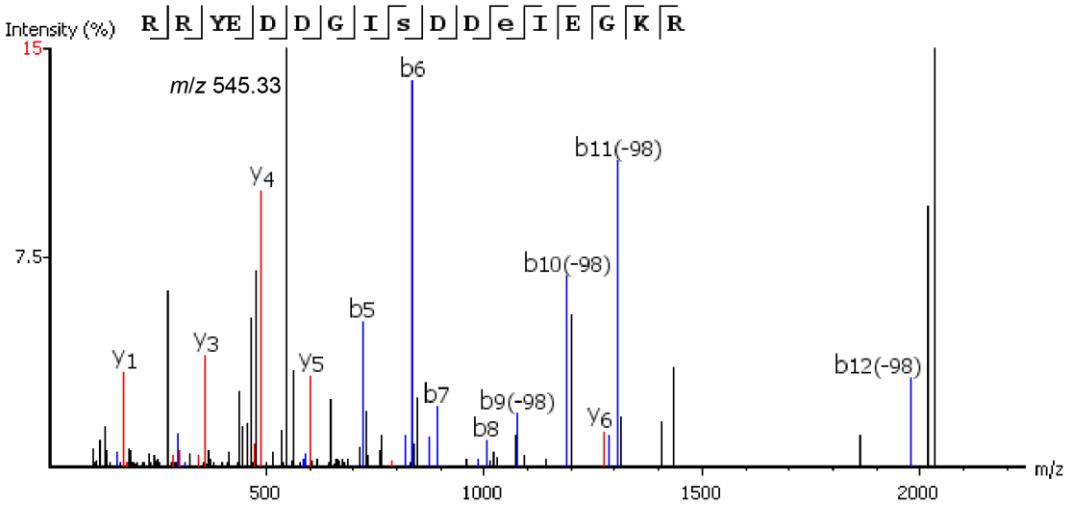

Figure 4.13 – *MS*/*MS* fragmentation pattern, showing labelling of residue E_{31}. An intense peak corresponding to fragmentation of the bond formed by photo-crosslinking of **230** and KDM2A is also present (*m*/*z* = 545.33).

While the results appear to imply that the photoaffinity inhibitor **230** binds KDM2A at a site near the enzyme's *N*-terminus, they also highlight a substantial degree of apparently random, non-specific labelling. In particular, we noted that the majority of covalently-modified residues are acidic (65% of labelled residues are either Asp or Glu), although some regions with high densities of acidic residues but no labelling were also observed. A possible explanation for the apparently preferred photo-crosslinking of acidic residues may be related to the unique photochemistry of aliphatic diazirines.

It has been shown both theoretically and experimentally that diazirines isomerize to diazo-compounds upon irradiation with UV-light (Scheme 4.7).[150] Diazo-compounds can fragment to release N_2 and a highly reactive and short-lived singlet carbene species, which is expected to react instantaneously with residues in the protein binding site or with the solvent (carbene lifetime: 10^{-10} - 10^{-9} sec).[151] Alternatively, diazo-compounds can undergo protonation to form diazonium ions, which may be sufficiently long-lived to dissociate from the binding site and react relatively non-selectively with particularly nucleophilic and/or negatively-charged sidechains (diazonium lifetime: approx. 10^{-1} sec).[152] Indeed, J. B. Cohen and co-workers attributed the labelling of principally Asp, Glu, and Tyr residues on the nicotinic acetylcholine receptor by a diazirine-containing etomidate derivative to the generation of a relatively long-lived electrophilic species such as a diazonium ion or stabilized carbocation.[153] Moreover, the chemoselective alkylation of protein carboxyl groups by diazo compounds has been demonstrated by R. T. Raines.[154]

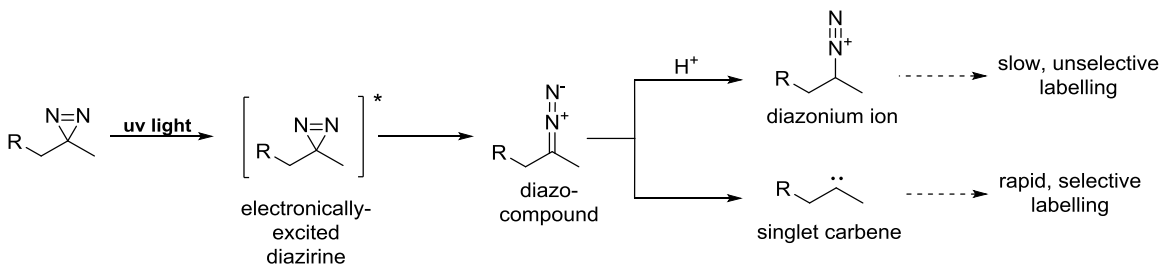

Scheme 4.7 – Photolysis of diazirines *via* diazo-intermediate.

To estimate the relative magnitudes of selective and unselective covalent labelling of KDM2A by **230**, an excess of the non-photoreactive inhibitor **108** (IC_{50} 0.25 μM) was added to the photo-crosslinking solution (Figure 4.14). **230** and **108** are predicted to compete for binding to the enzyme; however, only a minor reduction in the photolabelling efficiency was observed as a result of addition of **108** (9% vs. 12%). This suggests that the perceived distribution of covalently modified residues largely reflects non-selective reactions involving a positively-charged, long-lived electrophilic species derived from diazirine **230** and either negatively-charged or nucleophilic side chains of KDM2A.

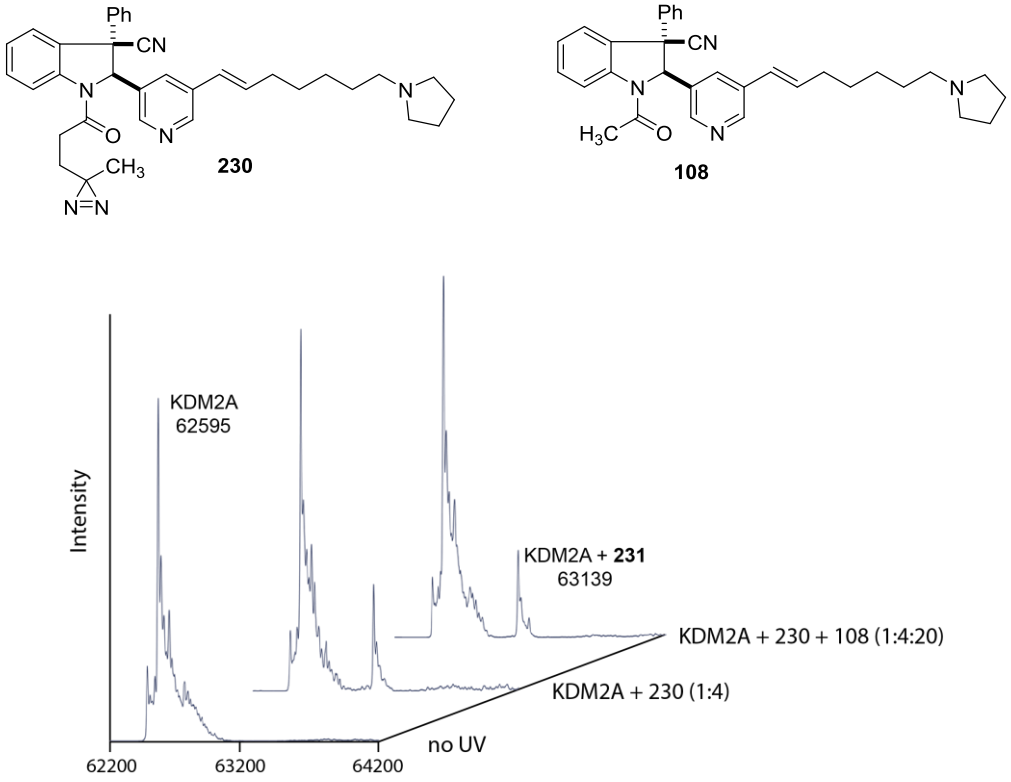

Figure 4.14 – Photocrosslinking competition involving **230** and **108** – KDM2A (1 μM), **230** (4 μM), $NiCl_2$ (50 μM), and 2-OG (10 μM) and **108** (20 μM) in MES buffer (pH 7.0) and was irradiated at 350 nm for 12 min.

We postulate that it may be possible to distinguish between selective and non-selective covalent modifications of KDM2A by monitoring changes in the distribution of photo-crosslinked residues as a function of irradiation time or due to the presence of a

competitive binder such as **108**. However, a different photoreactive functional group is ultimately required to provide a clear indication of the location of the inhibitor binding site. F.M. Richards first reported the use of 3-trifluoromethyl-3-aryldiazirine (TFMD) as a photoreactive group in photo-crosslinking studies.[155] It is reasoned that the diazo-compound derived from this functionality is less readily protonated to afford a long-lived diazonium species and is therefore more likely to bring about selective labelling of binding site residues.[140] We therefore propose that the trifluoromethyl-diazirine **242** might be a more suitable photoaffinity probe for future work on this project (Figure 4.15). To complement these studies, H-D exchange MS could also be used to reveal conformational changes upon inhibitor binding to KDM2A and thus hopefully provide a clear picture of the dynamics of this interaction.

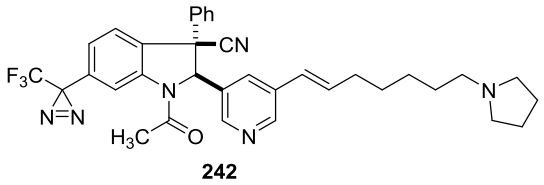

242

Figure 4.15 – Potential TFMD-based photoaffinity probe for more selective photo-crosslinking of KDM2A.

4.3.4 Project Conclusion and Prospects for Future Work

The aim of this project was to develop a chemical probe for the histone lysine demethylase KDM2A that would satisfy the SGC criteria regarding potency, selectivity, and cellular activity (Subsection 2.2.1). After identifying a promising hit in a screen of known binders to methyl-lysine reading domains and HMTs, we synthesized a library of chiral indoline-based KDM2A inhibitors and explored key SARs around this scaffold. Synthetic methodology relying on enantioselective phase-transfer catalysis was subsequently applied to the asymmetric synthesis of lead compounds, and we ultimately discovered a

novel inhibitor of KDM2A that displays very promising *in vitro* potency and selectivity towards this target (IC_{50} 0.16 µM, > 70-fold selectivity). A subsequent evaluation of the cellular compound activity focused on inhibition of H3K36me2 demethylation and made use of transcriptomics to explore the resulting impact on gene expression patterns. We attempted to address important limitations associated with compound cytotoxicity and promiscuity using a rational approach based on computational docking and an analysis of key physical properties. Finally, we investigated the mechanism of KDM2A inhibition using a variety of experimental techniques, including enzyme kinetics studies, native mass spectrometry, and photo-crosslinking with a photoreactive inhibitor. Although a number of questions regarding the nature of the protein-inhibitor interaction still remain unanswered, notably the actual strength of inhibitor-KDM2A association and the precise location of the inhibitor binding site, we identified potential strategies for resolving these issues.

To our knowledge, **(*S*,*S*)-108** is the first KDM2A-selective inhibitor to demonstrate a significant effect on cellular H3K36me2 levels at sub-micromolar doses (Subsection 3.1.1). However, its cytotoxicity and off-target activity at higher concentrations compromise its suitability as a chemical probe. As a potential strategy to overcome this problem, we identified the indoline *N*-acyl group as a promising handle for modulating compound lipophilicity. Polar follow-up candidates that are possibly more stable to hydrolytic decomposition than indoline **213** (*c*log*P* 4.64, IC_{50} 0.12 µM) are illustrated in Figure 4.15.

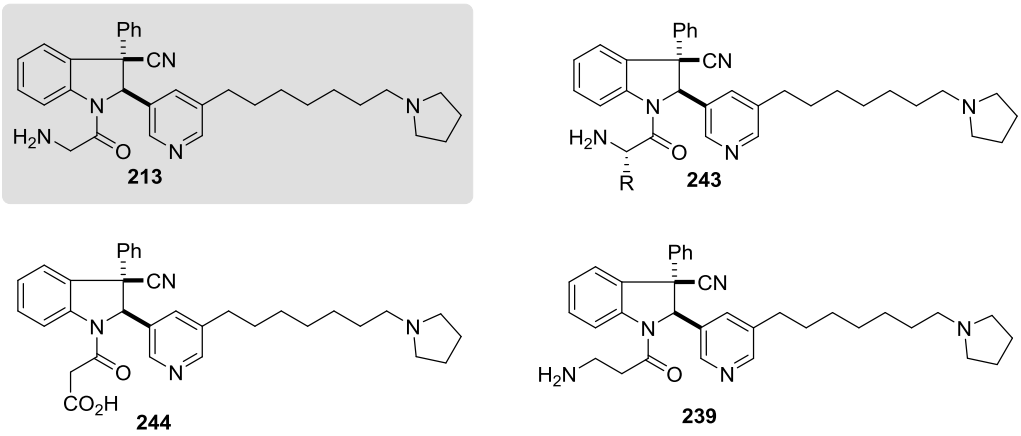

Figure 4.15 – Follow-up candidates to **213**: A series of α-amino acid derivatives (**243**) might be stabilized towards amide hydrolysis due to steric hindrance around the *N*-acyl bond. The α-carboxyacetyl indoline **244** is expected to exist as a zwitterion at neutral pH and may therefore retain membrane permeability. The β-aminoacetyl indoline **239** has already been synthesized as an intermediate towards diazirine **240** (Scheme 4.6).

The discovery of a completely novel class of selective KDM2A inhibitors that display an apparently unique inhibitory mechanism illustrates the successful application of asymmetric organocatalysis to an exciting area of research within chemical biology – epigenetics. In this project, the availability of robust, enantioselective synthetic methodology was essential for the efficient synthesis of optically-pure lead compounds. The next chapter of this thesis therefore focuses on the development of new chiral cation-directed reactions, which provide access to three-dimensional scaffolds that could potentially form the basis of future chemical probe discovery programs.

5. ENANTIOSELECTIVE SYNTHESIS OF POISED FRAGMENTS

5.1 Background

5.1.1 3-D Poised Fragments

Recent years have witnessed a growing interest in the development of asymmetric fragments for drug discovery. The creation of international collaborative projects such as the 3-D fragment consortium[156] and the European Lead Factory,[157] which aim to address the current need for small, chiral scaffolds, is testament to the importance of such compounds for the discovery of novel biologically-active molecules. We regard the development of new enantioselective synthetic methodology as a potentially valuable contribution to these efforts.

In the context of drug discovery, a *fragment* may be defined as a molecule with a molecular weight < 300 $gmol^{-1}$ and log*P* < 3.[158] An alternative characterization of overall fragment size based on the total number of "heavy" (*i.e.* non-hydrogen) atoms is also commonly adopted. In order for a molecule to qualify as a fragment according to this definition, the total number of atoms other than H ≤ 15.[159] The principle advantage of screening molecules of this size as opposed to larger, more drug-like compounds is the ability of fragment libraries to statistically cover a larger proportion of the available chemical space and thus give rise to higher hit-discovery rates.[160] Fragments that are found to interact independently with the desired biological target may subsequently be linked to

afford potent and selective lead compounds. One of the challenges associated with this approach is the requirement for sensitive biophysical techniques to measure the relatively weak affinities of proteins for fragment-sized molecules (μM to mM levels).[161]

The discovery of the anti-cancer drug Navitoclax by Abbott Laboratories provides an elegant example of the promise of fragments in chemical biology. As illustrated in Figure 5.1, two small molecules that were found to bind weakly to the surface of the anti-apoptotic transmembrane protein Bcl-X_L were connected and subsequently elaborated to afford a highly potent series of inhibitors of the Bcl proteins.[162]

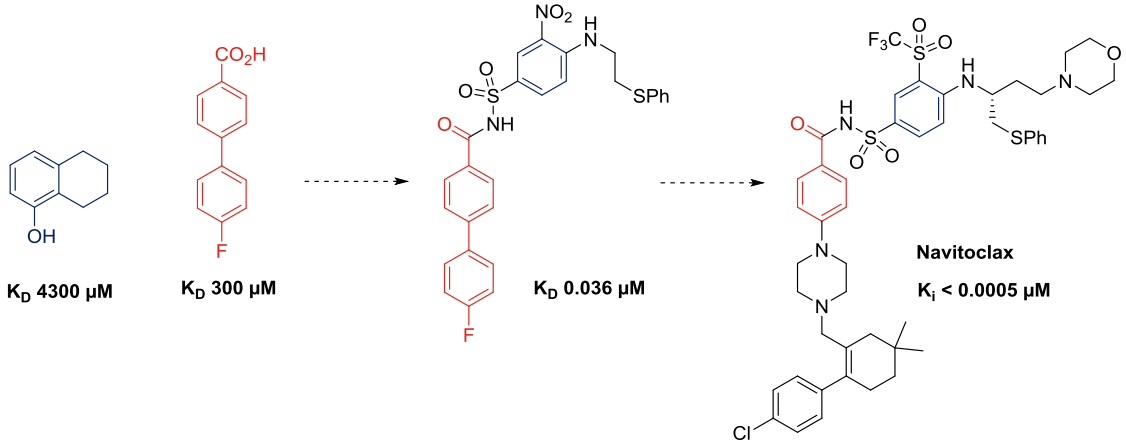

Figure 5.1 – Fragment-based discovery of the potent anti-cancer drug Navitoclax. K_D and K_i values indicate activity towards Bcl-X_L.

In order to realize the full potential of fragment-based drug discovery (FBDD), it is crucial that fragment libraries maximize their coverage of available chemical space. Consequently, a combination of both sp^2-rich ("flatland") and sp^3-rich (3-D) fragments is desirable. The generation of *chiral* fragments poses a particular challenge, as an effective control of their absolute stereochemistry is ultimately required for the development of enantiopure drug candidates. In addition, the ideal fragment contains multiple reactively-orthogonal functional groups that serve as "handles" for connection to other chemical entities.[163] With this in mind, we sought to expand the scope of cation-directed enantioselective *C*-acylation reactions recently developed within the Smith group to access

unique, enantioenriched 3-D fragments that would be "poised" to react *via* one or more reactive sites.

5.1.2 Enantioselective C-Acylation of Enolates

The principle challenge associated with enantioselective *C*-acylation of enolate anions is their ambident reactivity, which gives rise to mixtures of regioisomeric products resulting from acylation on either oxygen or carbon. In general, *O*-acylation is kinetically favored in both the gas phase and in solution.[164-166] To overcome this intrinsic preference, strategies have been developed based on the use of preformed enolate derivatives such as silyl ketene acetals by G. C. Fu,[167] A. D. Smith,[168] and E. N. Jacobsen[169] (Figure 5.2 – A-C). More recently, intermolecular enantioselective *C*-acylation of 3-substituted lactams has also been accomplished by B. M. Stoltz and co-workers *via* a Ni-catalyzed 3-component coupling reaction (Figure 5.2 – D).[170]

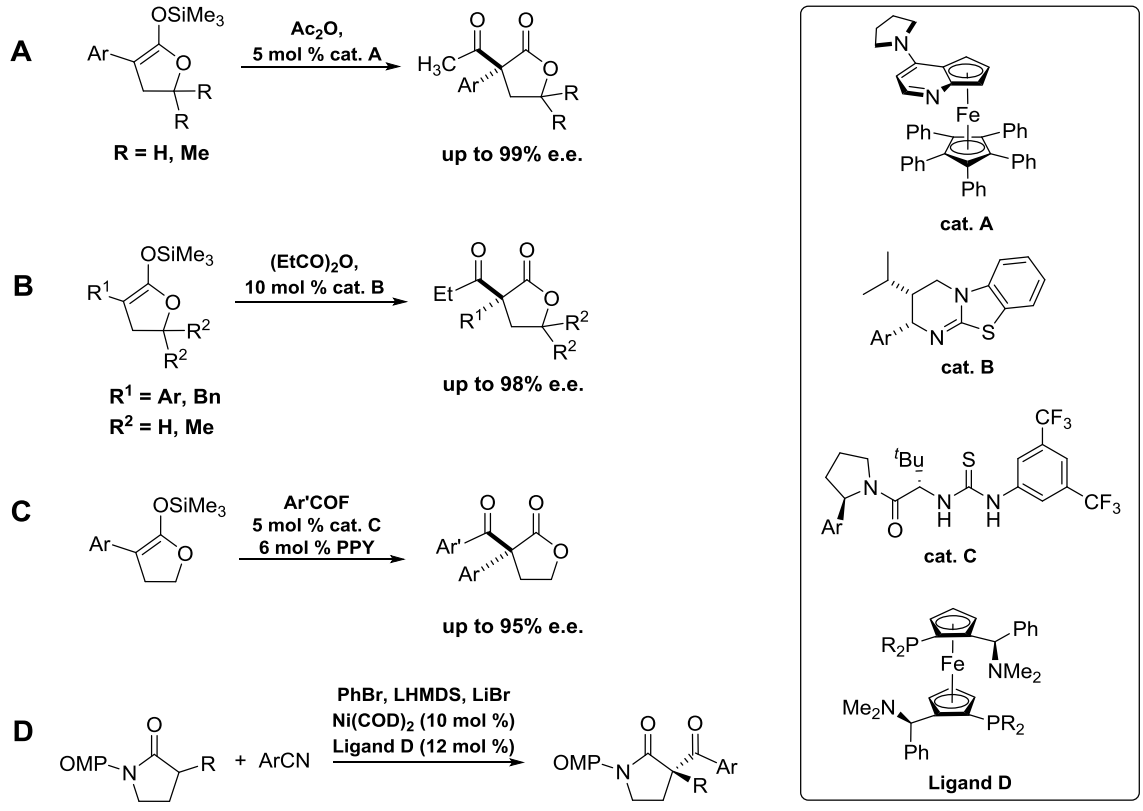

Figure 5.2 – Previous approaches to enantioselective *C*-acylation of enolate derivatives.

Within the Smith group, the enantioselective synthesis of a series of spirobiindanones was recently achieved using an organocatalytic approach (Figure 5.3 – A).[171] This reaction proceeds through chiral cation-directed *C*-acylation of the indanone substrate with an intramolecular ester. We anticipated that the principles of this approach could potentially be applied to the enantioselective synthesis of a unique poised spirolactam fragment (Figure 5.3 –B).

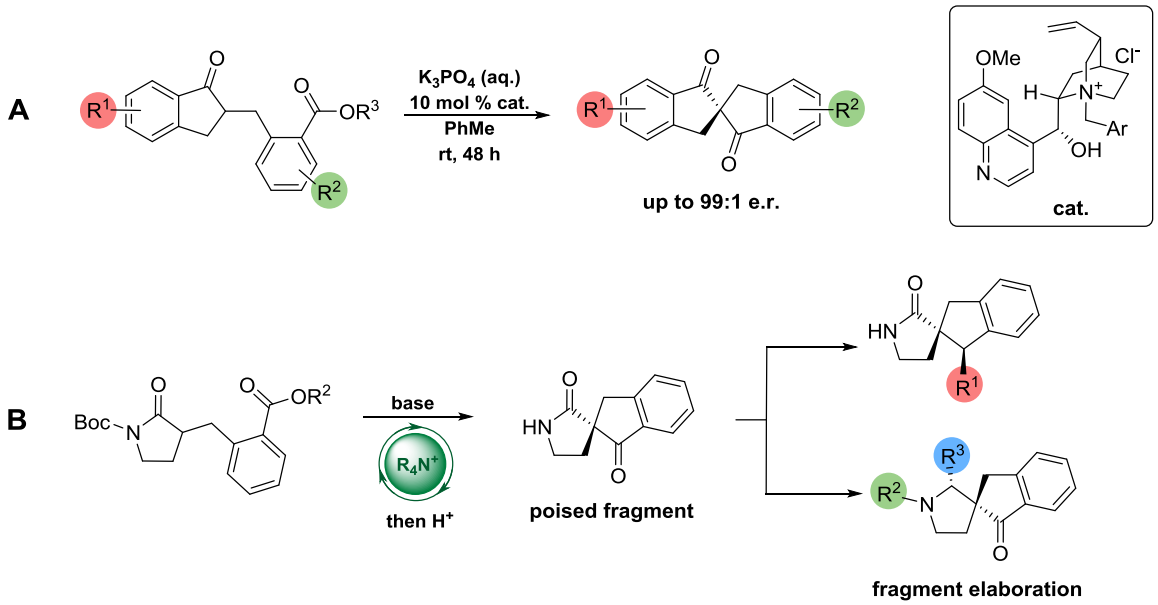

Figure 5.3 – A) Chiral cation-directed enantioselective synthesis of spirobiindanones. B) Proposed enantioselective synthesis of a poised spirolactam fragments and potential approaches to fragment elaboration.

5.2 Development of a Poised Spirolactam Fragment

5.2.1 Substrate Synthesis

The synthesis of phenyl 2-(bromomethyl)benzoate **247** is illustrated in Scheme 5.1. Phenyl ester **246** was easily prepared from commercially-available *o*-toluic acid, and subsequent radical bromination afforded benzyl bromide **247** in good yield. We envisaged

alkylating an *N*-protected pyrrolidinone with this compound to obtain a substrate for cyclization.

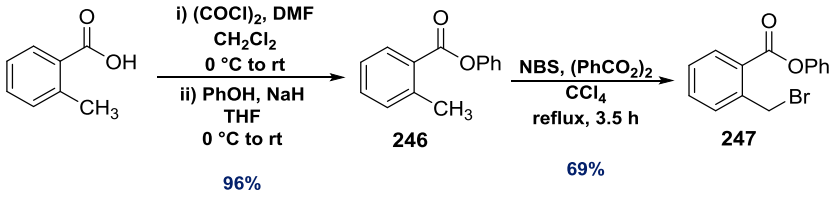

Scheme 5.1 – Synthesis of 2-(bromomethyl)benzoate **247** for alkylation of pyrrolidinone.

Initial attempts to alkylate *N*-benzylpyrrolidinone **248** with **247** proved unsuccessful, affording a complex mixture of products in addition to largely unreacted pyrrolidinone starting material (Scheme 5.2 – A). Deprotonation of **248** by lithium amide bases has been documented in the literature,[172] and we therefore postulate that the resulting lithium-enolate irreversibly deprotonates alkyl bromide **247** at the benzylic position rather than undergoing alkylation. By contrast, the less basic lithium enolate of *N*-Boc-pyrrolidinone **249** was found to react smoothly with **247**, affording the cyclization substrate **250** in moderate yield (Scheme 5.2 – B).

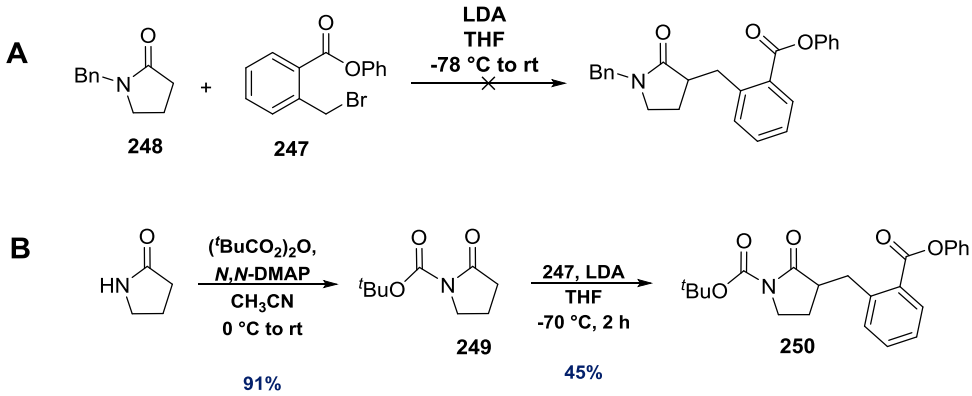

Scheme 5.2 – A) Attempted alkylation of *N*-benzylpyrrolidinone **248** with bromide **247**. B) Successful alkylation of *N*-Boc-pyrrolidinone **249** with benzyl bromide **247**.

250 was found to undergo cyclization to the desired spirolactam **251** in the presence of KO^{t}Bu or alternatively a combination of solid Cs_2CO_3 and TBAB (Scheme 5.3). However, under either set of reaction conditions, conversion of substrate to product appeared to

plateau at approximately 40%. To investigate whether this was a consequence of a retro-acylation process induced by the released phenoxide, we monitored a mixture of **251**, phenol, and KO^{t}Bu at rt. The reversibility of *C*-acylation was confirmed by the recovery of an approximately equimolar mixture of **250** and **251** after 48 h. We concluded that an alternative substrate would therefore be required to achieve a favorable cyclization yield and ultimately a high degree of enantiocontrol under asymmetric reaction conditions.

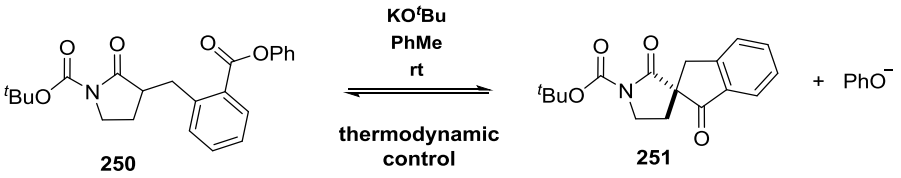

Scheme 5.3 – Cyclization of phenyl ester **250** afforded spirolactam **251**, but the phenoxide leaving group was found to induce retro-acylation.

Issues associated with the reactivity of phenoxide had also been encountered in the course of the development of methodology towards enantiomerically-enriched spirobiindanones. These problems were eventually overcome by replacing the substrate's phenyl ester with a pentafluorophenyl ester, which generates a less nucleophilic phenoxide byproduct. Thus, we focused on the synthesis of the pentafluorophenyl ester equivalent of **250**. Unfortunately, alkylation of *N*-Boc pyrrolidinone **249** by alkyl bromide **254** afforded a complex mixture of products (Scheme 5.4), possibly as a result of competitive deprotonation of **254** by the lithium enolate of **249** or competitive reactions involving the pentafluorophenyl ester.

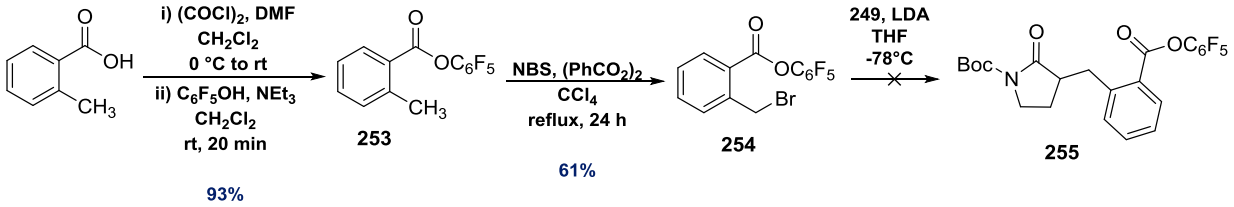

Scheme 5.4 – Attempted direct alkylation of *N*-Boc-pyrrolidine **249** by bromide **254**.

We therefore envisaged an alternative route to the desired pentafluorophenyl ester substrate *via* an ester coupling of the corresponding benzoic acid. Alkylation of **249** by methyl 2-(bromomethyl)benzoate **256** afforded pyrrolidinone **257** in good yield. However, attempted deprotection of the methyl ester by LiOH or KOTMS to access benzoic acid **258** resulted in preferential hydrolysis of the lactam (Scheme 5.5).

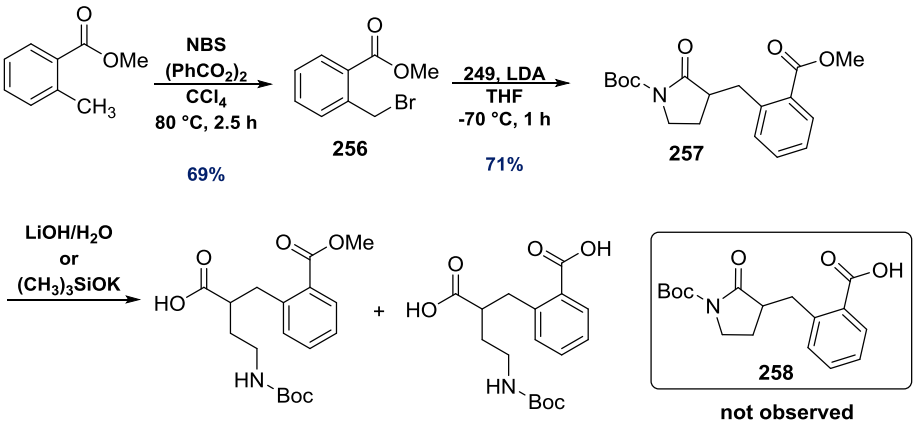

Scheme 5.5 – Synthesis of pyrrolidinone **257** and lack of chemoselectivity with respect to hydrolysis of its methyl ester.

Benzoic acid **258** was eventually synthesized by hydrogenolysis of the corresponding benzyl ester **261**. Subsequent carbodiimide coupling of the acid with pentafluorophenol afforded pyrrolidinone **255** in good yield (Scheme 5.6).

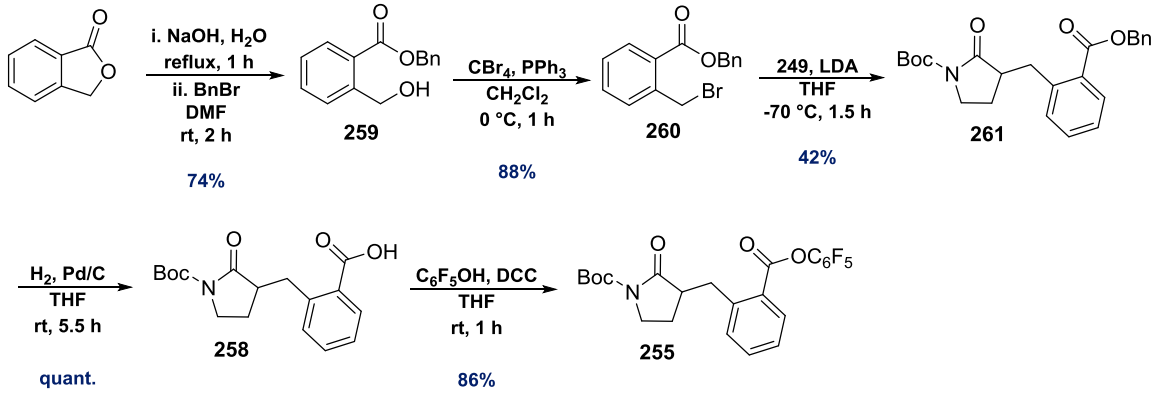

Scheme 5.6 – Synthesis of pentafluorophenyl ester cyclization substrate **255**.

5.2.2 Attempted Enantioselective cyclization

Encouragingly, pyrrolidinone **255** was found to undergo efficient cyclization to spirolactam **251** in the presence of KO^{t}Bu, although purification of the reaction product proved challenging due to its lack of stability towards silica gel column chromatography (Scheme 5.7).

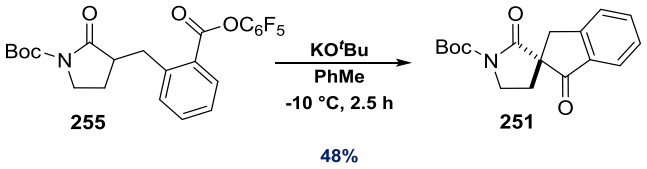

Scheme 5.7 – Racemic cyclization of pyrrolidinone **255** to spirolactam **251**.

We estimate the pKa of **255** to be close to the empirical upper limit for interfacial phase-transfer catalysis (approx. 23).[173] Nonetheless, we proceeded with a screen of asymmetric reaction conditions using *N*-benzyl quinidinium **A** as the catalyst (Table 5.1).

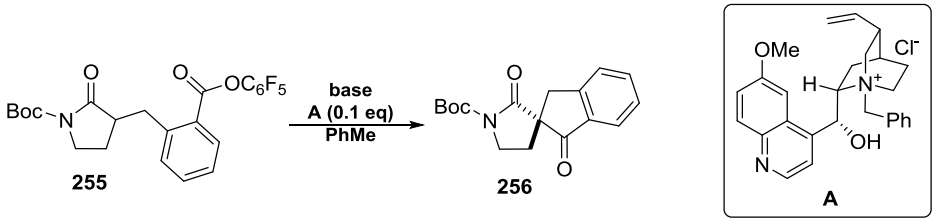

Base	Temp.	Duration	Outcome
K_2CO_3 (aq., 10 eq.)	rt	48 h	Recovered SM
Cs_2CO_3 (aq., 10 eq.)	rt	48 h	Recovered SM
K_3PO_4 (aq., 10 eq.)	rt	48 h	Recovered SM
KOH (aq., 10 eq.)	rt	10 h	Decomposition[i]
Cs_2CO_3 (s., 10 eq.)	rt	48 h	Trace product[i]
K_3PO_4 (s., 10 eq.)	rt	48 h	Trace product[i]
KOH (s. 10 eq.)	rt	48 h	5% (e.r. 47:53)[ii]
$CsOH{\cdot}H_2O$ (s., 10 eq.)	rt	6 h	Decomposition[i]
$CsOH{\cdot}H_2O$ (s., 2 eq.)	0 °C	10 h	Recovered SM
KOH (s. 4 eq.), [18]crown-6 (0.1 eq.)	rt	24 h	Trace product[i]
BTTP (3 eq.)	rt	48 h	12% (e.r. 50:50)[ii]

Table 5.1 – [i] As determined by TLC. [ii] As determined by analysis of the crude ^{1}H NMR spectrum.

Unfortunately, conversion levels were found to be exceptionally poor with all bases screened. Enantiomeric ratios could be measured after cyclization with $KOH_{(s)}$ and the phosphazene base BTTP,[174] but an essentially racemic mixture of products was obtained in both cases. Finally, attempts to augment the basicity of KOH and thereby enhance the reaction rate by addition of a crown ether[175] failed to improve results. We concluded that pyrrolidinone **255** is not sufficiently reactive under the conditions attainable under enantioselective phase transfer catalysis and that an alternative, more acidic cyclization substrate is required. We considered that cyclization of the corresponding oxindole would be instructive, despite the fact that the resulting spiro-oxindole product would no longer qualify as a true fragment.

5.3 Spiro-Oxindoles

5.3.1 Substrate Synthesis

Spiro-oxindoles feature in a broad range of natural products and biologically-active molecules, and a variety of synthetic strategies towards these privileged scaffolds have therefore been developed.[176, 177] However, to the best of our knowledge, enantioselective acylation at the oxindole *C*3 position has not been reported. A notable recent contribution to spiro-oxindole synthetic methodology is the discovery of a reaction involving the enantioselective C-H oxidation of an achiral spirocyclic substrate by a supramolecular ruthenium complex within the group of T. Bach (Scheme 5.8).[178] Unfortunately, racemization of the initial alcohol product of oxidation *via* a retro-aldol process leads to a trade-off between enantioselectivity and overall yield.

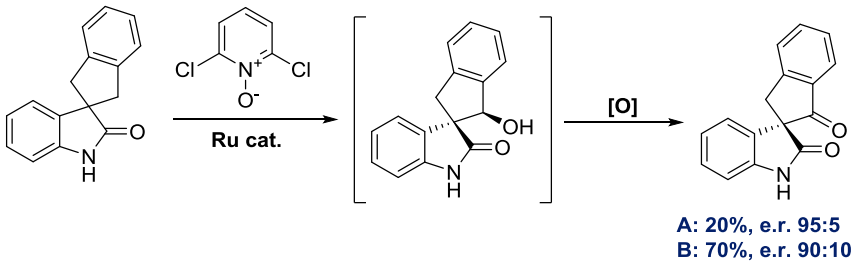

Scheme 5.8 – Enantioselective C-H oxidation to form spiro-oxindoles developed by T. Bach and co-workers.

Synthesis of the pentafluorophenyl ester cyclization substrate **263** is illustrated in Scheme 5.9. *N*-methyloxindole **258** was accessed *via* a Wolff-Kishner reduction[179] of *N*-methylisatin and subjected to a Knoevenagel condensation[180] with benzaldehyde **259** to afford oxindole **260** as a 1:3 mixture of *E*- and *Z*-olefins. Hydrogenation of this mixture with a palladium on carbon catalyst cleanly afforded benzoic acid **261**. The fact that lactone **262** was not observed suggests that reduction of the alkene function proceeds more rapidly than hydrogenolysis of the benzyl ester moiety. Finally, carbodiimide coupling of acid **261** with pentafluorophenol afforded **263** in good yield.

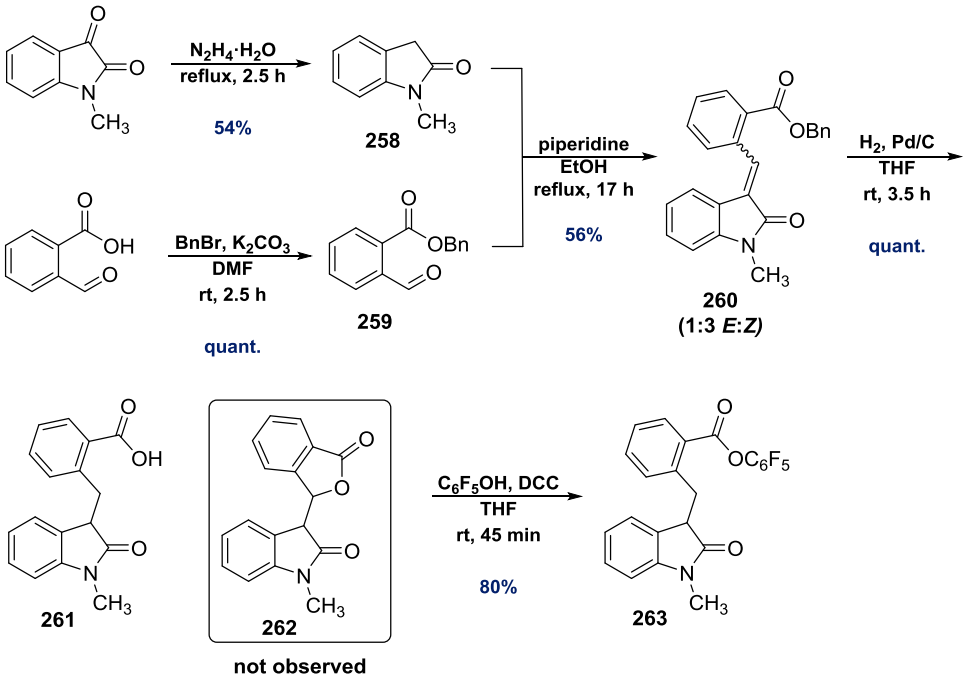

Scheme 5.9 – Synthesis of oxindole cyclization precursor **263**.

5.3.2 Enantioselective Cyclization

Oxindole **263** was found to cyclize cleanly to the desired racemic spiro-oxindole product **264** in the presence of aqueous K_2CO_3 and TBAB (Scheme 5.10). Encouraged by the markedly greater reactivity of this scaffold towards intramolecular *C*-acylation relative to the previous pyrrolidinone system, we envisaged a methodical screen of enantioselective reaction conditions. In order to expedite screening, reactions were performed on a relatively small scale (15 mg **263**), and only the enantioselectivity of each reaction was initially evaluated.

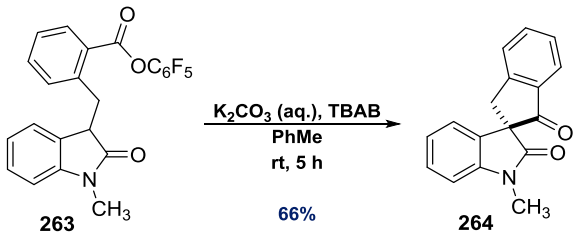

Scheme 5.10 – Racemic cyclization of oxindole **263** to spiro-oxindole **264**.

To begin, phase-transfer catalysts based on the four commercially-available *N*-benzyl cinchona alkaloid scaffolds were investigated together with a selection of aqueous bases. We hoped that this limited screen would provide an initial insight into the sensitivity of the reaction towards modifying these components. The cinchonidinium salt (**D**) performed marginally better than its stereoisomeric analogues (entries 1-4), giving rise to a very promising level of enantioenrichment (e.r. 75:25). The identity of the aqueous base was found to have only a minor effect on enantioselectivity (entries 5-10), suggesting that the base's metallic counterion is readily displaced from the deprotonated substrate by the ammonium species and likely does not feature in the cyclization transition state (Table 5.2).

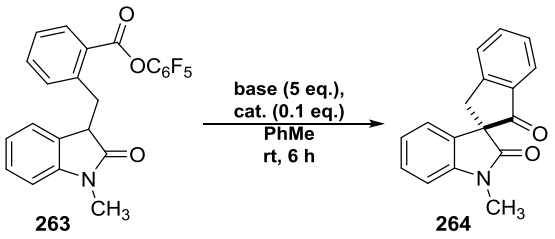

263 264

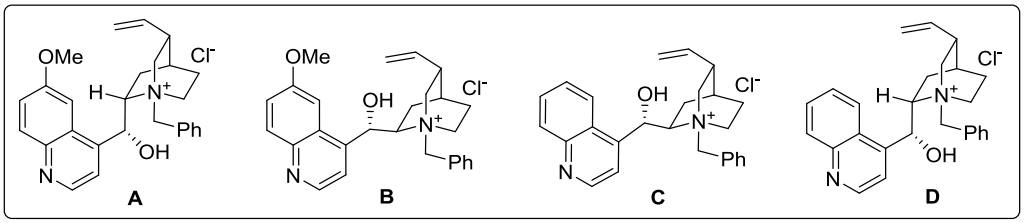

A B C D

Entry	Base	Catalyst	e.r.
1	**K_2CO_3 (50% aq.)**	**A**	72:28
2	**K_2CO_3 (50% aq.)**	**B**	27:73
3	**K_2CO_3 (50% aq.)**	**C**	70:30
4	**K_2CO_3 (50% aq.)**	**D**	25:75
5	**$KHCO_3$ (25% aq.)**	**D**	26:74
6	**K_3PO_4 (50% aq.)**	**D**	25:75
7	**KOH (50% aq.)**	**D**	29:71
8	**CsOH (50% aq.)**	**D**	27:73
9	**Cs_2CO_3 (50% aq.)**	**D**	26:74
10	**Na_2CO_3 (50% aq.)**	**D**	25:75

Table 5.2 – Primary screen of main cinchona alkaloid scaffolds and aqueous bases.

Next, we conducted an extensive screen of chiral phase-transfer catalysts (Figure 5.4). The presence of a free hydroxyl group at the *C*9 position of the cinchona catalyst scaffold was found to be essential for attaining high levels of enantioenrichment (**D** vs. **E**, **K** vs. **O**), implying a possible substrate-catalyst H-bonding interaction. In addition, polyaromatic substituents such as naphthyl and anthracenyl ring systems were found to enhance enantioselectivity (**J** – **M**). The most favorable result was ultimately achieved with quininium-based catalyst **N**, which gave rise to a 92:8 mixture of enantiomers. Alternative catalysts based on dual quaternary- ammonium/H-bonding functionality (**Q**) or a chiral biaryl scaffold (**R**) did not perform well.

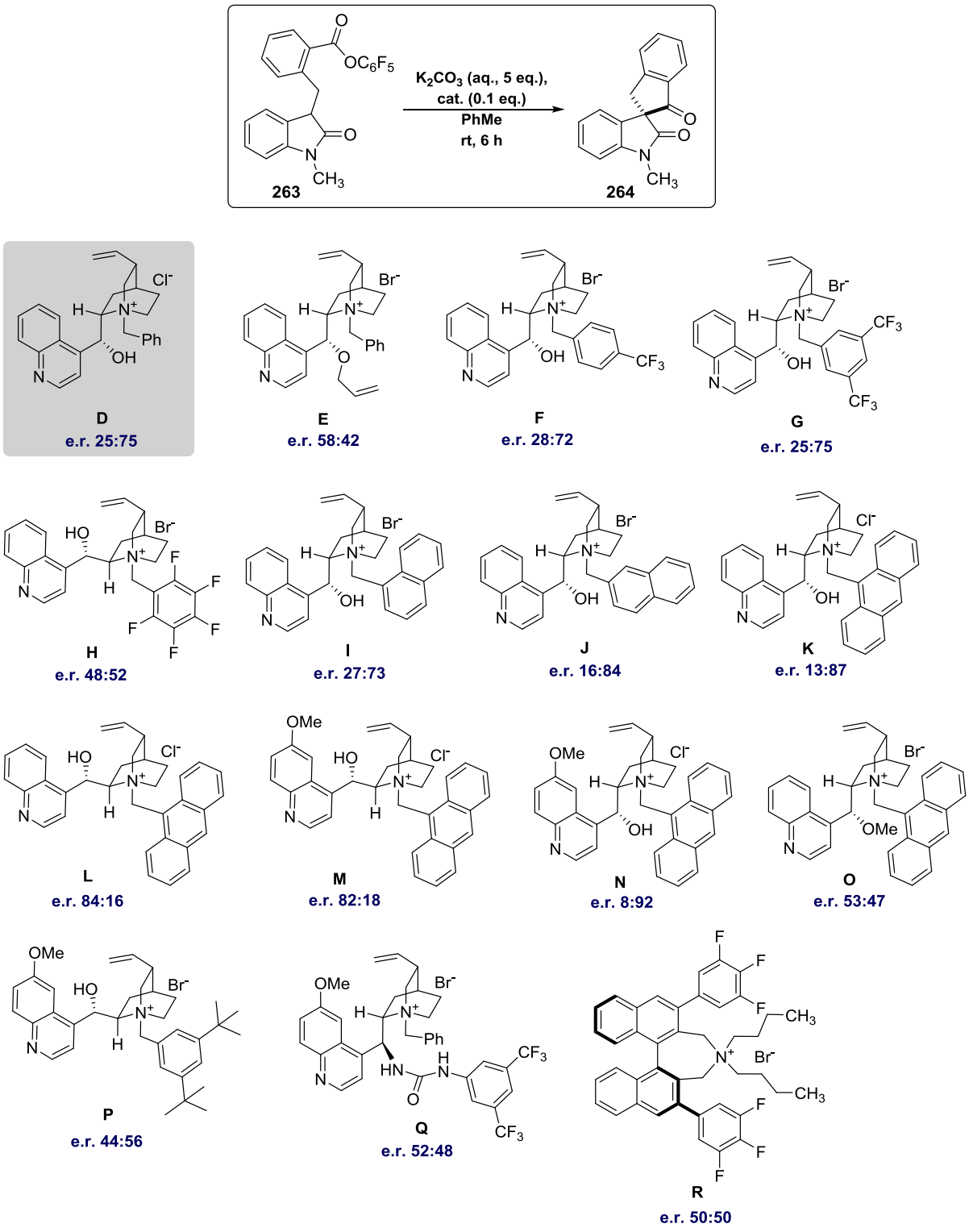

Figure 5.4 – Screen of phase-transfer catalysts for the cyclization of **263** to **264**.

Having identified a selective catalyst, we investigated the impact of varying substrate concentration, catalyst loading, and water content on enantioselectivity. Key findings are summarized here and in Tables 5.3 and 5.4.

1. Lowering the concentration of **263** from 0.05 M to 0.025 M led to a marginal improvement in the e.r. (entries 1 vs. 2).

2. Reducing the catalyst loading from 10 to 5 mol % did not affect enantioselectivity but resulted in a markedly slower reaction rate based on TLC analysis (entries 1 vs. 3).

3. Aqueous bases gave rise to higher e.r. values than their solid equivalents (entries 4-7). Raising the water content did not have a significant impact on enantioselectivity (entries 3 vs. 4)

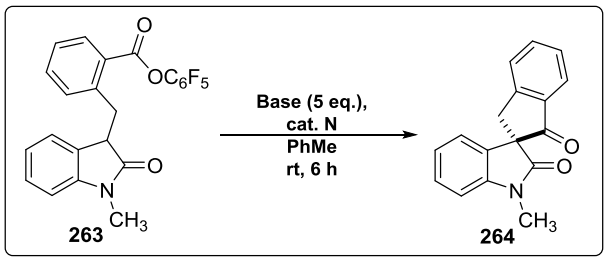

Entry	Base	Concentration of 263	Catalyst loading	e.r.
1	**K_2CO_3 (50% aq.)**	0.05 M	0.1 eq.	92:8
2	**K_2CO_3 (50% aq.)**	0.025 M	0.1 eq.	93:7
3	**K_2CO_3 (50% aq.)**	0.05 M	0.05 eq.	92:8
4	**K_2CO_3 (25% aq.)**	0.05 M	0.1 eq.	92:8
5	**K_3PO_4 (50% aq.)**	0.05 M	0.1 eq.	91:9
6	**K_2CO_3 (s.)**	0.05 M	0.1 eq.	88:12
7	**K_3PO_4 (s.)**	0.05 M	0.1 eq.	88:12

Table 5.3 – Effect of substrate concentration, catalyst loading, and use of solid/aqueous bases on reaction enantioselectivity.

The reaction medium was found to have a substantial effect on the degree of enantiocontrol, and non-polar, aromatic solvents generally gave rise to higher product e.r. values (Table 5.4). Finally, lowering the reaction temperature to 0 °C resulted in a further improvement of enantioselectivity (to 94:6), although the reaction was found to slow down considerably under these conditions based on TLC analysis.

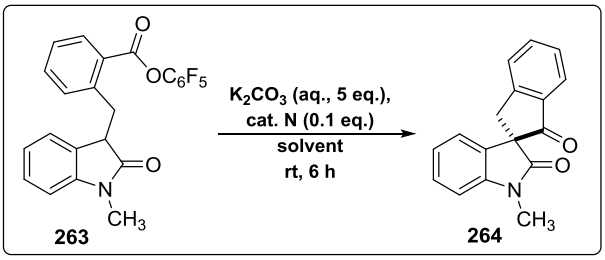

Solvent	e.r.
Toluene	92:8
Benzene	91:9
THF	66:34
CCl_4	90:10
m-Xylene	93:7
Chlorobenzene	91:9
1,1,1-Trifluorotoluene	88:12
Diisopropyl-ether	78:22
TBME	79:21
1:1 Hexane/Benzene	83:17

Table 5.4 – Effect of reaction solvent on enantioselectivity.

Guided by these screening results, we were ultimately able to obtain **264** in good yield and with an e.r. of 95:5 (Scheme 5.11). Product enantioenrichment could subsequently be augmented to 98:2 by recrystallization. The high level of enantiocontrol exhibited by this reaction demonstrates the potential of cation-directed intramolecular *C*-acylation as an approach to the asymmetric synthesis of spirocyclic compounds.

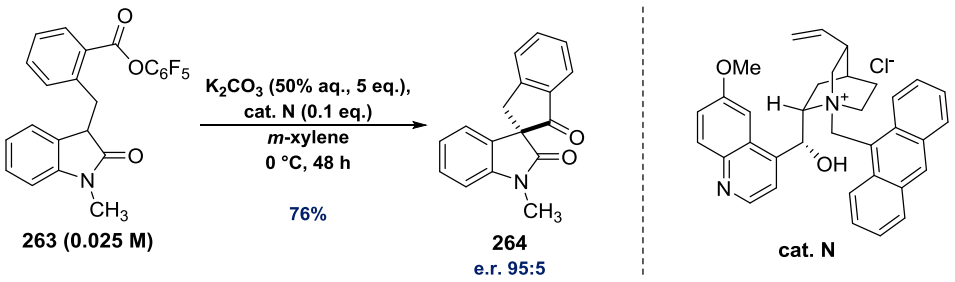

Scheme 5.11 – Optimized enantioselective reaction conditions for cyclization of **263** to **264**.

5.3.3 Prospects for Future Work

Derivitization of spiro-oxindole **264** proved challenging. Given the insights of T. Bach and co-workers regarding the tendency of alcohol **265** to undergo racemization *via* a retro-aldol reaction, we anticipated that nucleophilic addition to the ketone carbonyl would probably afford a mixture of products and ultimately lead to an erosion of enantioenrichment (Scheme 5.12). In addition, protection *via* formation of a ketal was not accomplished, probably as a result of the neopentylic nature of the ketone.

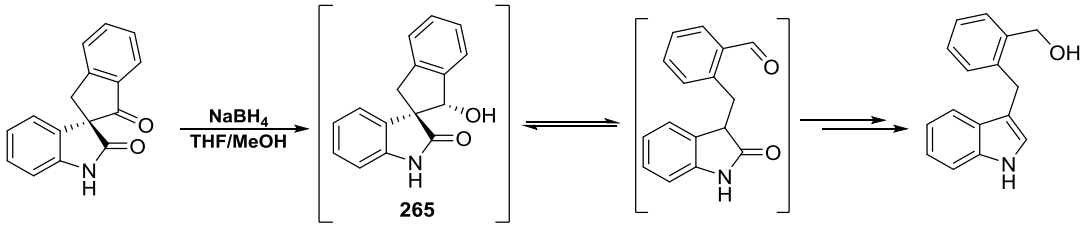

Scheme 5.12 – Lability of alcohol **265** as observed by T. Bach and co-workers.[178]

The chemoselective functionalization of amides using catalytic In^{I} complexes has been reported by H. Nagashima,[181] D. J. Dixon,[182] and P. Huang.[183] Unfortunately, attempts to apply this methodology to either reduction or reductive alkynylation of the amide carbonyl of **264** were unsuccessful (Scheme 5.13). We postulate that this is a result of electronic deactivation of the amide by the oxindole aromatic ring. We were also unable to activate the amide carbonyl with more potent electrophilic reagents such as trifluoromethanesulphonic anhydride (Tf_2O) and phosphorus oxychloride ($POCl_3$).

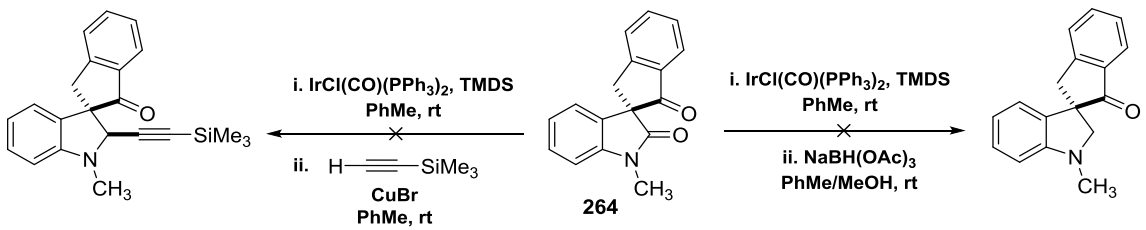

Scheme 5.13 – Attempted functionalization of amide carbonyl using Ir^{I} catalysis.

Finally, we anticipated that removal of the *N*-methyl group to afford the secondary amide would facilitate functionalization. However, attempts to effect this transformation using BBr_3, HBr, and high-pressure hydrogenation[184] over a palladium on charcoal catalyst were unsuccessful, resulting in either recovery of the unreacted starting material or extensive decomposition.

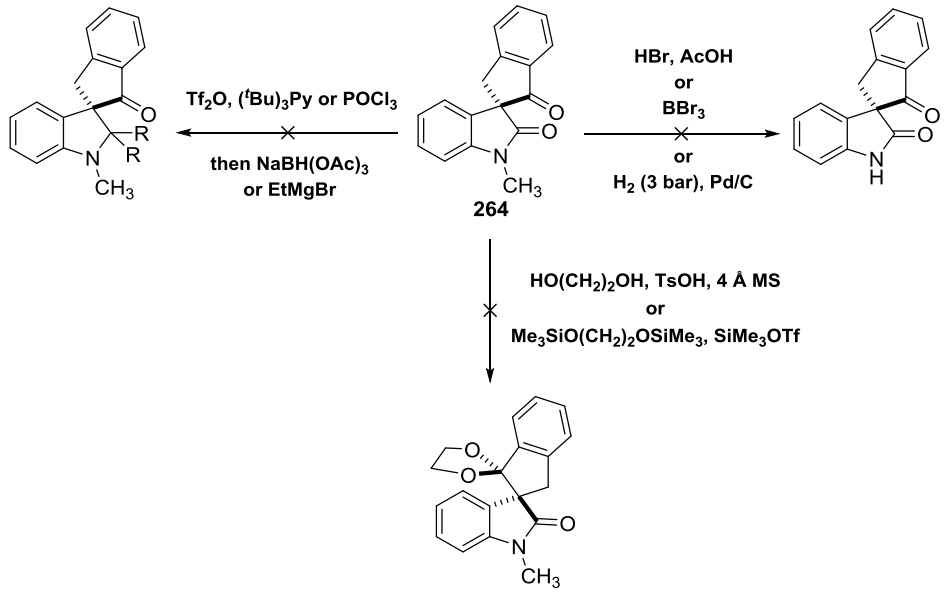

Scheme 5.14 – Further attempted reactions of spiro-oxindole **264**.

Despite these setbacks regarding the derivatization of spiro-oxindole **264**, we anticipate that a range of alternative poised chiral fragments could potentially be synthesized *via* an enantioselective *C*-acylation approach. The lessons learned in the course of this project will hopefully provide a valuable insight for future work within the group. In particular, we confirmed the importance of employing a pentafluorophenyl ester acylating agent, and we explored the limits of base-induced interfacial phase-transfer catalysis with respect to the substrate pKa. Potential substrates for cation-directed intramolecular *C*-acylation to afford 3-D fragments are depicted in Figure 5.5.

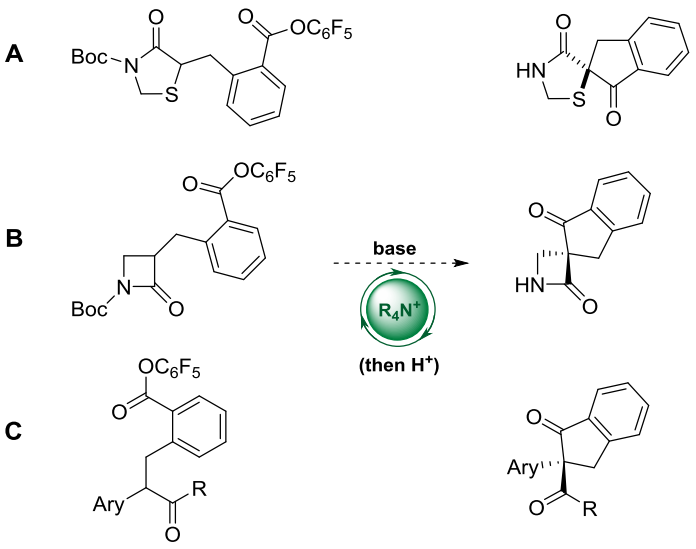

Figure 5.5 – Potential substrates for cation-directed enantioselective *C*-acylation: A) *N*-Boc-4-Thiazolidinone scaffold is expected to be more acidic than its pyrrolidinone equivalent due to carbanion-stabilization by sulfur.[185] B) *N*-Boc-β-lactam is expected to be more acidic than its pyrrolidinone equivalent due to the smaller ring size.[186] C) Potential acyclic substrate.

6. EXPERIMENTAL

6.1 General Experimental

6.1.1 General Synthetic Procedures I

Reaction Conditions

Reactions were carried out in flame-dried glassware under an atmosphere of argon unless stated otherwise. Room temperature (rt) refers to 20-25 °C. Temperatures of 0 °C were obtained using an ice/water bath. Temperatures of -78 °C were obtained using a dry ice/acetone bath. Reflux conditions were obtained using an oil bath or a Drysyn® heating block equipped with a contact thermometer. Temperatures of 0 °C or below which had to be maintained for extended periods of time were obtained using a Julabo FT902 immersion cooler.

Solvents

Acetonitrile, dichloromethane, diethyl ether, methanol, toluene, and tetrahydrofuran were purified by filtration through activated alumina columns employing the method of Grubbs *et al*.[187] Dimethylsulfoxide, dimethylformamide, and *N*-methylpyrrolidinone were purchased as anhydrous solvents in a Sure/Seal™ bottle from Sigma-Aldrich. All other solvents were used as supplied without prior purification.

Reagents and Catalysts

All reagents were used directly as supplied by major chemical suppliers or following purification procedures described by Perrin and Armarego.[188]

Chromatography

Thin layer chromatography was performed on Merck Kieselgel 60 F_{254} 0.25 mm pre-coated aluminium plates. Product spots were visualized under UV light (λ = 254 nm) and/or by staining with potassium permanganate solution, vanillin solution, or ninhydrin solution. Flash pressure column chromatography was performed using VWR silica gel 60 (40-63 µm particle size) using head pressure by means of a nitrogen line.

Nuclear Magnetic Resonance Spectrometry

NMR spectroscopy was carried out using Bruker Avance spectrometers in the deuterated solvent stated, using the residual non-deuterated solvent signal as an internal reference. ^{19}F NMR spectra were referenced externally to $CFCl_3$ in $CDCl_3$. Magnetic field strengths are quoted in MHz and refer to the resonance frequency of the relevant nucleus. Chemical shifts are quoted in ppm with signal splittings recorded as singlet (s), doublet (d), triplet (t), quartet (q), quintet (quin), sextet (sex), septet (sept), octet (oct), nonet (non) and multiplet (m). The abbreviation br. is to denote broad, app. to denote apparent, Ph to denote phenyl, and C=O to denote carbonyl groups. Coupling constants, *J*, are measured to the nearest 0.1 Hz for ^{1}H NMR spectra and to the nearest 1 Hz for ^{13}C NMR spectra and are presented as observed. For rotameric molecules, spectra were obtained at 348 K in deuterated benzene or deuterated dimethylsulfoxide.[*] Assignment of spectra was assisted by the results of COSY, HSQC, and HMBC experiments. A forward slash (/) separates ambiguous assignments for a particular peak.

Infrared Spectroscopy

Infrared spectra were recorded neat or as a film on a Bruker Tensor 27 FTIR spectrometer equipped with an attenuated total reflectance attachment with internal calibration. Absorption maxima (λ_{max}) are quoted in wavenumbers (cm^{-1}).

[*] VT-NMR spectra were obtained by Dr Barbara Odell.

Mass Spectrometry

Low resolution mass spectra were recorded on a Micromass LCT Premier spectrometer under conditions of electrospray ionization (ESI). High resolution mass spectra were recorded on Bruker MicroTOF and Micromass GCT spectrometers under conditions of electrospray ionization (ESI), field ionization (FI), or chemical ionization (CI). Values are reported as a ratio of mass to charge in Daltons.

Melting Points

Melting points were determined using a Reichert melting point apparatus and are uncorrected.

Polarimetry

Optical rotations were recorded on a Perkin-Elmer 241 polarimeter with a path length of 1 dm (using the sodium D line, 589 nm). Concentrations are reported in g/100 mL. Temperatures are reported in °C.

HPLC

Analytical chiral HPLC was performed on a Dionex UltiMate 3000 system comprising a Dionex LPG-3400A pump, WPS-3000SL autosampler, TCC-3000SD column compartment, DAD-3000 diode-array detector, fitted with the appropriate Daicel Chiralpak column (dimensions: 0.46 cm ø x 25 cm) and corresponding guard column (0.4 cm ø x 1 cm). Wavelengths (λ) are reported in nm, retention times (τ_R) are reported in minutes and solvent flow rates are reported in mL min^{-1}. Semi-preparatory HPLC was performed on the same system, fitted with a YMC Chiral amylose-SA S-5µm column (dimensions: 250 x 10.0 mml.D).

6.1.2 General Synthetic Procedures II

General Procedure 1 – Racemic cyclization of imines to form indolines

KO^tBu (1.1-1.8 eq.) was added to a solution of imine (1 eq.) in toluene and stirred at 0 °C until completion. NH_4Cl (saturated aq., approx. 10 mL/mmol imine) was added, and the mixture was extracted with EtOAc. The combined organic extracts were washed with brine, dried over Na_2SO_4, filtered, and concentrated.

General Procedure 2 – Acylation of indolines with acyl chlorides or chloroformates

Acyl chloride (2-5 eq.) was added portionwise/dropwise to a solution of indoline (1 eq.) and pyridine (2-5 eq.) in CH_2Cl_2. The reaction mixture was stirred at rt until completion. $NaHCO_3$ (saturated aq., approx. 10 mL/mmol indoline) was added, and the mixture was extracted with CH_2Cl_2. The combined organic extracts were washed with brine, dried over Na_2SO_4, filtered, and concentrated.

General Procedure 3 – Hydrogenation and hydrogenolysis over Pd/C

Pd/C (wet degussa type, 10% w/w substrate) was added to a solution of the substrate in the specified solvent. The suspension was first degassed three times with N_2 using a pump-flood procedure and then degassed three times with H_2 using a pump-flood procedure. The reaction mixture was stirred under a H_2 atmosphere until completion and flushed with N_2. The suspension was filtered through Celite™, eluted with EtOAc, and concentrated.

General procedure 4 – Stille cross-coupling

A solution of aryl bromide/triflate (1 eq.) and vinyl stannane (1.2 eq.) in NMP was degassed with Ar. $Pd(Ph_3)_4$ (0.1 eq.) was added, and the mixture was stirred at the specified temperature until completion. The reaction mixture was allowed to cool to rt, diltuted with CH_2Cl_2, and washed three times with H_2O, then brine. The organic layer was dried over Na_2SO_4, filtered, and concentrated.

General procedure 5 – Sonogashira cross-coupling in *N*,*N*-diisopropylamine

Indoline (1 eq.), $PdCl_2(PPh_3)_2$ (0.05 eq.), and CuI (0.05 eq.) were degassed three times in a Schlenk tube with Ar. A degassed solution of alkyne (1.2 eq.) in *N*,*N*-diisopropylamine was added, and the reaction mixture was stirred at the specified temperature until completion. The reaction mixture was allowed to cool to rt, filtered through Celite™ and eluted with EtOAc. The filtrate was washed 3 times with H_2O, then brine, dried over Na_2SO_4, filtered, and concentrated.

6.2 Experimental Procedures

6.2.1 Chemical Synthesis

2-Phenylacetonitrile nitrobenzene **46**

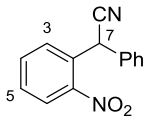

Nitrile **46** was prepared according to a modified literature procedure.[86] NaOH (aq., 50% w/w, 12 mL, 150 mmol) was added to a suspension of 1-fluoro-2-nitrobenzene (3.2 mL, 30 mmol), benzyl cyanide (3.5 mL, 30 mmol), and tetrabutylammonium bisulfate (10.2 g, 30.0 mmol) in toluene (80 mL). The mixture was stirred at 0 °C for 60 min. HCl (aq., 1 M, 150 mL) was added, and the mixture was extracted with CH_2Cl_2. The combined organic extracts were washed with brine, dried over $MgSO_4$, filtered, and concentrated. Purification by flash pressure column chromatography (10% EtOAc/petroleum ether) afforded nitrile **46** as a yellow solid (3.34 g, 14.0 mmol, 47%).

^{1}H (400 MHz, $CDCl_3$): δ 8.08 (1H, dd, *J* 8.3, 1.3, *H*6), 7.68-7.77 (2H, m, *H*3, *H*4), 7.53-7.59 (1H, ddd, *J* 8.3, 7.4, 1.3, *H*5), 7.30-7.41 (5H, m, *Ph*), 6.18 (1H, s, *H*7).

^{13}C (101 MHz, $CDCl_3$): δ 147.6 (*C*1), 134.1 (*C*4), 134.1 (*i-Ph*), 130.9 (*C*3), 130.5 (*C*2), 129.7 (*C*5), 129.3 (*Ph*), 128.7 (*Ph*), 127.9 (*Ph*), 125.8 (*C*6), 118.6 (*C*N), 38.3 (*C*7).

HRMS (ES^+): $C_{14}H_{10}N_2NaO_2^+$ ($[M+Na]^+$) requires 261.0634; found 261.0640.

IR: ν_{max} (film)/cm^{-1} 3065, 3033, 2867, 2242, 1527, 1347, 736, 699.

MP: 47-48 °C.

2-(3-Nitropyridin-4-yl)-2-phenylacetonitrile **176**

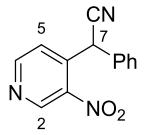

Nitrile **176** was prepared according to a modified literature procedure.[125] Benzyl cyanide (1.20 mL, 10.4 mmol) was added to a suspension of tris[2-(2-methoxyethoxy)ethyl]amine (3.0 mL, 9.4 mmol) and KOH (2.33 g, 41.6 mmol) in THF (25 mL). The mixture was stirred at 50 °C for 10 min, and a solution of 3-nitro-4-chloropyridine (1.48 g, 9.36 mmol) in THF (15 mL) was added over 1 h by syringe pump. The mixture was stirred at 50 °C for a further 30 min, then allowed to cool to rt and quenched with NH_4Cl (saturated aq., 50 mL). The mixture was extracted with EtOAc, and the combined organic extracts were washed with pH 6 phosphate buffer, then brine, dried over $MgSO_4$, filtered, and concentrated. Purification by flash pressure column chromatography (22% EtOAc/petroleum ether) afforded nitrile **176** as a brown solid (1.23 g, 5.14 mmol, 55%).

^{1}H (400 MHz, $CDCl_3$): δ 9.28 (1H, s, *H*2), 8.92 (1H, d, *J* 5.1, *H*6), 7.72 (1H, d, *J* 5.1, *H*5), 7.36-7.45 (3H, m, Ph), 7.29-7.35 (2H, m, Ph), 6.22 (1H, s, *H*7).

^{13}C (101 MHz, $CDCl_3$): δ 154.7 (*C*6), 146.8 (*C*2), 143.3, 139.4, 132.4, 129.7 (Ph), 129.3 (Ph), 128.0 (Ph), 124.4 (*C*5), 117.3 (*C*N), 38.0 (*C*7).

HRMS (ES$^+$): $[C_{13}H_9O_2N_3Na]^+$ ([M+Na]$^+$) requires 262.05870; found 262.05884.

IR: ν_{max} (film)/cm^{-1} 3081, 2248, 1595, 1568, 1530, 1348, 824, 762, 698.

MP: 52-54 °C.

2-(3-Nitropyridin-2-yl)-2-phenylacetonitrile **174**

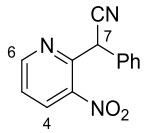

Nitrile **174** was prepared according to a modified literature procedure.[125] Benzyl cyanide (1.20 mL, 10.4 mmol) was added to a suspension of tris[2-(2-methoxyethoxy)ethyl]amine (3.0 mL, 9.4 mmol) and KOH (2.33 g, 41.6 mmol) in THF (25 mL). The mixture was stirred at 50 °C for 10 min, and a solution of 2-chloro-3-nitropyridine (1.48 g, 9.36 mmol) in THF (15 mL) was added over 1 h by syringe pump. The mixture was stirred at 50 °C for a further 30 min, then allowed to cool to rt and quenched with NH_4Cl (saturated aq., 50 mL). The mixture was extracted with EtOAc, and the combined organic extracts were washed with pH 6 phosphate buffer, then brine, dried over $MgSO_4$, filtered, and concentrated. Purification by flash pressure column chromatography (22% EtOAc/petroleum ether) afforded nitrile **174** as a yellow solid (1.02 g, 4.26 mmol, 46%).

^{1}H (400 MHz, $CDCl_3$): δ 8.89 (1H, dd, *J* 4.6, 1.5, *H*6), 8.32 (1H, dd, *J* 8.3, 1.7, *H*4), 7.48 (1H, dd, *J* 8.3, 4.6, *H*5), 7.38-7.44 (2H, m, Ph), 7.24-7.32 (3H, m, Ph), 6.25 (1H, s, *H*7).

^{13}C (101 MHz, $CDCl_3$): δ 153.7 (*C*6), 149.5, 143.9, 133.8 (*C*4), 133.2, 129.2 (Ph), 128.9 (Ph), 128.3 (Ph), 124.2 (*C*5), 118.0 (*C*N), 42.0 (*C*7).

HRMS (ES^+): $[C_{13}H_9O_2N_3Na]^+$ ($[M+Na]^+$) requires 262.0587; found 262.0588.

IR: ν_{max} (film)/cm^{-1} 3109, 2250, 1597, 1528, 1350, 1207, 849, 748, 696.

MP: 96-98 °C.

Ethyl 2-cyano-2-(nitrophenyl)acetate **73**

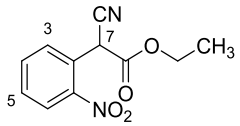

Ethyl cyanoacetate (4.3 mL, 40 mmol) was added dropwise to a suspension of KO^{t}Bu (4.9 g, 44 mmol) in THF (50 mL) and stirred at 0 °C for 10 min. 1-Fluoro-2-nitrobenzene (2.1 mL, 20 mmol) was added dropwise and stirred at 60 °C for 16 h. The mixture was diluted with EtOAc, and HCl (aq., 1 M, 30 mL) was added. The solution with extracted with EtOAc. The combined organic extracts were washed with brine, dried over $MgSO_4$, filtered, and concentrated. Purification by flash pressure column chromatography (45% Et_2O/hexane) afforded nitrile **73** as a yellow oil (1.9 g, 8.0 mmol, 40%).

^{1}H (400 MHz, $CDCl_3$): δ 8.23 (1H, d, *J* 7.8, *H*6), 7.74-7.81 (2H, m, *H*3, *H*4), 7.65 (1H, m, *H*5), 5.66 (1H, s, *H*7), 4.30 (2H, q, *J* 7.1, C*H*$_2$CH$_3$), 1.32 (3H, t, *J* 7.1, CH$_2$C*H*$_3$).

^{13}C (101 MHz, $CDCl_3$): δ 163.5 (*C*=O), 147.3 (*C*1), 134.5 (*C*3/*C*4), 131.5 (*C*3/*C*4), 130.6 (*C*5), 126.0 (*C*6), 125.2 (*C*2), 114.4 (*C*N), 63.8 (*C*7), 41.2 (*C*H$_2$CH$_3$), 13.8 (CH$_2$*C*H$_3$).

HRMS (ES$^+$): $C_{11}H_{10}NaN_2O_4^+$ ([M+Na]$^+$) requires 257.0538; found 257.0541.

IR: ν_{max} (film)/cm^{-1} 3034, 2841, 2241, 1746 (C=O), 1528, 1347, 1216, 1023, 789, 739, 699.

Methyl 2-(nitrophenyl)-2-phenylacetate **62**

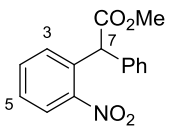

A solution of methyl phenylacetate (0.56 mL, 4.0 mmol) in THF (20 mL) was added to a solution of KHMDS (0.5 M in toluene, 16.8 mL, 8.40 mmol) in THF (20 mL) and stirred at -78 °C for 10 min. 1-Fluoro-2-nitrobenzene (0.42 mL, 4.0 mmol) was added dropwise, and the mixture was stirred at -60 °C for 30 min. The solution was allowed to warm to 0 °C, and H_2O (10 mL) was added. The

mixture was extracted with EtOAc. Purification by flash pressure column chromatography (10% Et_2O/petroleum ether) afforded ester **62** as a pale yellow oil (335 mg, 1.24 mmol, 31%).

^{1}H (400 MHz, $CDCl_3$): δ 7.56 (1H, dd, *J* 7.9, 1.3, *H*6), 6.95-7.14 (6H, m, *H*3, *Ph*), 6.72 (1H, app td, *J* 7.9, 1.3, *H*4), 6.58 (1H, app td, *J* 7.9, 1.2, *H*5), 5.75 (1H, s, *H*7), 3.31 (3H, s, CH_3).

^{13}C (101 MHz, $CDCl_3$): δ 172.1 (*C*O_2Me), 149.9 (*C*1), 137.5 (*i-Ph*), 134.6 (*C*2), 133.0 (*C*4), 132.0 (*C*3), 130.0 (*Ph*), 129.6 (*Ph*), 128.3 (*Ph*), 128.2 (*C*5), 125.2 (*C*6), 54.0 (*C*7), 52.4 (*C*H_3).

HRMS (ES^+): $C_{15}H_{13}NaNO_4^+$ ([M+Na]$^+$) requires 294.0742; found 294.0745.

IR: ν_{max} (film)/cm^{-1} 2872, 1737 (C=O), 1526, 1350, 1204, 1165, 1009, 737, 703.

Methyl 2-(nitrophenyl)acetate **82**

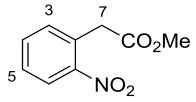

Ester **82** was prepared according to a literature procedure.[189] Two drops of concentrated H_2SO_4 were added to a stirred solution of 2-nitrophenylacetic acid (6.0 g, 33 mmol) in CH_3OH. The solution was stirred at 60 °C for 16 h, then concentrated. The resulting residue was dissolved in EtOAc and washed with H_2O, then with brine. The organic layer was dried over $MgSO_4$, filtered, and concentrated to afford ester **82** as a colorless oil (6.6 g, 33 mmol, quant). The spectral data matched those previously reported in the literature.

^{1}H (400 MHz, $CDCl_3$): δ 8.12 (1H, dd, *J* 8.0, 1.3, *H*6), 7.61 (1H, app td, *J* 7.5, 1.2, *H*4), 7.49 (1H, app td, *J* 8.0, 1.3, *H*5), 7.37 (1H, dd, *J* 7.5, 1.2, *H*3), 4.04 (2H, s, *H*7), 3.72 (3H, s, CO_2CH_3).

^{13}C (101 MHz, $CDCl_3$): δ 170.4 (*C*=O), 148.7 (*C*1), 133.6 (*C*4), 133.3 (*C*3), 129.7 (*C*2), 128.6 (*C*5), 125.3 (*C*6), 52.2 (CO_2CH_3), 39.5 (*C*7).

LCMS (ES^+): 218.1 ([M+Na$^+$]).

IR: ν_{max} (film)/cm^{-1} 3004, 2955, 1737 (C=O), 1524, 1347, 1196, 1171, 713.

Methyl 2-(nitrophenyl)acrylate **83**

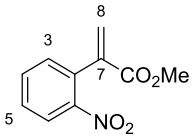

Ester **83** was prepared according to a literature procedure.[190] A mixture of ester **82** (5.0 g, 26 mmol), paraformaldehyde (3.08 g, 103 mmol), tetrabutylammonium iodide (380 mg, 1.03mmol), and K_2CO_3 (14.2 g, 103 mmol) in toluene (50 mL) was stirred at 50 °C for 5 h. The reaction was quenched with H_2O, and the mixture was extracted with toluene. The combined organic extracts were washed with brine, dried over $MgSO_4$, filtered, and concentrated. Purification by flash pressure column chromatography (10% EtOAc/petroleum ether) afforded ester **83** as a pale yellow oil (4.97 g, 24.1 mmol, 94%). The spectral data matched those previously reported in the literature.

^{1}H (400 MHz, $CDCl_3$): δ 8.12 (1H, d, *J* 7.9, *H*6), 7.66 (1H, app t, *J* 7.5, *H*4), 7.54 (1H, app t, *J* 7.9, *H*5), 7.40 (1H, d, *J* 7.5, *H*3), 6.55 (1H, app s, *H*8a), 5.89 (1H, app s, *H*8b), 3.73 (3H, s, CO_2CH_3).

^{13}C (101 MHz, $CDCl_3$): δ 165.2 (*C*=O), 147.8 (*C*1), 139.7 (*C*7), 133.7 (*C*4), 132.9 (*C*2), 132.1 (*C*3), 129.3 (*C*5), 127.5 (*C*8), 124.5 (*C*6), 52.3 (CO_2CH_3).

LRMS (ES^+): 208.1 ([M+H$^+$]), 230.1 ([M+Na$^+$]).

IR: ν_{max} (film)/cm^{-1} 2954, 1721 (C=O), 1524, 1347, 1208, 812, 788.

2-Phenylnitrile aniline **47**

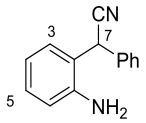

Aniline **47** was prepared according to a modified literature procedure.[87] Zinc powder (8.24 g, 126 mmol) and NH_4Cl (10.1 g, 189 mmol) were added to a solution of nitrile **46** (3.00 g, 12.6 mmol) in 5:1 acetone/H_2O (240 mL). The mixture was stirred at rt for 20 min, then filtered through Celite™, eluted with EtOAc, and washed with water, then brine. The organic layer was dried over $MgSO_4$,

filtered, and concentrated. Purification by flash pressure column chromatography (13% EtOAc/petroleum ether) afforded aniline **47** as an orange solid (2.16 g, 10.4 mmol, 82%).

^{1}H (400 MHz, $CDCl_3$): δ 7.30-7.44 (6H, m, *H*3, *Ph*), 7.21 (1H, app td, *J* 7.8, 1.2, *H*5), 6.89 (1H, app td, *J* 7.8, 1.2, *H*4), 6.74 (1H, dd, *J* 7.8, 1.2, *H*6), 5.19 (1H, s, *H*7), 3.54 (2H, br s, NH_2).

^{13}C (101 MHz, $CDCl_3$): δ 143.8 (*C*1), 133.9 (*i-Ph*), 129.6 (*C*5), 129.5 (C3), 129.4 (*Ph*), 128.5 (*Ph*), 127.7 (*Ph*), 120.0 (*C*2), 119.5 (C4), 118.9 (*C*N), 117.5 (C6), 39.0 (*C*7).

HRMS (ES^+): $C_{14}H_{12}N_2Na^+$ ($[M+Na]^+$) requires 231.0893; found 231.0901.

IR: ν_{max} (film)/cm^{-1} 3482, 3374, 3076, 3014, 2259, 1628, 1496, 1455, 751, 698.

MP: 72-73 °C.

2-(3-aminopyridin-4-yl)-2-phenylacetonitrile **177**

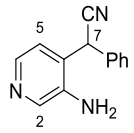

Aniline **177** was prepared according to a modified literature procedure.[87] Zinc powder (2.73 g, 41.8 mmol) and NH_4Cl (3.35 g, 62.7 mmol) were added to a solution of nitrile **176** (1.00 g, 4.18 mmol) in 5:1 acetone/H_2O (25 mL). The mixture was stirred at rt for 20 min, then filtered through Celite™, eluted with EtOAc, and washed with water, then brine. The organic layer was dried over $MgSO_4$, filtered, and concentrated. Purification by flash pressure column chromatography (3% MeOH/CH_2Cl_2) afforded aniline **177** as a yellow solid (443 mg, 2.12 mmol, 51%).

^{1}H (400 MHz, $CDCl_3$): δ 8.09-8.16 (2H, m, *H*2, *H*6), 7.38-7.45 (3H, m, Ph), 7.31-7.36 (2H, m, Ph), 7.23 (1H, d, *J* 4.9, *H*5), 5.15 (1H, s, *H*7), 3.66 (2H, br s, NH_2).

^{13}C (101 MHz, $CDCl_3$): δ 140.9 (*C*2/*C*6), 139.9, 139.6 (*C*2/*C*6), 132.3, 129.7 (Ph), 129.1 (Ph), 127.7 (Ph), 127.3, 123.0 (*C*5), 117.7 (*C*N), 38.4 (*C*7).

HRMS (ES$^+$): $[C_{13}H_{12}N_3]^+$ ([M+H]$^+$) requires 210.10257; found 210.10274.

IR: ν_{max} (film)/cm^{-1} 3391, 3208, 2251, 1636, 1566, 1495, 1422, 1331, 1072, 733, 698.

MP: 110-112 °C.

(*E*)-(((5'-Bromopyridin-3'-yl)methylene)amino)phenyl-2-phenylacetonitrile **48**

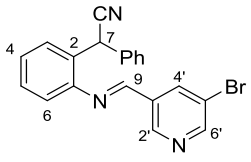

5-Bromo-3-pyridinecarboxaldehyde (800 mg, 4.30 mmol) was added to a suspension of aniline **47** (597 mg, 2.87 mmol) and $MgSO_4$ (1.73 g, 14.3 mmol) in dry toluene (25 mL). The mixture was stirred at rt for 2 h, then filtered and concentrated. The crude product was triturated with ice-cooled Et_2O to afford imine **48** as a yellow solid (1.02 g, 2.71 mmol, 94%).

^{1}H (400 MHz, $CDCl_3$): δ 8.85 (1H, d, *J* 1.7, *H*2'/*H*6'), 8.74 (1H, d, *J* 2.2, *H*2'/*H*6'), 8.33-8.39 (2H, m, *H*9, *H*4'), 7.45 (1H, dd, *J* 7.6, 1.5, *H*3), 7.35 (1H, app td, *J* 7.7, 1.5, *H*5), 7.19-7.33 (6H, m, *Ph*, *H*4), 7.05 (1H, dd, *J* 7.7, 1.2, *H*6), 5.83 (1H, s, *H*7).

^{13}C (101 MHz, $CDCl_3$): δ 156.1 (*C*9), 153.4 (*C*2'/*C*6'), 148.9 (*C*2'/*C*6'), 147.8 (*C*1), 137.2 (*C*4'), 135.8, 132.9, 131.2, 129.7 (*C*5), 129.0 (*Ph*/*C*4), 128.9 (*C*3), 128.0 (*Ph*/*C*4), 127.9 (*Ph*/*C*4), 127.7 (*Ph*/*C*4), 121.4 (*C*5'), 119.8 (*C*N), 117.8 (*C*6), 37.7 (*C*7).

HRMS (ES$^+$): $C_{20}H_{14}{}^{79}BrN_3Na^+$ ([M+Na]$^+$) requires 398.0263; found 398.0265.

IR: ν_{max} (film)/cm^{-1} 3061, 2894, 2244, 1629, 1551, 1493, 1452, 764, 696.

MP: 115-118 °C.

(*E*)-2-(2-((3-Bromobenzylidene)amino)phenyl)-2-phenylacetonitrile **123**

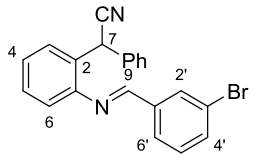

3-Bromobenzaldehyde (0.25 mL, 2.1 mmol) was added to a suspension of aniline **47** (370 mg, 1.78 mmol) and $MgSO_4$ (1.07 g, 8.89 mmol) in dry toluene (12 mL). The mixture was stirred at rt for 16 h, then filtered and concentrated. Purification by flash pressure column chromatography (8-15% Et_2O/petroleum ether) afforded imine **123** as a yellow solid (497 mg, 1.32 mmol, 74%).

^{1}H (400 MHz, C_6D_6): δ 7.78 (1H, app t, *J* 1.4, *H*2'), 7.55 (1H, s, *H*9), 7.48 (1H, dd, *J* 7.6, 1.4, *H*3), 7.41 (1H, app dt, *J* 7.8, 1.4, *H*6'), 7.21-7.27 (3H, m, *H*4', *o*-Ph), 6.85-7.01 (5H, m, *m*-Ph, *p*-Ph, *H*4, *H*5), 6.74 (1H, app t, *J* 7.8, *H*5'), 6.53 (1H, dd, *J* 7.6, 1.4, *H*6), 5.66 (1H, s, *H*7).

^{13}C (101 MHz, C_6D_6): δ 159.3 (*C*9), 149.0 (*C*1), 138.6 (*C*1'), 137.2 (*i*-Ph), 134.9 (*C*4'), 132.6 (*C*2'), 132.2 (*C*2), 130.8 (*C*5'), 129.8 (*C*5), 129.4 (*p*-Ph), 129.2 (*C*3), 128.5 (*o*-Ph), 128.1 (*p*-Ph), 127.8 (*C*4), 127.8 (*C*6'), 123.6 (*C*3'), 120.4 (*C*N), 118.5 (*C*6), 38.5 (*C*7).

HRMS (ES$^+$): $C_{21}H_{16}{}^{79}BrN_2{}^+$ ([M+H]$^+$) requires 375.0497; found 375.0488.

IR: ν_{max} (film)/cm^{-1} 3062, 3029, 2900, 2243, 1627, 1563, 1487, 1193, 786, 698.

MP: 123-126 °C.

(*E*)-2-(2-(((5-Bromofuran-2-yl)methylene)amino)phenyl)-2-phenylacetonitrile **138**

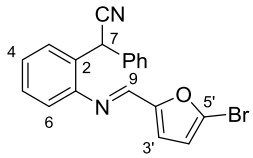

5-Bromo-2-furaldehyde (333 mg, 1.90 mmol) was added to a suspension of aniline **47** (330 mg, 1.58 mmol) and $MgSO_4$ (954 mg, 7.92 mmol) in CH_2Cl_2 (12 mL). The mixture was stirred at rt for 16 h, then filtered and concentrated. Purification by flash pressure column chromatography

(20% Et_2O/petroleum ether) afforded imine **138** as a yellow oil (398 mg, 1.09 mmol, 69%).

^1H (400 MHz, C_6D_6): δ 7.41-7.48 (2H, m, *H*3, *H*9), 7.29-7.35 (2H, m, *o*-Ph), 6.86-6.99 (5H, m, *H*4, *H*5, *m*-Ph, *p*-Ph), 6.47 (1H, dd, *J* 7.3, 1.9, *H*6), 6.28 (1H, d, *J* 3.4, *H*3'/*H*4'), 5.84-5.91 (2H, m, *H*7, *H*3'/*H*4').

^{13}C (101 MHz, C_6D_6): δ 154.9 (*C*2'), 148.7 (*C*1), 147.1 (*C*9), 137.4 (*i*-Ph), 132.7 (*C*2), 129.7 (*C*5), 129.4 (*m*-Ph/*p*-Ph), 129.2 (*C*3), 128.6 (*o*-Ph), 127.8 (*C*4), 127.4 (*C*5'), 120.6 (*C*N), 118.0 (*C*6), 117.8 (*C*3'/*C*4'), 114.7 (*C*3'/*C*4'), 38.1 (*C*7).ł

HRMS (ES^+): $C_{19}H_{13}{}^{79}BrNaN_2O^+$ ($[M+Na]^+$) requires 387.0109; found 387.0096.

IR: ν_{max} (film)/cm^{-1} 3029, 2914, 2244, 1628, 1466, 1018, 753, 697.

ł 1 peak obscured by solvent signal.

(*E*)-2-(2-(((4-Bromofuran-2-yl)methylene)amino)phenyl)-2-phenylacetonitrile **132**

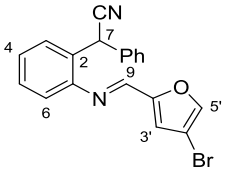

Imine **132** was prepared according to a modified literature procedure.[100] Pyrrolidine (14 µL, 0.17 mmol) was added to a stirred slurry of aniline **47** (350 mg, 1.68 mmol), 4-bromo-2-furaldehyde (382 mg, 2.18 mmol), and 3 Å molecular sieves (1.7 g) in CH_2Cl_2 (10 mL). The mixture was stirred at 50 °C for 18 h, then filtered through Celite™, eluted with CH_2Cl_2, and concentrated. Purification by flash pressure column chromatography (10-45% Et_2O/petroleum ether) afforded imine **132** as an orange oil (359 mg, 0.98 mmol, 59%).

^1H (400 MHz, C_6D_6): δ 7.41-7.47 (2H, m, *H*3, *H*9), 7.29-7.34 (2H, m, *o*-Ph), 6.86-6.98 (6H, m, *H*4, *H*5, *H*5', *m*-Ph, *p*-Ph), 6.54 (1H, s, *H*3'), 6.43 (1H, app m, *H*6), 5.89 (1H, s, *H*7).

^{13}C (101 MHz, C_6D_6): δ 153.6 (*C*2'), 148.4 (*C*1), 147.5 (*C*9), 144.3 (*C*5'), 137.3 (*i*-Ph), 132.8 (*C*2), 129.7 (*C*5), 129.4 (*m*-Ph/*p*-Ph), 129.2 (*C*3), 128.5 (*o*-Ph), 128.0 (*C*4), 120.5 (*C*N), 118.0 (*C*6), 117.8 (*C*3'),

102.7 (*C*4'), 38.0 (*C*7).[ł]

HRMS (ES$^+$): $C_{19}H_{13}{}^{79}BrNaN_2O^+$ ([M+Na]$^+$) requires 387.0109; found 387.0095.

IR: ν_{max}(film)/cm^{-1} 3141, 2922, 2244, 1626, 1493, 1213, 925, 754, 697.

ł 1 peak obscured by solvent signal.

(*E*)-2-(2-(((5-Bromopyridin-3-yl)methylene)amino)phenyl)-2-phenylacetonitrile **64**

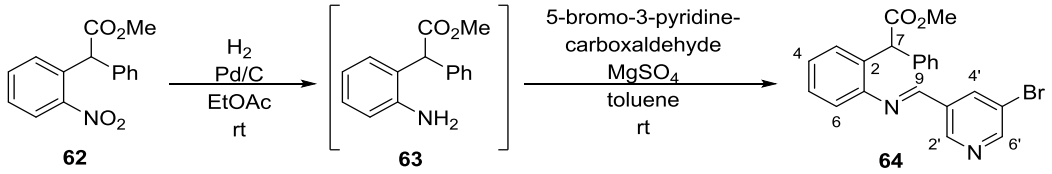

Pd/C (wet degussa type, 16 mg) was added to a solution of ester **62** (160 mg, 0.59 mmol) in EtOAc (6 mL). The suspension was degassed 3 times with hydrogen using a pump-flood procedure and placed under hydrogen for 2.5 h. The mixture was filtered through Celite^{TM}, eluted with EtOAc, and concentrated at 26 °C. The resulting residue was dissolved in toluene (6 mL), and $MgSO_4$ (355 mg, 2.95 mmol) and 5-Bromo-3-pyridinecarboxaldehyde (120 mg, 0.65 mmol) were added. The mixture was stirred at rt for 16 h, then filtered and concentrated. Purification by flash pressure column chromatography (17% EtOAc/petroleum ether) afforded imine **64** as a yellow oil (220 mg, 0.54 mmol, 91%).

^{1}H (400 MHz, C_6D_6): δ 8.63 (1H, d, *J* 2.0, *H*2'/*H*6'), 8.59 (1H, d, *J* 2.0, *H*2'/*H*6'), 8.12 (1H, app t, *J* 2.0, *H*4'), 7.59 (1H, s, *H*9), 7.34-7.44 (3H, m, *H*3, *o-Ph*), 6.98-7.14 (5H, m, *H*4, *H*5, *m-Ph, p-Ph*), 6.67 (1H, dd, *J* 7.6, 1.5, *H*6), 5.74 (1H, s, *H*7), 3.32 (3H, s, CO_2CH_3).

^{13}C (101 MHz, C_6D_6): δ 173.3 (*C*=O), 155.6 (*C*9), 153.5 (*C*2'/*C*6'), 149.5 (*C*2'/*C*6'), 149.4 (*C*1), 138.7, 137.4 (*C*4'), 135.6, 133.9, 130.0 (*C*3/*o-Ph*), 129.8 (*C*3/*o-Ph*), 129.3 (*C*5), 128.6 (*Ph*/*C*4), 127.9 (*Ph*/*C*4), 127.8 (*Ph*/*C*4), 121.9 (*C*5'), 117.7 (*C*6), 53.6 (*C*7), 52.1 (CO_2CH_3).

HRMS (ES$^+$): $C_{21}H_{17}{}^{79}BrNaN_2O_2{}^+$ ([M+Na]$^+$) requires 431.0371; found 431.0364.

IR: ν_{max}(film)/cm^{-1} 3024, 2949, 1735 (C=O), 1628, 1199, 1153, 1018, 765, 698.

Methyl (*E*)-2-(2-(((5-Bromopyridin-3-yl)methylene)amino)phenyl)propanoate **85**

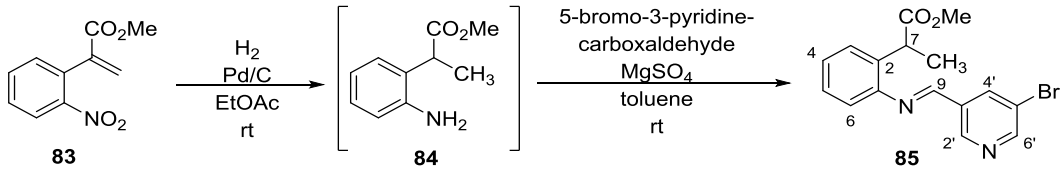

Pd/C (wet degussa type, 120 mg) was added to a solution of ester **83** (1.2 g, 5.8 mmol) in EtOAc (35 mL). The suspension was degassed 3 times with hydrogen using a pump-flood procedure and placed under hydrogen for 2 h. The mixture was filtered through Celite™, eluted with EtOAc, and concentrated at 26 °C. The resulting residue was dissolved in toluene (40 mL), and powdered $MgSO_4$ (3.8 g, 32 mmol) and 5-Bromo-3-pyridinecarboxaldehyde (1.2 g, 6.4 mmol) were added. The mixture was stirred at rt for 1 h, then filtered and concentrated. Purification by flash pressure column chromatography (32% Et_2O/petroleum ether) afforded imine **85** as a pale yellow solid (1.2 g, 3.4 mmol, 58%).

^{1}H (400 MHz, $CDCl_3$): δ 8.90 (1H, d, *J* 2.0, *H*6'), 8.77 (1H, d, *J* 2.0, *H*2'), 8.46 (1H, app t, *J* 2.0, *H*4'), 8.44 (1H, s, *H*9), 7.35 (1H, app m, *H*3), 7.28-7.33 (2H, m, *H*4, *H*5), 7.06 (1H, dd, *J* 7.5, 1.4, *H*6), 4.23 (1H, q, *J* 7.2, *H*7), 3.63 (3H, s, CO_2CH_3), 1.51 (3H, d, *J* 7.2, *H*8).

^{13}C (101 MHz, $CDCl_3$): δ 175.3 (*C*=O), 154.8 (*C*9), 153.0 (*C*2'), 148.9 (*C*6'), 148.2 (*C*1), 137.2 (*C*4'), 136.0 (*C*2), 133.4 (*C*3'), 128.1 (*C*4/*C*5), 128.0 (*C*3), 127.5 (*C*4/*C*5), 121.4 (*C*5'), 117.3 (*C*6), 51.9 (CO_2CH_3), 41.0 (*C*7), 17.8 (*C*8).

HRMS (ES^+): $C_{16}H_{15}{}^{79}BrNaN_2O_2^+$ ($[M+Na]^+$) requires 369.0215; found 369.0220.

IR: ν_{max} (film)/cm^{-1} 2982, 2948, 1732 (C=O), 1628, 1208, 743, 696.

MP: 65-66 °C.

(E)-2-(2-(((5-(Benzyloxy)pyridin-3-yl)methylene)amino)phenyl)-2-phenylacetonitrile **92**

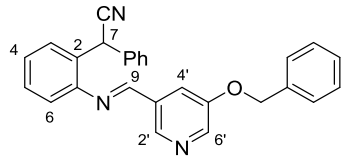

A solution of aldehyde **91** (4.86 g, 22.8 mmol) in toluene (25 mL) was added to a slurry of aniline **47** (4.0 g, 19 mmol) and $MgSO_4$ (11.4 g, 94.7 mmol) in toluene (75 mL). The mixture was stirred at rt for 16 h, filtered, and concentrated. Purification by flash pressure column chromatography (30% EtOAc/petroleum ether) afforded imine **92** as a pale yellow solid (6.05 g, 15.0 mmol, 79%).

^{1}H (500 MHz, C_6D_6): δ 8.59 (1H, d, *J* 2.9, *H*6'), 8.41 (1H, d, *J* 1.6, *H*2'), 7.74 (1H, dd, *J* 2.9, 1.6, *H*4'), 7.63 (1H, s, *H*9), 7.43 (1H, dd, *J* 7.5, 1.7, *H*6), 7.18-7.24 (4H, m, *Ph*), 7.13 (2H, app t, *J* 7.6, *Ph*), 7.05 (1H, app t, *J* 7.4, *Ph*), 6.84-7.00 (5H, m, *H*4, *H*5, *Ph*), 6.50 (1H, dd, *J* 7.8, 1.4, *H*3), 5.65 (1H, s, *H*7), 4.72 (1H, d, *J* 12.0, OCH_aH$_b$Ph), 4.67 (1H, d, *J* 12.0, OCH$_a$$H_b$Ph).

^{13}C (126 MHz, C_6D_6): δ 157.6 (*C*9), 155.4 (*C*5'), 148.5 (*C*1), 144.7 (*C*2'), 142.9 (*C*6'), 136.8 (*i-Ph*), 136.5 (*i-Ph*), 132.4 (*C*3'), 131.8 (C2), 129.5 (*C*4/*C*5/*Ph*), 129.1 (*C*4/*C*5/*Ph*), 128.9 (*C*6), 128.6 (*Ph*), 128.5 (*Ph*), 127.7 (*C*4/*C*5/*Ph*), 127.5 (*C*4/*C*5/*Ph*), 120.0 (*C*N), 118.2 (*C*3), 117.9 (*C*4'), 70.3 (O*C*H$_2$Ph), 38.3 (*C*7).‡

‡ 2 peaks obscured.

HRMS (ES$^+$): $[C_{27}H_{22}ON_3]^+$ ([M+H]$^+$) requires 404.17574; found 404.17587.

IR: ν_{max} (film)/cm^{-1} 3063, 2879, 2243, 1628, 1589, 1454, 1425, 1317, 1283, 1175, 737, 696.

MP: 78-80 °C.

(E)-2-(3-(((5-Bromopyridin-3-yl)methylene)amino)pyridin-2-yl)-2-phenylacetonitrile **178**

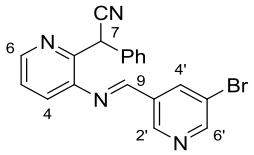

5-Bromopyridinecarboxaldehyde (289 mg, 1.55 mmol) was added to a suspension of aniline **175** (250 mg, 1.19 mmol) and $MgSO_4$ (719 mg, 5.97 mmol) in toluene (10 mL) and stirred at rt for 24 h. The mixture was filtered and concentrated. The crude product was triturated three times with ice-cooled Et_2O to afford imine **178** as a yellow solid. (265 mg, 0.70 mmol, 59%, contains minor impurities).

^{1}H (400 MHz, $CDCl_3$): δ 8.69 (1H, d, *J* 2.0, *H*2'/*H*6'), 8.61 (1H, d, *J* 2.0, *H*2'/*H*6'), 8.36 (1H, dd, *J* 4.8, 1.6, *H*6), 8.21 (1H, app t, *J* 2.0, *H*4'), 8.16 (1H, s, *H*9), 7.17-7.25 (3H, m, *H*4, *Ph*), 7.11-7.16 (1H, dd, *J* 7.8, 4.8, *H*5), 6.98-7.10 (3H, m, *Ph*), 5.74 (1H, s, *H*7).

^{13}C (101 MHz, $CDCl_3$): δ 158.0 (*C*9), 153.8 (*C*2'/*C*6'), 150.1, 149.0 (*C*2'/*C*6'), 148.4 (*C*6), 143.4, 137.4 (*C*4'), 134.7, 132.4, 128.9 (*Ph*), 128.1 (*Ph*), 127.8 (*C*4/*Ph*), 125.5 (*C*4/*Ph*), 124.4 (*C*5), 121.5 (*C*5'), 118.9 (*C*N), 41.1 (*C*7).

HRMS (ES^+): $[C_{19}H_{14}N_4{}^{79}Br]^+$ ($[M+H]^+$) requires 377.0396; found 377.0400.

IR: ν_{max} (film)/cm^{-1} 3059, 2245, 1626, 1493, 1437, 1200, 1018, 748, 696.

MP: 116-118 °C.

(2*RS*, 3*SR*)-2-(5'-Bromopyridin-3'-yl)-3-phenylindoline-3-carbonitrile **49** and (2*RS*, 3*RS*)-2-(5'-bromopyridin-3'-yl)-3-phenylindoline-3-carbonitrile **50**

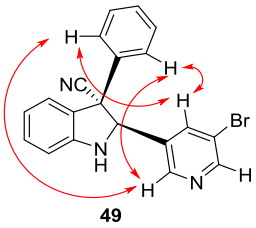

49

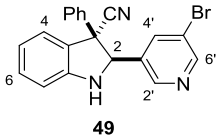

49

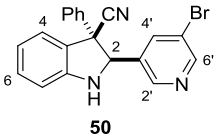

50

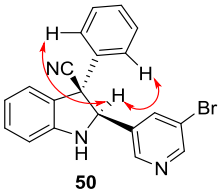

50

Indolines **49** and **50** were prepared according to general procedure 1, using KO^{t}Bu (656 mg, 5.85 mmol), imine **48** (1.10 g, 2.92 mmol) in toluene (50 mL). The reaction mixture was stirred at 0 °C for 20 min. Purification by flash pressure column chromatography (18% EtOAc/petroleum ether) afforded separately indoline **49** as a colorless solid (338 mg, 0.90 mmol, 31%) and indoline **50** as a colorless solid (580 mg, 1.54 mmol, 53%).

N.B. Stereochemistry assigned by nOe analysis, with red arrows indicating through-space interactions.

(2*RS*,3*SR*)-2-(5-Bromopyridin-3-yl)-3-phenylindoline-3-carbonitrile **49**

^{1}H (500 MHz, C_6D_6): δ 8.46 (1H, d, *J* 2.0, H2'), 8.36 (1H, d, *J* 2.0, H6'), 7.16 (1H, app s H4'), 7.05 (1H, app td, *J* 7.7, 1.2, H6), 6.99 (1H, app d, *J* 7.7, H4), 6.69-6.75 (3H, m, *o*-, *p*-Ph), 6.60-6.68 (3H, m, H5, *m*-Ph), 6.41 (1H, app d, *J* 7.7, H7), 4.69 (1H, d, *J* 3.4, H2), 2.72 (1H, d, *J* 3.4, NH).

^{13}C (126 MHz, C_6D_6): δ 151.4 (*C*6'), 150.4 (*C*7a), 147.8 (*C*2'), 137.8 (*C*4'), 134.7 (*i-Ph*), 134.4 (*C*3'), 130.7 (*C*6), 128.9 (*Ph*), 128.9 (*Ph*), 128.7 (*Ph*), 128.2 (*C*3a) 126.1 (*C*4), 121.8 (*C*5), 121.5 (*C*N), 120.7 (*C*5'), 111.0 (*C*7), 71.9 (*C*2), 56.0 (*C*3).

HRMS (ES$^+$): $C_{20}H_{14}{}^{79}BrN_3Na^+$ ([M+Na]$^+$) requires 398.0263; found 398.0270.

IR: ν_{max}(film)/cm^{-1} 3354, 3059, 2242, 1608, 1485 1262, 752, 701.

MP: 133-136 °C.

(2*RS*,3*RS*)-2-(5-Bromopyridin-3-yl)-3-phenylindoline-3-carbonitrile **50**

^{1}H (500 MHz, C_6D_6): δ 8.65 (1H, app s, H6'), 8.08 (1H, app s, H2'), 7.91 (1H, app t, *J* 1.9, H4'), 7.17-

7.20 (2H, m, *o*-Ph), 6.95-7.04 (4H, m, H6, *m-Ph*, *p-Ph*), 6.67 (1H, app d, *J* 7.7, H4), 6.60 (1H, app td, *J* 7.7, 0.9, H5), 6.43 (1H, app d, *J* 7.7, H7), 4.21 (1H, d, *J* 3.2, H2), 2.93 (1H, d, *J* 3.2, NH).

^{13}C (126 MHz, C_6D_6): δ 152.3 (*C*6'), 150.6 (*C*7a), 148.1 (*C*2'), 138.5 (*C*4'), 137.4 (*i-Ph*), 134.6 (*C*3'), 130.7 (*C*6), 129.5 (*Ph*), 129.2 (*Ph*), 128.7 (*Ph*), 127.5 (*C*3a), 126.2 (*C*4), 121.5 (*C*5), 121.4 (*C*5') 118.8 (*C*N), 111.2 (*C*7), 75.4 (*C*2), 58.9 (*C*3).

HRMS (ES$^+$): $C_{20}H_{14}{}^{79}BrN_3Na^+$ ([M+Na]$^+$) requires 398.0263; found 398.0270.

IR: ν_{max} (film)/cm^{-1} 3343, 3058, 2242, 1607, 1484, 1470, 1257, 752, 702.

MP: 69-70 °C.

Ethyl (2*RS*, 3*RS*)-2-(5-bromopyridin-3-yl)-3-cyanoindoline-3-carboxylate **77**

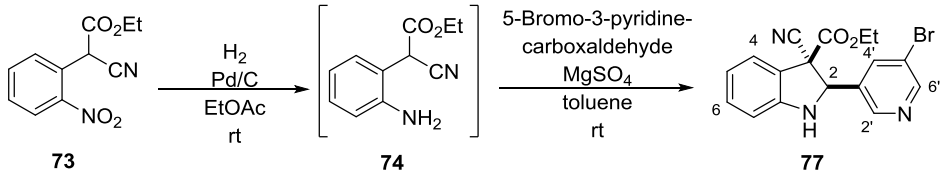

Pd/C (wet degussa type, 10% palladium by weight, 80 mg) was added to a solution of nitrile **73** (800 mg, 3.42 mmol) in EtOAc (20 mL). The suspension was degassed 3 times with hydrogen using a pump-flood procedure and placed under hydrogen for 45 min. The mixture was filtered through Celite™, eluted with EtOAc, and concentrated at 26 °C. The resulting residue was dissolved in toluene (24 mL), and $MgSO_4$ (2.06 g, 17.1 mmol) and 5-Bromo-3-pyridinecarboxaldehyde (699 mg, 3.76 mmol) were added. The mixture was stirred at rt for 16 h, then filtered and concentrated. Purification by flash pressure column chromatography (28% EtOAc/petroleum ether) afforded indoline **77** as a 97:3 mixture of diastereoisomers as a pale yellow solid (889 mg, 2.38 mmol, 68%).

N.B. Stereochemistry assigned by X-ray crystallography. Major diastereoisomer (as drawn):

^{1}H (400 MHz, C_6D_6): δ 8.69 (1H, d, *J* 1.9, *H*2'), 8.60 (1H, d, *J* 2.2, *H*6'), 7.85 (1H, app t, *J* 2.0, *H*4'), 7.09 (1H, app d, *J* 7.9, *H*4), 6.98 (1H, app td, *J* 7.7, 1.2, *H*6), 6.62 (1H, app td, *J* 7.7, 1.0, *H*5), 6.34 (1H, app

d, *J* 7.9, *H*7), 4.66 (1H, d, *J* 3.4, *H*2), 3.35 (2H, q, *J* 7.1, OC*H*$_2$CH$_3$), 2.72 (1H, d, *J* 3.4, N*H*), 0.42 (3H, t, *J* 7.1, OCH$_2$C*H*$_3$).

^{13}C (101 MHz, C_6D_6): δ 164.7 (*C*=O), 152.0 (*C*6'), 150.8 (*C*7a), 148.1 (*C*2'), 138.0 (*C*4'), 134.4 (*C*3'), 131.2 (*C*6), 125.5 (*C*4), 124.6 (*C*3a), 121.4 (*C*5), 121.1 (*C*5'), 118.4 (*C*N), 111.5 (*C*7), 70.2 (*C*2), 63.2 (O*C*H$_2$CH$_3$), 57.5 (*C*3), 13.7 (OCH$_2$*C*H$_3$).

HRMS (ES$^+$): $C_{17}H_{14}{}^{79}BrNaN_3O_2^+$ ([M+Na]$^+$) requires 394.0167; found 394.0169.

IR: ν_{max}(film)/cm^{-1} 3355, 2989, 2254, 1741 (C=O), 1607, 1487, 1229, 1022, 752.

MP: 100-102 °C.

Methyl (2*RS*,3*SR*)-2-(5-bromopyridin-3-yl)-3-phenylindoline-3-carboxylate **65** and Methyl (2*RS*,3*RS*)-2-(5-bromopyridin-3-yl)-3-phenylindoline-3-carboxylate **66**

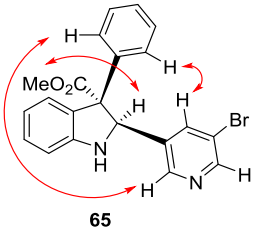

65

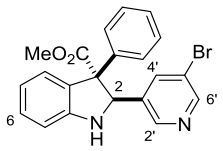

65

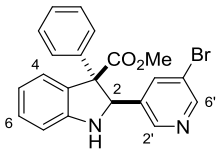

66

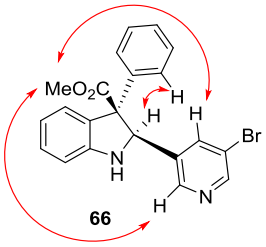

66

Indolines **65** and **66** were prepared according to general procedure 1, using KO^{t}Bu (72 mg, 0.65 mmol), and imine **64** (240 mg, 0.59 mmol) in toluene (11 mL). The reaction mixture was stirred at 0 °C for 20 min. Purification by flash pressure column chromatography (18% EtOAc/petroleum ether) afforded separately indoline **65** as a colorless solid (76 mg, 0.19 mmol, 31%) and indoline **66** as a colorless solid (66 mg, 0.16 mmol, 27%).

N.B. Stereochemistry assigned by nOe analysis, with red arrows indicating through-space interactions.

Methyl (2*RS*,3*SR*)-2-(5-bromopyridin-3-yl)-3-phenylindoline-3-carboxylate **65**

^{1}H (500 MHz, C_6D_6): δ 8.68 (1H, d, *J* 1.7, *H*2'), 8.52 (1H, d, *J* 2.4, *H*6'), 7.51 (1H, app d, *J* 7.6, *H*4), 7.40

(1H, app t, *J* 1.9, *H*4'), 7.16 (1H, obscured, *H*6), 6.83 (1H, app td, *J* 7.6, 1.0, *H*5), 6.69-6.79 (3H, m, *m*-*Ph*, *p*-*Ph*), 6.50 (1H, app d, *J* 7.7, *H*7), 6.44 (2H, m, *o*-*Ph*), 5.55 (1H, d, *J* 3.6, *H*2), 3.26 (3H, s, CO_2CH_3), 2.91 (1H, d, *J* 3.3, N*H*).

^{13}C (126 MHz, C_6D_6): δ 173.7 (*C*=O), 151.2 (*C*7a), 150.4 (*C*6'), 149.1 (*C*2'), 138.8 (*i*-*Ph*), 138.8 (*C*4'), 137.4 (*C*3'), 130.0 (*C*6), 128.6 (*o*-*Ph*), 128.4 (*m*-*Ph*/*p*-*Ph*), 127.9 (*m*-*Ph*/*p*-*Ph*), 127.4 (*C*4), 120.5 (*C*5), 120.5 (*C*5'), 110.5 (*C*7), 67.8 (*C*2), 67.2 (*C*3), 52.6 (CH_3).‡

‡ 1 peak obscured by solvent signal.

HRMS (ES$^+$): $[C_{21}H_{18}{}^{79}BrN_2O_2]^+$ ($[M+H]^+$) requires 409.0546; found 409.0538.

IR: ν_{max} (film)/cm^{-1} 3361, 1730 (C=O), 1605, 1483, 1237, 1041, 712, 699.

MP: 118-121 °C.

Methyl (2*RS*,3*RS*)-2-(5-bromopyridin-3-yl)-3-phenylindoline-3-carboxylate **66**

^{1}H (500 MHz, C_6D_6): δ 8.64 (1H, d, *J* 2.2, *H*6'), 8.34 (1H, d, *J* 1.7, *H*2'), 7.79 (1H, app t, *J* 2.1, *H*4'), 7.37 (1H, app d, *J* 7.4, *H*4), 7.32 (2H, m, *o*-*Ph*), 7.01-7.11 (4H, m, *H*6, *m*-*Ph*, *p*-*Ph*), 6.77 (1H, app td, *J* 7.5, 1.0, *H*5), 6.46 (1H, app d, *J* 7.7, *H*7), 4.57 (1H, d, *J* 2.4 Hz, *H*2), 3.06 (1H, app s, N*H*), 2.89 (3H, s, CH_3).

^{13}C (126 MHz, C_6D_6): δ 171.0 (*C*=O), 151.0 (*C*7a), 150.9 (*C*6'), 148.4 (*C*2'), 142.8 (*i*-*Ph*), 138.7 (*C*4'), 137.7 (*C*3'), 129.7 (*C*6), 129.5 (*C*3a), 129.1 (*m*-*Ph*/*p*-*Ph*), 128.5 (*C*4), 128.4 (*o*-*Ph*), 128.4 (*m*-*Ph*/*p*-*Ph*), 120.7 (*C*5'), 120.5 (*C*5), 110.6 (*C*7), 73.0 (*C*2), 67.4 (*C*3), 51.8 (CH_3).

HRMS (ES$^+$): $[C_{21}H_{18}{}^{79}BrN_2O_2]^+$ ($[M+H]^+$) requires 409.0546; found 409.0536.

IR: ν_{max} (film)/cm^{-1} 3354, 1735 (C=O), 1604, 1484, 1260, 886, 752, 703.

MP: 72-76 °C.

(2*RS*,3*SR*)-2-(3-Bromophenyl)-3-phenylindoline-3-carbonitrile **124** and (2*RS*,3*RS*)-2-(3-bromophenyl)-3-phenylindoline-3-carbonitrile **125**

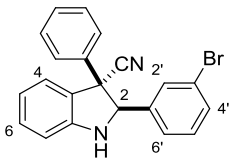

124

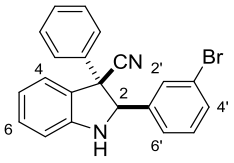

125

Indolines **124** and **125** were prepared according to general procedure 1, using KO^{t}Bu (278 mg, 2.48 mmol) and imine **123** (465 mg, 1.24 mmol) in toluene (20 mL). The reaction mixture was stirred at 0 °C for 15 min. Purification by flash pressure column chromatography (13% Et_2O/petroleum ether) afforded separately indoline **124** as a colorless solid (118 mg, 0.31 mmol, 25%) and indoline **125** as a colorless solid (194 mg, 0.52 mmol, 42%).

N.B. Stereochemistry assigned by analogy to previously reported similar indolines.[74]

(2*RS*,3*SR*)-2-(3-Bromophenyl)-3-phenylindoline-3-carbonitrile **124**

^{1}H (500 MHz, C_6D_6): δ 7.14 (1H, app t, *J* 1.8, *H*2'), 7.02-7.09 (3H, m, *H*4, *H*6, *H*4'), 6.90 (1H, app d, *J* 7.8, *H*6'), 6.68-6.82 (5H, m, *Ph*), 6.65 (1H, app td, *J* 7.5, 1.0, *H*5), 6.57 (1H, app t, *J* 7.8, *H*5'), 6.41 (1H, app d, *J* 7.6, *H*7), 4.84 (1H, d, *J* 3.3, *H*2), 2.78 (1H, d, *J* 3.3, N*H*).

^{13}C (126 MHz, C_6D_6): δ 150.7 (*C*7a), 139.1 (*C*1'), 135.1 (*i*-Ph), 131.8 (*C*4'), 131.3 (*C*2'), 130.5 (*C*6), 129.9 (*C*5'), 129.0 (*C*3a), 128.7 (*o*/*m*/*p*-Ph), 128.7 (*o*/*m*/*p*-Ph), 128.4 (*o*/*m*/*p*-Ph), 126.8 (*C*6'), 126.1 (*C*4), 122.8 (*C*3'), 122.0 (*C*N), 121.5 (*C*5), 110.8 (*C*7), 74.4 (*C*2), 55.9 (*C*3).

HRMS (ES$^+$): $C_{21}H_{16}{}^{79}BrN_2^+$ ([M+H]$^+$) requires 375.0497; found 375.0485.

IR: ν_{max}(film)/cm^{-1} 3360, 3060, 2854, 2241, 1608, 1484, 1469, 1204, 791, 751, 698.

MP: 140-143 °C.

(2*RS*,3*RS*)-2-(3-bromophenyl)-3-phenylindoline-3-carbonitrile **125**

^{1}H (500 MHz, C_6D_6): δ 7.40 (1H, app t, *J* 1.8, *H*2'), 7.22-7.30 (3H, m, *H*4', *o*-Ph), 6.97-7.06 (5H, m, *H*6, *H*6', *m*-Ph, *p*-Ph), 6.69-6.78 (2H, m, *H*4, *H*5'), 6.60 (1H, app dt, *J* 7.5, 0.9, *H*5), 6.42 (1H, app d, *J* 7.9,

*H*7), 4.35 (1H, d, *J* 3.0, *H*2), 3.01 (1H, d, *J* 3.0, N*H*).

^{13}C (126 MHz, C_6D_6): δ 150.3 (*C*7a), 139.6 (*C*1'), 138.3 (*i*-Ph), 132.6 (*C*4'), 131.7 (*C*2'), 130.6 (*C*6), 130.5 (*C*5'), 129.4 (*m*-Ph), 129.0 (*p*-Ph), 128.4 (*o*-Ph), 128.0 (*C*3a), 127.0 (C6'), 126.2 (*C*4), 123.0 (*C*3'), 121.2 (*C*5), 118.9 (*C*N), 111.0 (*C*7), 77.8 (*C*2), 58.9 (*C*3).

HRMS (ES$^+$): $C_{21}H_{16}{}^{79}BrN_2^+$ ([M+H]$^+$) requires 375.0497; found 375.0484.

IR: ν_{max} (film)/cm^{-1} 3359, 3059, 2868, 2237, 1607, 1483, 1470, 1254, 751, 700.

MP: 120-122 °C.

(2*SR*,3*RS*)-2-(4-Bromofuran-2-yl)-3-phenylindoline-3-carbonitrile **133**

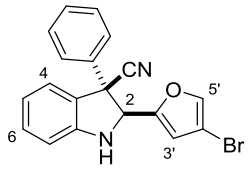

Indoline **133** was prepared according to general procedure 1, using KO^{t}Bu (109 mg, 0.98 mmol) and imine **132** (325 mg, 0.89 mmol) in toluene (12 mL). The reaction mixture was stirred at 15 °C for 15 min. Purification by flash pressure column chromatography (15% Et_2O/petroleum ether) afforded indoline **133** as a colorless solid (240 mg, 0.65 mmol, 73%).

N.B. Stereochemistry assigned by analogy to previously reported similar indolines.[74]

^{1}H (400 MHz, C_6D_6): δ 7.32-7.41 (2H, m, *o*-Ph), 6.94-7.06 (4H, m, *H*6, *p-Ph*, *m-Ph*), 6.87 (1H, d, *J* 0.7, *H*5'), 6.80 (1H, app d, *J* 7.5, *H*4), 6.57 (1H, app td, *J* 7.5, 0.8, *H*5), 6.38 (1H, app d, *J* 7.8, *H*7), 6.33 (1H, app s, *H*3'), 4.47 (1H, d, *J* 2.5, *H*2), 3.10 (1H, d, *J* 2.5, N*H*).

^{13}C (101 MHz, C_6D_6): δ 153.4 (*C*2'), 150.3 (*C*7a), 141.9 (*C*5'), 139.2 (*i-Ph*), 130.6 (*C*6), 129.5 (*m*-Ph), 129.0 (*p-Ph*), 127.8 (*C*3a), 127.7 (*o*-Ph), 126.1 (*C*4), 121.3 (*C*5), 119.0 (*C*N), 112.9 (*C*3'), 110.9 (*C*7), 101.1 (*C*4'), 71.1 (*C*2), 57.7 (*C*3).

HRMS (ES$^+$): $C_{19}H_{13}{}^{79}BrNaN_2O^+$ ([M+Na]$^+$) requires 387.0109; found 387.0097.

IR: ν_{max} (film)/cm^{-1} 3356, 2239, 1606, 1484, 1469, 1256, 1126, 924, 745.

MP: 137-140 °C.

(2*R*,3*R*)/(2*S*,*S*)-2-(5-(Benzyloxy)pyridin-3-yl)-3-phenylindoline-3-carbonitrile **93**

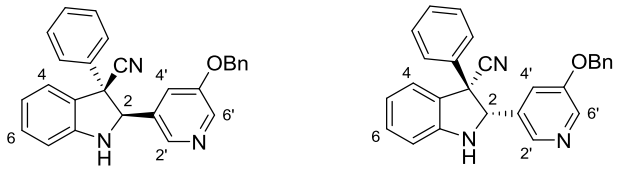

(*R*,*R*)-93 **(*S*,*S*)-93**

(2*R*,3*R*)-2-(5-(Benzyloxy)pyridin-3-yl)-3-phenylindoline-3-carbonitrile **(*R*,*R*)-93**

The catalyst (70 mg, 0.11 mmol) was added to a solution of imine **92** (880 mg, 2.18 mmol) in toluene (33 mL), and the suspension was stirred at -30 °C for 30 min. $CsOH{\cdot}H_2O$ (732 mg, 4.36 mmol) was added and stirred at -30 °C for 16 h. The mixture was diluted with EtOAc (40 mL), and NH_4Cl (sat. aq., 40 mL) was added. The mixture was allowed to warm to rt, the organic and aqueous layers were separated, and the aqueous layer was extracted with EtOAc. The combined organic layers were washed with brine, dried over Na_2SO_4, filtered, and concentrated. Purification by flash pressure column chromatography (35% EtOAc/petroleum ether) afforded indoline **93** as a 85:15 mixture of enantiomers as a colorless solid (787 mg, 1.95 mmol, 89%). Resolution by semi-preparatory chiral HPLC (YMC chiral amylose SA, 5% ^{i}PrOH, 95% hexane, 5.0 mL/min) afforded indoline **(*R*,*R*)-93** as a colorless solid (e.r. > 99:1).

(2*S*,3*S*)-2-(5-(Benzyloxy)pyridin-3-yl)-3-phenylindoline-3-carbonitrile **(*S*,*S*)-93**

Indoline **(*S*,*S*)-93** was prepared in an analogous manner to indoline **(*R*,*R*)-93** using a pseudoenantiomeric catalyst (47 mg, 0.074 mmol), imine **92** (600 mg, 1.49 mmol), and $CsOH{\cdot}H_2O$ (500 mg, 2.97 mmol) in toluene (19 mL). The reaction mixture was stirred at -30 °C for 16 h. Purification by flash pressure column chromatography (35% EtOAc/petroleum ether) afforded indoline **93** as a 89:11 mixture of enantiomers as a colorless solid (538 mg, 1.33 mmol, 90%). Resolution by semi-preparatory chiral HPLC (YMC chiral amylose SA, 5% ^{i}PrOH, 95% hexane, 5.0

mL/min) afforded indoline **(*S*,*S*)-93** as a colorless solid (e.r. > 99:1).

N.B. Stereochemistry assigned by x-ray crystallography of indoline **(*S*,*S*)-93**.

^{1}H (400 MHz, C_6D_6): δ 8.58 (1H, d, *J* 2.9, *H*2'/*H*6'), 7.91 (1H, d, *J* 1.4, *H*2'/*H*6'), 7.63 (1H, app t, *J* 2.0, *H*4'), 7.27 (2H, m, *Ph*), 6.93-7.14 (7H, m, *H*6, *Ph*), 6.74 (1H, app d, *J* 7.6, *H*4), 6.61 (1H, app t, *J* 7.6, *H*5), 6.44 (1H, app d, *J* 8.0, *H*7), 4.73 (1H, d, *J* 11.8, OC$H_a$$H_b$Ph), 4.69 (1H, d, *J* 11.8, OC$H_a$$H_b$Ph), 4.40 (1H, d, *J* 3.2, *H*2), 3.06 (1H, d, *J* 3.0, N*H*).ǂ

^{13}C (101 MHz, C_6D_6): δ 155.3 (*C*5'), 150.6 (*C*7a), 142.2 (*C*2'/*C*6'), 140.1 (*C*2'/*C*6'), 137.5, 136.8, 133.0, 130.3 (*C*6/*Ph*), 129.1 (*C*6/*Ph*), 128.7 (*C*6/*Ph*), 128.6 (*C*6/*Ph*), 127.5, 125.9 (*C*4), 121.0 (*C*5), 120.5 (*C*4'), 119.0 (*C*N), 110.8 (*C*7), 75.7 (*C*2), 70.4 (O*C*H_2Ph), 58.6 (*C*3).‡

ǂ Remaining 2 peaks obscured.

‡ Remaining 3 peaks obscured.

HRMS (ES$^+$): $[C_{27}H_{22}ON_3]^+$ ([M+H]$^+$) requires 404.1757; found 404.1763.

IR: ν_{max} (film)/cm^{-1} 3355, 2925, 2248, 1606, 1470, 1435, 1322, 1171, 1026, 745, 698.

MP: 48-50 °C.

$[\alpha]_D^{25.0}$ (*R*,*R*) = +26 (*c* = 0.1, $CHCl_3$); $[\alpha]_D^{25.0}$ (*S*,*S*) = -19 (*c* = 0.1, $CHCl_3$).

Chiral HPLC: (Chiralpak IA, 10% ^{i}PrOH, 90% hexane, 1.0 mL/min, λ = 254 nm, 20 µL injection) τ_R (*R*,*R*) = 33.2 min, τ_R (*S*,*S*) = 27.5 min.

(2*S*,3*S*)-2-(5-Hydroxypyridin-3-yl)-3-phenylindoline-3-carbonitrile **266**

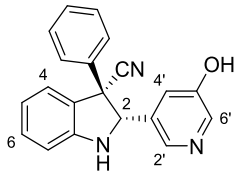

Indoline **266** was prepared according to general procedure 3 using indoline **(*S*,*S*)-93** (195 mg, 0.49 mmol) and Pd/C (wet degussa type, 20 mg) in MeOH (14 mL). The reaction mixture was stirred under a H_2 atmosphere for 2 h. The reaction mixture was filtered through Celite and concentrated to afford indoline **266** as a colorless solid (154 mg, 0.49 mmol, quant).

^{1}H (500 MHz, CD_3OD): δ 8.06 (1H, d, *J* 2.6, *H*2'/*H*6'), 7.72 (1H, d, *J* 1.6, *H*2'/*H*6'), 7.37-7.52 (5H, m, *Ph*), 7.21-7.32 (2H, m, *H*4', *H*6), 6.92 (2H, app d, *J* 8.5, *H*4, *H*7), 6.84 (1H, app t, *J* 7.5, *H*5), 5.08 (1H, app s, *H*2), 3.35 (1H, app s, N*H*).ǂ

^{13}C (126 MHz, CD_3OD): δ 155.8 (*C*5'), 152.7 (*C*7a), 140.0 (*C*2'/*C*6'), 138.8 (*C*2'/*C*6'), 138.5, 136.0, 131.5 (*C*6), 130.1 (*Ph*), 129.9 (*Ph*), 128.7 (*Ph*), 128.4, 126.1 (*C*4), 123.6 (*C*4'), 121.1 (*C*5), 120.0 (*C*N), 111.9 (*C*7), 76.3 (*C*2), 59.8 (*C*3).

ǂ OH peak not observed due to exchange with MeOD.

HRMS (ES^+): $[C_{20}H_{16}ON_3]^+$ ($[M+H]^+$) requires 314.1288; found 314.1287.

IR: ν_{max}(film)/cm^{-1} 3348, 2922, 2241, 1608, 1428, 1299, 1214, 1136, 994, 756.

MP: 110-112 °C.

$[\alpha]_D^{25.0}$ = +12 (*c* = 0.1, $CHCl_3$).

5-((2*S*,3*S*)-3-Cyano-3-phenylindolin-2-yl)pyridin-3-yl trifluoromethanesulfonate **267**

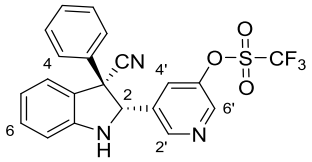

N,*N*-diisopropylethylamine (156 µL, 0.89 mmol) was added to a solution of indoline **266** (140 mg, 0.45 mmol) and *N*-phenyl-bis(trifluoromethanesulfonimide) (176 mg, 0.49 mmol) in CH_2Cl_2 (10 mL) at 0 °C. The reaction mixture was allowed to warm to rt and stirred for 1 h. H_2O (10 mL) was added, the layers separated, and the aqueous layer was extracted 3 times with CH_2Cl_2. The combined organic extracts were washed with brine, dried over Na_2SO_4, filtered, and concentrated. Purification by flash pressure column chromatography (3.5% EtOAc/petroleum ether) afforded indoline **267** as a colorless hygroscopic solid (170 mg, 0.38 mmol, 85%).

^{1}H (400 MHz, C_6D_6): δ 8.36 (1H, d, *J* 2.7, *H*2'/*H*6'), 8.11 (1H, d, *J* 1.7, *H*2'/*H*6'), 7.63 (1H, app t, *J* 2.1, *H*4'), 6.92-7.06 (4H, m, *H*6, *Ph*), 6.63 (1H, dd, *J* 7.9, 1.4, *H*4), 6.59 (1H, app td, *J* 7.5, 0.9, *H*5), 6.41 (1H, app d, *J* 8.2, *H*7), 4.21 (1H, d, *J* 3.4, *H*2), 2.83 (1H, d, *J* 3.4, N*H*).ǂ

^{13}C (101 MHz, C_6D_6): δ 150.0 (*C*5'), 149.1 (*C*2'/*C*6'), 146.9 (*C*7a), 143.6 (*C*2'/*C*6'), 136.8, 134.8, 130.4 (*C*6/*Ph*), 129.3 (*C*6/*Ph*), 129.0 (*Ph*), 128.6 (*C*4'), 127.0, 125.8 (*C*4), 121.5 (*C*5), 119.2 (q, *J* 321.2, *C*F_3), 118.1 (*C*N), 111.1 (*C*7), 74.8 (*C*2), 58.5 (*C*3).‡

ǂ 1 peak obscured by solvent signal.

‡ 1 peak obscured by solvent signal.

^{19}F (377 MHz, C_6D_6): δ -73.1.

HRMS (ES$^+$): $[C_{21}H_{15}O_3N_3F_3{}^{32}S]^+$ ([M+H]$^+$) requires 446.0781; found 446.0780.

IR: ν_{max} (film)/cm^{-1} 3059, 2249, 1607, 1427, 1217, 1138, 837, 756, 700.

$[\alpha]_D^{25.0}$ = +31 (*c* = 0.1, $CHCl_3$).

(2*RS*, 3*SR*)-1-Acetyl-2-(5'-bromopyridin-3'-yl)-3-phenylindoline-3-carbonitrile **52**

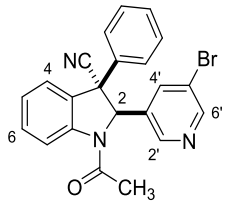

Indoline **52** was prepared according to general procedure 2, using indoline **49** (250 mg, 0.66 mmol), acetyl chloride (57 µL, 0.80 mmol), and pyridine (64 µL, 0.80 mmol) in CH_2Cl_2 (13 mL). The reaction mixture was stirred at rt for 15 min. Purification by flash pressure column chromatography (30% EtOAc/petroleum ether) afforded indoline **52** as a colorless solid (270 mg, 0.65 mmol, 98%).

^{1}H (500 MHz, C_6D_6, 348 K): δ 8.23 (1H, d, *J* 2.2, *H*6'), 8.10 (1H, app br s, *H*7), 7.87 (1H, app s, *H*2'), 7.08 (1H, app t, *J* 7.8, *H*6), 6.88 (2H, m, *o-Ph*), 6.71-6.84 (6H, m, *H*4, *H*4', *H*5, *m-Ph, p-Ph*), 5.62 (1H, s, *H*2), 1.64 (3H, s, C*H*$_3$).

^{13}C (126 MHz, C_6D_6, 348 K): δ 168.2 (*C*=O), 151.3 (*C*6'), 146.9 (*C*2'), 144.6 (*C*7a), 137.4 (*C*4'), 134.3 (*C*3'), 133.7 (*C*3a/*i-Ph*), 131.6 (*C*6), 129.5 (*m-Ph*/*p-Ph*), 129.1 (*m-Ph*/*p-Ph*), 129.1 (*o-Ph*), 126.8 (*C*4), 125.7 (*C*5), 121.4 (*C*N), 120.8 (*C*5'), 117.6 (*C*7), 72.9 (*C*2), 55.8 (*C*3), 24.0 (*C*H$_3$).ł

ł 1 peak obscured by solvent signal.

HRMS (ES$^+$): $C_{22}H_{16}{}^{79}BrN_3NaO^+$ ([M+Na]$^+$) requires 440.0369; found 440.0371.

IR: ν_{max}(film)/cm^{-1} 3062, 2361, 2236, 1677 (C=O), 1478, 1385, 1020, 756, 699.

MP: 126-128 °C.

(2*RS*, 3*RS*)-1-Acetyl-2-(5'-bromopyridin-3'-yl)-3-phenylindoline-3-carbonitrile **53**

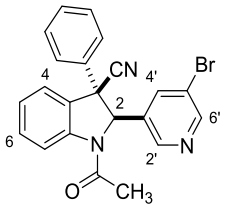

Indoline **53** was prepared according to general procedure 2, using indoline **50** (400 mg, 1.06 mmol), acetyl chloride (91 µL, 1.3 mmol), and pyridine (103 µL, 1.28 mmol) in CH_2Cl_2 (20 mL). The reaction mixture was stirred at rt for 15 min. Purification by flash pressure column chromatography (30% EtOAc/petroleum ether) afforded indoline **53** as a colorless solid (379 mg, 0.91 mmol, 85%).

^{1}H (500 MHz, C_6D_6, 348 K): δ 8.56 (1H, d, *J* 2.2, *H*6'), 8.41 (1H, d, *J* 1.6, *H*2'), 8.04 (1H, app br s, *H*7), 7.55 (1H, app t, *J* 1.8, *H*4'), 7.17 (2H, m, *o-Ph*), 7.06 (1H, app t, *J* 7.8, *H*6), 6.96-7.03 (4H, m, *H*4, *m-Ph*, *p-Ph*), 6.74 (1H, app t, *J* 7.8, *H*5), 5.18 (1H, br s, *H*2), 1.49 (3H, s, CH_3).

^{13}C (126 MHz, C_6D_6, 348 K): δ 167.9 (*C*=O), 152.9 (*C*6'), 147.1 (*C*2'), 143.4 (*C*7a), 140.8 (*i-Ph*), 136.8 (*C*4'), 136.0 (*C*3'), 131.4 (*C*6), 130.2 (*m-Ph*/*p-Ph*), 129.8 (*C*3a), 129.5 (*m-Ph*/*p-Ph*), 126.5 (*C*4), 126.2 (*o-Ph*), 126.1 (*C*5), 121.8 (*C*5'), 118.9 (*C*N), 117.5 (*C*7), 74.0 (*C*2), 57.9 (*C*3), 23.7 (*C*H_3).

HRMS (ES$^+$): $C_{22}H_{16}{}^{79}BrN_3NaO^+$ ([M+Na]$^+$) requires 440.0369; found 440.0370.

IR: ν_{max} (film)/cm^{-1} 3011, 2236, 1679 (C=O), 1479, 1389, 1020, 756, 700.

MP: 90-94 °C.

(2*RS*,3*SR*)-1-Acetyl-3-phenyl-2-(5'-((trimethylsilyl)ethynyl)pyridin-3'-yl)indoline-3-carbonitrile **116**

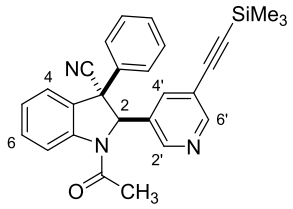

A suspension of indoline **52** (120 mg, 0.29 mmol), $PdCl_2(PPh_3)_2$ (10 mg, 0.014 mmol), and CuI (3.0 mg, 0.014 mmol) in diisopropylamine (4 mL) was degassed and placed under an Ar atmosphere before ethynyltrimethylsilane (50 µL, 0.34 mmol) was added. The mixture was stirred at 65 °C for 5.5 h, then filtered through Celite and eluted with CH_2Cl_2. The filtrate was washed with water, then with brine, dried over $MgSO_4$, filtered, and concentrated. Purification by flash pressure column chromatography (30% EtOAc/petroleum ether) afforded alkyne **116** as a pale yellow solid (121 mg, 0.28 mmol, 96%).

^{1}H (500 MHz, C_6D_6, 348 K): δ 8.43 (1H, app s, *H*6'), 8.15 (1H, app br s, *H*7), 7.85 (1H, app s, *H*2'), 7.06 (1H, app td, *J* 7.8, 1.4, *H*6), 6.85-6.94 (3H, m, *H*4', *o-Ph*), 6.67-6.83 (5H, m, *H*4, *H*5, *m-Ph*, *p-Ph*), 5.62 (1H, s, *H*2), 1.60 (3H, s, CH_3), 0.12 (9H, s, Si(CH_3)$_3$).

^{13}C (126 MHz, C_6D_6, 348 K): δ 168.2 (*C*=O), 153.0 (*C*6'), 148.2 (*C*2'), 144.8 (*C*7a), 137.1, 133.9 (*C*4'), 132.2, 131.5 (*C*6), 129.4 (*m-Ph*/*p-Ph*), 129.2 (*m-Ph*/*p-Ph*), 129.1 (*o-Ph*), 126.7 (*C*4), 125.6 (*C*5), 121.5 (*C*N), 120.5 (*C*5'), 117.7 (*C*7), 102.0 (*C*8/*C*9), 99.5 (*C*8/*C*9), 73.3 (*C*2), 55.9 (*C*3), 24.0 (*C*H$_3$), 0.02 (Si(*C*H$_3$)$_3$).‡

‡ 1 peak obscured by solvent signal.

HRMS (ES$^+$): $C_{27}H_{25}N_3NaOSi^+$ ([M+Na]$^+$) requires 458.1659; found 458.1655.

IR: ν_{max}(film)/cm^{-1} 3040, 2961, 2160, 2158, 1678 (C=O), 1600, 1479, 1385, 1127, 846, 758, 698.

MP: 125-127 °C.

(2*RS*,3*RS*)-1-Acetyl-3-phenyl-2-(5-((trimethylsilyl)ethynyl)pyridin-3-yl)indoline-3-carbonitrile **117**

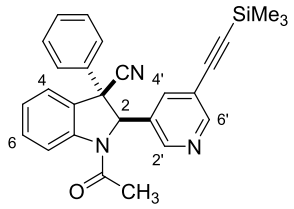

A suspension of indoline **53** (150 mg, 0.36 mmol), $PdCl_2(PPh_3)_2$ (13 mg, 0.018 mmol), and CuI (3.5 mg, 0.018 mmol) in diisopropylamine (4 mL) was degassed and placed under an Ar atmosphere before ethynyltrimethylsilane (61 µL, 0.43 mmol) was added. The mixture was stirred at 65 °C for 5.5 h, then filtered through Celite™. The filtrate was washed three times with water, then with brine, dried over $MgSO_4$, filtered, and concentrated. Purification by flash pressure column chromatography (30% EtOAc/petroleum ether) afforded alkyne **117** as a colorless solid (141 mg, 0.32 mmol, 89%).

^{1}H (500 MHz, C_6D_6, 348 K): δ 8.78 (1H, app s, H2'/*H*6'), 8.47 (1H, app s, *H*2'/*H*6'), 8.10 (1H, app br s, *H*7), 7.59 (1H, app s, *H*4'), 7.13-7.18 (2H, obscured, *o-Ph*), 7.03 (1H, app t, *J* 7.8, *H*6), 6.95-7.01 (4H, m, *H*4, *m-Ph*, *p-Ph*), 6.71 (1H, app t, *J* 7.8, *H*5), 5.16 (1H, s, *H*2), 1.47 (3H, s, CH_3), 0.14 (9H, s, Si(CH_3)$_3$).

^{13}C (126 MHz, C_6D_6, 348 K): δ 167.9 (*C*=O), 154.6 (*C*2'/*C*6'), 148.0 (*C*2'/*C*6'), 143.6 (*C*7a), 141.1, 136.6 (*C*4'), 134.0, 131.3 (*C*6), 130.2 (*m-Ph*/*p-Ph*), 129.7, 129.4 (*m-Ph*/*p-Ph*), 126.4 (*C*4), 126.2 (*o-Ph*), 126.0 (*C*5), 118.9 (*C*N), 117.6 (*C*7), 102.2 (*C*8/*C*9), 99.9 (*C*8/*C*9), 74.5 (*C*2), 58.0 (*C*3), 23.6 (*C*H_3), 0.04 (Si(*C*H_3)$_3$).‡

‡ 1 peak obscured by solvent signal.

HRMS (ES$^+$): $[C_{27}H_{26}N_3OSi]^+$ ([M+H]$^+$) requires 436.1840; found 436.1850.

IR: ν_{max} (film)/cm^{-1} 2961, 2160, 1680 (C=O), 1479, 1385, 1250, 847, 759, 698.

MP: 155-157 °C.

(2*RS*,3*SR*)-1-acetyl-2-(5-ethynylpyridin-3-yl)-3-phenylindoline-3-carbonitrile **118**

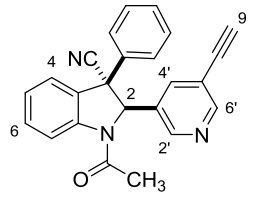

TBAF (1.0 M in THF, 0.3 mL, 0.3 mmol) was added dropwise to a solution of alkyne **116** (110 mg, 0.25 mmol) in THF (5 mL) at 0 °C and stirred at rt for 15 min. The mixture was diluted with EtOAc (10 mL) and washed three times with water, then with brine, dried over $MgSO_4$, filtered, and concentrated. Purification by flash pressure column chromatography (36% EtOAc/petroleum ether) afforded alkyne **118** as a colorless oil (90 mg, 0.25 mmol, 99%).

^{1}H (500 MHz, C_6D_6, 348 K): δ 8.36 (1H, app s, *H*2'/*H*6'), 8.17 (1H, app br s, *H*7), 7.86 (1H, app s , *H*2'/*H*6'), 7.07 (1H, app t, *J* 7.8, *H*6), 6.89 (2H, m, *o-Ph*), 6.83 (1H, app s, *H*4'), 6.70-6.81 (5H, m, *H*4, *H*5, *m-Ph*, *p-Ph*), 5.61 (1H, s, *H*2), 2.58 (1H, s, *H*9), 1.60 (3H, s, CH_3).

^{13}C (126 MHz, C_6D_6, 348 K): δ 168.2 (*C*=O), 153.0 (*C*2'/*C*6'), 148.5 (*C*2'/*C*6'), 144.8 (*C*7a), 137.5, 133.8 (*C*4'), 132.3, 131.5 (*C*6), 129.4 (*m-Ph*/*p-Ph*), 129.1 (*m-Ph*/*p-Ph*), 129.1 (*o-Ph*), 126.7 (*C*4), 125.6 (*C*5), 121.4 (*C*N), 119.5 (*C*5'), 117.7 (*C*7), 81.6 (*C*8/*C*9), 80.3 (*C*8/*C*9), 73.2 (*C*2), 55.9 (*C*3), 24.0 (*C*H_3).‡

‡ 1 peak obscured by solvent signal.

HRMS (ES$^+$): $[C_{24}H_{17}N_3NaO]^+$ ([M+Na]$^+$) requires 386.1264; found 386.1268.

IR: ν_{max} (film)/cm^{-1} 3285, 3023, 2261, 1676 (C=O), 1478, 1386, 1025, 757, 700.

(2*RS*,3*RS*)-1-Acetyl-2-(5-ethynylpyridin-3-yl)-3-phenylindoline-3-carbonitrile **119**

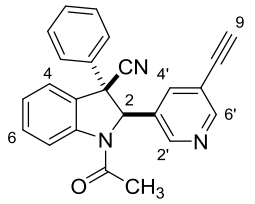

TBAF (1.0 M in THF, 0.35 mL, 0.35 mmol) was added dropwise to a solution of alkyne **117** (120 mg, 0.28 mmol) in THF (5 mL) at 0 °C and stirred at rt for 15 min. The mixture was diluted with EtOAc (10 mL) and washed three times with water, then with brine, dried over $MgSO_4$, filtered, and concentrated. Purification by flash pressure column chromatography (36% EtOAc/etroleum ether) afforded alkyne **119** as a colorless oil (94 mg, 0.26 mmol, 92%).

^{1}H (500 MHz, C_6D_6, 348 K): δ 8.71 (1H, app s, *H*2'/*H*6'), 8.46 (1H, app s, *H*2'/*H*6'), 8.12 (1H, app br s, *H*7), 7.53 (1H, app s, *H*4'), 7.14-7.20 (2H, obscured, *o-Ph*), 7.05 (1H, app t, *J* 7.9, *H*6), 6.95-7.03 (4H, m, *H*4, *m-Ph*, *p-Ph*), 6.73 (1H, app t, *J* 7.6, *H*5), 5.16 (1H, s, *H*2), 2.66 (1H, s, *H*9), 1.45 (3H, s, CH_3).

^{13}C (126 MHz, C_6D_6, 348 K): δ 167.9 (*C*=O), 154.5 (*C*2'/*C*6'), 148.3 (*C*2'/*C*6'), 143.6 (*C*7a), 141.0, 137.0 (*C*4'), 133.9, 131.3 (*C*6), 130.2 (*m-Ph*/*p-Ph*), 129.7, 129.4 (*m-Ph*/*p-Ph*), 126.4 (*C*4), 126.2 (*o-Ph*), 126.0 (*C*5), 120.5 (*C*5'), 118.9 (*C*N), 117.5 (*C*7), 82.1 (*C*8/*C*9), 80.5 (*C*8/*C*9), 74.4 (*C*2), 58.0 (*C*3), 23.6 (*C*H_3).

HRMS (ES$^+$): $[C_{24}H_{17}N_3NaO]^+$ ([M+Na]$^+$) requires 386.1264; found 386.1265.

IR: ν_{max} (film)/cm^{-1} 3286, 3021, 2260, 1675 (C=O), 1480, 1385, 1025, 753, 697.

Ethyl (2*RS*,3*RS*)-1-acetyl-2-(5-bromopyridin-3-yl)-3-cyanoindoline-3-carboxylate **78**

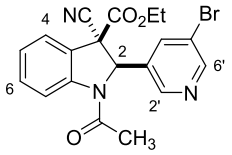

Indoline **78** was prepared according to general procedure 2, using indoline **77** (840 mg, 2.26 mmol), acetyl chloride (0.20 mL, 2.7 mmol), and pyridine (0.20 mL, 2.7 mmol) in CH_2Cl_2 (35 mL). The reaction mixture was stirred at rt for 15 min. Purification by flash pressure column chromatography (36% EtOAc/petroleum ether) afforded indoline **78** as a colorless solid (819 mg, 1.97 mmol, 87%).

^{1}H (500 MHz, C_6D_6, 348 K): δ 8.44 (1H, d, *J* 1.8, *H*6'), 8.25 (1H, d, *J* 1.6, *H*2'), 7.72 (1H, app br s, *H*7), 7.36 (1H, app t, *J* 1.8, *H*4'), 7.00 (1H, app t, *J* 7.8, *H*6), 6.77 (1H, app t, *J* 7.6, *H*5), 5.73 (1H, s, *H*2), 3.48 (2H, q, *J* 7.1, OC*H*$_2$CH$_3$), 1.55 (3H, s, C*H*$_3$), 0.63 (3H, t, *J* 7.1, OCH$_2$C*H*$_3$).ǂ

^{13}C (126 MHz, C_6D_6, 348 K): δ 167.3 (*C*=O), 163.9 (*C*=O), 152.1 (*C*6'), 147.2 (*C*2'), 143.5 (*C*7a), 137.2 (*C*4'), 133.6 (*C*3'), 131.4 (*C*6), 127.1 (*C*4), 125.2 (*C*5), 125.0 (*C*3a), 120.8 (*C*5'), 117.5 (*C*N), 116.7 (*C*7), 69.5 (*C*2), 63.6 (O*C*H$_2$CH$_3$), 55.6 (*C*3), 13.4 (*C*H$_3$), 13.3 (OCH$_2$*C*H$_3$).

ǂ 1 peak obscured by solvent signal.

HRMS (ES$^+$): [$C_{19}H_{16}{}^{79}BrNaN_3O_3$]$^+$ ([M+Na]$^+$) requires 436.0273; found 436.0276.

IR: ν_{max} (film)/cm^{-1} 2984, 2248, 1754, 1677 (C=O), 1481, 1385, 1253, 1021, 755, 705.

MP: 91-93 °C.

Methyl (2*RS*,3*SR*)-1-acetyl-2-(5-bromopyridin-3-yl)-3-phenylindoline-3-carboxylate **67**

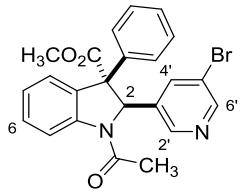

Indoline **67** was prepared according to general procedure 2, using indoline **65** (65 mg, 0.16 mmol), acetyl chloride (14 µL, 0.19 mmol), and pyridine (15 µL, 0.19 mmol) in CH_2Cl_2 (5 mL). The reaction mixture was stirred at rt for 15 min. Purification by flash pressure column chromatography (30% EtOAc/petroleum ether) afforded indoline **67** as a colorless paste (72 mg, 0.16 mmol, 99%).

^{1}H (500 MHz, C_6D_6, 348 K): δ 8.41 (1H, app br s, *H*7), 8.24 (1H, d, *J* 2.1, *H*2'/*H*6'), 8.02 (1H, d, *J* 1.4, *H*2'/*H*6'), 7.30 (1H, app d, *J* 7.7, *H*4), 7.15 (1H, obscured, *H*5), 7.00 (1H, app s, *H*4'), 6.90 (1H, app td, *J* 7.7, 1.0, *H*6), 6.77-6.81 (3H, m, *Ph*), 6.72-6.77 (2H, m, *Ph*), 6.31 (1H, s, *H*2), 3.19 (3H, s, CO_2CH_3), 1.83 (3H, s, CH_3).

^{13}C (126 MHz, C_6D_6, 348 K): δ 172.6 (*C*=O), 167.9 (*C*=O), 150.3 (*C*2'/*C*6'), 147.1 (*C*2'/*C*6'), 144.7 (*C*7a), 137.1 (*C*4'), 136.9, 136.2, 130.4 (*C*6), 129.5, 128.6 (*Ph*), 128.1 (*Ph*), 127.9 (*Ph*), 124.4 (*C*5), 120.4 (*C*5'), 117.5 (*C*7), 69.6 (*C*2), 67.9 (CO_2CH_3), 52.8 (C3), 23.7 (CH_3).‡

‡ 1 peak obscured by solvent signal.

HRMS (ES$^+$): $[C_{23}H_{20}{}^{79}BrO_3N_2]^+$ ([M+H]$^+$) requires 451.0652; found 451.0651.

IR: ν_{max}(film)/cm^{-1} 3044, 1731, 1673 (C=O), 1477, 1389, 1231, 939, 730, 699, 662.

(2*RS*,3*SR*)-1-Acetyl-2-(3-bromophenyl)-3-phenylindoline-3-carbonitrile **126**

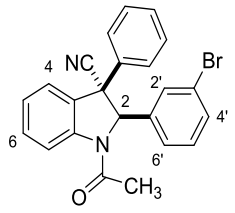

Indoline **126** was prepared according to general procedure 2, using indoline **124** (100 mg, 0.27 mmol), acetyl chloride (23 µL, 0.32 mmol), and pyridine (26 µL, 0.32 mmol) in CH_2Cl_2 (6 mL). The reaction mixture was stirred at rt for 25 min. Purification by flash pressure column chromatography (15% EtOAc/petroleum ether) afforded indoline **126** as a colorless solid (97 mg, 0.23 mmol, 87%).

^{1}H (500 MHz, C_6D_6, 348 K): δ 8.48 (1H, app br s, *H*7), 7.13 (1H, app td, *J* 7.7, 1.4, *H*6), 6.93 (2H, app d, *J* 7.3, *o*-*Ph*), 6.73-6.88 (6H, m, *m*-*Ph*, *p*-*Ph*, *H*4, *H*4', *H*5), 6.61 (1H, app br s, *H*2'), 6.40 (1H, app d, *J* 7.8, *H*6'), 6.33 (1H, app t, *J* 7.8, *H*5'), 5.52 (1H, s, *H*2), 1.62 (3H, s, *C*H_3).

^{13}C (126 MHz, C_6D_6, 348 K): δ 168.6 (*C*=O), 145.2 (*C*7a), 139.2, 134.2, 131.8, 131.4, 131.3 (*C*6), 130.3, 129.2, 128.8, 128.8, 126.6, 125.7, 125.5 (*C*5), 123.1 (*C*N), 121.7 (*C*3'), 117.9 (*C*7), 75.1 (*C*2), 56.2 (*C*3), 24.1 (*C*H_3).‡

‡ 1 peak obscured by solvent signal.

HRMS (ES$^+$): $C_{23}H_{17}{}^{79}BrNaN_2O^+$ ([M+Na]$^+$) requires 439.0422; found 439.0415.

IR: ν_{max}(film)/cm^{-1} 3064, 2236, 1677 (C=O), 1478, 1387, 1282, 757, 728, 694.

MP: 125-128 °C.

(2*RS*,3*RS*)-1-Acetyl-2-(3-bromophenyl)-3-phenylindoline-3-carbonitrile **127**

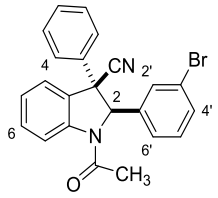

Indoline **127** was prepared according to general procedure 2, using indoline **125** (170 mg, 0.45 mmol), acetyl chloride (39 µL, 0.54 mmol), and pyridine (44 µL, 0.54 mmol) in CH_2Cl_2 (10 mL). The reaction mixture was stirred at rt for 25 min. Purification by flash pressure column chromatography (16% EtOAc/petroleum ether) afforded indoline **127** as a colorless solid (179 mg, 0.43 mmol, 95%).

^{1}H (500 MHz, C_6D_6, 348 K): δ 8.42 (1H, app br s, *H*7), 7.37 (1H, app s, *H*2'), 7.20-7.25 (2H, m, *o-Ph*), 7.19 (1H, app d, *J* 8.2, *H*4'), 7.13 (1H, app t, *J* 7.9, *H*6), 7.06 (1H, app d, *J* 7.6, *H*4), 6.96-7.04 (3H, m, *m-Ph*, *p-Ph*), 6.90 (1H, app d, *J* 7.9, *H*6'), 6.77 (1H, app t, *J* 7.6, *H*5), 6.68 (1H, app t, *J* 7.9, *H*5'), 5.08 (1H, s, *H*2), 1.48 (3H, s, CH_3).

^{13}C (126 MHz, C_6D_6, 348 K): δ 168.3 (*C*=O), 144.1 (*C*7a), 141.6 (*i-Ph*), 141.0 (*C*1'), 133.2 (*C*4'), 131.6 (*C*5'), 131.2 (*C*6), 130.5 (*C*2'), 130.2 (*m-Ph*/*p-Ph*), 130.0 (*C*3a), 129.3 (*m-Ph*/*p-Ph*), 126.4 (*C*4), 126.2 (*o-Ph*), 125.9 (*C*5), 125.3 (*C*6'), 124.0 (*C*3'), 118.8 (*C*N), 117.7 (*C*7), 76.4 (*C*2), 58.4 (*C*3), 23.8 (*C*H_3).

HRMS (ES$^+$): $[C_{23}H_{17}{}^{79}BrNaN_2O]^+$ ($[M+Na]^+$) requires 439.0422; found 439.0414.

IR: ν_{max} (film)/cm^{-1} 3063, 2238, 1676 (C=O), 1463, 1387, 1242, 757, 738, 696.

MP: 149-152 °C.

(2*RS*,3*RS*)-1-Acetyl-2-(5-bromofuran-2-yl)-3-phenylindoline-3-carbonitrile **139** and (2*RS*,3*SR*)-1-Acetyl-2-(5-bromofuran-2-yl)-3-phenylindoline-3-carbonitrile **140**

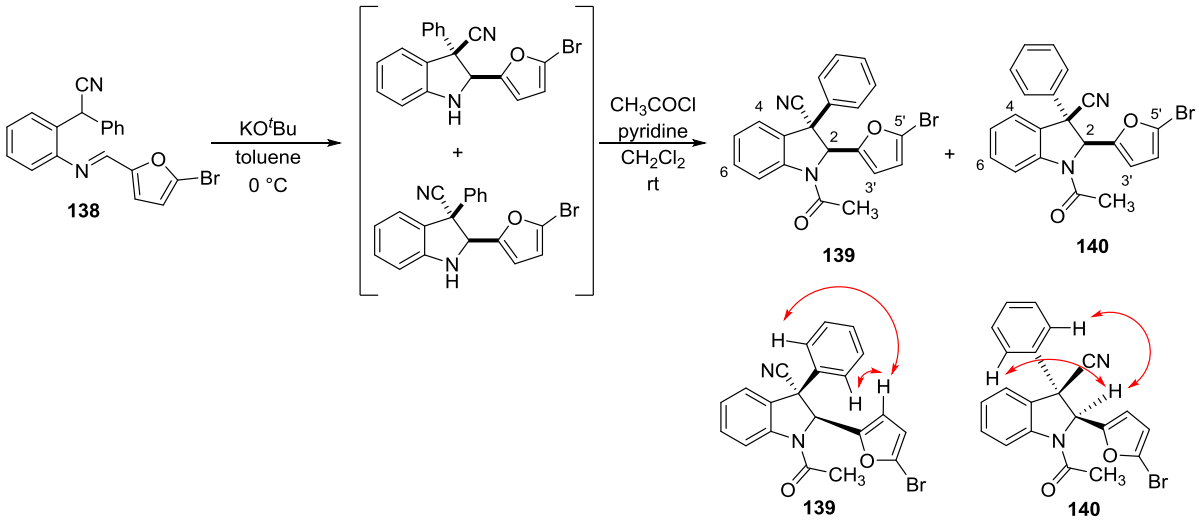

KO^{t}Bu (68 mg, 0.60 mmol) was added to a solution of imine **138** (200 mg, 0.55 mmol) in toluene (8 mL) and stirred at 0 °C for 10 min. NH_4Cl (saturated aq., 6 mL) was added, and the mixture was extracted with EtOAc. The combined organic extracts were washed with brine, dried over $MgSO_4$, and filtered. The resulting residue (200 mg) was dissolved in CH_2Cl_2 (10 mL) with pyridine (53 µL, 0.66 mmol). Acetyl chloride (47 µL, 0.66 mmol) was added dropwise, and the solution was stirred at rt for 10 min. $NaHCO_3$ (saturated aq., 5 mL) was added, and the mixture was extracted with CH_2Cl_2. The combined organic extracts were washed with brine, dried over $MgSO_4$, filtered, and concentrated. Purification by flash pressure column chromatography (3.5% Et_2O/toluene) afforded separately indoline **140** as a colorless oil (115 mg, 0.28 mmol, 52%) and indoline **139** as a colorless oil (71 mg, 0.17 mmol, 32%).

N.B. Stereochemistry assigned by nOe analysis, with red arrows indicating through-space interactions.

(2*RS*,3*RS*)-1-Acetyl-2-(5-bromofuran-2-yl)-3-phenylindoline-3-carbonitrile **140**

^{1}H (500 MHz, C_6D_6, 348 K): δ 8.30 (1H, app br s, *H*7), 7.18-7.23 (2H, m, *o*-Ph), 7.06-7.13 (2H, m, *H*4, *H*6), 6.93-7.01 (3H, m, *m*-Ph, *p*-Ph), 6.77 (1H, app td, *J* 7.6, 0.8, *H*5), 5.85 (1H, d, *J* 3.4, *H*3'/*H*4'), 5.80 (1H, d, *J* 3.4, *H*3'/*H*4'), 5.27 (1H, br s, *H*2), 1.53 (3H, s, C*H*$_3$).

^{13}C (126 MHz, C_6D_6, 348 K): δ 168.0 (*C*=O), 153.2 (*C*2'), 143.4 (*C*7a), 140.5 (*i-Ph*), 131.0 (*C*6), 130.1 (*m*-Ph), 130.0 (*p*-Ph), 129.4 (*C*3a), 126.3 (*o*-Ph), 126.2 (*C*4), 125.7 (*C*5), 123.9 (*C*5'), 118.7 (*C*N), 118.0 (*C*7), 113.4 (*C*3'/*C*4'), 111.9 (*C*3'/*C*4'), 70.9 (*C*2), 56.9 (*C*3), 23.2 (CH_3).

HRMS (ES^+): $[C_{21}H_{16}{}^{79}BrN_2O_2]^+$ ($[M+H]^+$) requires 407.0390; found 407.0382.

IR: ν_{max} (film)/cm^{-1} 3128, 3064, 2241, 1677 (C=O), 1600, 1479, 1387, 1351, 1122, 735, 668.

(2*RS*,3*SR*)-1-Acetyl-2-(5-bromofuran-2-yl)-3-phenylindoline-3-carbonitrile **139**

^{1}H (500 MHz, C_6D_6, 348 K): δ 8.35 (1H, app br s, *H*7), 7.13-7.14 (2H, m, *o*-Ph), 7.10 (1H, app td, *J* 7.7, 1.2, *H*6), 6.91-7.02 (3H, m, *m*-Ph, *p*-Ph), 6.82 (1H, app d, *J* 7.7, *H*4), 6.74 (1H, app td, *J* 7.7, 0.9, *H*5), 5.60 (1H, s, *H*2), 5.48 (1H, d, *J* 3.2, *H*4'), 5.43 (1H, d, *J* 3.2, *H*3'), 1.63 (3H, s, CH_3).

^{13}C (126 MHz, C_6D_6, 348 K): δ 168.2 (*C*=O), 151.5 (*C*2'), 144.7 (*C*7a), 134.0 (*i*-Ph), 131.2 (*C*6), 130.1 (*C*3a), 129.4 (*p*-Ph), 128.9 (*m*-Ph), 128.9 (*o*-Ph), 126.4 (*C*4), 125.3 (*C*5), 123.2 (*C*5'), 121.0 (*C*N), 118.1 (*C*7), 112.7 (*C*3'), 112.5 (*C*4'), 70.1 (*C*2), 55.4 (*C*3), 23.5 (*C*H_3).

HRMS (ES^+): $[C_{21}H_{16}{}^{79}BrN_2O_2]^+$ ($[M+H]^+$) requires 407.0390; found 407.0382.

IR: ν_{max} (film)/cm^{-1} 3065, 2236, 1678 (C=O), 1600, 1478, 1386, 1351, 1125, 755, 698.

(2*SR*,3*RS*/*SR*)-1-Acetyl-2-(4-bromofuran-2-yl)-3-phenylindoline-3-carbonitrile **134**

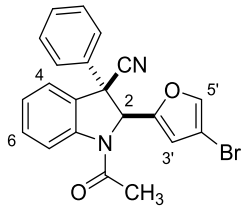

Indoline **134** was prepared according to general procedure 2, using indoline **133** (133 mg, 0.36 mmol), acetyl chloride (31 μL, 0.44 mmol), and pyridine (35 μL, 0.44 mmol) in CH_2Cl_2 (7 mL). The reaction mixture was stirred at rt for 10 min. Purification by flash pressure column chromatography (15% EtOAc/petroleum ether) afforded indoline **134** as a yellow oil (144 mg, 0.38 mmol, 97%).

^{1}H (500 MHz, C_6D_6, 348 K): δ 8.26 (1H, app br s, *H*7), 7.20-7.25 (2H, m, *o*-Ph), 7.07-7.13 (2H, m, *H*4, *H*6), 6.94-7.02 (3H, m, *m*-Ph, *p*-Ph), 6.92 (1H, s, *H*5'), 6.78 (1H, app t, *J* 7.6, *H*5), 6.08 (1H, s, *H*3'), 5.25 (1H, br s, *H*2), 1.52 (3H, s, CH_3).

^{13}C (126 MHz, C_6D_6, 348 K): δ 167.8 (*C*=O), 152.2 (*C*2'), 143.3 (*C*7a), 142.6 (*C*5'), 140.5 (*i-Ph*), 131.0 (*C*6), 130.2 (*m*-Ph), 129.4 (*p*-Ph), 128.9 (*C*3a), 126.3 (*o-Ph*), 126.1 (*C*4), 125.8 (*C*5), 118.6 (*C*N), 118.0 (*C*7), 112.9 (*C*3'), 101.3 (*C*4'), 70.8 (*C*2), 56.7 (*C*3), 23.2 (*C*H_3).

HRMS (ES$^+$): $[C_{21}H_{16}{}^{79}BrN_2O_2]^+$ ([M+H]$^+$) requires 407.0390; found 407.0383.

IR: ν_{max} (film)/cm^{-1} 3061, 2236, 1677 (C=O), 1479, 1387, 1352, 924, 755, 697.

(2*RS*,3*RS*)-1-acetyl-2-(5-(benzyloxy)pyridin-3-yl)-3-phenylindoline-3-carbonitrile **95** and (2*RS*,3*SR*)-1-Acetyl-2-(5-(benzyloxy)pyridin-3-yl)-3-phenylindoline-3-carbonitrile **94**

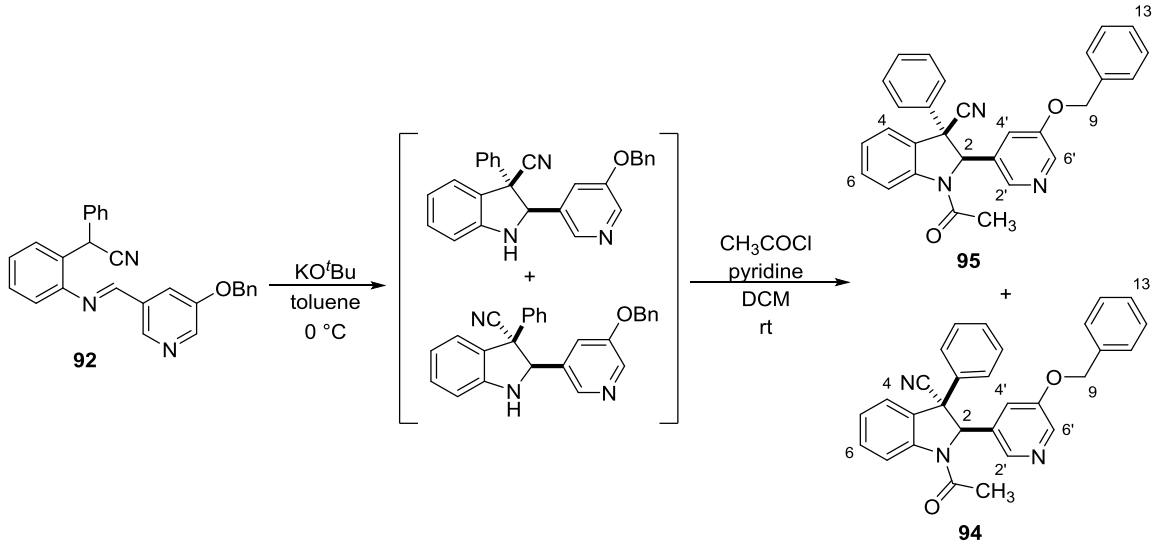

Racemic:

^{t}BuOK (706 mg, 6.29 mmol) was added to a solution of imine **92** (1.27 g, 3.15 mmol) in toluene (60 mL) and stirred at 0 °C for 25 min. NH_4Cl (saturated aq., 60 mL) was added, and the mixture was extracted 3 times with EtOAc. The combined organic extracts were washed with brine, dried over Na_2SO_4, filtered, and concentrated. Purification by flash pressure column chromatography (30% EtOAc/petroleum ether) afforded an inseparable mixture of diastereomers (853 mg,

2.11 mmol, 67%). This mixture (755 mg, 1.87 mmol) was dissolved in CH_2Cl_2 (40 mL) with pyridine (212 µL, 2.63 mmol). Acetyl chloride (181 µL, 2.53 mmol) was added dropwise, and the solution was stirred at rt for 30 min. $NaHCO_3$ (saturated aq., 40 mL) was added, and the mixture was extracted with CH_2Cl_2. The combined organic extracts were washed with brine, dried over $MgSO_4$, filtered, and concentrated. Purification by flash pressure column chromatography (15% EtOAc/petroleum ether) afforded separately diastereomers **95** as a colorless solid (376 mg, 0.84 mmol, 45%) and **94** as a colorless solid (167 mg, 0.38 mmol, 20%).

Asymmetric:

Indolines **(*R,R*)-95** and **(*S,S*)-95** were prepared according to general procedure 2 using indoline **(*R,R*)-93** (157 mg, 0.39 mmol), acetyl chloride (33 µL, 0.47 mmol), and pyridine (38 µL, 0.47 mmol) in CH_2Cl_2 (8.5 mL) and indoline **(*S,S*)-93** (216 mg, 0.54 mmol), acetyl chloride (46 µL, 0.64 mmol), and pyridine (52 µL, 0.64 mmol) in CH_2Cl_2 (10 mL). Purification by flash pressure column chromatography (50% EtOAc/petroleum ether) afforded indolines **(*R,R*)-95** (165 mg, 0.37 mmol, 95%) and **(*S,S*)-95** (230 mg, 0.52 mmol, 96%) respectively.

(2*RS*,3*RS*)-1-acetyl-2-(5-(benzyloxy)pyridin-3-yl)-3-phenylindoline-3-carbonitrile **95**

^{1}H (500 MHz, C_6D_6, 348 K): δ 8.45 (1H, app s, *H*2'/*H*6'), 8.33 (1H, app br s, *H*7), 8.26 (1H, app s, *H*2'/*H*6'), 7.22 (2H, app d, *J* 7.6, *o-Ph*), 6.97-7.13 (11H, m, *H*4, *H*4', *H*6, *m-Ph*, *p-Ph*, *H*11, *H*12, *H*13), 6.77 (1H, app t, *J* 7.6, *H*5), 5.20 (1H, br s, *H*2), 4.50-4.61 (2H, d, *J* 12.5, *H*9), 1.48 (3H, br s, C*H*$_3$).

^{13}C (126 MHz, C_6D_6, 348 K): δ 168.2 (*C*=O), 156.1 (*C*5'), 144.0 (*C*7a), 141.7 (*C*2'/*C*6'), 141.3, 140.9 (*C*2'/*C*6'), 136.8 (*C*10), 134.8, 131.2, 130.2, 129.9, 129.4, 129.1, 126.4, 126.3 (*o-Ph*), 125.9 (*C*5), 119.7 (*C*4'), 119.0 (*C*N), 117.7 (*C*7), 74.7 (*C*2), 71.2 (*C*9), 58.3 (*C*3), 23.7 (*C*H$_3$).‡

‡ 2 peaks obscured.

HRMS (ES$^+$): $[C_{29}H_{24}N_3O_2]^+$ ([M+H]$^+$) requires 446.1863; found 446.1854.

IR: ν_{max} (film)/cm^{-1} 2981, 2241, 1675 (C=O), 1479, 1386, 1277, 753, 669.

MP: 61-64 °C.

$[\alpha]_D^{25.0}$ (*R*,*R*) = +76 (*c* = 0.1, $CHCl_3$); $[\alpha]_D^{25.0}$ (*S*,*S*) = -84 (*c* = 0.1, $CHCl_3$).

(2*RS*,3*SR*)-1-Acetyl-2-(5-(benzyloxy)pyridin-3-yl)-3-phenylindoline-3-carbonitrile **94**

^{1}H (500 MHz, C_6D_6, 348 K): δ 8.61 (1H, app br s, *H*7), 8.45 (1H, d, *J* 2.7, *H*2'/*H*6'), 8.28 (1H, app s, *H*2'/*H*6'), 7.19-7.24 (2H, m, *o*-*Ph*), 6.87-7.12 (11H, m, *H*4, *H*4', *H*6, *m*-*Ph*, *p*-*Ph*, *H*11, *H*12, *H*13), 6.70 (1H, app td, *J* 7.6, 1.0, *H*5), 5.09 (1H, br s, *H*2), 4.42 (1H, d, *J* 11.7, *H*9), 4.38 (1H, d, *J* 11.7, *H*9'), 1.36 (3H, br s, C*H*$_3$).

^{13}C (126 MHz, C_6D_6, 348 K): δ 168.0 (*C*=O), 155.5 (*C*5'), 143.5 (*C*7a), 141.1 (*C*2'/*C*6'), 140.7, 140.0 (*C*2'/*C*6'), 136.1, 134.4, 130.9, 129.8, 129.0, 128.7, 127.9, 126.0, 125.9, 125.7 (*C*5), 118.8 (*C*4'/*C*N), 118.7 (*C*4'/*C*N), 117.3 (*C*7), 73.9 (*C*2), 70.3 (*C*9), 57.8 (*C*3), 23.3 (*C*H$_3$).‡

‡ 2 peaks obscured.

HRMS (ES$^+$): $[C_{29}H_{24}N_3O_2]^+$ ([M+H]$^+$) requires 446.1863; found 446.1860.

IR: ν_{max}(film)/cm^{-1} 3033, 2239, 1675 (C=O), 1594, 1479, 1385, 1277, 738, 698.

MP: 63-68 °C.

(2*RS*,3*SR*)-1-Acetyl-2-(5-hydroxypyridin-3-yl)-3-phenylindoline-3-carbonitrile **96**

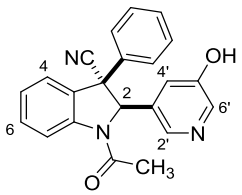

Indoline **96** was prepared according to general procedure 3, using indoline **94** (150 mg, 0.34 mmol) and Pd/C (wet degussa type, 15 mg) in MeOH (10 mL). The reaction mixture was stirred under a H_2 atmosphere for 5.5 h. The crude residue was triturated with toluene to afford indoline **96** as a colorless solid (75 mg, 0.21 mmol, 63%).

^{1}H NMR (500 MHz, CD_3OD): δ 8.28 (1H, app br s, *H*7), 7.77 (1H, d, *J* 2.4, *H*6'), 7.59 (1H, app td, *J* 7.8, 1.1, *H*6), 7.38 (1H, d, *J* 1.3, *H*2'), 7.31 (1H, app td, *J* 7.8, 1.1, *H*5), 7.19-7.28 (4H, m, *H*4, *Ph*), 7.15 (2H,

m, *Ph*), 6.61 (1H, app t, *J* 1.9, *H*4'), 6.30 (1H, s, *H*2), 2.16 (3H, br s, C*H*$_3$).ł

^{13}C NMR (126 MHz, CD_3OD): δ 171.5 (*C*=O), 155.7 (*C*5'), 145.3 (*C*7a), 140.0 (*C*2'), 138.5 (*C*6'), 134.5 (*C*3'), 133.7 (*i-Ph*), 132.4 (*C*6), 130.4 (*Ph*), 129.8 (*Ph*), 129.8 (*Ph*), 127.6 (*C*4), 127.0 (*C*5), 122.5 (*C*4'), 122.3 (*C*N), 118.8 (*C*7), 72.9 (*C*2), 56.6 (*C*3), 24.2 (*C*H_3).‡

ł O*H* peak not observed due to exchange with MeOD.

‡ 1 peak obscured.

HRMS (ES$^+$): $[C_{22}H_{18}N_3O_2]^+$ ($[M+H]^+$) requires 356.1394; found 356.1390.

IR: ν_{max} (film)/cm^{-1} 3065, 2236, 1671 (C=O), 1591, 1479, 1388, 1280, 700, 625.

MP: 132-136 °C.

(2*RS*,3*SR*)-1-Acetyl-2-(5-hydroxypyridin-3-yl)-3-phenylindoline-3-carbonitrile **100**

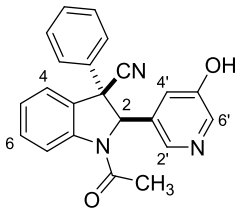

Indoline **100** was prepared according to general procedure 3, using indoline **95** (390 mg, 0.88 mmol) and Pd/C (wet degussa type, 36 mg) in MeOH (24 mL). The reaction mixture was stirred under a H_2 atmosphere for 5 h. The crude residue was triturated with toluene to afford indoline **100** as a colorless solid (308 mg, 0.87 mmol, 98%). The non-racemic forms of indoline **100** were prepared from **(*R,R*)-95** and **(*S,S*)-95**, following an identical protocol.

^{1}H NMR (500 MHz, CD_3OD): δ 8.33 (1H, app br s, *H*7), 8.15 (1H, app br s, *H*6'), 8.06 (1H, app br s, *H*2'), 7.57 (1H, app t, *J* 7.7, *H*6), 7.36-7.46 (4H, m, *H*4, *m-Ph*, *p-Ph*), 7.32 (1H, app t, *J* 7.7, *H*5), 7.28 (2H, m, *o-Ph*), 7.05 (1H, app t, *J* 2.0, *H*4'), 5.75 (1H, s, *H*2), 1.99 (3H, br s, C*H*$_3$).ł

^{13}C NMR (126 MHz, CD_3OD): δ 171.2 (*C*=O), 156.3 (*C*5'), 144.2 (*C*7a), 141.0 (*i-Ph*), 140.0 (*C*6'), 139.6

(*C*2'), 136.6 (*C*3'), 132.2 (*C*6), 130.9 (*m-Ph*/*p-Ph*), 130.4 (*m-Ph*/*p-Ph*), 127.2 (*C*5), 127.2 (*C*4), 126.9 (*o-Ph*), 121.7 (*C*4'), 119.8 (*C*N), 118.5 (*C*7), 74.1 (*C*2), 58.8 (*C*3), 24.0 (CH_3).‡

ł O*H* peak not observed due to exchange with MeOD.

‡ 1 peak obscured.

HRMS (ES^+): $[C_{22}H_{18}N_3O_2]^+$ ($[M+H]^+$) requires 356.1394; found 356.1389.

IR: ν_{max}(film)/cm^{-1} 3062, 2234, 1671 (C=O), 1591, 1480, 1387, 1278, 757, 673.

MP: 120-125 °C.

$[\alpha]_D^{25.0}$ (*R*,*R*) = +72 (*c* = 0.1, $CHCl_3$); $[\alpha]_D^{25.0}$ (*S*,*S*) = -73 (*c* = 0.1, $CHCl_3$).

5-((2*R*,3*R*)/(2*S*,3*S*)-1-Acetyl-3-cyano-3-phenylindolin-2-yl)pyridin-3-yl trifluoromethanesulfonate

157

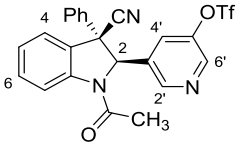

(***R*,*R*)-157**

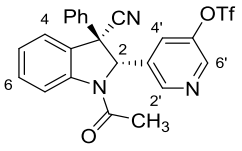

(***S*,*S*)-157**

5-((2*R*,3*R*)-1-Acetyl-3-cyano-3-phenylindolin-2-yl)pyridin-3-yl trifluoromethanesulfonate **157**

Diisopropylethylamine (49 µL, 0.28 mmol) was added to a solution of indoline **(*R*,*R*)-100** (50 mg, 0.14 mmol) and *N*-phenyl-bis(trifluoromethylsulfonimide) (100 mg, 0.28 mmol) in CH_2Cl_2 (4 mL) at 0 °C. The reaction mixture was allowed to warm to rt and stirred for 3 h. H_2O (10 mL) was added, and the mixture was extracted with CH_2Cl_2. The combined organic extracts were washed with brine, dried over Na_2SO_4, filtered, and concentrated. Purification by flash pressure column chromatography (30% EtOAc/petroleum ether) afforded indoline **(*R*,*R*)-157** as a colorless hygroscopic solid (53 mg, 0.11 mmol, 79%).

5-((2*S*,3*S*)-1-acetyl-3-cyano-3-phenylindolin-2-yl)pyridin-3-yl trifluoromethanesulfonate **157**

Indoline **(*S*,*S*)-157** was prepared in an analogous manner to indoline **(*R*,*R*)-157**, using indoline **(*S*,*S*)-100** (148 mg, 0.42 mmol), diisopropylethylamine (0.15 mL, 0.83 mmol), and *N*-phenyl-bis(trifluoromethylsulfonimide) (298 mg, 0.83 mmol) in CH_2Cl_2 (12 mL). The reaction mixture was stirred at rt for 3 h. Purification by flash pressure column chromatography (30% EtOAc/petroleum ether) afforded indoline **(*S*,*S*)-157** as a colorless hygroscopic solid (189 mg, 0.39 mmol, 93%).

Alternatively, indoline **(*S*,*S*)-157** was prepared according to general procedure 2, using indoline **267** (52 mg, 0.12 mmol), acetyl chloride (17 µL, 0.23 mmol), and pyridine (19 µL, 0.23 mmol) in CH_2Cl_2 (2 mL). The reaction mixture was stirred at rt for 20 min. Purification by flash pressure column chromatography (30% EtOAc/petroleum ether) afforded indoline **(*S*,*S*)-157** as a colorless hygroscopic solid (52 mg, 0.11 mmol, 92%).

^{1}H (500 MHz, C_6D_6, 348 K): δ 8.44 (1H, app s, *H*2'/*H*6'), 8.34 (1H, d, *J* 2.1, *H*2'/*H*6'), 7.96 (1H, app br s, *H*7), 7.24 (1H, app s, *H*4'), 7.11-7.21 (2H, obscured, *o-Ph*), 7.06 (1H, app t, *J* 7.9, *H*6), 6.94-7.03 (4H, m, *H*4, *m-Ph*, *p-Ph*), 6.74 (1H, app t, *J* 7.6, *H*5), 5.23 (1H, s, *H*2), 1.50 (3H, s, CH_3).

^{13}C (126 MHz, C_6D_6, 348 K): δ 167.7 (*C*=O), 148.4 (*C*2'/*C*6'), 147.4, 144.2 (*C*2'/*C*6'), 143.2, 140.4, 136.2, 131.4 (*C*6), 130.3 (*m-Ph*/*p-Ph*), 129.7, 129.6 (*m-Ph*/*p-Ph*), 127.1 (*C*4'), 126.6 (*C*4), 126.2 (*o-Ph*), 126.2 (*C*5), 118.6 (*C*N), 117.2 (*C*7), 73.6 (*C*2), 57.7 (*C*3), 23.5 (*C*H_3).‡

‡ CF_3 signal obscured due to insufficient signal-to-noise ratio.

^{19}F (377 MHz, C_6D_6): δ -72.7.

HRMS (ES^+): $[C_{23}H_{17}O_4N_3F_3{}^{32}S]^+$ ($[M+H]^+$) requires 488.0886; found 488.0887.

IR: ν_{max}(film)/cm^{-1} 2981, 2236, 1678 (C=O), 1479, 1429, 1385, 1219, 1138, 835, 752, 698.

$[\alpha]_D^{25.0}$ (*R*,*R*) = +51 (*c* = 0.1, $CHCl_3$), $[\alpha]_D^{25.0}$ (*S*,*S*) = -60 (*c* = 0.1, $CHCl_3$).

(2*RS*,3*SR*)-1-Acetyl-2-(5-bromopyridin-3-yl)-3-phenyl-2,3-dihydro-1H-pyrrolo[3,2-b]pyridine-3-carbonitrile **180**

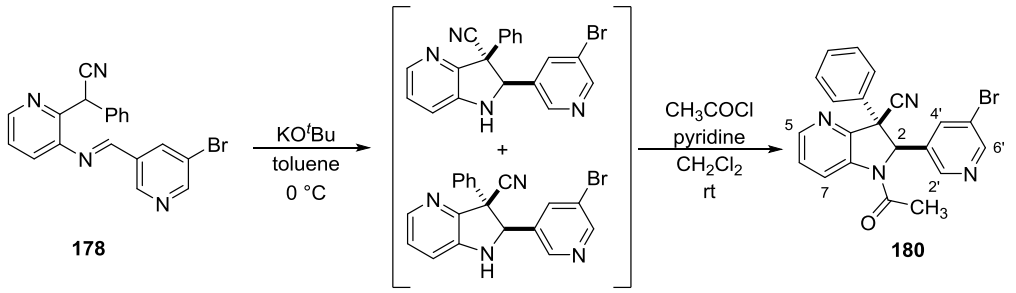

KO^{t}Bu (65 mg, 0.58 mmol) was added to a solution of imine **178** (200 mg, 0.53 mmol) in toluene and stirred at 0 °C for 20 min. NH_4Cl (saturated aq., 20 mL) was added, and the mixture was extracted with EtOAc. The combined organic extracts were washed with brine, dried over Na_2SO_4, filtered, and concentrated. Purification by flash pressure column chromatography (50% EtOAc/petroleum ether) afforded a 1:1.2 inseparable mixture of diastereoisomers (87 mg, 0.23 mmol, 44%). 60 mg (0.16 mmol) of the residue was dissolved in CH_2Cl_2 (6 mL). Pyridine (19 µL, 0.24 mmol) was added, followed by acetyl chloride (17 µL, 0.24 mmol). The mixture was stirred at rt for 2 h. $NaHCO_3$ (saturated aq., 6 mL) was added, and the mixture was extracted with CH_2Cl_2. The combined organic extracts were washed with brine, dried over Na_2SO_4, filtered and concentrated. Purification by flash pressure column chromatography afforded indoline **180** as a colorless hygroscopic solid as a 19:1 mixture of diastereoisomers (38 mg, 0.09 mmol, 57%).

N.B. Stereochemistry assigned by analogy to indolines **52** and **53**.

^{1}H (500 MHz, C_6D_6, 348 K): δ 8.57 (1H, d, *J* 1.9, *H*2'/*H*6'), 8.33 (1H, d, *J* 1.9, *H*2'/*H*6'), 8.19 (1H, app br s, *H*7), 7.98 (1H, dd, *J* 4.7, 1.3, *H*5), 7.48 (1H, app t, *J* 1.9, *H*4'), 7.23 (2H, app d, *J* 8.0, Ph), 6.93-7.03 (3H, m, Ph), 6.63 (1H, dd, *J* 8.2, 4.7, *H*6), 5.17 (1H, s, *H*2), 1.41 (3H, s, C*H*$_3$).

^{13}C (126 MHz, C_6D_6, 348 K): δ 168.6 (*C*=O), 153.1 (*C*2'/*C*6'), 149.8, 147.4 (*C*5), 146.9 (*C*2'/*C*6'), 139.8, 137.5, 136.7 (*C*4'), 135.5, 130.3 (Ph), 129.5 (Ph), 126.2 (Ph), 125.0 (*C*6), 124.3 (*C*5'), 121.9 (*C*N), 117.5 (*C*7), 72.3 (*C*2), 59.4 (*C*3), 23.2 (*C*H$_3$).

HRMS (ES$^+$): $[C_{21}H_{16}{}^{79}BrN_4O]^+$ ([M+H]$^+$) requires 419.0502; found 419.0504.

IR: ν_{max} (film)/cm^{-1} 3035, 2241, 1682 (C=O), 1439, 1354, 1227, 701, 683.

1-(5'-Azidopentyl)pyrrolidine **114**

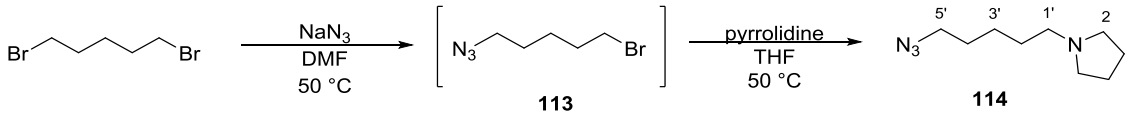

Azide **113** was prepared according to a literature procedure.[191] NaN_3 (286 mg, 4.42 mmol) was added to a solution of 1,5-dibromopentane (1.2 mL, 8.8 mL) in DMF (30 mL) and stirred at 50 °C for 3 h. The mixture was allowed to cool to rt, diluted with EtOAc, and washed with H_2O, then brine. The organic layer was dried over Na_2SO_4, filtered, and concentrated. Purification by flash pressure column chromatography (3.5% Et_2O/hexane) afforded **113** as a colorless liquid (557 mg, 2.90 mmol, 66%). Azide **113** was not fully characterized due to concerns about its toxicity and stability.

A solution of azide **113** (200 mg, 1.04 mmol) in dry THF (2 mL) was added dropwise to a solution of pyrrolidine (0.96 mL, 12 mmol) in dry THF (3 mL) and stirred at 50 °C for 1 h. Water (5 mL) was added, and the mixture was extracted with Et_2O. The combined organic extracts were washed with brine, dried over $MgSO_4$, filtered, and concentrated to afford azide **114** as a yellow liquid (171 mg, 0.94 mmol, 90%).

^{1}H (400 MHz, $CDCl_3$): δ 3.27 (2H, t, *J* 7.0, *H*5'), 2.37-2.55 (6H, m, *H*1', *H*2), 1.81 (4H, m, *H*3), 1.49-1.68 (4H, m, *H*2', *H*4'), 1.41 (2H, app m, *H*3').

^{13}C (101 MHz, $CDCl_3$): δ 56.4 (*C*1'), 54.3 (*C*2), 51.5 (*C*5'), 28.9 (*C*2'/*C*4'), 28.5 (*C*2'/*C*4'), 24.9 (*C*3'), 23.5 (*C*3).

IR: ν_{max} (film)/cm^{-1} 3399, 2935, 2091 (N=N=N), 1459, 1266, 879.

HRMS: $[C_9H_{19}N_4]^+$ ($[M+H]^+$) requires 183.1604; found 183.1605.

(2*RS*,3*SR*)-1-Acetyl-3-phenyl-2-(5-(1-(5-(pyrrolidin-1-yl)pentyl)-1H-1,2,3-triazol-4-yl)pyridin-3-yl)indoline-3-carbonitrile **121**

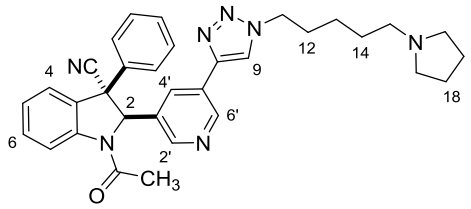

Indoline **121** was prepared according to a modified literature procedure.[192] $CuSO_4$ (aq., 2.5 mM, 0.55 mL, 0.0014 mmol) and sodium-L-ascorbate (aq., 12.5 mM, 0.55 mL, 0.0069 mmol) were added to a solution of alkyne **118** (25 mg, 0.070 mmol) and azide **114** (15 mg, 0.083 mmol) in ^{t}BuOH (1.1 mL). The mixture was stirred at rt for 16 h. H_2O (4 mL) was added, and the mixture was extracted with EtOAc. The combined organic extracts were washed with brine, dried over Na_2SO_4, filtered, and concentrated. Purification by preparatory TLC (6% MeOH/CH_2Cl_2 + 0.5% aq. NH_4OH) afforded indoline **121** as a colorless solid (9.3 mg, 0.017 mmol, 26%).

^{1}H (500 MHz, C_6D_6, 348 K): δ 8.75 (1H, d, *J* 2.0, *H*6'), 8.32 (1H, app br s, *H*7), 8.04 (1H, app s, *H*2'), 7.65 (1H, app t, *J* 2.0, *H*4'), 7.12 (1H, app td, *J* 7.8, 1.4, *H*6), 7.04-7.09 (2H, m, *Ph*), 6.84 (1H, dd, *J* 7.7, 0.9, *H*4), 6.72-6.82 (5H, m, *H*5, *H*9, *Ph*), 5.82 (1H, s, *H*2), 3.69 (2H, t, *J* 7.1, *H*11), 2.36 (4H, m, *H*17), 2.26 (2H, t, *J* 7.0, *H*15), 1.70 (3H, s, C*H*$_3$), 1.61 (4H, m, *H*18), 1.47 (2H, app quin, *J* 7.2, *H*12), 1.31 (2H, app quin, *J* 7.2, *H*14), 1.10 (2H, app quin, *J* 7.2, *H*13).

^{13}C (126 MHz, C_6D_6, 348 K): δ 168.5 (*C*=O), 148.4 (*C*6'), 147.6 (*C*9), 145.1 (*C*2'), 144.2 (*C*7a), 134.2, 132.9 (*C*4'), 131.7, 131.5 (*C*6), 129.3 (*Ph*), 129.3, 129.1 (*Ph*), 128.9 (*Ph*), 127.6, 126.7 (*C*4), 125.6 (*C*5), 121.7, 120.0, 117.9 (*C*7), 73.7 (*C*2), 56.3 (*C*15), 56.1 (*C*3), 54.6 (*C*17), 50.4 (*C*11), 30.5 (*C*12), 28.9 (*C*14), 24.9 (*C*13), 24.4 (*C*18), 24.1 (*C*H$_3$).

HRMS (ES^{+}): $[C_{33}H_{36}N_7O]^{+}$ ([M+H]$^{+}$) requires 546.2976; found 546.2983.

IR: ν_{max}(film)/cm^{-1} 2937, 2793, 2261, 1674 (C=O), 1600, 1478, 1388, 1352, 1283, 733, 700.

MP: 116-123 °C.

(2*RS*,3*RS*)-1-Acetyl-3-phenyl-2-(5-(1-(5-(pyrrolidin-1-yl)pentyl)-1H-1,2,3-triazol-4-yl)pyridin-3-yl)indoline-3-carbonitrile **122**

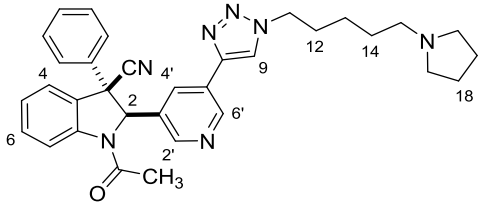

Indoline **122** was prepared according to a modified literature procedure.[192] $CuSO_4$ (aq., 10 mM, 0.33 mL, 0.0033 mmol) and sodium-L-ascorbate (aq., 50 mM, 0.13 mL, 0.0065 mmol) were added to a solution of alkyne **119** (24 mg, 0.070 mmol) and azide **114** (12 mg, 0.066 mmol) in 3:1 $^{t}BuOH/H_2O$ (1 mL). The mixture was stirred at rt for 16 h. H_2O (4 mL) was added, and the mixture was extracted with EtOAc. The combined organic extracts were washed with brine, dried over Na_2SO_4, filtered, and concentrated. Purification by preparatory TLC (6% $MeOH/CH_2Cl_2$ + 0.5% aq. NH_4OH) afforded indoline **122** as a colorless solid (9.5 mg, 0.017 mmol, 26%).

^{1}H (500 MHz, C_6D_6, 348 K): δ 9.06 (1H, d, *J* 2.0, *H*6'), 8.61 (1H, d, *J* 2.0, *H*2'), 8.36 (1H, app t, *J* 2.0, *H*4'), 8.32 (1H, app br s, *H*7), 7.25 (2H, m, *Ph*), 7.11 (1H, app t, *J* 7.6, *H*6), 7.08 (1H, app d, *J* 7.5, *H*4), 6.95-7.05 (3H, m, *Ph*), 6.88 (1H, s, *H*9), 6.76 (1H, app t, *J* 7.5, *H*5), 5.35 (1H, s, *H*2), 3.72 (2H, t, *J* 7.3, *H*11), 2.37 (4H, m, *H*17), 2.27 (2H, t, *J* 7.3, *H*15), 1.62 (4H, m, *H*18), 1.55 (3H, s, CH_3), 1.50 (2H, app quin, *J* 7.5, *H*12), 1.33 (2H, app quin, *J* 7.3, *H*14), 1.13 (2H, app quin, *J* 7.3, *H*13).

^{13}C (126 MHz, C_6D_6, 348 K): δ 168.2 (*C*=O), 149.1 (*C*6'), 148.0 (*C*2'), 144.4, 144.0, 141.2, 134.7 (*C*4'), 131.3 (*C*6/*C*9), 131.2 (*C*6/*C*9), 130.2 (*Ph*), 129.8, 129.3 (*Ph*), 126.4 (*C*4), 126.3 (*Ph*), 125.9 (*C*5), 120.4, 119.2, 117.8 (*C*7), 75.0 (*C*2), 58.3 (*C*3), 56.3 (*C*15), 54.6 (*C*17), 50.5 (*C*11), 30.5 (*C*12), 28.9 (*C*14), 25.0 (*C*13), 24.4 (*C*18), 23.7 (*C*H_3).‡

‡ 1 peak obscured.

HRMS (ES^+): $[C_{33}H_{36}N_7O]^+$ ($[M+H]^+$) requires 546.2976; found 546.2980.

IR: ν_{max} (film)/cm^{-1} 2935, 2793, 2261, 1673 (C=O), 1600, 1478, 1386, 1353, 912, 734.

MP: 109-114 °C.

(*E*)-7-(Tributylstannyl)hept-6-en-1-ol **55**

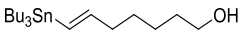

Vinylstannane **55** was prepared according to a literature procedure.[193] Pd_2dba_3 (16 mg, 0.018 mmol), cyc_3PHBF_4 (26 mg, 0.071 mmol), and DIPEA (25 μL, 0.14 mmol) were added to a solution of CH_2Cl_2 (15 mL) and stirred at rt for 10 min. 6-Heptyn-1-ol (400 mg, 3.57 mmol) was added, and the mixture was cooled to 0 °C. A solution of Bu_3SnH (1.15 mL, 4.28 mmol) in CH_2Cl_2 (5 mL) was added dropwise over 5 min and stirred at 0 °C for 2.5 h. The mixture was concentrated and the residue purified by flash pressure column chromatography (10% EtOAc/petroleum ether) to afford vinylstannane **55** as a colorless liquid (1.20 g, 2.98 mmol, 84%). The spectral data matched those previously reported in the literature.

^{1}H (400 MHz, $CDCl_3$): δ 5.93 (1H, app dt, *J* 19.0, 5.6, *H*6), 5.86 (1H, app d, *J* 19.0, *H*7), 3.65 (2H, app td, *J* 6.6, 5.4, *H*1), 2.15 (2H, td, *J* 6.9, 5.6, *H*5), 1.28-1.63 (20H, m), 0.74-0.98 (15H, m).

^{13}C (101 MHz, $CDCl_3$): δ 149.4 (*C*6), 127.3 (*C*7), 63.0 (*C*1), 37.8 (*C*5), 32.7, 29.1, 28.7, 27.3, 25.2, 13.7, 9.4.

LCMS (ES^+): 291.1 ([M(^{120}Sn)-2(C_4H_9)+H^+]), 427.2 ([M(^{120}Sn)+Na^+]).

(*E*)-1-(7-(Tributylstannyl)hept-6-en-1-yl)pyrrolidine **57**

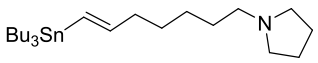

PPh_3 (972 mg, 3.71 mmol) was added portionwise to a solution of vinylstannane **55** (1.15 g, 2.85 mmol) and CBr_4 (1.23 g, 3.71 mmol) in CH_2Cl_2 (20 mL), and the mixture was stirred at 0 °C for 1 h. Ice-cooled pentane (50 mL) was added. The white precipitate was removed by filtration, and the filtrate was concentrated. The resulting residue was dissolved in THF (10 mL) and added to a solution of pyrrolidine (1.20 mL, 13.9 mmol) in THF (10 mL). The mixture was stirred at 50 °C for 4 h. H_2O (20 mL) was added and the mixture was extracted with EtOAc. The combined organic

extracts were washed with brine, dried over Na_2SO_4, filtered, and concentrated. Purification by flash pressure column chromatography (5% MeOH/CH_2Cl_2 + 0.5% aq. NH_4OH) afforded vinylstannane **57** as a yellow oil (413 mg, 0.90 mmol, 32%).

^{1}H (400 MHz, $CDCl_3$): δ 5.96 (1H, app dt, *J* 18.9, 5.8, *H*6), 5.86 (1H, app d, *J* 18.9, *H*7), 2.49 (4H, m, *H*2'), 2.42 (2H, t, *J* 7.1, *H*1), 2.14 (2H, app q, *J* 6.7, *H*5), 1.78 (4H, m, *H*3'), 1.39-1.55 (10H, m), 1.23-1.37 (8H, m), 0.82-0.93 (15H, m).

^{13}C (101 MHz, $CDCl_3$): δ 149.6 (*C*6), 127.1 (*C*7), 56.7 (*C*1), 54.2 (*C*2'), 37.8 (*C*5), 29.1, 29.0, 28.9, 27.3, 27.2, 23.4 (*C*3'), 13.7, 9.4.

HRMS (ES^+): $[C_{23}H_{48}N^{120}Sn]^+$ ($[M+H]^+$) requires 458.2807; found 458.2809.

IR: ν_{max} (film)/cm^{-1} 2956, 2926, 2872, 2853, 1457, 1146, 989.

(2*RS*,3*SR*)-1-Acetyl-3-phenyl-2-(5-((E)-7-(pyrrolidin-1-yl)hept-1-en-1-yl)pyridin-3-yl)indoline-3-carbonitrile **58**

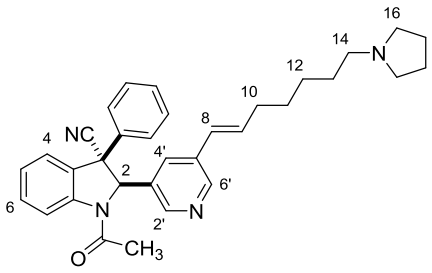

Indoline **58** was prepared according to general procedure 4, using indoline **52** (60 mg, 0.14 mmol), vinylstannane **57** (78 mg, 0.17 mmol), and $Pd(PPh_3)_4$ (17 mg, 0.014 mmol) in NMP (1.5 mL). The reaction mixture was stirred at 85 °C for 1.5 h. Purification by flash pressure column chromatography (4.5% MeOH/CH_2Cl_2 + 0.5% aq. NH_4OH) afforded indoline **58** as a pale yellow oil (38 mg, 0.075 mmol, 54%).

^{1}H (500 MHz, C_6D_6, 348 K): δ 8.41 (1H, app br s, *H*7), 8.29 (1H, d, *J* 2.0, *H*6'), 7.91 (1H, app s, *H*2'), 7.13 (1H, obscured, *H*6), 7.00 (2H, m, *o-Ph*), 6.68-6.88 (6H, m, *H*4, *H*4', *H*5, *m-Ph*, *p-Ph*), 5.86 (1H, d,

J 16.1, *H*8) 5.89 (1H, dt, *J* 16.1, 6.2, *H*9), 5.71 (1H, s, *H*2), 2.42 (4H, m, *H*16), 2.37 (2H, t, *J* 7.2, *H*14) 1.93 (2H, app q, *J* 6.9, *H*10), 1.67 (3H, s, CH_3), 1.63 (4H, m, *H*17), 1.49 (2H, app quin, *J* 7.1, *H*13), 1.23-1.35 (4H, m, *H*11, *H*12).

^{13}C (126 MHz, C_6D_6, 348 K): δ 168.4 (*C*=O), 148.4 (*C*6'), 147.2 (*C*2'), 145.1 (*C*7a), 134.5 (*C*9), 134.1, 133.4, 132.1, 131.4 (*C*6), 131.3, 129.2, 128.9, 126.5 (*C*8), 126.5 (*C*4), 125.5 (*C*5), 121.6 (*C*N), 117.8 (*C*7), 73.6 (*C*2), 56.6 (*C*3), 56.0 (*C*14), 54.5 (*C*16), 33.4 (*C*10), 29.5 (*C*11/*C*12/*C*13), 29.5 (*C*11/*C*12/*C*13), 27.6 (*C*11/*C*12), 24.3 (*C*17), 24.0 (*C*H_3).‡

‡ 2 peaks obscured.

HRMS (ES$^+$): $[C_{33}H_{37}N_4O]^+$ ([M+H]$^+$) requires 505.2962; found 505.2962.

IR: ν_{max} (film)/cm^{-1} 2931, 2787, 2260, 1679 (C=O), 1478, 1387, 1024, 756, 731, 696.

(2*RS*,3*RS*)-1-Acetyl-3-phenyl-2-(5-((E)-7-(pyrrolidin-1-yl)hept-1-en-1-yl)pyridin-3-yl)indoline-3-carbonitrile **59**

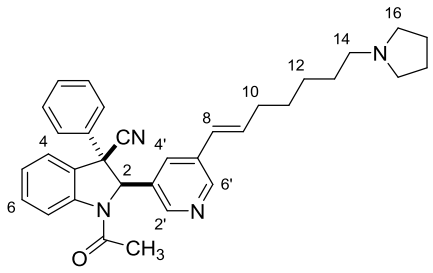

Indoline **59** was prepared according to general procedure 4, using indoline **53** (40 mg, 0.095 mmol), vinylstannane **57** (48 mg, 0.11 mmol), and $Pd(PPh_3)_4$ (11 mg, 0.0095 mmol) in NMP (1.2 mL). The reaction mixture was stirred at 85 °C for 2 h. Purification by flash pressure column chromatography (5% MeOH/CH_2Cl_2 + 0.5% aq. NH_4OH) afforded indoline **59** as a pale yellow oil (19 mg, 0.038 mmol, 40%).

^{1}H (500 MHz, C_6D_6, 348 K): δ 8.66 (1H, d, *J* 2.0, *H*6'), 8.45 (1H, d, *J* 2.0, *H*2'), 8.39 (1H, app br s, *H*7), 7.42 (1H, app t, *J* 2.0, *H*4'), 7.21-7.30 (2H, m, *o-Ph*), 7.12 (1H, obscured, *H*6), 7.07 (1H, app d, *J* 7.6,

*H*4), 6.95-7.04 (3H, m, *m-Ph*, *p-Ph*), 6.77 (1H, app t, *J* 7.6, *H*5), 5.94-6.10 (2H, m, *H*8, *H*9),ǂ 5.24 (1H, s, *H*2), 2.43 (4H, m, *H*17), 2.38 (2H, t, *J* 7.1, *H*14), 1.93 (2H, app q, *J* 6.9, *H*10), 1.64 (4H, m, *H*17), 1.42-1.56 (5H, m, *H*13, CH_3), 1.24-1.35 (4H, m, *H*11, *H*12).

ǂ ^{1}H NMR (500 MHz, C_6D_6): 5.96 (1H, dt, *J* 16.1, 6.7, *H*9), 5.86 (1H, d, *J* 16.1, *H*8).

^{13}C (126 MHz, C_6D_6, 348 K): δ 168.3 (*C*=O), 149.9 (*C*6‘), 147.3 (*C*2‘), 144.1 (*C*7a), 141.4, 135.1 (*C*9), 134.8, 134.1, 131.3 (*C*6), 130.6, 130.2 (*m-Ph*/*p-Ph*), 129.4 (*m-Ph*/*p-Ph*), 126.8 (*C*8), 126.5 (*C*4), 126.3 (*o-Ph*), 126.0 (*C*5), 119.1 (*C*N), 117.7 (*C*7), 74.9 (*C*2), 58.3 (*C*3), 56.8 (*C*14), 54.7 (*C*16), 33.7 (*C*10), 29.6 (*C*11/*C*12/*C*13), 29.6 (*C*11/*C*12/*C*13), 27.9 (*C*11/*C*12), 24.5 (*C*17), 23.7 (*C*H_3).‡

‡ 1 peak obscured.

HRMS (ES$^+$): $[C_{33}H_{37}N_4O]^+$ ($[M+H]^+$) requires 505.2962; found 505.2967.

IR: ν_{max} (film)/cm^{-1} 3028, 2931, 2791, 2261, 1678 (C=O), 1479, 1386, 1239, 1176, 1133, 756, 680.

Ethyl (2*RS*,3*RS*)-1-acetyl-3-cyano-2-(5-((E)-7-(pyrrolidin-1-yl)hept-1-en-1-yl)pyridin-3-yl)indoline-3-carboxylate **79**

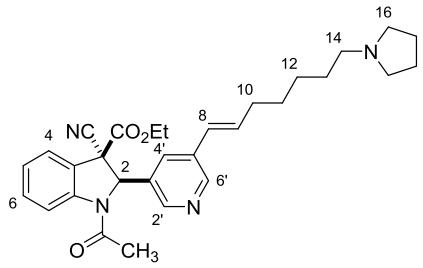

Indoline **79** was prepared according to general procedure 4, using indoline **78** (70 mg, 0.17 mmol), vinylstannane **57** (108 mg, 0.24 mmol), and $Pd(PPh_3)_4$ (20 mg, 0.017 mmol) in NMP (2.0 mL). The reaction mixture was stirred at 85 °C for 1 h. Purification by flash pressure column chromatography (5% MeOH/CH_2Cl_2 + 0.5% aq. NH_4OH) afforded indoline **79** as a pale yellow oil (30 mg, 0.060 mmol, 36%, contains minor impurities).

^{1}H (500 MHz, C_6D_6, 348 K): δ 8.51 (1H, d, *J* 2.2, *H*6’), 8.31 (1H, d, *J* 2.2, *H*2’), 8.12 (1H, app br s, *H*7), 7.26 (1H, app s, *H*4’), 7.22 (1H, app d, *J* 7.5, *H*4), 7.08 (1H, app td, *J* 7.7, 1.3, *H*6), 6.82 (1H, app td, *J*

7.7, 0.9, *H*5), 5.97 (1H, dt, *J* 16.1, 6.4, *H*9), 5.91 (1H, d, *J* 16.1, *H*8), 5.81 (1H, br s, *H*2), 3.51 (2H, q, *J* 7.0, C*H*$_2$CH$_3$), 2.41 (4H, m, *H*16), 2.37 (2H, t, *J* 7.1, *H*14), 1.90 (2H, app q, *J* 6.4, *H*10), 1.64 (4H, m, *H*17), 1.59 (3H, s, COC*H*$_3$), 1.46 (2H, app quin, *J* 7.1, *H*13), 1.20-1.32 (4H, m, *H*11, *H*12), 0.65 (3H, t, *J* 7.0, CH$_2$C*H*$_3$).

^{13}C (126 MHz, C_6D_6, 348 K): δ 168.0 (N*C*OCH$_3$), 164.4 (*C*O$_2$Et), 149.5 (*C*6'), 147.8 (*C*2'), 144.5 (*C*7a), 135.3 (*C*9), 134.2 (*C*3'/*C*5'), 132.0 (*C*3'/*C*5'), 131.7 (*C*6), 131.4 (*C*4'), 127.4 (*C*4), 126.4 (*C*8), 125.4 (*C*5), 125.4 (*C*3a) 118.3 (*C*N), 117.4 (*C*7), 70.6 (*C*2), 63.8 (*C*H$_2$CH$_3$), 56.8 (*C*14), 56.4 (*C*3), 54.7 (*C*16), 33.6 (*C*10), 29.6 (*C*13), 29.5 (*C*11/*C*12), 27.8 (*C*11/*C*12), 24.5 (*C*17), 23.9 (NCO*C*H$_3$), 13.7 (CH$_2$*C*H$_3$).

HRMS (ES$^+$): $[C_{30}H_{37}N_4O_3]^+$ ([M+H]$^+$) requires 501.2860; found 501.2847.

IR: ν_{max} (film)/cm^{-1} 2932, 2788, 2260, 1757 (C=O), 1680 (C=O), 1481, 1463, 1387, 1252, 1024, 754.

Methyl (2*RS*,3*SR*)-1-acetyl-3-phenyl-2-(5-((E)-7-(pyrrolidin-1-yl)hept-1-en-1-yl)pyridin-3-yl)indoline-3-carboxylate **69**

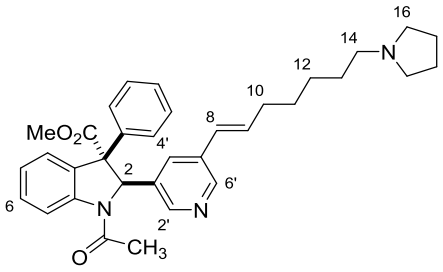

Indoline **69** was prepared according to general procedure 4, using indoline **67** (50 mg, 0.11 mmol), vinylstannane **57** (71 mg, 0.16 mmol), and Pd(PPh$_3$)$_4$ (13 mg, 0.011 mmol) in NMP (1.5 mL). The reaction mixture was stirred at 85 °C for 1.2 h. Purification by flash pressure column chromatography (6.5% MeOH/CH_2Cl_2 + 0.5% aq. NH_4OH) afforded indoline **69** as a pale yellow oil (40 mg, 0.074 mmol, 67%).

^{1}H (500 MHz, C_6D_6, 348 K): δ 8.64 (1H, app br s, *H*7), 8.29 (1H, app s, *H*2'/*H*6'), 8.07 (1H, app s, *H*2'/*H*6'), 7.36 (1H, app d, *J* 7.7, *H*4), 7.21 (1H, app td, *J* 7.7, 1.3, *H*5), 6.77-6.95 (7H, m, *H*4', *H*6, *Ph*), 6.45 (1H, s, *H*2), 5.90 (1H, d, *J* 16.0, *H*8), 5.84 (1H, dt, *J* 16.0 Hz, 6.1, *H*9), 3.23 (3H, s, CO$_2$C*H*$_3$), 2.42

(4H, m, *H*16), 2.39 (2H, t, *J* 7.2, *H*14), 1.88-1.99 (5H, m, *H*10, CH_3), 1.64 (4H, m, *H*17), 1.49 (2H, app quin, *J* 6.8, *H*13), 1.23-1.39 (4H, m, *H*11, *H*12).

^{13}C (126 MHz, C_6D_6, 348 K): δ 173.2 (*C*=O), 168.6 (*C*=O), 147.9 (*C*2'/*C*6'), 147.9 (*C*2'/*C*6'), 145.5 (*C*7a), 137.7, 134.3, 134.1, 133.4, 131.4, 130.7 (*C*6), 130.2, 129.0 (*Ph*), 128.8 (*Ph*), 127.0 (*Ph*), 124.6 (*C*5), 118.0 (*C*7), 70.6 (*C*2), 68.4 (CO_2CH_3), 56.8 (*C*3), 54.7 (*C*14/C16), 53.1 (*C*14/C16), 33.6 (*C*10), 29.7 (*C*11/*C*12/*C*13), 29.7 (*C*11/*C*12/*C*13), 27.8 (*C*11/*C*12), 24.5 (*C*17), 24.1 (CH_3).‡

‡ 2 peaks obscured.

HRMS (ES$^+$): $[C_{34}H_{40}N_3O_3]^+$ ([M+H]$^+$) requires 538.3064; found 538.3058.

IR: ν_{max} (film)/cm^{-1} 2931, 2786, 1731 (C=O), 1673 (C=O), 1478, 1390, 1229, 729.

Methyl (2*RS*,3*RS*)-1-acetyl-3-phenyl-2-(5-((E)-7-(pyrrolidin-1-yl)hept-1-en-1-yl)pyridin-3-yl)indoline-3-carboxylate **70**

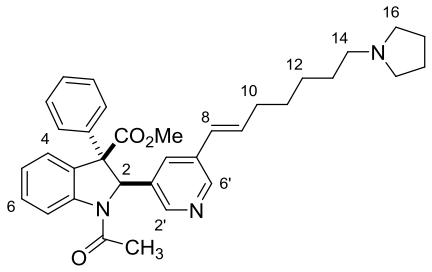

Indoline **70** was prepared according to general procedure 4, using indoline **68** (40 mg, 0.089 mmol), vinylstannane **57** (57 mg, 0.12 mmol), and $Pd(PPh_3)_4$ (10 mg, 0.0087 mmol) in NMP (2.0 mL). The reaction mixture was stirred at 85 °C for 4.5 h. Purification by flash pressure column chromatography (5% MeOH/CH_2Cl_2 + 0.5% aq. NH_4OH) afforded indoline **70** as a pale yellow oil (20 mg, 0.037 mmol, 41%).

^{1}H (500 MHz, dmso-D_6, 363 K): δ 8.49 (1H, d, *J* 1.9, *H*2'/*H*6'), 8.19 (1H, d, *J* 1.9, *H*2'/*H*6'), 7.99 (1H, app br s, *H*7), 7.63 (1H, app d, *J* 7.6, *H*4), 7.53 (1H, app s, *H*4'), 7.44 (2H, app d, *J* 7.6, *o-Ph*), 7.37 (3H, m, *m-Ph*, *p-Ph*), 7.30 (1H, app t, *J* 7.3, *H*5), 7.19 (1H, app t, *J* 7.6, *H*6), 6.35 (1H, d, *J* 16.0, *H*8), 6.26

(1H, dt, *J* 16.0, 6.7, *H*9), 6.18 (1H, s, *H*2), 3.23 (3H, s, CO_2CH_3), 2.42 (4H, m, *H*16), 2.38 (2H, t, *J* 7.3, *H*14), 2.19 (2H, app q, *J* 7.2, *H*10), 2.15 (3H, s, CH_3), 1.67 (4H, m, *H*17), 1.40-1.51 (4H, m, *H*11/*H*12/*H*13), 1.33-1.39 (2H, app quin, *J* 6.9, *H*11/*H*12/*H*13).

^{13}C (126 MHz, dmso-D_6, 363 K): δ 169.3 (*C*=O), 167.4 (*C*=O), 146.9 (*C*2'/*C*6'), 146.0 (*C*2'/*C*6'), 141.6 (*C*7a), 141.3, 133.5, 133.5, 133.3, 132.1, 130.6, 128.4, 128.3, 127.3, 127.1, 125.3, 123.5, 115.5 (*C*7), 69.1 (CO_2CH_3), 55.1 (*C*3), 53.0 (*C*16), 51.2 (*C*14), 31.7 (*C*10), 27.9 (*C*11/*C*12/*C*13), 27.7 (*C*11/*C*12/*C*13), 26.1 (*C*11/*C*12/*C*13), 23.2 (CH_3), 22.8 (*C*17).‡

‡ 2 peaks obscured.

HRMS (ES^+): $[C_{34}H_{40}N_3O_3]^+$ ($[M+H]^+$) requires 538.3064; found 538.3066.

IR: ν_{max}(film)/cm^{-1} 2929, 1741 (C=O), 1671 (C=O), 1479, 1389, 1223, 966, 716, 697.

(2*RS*,3*SR*)-1-Acetyl-3-phenyl-2-(3-((E)-7-(pyrrolidin-1-yl)hept-1-en-1-yl)phenyl)indoline-3-carbonitrile **128**

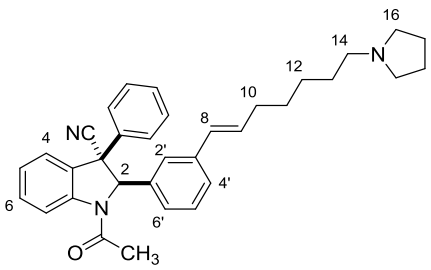

Indoline **128** was prepared according to general procedure 4, using indoline **126** (38 mg, 0.091 mmol), vinylstannane **57** (66 mg, 0.15 mmol), and $Pd(PPh_3)_4$ (11 mg, 0.0095 mmol) in NMP (1.6 mL). The reaction mixture was stirred at 85 °C for 2.5 h. Purification by flash pressure column chromatography (5% MeOH/CH_2Cl_2 + 0.5% aq. NH_4OH) afforded indoline **128** as a pale yellow oil (27 mg, 0.054 mmol, 59%).

^{1}H (500 MHz, C_6D_6, 348 K): δ 8.69 (1H, app d, *J* 8.2, *H*7), 7.12-7.20 (1H, obscured, *H*6), 7.03 (2H, m, *o-Ph*), 6.74-6.88 (6H, m, *m-Ph*, *p-Ph*, *H*4, *H*4', *H*5), 6.64 (1H, app t, *J* 7.5, *H*5'), 6.55 (1H, br s, *H*2'),

6.43 (1H, app d, *J* 7.5, *H*6'), 6.00 (1H, d, *J* 15.8, *H*8), 5.84 (1H, dt, *J* 15.8, 6.8, *H*9), 5.64 (1H, s, *H*2), 2.35-2.49 (6H, m, *H*14, *H*16), 2.00 (2H, app q, *J* 6.8, *H*10), 1.69 (3H, s, CH_3), 1.59-1.67 (4H, m, *H*17), 1.50 (2H, app quin, *J* 6.8, *H*13), 1.35 (4H, m, *H*11, *H*12).

^{13}C (126 MHz, C_6D_6, 348 K): δ 169.2 (*C*=O), 145.4 (*C*7a), 138.8, 136.8, 134.3, 132.3 (*C*9), 131.4, 129.8 (*C*8), 129.2, 129.1, 128.9, 127.9, 126.5, 126.2, 125.5, 122.1, 117.9 (*C*7), 75.4 (*C*2), 56.8 (*C*14/*C*16), 56.1 (*C*3), 54.7 (*C*14/*C*16), 33.6 (*C*10), 29.9 (*C*11/*C*12), 29.7 (*C*13), 27.8 (*C*11/*C*12), 24.3 (*C*17), 24.3 (*C*H_3).‡

‡ 3 peaks obscured.

HRMS (ES$^+$): $[C_{34}H_{38}N_3O]^+$ ([M+H]$^+$) requires 504.3009; found 504.2998.

IR: ν_{max} (film)/cm^{-1} 2930, 2789, 1677 (C=O), 1477, 1352, 1281, 728, 697.

(2*RS*,3*RS*)-1-Acetyl-3-phenyl-2-(3-((E)-7-(pyrrolidin-1-yl)hept-1-en-1-yl)phenyl)indoline-3-carbonitrile **129**

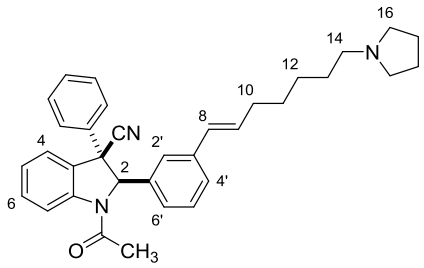

Indoline **129** was prepared according to general procedure 4, using indoline **127** (50 mg, 0.12 mmol), vinylstannane **57** (77 mg, 0.17 mmol), and $Pd(PPh_3)_4$ (14 mg, 0.012 mmol) in NMP (2.0 mL). The reaction mixture was stirred at 85 °C for 1.5 h. Purification by flash pressure column chromatography (4.5% MeOH/CH_2Cl_2 + 0.5% aq. NH_4OH) afforded indoline **129** as a pale yellow oil (35 mg, 0.070 mmol, 58%).

^{1}H (500 MHz, C_6D_6, 348 K): δ 8.62 (1H, app d, *J* 7.8, *H*7), 7.33 (2H, m, *o-Ph*), 7.24 (1H, app s, *H*2'), 7.17-7.22 (2H, m, *H*4', *H*6), 7.11 (1H, app d, *J* 7.6, *H*4), 6.98-7.07 (4H, m, *m-Ph*, *p-Ph*, *H*5'), 6.95 (1H,

app d, *J* 7.3, *H*6'), 6.80 (1H, app t, *J* 7.6, *H*5), 6.25 (1H, d, *J* 15.6, *H*8), 6.11 (1H, dt, *J* 15.6, 6.8, *H*9), 5.22 (1H, s, *H*2), 2.35-2.47 (6H, m, *H*14, *H*16), 2.05 (2H, app q, *J* 6.7, *H*10), 1.60-1.68 (4H, m, *H*17), 1.57 (3H, s, CH_3), 1.51 (2H, app quin, *J* 6.9, *H*13), 1.37 (4H, m, *H*11, *H*12).

^{13}C (126 MHz, C_6D_6, 348 K): δ 168.9 (*C*=O), 144.4 (*C*7a), 141.9, 139.9, 138.9, 132.7 (*C*9), 131.2 (*C*6), 130.2 (*m*-*Ph*/*p*-*Ph*/*C*5'), 130.1 (*C*8), 130.1 (*m*-*Ph*/*p*-*Ph*/*C*5'), 129.2 (*m*-*Ph*/*p*-*Ph*/*C*5'), 128.9, 127.3 (*C*2'), 126.4 (*C*4), 126.3 (*o*-*Ph*), 125.8 (*C*5), 125.2 (*C*6'), 125.0 (*C*4'), 119.1 (*C*N), 117.7 (*C*7), 77.1 (*C*2), 58.5 (*C*3), 56.8 (*C*14), 54.7 (*C*16), 33.7 (*C*10), 29.8 (*C*11/*C*12), 29.7 (*C*13), 27.9 (*C*11/*C*12), 24.3 (*C*17), 24.0 (*C*H_3).

HRMS (ES$^+$): $[C_{34}H_{38}N_3O]^+$ ([M+H]$^+$) requires 504.3009; found 504.2993.

IR: ν_{max} (film)/cm^{-1} 2930, 2790, 1678 (C=O), 1478, 1387, 1282, 729, 697.

7-Bromohept-1-yne **104**

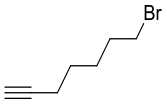

Alkyne **104** was prepared according to a literature procedure.[194] PPh_3 (1.22 g, 4.64 mmol) was added portionwise to a solution of 6-heptyn-1-ol (400 mg, 3.57 mmol) and CBr_4 (1.54 g, 4.64 mmol) in CH_2Cl_2 (8 mL), and the mixture was stirred at 0 °C for 1.5 h. Ice-cooled hexane (30 mL) was added. The white precipitate was removed by filtration, and the filtrate was concentrated. Purification by flash pressure column chromatography (100% petroleum ether) afforded alkyne **104** as a colorless liquid (537 mg, 3.07 mmol, 86%). The spectral data matched those reported in the literature.

^{1}H (400 MHz, $CDCl_3$): δ 3.42 (2H, t, *J* 6.8, *H*7), 2.22 (2H, app m, *H*3), 1.96 (1H, t, *J* 2.7, *H*1), 1.89 (2H, app m, *H*6), 1.48-1.64 (4H, m, *H*4, *H*5).

^{13}C (101 MHz, $CDCl_3$): δ 84.1 (*C*2), 68.5 (*C*1), 33.5 (*C*7), 32.3 (*C*6), 27.6 (*C*4/*C*5), 27.3 (*C*4/*C*5), 18.3 (*C*3).

7-Pyrrolidine-hept-1-yne **105**

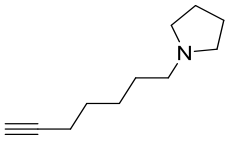

A solution of alkyne **104** (280 mg, 1.60 mmol) in THF (4 mL) was added to a solution of pyrrolidine (1.3 mL, 16 mmol) in THF (4 mL). The mixture was stirred at 50 °C for 1.5 h. H_2O was added, and the mixture was extracted with Et_2O. The combined organic extracts were washed with brine, dried over Na_2SO_4, filtered, and concentrated. Purification by flash pressure column chromatography (5% MeOH/CH_2Cl_2 + 0.5% aq. NH_4OH) afforded alkyne **105** as a yellow liquid (245 mg, 1.48 mmol, 41%).

^{1}H (400 MHz, $CDCl_3$): δ 2.37-2.53 (6H, m, *H*7, *H*9), 2.18 (2H, td, *J* 7.0, 2.7, *H*3), 1.93 (1H, t, *J* 2.7, *H*1), 1.76 (4H, m, *H*10), 1.47-1.61 (4H, m, *H*4, *H*6), 1.43 (2H, app quin, *J* 7.1, *H*5).

^{13}C (101 MHz, $CDCl_3$): δ 84.6 (*C*2), 68.1 (*C*1), 56.5 (*C*7/*C*9), 54.2 (*C*7/*C*9), 28.6 (*C*4/*C*6), 28.4 (*C*4/*C*6), 26.8 (*C*5), 23.4 (*C*10), 18.3 (*C*3).

HRMS (ES$^+$): $[C_{11}H_{20}N]^+$ ($[M+H]^+$) requires 166.1590; found 166.1592.

IR: ν_{max} (film)/cm^{-1} 3311 (C-H), 2936, 2787, 1461, 1147, 734, 631.

(2*RS*,3*SR*)-1-Acetyl-3-phenyl-2-(5-(7-(pyrrolidin-1-yl)hept-1-yn-1-yl)pyridin-3-yl)indoline-3-carbonitrile **106**

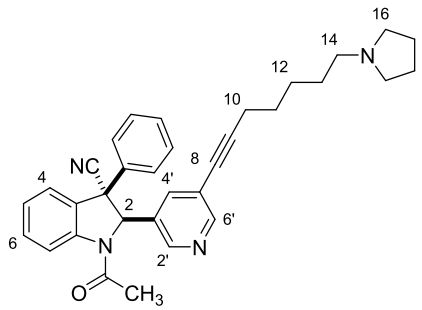

Indoline **106** was prepared according to general procedure 5, using indoline **52** (70 mg, 0.17 mmol), alkyne **105** (41 mg, 0.25 mmol), $PdCl_2(PPh_3)_2$ (5.9 mg, 0.0084 mmol), and CuI (1.6 mg, 0.0084 mmol)

in *N*,*N*-diisopropylamine (2.5 mL). The reaction mixture was stirred at 70 °C for 1 h. Purification by flash pressure column chromatography (5% MeOH/CH_2Cl_2 + 0.5% aq. NH_4OH) afforded indoline **106** as a pale yellow oil (55 mg, 0.11 mmol, 66%).

^{1}H (500 MHz, C_6D_6, 348 K): δ 8.45 (1H, d, *J* 1.9, *H*6'), 8.26 (1H, app br s, *H7*) 7.84 (1H, app br s, *H*2'), 7.08 (1H, app td, *J* 7.7, 1.3, *H*6), 6.89-6.99 (3H, m, *H*4', *o-Ph*), 6.76-6.86 (4H, m, *H*4, *m-Ph*, *p-Ph*), 6.73 (1H, app t, *J* 7.7, *H*5), 5.63 (1H, s, *H*2), 2.39 (4H, m, *H*16), 2.33 (2H, t, *J* 6.9, *H*14), 2.09 (2H, t, *J* 6.6, *H*10), 1.57-1.67 (7H, m, *H*17, C*H*$_3$), 1.32-1.44 (6H, m, *H*11, *H*12, *H*13).

^{13}C (126 MHz, C_6D_6): δ 168.4 (*C*=O), 152.7 (*C*6'), 147.5 (*C*2'), 144.7 (*C*7a), 137.9, 136.8, 133.5 (*C*4'), 132.0, 131.5 (*C*6), 129.4 (*Ph*), 129.1 (*Ph*), 128.9 (*Ph*), 126.6, 125.7, 121.6 (*C*5'/*C*N), 121.4 (*C*5'/*C*N), 117.8 (*C7*), 95.4 (*C*8/*C*9), 77.7 (*C*8/*C*9), 72.8 (*C*2), 56.6 (*C*14), 55.7 (*C*3), 54.6 (*C*16), 29.1 (*C*11/*C*12/*C*13), 28.9 (*C*11/*C*12/*C*13), 27.4 (*C*11/*C*12/*C*13), 24.3 (*C*17), 24.1 (*C*H$_3$), 19.9 (*C*10).

HRMS (ES$^+$): $[C_{33}H_{35}N_4O]^+$ ([M+H]$^+$) requires 503.2805; found 503.2792.

IR: ν_{max} (film)/cm^{-1} 2935, 2790, 2232, 1680 (C=O), 1478, 1387, 1024, 757, 700.

(2*RS*,3*RS*)-1-Acetyl-3-phenyl-2-(5-(7-(pyrrolidin-1-yl)hept-1-yn-1-yl)pyridin-3-yl)indoline-3-carbonitrile **107**

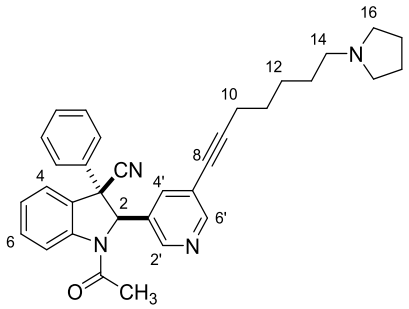

Indoline **107** was prepared according to general procedure 5, using indoline **53** (70 mg, 0.17 mmol), alkyne **105** (41 mg, 0.25 mmol), $PdCl_2(PPh_3)_2$ (5.9 mg, 0.0084 mmol), and CuI (1.6 mg, 0.0084 mmol) in *N*,*N*-diisopropylamine (2.5 mL). The reaction mixture was stirred at 70 °C for 1.25 h. Purification by flash pressure column chromatography (5% MeOH/CH_2Cl_2 + 0.5% aq. NH_4OH) afforded indoline

107 as a pale yellow oil (66 mg, 0.092 mmol, 79%). The non-racemic form of indoline **107** was prepared from **(*S,S*)-157**, following an identical protocol.

^{1}H (500 MHz, C_6D_6, 348 K): δ 8.81 (1H, d, *J* 1.9, *H*6'), 8.46 (1H, d, *J* 2.2, *H*2'), 8.21 (1H, app br s, *H*7), 7.60 (1H, app s, *H*4'), 7.19 (2H, m, *o-Ph*), 7.06 (1H, app t, *J* 7.7, *H*6), 6.95-7.04 (4H, m, *H*4, *m-Ph*, *p-Ph*), 6.73 (1H, app t, *J* 7.7, *H*5), 5.18 (1H, br s, *H*2), 2.40 (4H, app br s, *H*16), 2.33 (2H, t, *J* 6.9, *H*14), 2.13 (2H, t, *J* 6.8, *H*10), 1.62 (4H, m, *H*17), 1.47 (3H, s, C*H*$_3$), 1.34-1.45 (6H, m, *H*11, *H*12, *H*13).

^{13}C (126 MHz, C_6D_6): δ 168.1 (*C*=O), 154.4 (*C*6'), 147.2 (*C*2'), 143.6 (*C*7a), 140.9 (*C*3'/*i-Ph*), 136.1 (*C*4'), 133.8 (*C*3'/*i-Ph*), 131.3 (*C*3a), 130.6 (*C*6), 130.2 (*C*4/*m-Ph*/*p-Ph*), 129.4 (*C*4/*m-Ph*/*p-Ph*), 126.4 (*C*4/*m-Ph*/*p-Ph*), 126.3 (*o-Ph*), 126.1 (*C*5), 119.0 (*C*5'/*C*N), 118.3 (*C*5'/*C*N), 117.7 (*C*7), 96.0 (*C*8/*C*9), 77.9 (*C*8/*C*9), 74.2 (*C*2), 58.0 (*C*3), 56.5 (*C*14), 54.6 (*C*16), 29.1 (*C*11/*C*12/*C*13), 28.9 (*C*11/*C*12/*C*13), 27.4 (*C*11/*C*12/*C*13), 24.3 (*C*17), 23.7 (*C*H$_3$), 20.0 (*C*10).

HRMS (ES$^+$): $[C_{33}H_{35}N_4O]^+$ requires 503.2805; found 503.2790.

IR: ν_{max} (film)/cm^{-1} 2934, 2789, 2232, 2341, 1678 (C=O), 1479, 1389, 1275, 755, 705.

$[\alpha]_D^{25.0}$ (*S,S*) = -55 (*c* = 0.1, $CHCl_3$).

(2*SR*,3*RS*)-1-Acetyl-3-phenyl-2-(5-(7-(pyrrolidin-1-yl)hept-1-yn-1-yl)furan-2-yl)indoline-3-carbonitrile **143**

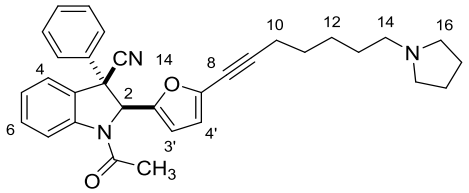

Indoline **143** was prepared according to general procedure 5, using indoline **140** (50 mg, 0.12 mmol), alkyne **105** (26 mg, 0.16 mmol), $PdCl_2(PPh_3)_2$ (4 mg, 0.006 mmol), and CuI (1 mg, 0.006 mmol) in *N,N*-diisopropylamine (5 mL). The reaction mixture was stirred at 70 °C for 2.5 h. Purification by flash pressure column chromatography (4.5 % MeOH/CH_2Cl_2 + 0.5% aq. NH_4OH) afforded indoline **143** as a pale yellow oil (51 mg, 0.10 mmol, 83%).

^{1}H (500 MHz, C_6D_6, 348 K): δ 8.39 (1H, app br s, *H*7), 7.20-7.27 (2H, m, *o-Ph*), 7.08-7.14 (2H, m, *H*4, *H*6), 6.92-7.01 (3H, m, *m-Ph*, *p-Ph*), 6.77 (1H, app td, *J* 7.6 Hz, 0.9, *H*5), 6.22 (1H, d, *J* 3.4, *H*3'/*H*4'), 5.90 (1H, d, *J* 3.4, *H*3'/*H*4'), 5.31 (1H, br s, *H*2), 2.38 (4H, m, *H*16), 2.31 (2H, t, *J* 6.9, *H*14), 2.13 (2H, t, *J* 6.8, *H*10), 1.62 (4H, m, *H*17), 1.55 (3H, s, CH_3), 1.33-1.42 (6H, m, *H*11, *H*12, *H*13).

^{13}C (126 MHz, C_6D_6): δ 168.3 (*C*=O), 150.9, 143.4, 140.5, 139.7, 131.0 (*C*6), 130.1 (*m-Ph*/*p-Ph*), 129.3 (*m-Ph*/*p-Ph*), 126.4 (*o-Ph*), 126.2 (*C*4), 125.7 (*C*5), 118.8 (*C*N), 118.1 (*C*7), 115.6 (*C*3'), 110.2 (*C*4'), 96.8 (*C*8/*C*9), 71.8 (*C*8/*C*9), 71.0 (*C*2), 57.0 (*C*3), 56.6 (*C*14), 54.6 (*C*16), 29.2 (*C*11/*C*12/*C*13), 28.8 (*C*11/*C*12/*C*13), 27.4 (*C*11/*C*12/*C*13), 24.3 (*C*17), 23.3 (*C*H_3), 20.0 (*C*10).‡

‡ 1 peak obscured.

HRMS (ES$^+$): $[C_{32}H_{34}N_3O_2]^+$ ([M+H]$^+$) requires 492.2645; found 492.2639.

IR: ν_{max} (film)/cm^{-1} 2935, 2792, 2260, 1680 (C=O), 1478, 1388, 1352, 1022, 756, 698.

(2*SR*,3*SR*)-1-Acetyl-3-phenyl-2-(5-(7-(pyrrolidin-1-yl)hept-1-yn-1-yl)furan-2-yl)indoline-3-carbonitrile **141**

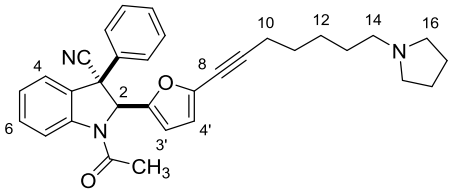

Indoline **141** was prepared according to general procedure 5, using indoline **139** (50 mg, 0.12 mmol), alkyne **105** (26 mg, 0.16 mmol), $PdCl_2(PPh_3)_2$ (4 mg, 0.006 mmol), and CuI (1 mg, 0.006 mmol) in *N*,*N*-diisopropylamine (5 mL). The reaction mixture was stirred at 70 °C for 1.5 h. Purification by flash pressure column chromatography (4% MeOH/CH_2Cl_2 + 0.5% aq. NH_4OH) afforded indoline **141** as a pale yellow oil (50 mg, 0.10 mmol, 82%).

^{1}H (500 MHz, C_6D_6, 348 K): δ 8.75 (1H, app br s, *H*7), 7.23 (2H, m, *o-Ph*), 7.07 (1H, app t, *J* 7.5, *H*6), 6.94-7.03 (3H, m, *m-Ph*, *p-Ph*), 6.74 (1H, dd, *J* 7.6, 1.2, *H*4), 6.69 (1H, app td, *J* 7.6, 1.0, *H*5), 5.84 (1H,

d, *J* 3.4, *H*3'/*H*4'), 5.55 (1H, br s, *H*2), 5.39 (1H, d, *J* 3.4, *H*3'/*H*4'), 2.35 (4H, m, *H*16), 2.27 (2H, t, *J* 7.1, *H*14), 1.98 (2H, t, *J* 6.5, *H*10), 1.62 (4H, m, *H*17), 1.54 (3H, br s, CH_3), 1.34 (2H, app quin, *J* 6.7, *H*11/*H*12/*H*13), 1.21-1.30 (4H, m, *H*11/*H*12/*H*13).

^{13}C (126 MHz, C_6D_6): δ 168.4 (*C*=O), 149.2, 144.6, 139.0, 133.9, 131.2 (*C*6), 129.3 (*m-Ph*/*p-Ph*), 128.9 (*m-Ph*/*p-Ph*), 128.7 (*o-Ph*), 126.3 (*C*4), 125.3 (*C*5), 121.2 (*C*N), 118.2 (*C*7), 114.7 (*C*3'/*C*4'), 111.1 (*C*3'/*C*4'), 96.0 (*C*8/*C*9), 71.3 (*C*8/*C*9), 69.9 (*C*2), 56.5 (*C*14), 55.3 (*C*3), 54.6 (*C*16), 29.0 (*C*11/*C*12/*C*13), 28.7 (*C*11/*C*12/*C*13), 27.3 (*C*11/*C*12/*C*13), 24.2 (*C*17), 23.6 (*C*H_3), 19.8 (*C*10).‡

‡ 1 peak obscured.

HRMS (ES$^+$): $[C_{32}H_{34}N_3O_2]^+$ ([M+H]$^+$) requires 492.2645; found 492.2634.

IR: ν_{max} (film)/cm^{-1} 2934, 2789, 2259, 1679 (C=O), 1479, 1387, 1351, 1021, 756, 697.

(2*SR*,3*RS*)-1-Acetyl-3-phenyl-2-(4-(7-(pyrrolidin-1-yl)hept-1-yn-1-yl)furan-2-yl)indoline-3-carbonitrile **135**

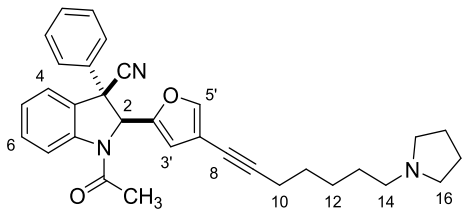

Indoline **135** was prepared according to general procedure 5, using indoline **134** (50 mg, 0.12 mmol), alkyne **105** (28 mg, 0.17 mmol), $PdCl_2(PPh_3)_2$ (4 mg, 0.006 mmol), and CuI (1 mg, 0.006 mmol) in *N*,*N*-diisopropylamine (5 mL). The reaction mixture was stirred at 70 °C for 16 h. Purification by flash pressure column chromatography (4.5% MeOH/CH_2Cl_2 + 0.5% aq. NH_4OH) afforded indoline **135** as a pale yellow oil (15 mg, 0.031 mmol, 24%).

^{1}H (500 MHz, C_6D_6): δ 8.68 (1H, app br s, *H*7), 7.24 (2H, m, *o-Ph*), 7.20 (1H, s, *H*5'), 7.00-7.13 (2H, m, *H*4, *H*6), 6.90-6.97 (3H, m, *m-Ph*, *p-Ph*), 6.72 (1H, app td, *J* 7.5, 1.1, *H*5), 6.21 (1H, br s, *H*3'), 5.08 (1H, br s, *H*2), 2.37 (4H, m, *H*16), 2.31 (2H, t, *J* 7.0, *H*14), 2.19 (2H, t, *J* 6.7, *H*10), 1.61 (4H, m, *H*17),

1.33-1.49 (9H, m, *H*11, *H*12, *H*13, CH_3).

^{13}C (126 MHz, C_6D_6): δ 168.2 (*C*=O), 150.8, 146.6 (*C*5'), 143.4, 140.4, 131.0 (*C*4/*C*6), 130.1 (*m-Ph*/*p-Ph*), 129.4 (*m-Ph*/*p-Ph*), 126.3 (*o-Ph*), 125.9 (*C*4/*C*6), 125.7 (*C*5), 118.8 (*C*N), 118.2 (*C*7), 112.6 (*C*3'), 110.4 (*C*8/*C*9), 93.4 (*C*8/*C*9), 70.6 (*C*2), 56.7 (*C*3), 56.6 (*C*14), 54.6 (*C*16), 29.2 (*C*11/*C*12/*C*13), 29.1 (*C*11/*C*12/*C*13), 27.4 (*C*11/*C*12/*C*13), 24.2 (*C*17), 23.3 (*C*H_3), 20.0 (*C*10).‡

‡ 2 peaks obscured.

HRMS (ES$^+$): $[C_{32}H_{34}O_2N_3]^+$ ([M+H]$^+$) requires 492.2646; found 492.2644.

IR: ν_{max}(film)/cm^{-1} 2948, 2248, 1676 (C=O), 1479, 1387, 1352, 1275, 756, 698.

(2*RS*,3*RS*)-1-Acetyl-3-phenyl-2-(5-(7-(pyrrolidin-1-yl)heptyl)pyridin-3-yl)indoline-3-carbonitrile **108**

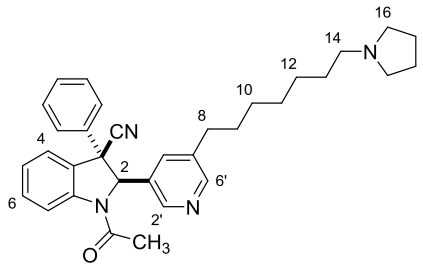

Indoline **108** was prepared according to general procedure 3, using indoline **107** (50 mg, 0.099 mmol) and Pd/C (wet degussa type, 5 mg) in MeOH (2.5 mL). The reaction mixture was stirred under a H_2 atmosphere for 4.5 h. Purification by flash pressure column chromatography (5% MeOH/CH_2Cl_2 + 0.5% aq. NH_4OH) afforded indoline **108** as a colorless oil (37 mg, 0.073 mmol, 74%). The non-racemic form of indoline **108** was prepared from **(*S,S*)-107**, following an identical protocol (e.r. >99:1).

^{1}H (500 MHz, C_6D_6): δ 8.69 (1H, app br s, *H*7), 8.50 (1H, d, *J* 2.0, *H*6'), 8.46 (1H,d, *J* 1.7, *H*2'), 7.20-7.28 (3H, m, *H*4', *o-Ph*), 7.10 (1H, app t, *J* 7.7, *H*6), 7.03 (1H, app d, *J* 7.7, *H*4), 6.94-7.01 (3H, m, *m-Ph*, *p-Ph*), 6.74 (1H, app td, *J* 7.5, 0.9, *H*5), 5.13 (1H, br s, *H*2), 2.36-2.48 (6H, m, *H*14, *H*16), 2.09 (2H, t, *J* 7.3, *H*8), 1.65 (4H, m, *H*17), 1.38-1.55 (5H, m, *H*13, CH_3), 1.22-1.33 (4H, m, *H*9, *H*12), 0.98-1.17

(4H, m, *H*10, *H*11).

^{13}C (126 MHz, C_6D_6): δ 168.5 (*C*=O), 152.3 (*C*6'), 146.6 (*C*2'), 144.0 (*C*7a), 141.1, 139.2, 133.7, 133.3 (*C*4'), 131.3 (*C*6), 130.2 (*m-Ph*/*p-Ph*), 129.4 (*m-Ph*/*p-Ph*), 126.4 (*C*4), 126.3 (*o-Ph*), 126.0 (*C*5), 119.1 (*C*N), 117.7 (*C*7), 74.5 (*C*2), 58.2 (*C*3), 57.0 (*C*14/*C*16), 54.8 (*C*14/*C*16), 33.1 (*C*8), 31.4 (*C*9/*C*12), 29.9 (*C*10/*C*11), 29.9 (*C*13), 29.6 (*C*10/*C*11), 28.2 (*C*9/*C*12), 24.3 (*C*17), 23.8 (*C*H$_3$).‡

‡ 1 peak obscured.

HRMS (ES$^+$): $[C_{33}H_{39}N_4O]^+$ ([M+H]$^+$) requires 507.3118; found 507.3106.

IR: ν_{max} (film)/cm^{-1} 2929, 2787, 2261, 1677 (C=O), 1479, 1385, 1239, 1028, 755, 669.

$[\alpha]_D^{25.0}$ (*S*,*S*) = -87 (*c* = 0.1, $CHCl_3$).

Chiral HPLC: (Chiralpak ODH, 15% ^{i}PrOH, 85% hexane, 1.3 mL/min, λ = 254 nm, 20 µL injection) τ_R (*R*,*R*) = 8.7 min, τ_R (*S*,*S*) = 11.4 min.

(2*SR*,3*RS*)-1-Acetyl-3-phenyl-2-(5-(7-(pyrrolidin-1-yl)heptyl)furan-2-yl)indoline-3-carbonitrile **144**

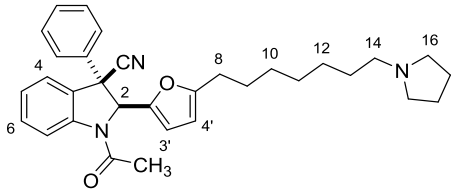

Indoline **144** was prepared according to general procedure 3, using indoline **143** (41 mg, 0.083 mmol) and Pd/C (wet degussa type, 4 mg) in MeOH (1.5 mL). The reaction mixture was stirred under a H_2 atmosphere for 4.5 h. Purification by flash pressure column chromatography (4.5% MeOH/CH_2Cl_2 + 0.5% aq. NH_4OH) afforded indoline **144** as a colorless oil (23 mg, 0.046 mmol, 56%).

^{1}H (500 MHz, C_6D_6): δ 8.77 (1H, app br s, *H*7), 7.31 (2H, m, *o-Ph*), 7.04-7.15 (2H, m, *H*4, *H*6), 6.0-7.0 (3H, m, *m-Ph*, *p-Ph*), 6.75 (1H, app td, *J* 7.6, 0.9, *H*5), 5.93 (1H, app br s, *H*3'), 5.73 (1H, d, *J* 3.3, *H*4'), 5.23 (1H, br s, *H*2), 2.35-2.48 (8H, m, *H*8, *H*14, *H*16), 1.64 (4H, m, *H*17), 1.47-1.60 (7H, m, *H*9, *H*13, C*H*$_3$), 1.33 (2H, app quin, *J* 7.4, *H*10/*H*11/*H*12), 1.17-1.28 (4H, m, *H*10/*H*11/*H*12).

^{13}C (126 MHz, C_6D_6): δ 168.4 (*C*=O), 158.7, 148.8, 143.6, 140.8, 130.9 (*C*4/*C*6), 130.0 (*m-Ph*/*p-Ph*), 129.2 (*m-Ph*/*p-Ph*), 126.3 (*o-Ph*), 126.0 (*C*4/*C*6), 125.6 (*C*5), 119.0 (*C*N), 118.1 (*C*7), 110.2 (*C*3'), 106.7 (*C*4'), 71.2 (*C*2), 57.0 (*C*14), 57.0 (*C*3), 54.7 (*C*16), 30.0 (*C*10/*C*11/*C*12), 29.9 (*C*9/*C*13), 29.7 (*C*10/*C*11/*C*12), 28.6 (*C*8), 28.5 (*C*9/*C*13), 28.2 (*C*10/*C*11/*C*12), 24.3 (*C*17), 23.4 (*C*H_3).‡

‡ 1 peak obscured.

HRMS (ES$^+$): $[C_{32}H_{38}N_3O_2]^+$ ([M+H]$^+$) requires 496.2959; found 496.2940.

IR: ν_{max} (film)/cm^{-1} 2933, 2789, 2263, 1673 (C=O), 1479, 1384, 1351, 1022, 756, 698.

(2*SR*,3*SR*)-1-Acetyl-3-phenyl-2-(5-(7-(pyrrolidin-1-yl)heptyl)furan-2-yl)indoline-3-carbonitrile **142**

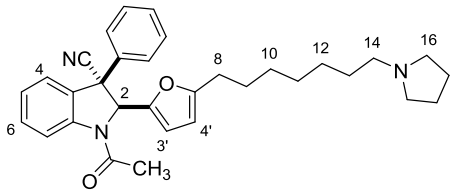

Indoline **142** was prepared according to general procedure 3, using indoline **141** (40 mg, 0.081 mmol) and Pd/C (wet degussa type, 4 mg) in MeOH (1.5 mL). The reaction mixture was stirred under a H_2 atmosphere for 1 h. Purification by flash pressure column chromatography (4% MeOH/CH_2Cl_2 + 0.5% aq. NH_4OH) afforded indoline **142** as a colorless oil (26 mg, 0.052 mmol, 64%).

^{1}H (500 MHz, C_6D_6): δ 8.54 (1H, app br s, *H*7), 7.24 (2H, app d, *J* 7.5, *o-Ph*), 7.14 (1H, app t, *J* 7.7, *H*6), 6.95-7.02 (3H, m, *m-Ph*, *p-Ph*), 6.86 (1H, app d, *J* 7.7, *H*4), 6.78 (1H, app t, *J* 7.7, *H*5), 5.70 (1H, s, *H*2), 5.60 (1H, d, *J* 3.0, *H*3'), 5.38 (1H, d, *J* 3.0, *H*4'), 2.38-2.48 (6H, m, *H*14, *H*16), 2.04 (2H, t, *J* 7.4, *H*8), 1.74 (3H, s, C*H*$_3$), 1.65 (4H, m, *H*17), 1.50 (2H, app quin, *J* 7.4, *H*13), 1.32 (2H, app quin, *J* 7.4, *H*12), 1.04-1.22 (4H, m, *H*9, *H*11), 1.00 (2H, app quin, *J* 7.1, *H*10).

^{13}C (126 MHz, C_6D_6): δ 168.6 (*C*=O), 157.9, 147.4, 145.1, 134.7, 131.1 (*C*6), 129.0 (*Ph*), 129.0 (*Ph*), 129.0 (*Ph*), 126.3 (*C*4), 125.1 (*C*5), 121.4 (*C*N), 118.2 (*C*7), 110.9 (*C*3'), 106.0 (*C*4'), 70.6 (*C*2), 56.9 (*C*14), 55.6 (*C*3), 54.7 (*C*16), 29.9 (*C*9/*C*10/*C*11/*C*13), 29.9 (*C*9/*C*10/*C*11/*C*13), 29.7

(*C*9/*C*10/*C*11/*C*13), 28.4 (*C*9/*C*10/*C*11/*C*13), 28.2 (*C*8/*C*12), 28.2 (*C*8/*C*12), 24.5 (*C*17), 23.6 (*C*H_3).‡

‡ 1 peak obscured.

HRMS (ES$^+$): $[C_{32}H_{38}N_3O_2]^+$ ([M+H]$^+$) requires 496.2959; found 496.2938.

IR: ν_{max} (film)/cm^{-1} 2933, 2789, 1671 (C=O), 1477, 1389, 1353, 1022, 757, 699.

(2*SR*,3*RS*)-1-Acetyl-3-phenyl-2-(4-(7-(pyrrolidin-1-yl)heptyl)furan-2-yl)indoline-3-carbonitrile **136**

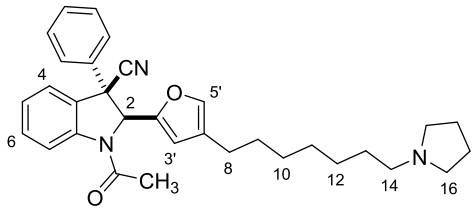

Indoline **136** was prepared according to general procedure 3, using indoline **135** (10 mg, 0.020 mmol) and Pd/C (wet degussa type, 1.5 mg) in MeOH (1.0 mL). The reaction mixture was stirred under a H_2 atmosphere for 16 h. Purification by flash pressure column chromatography (4% MeOH/CH_2Cl_2 + 0.5% aq. NH_4OH) afforded indoline **135** as a colorless oil (6.0 mg, 0.012 mmol, 60%).

^{1}H (500 MHz, C_6D_6): δ 8.80 (1H, app br s, *H*7) 7.31 (2H, *o-Ph*), 7.06-7.14 (2H, m, *H*4, *H*6), 6.91-6.98 (4H, m, *H*5', *m-Ph*, *p-Ph*), 6.74 (1H, app td, *J* 7.6, 0.9, *H*5), 6.01 (1H, br s, *H*3'), 5.22 (1H, br s, *H*2), 2.39-2.46 (6H, m, *H*14, *H*16), 2.06 (2H, t, *J* 7.6, *H*8), 1.65 (4H, m, *H*17), 1.48-1.59 (5H, m, *H*13, C*H*$_3$), 1.26-1.38 (4H, m, *H*9, *H*12), 1.14-1.25 (4H, m, *H*10, *H*11).

^{13}C (126 MHz, C_6D_6): δ 168.4 (*C*=O), 150.8, 143.7, 140.8, 140.4 (*C*5'), 131.0 (*C*6), 130.1 (*m-Ph*/*p-Ph*), 129.3 (*m-Ph*/*p-Ph*), 127.3, 126.3 (*o-Ph*), 126.1 (*C*4), 125.7 (*C*5), 118.9 (*C*N), 118.2 (*C*7), 110.8 (*C*3'), 71.2 (*C*2), 57.0 (*C*3), 57.0 (*C*14/*C*16), 54.8 (*C*14/*C*16), 30.2 (*C*9/*C*12), 30.0 (*C*10/*C*11), 30.0 (*C*10/*C*11), 29.9 (*C*13), 28.3 (*C*9/*C*12), 25.2 (*C*8), 24.3 (*C*17), 23.4 (*C*H_3).‡

‡ 1 peak obscured.

HRMS (ES$^+$): $[C_{32}H_{34}N_3O_2]^+$ ([M+H]$^+$) requires 492.2645; found 492.2638.

IR: ν_{max} (film)/cm^{-1} 2933, 2789, 2248, 1673 (C=O), 1479, 1384, 1351, 1022, 756, 698.

(2*RS*,3*SR*)-1-Acetyl-2-(5-((7-bromoheptyl)oxy)pyridin-3-yl)-3-phenylindoline-3-carbonitrile **98**

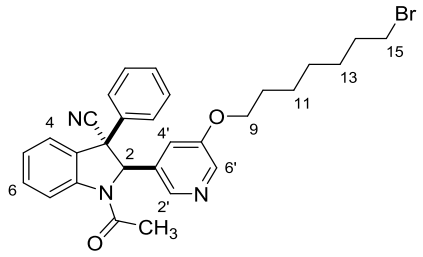

K_2CO_3 (146 mg, 1.06 mmol) was added to a solution of indoline **96** (75 mg, 0.21 mmol) in acetone (15 mL), followed by 1,7-dibromoheptane (140 µL, 0.84 mmol). The mixture was stirred under reflux for 16 h, allowed to cool to rt, and concentrated. The remaining residue was dissolved in EtOAc, washed three times with H_2O, then brine. The organic layer was dried over Na_2SO_4, filtered, and concentrated. Purification by flash pressure column chromatography (40% EtOAc/petroleum ether) afforded indoline **98** as a pale yellow oil (36 mg, 0.068 mmol, 32%, contains minor impurities).

^{1}H (500 MHz, C_6D_6, 348 K): δ 8.32 (1H, app br s, *H*7), 8.08 (1H, d, *J* 2.4, *H*6'), 7.72 (1H, app s, *H*2'), 7.11 (1H, app td, *J* 7.8, 1.3, *H*6), 7.02 (2H, app d, *J* 7.8, *o-Ph*), 6.78-6.87 (4H, m, *H*4, *m-Ph*, *p-Ph*), 6.76 (1H, app t, *J* 7.7, *H*5), 6.36 (1H, app s, *H*4'), 5.71 (1H, s, *H*2), 3.33 (2H, app m, *H*9), 3.00 (2H, t, *J* 7.0, *H*15), 1.69 (3H, s, C*H*$_3$), 1.33 (2H, app quin, *J* 7.4, *H*10), 1.15 (2H, app quin, *J* 7.4, *H*13), 1.07 (2H, app quin, *J* 7.0, *H*11), 0.99 (2H, app quin, *J* 7.0, *H*12).

^{13}C (126 MHz, C_6D_6, 348 K): δ 168.2 (*C*=O), 155.2 (*C*5'), 144.8 (*C*7a), 141.3 (*C*2'), 138.6 (*C*6'), 133.9 (*i-Ph*), 132.8 (*C*3'), 131.1 (*C*6), 129.0 (*Ph*), 128.9 (*Ph*), 128.6 (*Ph*), 126.3 (*C*4), 125.2 (*C*5), 121.3 (*C*N), 119.6 (*C*4'), 117.4 (*C*7), 73.2 (*C*2), 68.5 (*C*9), 55.8 (*C*3), 33.1 (*C*15), 32.9 (*C*14), 29.1 (*C*10), 28.5 (*C*12), 28.2 (*C*13), 25.9 (*C*11), 23.7 (*C*H$_3$).‡

‡ 1 peak obscured.

HRMS (ES$^+$): $[C_{29}H_{31}{}^{79}BrN_3O_3]^+$ ([M+H]$^+$) requires 532.1594; found 532.1592.

IR: ν_{max} (film)/cm^{-1} 3028, 2929, 2857, 1676 (C=O), 1599, 1497, 1387, 1321, 1188, 757, 701.

(2*RS*,3*RS*)-1-Acetyl-2-(5-((7-bromoheptyl)oxy)pyridin-3-yl)-3-phenylindoline-3-carbonitrile **101**

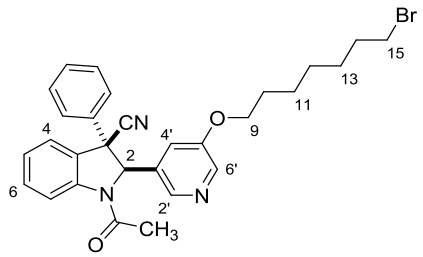

K_2CO_3 (214 mg, 1.55 mmol) was added to a solution of indoline **100** (110 mg, 0.31 mmol) in acetone (20 mL), followed by 1,7-dibromoheptane (0.20 mL, 1.2 mmol). The mixture was stirred under reflux for 8 h, allowed to cool to rt, and concentrated. The remaining residue was dissolved in EtOAc, washed three times with H_2O, then brine. The organic layer was dried over Na_2SO_4, filtered, and concentrated. Purification by flash pressure column chromatography (40% EtOAc/petroleum ether) afforded indoline **101** as a pale yellow oil (63 mg, 0.12 mmol, 38%, contains minor impurities). The non-racemic forms of indoline **101** were prepared from **(*R*,*R*)-100** and **(*S*,*S*)-100**, following an identical protocol.

^{1}H (500 MHz, C_6D_6, 348 K): δ 8.43 (1H, d, *J* 2.5, *H*6'), 8.38 (1H, app br s, *H*7), 8.28 (1H, d, *J* 1.9, *H*2'), 7.24 (2H, m, *o-Ph*), 7.10 (1H, app td, *J* 7.9, 1.2, *H*6), 7.06 (1H, app d, *J* 7.6, *H*4), 7.04 (1H, app t, *J* 2.2, *H*4'), 6.96-7.03 (3H, m, *m-Ph*, *p-Ph*), 6.76 (1H, app td, *J* 7.7, 0.9, *H*5), 5.23 (1H, s, *H*2), 3.47 (2H, app td, *J* 6.7, 1.6, *H*9), 2.99 (2H, t, *J* 6.8, *H*15), 1.44-1.57 (5H, m, *H*14, C*H*$_3$), 1.35 (2H, app quin, *J* 7.4, *H*10), 1.10 (2H, app quin, *J* 7.5, *H*13), 1.04 (2H, app quin, *J* 7.5, *H*11), 0.96 (2H, app quin, *J* 7.2, *H*12).

^{13}C (126 MHz, C_6D_6, 348 K): δ 168.4 (*C*=O), 156.2 (*C*5'), 143.8 (*C*7a), 141.2 (*C*2'), 140.9 (*i-Ph*), 139.8 (*C*6'), 134.8 (*C*3'), 131.3 (*C*6), 130.2 (*m-Ph*/*p-Ph*), 129.4 (*m-Ph*/*p-Ph*), 126.4 (*C*4), 126.2 (*o-Ph*), 126.0 (*C*5), 119.1 (*C*N), 118.6 (*C*4'), 117.6 (*C*7), 74.2 (*C*2), 68.5 (*C*9), 58.1 (*C*3), 34.0 (*C*15), 33.1 (*C*14), 29.3 (*C*10), 28.8 (*C*12), 28.4 (*C*13), 26.0 (*C*11), 23.7 (*C*H$_3$).‡

‡ 1 peak obscured.

HRMS (ES$^+$): $[C_{29}H_{31}{}^{79}BrN_3O_2]^+$ ([M+H]$^+$) requires 532.1594; found 532.1580.

IR: ν_{max} (film)/cm^{-1} 3063, 2935, 2258, 1676 (C=O), 1595, 1479, 1386, 1238, 927, 756, 698.

$[\alpha]_D^{25.0}$ (*R*,*R*) = +26 (*c* = 0.1, $CHCl_3$); $[\alpha]_D^{25.0}$ (*S*,*S*) = -34 (*c* = 0.1, $CHCl_3$).

(2*RS*,3*SR*)-1-acetyl-3-phenyl-2-(5-((7-(pyrrolidin-1-yl)heptyl)oxy)pyridin-3-yl)indoline-3-carbonitrile

99

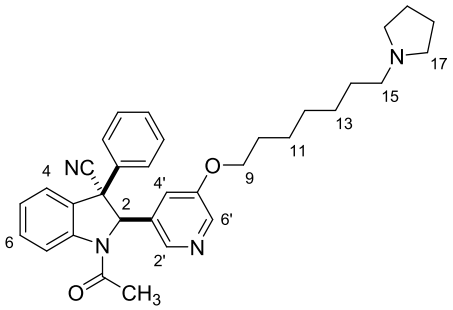

K_2CO_3 (29 mg, 0.21 mmol) was added to a solution of indoline **98** (22 mg, 0.04 mmol) in acetonitrile (3.0 mL), followed by pyrrolidine (14 µL, 0.17 mmol). The mixture was stirred at 60 °C for 2.5 h. H_2O was added, and the mixture was extracted with EtOAc. The combined organic extracts were washed with brine, dried over Na_2SO_4, filtered, and concentrated. Purification by flash pressure column chromatography (4.5-5% MeOH/CH_2Cl_2 + 0.5% aq. NH_4OH) afforded indoline **99** as a colorless oil (14 mg, 0.027 mmol, 65%).

^{1}H (500 MHz, C_6D_6, 348 K): δ 8.36 (1H, app br s, *H*7), 8.09 (1H, d, *J* 2.8, *H*6'), 7.72 (1H, app br s, *H*2'), 7.10 (1H, app td, *J* 7.7, 1.2, *H*6), 7.01 (2H, app d, *J* 7.3, *o-Ph*), 6.77-6.86 (4H, m, *H*4, *m-Ph*, *p-Ph*), 6.74 (1H, app td, *J* 7.7, 1.0, *H*5), 6.32 (1H, app br s, *H*4'), 5.67 (1H, br s, *H*2), 3.32 (2H, app m, *H*9), 2.39-2.46 (6H, m, *H*15, *H*17), 1.61-1.69 (7H, m, *H*18, C*H*$_3$), 1.50 (2H, app quin, *J* 7.3, *H*14), 1.39 (2H, app quin, *J* 6.8, *H*10), 1.32 (2H, app quin, *J* 6.9, *H*13), 1.15-1.23 (4 H, m, *H*11, *H*12).

^{13}C (126 MHz, C_6D_6, 348 K): δ 168.6 (*C*=O), 155.4 (*C*5'), 144.9 (*C*7a), 141.1 (*C*2'), 138.7 (*C*6'), 133.9 (*i-Ph*), 132.9 (*C*3'), 131.5 (*C*6), 129.2 (*Ph*), 129.2 (*Ph*), 129.0 (*Ph*), 126.6 (*C*4), 125.6 (*C*5), 121.7 (*C*N), 119.6 (*C*4'), 117.7 (*C*7), 73.0 (*C*2), 68.5 (*C*9), 56.9 (*C*15/*C*17), 55.8 (*C*3), 54.8 (*C*15/*C*17), 29.9 (*C*11/*C*12), 29.8 (*C*14), 29.5 (*C*10), 28.1 (*C*13), 26.5 (*C*11/*C*12), 24.3 (*C*18), 24.1 (*C*H$_3$).‡

‡ 1 peak obscured.

HRMS (ES$^+$): $[C_{33}H_{39}N_4O_2]^+$ ($[M+H]^+$) requires 523.3068; found 523.3068.

IR: ν_{max} (film)/cm^{-1} 2932, 2235, 1679 (C=O), 1478, 1387, 1183, 1030, 756, 699.

(2*RS*,3*SR*)-1-Acetyl-3-phenyl-2-(5-((7-(pyrrolidin-1-yl)heptyl)oxy)pyridin-3-yl)indoline-3-carbonitrile **102**

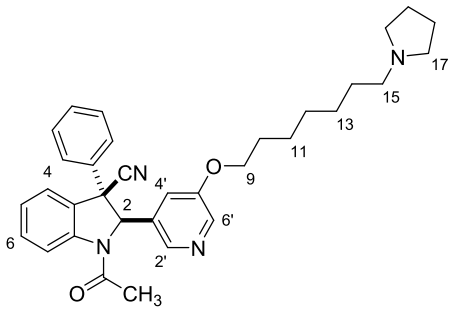

K_2CO_3 (58 mg, 0.42 mmol) was added to a solution of indoline **101** (45 mg, 0.085 mmol) in acetonitrile (6 mL), followed by pyrrolidine (28 µL, 0.34 mmol). The mixture was stirred at 60 °C for 3 h. H_2O was added, and the mixture was extracted with EtOAc. The combined organic extracts were washed with brine, dried over Na_2SO_4, filtered, and concentrated. Purification by flash pressure column chromatography (5% MeOH/CH_2Cl_2 + 0.5% aq. NH_4OH) afforded indoline **102** as a colorless oil (24 mg, 0.046 mmol, 54%). The non-racemic forms of indoline **102** were prepared from **(*R*,*R*)-101** and **(*S*,*S*)-101**, following an identical protocol (e.r. > 99:1).

^{1}H (500 MHz, C_6D_6, 348 K): δ 8.42 (1H, d, *J* 2.5, *H*6'), 8.39 (1H, app br s, *H*7), 8.28 (1H, d, *J* 1.2, *H*2'), 7.24 (2H, m, *o*-*Ph*), 7.05-7.13 (2H, m, *H*4, *H*6), 6.96-7.04 (4H, m, *H*4', *m*-*Ph*, *p*-*Ph*), 6.76 (1H, app td, *J* 7.6, 0.9, *H*5), 5.22 (1H, br s, *H*2), 3.50 (2H, app td, *J* 6.4, 1.7, *H*9), 2.37-2.48 (6H, m, *H*15, *H*17), 1.65 (4H, m, *H*18), 1.46-1.54 (5H, m, *H*14, C*H*$_3$), 1.43 (2H, app quin, *J* 6.8, *H*10), 1.29 (2H, app quin, *J* 7.1, *H*13), 1.18 (4H, m, *H*11, *H*12).

^{13}C (126 MHz, C_6D_6, 348 K): δ 168.5 (*C*=O), 156.3 (*C*5'), 143.9 (*C*7a), 141.1 (*C*2'), 141.0 (*i*-*Ph*), 139.9 (*C*6'), 134.8 (*C*3'), 131.3 (*C*6), 130.2 (*m*-*Ph*/*p*-*Ph*), 129.4 (*m*-*Ph*/*p*-*Ph*), 128.7 (*C*3a), 126.4 (*C*4), 126.3 (*o*-*Ph*), 126.0 (*C*5), 119.2 (*C*N), 118.7 (*C*4'), 117.6 (*C*7), 74.3 (*C*2), 68.7 (*C*9), 58.2 (*C*3), 56.9 (*C*15),

54.8(*C*17), 30.0 (*C*11/*C*12), 29.8 (*C*14), 29.6 (*C*10), 28.1 (*C*13), 26.4 (*C*11/*C*12), 24.3 (*C*18), 23.8 (*C*H_3).

HRMS (ES^+): $[C_{33}H_{39}N_4O_2]^+$ ($[M+H]^+$) requires 523.3068; found 523.3063.

IR: ν_{max}(film)/cm^{-1} 2932, 2789, 1677 (C=O), 1595, 1479, 1386, 1278, 1032, 873, 755, 698.

$[\alpha]_D^{25.0}$ (*R*,*R*) = +57 (*c* = 0.1, $CHCl_3$); $[\alpha]_D^{25.0}$ (*S*,*S*) = -48 (*c* = 0.1, $CHCl_3$).

Chiral HPLC: (Chiralpak ODH, 15% ^{i}PrOH, 85% hexane, 1.3 mL/min, λ = 254 nm, 20 μL)

τ_R (*R*,*R*) = 11.8 min, τ_R (*S*,*S*) = 16.7 min.

(2*RS*,3*RS*)-1-Acetyl-2-(5-((7-(dimethylamino)heptyl)oxy)pyridin-3-yl)-3-phenylindoline-3-carbonitrile **216**

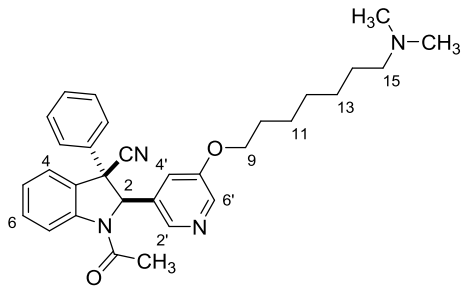

Dimethylamine hydrochloride (20 mg, 0.23 mmol) was added to a solution of indoline **101** (30 mg, 0.056 mmol) in acetonitrile, followed by K_2CO_3 (40 mg, 0.28 mmol). The mixture was stirred 50 °C for 4.5 h. H_2O was added, and the mixture was extracted with EtOAc. The combined organic extracts were washed with brine, dried over Na_2SO_4, filtered, and concentrated. Purification by flash pressure column chromatography (5% MeOH/CH_2Cl_2 + 0.5% aq. NH_4OH) afforded indoline **216** as a colorless oil (19 mg, 0.038 mmol, 68%).

^{1}H (500 MHz, C_6D_6, 348 K): δ 8.42 (1H, d, *J* 2.2, *H*6'), 8.35 (1H, app br s, *H*7), 8.27 (1H, app s, *H*2'), 7.24 (2H, app d, *J* 7.6, Ph), 7.06-7.13 (2H, m, *H*4, *H*6), 6.95-7.05 (4H, m, *H*4', Ph), 6.77 (1H, app t, *J* 7.6, *H*5), 5.24 (1H, s, *H*2), 3.54 (2H, t, *J* 6.5, *H*9), 2.18 (2H, t, *J* 7.1, *H*15), 2.13 (6H, s, *H*17), 1.54 (3H, s, CH_3), 1.46 (2H, app quin, *J* 7.3, *H*10), 1.40 (2H, app quin, *J* 7.2, *H*14), 1.25 (2H, app quin, *J* 7.5, *H*13), 1.11-1.21 (4H, m, *H*11, *H*12).

^{13}C (126 MHz, C_6D_6, 348 K): δ 168.3 (*C*=O), 156.5 (*C*5'), 144.1 (*C*7a), 141.3 (*C*2'), 141.3, 140.4 (*C*6'), 134.8, 131.3 (*C*6), 130.2 (Ph), 130.0, 129.4 (Ph), 126.4 (*C*4), 126.3 (Ph), 125.9 (*C*5), 119.2 (*C*4'), 119.1 (*C*N), 117.7 (*C*7), 74.8 (*C*2), 69.2 (*C*9), 60.4 (*C*15), 58.3 (*C*3), 45.9 (*C*17), 29.9 (*C*11/*C*12), 29.6 (*C*10), 28.4 (*C*14), 28.0 (*C*13), 26.5 (*C*11/*C*12), 23.7 (CH_3).

HRMS (ES$^+$): $[C_{31}H_{37}N_4O_2]^+$ ([M+H]$^+$) requires 497.2911; found 497.2909.

IR: ν_{max} (film)/cm^{-1} 2937, 2858, 1678 (C=O), 1595, 1479, 1387, 1279, 1032, 756.

(2*RS*,3*RS*)-1-Acetyl-2-(5-(2-(2-(2-bromoethoxy)ethoxy)ethoxy)pyridin-3-yl)-3-phenylindoline-3-carbonitrile **158**

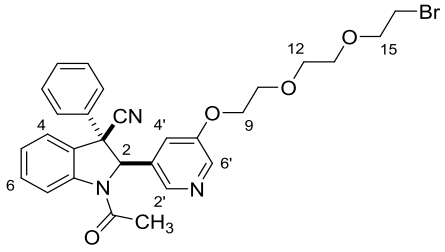

K_2CO_3 (272 mg, 1.97 mmol) was added to a solution of indoline **100** (140 mg, 0.39 mmol) in acetone (25 mL), followed by 1,2-bis(2-bromoethoxy)ethane (410 mg, 1.58 mmol). The mixture was stirred at 50 °C for 2 h, allowed to cool to rt, and concentrated. The remaining residue was dissolved in EtOAc, washed three times with H_2O, then brine. The organic layer was dried over Na_2SO_4, filtered, and concentrated. Purification by flash pressure column chromatography (3.5% MeOH/CH_2Cl_2) afforded indoline **158** as an orange paste (80 mg, 0.15 mmol, 37%, contains minor impurities).

^{1}H (500 MHz, C_6D_6, 348 K): δ 8.41 (1H, d, *J* 2.3, *H*6'), 8.33 (1H, app br s, *H*7), 8.26 (1H, app s, *H*2'), 7.23 (2H, app d, *J* 7.7, *o-Ph*), 7.11 (1H, app t, *J* 7.8, *H*6), 7.04-7.08 (2H, m, *H*4, *H*4'), 6.95-7.04 (3H, m, *m-Ph*, *p-Ph*), 6.77 (1H, app t, *J* 7.6, *H*5), 5.22 (1H, s, *H*2), 3.65 (2H, app m, *H*9), 3.41 (2H, t, *J* 6.3, *H*15), 3.35 (2H, app s, *H*10), 3.24-3.33 (4H, m, *H*12, *H*13), 3.06 (2H, t, *J* 6.3, *H*16), 1.53 (3H, s, CH_3).

^{13}C (126 MHz, C_6D_6, 348 K): δ 168.4 (*C*=O), 156.1 (*C*5'), 143.8 (*C*7a), 141.3 (*C*2'), 141.0 (*i-Ph*), 139.8 (*C*6'), 134.7 (*C*3'), 131.2 (*C*6), 130.1 (*m-Ph*/*p-Ph*), 129.3 (*m-Ph*/*p-Ph*), 126.2 (*C*4), 126.2 (*o-Ph*), 125.9

(*C*5), 119.2 (*C*4'), 119.1 (*C*N), 117.6 (*C*7), 74.2 (*C*2), 71.6 (*C*15), 71.2 (*C*10), 70.9 (*C*12/*C*13), 69.9 (*C*12/*C*13), 68.2 (*C*9), 58.1 (*C*3), 31.0 (*C*16), 23.7 (CH_3).‡

‡ 1 peak obscured.

HRMS (ES^+): $[C_{28}H_{29}{}^{79}BrN_3O_4]^+$ ($[M+H]^+$) requires 550.1336; found 550.1326.

IR: ν_{max}(film)/cm^{-1} 3026, 2923, 2249, 1674 (C=O), 1598, 1479, 1479, 1384, 1279, 1061, 735, 697.

(2*RS*,3*RS*)-1-Acetyl-3-phenyl-2-(5-(2-(2-(2-(pyrrolidin-1-yl)ethoxy)ethoxy)ethoxy)pyridin-3-yl)indoline-3-carbonitrile **159**

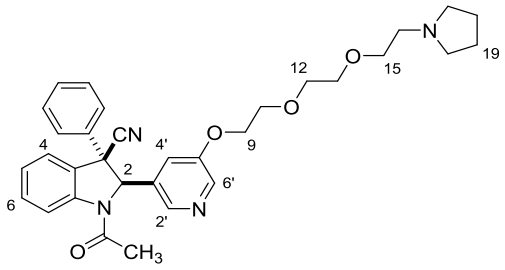

K_2CO_3 (63 mg, 0.45 mmol) was added to a solution of indoline **158** (50 mg, 0.091 mmol) in acetonitrile (6 mL), followed by pyrrolidine (30 µL, 0.36 mmol). The mixture was stirred at 60 °C for 3 h. H_2O was added, and the mixture was extracted with EtOAc. The combined organic extracts were washed with brine, dried over Na_2SO_4, filtered, and concentrated. Purification by flash pressure column chromatography (5% MeOH/CH_2Cl_2 + 0.5% aq. NH_4OH) afforded indoline **159** as a pale yellow oil (38 mg, 0.070 mmol, 77%).

^{1}H (500 MHz, C_6D_6, 348 K): δ 8.41 (1H, d, *J* 2.8, *H*6'), 8.33 (1H, app br s, *H*7), 8.26 (1H, app s, *H*2'), 7.24 (2H, m, *o-Ph*), 7.12 (1H, app t, *J* 8.0, *H*6), 6.96-7.09 (5H, m, *H*4, *H*4', *m-Ph*, *p-Ph*), 6.78 (1H, app t, *J* 7.4, *H*5), 5.24 (1H, s, *H*2), 3.69 (2H, app m, *H*9), 3.51 (2H, t, *J* 6.0, *H*15), 3.36-3.47 (6H, m, *H*10, *H*12, *H*13), 2.63 (2H, t, *J* 6.0, *H*16), 2.46 (4H, m, *H*18), 1.56-1.64 (4H, m, *H*19), 1.55 (3H, s, C*H*$_3$).

^{13}C (126 MHz, C_6D_6, 348 K): δ 168.3 (*C*=O), 156.3 (*C*5'), 144.0 (*C*7a), 141.5 (*C*2'), 141.3 (*i-Ph*), 140.5 (*C*6'), 134.8 (*C*3'), 131.3 (*C*6), 130.2 (*m-Ph*/*p-Ph*), 129.9 (*C*3a), 129.4 (*m-Ph*/*p-Ph*), 126.4 (*C*4), 126.3

(*o-Ph*), 125.9 (*C*5), 119.7 (*C*4'), 119.1 (*C*N), 117.7 (*C*7), 74.7 (*C*2), 71.6 (*C*15), 71.5 (*C*10/*C*12/*C*13), 71.2 (*C*10/*C*12/*C*13), 70.1 (*C*10/*C*12/*C*13), 68.9 (*C*9), 58.3 (*C*3), 56.4 (*C*16), 55.1 (*C*18), 24.5 (*C*19), 23.7 (CH_3).

HRMS (ES^+): $[C_{32}H_{37}N_4O_4]^+$ ($[M+H]^+$) requires 541.2809; found 541.2788.

IR: ν_{max} (film)/cm^{-1} 2875, 2842, 1675 (C=O), 1595, 1479, 1387, 1279, 1124, 757.

(2*RS*,3*RS*)-1-Acetyl-2-(5-((Z)-7-hydroxyhept-1-en-1-yl)pyridin-3-yl)-3-phenylindoline-3-carbonitrile

110

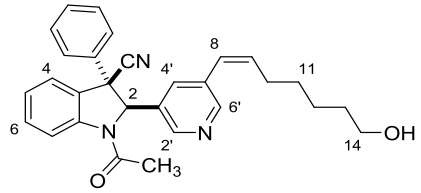

Indoline **110** was prepared according to a modified literature procedure.[97] $InCl_3$ (66 mg, 0.30 mmol) was dissolved in THF (0.9 mL) and cooled to -78 °C. DIBAL-H (1.0 M in hexanes, 0.28 mL, 0.28 mmol) was added and stirred at -78 °C for 45 min. A solution of 6-heptyn-1-ol (22 mg, 0.20 mmol) in THF (0.6 mL) was added, followed by Et_3B (1.0 M in hexanes, 0.19 mL, 0.19 mmol), and the mixture was stirred at -78 °C or 4 h. The reaction was allowed to warm to rt, and a solution of indoline **53** (110 mg, 0.26 mmol) in DMF (0.9 mL) was added, followed by a solution of $Pd(PPh_3)_4$ in THF (4.6 mM, 0.35 mL, 0.0016 mmol). The reaction mixture was stirred at 60 °C for 7 h, then diluted with EtOAc, washed with $NaHCO_3$ (saturated aq), and extracted with EtOAc. The combined organic extracts were washed with brine, dried over Na_2SO_4, filtered, and concentrated. Purification by flash pressure column chromatography (3.5% MeOH/CH_2Cl_2) afforded indoline **110** as a colorless oil (42 mg, 0.093 mmol, 58%, contains minor impurities).

^{1}H (500 MHz, C_6D_6, 348 K): δ 8.59 (1H, app s, *H*6'), 8.46 (1H, app s, *H*2'), 8.34 (1H, app br s, *H*7), 7.42 (1H, app s, *H*4'), 7.24 (2H, m, Ph), 7.14 (1H, app t, *J* 7.8, *H*6), 7.08 (1H, app d, *J* 7.6, *H*4), 6.96-7.05 (3H, m, Ph), 6.80 (1H, app t, *J* 7.6, *H*5), 6.07 (1H, d, *J* 11.7, *H*8), 5.53 (1H, dt, *J* 11.7, 7.6, *H*9), 5.24

(1H, s, *H*2), 3.38 (2H, app q, *J* 6.3, *H*14), 2.02 (2H, app q, *J* 7.4, *H*10), 1.52 (3H, s, C*H*$_3$), 1.33 (2H, app quin, *J* 6.7, *H*13), 1.13-1.24 (4H, m, *H*11, *H*12), 0.94 (1H, t, *J* 5.5, O*H*).

^{13}C (126 MHz, C_6D_6, 348 K): δ 168.3 (*C*=O), 152.2 (*C*6'), 147.1 (*C*2'), 144.0 (*C*7a), 141.2, 136.9 (*C*9), 134.7, 133.7, 133.2 (*C*4'), 131.3 (*C*6), 130.2 (Ph), 129.9, 129.4 (Ph), 126.5 (*C*4), 126.3 (Ph), 126.0 (*C*5), 125.6 (*C*8), 119.1 (*C*N), 117.7 (*C*7), 74.8 (*C*2), 63.0 (*C*14), 58.3 (*C*3), 33.3 (*C*13), 30.0 (*C*11/*C*12), 29.0 (*C*10), 26.1 (*C*11/*C*12), 23.7 (*C*H$_3$).

HRMS (ES$^+$): $[C_{29}H_{30}N_3O_2]^+$ ([M+H]$^+$) requires 452.2333; found 452.2326.

IR: ν_{max} (film)/cm^{-1} 3420 (O-H), 3061, 2243, 1676 (C=O), 1479, 1385, 978, 755, 700.

(*Z*)-7-(5-((2*RS*,3*RS*)-1-Acetyl-3-cyano-3-phenylindolin-2-yl)pyridin-3-yl)hept-6-en-1-yl 4-methylbenzenesulfonate **111**

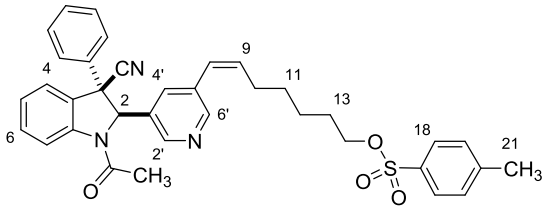

p-Toluenesulfonyl chloride (38 mg, 0.20 mmol) was added to a solution of indoline **110** (30 mg, 0.066 mmol) and pyridine (32 µL, 0.41 mmol) in CH_2Cl_2 (5 mL) at 0 °C. The reaction mixture was stirred at 0 °C for 10 min, allowed to warm to rt, and stirred for a further 20 h. H_2O (5 ml) was added, and the mixture was extracted 3 times with CH_2Cl_2. The combined organic extracts were washed with H_2O, then brine, dried over Na_2SO_4, filtered, and concentrated. Purification by flash pressure column chromatography (55% EtOAc/petroleum ether) afforded indoline **111** as a colorless solid (41 mg, 0.068 mmol, 95%).

^{1}H (500 MHz, C_6D_6, 348 K): δ 8.56 (1H, d, *J* 1.6, *H*6'), 8.46 (1H, d, *J* 1.9, *H*2'), 8.32 (1H, app br s, *H*7), 7.77 (2H, app d, *J* 8.2, *H*18), 7.38 (1H, app s, *H*4'), 7.24 (2H, app d, *J* 8.2, Ph), 7.13-7.18 (1H, obscured, *H*6), 7.10 (1H, app d, *J* 7.6, *H*4), 6.97-7.06 (3H, m, Ph), 6.76-6.88 (3H, m, *H*5, *H*19), 6.04 (1H, d, *J* 11.3,

*H*8), 5.42 (1H, dt, *J* 11.7, 7.4, *H*9), 5.25 (1H, s, *H*2), 3.88 (2H, t, *J* 6.5, *H*14), 1.86-1.95 (5H, m, *H*10, *H*21), 1.53 (3H, s, CH_3), 1.32 (2H, app quin, *J* 6.9, *H*13), 0.93-1.11 (4H, m, *H*11, *H*12).

^{13}C (126 MHz, C_6D_6, 348 K): δ 168.2 (*C*=O), 152.1 (*C*6'), 147.2 (*C*2'), 144.4, 144.0 (*C*7a), 141.2, 136.4 (*C*9), 135.7, 134.5, 133.7, 133.2 (*C*4'), 131.3 (*C*6), 130.2 (Ph), 130.2 (*C*19), 129.4 (Ph), 126.5 (*C*4), 126.3 (Ph), 126.0 (*C*5), 125.8 (*C*8), 119.1 (*C*N), 117.6 (*C*7), 74.7 (*C*2), 70.5 (*C*14), 58.3 (*C*3), 29.5 (*C*11/*C*12), 29.4 (*C*13), 28.8 (*C*10), 25.6 (*C*11/*C*12), 23.7 (*C*H_3), 21.4 (*C*21).‡

‡ 2 peaks obscured.

HRMS (ES$^+$): $[C_{36}H_{36}N_3O_4S]^+$ ($[M+H]^+$) requires 606.2421; found 606.2414.

IR: ν_{max} (film)/cm^{-1} 3029, 2927, 1677 (C=O), 1479, 1387, 1189, 1033, 1011, 665.

MP: 104-106°C.

(2*RS*,3*RS*)-1-Acetyl-3-phenyl-2-(5-((*Z*)-7-(pyrrolidin-1-yl)hept-1-en-1-yl)pyridin-3-yl)indoline-3-carbonitrile **109**

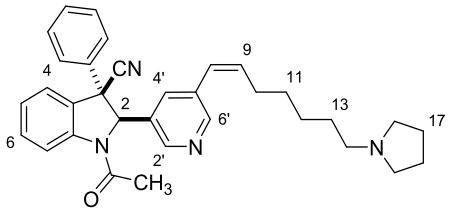

Pyrrolidine (23 µL, 0.28 mmol) was added to a solution of indoline **111** (17 mg, 0.028 mmol) in CH_3CN (2 mL). The reaction mixture was stirred at 50 °C for 1 h, then allowed to cool to rt and diluted with EtOAc. The solution was washed twice with H_2O, then with brine. The organic layer was dried over Na_2SO_4, filtered, and concentrated. Purification by flash pressure column chromatography (5% MeOH/CH_2Cl_2 + 0.5% aq. NH_4OH) to afford indoline **109** as a pale yellow oil (9.2 mg, 0.018 mmol, 64%).

^{1}H (500 MHz, C_6D_6, 348 K): δ 8.61 (1H, d, *J* 1.5, *H*6'), 8.46 (1H, d, *J* 1.9, *H*2'), 8.36 (1H, app br s, *H*7), 7.43 (1H, app s, *H*4'), 7.25 (2H, m, Ph), 7.13-7.18 (1H, obscured, *H*6), 7.10 (1H, app d, *J* 7.6, *H*4),

6.94-7.06 (3H, m, Ph), 6.81 (1H, app t, *J* 7.6, *H*5), 6.07 (1H, d, *J* 11.7, *H*8), 5.57 (1H, dt, *J* 11.6, 7.4, *H*9), 5.23 (1H, s, *H*2), 2.43 (4H, m, *H*16), 2.38 (2H, t, *J* 7.3, *H*14), 2.07 (2H, app q, *J* 7.0, *H*10), 1.64 (4H, m, *H*17), 1.52 (3H, s, CH_3), 1.45 (2H, app quin, *J* 7.1, *H*13), 1.22-1.33 (4H, m, *H*11, *H*12).

^{13}C (126 MHz, C_6D_6, 348 K): δ 168.2 (*C*=O), 152.2 (*C*6'), 147.1 (*C*2'), 144.1 (*C*7a), 141.3, 137.0 (*C*9), 134.7, 133.7, 133.2 (*C*4'), 131.3 (*C*6), 130.2 (Ph), 129.9, 129.4 (Ph), 126.4 (*C*4), 126.3 (Ph), 125.9 (*C*5), 125.5 (*C*8), 119.1 (*C*N), 117.7 (*C*7), 74.8 (*C*2), 58.3 (*C*3), 56.9 (*C*14), 54.7 (*C*16), 30.4 (*C*11/*C*12), 29.7 (*C*13), 29.3 (*C*10), 27.9 (*C*11/*C*12), 24.5 (*C*17), 23.7 (*C*H_3).

HRMS (ES$^+$): $[C_{33}H_{37}ON_4]^+$ ([M+H]$^+$) requires 505.2962; found 505.2961.

IR: ν_{max}(film)/cm^{-1} 3028, 2931, 2242, 1676 (C=O), 1479, 1387, 1026, 755, 698.

(2*RS*,3*SR*)-1-Acetyl-3-phenyl-2-(5-((E)-7-(pyrrolidin-1-yl)hept-1-en-1-yl)pyridin-3-yl)-2,3-dihydro-1H-pyrrolo[3,2-b]pyridine-3-carbonitrile **181**

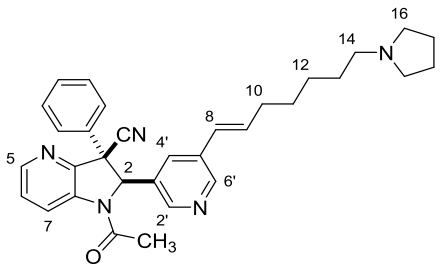

Indoline **181** was prepared according to general procedure 4 using indoline **180** (30 mg, 0.072 mmol), vinylstannane **57** (42 mg, 0.093 mmol), and Pd(PPh$_3$)$_4$ (8 mg, 0.007 mmol) in NMP (1.5 mL). The reaction mixture was stirred at 85 °C for 1.5 h. Purification by flash pressure column chromatography (4.5% MeOH/CH_2Cl_2 + 0.5% aq. NH_4OH) afforded indoline **181** as a pale yellow oil (20 mg, 0.040 mmol, 55%).

^{1}H (500 MHz, C_6D_6, 348 K): δ 8.66 (1H, d, *J* 1.8, *H*2'/*H*6'), 8.44 (1H, app br s, *H*7), 8.38 (1H, d, *J* 2.0, *H*2'/*H*6'), 8.03 (1H, dd, *J* 4.8 Hz, 1.3, *H*5), 7.35 (1H, app s, *H*4'), 7.31 (2H, m, *Ph*), 6.95-7.05 (3H, m, *Ph*), 6.70 (1H, dd, *J* 8.2, 4.8, *H*6), 5.98-6.08 (2H, m, *H*8, *H*9),[‡] 5.29 (1H, s, *H*2), 2.43 (4H, m, *H*16), 2.39 (2H, t, *J* 7.2, *H*14), 1.96 (2H, app br s, *H*10), 1.64 (4H, m, *H*17), 1.44-1.53 (5H, m, *H*13, CH_3), 1.28-

1.36 (4H, m, *H*11, *H*12).

^{13}C (126 MHz, C_6D_6, 348 K): δ 169.0 (*C*=O), 150.0, 147.2 (*C*2'/*C*6'), 147.0 (*C*5), 140.2 (*C*2'/*C*6'), 140.0, 135.4 (*C*8/*C*9), 134.8, 133.6, 130.6 (*C*4'), 130.2 (*Ph*), 129.4 (*Ph*), 126.7 (*C*8/*C*9), 126.3 (*Ph*), 124.9 (*C*6), 124.3 (*C*N), 117.6 (*C*7), 73.2 (*C*2), 59.6 (*C*3), 56.7 (*C*14), 54.7 (*C*16), 33.6 (*C*10), 29.6 (*C*11/*C*12/*C*13), 29.5 (*C*11/*C*12/*C*13), 27.9 (*C*11/*C*12/*C*13), 24.5 (*C*17), 23.3 (CH_3).‡

ł ^{1}H NMR (400 MHz, C_6D_6): δ 5.98 (1H, dt, *J* 16.0, 6.5, *H*9), 5.88 (1H, d, *J* 16.0, *H*8).

‡ 1 peak obscured.

HRMS (ES$^+$): $[C_{23}H_{36}N_5O]^+$ ($[M+H]^+$) requires 506.2914; found 506.2914.

IR: ν_{max} (film)/cm^{-1} 2931, 2790, 2261, 1682 (C=O), 1439, 1381, 1277, 1024, 969, 804, 698.

2-(2-Nitrophenyl)-2-(thiazol-2-yl)acetonitrile **182**

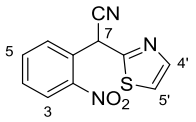

Thiazole **182** was prepared according to a modified literature procedure.[195] A solution of 2-nitrophenylacetonitrile (800 mg, 4.93 mmol) in DMSO (8 mL) was added dropwise to a suspension of 2-chlorothiazole (0.42 mL, 4.9 mmol) and Cs_2CO_3 (3.54 g, 10.9 mmol) in DMSO (8 mL) and stirred at 80 °C for 16 h. The mixture was allowed to cool to rt, and NH_4Cl (saturated aq.) was added. The mixture was extracted with CH_2Cl_2. The combined organic extracts were washed three times with H_2O, then brine, dried over Na_2SO_4, filtered, and concentrated. Purification by flash pressure column chromatography (20% EtOAc/petroleum ether) afforded nitrile **182** as an orange solid (344 mg, 1.40 mmol, 28%).

^{1}H (400 MHz, $CDCl_3$): δ 8.18 (1H, dd, *J* 7.8, 1.2, *H*3), 7.97 (1H, dd, *J* 7.8, 1.3, *H*6), 7.74-7.83 (2H, m, *H*5, *H*4'), 7.63 (1H, app td, *J* 7.8, 1.3, *H*4), 7.39 (1H, d, *J* 3.4, *H*5'), 6.61 (1H, s, *H*7).

^{13}C (101 MHz, $CDCl_3$): δ 161.3, 147.1, 143.6 (*C*5/*C*4'), 134.6 (*C*5/*C*4'), 131.2 (*C*6), 130.5 (*C*4), 128.2, 125.9 (*C*3), 121.2 (*C*5'), 116.7 (*C*N), 37.2 (*C*7).

HRMS (ES$^+$): $[C_{11}H_7O_2Na^{32}S]^+$ ([M+Na]$^+$) requires 268.01512; found 268.01512.

IR: ν_{max}(film)/cm^{-1} 3118, 2947, 2249, 1526, 1497, 1346, 787, 735.

MP: 40-41 °C.

(2*RS*,3*RS*)-2-(5-Bromopyridin-3-yl)-3-(thiazol-2-yl)indoline-3-carbonitrile **189**

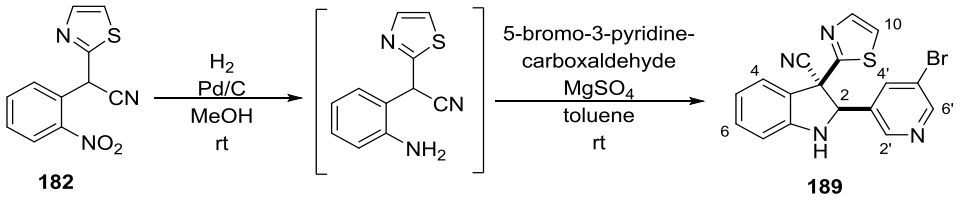

Pd/C (wet Degussa type, 30 mg) was added to a solution of nitrile **182** (300 mg, 1.22 mmol) in MeOH (12 mL). The suspension was first degassed 3 times with N_2 and then 3 times with H_2 using a pump-flood procedure. The mixture was stirred under a H_2 atmosphere for 18 h, then flushed with N_2 before being filtered through Celite^{TM}, eluted with EtOAc, and concentrated. Purification by flash pressure column chromatography (25% EtOAc/petroleum ether) afforded an orange solid (150 mg, impure), which was re-dissolved in toluene (6 mL). $MgSO_4$ (414 mg, 3.44 mmol) and 5-bromo-3-pyridinecarboxaldehyde (166 mg, 0.89 mmol) were added, and the mixture was stirred at rt for 48 h. The mixture was filtered and concentrated. Purification by flash pressure column chromatography (40% EtOAc/petroleum ether) afforded indoline **189** as a yellow solid (62 mg, 0.16 mmol, 13%).

N.B. Stereochemistry was assigned by analogy to indolines **49** and **50**.

^{1}H (500 MHz, C_6D_6): δ 8.54 (1H, d, *J* 2.4, *H*6'), 8.46 (1H, d, *J* 1.9, *H*2'), 7.42 (1H, app t, *J* 2.1, *H*4'), 7.07 (1H, d, *J* 3.3, *H*11), 6.98-7.05 (2H, m, *H*4, *H*6), 6.62 (1H, app td, *J* 7.6, 0.9, *H*5), 6.38 (1H, app d, *J* 7.9, *H*7), 6.16 (1H, d, *J* 3.3, *H*10), 4.72 (1H, d, *J* 3.5 *H*2), 2.79 (1H, d, *J* 3.3, N*H*).

^{13}C (126 MHz, C_6D_6): δ 164.5 (*C*8), 151.7 (*C*6'), 150.3 (*C*7a), 147.9 (*C*2'), 143.8 (*C*11), 137.6 (*C*4'), 133.8 (*C*3'), 131.5 (*C*4/*C*6), 127.4 (*C*3a), 126.2 (*C*4/*C*6), 121.6 (*C*5), 121.3 (*C*10), 120.8 (*C*5'), 119.4

(*C*N), 111.5 (*C*7), 72.0 (*C*2), 54.7 (*C*3).

HRMS (ES^+): $[C_{17}H_{12}N_4{}^{79}Br^{32}S]^+$ ($[M+H]^+$) requires 382.9961; found 382.9963.

IR: ν_{max} (film)/cm^{-1} 3187, 2952, 1609, 1485, 1423, 1261, 1022, 885, 748, 706.

MP: 152-155 °C.

(2*RS*,3*RS*)-1-Acetyl-2-(5-bromopyridin-3-yl)-3-(thiazol-2-yl)indoline-3-carbonitrile **192**

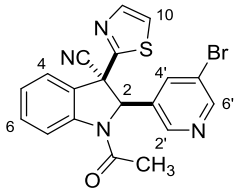

Indoline **192** was prepared according to general procedure 2, using indoline **189** (52 mg, 0.14 mmol), acetyl chloride (24 μL, 0.33 mmol), and pyridine (26 μL, 0.33 mmol) in CH_2Cl_2 (3 mL). The reaction mixture was stirred at rt for 1 h. $NaHCO_3$ (saturated aq., 3 mL) was added, and the mixture was stirred at rt for a further 10 min. Purification by flash pressure column chromatography (42% EtOAc/petroleum ether) afforded indoline **192** as a pale yellow solid (55 mg, 0.13 mmol, 92%).

^{1}H NMR (400 MHz, $CDCl_3$): δ 8.43 (1H, d, *J* 1.3, *H*6'), 8.36 (1H, app br s, *H*7), 8.07 (1H, d, *J* 1.9, *H*2'), 7.80 (1H, d, *J* 3.3, *H*11), 7.61 (1H, app td, *J* 7.9, 1.2, *H*6), 7.49 (1H, app d, *J* 7.6, *H*4), 7.28-7.35 (2H, m, *H*4', *H*5), 7.24 (1H, d, *J* 3.3, *H*10), 6.08 (1H, br s, *H*2), 2.24 (3H, br s, CH_3).

^{13}C NMR (100.6 MHz, $CDCl_3$): δ 168.0 (*C*=O), 162.2 (*C*8), 151.3 (*C*6'), 146.3 (*C*2'), 143.9 (*C*11), 143.3 (*C*7a), 136.9 (*C*4'), 132.4 (*C*6), 132.2 (*C*3'), 126.4 (*C*4), 125.8 (*C*5), 121.9 (*C*10), 120.5 (*C*5'), 118.6 (*C*N), 117.7 (*C*7), 71.5 (*C*2), 53.2 (*C*3), 24.2 (*C*H_3).[ł]

ł 1 peak obscured.

HRMS (ES^+): $[C_{19}H_{14}{}^{79}BrN_4OS]^+$ ($[M+H]^+$) requires 425.0066; found 425.0066.

IR: ν_{max} (film)/cm^{-1} 3051, 2248, 1677 (C=O), 1478, 1384, 1219, 1020, 756, 704.

MP: 188-190 °C.

(2*RS*,3*RS*)-1-Acetyl-2-(5-((*E*)-7-(pyrrolidin-1-yl)hept-1-en-1-yl)pyridin-3-yl)-3-(thiazol-2-yl)indoline-3-carbonitrile **193**

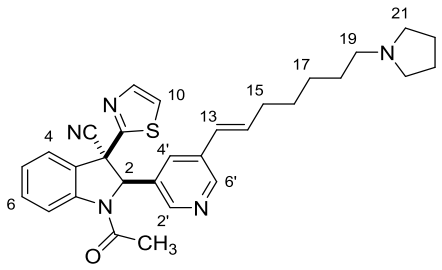

Indoline **193** was prepared according to general procedure 4 using indoline **192** (40 mg, 0.094 mmol), vinylstannane **57** (55 mg, 0.12 mmol), and $Pd(PPh_3)_4$ (14 mg, 0.012 mmol) in NMP (1.5 mL). The reaction mixture was stirred at 85 °C for 2 h. Purification by flash pressure column chromatography (4.5% MeOH/CH_2Cl_2 + 0.5% aq. NH_4OH) afforded indoline **193** as a pale yellow oil (29 mg, 0.057 mmol, 60%).

^{1}H NMR (500 MHz, C_6D_6): δ 8.68 (1H, app br s, *H*7), 8.37 (1H, d, *J* 2.0, *H*6'), 8.09 (1H, app s, *H*2'), 7.33 (1H, d, *J* 3.3, *H*11), 7.07 (1H, app t, *J* 7.7, *H*6), 6.97 (1H, app br s, *H*4'), 6.93 (1H, app d, *J* 7.9, *H*4), 6.71 (1H, app td, *J* 7.6, 0.9, *H*5), 6.20 (1H, d, *J* 3.3, *H*10), 5.88 (1H, dt, *J* 16.0, 6.5, *H*14), 5.83 (1H, br s, *H*2), 5.78 (1H, d, *J* 16.0, *H*13), 2.32-2.44 (6H, m, *H*19, *H*21), 1.88 (2H, app q, *J* 6.8, *H*15), 1.64 (4H, m, *H*22), 1.38-1.55 (5H, m, *H*18, C*H*$_3$), 1.27 (4H, m, *H*16, *H*17).

^{13}C NMR (126 MHz, C_6D_6): δ 168.5 (*C*=O), 163.6 (*C*8), 148.7 (*C*6'), 147.3 (*C*2'), 144.8 (*C*7a), 143.8 (*C*11), 134.8 (*C*14), 133.5 (*C*5'), 132.4 (*C*6), 131.5 (*C*4'), 131.1 (*C*3'), 126.7 (*C*4), 126.2 (*C*13), 125.6 (*C*5), 121.9 (*C*10), 119.8 (*C*N), 118.0 (*C*7), 72.7 (*C*2), 56.8 (*C*19), 54.7 (*C*21), 54.3 (*C*3), 33.7 (*C*15), 29.6 (*C*18), 29.6 (*C*16/*C*17), 27.8 (*C*16/*C*17), 24.3 (*C*22), 24.0 (*C*H$_3$).ǂ

ǂ 1 peak obscured.

HRMS (ES$^+$): $[C_{30}H_{34}N_5OS]^+$ ([M+H]$^+$) requires 512.2479; found 512.2478.

IR: ν_{max}(film)/cm^{-1} 2931, 2790, 2194, 1679 (C=O), 1478, 1386, 1351, 1024, 756.

(*R*)-1-(But-3-yn-1-yloxy)-3-(pyrrolidin-1-yl)propan-2-ol **164**

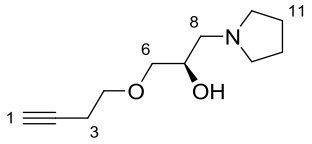

Alkyne **164** was prepared according to a modified literature procedure.[122] NaOH (50% w/w aq., 0.64 mL, 24 mmol) and tetrabutylammonium bromide (341 mg, 1.06 mmol) were added to a solution of 3-butyn-1-ol (0.80 mL, 11 mmol) in hexane (20 mL). *R*-(-)-epichlorohydrin (1.9 mL, 24 mmol) was added dropwise, and the mixture was stirred at 45 °C for 3 h. The mixture was allowed to cool to rt, diluted with Et_2O, and washed three times with H_2O, then brine. The organic layer was dried over Na_2SO_4, filtered, and concentrated to afford a pale yellow liquid (1.13 g). The crude product (250 mg) was dissolved in a solution of pyrrolidine (1.65 mL, 19.8 mmol) in EtOH (10 mL), and the mixture was stirred at 100 °C for 2.5 h. The solution was allowed to cool to rt, NH_4Cl (saturated aq., 25 mL) was added, and the mixture was extracted with EtOAc. The combined organic extracts were washed three times with H_2O, then brine, dried over Na_2SO_4, filtered, and concentrated. Purification by flash pressure column chromatography afforded alkyne **164** as a yellow hygroscopic solid (165 mg, 0.84 mmol, 42%).

^{1}H (400 MHz, $CDCl_3$): δ 3.86 (1H, app qt, *J* 9.6, 6.0, 3.8, *H*7), 3.61 (2H, t, *J* 7.2, *H*4), 3.52 (1H, dd, *J* 10.0, 3.8, *H*6), 3.44 (1H, dd, *J* 10.0, 6.0, *H*6'), 3.39 (1H, br s, O*H*), 2.59-2.71 (3H, m, *H*8, *H*10), 2.42-2.54 (4H, m, *H*3, *H*10'), 2.36 (1H, dd, *J* 12.1, 3.8, *H*8'), 1.97 (1H, t, *J* 2.7, *H*1), 1.70-1.82 (4H, m, *H*11).

^{13}C (101 MHz, $CDCl_3$): δ 81.2 (*C*2), 73.6 (*C*6), 69.4 (*C*1), 69.3 (*C*4), 67.9 (*C*7), 58.4 (*C*8), 54.1 (*C*10), 23.5 (*C*11), 19.7 (*C*3).

HRMS (ES^+): $[C_{11}H_{20}O_2N]^+$ ($[M+H]^+$) requires 198.1489; found 198.1490.

IR: ν_{max} (film)/cm^{-1} 3480 (br, O-H), 3300 (sharp, C-H), 2876, 2803, 1117, 1063.

$[\alpha]_D^{25.0}$ = -26 (*c* = 0.1, $CHCl_3$).

(*S*)-1-(But-3-yn-1-yloxy)-3-(pyrrolidin-1-yl)propan-2-ol **163**

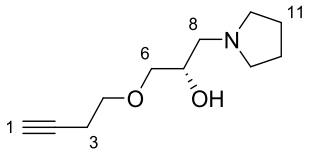

Alkyne **163** was prepared according to the same procedure as **164**,[122] using NaOH (50% w/w aq., 0.64 mL, 24 mmol), tetrabutylammonium bromide (341 mg, 1.06 mmol), 3-butyn-1-ol (0.80 mL, 11 mmol), and *S*-(+)-epichlorohydrin (1.9 mL, 24 mmol) in hexane (20 mL). The reaction mixture was stirred at 45 °C for 4 h. The crude product (600 mg) was dissolved in a solution of pyrrolidine (4.0 mL, 48 mmol) in EtOH (25 mL), and the mixture was stirred at 100 °C for 2 h. The solution was allowed to cool to rt, and NH_4Cl (saturated aq., 50 mL) was added, and the mixture was extracted with EtOAc. The combined organic extracts were washed three times with H_2O, then brine, dried over Na_2SO_4, filtered, and concentrated. Purification by flash pressure column chromatography afforded alkyne **163** as a yellow hygroscopic solid (419 mg, 2.12 mmol, 45%).

The spectral and mass properties of alkyne **163** are identical to those of alkyne **164**.

$[\alpha]_D^{25.0}$ = +19 (*c* = 0.1, $CHCl_3$).

(2*R*,3*R*)-1-Acetyl-2-(5-(4-((S)-2-hydroxy-3-(pyrrolidin-1-yl)propoxy)but-1-yn-1-yl)pyridin-3-yl)-3-phenylindoline-3-carbonitrile **165**

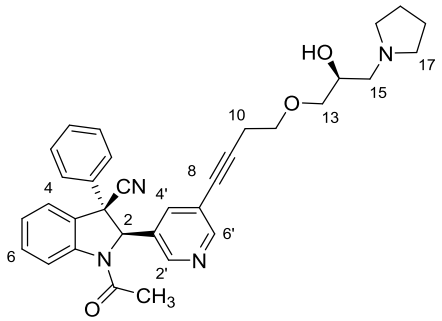

Indoline **165** was prepared according to general procedure 5 using indoline **(*R*,*R*)-157** (25 mg, 0.051 mmol), alkyne **163** (14 mg, 0.072 mmol), $PdCl_2(PPh_3)_2$ (1.8 mg, 0.0026 mmol), and CuI (< 1 mg) in diisopropylamine (1.2 mL). The reaction mixture was stirred at 70 °C for 2.5 h. Purification by

flash pressure column chromatography (4.5% MeOH/CH_2Cl_2 + 0.5% aq. NH_4OH) afforded indoline **165** as a pale yellow gum (14 mg, 0.026 mmol, 51%).

^{1}H NMR (500 MHz, C_6D_6, 348 K): δ 8.79 (1H, d, *J* 1.7, *H*6'), 8.46 (1H, d, *J* 1.8, *H*2'), 8.22 (1H, app br s, *H*7), 7.58 (1H, app s, *H*4'), 7.18-7.22 (2H, m, *o-Ph*), 7.07 (1H, app t, *J* 7.9, *H*6), 6.95-7.05 (4H, m, *H*4, *m-Ph*, *p-Ph*), 6.73 (1H, app t, *J* 7.5, *H*5), 5.18 (1H, br s, *H*2), 3.84 (1H, app sex, *J* 4.8, *H*14), 3.32-3.51 (4H, m, *H*11, *H*13), 2.58 (1H, dd, *J* 12.1, 8.7, *H*15), 2.45 (2H, m, *H*17), 2.35-2.42 (3H, m, *H*10, *H*15'), 2.31 (2H, m, *H*17'), 1.52 (4H, m, *H*18), 1.48 (3H, s, CH_3).‡

^{13}C NMR (126 MHz, C_6D_6, 348 K): δ 168.0 (*C*=O), 154.4 (*C*6'), 147.4 (*C*2'), 143.7 (*C*7a), 141.1 (*C*3'/*i-Ph*), 136.4 (*C*4'), 133.9 (*C*3'/*i-Ph*), 131.3 (*C*6), 130.2 (*C*4/*m-Ph*/*p-Ph*), 129.7 (*C*3a), 129.4 (*C*4/*m-Ph*/*p-Ph*), 126.4 (*C*4/*m-Ph*/*p-Ph*), 126.3 (*o*-Ph), 126.0 (*C*5), 122.2 (*C*5'/*C*N), 119.0 (*C*5'/*C*N), 117.6 (*C*7), 92.9 (*C*8/*C*9), 78.8 (*C*8/*C*9), 74.7 (*C*11/*C*13), 74.5 (*C*2), 70.0 (*C*11/*C*13), 69.1 (*C*14), 59.7 (*C*15), 58.0 (*C*3), 54.9 (*C*17), 24.4 (*C*18), 23.7 (*C*H_3), 21.6 (*C*10).

‡ O*H* signal not observed.

HRMS (ES^+): $[C_{33}H_{35}O_3N_4]^+$ ($[M+H]^+$) requires 535.2704; found 535.2706.

IR: ν_{max} (film)/cm^{-1} 3412 (br, O-H), 2934, 2882, 2249, 1676 (C=O), 1479, 1387, 1119, 758, 698.

$[\alpha]_D^{25.0}$ = -74 (*c* = 0.1, $CHCl_3$).

(2*R*,3*R*)-1-Acetyl-2-(5-(4-((*R*)-2-hydroxy-3-(pyrrolidin-1-yl)propoxy)but-1-yn-1-yl)pyridin-3-yl)-3-phenylindoline-3-carbonitrile **167**

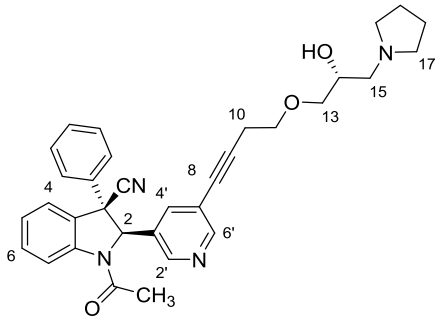

Indoline **167** was prepared according to general procedure 5 using indoline **(*R*,*R*)-157** (25 mg, 0.051 mmol), alkyne **164** (14 mg, 0.072 mmol), $PdCl_2(PPh_3)_2$ (1.8 mg, 0.0026 mmol), and CuI (< 1 mg) in diisopropylamine (1.2 mL). The reaction mixture was stirred at 70 °C for 1.5 h. Purification by flash pressure column chromatography (4.5% MeOH/CH_2Cl_2 + 0.5% aq. NH_4OH) afforded indoline **167** as a pale yellow gum (17 mg, 0.032 mmol, 62%).

^{1}H NMR (500 MHz, C_6D_6, 348 K): δ 8.80 (1H, d, *J* 1.8, *H*6'), 8.45 (1H, d, *J* 2.3, *H*2'), 8.22 (1H, app br s, *H*7), 7.58 (1H, app t, *J* 1.9, *H*4'), 7.16-7.25 (2H, m, *o-Ph*), 7.06 (1H, app t, *J* 7.8, *H*6), 6.94-7.04 (4H, m, *H*4, *m-Ph*, *p-Ph*), 6.72 (1H, app t, *J* 7.6, *H*5), 5.17 (1H, s, *H*2), 3.83 (1H, app sex, *J* 4.6, *H*14), 3.34-3.49 (4H, m, *H*11, *H*13), 2.58 (1H, dd, *J* 12.1, 8.7, *H*15), 2.44 (2H, m, *H*17), 2.34-2.41 (3H, m, *H*10, *H*15'), 2.26-2.34 (2H, m, *H*17'), 1.51 (4H, m, *H*18), 1.46 (3H, s, C*H*$_3$).‡

^{13}C NMR (126 MHz, C_6D_6, 348 K): δ 168.0 (*C*=O), 154.3 (*C*6'), 147.4 (*C*2'), 143.7 (*C*7a), 141.1 (*C*3'/*i-Ph*), 136.3 (*C*4'), 133.8 (*C*3'/*i-Ph*), 131.2 (*C*6), 130.2 (*C*4/*m-Ph*/*p-Ph*), 129.7 (*C*3a), 129.3 (*C*4/*m-Ph*/*p-Ph*), 126.4 (*C*4/*m-Ph*/*p-Ph*), 126.2 (*o*-Ph), 126.0 (*C*5), 122.2 (*C*5'/*C*N), 118.9 (*C*5'/*C*N), 117.6 (*C*7), 92.9 (*C*8/*C*9), 78.8 (*C*8/*C*9), 74.6 (*C*11/*C*13), 74.5 (*C*2), 70.0 (*C*11/*C*13), 69.0 (*C*14), 59.7 (*C*15), 58.0 (*C*3), 54.8 (*C*17), 24.4 (*C*18), 23.6 (*C*H$_3$), 21.6 (*C*10).

‡ O*H* peak not observed.

HRMS (ES$^+$): $[C_{33}H_{35}O_3N_4]^+$ ([M+H]$^+$) requires 535.27037; found 535.27063.

IR: ν_{max} (film)/cm^{-1} 3415 (br, O-H), 2923, 2247, 1676 (C=O), 1479, 1385, 1275, 1117, 1024, 750, 696.

$[\alpha]_D^{25.0}$ = +52 (*c* = 0.1, $CHCl_3$).

(2*S*,3*S*)-1-Acetyl-2-(5-(4-((S)-2-hydroxy-3-(pyrrolidin-1-yl)propoxy)but-1-yn-1-yl)pyridin-3-yl)-3-phenylindoline-3-carbonitrile **169**

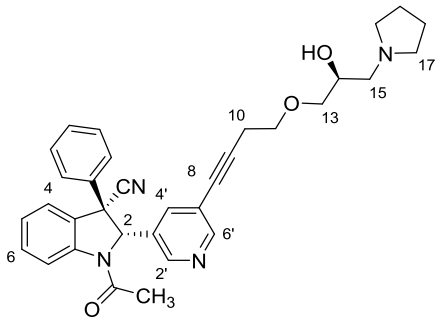

Indoline **169** was prepared according to general procedure 5 using indoline **(*S*,*S*)-157** (60 mg, 0.12 mmol), alkyne **105** (26 mg, 0.14 mmol), $PdCl_2(PPh_3)_2$ (4.3 mg, 0.0060 mmol), and CuI (< 1 mg) in diisopropylamine (2.5 mL). The reaction mixture was stirred at 70 °C for 2 h. Purification by flash pressure column chromatography (4.5% MeOH/CH_2Cl_2 + 0.5% aq. NH_4OH) afforded indoline **169** as a pale yellow gum (42 mg, 0.079 mmol, 64%).

The spectral and mass properties of indoline **169** are identical to those of indoline **167**.

$[\alpha]_D^{25.0}$ = -60 (*c* = 0.1, $CHCl_3$).

(2*S*,3*S*)-1-Acetyl-2-(5-(4-((*R*)-2-hydroxy-3-(pyrrolidin-1-yl)propoxy)but-1-yn-1-yl)pyridin-3-yl)-3-phenylindoline-3-carbonitrile **171**

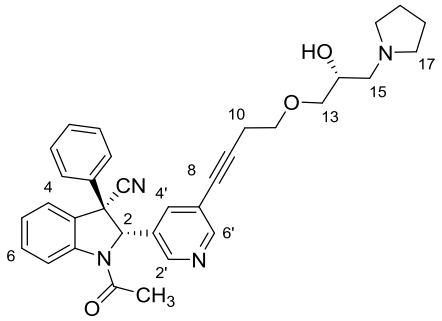

Indoline **171** was prepared according to general procedure 5 using indoline **(*S*,*S*)-157** (60 mg, 0.12 mmol), alkyne **164** (26 mg, 0.14 mmol), $PdCl_2(PPh_3)_2$ (4.3 mg, 0.0060 mmol), and CuI (< 1 mg) in diisopropylamine (2.5 mL). The reaction mixture was stirred at 70 °C for 2 h. Purification by flash

pressure column chromatography (4.5% MeOH/CH_2Cl_2 + 0.5% aq. NH_4OH) afforded indoline **171** as a pale yellow gum (42 mg, 0.079 mmol, 64%).

The spectral and mass properties of indoline **171** are identical to those of indoline **165**.

$[\alpha]_D^{25.0}$ = -85 (*c* = 0.1, $CHCl_3$).

(2*R*,3*R*)-1-Acetyl-2-(5-(4-((*S*)-2-hydroxy-3-(pyrrolidin-1-yl)propoxy)butyl)pyridin-3-yl)-3-phenylindoline-3-carbonitrile **166**

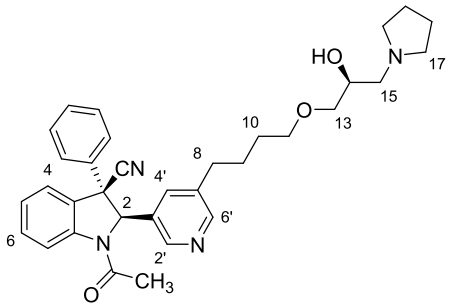

Indoline **166** was prepared according to general procedure 3 using indoline **165** (12 mg, 0.022mmol) and Pd/C (wet degussa type, 2 mg) in MeOH (1.2 mL). The reaction mixture was stirred at rt under a H_2 atmosphere for 3 h. Purification by flash pressure column chromatography (4.5% MeOH/CH_2Cl_2 + 0.5% aq. NH_4OH) afforded indoline **166** as a pale yellow oil (8.2 mg, 0.015 mmol, 69%).

^{1}H NMR (500 MHz, C_6D_6, 348 K): δ 8.49 (1H, d, *J* 1.8, *H*6'), 8.45 (1H, d, *J* 1.8, *H*2'), 8.41 (1H, app br s, *H*7), 7.21-7.30 (3H, m, *H*4', *o-Ph*), 7.17 (1H, app td, *J* 7.8, 1.2, *H*6), 7.08 (1H, app d, *J* 7.8, *H*4), 6.96-7.05 (3H, m, *m-Ph*, *o-Ph*), 6.78 (1H, app td, *J* 7.5, 0.9, *H*5), 5.22 (1H, s, *H*2), 3.89 (1H, app sex, *J* 4.4, *H*14), 3.42 (2H, m, *H*13, *H*13'), 3.26 (2H, app td, *J* 6.5, 2.5, *H*11), 2.61 (1H, dd, *J* 12.2, 8.6, *H*15), 2.45-2.52 (2H, m, *H*17), 2.43 (1H, dd, *J* 12.2, 4.4, *H*15'), 2.34 (2H, m, *H*17'), 2.23 (2H, t, *J* 7.4, *H*8), 1.49-1.57 (7H, m, *H*18, C*H*$_3$), 1.45 (2H, app quin, *J* 7.4, *H*9), 1.37 (2H, app quin, *J* 7.1, *H*10).[ŧ]

^{13}C NMR (126 MHz, C_6D_6, 348 K): δ 168.3 (*C*=O), 152.3 (*C*6'), 146.6 (*C*2'), 144.0 (*C*7a), 141.3, 138.8, 133.7, 133.6 (*C*4'), 131.2 (*C*6), 130.1 (*m-Ph*/*p-Ph*), 129.3 (*m-Ph*/*p-Ph*), 126.4 (*C*4), 126.2 (*o-Ph*), 125.9 (*C*5), 119.0 (*C*N), 117.7 (*C*7), 74.9 (*C*2), 74.6 (*C*13), 71.6 (*C*11), 69.1 (*C*14), 59.9 (*C*15), 58.3 (*C*3), 54.8

(*C*17), 32.9 (*C*8), 29.6 (*C*10), 27.9 (*C*9), 24.4 (*C*18), 23.7 (*C*H_3).‡

ł O*H* peak not observed.

‡ 1 peak obscured.

HRMS (ES$^+$): $[C_{33}H_{39}O_3N_4]^+$ ([M+H]$^+$) requires 539.3017; found 539.3010.

IR: ν_{max}(film)/cm^{-1} 3418 (br, O-H), 2927, 2247, 1678 (C=O), 1479, 1385, 1275, 1119, 750, 706.

$[\alpha]_D^{25.0}$ = +52 (*c* = 0.1, $CHCl_3$).

(2*R*,3*R*)-1-Acetyl-2-(5-(4-((*R*)-2-hydroxy-3-(pyrrolidin-1-yl)propoxy)butyl)pyridin-3-yl)-3-phenylindoline-3-carbonitrile **168**

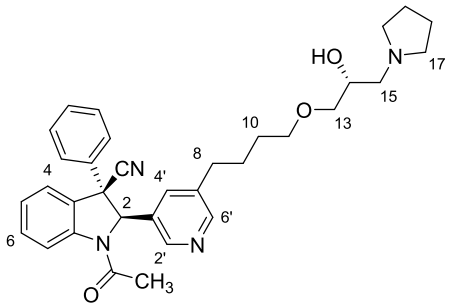

Indoline **168** was prepared according to general procedure 3 using indoline **167** (13 mg, 0.024 mmol) and Pd/C (wet degussa type, 2 mg) in MeOH (1.2 mL). The reaction mixture was stirred at rt under a H_2 atmosphere for 2.5 h. Purification by flash pressure column chromatography (4.5% MeOH/CH_2Cl_2 + 0.5% aq. NH_4OH) afforded indoline **168** as a pale yellow oil (8.3 mg, 0.015 mmol, 64%).

^{1}H NMR (500 MHz, C_6D_6, 348 K): δ 8.49 (1H, d, *J* 2.0, *H*6'), 8.45 (1H, d, *J* 2.1, *H*2'), 8.41 (1H, app br s, *H*7), 7.22-7.30 (3H, m, *H*4', *o-Ph*), 7.14 (1H, app t, *J* 8.2, *H*6), 7.08 (1H, app d, *J* 7.4, *H*4), 6.96-7.05 (3H, m, *m-Ph*, *p-Ph*), 6.79 (1H, app td, *J* 7.6, 0.9, *H*5), 5.23 (1H, s, *H*2), 3.89 (1H, app sex, *J* 4.5, *H*14), 3.42 (2H, m, *H*13, *H*13'), 3.26 (2H, app t, *J* 6.3, *H*11), 2.61 (1H, dd, *J* 12.0, 8.6, *H*15), 2.39-2.52 (3H, m, *H*15', *H*17), 2.35 (2H, m, *H*17'), 2.23 (2H, t, *J* 7.4, *H*8), 1.49-1.59 (7H, m, *H*18, C*H*$_3$), 1.45 (2H, app quin, *J* 7.3, *H*9), 1.37 (2H, app quin, *J* 7.3, *H*10).‡

^{13}C NMR (126 MHz, C_6D_6, 348 K): δ 168.3 (*C*=O), 152.3 (*C*6'), 146.7 (*C*2'), 144.1 (*C*7a), 141.3, 138.9, 133.8, 133.6 (*C*4'), 131.3 (*C*6), 130.2 (*m-Ph*, *p-Ph*), 129.9, 129.3 (*m-Ph*, *p-Ph*), 126.4 (*C*4), 126.3 (*o-Ph*), 125.9 (*C*5), 119.1 (*C*N), 117.7 (*C*7), 74.9 (*C*2), 74.6 (*C*13), 71.7 (*C*11), 69.2 (*C*14), 59.9 (*C*15), 58.4 (*C*3), 54.9 (*C*17), 33.0 (*C*8), 29.7 (*C*10), 28.0 (*C*9), 24.5 (*C*18), 23.8 (*C*H_3).

‡ O*H* peak not observed.

HRMS (ES$^+$): $[C_{33}H_{39}O_3N_4]^+$ ([M+H]$^+$) requires 539.3017; found 539.3010.

IR: ν_{max}(film)/cm^{-1} 3422 (br, O-H), 2947, 2246, 1676 (C=O), 1479, 1387, 1117, 751, 698.

$[\alpha]_D^{25.0}$ = +55 (*c* = 0.1, $CHCl_3$).

(2*S*,3*S*)-1-Acetyl-2-(5-(4-((*S*)-2-hydroxy-3-(pyrrolidin-1-yl)propoxy)butyl)pyridin-3-yl)-3-phenylindoline-3-carbonitrile **170**

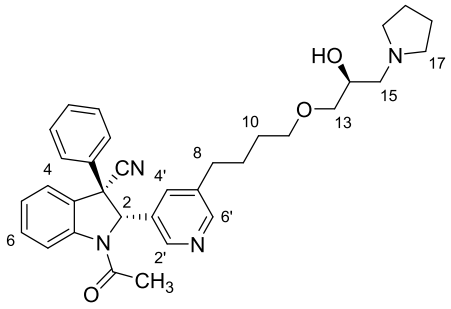

Indoline **170** was prepared according to general procedure 3 using indoline **169** (22 mg, 0.041 mmol) and Pd/C (wet degussa type, 2.5 mg) in MeOH (1.8 mL). The reaction mixture was stirred at rt under a H_2 atmosphere for 2.5 h. Purification by flash pressure column chromatography (4.5% MeOH/CH_2Cl_2 + 0.5% aq. NH_4OH) afforded indoline **170** as a pale yellow oil (15 mg, 0.028 mmol, 68%).

The spectral and mass properties of indoline **170** are identical to those of indoline **168**.

$[\alpha]_D^{25.0}$ = -47 (*c* = 0.1, $CHCl_3$).

(2*S*,3*S*)-1-Acetyl-2-(5-(4-((*R*)-2-hydroxy-3-(pyrrolidin-1-yl)propoxy)butyl)pyridin-3-yl)-3-phenylindoline-3-carbonitrile **172**

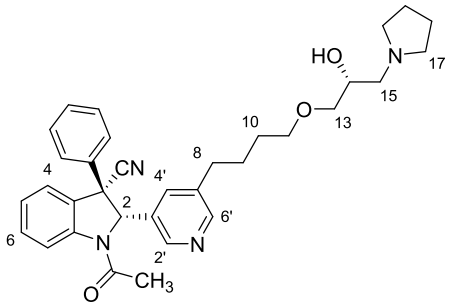

Indoline **172** was prepared according to general procedure 3 using indoline **171** (30 mg, 0.056 mmol) and Pd/C (wet degussa, 3 mg) in MeOH (1.8 mL). The reaction mixture was stirred at rt under a hydrogen atmosphere for 2 h. Purification by flash pressure column chromatography (4.5% MeOH/CH_2Cl_2 + 0.5% aq. NH_4OH) afforded indoline **172** as a pale yellow oil (22 mg, 0.041 mmol, 73%).

The spectral and mass properties of indoline **172** are identical to those of indoline **166**.

$[\alpha]_D^{25.0}$ = -52 (*c* = 0.1, $CHCl_3$).

(2*RS*,3*RS*)-1-(2-(Benzyloxy)acetyl)-2-(5-bromopyridin-3-yl)-3-phenylindoline-3-carbonitrile **198**

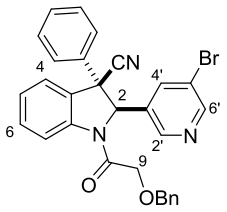

Indoline **198** was prepared according to general procedure 2, using indoline **50** (60 mg, 0.16 mmol), benzyloxyacetyl chloride (38 µL, 0.24 mmol), and pyridine (19 µL, 0.24 mmol) in CH_2Cl_2 (5 mL). The reaction mixture was stirred at rt for 2 h. Purification by flash pressure column chromatography (25% EtOAc/petroleum ether) afforded indoline **198** as a colourless paste (62 mg, 0.12 mmol, 74%).

^{1}H NMR (500 MHz, C_6D_6, 348 K): δ 8.54 (1H, d, *J* 1.8, *H*6'), 8.39 (1H, d, *J* 1.5, *H*2'), 8.31 (1H, app br s, *H*7), 7.50 (1H, app s, *H*4'), 7.12-7.25 (2H, obscured, *Ph*), 7.00-7.10 (5H, m, *H*4, *H*6, *Ph*), 6.91-6.99

(3H, m, *Ph*), 6.83-6.91 (2H, m, *Ph*), 6.74 (1H, app t, *J* 7.5, *H*5), 5.68 (1H, s, *H*2), 4.10 (1H, d, *J* 11.7, *H*9), 3.96 (1H, d, *J* 11.7, *H*9'), 3.64 (2H, s, OCH_2Ph).

^{13}C NMR (126 MHz, C_6D_6, 348 K): δ 167.5 (*C*=O), 152.8 (*C*6'), 147.0 (*C*2'), 143.4 (*C*7a), 140.5, 137.4, 136.8 (*C*4'), 136.0, 131.4 (*C*6), 130.1 (*Ph*), 129.6, 129.4 (*Ph*), 129.0 (*Ph*), 128.9 (*Ph*), 128.5 (*Ph*), 126.7 (*C*5), 126.4 (*C*4), 126.3 (*Ph*), 121.7 (*C*5'), 118.8 (*C*N), 118.0 (*C*7), 73.7 (*C*9), 72.5 (*C*2), 71.2 (O*C*H_2Ph), 58.2 (*C*3).

HRMS (ES$^+$): [$C_{29}H_{23}O_2N_3{}^{79}Br$]$^+$ ([M+H]$^+$) requires 524.0968; found 524.0971.

IR: ν_{max}(film)/cm^{-1} 3079, 2896, 1676 (C=O), 1599, 1479, 1393, 1099, 1020, 750, 696.

(2*RS*,3*RS*)-1-(2-(Benzyloxy)acetyl)-3-phenyl-2-(5-(7-(pyrrolidin-1-yl)hept-1-yn-1-yl)pyridin-3-yl)indoline-3-carbonitrile **199**

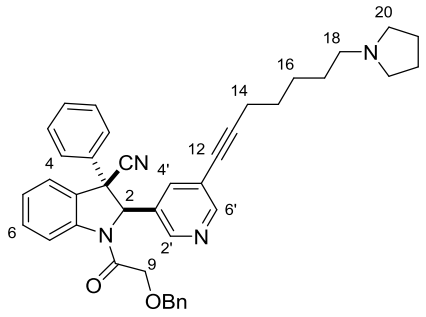

Indoline **199** was prepared according to general procedure 5, using indoline **198** (45 mg, 0.086 mmol), alkyne **105** (16 mg, 0.094 mmol), $PdCl_2(PPh_3)_2$ (3 mg, 0.004 mmol), and CuI (< 1 mg) in *N*,*N*-diisopropylamine (2 mL). The reaction mixture was stirred at 70 °C for 5 h. Purification by flash pressure column chromatography (4.5% MeOH/CH_2Cl_2 + 0.5% aq. NH_4OH) afforded indoline **199** as a yellow oil (15 mg, 0.025 mmol, 29%).

^{1}H NMR (500 MHz, C_6D_6, 348 K): δ 8.79 (1H, d, *J* 1.8, *H*6'), 8.45 (1H, d, *J* 2.1, *H*2'), 8.39 (1H, app d, *J* 7.8, *H*7), 7.57 (1H, app t, *J* 2.0, *H*4'), 7.16-7.23 (4H, m, *Ph*), 7.02-7.12 (4H, m, *H*4, *H*6, *Ph*), 6.85-6.98 (4H, m, *Ph*), 6.74 (1H, app td, *J* 7.8, 0.8, *H*5), 5.77 (1H, s, *H*2), 4.13 (1H, d, *J* 11.7, *H*9), 3.99 (1H, d, *J* 11.7, *H*9'), 3.67 (2H, d, *J* 13.6, OCH_2Ph), 2.40 (4H, m, *H*20), 2.34 (2H, t, *J* 6.9, *H*18), 2.12 (2H, t, *J* 6.7,

*H*14), 1.63 (4H, m, *H*21), 1.33-1.46 (6H, m, *H*15, *H*16, *H*17).

^{13}C NMR (126 MHz, C_6D_6, 348 K): δ 167.6 (*C*=O), 154.4 (*C*6'), 147.3 (*C*2'), 143.7, 140.9, 137.6, 136.3 (*C*4'), 133.9, 131.3 (*C*4/*C*6/*Ph*), 130.1 (*Ph*), 129.7, 129.3 (*Ph*), 129.0 (*C*4/*C*6/*Ph*), 128.9 (Ph) 126.5 (*C*5), 126.4 (*C*4/*C*6/*Ph*), 126.3 (*Ph*), 122.5 (*C*5'/*C*N), 118.9 (*C*5'/*C*N), 118.0 (*C*7), 95.9 (*C*12/*C*13), 78.1 (*C*12/*C*13), 73.6 (*C*9), 72.8 (*C*2), 71.3 (O*C*H$_2$Ph), 58.3 (*C*3), 56.6 (*C*18), 54.7 (*C*20), 29.3 (*C*15/*C*16/*C*17), 29.1 (*C*15/*C*16/*C*17), 27.6 (*C*15/*C*16/*C*17), 24.5 (*C*21), 20.1 (*C*14).‡

‡ 1 peak obscured.

HRMS (ES$^+$): $[C_{40}H_{41}O_2N_4]^+$ ([M+H]$^+$) requires 609.3224; found 609.3224.

IR: ν_{max} (film)/cm^{-1} 2928, 2439, 1680 (C=O), 1479, 1395, 1105, 1024, 754, 698.

Tert-butyldimethylsilyl 2-((tert-butyldimethylsilyl)oxy)acetate **202**

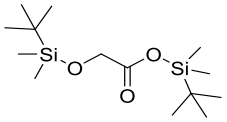

Ester **202** was prepared according to a literature procedure.[196] Imidazole (3.76 g, 55.2 mmol) was added to a solution of glycolic acid (1.0 g, 13 mmol) and *tert*-butyldimethylchlorosilane (4.16 g, 27.6 mmol) in *N*,*N*-DMF (15 mL) and stirred at rt for 18 h. The reaction mixture was poured onto H_2O and extracted with petroleum ether. The combined organic extracts were washed with $NaHCO_3$ (saturated aq.), then brine, dried over Na_2SO_4, filtered, and concentrated to afford ester **202** as a colourless liquid (2.14 g, 7.04 mmol, 54%). The spectral data matched those reported in the literature.

^{1}H NMR (400 MHz, $CDCl_3$): δ 4.19 (2H, s, C*H*$_2$), 0.93 (9H, s, SiC(C*H*$_3$)$_3$), 0.92 (9H, s, SiC(C*H*$_3$)$_3$), 0.29 (6H, s, Si(C*H*$_3$)$_2$), 0.11 (6H, s, Si(C*H*$_3$)$_2$).

^{13}C NMR (101 MHz, $CDCl_3$): δ 171.9 (*C*=O), 62.3 (*C*H$_2$), 25.8 (SiC(*C*H$_3$)$_3$), 25.5 (SiC(*C*H$_3$)$_3$), 17.7 (Si*C*(CH$_3$)$_3$), 3.6 (Si*C*(CH$_3$)$_3$), -4.8 (Si(*C*H$_3$)$_2$), -5.5 (Si(*C*H$_3$)$_2$).

(2*RS*,3*RS*)-2-(5-Bromopyridin-3-yl)-1-(2-((tert-butyldimethylsilyl)oxy)acetyl)-3-phenylindoline-3-carbonitrile **203**

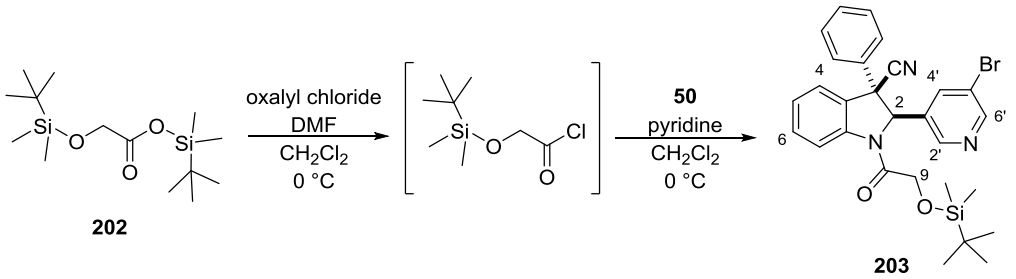

1 drop of DMF was added to a solution of ester **202** (0.50 g, 1.6 mmol) in CH_2Cl_2 (5 mL) at 0 °C. Oxalyl chloride (0.13 mL, 1.5 mmol) was added dropwise, and the mixture was stirred at 0 °C for 1 h and allowed to warm to rt. The reaction mixture was transferred to a solution of indoline **50** (80 mg, 0.21 mmol) and pyridine (0.10 mL, 1.3 mmol) in CH_2Cl_2 (5 mL) via cannula and stirred at 0 °C for 15 min. $NaHCO_3$ (saturated aq., 15 mL) was added, and the mixture was extracted with CH_2Cl_2. The combined organic extracts were washed with brine, dried over Na_2SO_4, filtered, and concentrated. Purification by flash pressure column chromatography (10-15% EtOAc/petroleum ether) afforded indoline **203** as a colorless paste (58 mg, 0.11 mmol, 50%).

^{1}H NMR (500 MHz, C_6D_6, 348 K): δ 8.59 (1H, d, *J* 2.0, *H*6'), 8.54 (1H, d, *J* 1.3, *H*2'), 8.28 (1H, app d, *J* 7.6, *H*7), 7.65 (1H, app t, *J* 2.0, *H*4'), 7.12-7.20 (2H, obscured, *Ph*), 7.07 (1H, app t, *J* 7.9, *H*6), 6.94-7.05 (4H, m, *H*4, *Ph*), 6.74 (1H, app t, *J* 7.5, *H*5), 5.77 (1H, s, *H*2), 3.93 (1H, d, *J* 13.9, *H*9), 3.83 (1H, d, *J* 13.9, *H*9'), 0.73 (9H, s, SiC(CH_3)$_3$), -0.14 (3H, s, Si(CH_3)$_2$), -0.15 (3H, s, Si(CH_3)$_2$).

^{13}C NMR (126 MHz, C_6D_6, 348 K): δ 168.8 (*C*=O), 152.9 (*C*6'), 147.2 (*C*2'), 143.5, 140.7, 136.8 (*C*4'), 136.1, 131.4 (*C*6), 130.2 (*C*4/*Ph*), 129.5, 129.4 (*C*4/*Ph*), 126.5 (*C*5), 126.5 (*C*4/*Ph*), 126.3 (*Ph*), 121.8 (*C*5'/*C*N), 118.9 (*C*5'/*C*N), 117.8 (*C*7), 72.3 (*C*2), 65.8 (*C*9), 58.2 (*C*3), 26.2 (SiC(*C*H_3)$_3$), 18.7 (Si*C*(CH$_3$)$_3$), -5.1 (Si*C*H$_3$), -5.2 (Si*C*H$_3$').

HRMS (ES$^+$): [$C_{28}H_{31}O_2N_3{}^{79}Br^{28}Si$]$^+$ ([M+H]$^+$) requires 548.1363; found 548.1364.

IR: ν_{max}(film)/cm^{-1} 2953, 2857, 1676 (C=O), 1479, 1391, 1256, 1099, 837, 781.

(2*RS*,3*RS*)-1-(2-((Tert-butyldimethylsilyl)oxy)acetyl)-3-phenyl-2-(5-(7-(pyrrolidin-1-yl)hept-1-yn-1-yl)pyridin-3-yl)indoline-3-carbonitrile **205**

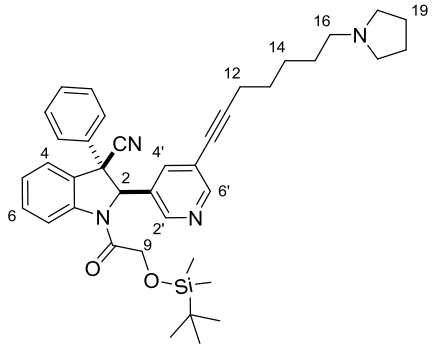

Indoline **203** (48 mg, 0.088 mmol), $PdCl_2(PPh_3)_2$ (6 mg, 0.009 mmol), and CuI (< 1 mg) were degassed 3 times in a Schlenk tube with Ar. A degassed solution of alkyne **105** (22 mg, 0.13 mmol) and triethylamine (30 µL, 0.22 mmol) in toluene (2 mL) was added, and the reaction mixture was stirred at 70 °C for 3.5 h. The reaction mixture was allowed to cool to rt, filtered through Celite™ and eluted with EtOAc. The filtrate was washed 3 times with H_2O, then brine, dried over Na_2SO_4, filtered, and concentrated. Purification by flash pressure column chromatography (4.5% MeOH/CH_2Cl_2 + 0.5% aq. NH_4OH) afforded indoline **205** as a pale yellow paste (21 mg, 0.033 mmol, 38%).

^{1}H NMR (500 MHz, C_6D_6): δ 8.88 (1H, d, *J* 2.0, *H*6'), 8.63 (1H, d, *J* 2.2, *H*2'), 8.47 (1H, app br s, *H*7), 7.73 (1H, app t, *J* 2.1, *H*4'), 7.17-7.20 (2H, m, Ph), 7.03 (1H, app td, *J* 7.9, 1.4, *H*6), 6.97 (1H, app dd, *J* 7.6, 0.7, *H*4), 6.89-6.96 (3H, m, Ph), 6.67 (1H, app td, *J* 7.6, 1.0, *H*5), 5.83 (1H, s, *H*2), 3.87 (1H, d, *J* 14.0, *H*9), 3.75 (1H, d, *J* 14.0, *H*9'), 2.34-2.42 (4H, m, *H*18), 2.30 (2H, t, *J* 7.1, *H*16), 2.06 (2H, t, *J* 6.7, *H*12), 1.63 (4H, m, *H*19), 1.26-1.43 (6H, m, *H*13, *H*14, *H*15), 0.72 (9H, s, $SiC(CH_3)_3$), -0.15 (3H, s, $Si(CH_3)_2$), -0.16 (3H, s, $Si(CH_3)_2$).

^{13}C NMR (126 MHz, C_6D_6): δ 168.9 (*C*=O), 154.3 (*C*6'), 147.3 (*C*2'), 143.7, 140.7, 136.1 (*C*4'), 134.0, 131.3 (*C*6), 130.1 (Ph), 129.3 (Ph), 128.9, 126.5 (*C*5), 126.4 (*C*4), 126.3 (Ph), 122.6 (*C*5'), 119.1 (*C*N), 117.8 (*C*7), 96.0 (*C*10/*C*11), 77.9 (*C*10/*C*11), 72.2 (*C*2), 65.7 (*C*9), 58.2 (*C*3), 56.6 (*C*16), 54.6 (*C*18), 29.1 (*C*13/*C*14/*C*15), 28.9 (*C*13/*C*14/*C*15), 27.4 (*C*13/*C*14/*C*15), 26.2 ($SiC(CH_3)_3$), 24.3 (*C*19), 20.0 (*C*12), 18.6 ($SiC(CH_3)_3$), -5.11 ($Si(CH_3)$), -5.34 ($Si(CH_3)$').

HRMS (ES^+): $[C_{39}H_{49}N_4O_2{}^{28}Si]^+$ ($[M+H]^+$) requires 633.3625; found 633.2627.

IR: ν_{max} (film)/cm^{-1} 2988, 1670 (C=O), 1464, 1381, 1105, 1014, 742, 698.

(2*RS*,3*RS*)-2-(5-Bromopyridin-3-yl)-1-(2-cyanoacetyl)-3-phenylindoline-3-carbonitrile **194**

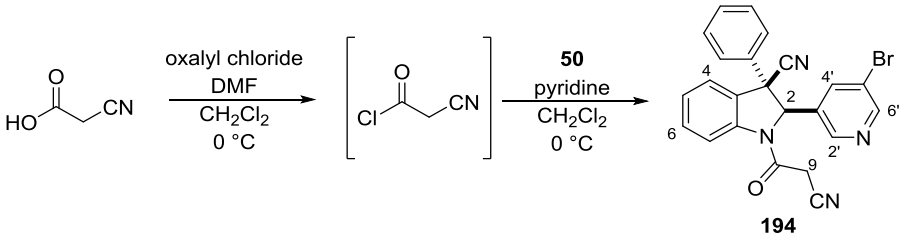

1 drop of DMF was added to a solution of cyanoacetic acid (200 mg, 2.35 mmol) in CH_2Cl_2 (8 mL), and the mixture was cooled to 0 °C. Oxalyl chloride (0.18 mL, 2.1 mmol) was added dropwise and the mixture was stirred at 0 °C for 1 h. 4 mL of the reaction mixture was transferred to a solution of indoline **50** (60 mg, 0.16 mmol) in CH_2Cl_2 (4 mL) at 0 °C, and the mixture was stirred at 0 °C for 25 min. $NaHCO_3$ (sat aq., 10 mL) was added, and the mixture was extracted with DCM. The combined organic extracts were washed with brine, dried over Na_2SO_4, filtered, and concentrated. Purification by flash pressure column chromatography (30% EtOAc/Petroleum ether) afforded indoline **194** as a colorless solid (56 mg, 0.13 mmol, 79%).

^{1}H NMR (500 MHz, C_6D_6, 348 K): δ 8.55 (1H, d, *J* 1.9, *H*6'), 8.28 (1H, d, *J* 1.6, *H*2'), 7.84 (1H, app br s, *H*7), 7.42 (1H, app s, *H*4'), 7.08 (2H, m, *Ph*), 6.95-7.04 (4H, m, *H*6, *Ph*), 6.93 (1H, app d, *J* 7.5, *H*4), 6.70 (1H, app t, *J* 7.6, *H*5), 5.01 (1H, s, *H*2), 2.30 (1H, d, *J* 18.5, *H*9), 2.24 (1H, d, *J* 18.5, *H*9').

^{13}C NMR (125.75 MHz, C_6D_6, 348 K): δ 160.0 (*C*=O), 153.5 (*C*6'), 146.7 (*C*2'), 142.2, 139.9, 136.6 (*C*4'), 134.5, 131.5 (*C*6/*Ph*), 130.4 (*C*6/*Ph*), 129.9 (*C*6/*Ph*), 127.3 (*C*5), 126.7 (*C*4), 126.1 (*Ph*), 122.0 (*C*5'), 118.4 (*C*N), 117.5 (*C*7), 112.5 (*C*N), 73.6 (*C*2), 58.2 (*C*3), 26.6 (*C*9).‡

‡ 1 peak obscured.

HRMS (ES$^+$): $[C_{23}H_{16}{}^{79}BrN_4O]^+$ ([M+H]$^+$) requires 443.0502; found 443.0502.

IR: ν_{max} (film)/cm^{-1} 3059, 2920, 2263, 2268, 1684 (C=O), 1482, 1389, 1281, 1226, 1281, 1226, 758.

MP: 93-95 °C.

(2*RS*,3*RS*)-1-(2-Cyanoacetyl)-3-phenyl-2-(5-(7-(pyrrolidin-1-yl)hept-1-yn-1-yl)pyridin-3-yl)indoline-3-carbonitrile **195**

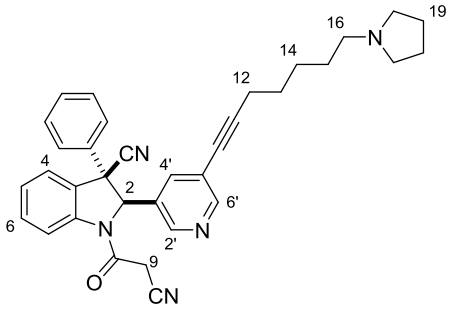

Indoline **195** was prepared according to general procedure 5 using indoline **194** (40 mg, 0.090 mmol), alkyne **105** (16 mg, 0.099 mmol), $PdCl_2(PPh_3)_2$ (3.2 mg, 0.0045 mmol), and CuI (< 1 mg) in diisopropylamine (2 mL). The reaction mixture was stirred at 70 °C for 4.5 h. Purification by flash pressure column chromatography (4.5% MeOH/CH_2Cl_2 + 0.5% aq. NH_4OH) afforded indoline **195** as a colorless oil (19 mg, 0.036 mmol, 40%, contains impurities).

^{1}H NMR (500 MHz, C_6D_6, 348 K): δ 8.80 (1H, d, *J* 1.5, *H*6'), 8.34 (1H, d, *J* 1.8, *H*2'), 8.01 (1H, app br s, *H*7) 7.47 (1H, app s, *H*4'), 7.12 (2H, m, *Ph*), 6.93-7.08 (5H, m, *H*4, *H*6, *Ph*), 6.72 (1H, app t, *J* 7.5, *H*5), 5.06 (1H, br s, *H*2), 2.40 (4H, m, *H*18), 2.28-2.37 (4H, m, *H*9, *H*16), 2.14 (2H, t, *J* 6.6, *H*12), 1.64 (4H, m, *H*19), 1.34-1.50 (6H, m, *H*13, *H*14, *H*15).

^{13}C NMR (126 MHz, C_6D_6, 348 K): δ 160.2 (*C*=O), 154.9 (*C*6'), 146.8 (*C*2'), 142.6, 140.3, 136.0 (*C*4'), 132.5, 131.5 (*C*4/*C*6/*Ph*), 130.4 (*C*4/*C*6/*Ph*), 129.7 (*C*4/*C*6/*Ph*), 127.2 (*C*5), 126.6 (*C*4/*C*6/*Ph*), 126.2 (*Ph*), 122.9 (*C*5'), 118.5 (*C*N), 117.7 (*C*7), 112.7 (*C*N), 96.6 (*C*10/*C*11), 77.8 (*C*10/*C*11), 74.1 (*C*2), 58.4 (*C*3), 56.6 (*C*9/*C*16), 54.7 (*C*18), 29.2 (*C*13/*C*14/*C*15), 29.0 (*C*13/*C*14/*C*15), 27.6 (*C*9/*C*16), 26.7 (*C*13/*C*14/*C*15), 24.5 (*C*19), 20.1 (*C*12).‡

‡ 1 peak obscured.

HRMS (ES^+): $[C_{34}H_{34}N_5O]^+$ ($[M+H]^+$) requires 528.2763; found 528.2762.

IR: ν_{max} (film)/cm^{-1} 3026, 2934, 2261, 1677 (C=O), 1480, 1394, 756, 698.

(2*RS*,3*RS*)-1-(2-Cyanoacetyl)-3-phenyl-2-(5-(7-(pyrrolidin-1-yl)heptyl)pyridin-3-yl)indoline-3-carbonitrile **196**

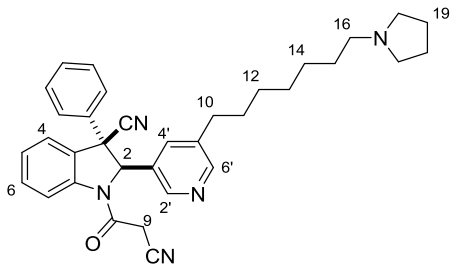

Indoline **196** was prepared according to general procedure 3 using indoline **195** (16 mg, 0.030 mmol) and Pd/C (wet degussa type, 2 mg) in MeOH (2 mL). The reaction mixture was stirred at rt under a H_2 atmosphere for 4 h. Purification by flash pressure column chromatography (4.5% MeOH/CH_2Cl_2 + 0.5% aq. NH_4OH) afforded indoline **196** as a colorless oil (14 mg, 0.026 mmol, 87%, contains minor impurities).

^{1}H NMR (500 MHz, C_6D_6, 348 K): δ 8.49 (1H, app s, *H*6'), 8.35 (1H, app s, *H*2'), 8.23 (1H, app br s, *H*7), 7.09 (1H, app t, *J* 7.9, *H*6), 6.97-7.06 (4H, m, *H*4, *Ph*), 6.78 (1H, app t, *J* 7.6, *H*5), 5.12 (1H, br s, *H*2), 2.37-2.49 (8H, m, *H*9, *H*16, *H*18), 2.21 (2H, t, *J* 7.6, *H*10), 1.65 (4H, m, *H*19), 1.50 (2H, app quin, *J* 7.4, *H*15), 1.27-1.41 (4H, m, *H*11, *H*14), 1.19 (2H, app quin, *J* 7.5, *H*13), 1.12 (2H, app quin, *J* 7.5, *H*12).ǂ

^{13}C NMR (126 MHz, C_6D_6, 348 K): δ 160.4 (*C*=O), 153.0 (*C*6'), 146.3 (*C*2'), 143.0, 140.5, 139.5, 133.3 (*C*4'), 132.5, 131.5 (*C*6), 130.4 (*C*4/*Ph*), 129.7 (*C*4/*Ph*), 127.1 (*C*5), 126.6 (*C*4/*Ph*), 126.3 (*Ph*), 118.6 (*C*N), 117.8 (*C*7), 112.8 (*C*N), 74.5 (*C*2), 58.7 (*C*3), 56.9 (*C*16), 54.7 (*C*18), 33.2 (*C*10), 31.1 (*C*11/*C*14), 29.9 (*C*13), 29.8 (*C*15), 29.5 (*C*12), 28.2 (*C*11/*C*14), 26.8 (*C*9), 24.5 (*C*19).‡

ǂ 3 peaks obscured.

‡ 1 peak obscured.

HRMS (ES$^+$): $[C_{34}H_{38}N_5O]^+$ ([M+H]$^+$) requires 532.3071; found 532.3073.

IR: ν_{max}(film)/cm^{-1} 3028, 2935, 2262, 1677 (C=O), 1480, 1461, 1393, 755, 698.

2-(1,3-Dioxoisoindolin-2-yl)acetyl chloride **209**

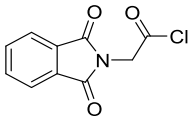

Acyl chloride **209** was prepared according to a literature procedure.[197] DMF (1 drop) was added to a suspension of *N*-phthaloylglycine (1.00 g, 4.87 mmol) in CH_2Cl_2 (35 mL) and cooled to 0 °C. Oxalyl chloride (0.82 mL, 9.8 mmol) was added dropwise, and the mixture was stirred at 0 °C for 1.5 h. The reaction mixture was concentrated at rt to afford acyl chloride **209** as a yellow solid (1.12 g, 5.01 mmol, quant). The spectral data matched those reported in the literature.

^{1}H NMR (400 MHz, $CDCl_3$): δ 7.88 (2H, m, *Ar*), 7.75 (2H, m, *Ar*), 4.79 (2H, s, C*H*$_2$).

^{13}C NMR (101 MHz, $CDCl_3$): δ 169.2 (*C*=O), 166.7 (*C*=O), 134.8 (*Ar*), 131.7 (*Ar*), 124.1 (*Ar*), 47.7 (*C*H$_2$).

(2*RS*,3*RS*)-2-(5-Bromopyridin-3-yl)-1-(2-(1,3-dioxoisoindolin-2-yl)acetyl)-3-phenylindoline-3-carbonitrile **210**

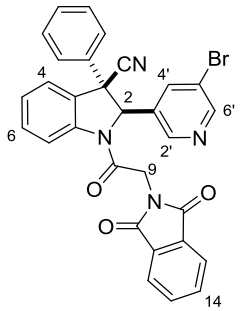

Indoline **210** was prepared according to general procedure 2, using indoline **50** (80 mg, 0.21 mmol), acyl chloride **209** (119 mg, 0.53 mmol), and pyridine (43 µL, 0.53 mmol) in CH_2Cl_2 (6.5 mL). The reaction mixture was stirred at rt for 16 h. Purification by flash pressure column chromatography (30-35% EtOAc/petroleum ether) afforded indoline **210** as a colorless solid (75 mg, 0.13 mmol, 63%).

^{1}H NMR (400 MHz, dmso-D_6): δ 8.79 (1H, d, *J* 1.9, *H*6'), 8.57 (1H, d, *J* 1.6, *H*2'), 8.11 (1H, app d, *J* 7.8, *H*7), 8.00 (1H, app s, *H*4'), 7.82-7.93 (4H, m, *H*13, *H*14), 7.60 (1H, app t, *J* 7.8, *H*6), 7.50-7.57 (2H, m,

Ph), 7.43-7.50 (2H, m, *H*4, *Ph*), 7.32-7.42 (3H, m, *H*5, *Ph*), 6.22 (1H, s, *H*2), 4.92 (1H, d, *J* 17.2, *H*9), 4.14 (1H, d, *J* 17.2, *H*9').

^{13}C NMR (101 MHz, dmso-D_6): δ 166.5 (*C*=O), 164.3 (*C*=O), 150.9 (*C*6'), 145.8 (*C*2'), 140.9, 138.1, 136.4 (*C*4'), 134.4, 134.2 (*C*13/*C*14), 131.1, 130.6 (*C*6), 129.1 (*Ph*), 128.6 (*C*4/*Ph*), 128.4, 127.7, 125.8 (*C*5/*Ph*), 125.3 (*C*4/*Ph*), 125.1 (*C*5/*Ph*), 122.8 (*C*13/*C*14), 119.8 (*C*5'/*C*N), 117.8 (*C*5'/*C*N), 116.4 (*C*7), 69.5 (*C*2), 56.4 (*C*3).

HRMS (ES$^+$): $[C_{30}H_{20}O_3N_4{}^{79}Br]^+$ ([M+H]$^+$) requires 563.0713; found 563.0714.

IR: ν_{max}(film)/cm^{-1} 2980, 1720, 1688, 1482, 1424, 1389, 733, 715.

MP: 250-252 °C.

(2*RS*,3*RS*)-1-(2-(1,3-Dioxoisoindolin-2-yl)acetyl)-3-phenyl-2-(5-(7-(pyrrolidin-1-yl)hept-1-yn-1-yl)pyridin-3-yl)indoline-3-carbonitrile **211**

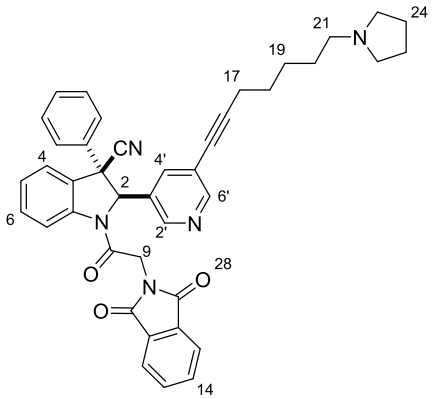

Indoline **211** was prepared according to general procedure 5 using indoline **210** (62 mg, 0.11 mmol), alkyne **105** (23 mg, 0.14 mmol), $Pd(Ph_3)_2Cl_2$ (4 mg, 0.006 mmol), and CuI (approx. 1 mg) in *N*,*N*-diisopropylamine (2 mL). The reaction mixture was stirred at 70 °C for 3 h. Purification by flash pressure column chromatography (4.5% MeOH/CH_2Cl_2 + 0.5% aq. NH_4OH) afforded indoline **211** as a pale yellow oil (34 mg, 0.053 mmol, 48%).

^{1}H NMR (400 MHz, C_6D_6, 348 K): δ 8.81 (1H, app s, *H*6'), 8.52 (1H, app s, *H*2'), 7.99 (1H, app br s,

*H*7), 7.68 (1H, app s, *H*4'), 7.37-7.50 (2H, m, *H*13/*H*14), 7.29 (2H, app d, *J* 7.4, *Ph*), 7.03-7.12 (2H, m, *Ph*), 6.95-7.03 (3H, m, *H*4, *H*6, *Ph*), 6.87-6.95 (2H, m, *H*13/*H*14), 6.70 (1H, app t, *J* 7.6, *H*5), 5.50 (1H, s, *H*2), 4.19 (1H, d, *J* 16.4, *H*9), 4.00 (1H, d, *J* 16.4, *H*9'), 2.40 (4H, m, *H*23), 2.33 (2H, t, *J* 7.0, *H*21), 2.13 (2H, t, *J* 6.7, *H*17), 1.62 (4H, m, *H*24), 1.32-1.51 (6H, m, *H*18, *H*19, *H*20).

^{13}C NMR (101 MHz, C_6D_6, 348 K): δ 167.5 (*C*=O), 164.9 (*C*=O), 154.6 (*C*6'), 147.2 (*C*2'), 142.9, 140.7, 136.4 (*C*4'), 134.0 (*C*13/*C*14), 133.1, 131.2 (*C*4/*C*6/*Ph*), 130.3 (*Ph*), 129.5 (*C*4/*C*6/*Ph*), 126.6 (*C*5), 126.3 (*C*4/*C*6/*Ph*), 126.1 (*Ph*), 123.7 (*C*13/*C*14), 122.7 (*C*5'/*C*N), 118.7 (*C*5'/*C*N), 117.9 (*C*7), 95.9 (*C*15/*C*16), 78.2 (*C*15/*C*16), 73.7 (*C*2), 58.6 (*C*3), 56.6 (*C*21), 54.6 (*C*23), 41.1 (*C*9), 29.0 (*C*18/*C*19/*C*20), 29.0 (*C*18/*C*19/*C*20), 27.5 (*C*18/*C*19/*C*20), 24.4 (*C*24), 20.1 (*C*17).‡

‡ 2 peaks obscured.

HRMS (ES$^+$): $[C_{41}H_{38}N_5O_3]^+$ ([M+H]$^+$) requires 648.2969; found 648.2963.

IR: ν_{max} (film)/cm^{-1} 2938, 2245, 1721, 1686, 1595, 1481, 1422, 1389, 954, 715.

(2*RS*,3*RS*)-1-(2-(1,3-Dioxoisoindolin-2-yl)acetyl)-3-phenyl-2-(5-(7-(pyrrolidin-1-yl)heptyl)pyridin-3-yl)indoline-3-carbonitrile **212**

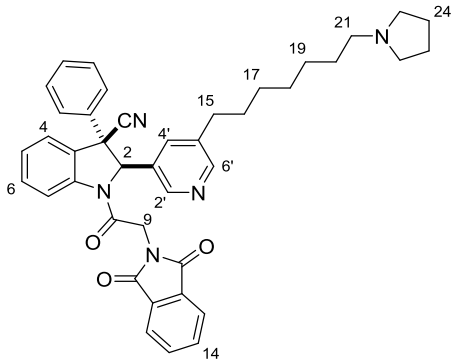

Indoline **212** was prepared according to general procedure 3, using indoline **211** (27 mg, 0.042 mmol) and Pd/C (wet degussa type, 3 mg) in MeOH (2.5 mL). The reaction mixture was stirred at rt under a H_2 atmosphere for 24 h. Purification by flash pressure column chromatography (4.5% MeOH/CH_2Cl_2 + 0.5% aq. NH_4OH) afforded indoline **212** as a colorless oil (17 mg, 0.026 mmol,

62%).

^{1}H NMR (400 MHz, C_6D_6, 348 K): δ 8.47-8.58 (2H, m, *H*2', *H*6'), 8.27 (1H, app br s, *H*7), 7.36-7.45 (3H, m, *H*4', *H*13/*H*14), 7.32 (2H, app d, *J* 7.6, *Ph*), 6.98-7.12 (5H, m, *H*4, *H*6, *Ph*), 6.88-6.96 (2H, m, *H*13/*H*14), 6.76 (1H, app t, *J* 7.6, *H*5), 5.51 (1H, s, *H*2), 4.19 (1H, d, *J* 16.4, *H*9), 3.99 (1H, d, *J* 16.4, *H*9'), 2.36-2.49 (6H, m, *H*21, *H*23), 2.28 (2H, t, *J* 6.9, *H*15), 1.64 (4H, m, *H*24), 1.40-1.56 (4H, m, *H*16, *H*20), 1.28-1.39 (2H, app quin, *J* 7.3, *H*19), 1.13-1.28 (4H, m, *H*17, *H*18).

^{13}C NMR (101 MHz, C_6D_6, 348 K): δ 167.5 (*C*=O), 165.1 (*C*=O), 152.6 (*C*2'/*C*6'), 146.8 (*C*2'/*C*6'), 143.4, 140.8, 139.4, 133.9 (*C*13/*C*14), 133.5 (*C*4'), 133.1, 132.9, 131.2 (*C*4/*C*6/*Ph*), 130.4, 130.3 (*C*4/*C*6/*Ph*), 129.4 (*C*4/*C*6/*Ph*), 126.5 (*C*5), 126.3 (*C*4/*C*6/*Ph*), 126.2 (*Ph*), 123.6 (*C*13/*C*14), 118.7 (*C*N), 117.9 (*C*7), 73.9 (*C*2), 59.0 (*C*3), 56.9 (*C*21), 54.7 (*C*23), 41.2 (*C*9), 33.3 (*C*15), 31.2 (*C*16/*C*20), 30.0 (*C*17/*C*18), 29.8 (*C*16/*C*20), 29.6 (*C*17/*C*18), 28.2 (*C*19), 24.4 (*C*24).

HRMS (ES$^+$): $[C_{41}H_{42}N_5O_3]^+$ ([M+H]$^+$) requires 652.3288; found 652.3281.

IR: ν_{max}(film)/cm^{-1} 2932, 2241, 1721, 1687, 1481, 1423, 1389, 1110, 734, 715.

(2*RS*,3*RS*)-1-Glycyl-3-phenyl-2-(5-(7-(pyrrolidin-1-yl)heptyl)pyridin-3-yl)indoline-3-carbonitrile **213**

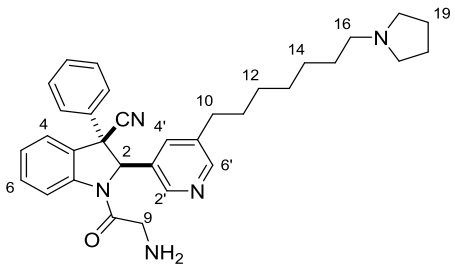

$N_2H_4{\cdot}H_2O$ (7.0 µL, 0.13 mmol) was added to a solution of indoline **212** (17 mg, 0.026 mmol) in EtOH (2 mL) and stirred at 60 °C for 1 h. The mixture was filtered and concentrated. CH_2Cl_2 was added to the remaining residue, the resulting precipitate was removed by filtration, and the filtrate was concentrated. This process was repeated 4 times. Purification by flash pressure column chromatography (5.5% MeOH/CH_2Cl_2 + 0.5% aq. NH_4OH) to afford indoline **213** as a pale yellow oil (9.4 mg, 0.018 mmol, 69%, contains minor impurities).

^{1}H NMR (400 MHz, C_6D_6): δ 8.53 (1H, app br s, *H*7), 8.50 (1H, d, *J* 2.0, *H*6'), 8.46 (1H, d, *J* 1.8, *H*2'), 7.19-7.24 (3H, m, *H*4', *Ph*), 7.10 (1H, app t, *J* 7.7, *H*6), 7.03 (1H, dd, *J* 7.7, 0.8, *H*4), 6.92-6.99 (3H, m, *Ph*), 6.73 (1H, app td, *J* 7.7, 1.0, *H*5), 5.20 (1H, br s, *H*2), 2.72 (2H, br s, *H*9), 2.36-2.48 (6H, m, *H*16, *H*18), 2.10 (2H, t, *J* 7.5, *H*10), 1.65 (4H, m, *H*19), 1.50 (2H, app quin, *J* 7.6, *H*15), 1.28 (4H, m, *H*11, *H*14), 1.12 (2H, app quin, *J* 7.2, *H*12/*H*13), 1.05 (2H, app quin, *J* 7.2, *H*12/*H*13), 0.77 (3H, br s, N*H*$_2$, includes H_2O).

^{13}C NMR (101 MHz, C_6D_6): δ 172.1 (*C*=O), 152.4 (*C*6'), 146.5 (*C*2'), 143.9, 141.0, 139.2, 133.5 (*C*4'), 133.3, 131.4 (*C*6), 130.2 (*Ph*), 129.4 (*Ph*), 126.5 (*C*4), 126.3 (*Ph*), 126.2 (*C*5), 119.1 (*C*N), 117.6 (*C*7), 73.1 (*C*2), 58.4 (*C*3), 57.0 (*C*16), 54.8 (*C*18), 46.2 (*C*9), 33.1 (*C*10), 31.3 (*C*11/*C*14), 30.0 (*C*12/*C*13), 29.8 (*C*15), 29.5 (*C*12/*C*13), 28.2 (*C*11/*C*14), 24.3 (*C*19).ǂ

ǂ 1 peak obscured.

HRMS (ES$^+$): $[C_{33}H_{40}N_5O]^+$ ([M+H]$^+$) requires 522.3227; found 522.3227.

IR: ν_{max} (film)/cm^{-1} 3378 (broad, N-H), 2241, 2930, 1681 (C=O), 1598, 1480, 1393, 1222, 772.

5-((2*S*,3*S*)-3-Cyano-1-(2-(1,3-dioxoisoindolin-2-yl)acetyl)-3-phenylindolin-2-yl)pyridin-3-yl trifluoromethanesulfonate **268**

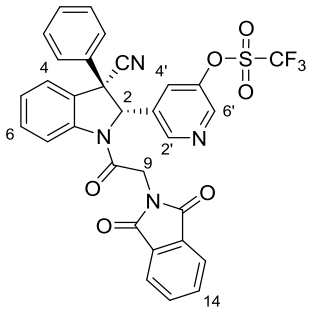

Indoline **268** was prepared according to general procedure 2, using indoline **267** (80 mg, 0.18 mmol), Acyl chloride **209** (240 mg, 1.07 mmol), and pyridine (87 μL, 1.1 mmol) in CH_2Cl_2 (3 mL). The reaction mixture was stirred at rt for 1 h. Purification by flash pressure column chromatography (8% EtOAc/$CHCl_3$) afforded indoline **268** as a colourless gum (108 mg, 0.17 mmol, 95%).

^{1}H NMR (500 MHz, C_6D_6, 348 K): δ 8.50 (1H, app s, *H*6'), 8.38 (1H, d, *J* 1.9, *H*2'), 7.76 (1H, app br s, *H*7), 7.40 (2H, m, *H*13), 7.33 (1H, app s, *H*4'), 7.27 (2H, app d, *J* 7.7, *o-Ph*), 7.04-7.12 (2H, m, *m*-Ph), 6.94-7.04 (3H, *H*4, *H*6, *p*-Ph), 6.90 (2H, m, *H*14), 6.71 (1H, app t, *J* 7.6, *H*5), 5.48 (1H, s, *H*2), 4.23 (1H, d, *J* 16.3, *H*9), 3.98 (1H, d, *J* 16.3, *H*9').

^{13}C NMR (126 MHz, C_6D_6, 348 K): δ 167.5 (*C*=O), 164.9, (*C*=O), 148.4 (*C*6'), 147.5, 144.5 (*C*2'), 142.2, 139.9, 135.3, 134.1 (*C*14), 132.9, 131.4 (*C*6), 130.4 (*m*-Ph), 129.7 (*p*-Ph), 127.2 (*C*4'), 126.9 (*C*5), 126.5 (*C*4), 126.0 (*o*-Ph), 123.7 (*C*13), 118.3 (*C*N), 117.4 (*C*7), 72.9 (*C*2), 58.1 (*C*3), 41.0 (*C*9).‡

^{19}F NMR (377 MHz, C_6D_6): -72.6 (s).

‡ 2 peaks obscured.

HRMS: $[C_{31}H_{20}O_6N_4F_3{}^{32}S]^+$ ($[M+H]^+$) requires 633.1050; found 633.1048.

IR: ν_{max}(film)/cm^{-1} 2921, 1721, 1689, 1427, 1301, 1220, 1025, 772.

$[\alpha]_D^{25.0}$ = +13 (*c* = 0.1, $CHCl_3$).

(2*S*,3*S*)-1-(2-(1,3-Dioxoisoindolin-2-yl)acetyl)-3-phenyl-2-(5-((E)-7-(pyrrolidin-1-yl)hept-1-en-1-yl)pyridin-3-yl)indoline-3-carbonitrile **269**

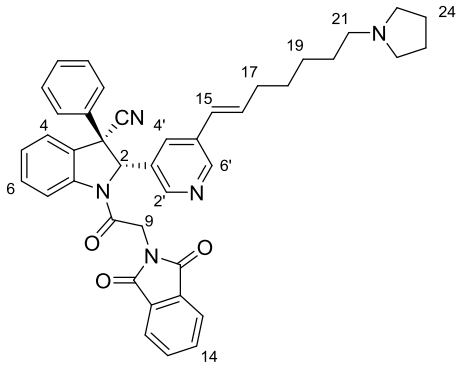

Indoline **269** was prepared according to general procedure 4, using indoline **268** (80 mg, 0.13 mmol), vinylstannane **57** (76 mg, 0.16 mmol), and $Pd(PPh_3)_4$ (15 mg, 0.013 mmol) in NMP (3 mL). The reaction mixture was stirred at 80 °C for 2.5 h. Purification by flash pressure column chromatography (5% MeOH/CH_2Cl_2 + 0.5% aq. NH_4OH) afforded indoline **269** as a colourless gum

(70 mg, 0.11 mmol, 85%).

^{1}H NMR (500 MHz, C_6D_6, 348 K): δ 8.68 (1H, app s, *H*6'), 8.52 (1H, app s, *H*2'), 8.21 (1H, app br s, *H*7), 7.55 (1H, app s, *H*4'), 7.40 (2H, m, *H*13), 7.34 (2H, app d, *J* 7.7, *o-Ph*), 6.96-7.10 (5H, m, *H*4, *H*6, *m-Ph*, *p-Ph*), 6.90 (2H, m, *H*14), 6.74 (1H, app t, *J* 7.6, *H*5), 6.01-6.15 (2H, m, *H*15, *H*16),ł 5.54 (1H, s, *H*2), 4.21 (1H, d, *J* 16.2, *H*9), 4.02 (1H, d, *J* 16.2, *H*9'), 2.43 (4H, m, *H*23), 2.37 (2H, t, *J* 7.2, *H*21), 1.96 (2H, app q, *J* 6.4, *H*17), 1.62 (4H, m, *H*24), 1.48 (2H, app quin, *J* 6.9, *H*20), 1.26-1.39 (4H, m, *H*18, *H*19).

^{13}C NMR (126 MHz, C_6D_6, 348 K): δ 167.6 (*C*=O), 165.2 (*C*=O), 150.2 (*C*6'), 147.3 (*C*2'), 143.3, 140.8, 135.2 (*C*15/*C*16), 135.0, 134.0 (*C*14), 133.2, 133.1, 131.2 (*C*6), 130.8 (*C*4'), 130.4 (*m-Ph*), 129.5 (*p-Ph*), 126.9 (*C*15/*C*16), 126.7 (*C*5), 126.4 (*o-Ph*), 126.2 (*C*4), 123.7 (*C*13), 118.8 (*C*N), 118.0 (*C*7), 74.0 (*C*2), 58.9 (*C*3), 56.7 (*C*21), 54.6 (*C*23), 41.3 (*C*9), 33.6 (*C*17), 29.5 (*C*18/*C*19), 29.3 (*C*20), 27.8 (*C*18/*C*19), 24.4 (*C*24).‡

ł ^{1}H NMR (400 MHz, C_6D_6): δ 6.05 (1H, dt, *J* 15.9, 6.6, *H*16), 5.94 (1H, d, *J* 15.9, *H*15).

‡ 1 peak obscured.

HRMS (ES^+): $[C_{41}H_{40}O_3N_5]^+$ ($[M+H]^+$) requires 650.3126; found 650.3120.

IR: ν_{max} (film)/cm^{-1} 2932, 2261, 1721 (C=O), 1688 (C=O), 1481, 1423, 1389, 715.

$[\alpha]_D^{25.0}$ = +17 (*c* = 0.1, $CHCl_3$).

(2*S*,3*S*)-1-Glycyl-3-phenyl-2-(5-((E)-7-(pyrrolidin-1-yl)hept-1-en-1-yl)pyridin-3-yl)indoline-3-carbonitrile **270**

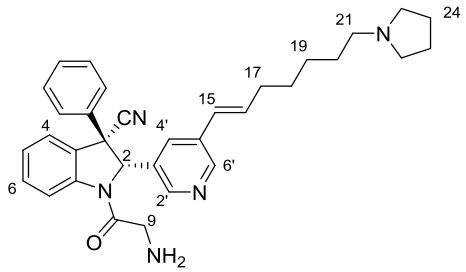

$N_2H_4{\cdot}H_2O$ (22 µL, 0.46 mmol) was added dropwise to a solution of indoline **269** (60 mg, 0.093 mmol) in EtOH (4.8 mL) and stirred at 60 °C for 1.5 h. The mixture was filtered and concentrated. CH_2Cl_2 was added to the remaining residue, the resulting precipitate was removed by filtration, and the filtrate was concentrated. This process was repeated 4 times. Purification by flash pressure column chromatography (7.5% MeOH/CH_2Cl_2 + 0.5% aq. NH_4OH) to afford indoline **270** as a pale yellow oil (29 mg, 0.056 mmol, 59%).

^{1}H NMR (500 MHz, C_6D_6, 348 K): δ 8.65 (1H, d, *J* 2.1, *H*6'), 8.44 (1H, d, *J* 2.1, *H*2'), 8.36 (1H, app br s, *H*7), 7.39 (1H, app t, *J* 1.9, *H*4'), 7.23 (2H, m, *o-Ph*), 7.10-7.19 (1H, obscured, *H*6), 7.07 (1H, app d, *J* 7.7, *H*4), 6.94-7.05 (3H, m, *m-Ph*, *p-Ph*), 6.77 (1H, app td, *J* 7.6, 1.0, *H*5), 5.94-6.10 (2H, m, *H*15, *H*16),ł 5.34 (1H, s, *H*2), 2.88 (1H, d, *J* 16.8, *H*9), 2.82 (1H, d, *J* 16.8, *H*9'), 2.42 (4H, m, *H*23), 2.38 (2H, t, *J* 7.10, *H*21), 1.94 (2H, app q, *J* 6.6, *H*17), 1.64 (4H, m, *H*24), 1.47 (2H, app quin, *J* 7.0, *H*20), 1.22-1.39 (4H, m, *H*18, *H*19), 0.95 (2H, br s, N*H*$_2$).

^{13}C NMR (126 MHz, C_6D_6, 348 K): δ 171.7 (*C*=O), 149.7 (*C*6'), 146.8 (*C*2'), 140.9, 134.8, 134.4 (*C*15/*C*16), 133.5, 131.0, 130.3 (*C*6), 129.9 (*C*4'), 129.6 (*m-Ph*/*p-Ph*), 129.0 (*m-Ph*/*p-Ph*), 126.5 (*C*15/*C*16), 126.2 (*C*4), 126.0 (*o-Ph*), 125.8 (*C*5), 118.7 (*C*N), 117.3 (*C*7), 73.1 (*C*2), 58.2 (*C*3), 56.5 (*C*21), 54.4 (*C*23), 46.1 (*C*9), 33.3 (*C*17), 29.3 (*C*18/*C*19/*C*20), 29.2 (*C*18/*C*19/*C*20), 27.6 (*C*18/*C*19), 24.2 (*C*24).‡

ł ^{1}H NMR (400 MHz, C_6D_6): δ 5.96 (1H, dt, *J* 16.0, 6.6, *H*16), 5.86 (1H, d, *J* 16.0, *H*15).

‡ 1 peak obscured.

HRMS: $[C_{33}H_{38}ON_5]^+$ ([M+H]$^+$) requires 520.3071; found 520.3069.

IR: ν_{max} (film)/cm^{-1} 3380 (br, N-H), 2931, 1681 (C=O), 1599, 1480, 1393, 1221, 773.

$[\alpha]_D^{25.0}$ = -63 (*c* = 0.1, $CHCl_3$).

(2*RS*,3*RS*)-3-Phenyl-2-(5-(7-(pyrrolidin-1-yl)hept-1-yn-1-yl)pyridin-3-yl)indoline-3-carbonitrile **207**

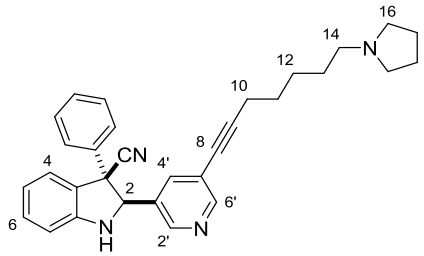

Indoline **207** was prepared according to general procedure 5, using indoline **50** (215 mg, 0.57 mmol), alkyne **105** (104 mg, 0.63 mmol), $Pd(PPh_3)_2Cl_2$ (20 mg, 0.03 mmol), and CuI (5 mg, 0.03 mmol) in *N*,*N*-diisopropylamine (5 mL). The reaction mixture was stirred at 60 °C for 3 h. Purification by flash pressure column chromatography (4.5% MeOH/CH_2Cl_2 + 0.5% aq. NH_4OH) afforded indoline **207** as a pale yellow oil (80 mg, 0.17 mmol, 31%).

^{1}H NMR (500 MHz, C_6D_6): δ 8.96 (1H, d, *J* 2.0, *H*6'), 8.18 (1H, d, *J* 2.0, *H*2'), 8.00 (1H, app t, *J* 2.0, *H*4'), 7.22 (2H, m, *Ph*), 6.93-7.06 (4H, m, *H*6, *Ph*), 6.73 (1H, app d, *J* 7.6, *H*4), 6.59 (1H, app td, *J* 7.6, 0.9, *H*5), 6.42 (1H, app d, *J* 7.6, *H*7), 4.29 (1H, d, *J* 3.2, *H*2), 2.99 (1H, d, *J* 3.2, N*H*), 2.38 (4H, m, *H*16), 2.33 (2H, t, *J* 6.9, *H*14), 2.15 (2H, t, *J* 6.6, *H*10), 1.63 (4H, m, *H*17), 1.33-1.50 (6H, m, *H*11, *H*12, *H*13).

^{13}C NMR (125.75 MHz, C_6D_6): δ 153.8 (*C*6'), 150.8 (*C*7a), 148.4 (*C*2'), 138.3 (*C*4'), 137.8, 132.3, 130.6 (*C*6/*Ph*), 129.5 (*C*6/*Ph*), 129.1 (*C*6/*Ph*), 127.7, 126.2 (*C*4), 121.8 (*C*5'), 121.3 (*C*5), 118.9 (*C*N), 111.1 (*C*7), 95.1 (*C*8/*C*9), 78.4 (*C*8/*C*9), 75.8 (*C*2), 58.9 (*C*3), 56.7 (*C*14), 54.7 (*C*16), 29.3 (*C*11/*C*12/*C*13), 29.1 (*C*11/*C*12/*C*13), 27.5 (*C*11/*C*12/*C*13), 24.3 (*C*17), 20.0 (*C*10).‡

‡ 1 peak obscured.

HRMS (ES$^+$): $[C_{31}H_{33}N_4]^+$ ([M+H]$^+$) requires 461.2700; found 461.2695.

IR: ν_{max} (film)/cm^{-1} 2936, 1726, 1607, 1470, 1450, 1263, 752.

(2*RS*,3*RS*)-3-phenyl-2-(5-(7-(pyrrolidin-1-yl)heptyl)pyridin-3-yl)indoline-3-carbonitrile **214**

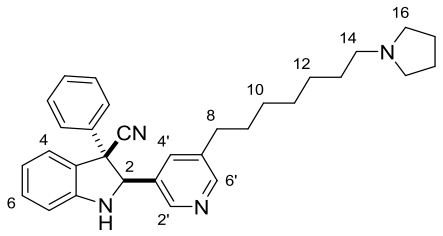

Indoline **214** was prepared according to general procedure 3 using indoline **207** (20 mg, 0.04 mmol) and Pd/C (degussa type, 2 mg) in MeOH (1.5 mL). The reaction mixture was stirred at rt under a H_2 atmosphere for 16 h. Purification by flash pressure column chromatography (5% MeOH/CH_2Cl_2 + 0.5% aq. NH_4OH) afforded indoline **214** as a colorless oil (14 mg, 0.029 mmol, 72%).

^{1}H NMR (500 MHz, C_6D_6): δ 8.57 (1H, d, *J* 2.0, *H*6'), 8.11 (1H, d, *J* 2.0, *H*2'), 7.83 (1H, app t, *J* 2.0, *H*4'), 7.28 (2H, m, *Ph*), 6.97-7.06 (4H, m, *H*6, *Ph*), 6.75 (1H, app d, *J* 7.6, *H*4), 6.61 (1H, app td, *J* 7.6, 0.9, *H*5), 6.47 (1H, app d, *J* 8.1, *H*7), 4.45 (1H, d, *J* 3.0, *H*2), 3.31 (1H, d, *J* 3.0, N*H*), 2.31-2.49 (8H, m, *H*8, *H*14, *H*16), 1.63 (4H, m, *H*17), 1.46-1.57 (4H, m, *H*9, *H*13), 1.35 (2H, app quin, *J* 7.5, *H*10/*H*11/*H*12), 1.17-1.29 (4H, m, *H*10/*H*11/*H*12).

^{13}C NMR (126 MHz, C_6D_6): δ 151.8 (*C*6'), 151.2 (*C*7a), 147.8 (*C*2'), 138.3, 138.0, 135.7 (*C*4'), 132.1, 130.6 (*C*6/*Ph*), 129.4 (*C*6/*Ph*), 129.0 (*C*6/*Ph*), 127.9, 126.3 (*C*4), 121.3 (*C*5), 119.3 (*C*N), 111.1 (*C*7), 76.4 (*C*2), 59.1 (*C*3), 57.0 (*C*14), 54.8 (*C*16), 33.5 (*C*8), 31.7 (*C*9/*C*13), 30.0 (*C*10/*C*11/*C*12), 29.8 (*C*9/*C*13), 29.7 (*C*10/*C*11/*C*12), 28.1 (*C*10/*C*11/*C*12), 24.3 (*C*17).ł

ł 1 peak obscured.

HRMS (ES$^+$): $[C_{31}H_{37}N_4]^+$ ([M+H]$^+$]) requires 465.3013; found 465.3013.

IR: ν_{max}(film)/cm^{-1} 3027, 2930, 2797, 1608, 1471, 1259, 1220, 749, 700.

(2*RS*,3*RS*)-3-Phenyl-2-(5-((E)-7-(pyrrolidin-1-yl)hept-1-en-1-yl)pyridin-3-yl)indoline-3-carbonitrile

271

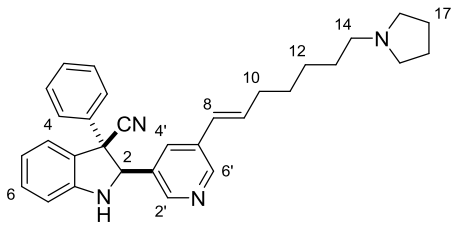

Indoline **271** was prepared according to general procedure 4, using indoline **50** (60 mg, 0.16 mmol), vinylstannane **57** (87 mg, 0.19 mmol), and $Pd(PPh_3)_4$ (18 mg, 0.016 mmol) in NMP (3.2 mL). The reaction mixture was stirred at 85 °C for 3 h. Purification by flash pressure column chromatography (4.5% $MeOH/CH_2Cl_2$ + 0.5% aq. NH_4OH) afforded indoline **271** as a colorless paste (42 mg, 0.091 mmol, 57%).

^{1}H (500 MHz, C_6D_6): δ 8.72 (1H, d, *J* 2.1, *H*6'), 8.11 (1H, d, *J* 2.1, *H*2'), 8.02 (1H, app t, *J* 2.1, *H*4'), 7.26 (2H, m, *o-Ph*), 6.96-7.06 (4H, m, *H*6, *m-Ph*, *p-Ph*), 6.75 (1H, app d, *J* 7.4, *H*4), 6.61 (1H, app td, *J* 7.5, 0.9, *H*5), 6.47 (1H, app d, *J* 7.9, *H*7), 6.17-6.23 (2H, m, *H*8, *H*9), 4.41 (1H, d, *J* 3.1, *H*2), 3.15 (1H, d, *J* 3.1, N*H*), 2.34-2.47 (6H, m, *H*14, *H*16), 2.00 (2H, app q, *J* 6.8, *H*10), 1.64 (4H, m, *H*17), 1.51 (2H, app quin, *J* 7.1, *H*13), 1.27-1.38 (4H, m, *H*11, *H*12).

^{13}C (126 MHz, C_6D_6): δ 151.0 (*C*7a), 149.7 (*C*6'), 148.4 (*C*2'), 137.8 (*i-Ph*), 134.6 (*C*9), 133.9 (*C*5'), 132.3 (*C*4'), 132.3 (*C*3'), 130.6 (*C*6), 129.4 (*m-Ph*), 129.0 (*p-Ph*), 128.4 (*o-Ph*), 127.9 (*C*3a), 126.9 (*C*8), 126.3 (*C*4), 121.3 (*C*5), 119.2 (*C*N), 111.2 (*C*7), 76.3 (*C*2), 59.0 (*C*3), 56.8 (*C*14), 54.7 (*C*16), 33.8 (*C*10), 29.7 (*C*13), 29.7 (*C*11/*C*12), 27.8 (*C*11/*C*12), 24.3 (*C*17).

HRMS: $[C_{31}H_{35}N_4]^+$ ($[M+H]^+$) requires 463.2856; found 463.2853.

IR: ν_{max} (film)/cm^{-1} 2933, 2798, 1608, 1472, 1260, 1220, 1026, 773, 645.

L-(+)-Isopropyl mandelate **146**

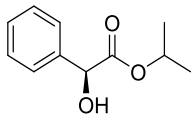

Ester **146** was prepared following a literature procedure.[101] Two drops of concentrated H_2SO_4 were added to a stirred solution of L-(+)-mandelic acid (1 g, 6.57 mmol) in ^{i}PrOH. The solution was stirred at 65 °C for 16 h, then concentrated. The resulting residue was dissolved in EtOAc and washed with H_2O, then with brine. The organic layer was dried over $MgSO_4$, filtered, and concentrated to afford ester **146** as a colorless solid (1.2 g, 5.57 mmol, 85%). The spectral data matched those reported in the literature.

^{1}H (400 MHz, $CDCl_3$): δ 7.29-7.46 (5H, m, *Ph*), 5.13 (1H, s, PhC*H*), 5.08 (1H, hept, *J* 6.3, OC*H*$(CH_3)_2$), 1.29 (3H, d, *J* 6.1, CH_3a), 1.12 (4 H, d, *J* 6.1, CH_3b).

^{13}C (101 MHz, $CDCl_3$): δ 173.2 ($CO_2{}^{i}$Pr), 138.5 (*i-Ph*), 128.5 (*Ph*), 128.3 (*Ph*), 126.4 (*Ph*), 72.9 (Ph*C*HOH), 70.2 (O*C*H$(CH_3)_2$), 21.7 (*C*H$_3$a), 21.4 (*C*H$_3$b).

LCMS (ES^+): 217.1 ([M+Na^+]).

IR: ν_{max}(film)/cm^{-1} 3484 (br, O-H), 2983, 2361, 1725 (C=O), 1265, 1183, 1105, 1067, 733, 700.

MP: 39-41 °C (lit 43 °C).

$[\alpha]_D^{20.0}$ = +109.1 ° (*c* = 1.0, $CHCl_3$), lit $[\alpha]_D^{22.0}$ = +103.6 ° (*c* = 1.0, $CHCl_3$).

Isopropyl (*S*)-2-((chlorocarbonyl)oxy)-2-phenylacetate **147**

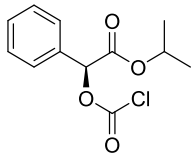

Chloroformate **147** was prepared following a literature procedure.[101] Triphosgene (1.15 g, 3.86 mmol) was added to a solution of ester **146** (1.00 g, 5.15 mmol) in toluene (5 mL) at 0 °C.

Quinoline (0.67 mL, 5.7 mmol) was added dropwise and stirred at rt for 2 h. The mixture was cooled to 0 °C, and HCl (aq. 1 M, 10 mL) was added. The mixture was extracted with Et_2O, and the combined organic extracts were washed with brine, dried over Na_2SO_4, filtered, and concentrated to afford chloroformate **147** as a brown, hygroscopic solid (1.32 g, 5.14 mmol, quant). The spectral data matched those reported in the literature.

^{1}H (400 MHz, $CDCl_3$): δ 7.39-7.50 (5H, m, *Ph*), 5.92 (1H, s, PHC*H*), 5.10 (1H, hept, *J* 6.3, OC*H*$(CH_3)_2$), 1.29 (3H, d, *J* 6.1, C*H*$_3$a), 1.16 (3 H, d, *J* 6.1, C*H*$_3$b).

^{13}C (101 MHz, $CDCl_3$): δ 166.4 (*C*$O_2{}^i$Pr), 150.6 (O*C*(O)Cl), 132.0 (*i-Ph*), 129.9 (*Ph*), 128.9 (*Ph*), 127.7 (*Ph*), 80.3 (PH*C*H), 70.4 (O*C*H$(CH_3)_2$), 21.6 (*C*H$_3$a), 21.3 (*C*H$_3$b).

LCMS (ES^+): 279.0 ([M(^{35}Cl)+Na^+]), 281.0 ([M(^{37}Cl)+Na^+]).

ν_{max} (film): 2984, 1776 (C=O), 1746 (C=O), 1139, 1101, 1008, 820, 734, 695.

$[\alpha]_D^{20.0}$ = +106.3 ° (*c* = 1.0, $CHCl_3$), lit $[\alpha]_D^{19.7}$ = +93.1 ° (*c* = 1.73, $CHCl_3$).

(S)-2-Isopropoxy-2-oxo-1-phenylethyl (2R,3R)-2-(5-bromopyridin-3-yl)-3-cyano-3-phenylindoline-1-carboxylate **148** and (S)-2-Isopropoxy-2-oxo-1-phenylethyl (2S,3S)-2-(5-bromopyridin-3-yl)-3-cyano-3-phenylindoline-1-carboxylate **149**

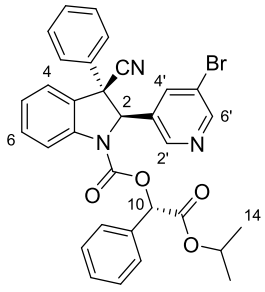

148

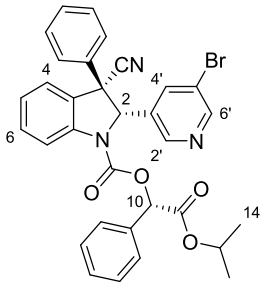

149

Indolines **148** and **149** were prepared according to general procedure 3 using indoline **50** (220 mg, 0.59 mmol), chloroformate **147** (330 mg, 1.29 mmol), and pyridine (0.12 mL, 1.5 mmol) in CH_2Cl_2 (12 mL). The reaction mixture was stirred at rt for 8 h. Purification by flash pressure column chromatography (5% EtOAc/petroleum ether) afforded separately indoline **148** as a colorless solid

(91 mg, 0.15 mmol, 25%) and indoline **149** as a colorless solid (99 mg, 0.17 mmol, 29%).

(S)-2-Isopropoxy-2-oxo-1-phenylethyl (2R,3R)-2-(5-bromopyridin-3-yl)-3-cyano-3-phenylindoline-1-carboxylate **148**

^{1}H NMR (500 MHz, C_6D_6): δ 8.69 (1H, app s, *H*6'), 8.53 (1H, app s, *H*2'), 8.29 (1H, app br s, *H*7), 7.74 (1H, app s, *H*4'), 7.12-7.18 (2H, obscured, *Ph*), 6.85-7.07 (10H, *H*4, *H*6, *Ph*), 6.65 (1H, app td, *J* 7.6, 1.0, *H*5), 5.81 (1H, s, *H*10), 5.32 (1H, br s, *H*2), 4.87 (1H, sept, *J* 6.3, *H*13), 0.92 (3H, d, *J* 6.3, *H*14), 0.77 (3H, d, *J* 6.3, *H*14').

^{13}C NMR (126 MHz, C_6D_6): δ 168.1 (*C*=O), 152.5 (*C*6'), 152.0 (*C*=O), 147.3 (*C*2'), 142.6 (*C*7a), 140.3 (*i-Ph*), 137.4 (*C*4'), 136.0 (*C*3'), 134.1 (*i-Ph*), 131.4 (*C*6), 130.1 (*Ph*), 129.9 (*Ph*), 129.4 (*Ph*), 129.3 (*Ph*), 126.4 (*Ph*), 126.4 (*C*4), 125.8 (*C*5), 121.6 (*C*5'), 118.8 (*C*N), 116.3 (*C*7), 77.7 (*C*10), 73.8 (*C*2), 69.9 (*C*13), 57.7 (*C*3), 21.8 (*C*14), 21.5 (*C*14').‡

‡ 2 peaks obscured.

HRMS (ES$^+$): $[C_{32}H_{27}O_4N_3{}^{79}Br]^+$ ([M+H]$^+$) requires 596.1180; found 596.1179.

IR: ν_{max}(film)/cm^{-1} 2972, 1722, 1485, 1393, 1217, 1103, 760, 696.

MP: 40-42 °C.

$[\alpha]_D^{25.0}$ = +102 (*c* = 0.1, $CHCl_3$).

(S)-2-Isopropoxy-2-oxo-1-phenylethyl (2S,3S)-2-(5-bromopyridin-3-yl)-3-cyano-3-phenylindoline-1-carboxylate **149**

^{1}H NMR (500 MHz, C_6D_6): δ 8.49 (1H, app s, *H*6'), 8.46 (1H, app br s, *H*2'), 8.27 (1H, app br d, *J* 7.4, *H*7), 7.54 (1H, app br s, *H*4'), 7.24 (2H, m, *Ph*), 6.91-7.07 (9H, m, *H*6, *Ph*), 6.88 (1H, dd, *J* 7.7, 0.8, *H*4), 6.64 (1H, app td, *J* 7.6, 1.0, *H*5), 6.01 (1H, s, *H*10), 5.62 (1H, s, *H*2), 4.87 (1H, sept, *J* 6.2, *H*13), 0.89 (3H, d, *J* 6.2, *H*14), 0.74 (3H, d, *J* 6.2, *H*14').

^{13}C NMR (126 MHz, C_6D_6): δ 168.4 (*C*=O), 152.3 (*C*6'), 151.8 (*C*=O), 147.0 (*C*2'), 142.4 (*C*7a), 140.4 (*i-Ph*), 136.9 (*C*4'), 136.1 (*C*3'), 134.1 (*i-Ph*), 131.4 (*C*6), 130.2 (*Ph*), 129.7 (*C*3a), 129.7 (*Ph*), 129.4

(*Ph*), 129.3 (*Ph*), 127.9 (*Ph*), 126.4 (*Ph*), 126.3 (*C*4), 125.8 (*C*5), 121.5 (*C*5‘), 118.8 (*C*N), 116.4 (*C*7), 76.8 (*C*10), 73.8 (*C*2), 70.1 (*C*13), 57.7 (*C*3), 21.8 (*C*14), 21.5 (*C*14‘).

HRMS (ES^+): $[C_{32}H_{27}O_4N_3{}^{79}Br]^+$ ($[M+H]^+$) requires 596.11780; found 596.1179.

IR: ν_{max} (film)/cm^{-1} 2978, 1722, 1485, 1391, 1221, 1103, 756, 696.

MP: 126-128 °C.

$[\alpha]_D^{25.0}$ = +3.0 (*c* =0.1, $CHCl_3$).

(2*RS*,3*RS*)-2-(5-Bromopyridin-3-yl)-1-(3-(3-methyl-3H-diazirin-3-yl)propanoyl)-3-phenylindoline-3-carbonitrile **229**

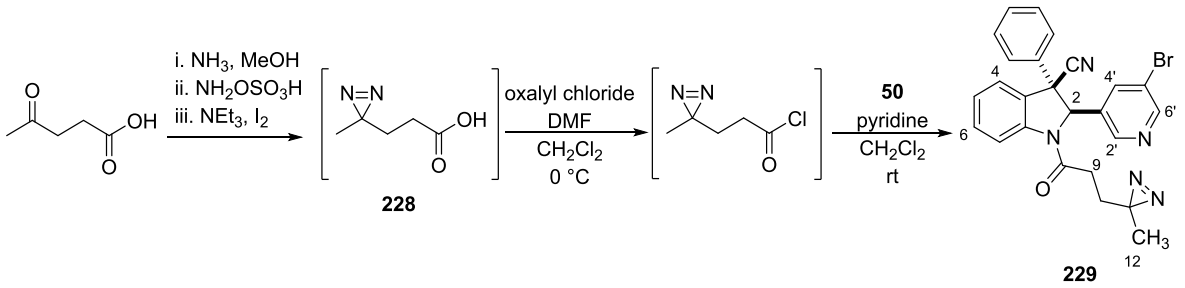

Diazirine **228** was prepared according to a modified literature procedure.[147] A solution of NH_3 in MeOH (7 N, 5.0 mL, 35 mmol) was added dropwise to a solution of levulinic acid (0.44 mL, 4.3 mmol) in MeOH (1 mL) at 0 °C and stirred for 3 h. A solution of hydroxylamine *O*-sulfonic acid (510 mg, 4.95 mmol) in MeOH (1.5 mL) was added and stirred at rt for 16 h. The excess NH_3 was removed by blowing the mixture down with N_2. The white precipitate was filtered off and the filtrate concentrated. The remaining residue was dissolved in MeOH (0.5 mL) and cooled to 0 °C. NEt_3 (0.90 mL, 6.5 mmol) was added and stirred at 0 °C for 5 min. I_2 was added portionwise until the yellow colour of the solution remained (approx. 1 g). The solution was diluted with EtOAc, washed with HCl (aq., 1 M), $Na_2S_2O_3$ (aq., 10% w/w), and brine. The organic layer was dried over Na_2SO_4, filtered, and concentrated.

The crude residue (210 mg) was dissolved in CH_2Cl_2 (12 mL) and 1 drop DMF was added. The solution

was cooled to 0 °C, and oxalyl chloride (0.30 mL, 3.3 mmol) was added dropwise. The reaction mixture was stirred at 0 °C for 1.5 h and concentrated.

The crude residue (78 mg) was dissolved in CH_2Cl_2 (1.5 mL) and added dropwise to a solution of indoline **50** (50 mg, 0.13 mmol) and pyridine (43 µL, 0.53 mmol) in CH_2Cl_2 (2 mL) and stirred at rt for 30 min. $NaHCO_3$ (saturated aq., 5 mL) was added, and the mixture was extracted with CH_2Cl_2. The combined organic extracts were washed with brine, dried over Na_2SO_4, filtered, and concentrated. Purification by flash pressure column chromatography (25% EtOAc/petroleum ether) afforded indoline **229** as a colourless gum (40 mg, 0.082 mmol, 62%).

^{1}H NMR (500 MHz, C_6D_6, 348 K): δ 8.56 (1H, d, *J* 2.1, *H*6'), 8.42 (1H, d, *J* 1.9, *H*2'), 8.06 (1H, app br s, *H*7), 7.56 (1H, app t, *J* 2.1, *H*4'), 7.20 (2H, m, *o-Ph*), 6.94-7.10 (5H, m, *H*4, *H*6, *m-Ph*, *p-Ph*), 6.73 (1H, app td, *J* 7.6, 0.8, *H*5), 5.25 (1H, s, *H*2), 1.57 (2H, app m, *H*9), 1.42 (2H, t, *J* 6.7, *H*10), 0.56 (3H, s, C*H*$_3$).

^{13}C NMR (126 MHz, C_6D_6, 348 K): δ 169.0 (*C*=O), 152.6 (*C*6'), 146.6 (*C*2'), 142.7, 140.3, 136.4 (*C*4'), 135.4, 130.9 (*C*6), 129.8 (*m-Ph*/*p-Ph*), 129.1 (*m-Ph*/*p-Ph*), 126.1 (*C*4), 125.9 (*C*5), 125.8 (*o-Ph*), 121.4 (*C*5'), 118.3 (*C*N), 117.2 (*C*7), 73.2 (*C*2), 57.5 (*C*3), 29.7 (*C*9/*C*10), 29.0 (*C*9/*C*10), 24.7 (*C*11), 19.7 (*C*12).‡

‡ 1 peak obscured.

HRMS (ES$^+$): $[C_{25}H_{21}ON_5{}^{79}Br]^+$ ([M+H]$^+$) requires 486.0924; found 486.0924.

IR: ν_{max}(film)/cm^{-1} 3069, 2933, 1672 (C=O), 1477, 1261, 1020, 737, 700.

(2*RS*,3*RS*)-1-(3-(3-Methyl-3H-diazirin-3-yl)propanoyl)-3-phenyl-2-(5-((E)-7-(pyrrolidin-1-yl)hept-1-en-1-yl)pyridin-3-yl)indoline-3-carbonitrile **230**

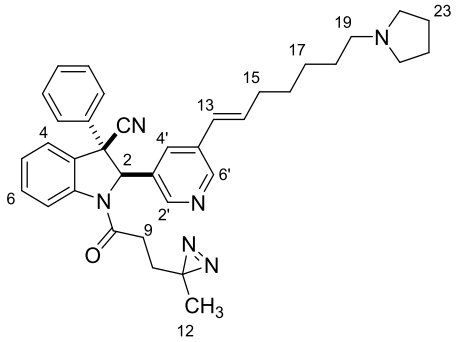

Indoline **230** was prepared according to general procedure 4 using indoline **229** (35 mg, 0.072 mmol), vinylstannane **57** (39 mg, 0.086 mmol), and $Pd(PPh_3)_4$ (8 mg, 0.007 mmol) in NMP (1.5 mL). The reaction mixture was stirred at 60 °C for 3.5 h. Purification by flash pressure column chromatography (6.5% MeOH/CH_2Cl_2 + 0.5% aq. NH_4OH) afforded indoline **230** as a pale yellow paste (14 mg, 0.024 mmol, 34%).

^{1}H NMR (500 MHz, C_6D_6, 348 K): δ 8.65 (1H, app s, *H*6'), 8.48 (1H, app s, *H*2'), 8.36 (1H, app br s, *H*7), 7.45 (1H, app s, *H*4'), 7.28 (2H, app d, *J* 7.5, *o-Ph*), 7.12 (1H, app t, *J* 7.9, *H*6), 7.08 (1H, app d, *J* 7.8, *H*4), 6.96-7.06 (3H, m, *m-Ph*, *p-Ph*), 5.98-6.10 (2H, m, *H*13, *H*14),ŧ 5.35 (1H, s, *H*2), 2.41 (4H, m, *H*22), 2.36 (2H, t, *J* 7.3, *H*19), 1.93 (2H, app q, *J* 6.4, *H*15), 1.56-1.73 (6H, m, *H*9, *H*23), 1.34-1.51 (4H, m, *H*10, *H*18), 1.22-1.34 (4H, m, *H*16, *H*17), 0.53 (3H, s, C*H*$_3$).

^{13}C NMR (126 MHz, C_6D_6, 348 K): δ 169.8 (*C*=O), 150.0 (*C*6'), 147.2 (*C*2'), 143.8, 141.2, 135.2 (*C*13/*C*14), 134.8, 133.9, 131.2 (*C*6), 130.8 (*C*4'), 130.2 (*m-Ph*/*p-Ph*), 129.4 (*m-Ph*/*p-Ph*), 126.8 (*C*13/*C*14), 126.5 (*C*4), 126.3 (*C*5), 126.1 (*o-Ph*), 118.9 (*C*N), 117.8 (*C*7), 74.5 (*C*2), 58.3 (*C*3), 56.7 (*C*19), 54.6 (*C*22), 33.6 (*C*15), 30.3 (*C*9), 29.6 (*C*10/*C*17/*C*18/*C*19), 29.6 (*C*10/*C*17/*C*18/*C*19), 29.5 (*C*10/*C*17/*C*18/*C*19), 27.8 (*C*17/*C*18), 25.1 (*C*11), 24.5 (*C*23), 20.0 (*C*H$_3$).ǂ

ŧ ^{1}H NMR (500 MHz, C_6D_6): δ 6.00 (1H, dt, *J* 15.9, 6.7, *H*14), 5.94 (1H, d, *J* 15.9, *H*13).

ǂ 1 peak obscured.

HRMS (ES$^+$): $[C_{36}H_{41}ON_6]^+$ ([M+H]$^+$) requires 573.3336; found 573.3339.

IR: ν_{max} (film)/cm^{-1} 2930, 2788, 2360, 1678 (C=O), 1479, 1350, 756, 669.

(2*RS*,3*RS*)-2-(5-Bromopyridin-3-yl)-1-(hex-5-ynoyl)-3-phenylindoline-3-carbonitrile **222**

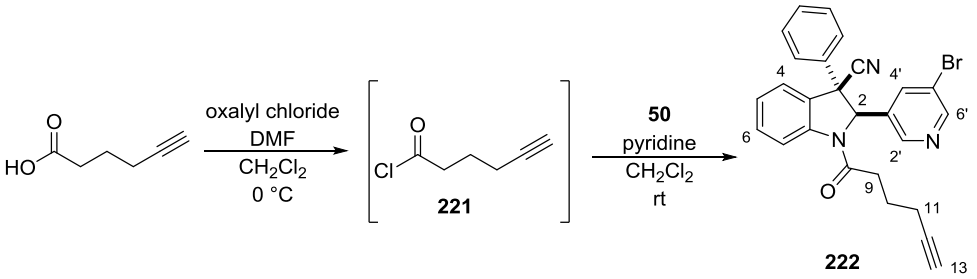

Oxalyl chloride (0.30 mL, 3.6 mmol) was added dropwise to a solution of 5-hexynoic acid (0.20 mL, 1.8 mmol) and DMF (1 drop) in CH_2Cl_2 (20 mL) at 0 °C and stirred for 1.5 h. The reaction mixture was allowed to warm to rt and concentrated to afford acyl chloride **221** as a yellow oil (224 mg, 1.72 mmol, 96%).

A solution of acyl chloride **221** (56 mg, 0.43 mmol) in CH_2Cl_2 (1 mL) was added to a solution of indoline **50** (80 mg, 0.21 mmol) and pyridine (34 µL, 0.43 mmol) in CH_2Cl_2 (3 mL) and stirred at rt for 1 h. $NaHCO_3$ (saturated aq., 3 mL) was added, and the mixture was extracted with EtOAc. The combined organic extracts were washed with brine, dried over Na_2SO_4, filtered, and concentrated. Purification by flash pressure column chromatography (25% EtOAc/petroleum ether) afforded indoline **222** as a pale yellow oil (94 mg, 0.20 mmol, 95%).

^{1}H NMR (500 MHz, C_6D_6, 348 K): δ 8.57 (1H, app s, *H*6'), 8.47 (1H, app s, *H*2'), 8.18 (1H, app br s, *H*7), 7.59 (1H, app s, *H*4'), 7.14-7.21 (2H, obscured, *o-Ph*), 7.07 (1H, app t, *J* 7.7, *H*6), 6.94-7.04 (4H, m, *H*4, *m-Ph*, *p-Ph*), 6.74 (1H, app t, *J* 7.7, *H*5), 5.33 (1H, s, *H*2), 1.99 (2H, app m, *H*9), 1.79-1.90 (2H, td, *J* 6.8, 2.5, *H*11), 1.56 (1H, t, *J* 2.6, *H*13), 1.52 (2H, app quin, 6.8, *H*10).

^{13}C NMR (126 MHz, C_6D_6, 348 K): δ 170.4 (*C*=O), 152.9 (*C*6'), 147.2 (*C*2'), 143.4 (*C*7a), 140.8 (*i-Ph*), 136.8 (*C*4'), 136.0 (*C*3'), 131.3 (*C*6), 130.2 (*m-Ph*/*p-Ph*), 129.5 (*m-Ph*/*p-Ph*), 126.5 (*C*4), 126.2 (*o-Ph*), 126.2 (*C*5), 121.8 (*C*5'), 118.9 (*C*N), 117.8 (*C*7), 83.5 (*C*12), 73.6 (*C*2), 69.9 (*C*13), 57.9 (*C*3), 34.2 (*C*9), 23.7 (*C*10), 17.9 (*C*11).‡

‡ 1 peak obscured.

HRMS (ES$^+$): $[C_{26}H_{21}ON_3{}^{79}Br]^+$ ($[M+H]^+$) requires 470.08625; found 470.08636.

IR: ν_{max}(film)/cm^{-1} 3288 (sharp, C-H), 3068, 2977, 1674 (C=O), 1479, 1391, 1271, 1020, 756, 698.

(2*RS*,3*RS*)-1-(Hex-5-ynoyl)-3-phenyl-2-(5-((E)-7-(pyrrolidin-1-yl)hept-1-en-1-yl)pyridin-3-yl)indoline-3-carbonitrile **223**

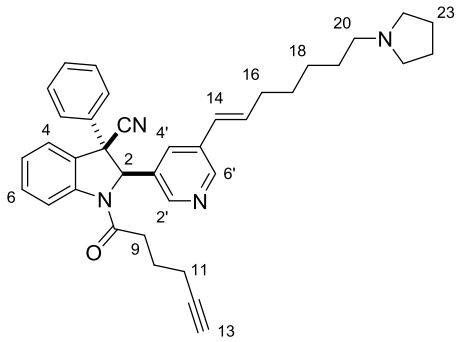

Indoline **223** was prepared according to general procedure 4, using indoline **222** (60 mg, 0.13 mmol), vinylstannane **57** (77 mg, 0.17 mmol), and $Pd(PPh_3)_4$ (15 mg, 0.013 mmol) in NMP (3 mL). The reaction mixture was stirred at 85 °C for 2.5 h. Purification by flash pressure column chromatography (5% MeOH/CH_2Cl_2 + 0.5% aq. NH_4OH) afforded indoline **223** as a pale yellow oil (32 mg, 0.057 mmol, 44%, contains minor impurities).

^{1}H NMR (500 MHz, C_6D_6, 348 K): δ 8.67 (1H, d, *J* 1.4, *H*6'), 8.54 (1H, d, *J* 1.7, *H*2'), 8.45 (1H, app br s, *H*7), 7.49 (1H, app s, *H*4'), 7.28 (2H, app d, *J* 7.4, *o-Ph*), 7.14 (1H, app t, *J* 8.0, *H*6), 7.10 (1H, app d, *J* 7.7, *H*4), 6.95-7.06 (3H, m, *m-Ph*, *p-Ph*), 6.79 (1H, app t, *J* 6.8, *H*5), 5.99-6.10 (2H, m, *H*14, *H*15),‡ 5.45 (1H, s, *H*2), 2.43 (4H, m, *H*22), 2.37 (2H, t, *J* 7.2, *H*20), 2.06 (2H, app m, *H*9), 1.89-1.97 (2H, app br s, *H*16), 1.85 (2H, td, *J* 6.8, 2.5, *H*11), 1.64 (4H, m, *H*23), 1.51-1.60 (3H, m, *H*10, *H*13), 1.48 (2H, app quin, *J* 7.0, *H*19), 1.22-1.35 (4H, m, *H*17, *H*18).

^{13}C NMR (126 MHz, C_6D_6, 348 K): δ 170.7 (*C*=O), 149.9 (*C*6'), 147.4 (*C*2'), 144.1, 141.3, 135.1 (*C*14/*C*15), 134.8, 134.1, 131.2 (*C*6), 130.7 (*C*4'), 130.2 (*m-Ph*/*p-Ph*), 129.4 (*m-Ph*/*p-Ph*), 126.9 (*C*14/*C*15), 126.5 (*C*4), 126.4 (*o-Ph*), 126.1 (*C*5), 119.1 (*C*N), 118.0 (*C*7), 83.6 (*C*12/*C*13), 74.5 (*C*2),

69.9 (*C*12/*C*13), 58.3 (*C*3), 56.7 (*C*20), 54.7 (*C*22), 34.4 (*C*9), 33.6 (*C*16), 29.5 (*C*17/*C*18/*C*19), 29.5 (*C*17/*C*18/*C*19), 27.8 (*C*17/*C*18/*C*19), 24.5 (*C*23), 23.9 (*C*10), 17.9 (*C*11).‡

ł ^{1}H NMR (400 MHz, C_6D_6): δ 5.97 (1H, dt, *J* 16.1, 6.6, *H*15), 5.87 (1H, d, *J* 16.1, *H*14).

‡ 1 peak obscured.

HRMS (ES^+): $[C_{37}H_{41}ON_4]^+$ ($[M+H]^+$) requires 557.32749; found 557.32733.

IR: ν_{max}(film)/cm^{-1} 2930, 2252, 1674 (C=O), 1599, 1479, 1391, 1273, 754.

N-(71-azido-3,6,9,12,15,18,21,24,27,30,33,36,39,42,45,48,51,54,57,60,63,66,69-Tricosaoxahenheptacontyl)-5-((3aS,4S,6aR)-2-oxohexahydro-1H-thieno[3,4-d]imidazol-4-yl)pentanamide **220**

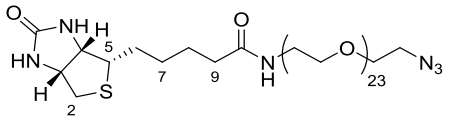

Azide **220** was prepared according to a modified literature procedure.[198] *N*-(3-Dimethylaminopropyl)-*N*'-ethylcarbodiimide hydrochloride (7.7 mg, 0.040 mmol) and 1-hydroxy-7-azabenzotriazole (5.4 mg, 0.039 mmol) were added to a solution of amino-$(PEG)_{23}$-azide (40 mg, 0.036 mmol) and D-biotin (8.9 mg, 0.036 mmol) in *N*,*N*-DMF (0.5 mL) and stirred at rt for 18 h. The reaction mixture was diluted with CH_2Cl_2 and washed 3 times with H_2O, then brine. The organic layer was dried over Na_2SO_4, filtered, and concentrated. Purification by flash pressure column chromatography (8% MeOH/CH_2Cl_2 + 1% aq. NH_4OH) afforded azide **220** as a colorless oil (37 mg, 0.028 mmol, 78%).

^{1}H NMR (500 MHz, $CDCl_3$): δ 6.69 (1H, s, N*H*), 5.77 (1H, app s, N*H*), 4.98 (1H, app s, N*H*), 4.51 (1H, dd, *J* 7.6, 5.0, *H*3), 4.33 (1H, dd, *J* 7.6, 4.8, *H*4), 3.60-3.71 (96H, m), 3.57 (2H, t, *J* 5.2), 3.42-3.47 (2H, t, *J* 5.5), 3.40 (2H, t, *J* 5.2, CH_2N_3), 3.16 (1H, ddd, *J* 8.0, 7.5, 4.6, *H*5), 2.92 (1H, dd, *J* 12.8, 5.0, *H*2), 2.74 (1H, d, *J* 12.8, *H*2'), 2.23 (2H, app m, *H*9), 1.62-1.80 (4H, m, *H*6, *H*8), 1.46 (2H, app quin, *J* 7.4, *H*7).

^{13}C NMR (126 MHz, $CDCl_3$): δ 173.1 (*C*=O), 163.2 (*C*=O), 70.7, 70.7, 70.6, 70.5, 70.4, 70.4, 70.1, 70.0, 69.9, 61.7 (*C*4), 60.1 (*C*3), 55.3 (*C*5), 50.7 (CH_2N_3), 40.5 (*C*2), 39.1 ($CONHCH_2$), 35.8 (*C*9), 28.0 (*C*6), 28.0 (*C*7), 25.5 (*C*8).

IR: ν_{max} (film)/cm^{-1} 2869, 2108 (N=N=N), 1702, 1457, 1349, 1251, 1104, 949.

N-(71-(4-(4-((2*RS*,3*RS*)-3-Cyano-3-phenyl-2-(5-((*E*)-7-(pyrrolidin-1-yl)hept-1-en-1-yl)pyridin-3-yl)indolin-1-yl)-4-oxobutyl)-1H-1,2,3-triazol-1-yl)-3,6,9,12,15,18,21,24,27,30,33,36,39,42,45,48,51,54,57,60,63,66,69-tricosaoxahenheptacontyl)-5-((3a*S*,4*S*,6a*R*)-2-oxohexahydro-1H-thieno[3,4-d]imidazol-4-yl)pentanamide **224**

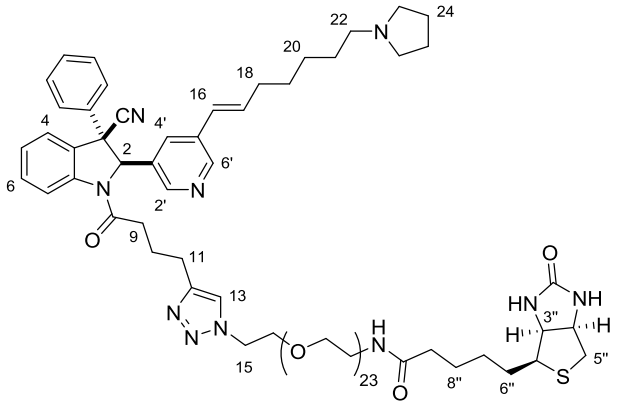

Indoline **224** was prepared according to a modified literature procedure.[192] $CuSO_4$ (5 mM aq., 175 µL, 0.88 µmol) and sodium-L-ascorbate (25 mM aq., 85 µL, 0.0021 mmol) were added to a solution of indoline **223** (12 mg, 0.018 mmol) and azide **220** (25 mg, 0.015 mmol) in 1:1 ^{t}BuOH/H_2O (1 mL) and stirred at 70 °C for 14 h. The reaction mixture was allowed to cool to rt, diluted with H_2O, and extracted with CH_2Cl_2. The combined organic extracts were washed with brine, dried over Na_2SO_4, filtered, and concentrated. Purification by flash pressure column chromatography (9% MeOH/CH_2Cl_2 + 1% aq. NH_4OH) afforded indoline **224** as a colorless oil (19 mg, 0.010 mmol, 56%, contains minor impurities).

^{1}H NMR (500 MHz, C_6D_6): δ 8.78 (1H, app br s, *H*7), 8.71 (1H, d, *J* 1.9, *H*6'), 8.63 (1H, d, *J* 1.9, *H*2'), 7.62 (1H, app s, *H*4'), 7.39 (2H, app d, *J* 7.6, *Ph*), 7.14-7.20 (1H, obscured, *H*6), 7.11 (1H, br t, N*H*),

7.05-7.10 (3H, m, *H*4, *Ph*), 6.97-7.04 (3H, m, *H*13, *Ph*), 6.76 (1H, app td, *J* 7.5, 0.8, *H*5), 6.09 (1H, dt, *J* 15.9, 6.8, *H*17), 5.99 (1H, d, *J* 15.9, *H*16), 5.79 (1H, br s, *H*2), 5.71 (1H, app s, N*H*), 4.06 (2H, t, *J* 5.2, *H*15), 3.95 (1H, dd, *J* 7.6, 4.8, *H*4''), 3.85 (1H, dd, *J* 7.6, 5.0, *H*3''), 3.30-3.58 (94H, m), 3.23-3.28 (2H, m), 2.77 (1H, ddd, *J* 8.2, 7.2, 4.7, *H*2''), 2.46-2.59 (4H, m), 2.44 (4H, m, *H*23), 2.38 (2H, t, *J* 7.40, *H*22), 2.26 (2H, m), 2.00 (1H, app oct, *J* 6.8), 1.92 (2H, app q, *J* 6.9, *H*18), 1.71-1.87 (3H, m, *H*6'', *H*21), 1.65 (5H, m, *H*6''', *H*24), 1.43-1.55 (2H, m), 1.23-1.42 (6H, m).

^{13}C NMR (126 MHz, $CDCl_3$): δ 173.4 (*C*=O), 171.6, 164.7 (*C*=O), 149.7 (*C*6'), 147.3 (*C*2'), 147.0, 140.9, 134.9 (*C*17), 134.6, 134.4, 131.3 (*C*6), 130.9 (*C*4'), 130.2 (*Ph*), 129.4 (*Ph*), 126.7 (*C*16), 126.6 (*Ph*), 126.5 (*C*4), 126.0 (*C*5), 122.5 (*C*13), 119.4 (*C*N), 117.9 (*C*7), 73.7 (*C*2), 71.4, 71.3, 71.3, 71.1, 71.1, 71.0, 70.9, 70.7, 70.6, 70.0, 62.1 (*C*3''), 60.8 (*C*4''), 56.8 (*C*22), 56.3 (*C*2''), 54.7 (*C*23), 50.3 (*C*15), 40.9 (*C*5''), 40.0, 36.4, 35.3, 33.8 (*C*18), 29.5, 29.5, 28.9, 28.9 (*C*6''), 27.9, 26.5, 25.2, 25.0, 24.3 (*C*24).

HRMS (ES^+): $[C_{95}H_{155}O_{26}N_{10}{}^{32}S]^{3+}$ ($[M+3H]^{3+}$) requires 628.3617; found 628.3614.

IR: ν_{max}(film)/cm^{-1} 2871, 1701, 1460, 1349, 1257, 1105, 949.

$[\alpha]_D^{25.0}$ = +8.6 (*c* = 0.1, $CHCl_3$).

4-Oxonon-8-ynoic acid **232**

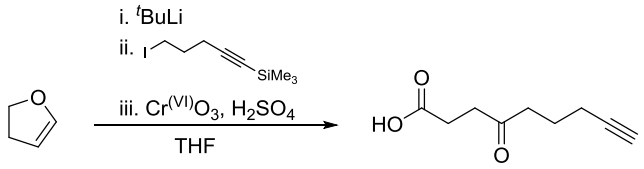

Acid **232** was prepared according to a literature procedure.[148] ^{t}BuLi (1.7 M in pentane, 8.5 mL, 14 mmol) was added dropwise to a solution of 2,3-dihydrofuran (1.3 mL, 17 mmol) in THF (16 mL) at -78 °C. The solution was allowed to warm to -5 °C over 1 h, then re-cooled to -78 °C. (5-Iodopent-1-yn-1-yl)trimethylsilane (3.2 g, 12.0 mmol) was added dropwise, and the reaction mixture was allowed to warm to rt and stirred for 16 h. The mixture was cooled to 0 °C, quenched with NH_4Cl (saturated aq.), and extracted with Et_2O. The combined organic extracts were washed

with brine, dried over Na_2SO_4, filtered, and concentrated. The resulting residue was dissolved in THF (32 mL), and Jones reagent (2 M, 18 mL, 36 mmol) was added dropwise with vigorous stirring. The mixture was stirred at rt for 4 h, diluted with Et_2O (35 mL) and H_2O (35 mL), and stirred for a further 30 min. The aqueous phase was extracted with Et_2O, and the combined organic extracts were washed with H_2O and extracted with NaOH (10% aq.). The basic extract was cooled to 0 °C, acidified to pH 2 with HCl (3M, aq.), and extracted with CH_2Cl_2. The combined organic extracts were washed with brine, dried over Na_2SO_4, filtered, and concentrated to afford acid **232** as a colorless solid (1.16 g, 6.90 mmol, 58%). The spectral data matched those reported in the literature.

^{1}H NMR (400 MHz, $CDCl_3$): δ 2.74 (2H, t, *J* 6.0, *H*2/*H*3), 2.57-2.68 (4H, m, *H*2/*H*3, *H*5), 2.23 (2H, td, *J* 7.0, 2.7, *H*7), 1.97 (1H, t, *J* 2.7, *H*9), 1.81 (2H, app quin, *J* 7.0, *H*6).ł

^{13}C NMR (101 MHz, $CDCl_3$): δ 208.1 (*C*=O), 178.7 (*C*=O), 83.4 (*C*8), 69.1 (*C*9), 40.9 (*C*2/*C*3/*C*5), 36.8 (*C*2/*C*3), 27.7 (*C*2/*C*3/*C*5), 22.1 (*C*6), 17.6 (*C*7).

ł CO_2H peak was not observed.

LCMS (ES^-): 167.1 ($[M-H]^-$).

IR: ν_{max} (film)/cm^{-1} 3289 (sharp, C-H), 1707, 1404, 1184, 1101, 929, 643.

MP: 42-44 °C (lit 45 °C).

3-(3-(Pent-4-yn-1-yl)-3H-diazirin-3-yl)propanoic acid **233**

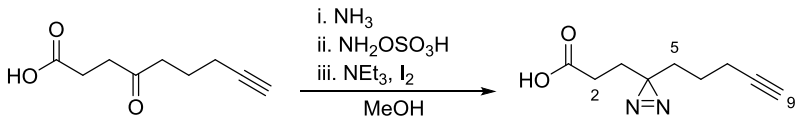

232 **233**

Diazirine **233** was prepared according to a modified literature procedure.[145] Anhydrous ammonia (approx. 4 mL) was condensed in a flask at -40 °C, and a solution of acid **232** (410 mg, 2.44 mmol) in MeOH (1.5 mL) was added dropwise. The mixture was stirred at -40 °C for 3.5 h. A solution of

hydroxylamine-*O*-sulphonic acid (317 mg, 2.80 mmol) in MeOH (2.5 mL) was added dropwise over 30 min. The reaction mixture was stirred at -35 °C for 1 h, then allowed to warm to rt and stirred for 14 h. The remaining ammonia was allowed to evaporate, and the crude residue was filtered and washed with MeOH. The filtrate was concentrated and dissolved in CH_2Cl_2 (1.5 mL). NEt_3 (0.40 mL, 2.9 mmol) was added, followed by a solution of I_2 in CH_2Cl_2 (0.5 g in 3 mL) until the yellow color persisted. The reaction mixture was diluted with EtOAc, washed with HCl (1 M aq.), $Na_2S_2O_3$ (aq., 10% w/w), and brine. The organic layer was dried over Na_2SO_4, filtered, and concentrated. Purification by flash pressure column chromatography (30% EtOAc/CH_2Cl_2) afforded diazirine **233** as a pale yellow oil (85 mg, 0.47 mmol, 19%).

^{1}H NMR (400 MHz, $CDCl_3$): δ 2.14-2.21 (4H, m, *H*2, *H*7), 1.96 (1H, t, *J* 2.7, *H*9), 1.77 (2H, t, *J* 7.7, *H*3), 1.56 (2H, t, *J* 7.4, *H*5), 1.34 (2H, app quin, 7.4, *H*6).

^{13}C NMR (101 MHz, $CDCl_3$): δ 177.5 (*C*=O), 83.2 (*C*8), 69.0 (*C*9), 31.5 (*C*5), 28.1 (*C*2), 27.9 (*C*3), 27.6 (*C*4), 22.6 (*C*6), 17.8 (*C*7).

HRMS (ES^-): $[C_9H_{11}N_2O_2]^-$ ([M-H]$^-$) requires 179.0826; found 179.0823.

IR: ν_{max}(film)/cm^{-1} 3299 (sharp, C-H), 3044, 1712 (C=O), 1585, 1435, 1289, 927, 646.

(2*RS*,3*RS*)-2-(5-Bromopyridin-3-yl)-1-(3-(1,3-dioxoisoindolin-2-yl)propanoyl)-3-phenylindoline-3-carbonitrile **237**

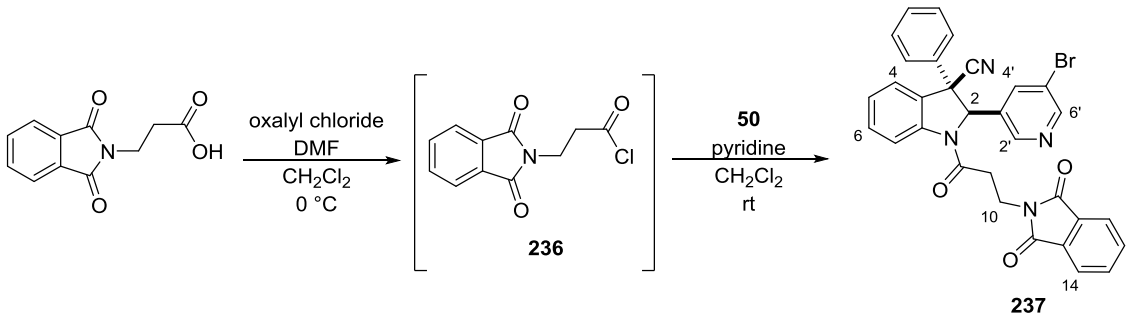

Acyl chloride **236** was prepared according to a modified literature procedure.[197] Oxalyl chloride (0.39 mL, 4.6 mmol) was added dropwise to a solution of 3-phthalimidopropionic acid (0.50 g,

2.3 mmol) and DMF (2 drops) in CH_2Cl_2 (20 mL) at 0 °C and stirred for 1 h. The reaction mixture was allowed to warm to rt and concentrated to afford acyl chloride **236** as a yellow solid (509 mg, 2.14 mmol, 94%).

Acyl chloride **236** (114 mg, 0.48 mmol) was added portionwise to a solution of indoline **50** (120 mg, 0.32 mmol) and pyridine (40 µL, 0.48 mmol) in CH_2Cl_2 (10 mL) and stirred at rt for 4 h. $NaHCO_3$ (saturated aq., 10 mL) was added, and the mixture was extracted with EtOAc. The combined organic extracts were washed with brine, dried over Na_2SO_4, filtered, and concentrated. Purification by flash pressure column chromatography (12% EtOAc/$CHCl_3$) afforded indoline **237** as a colorless solid (142 mg, 0.23 mmol, 72%).

^{1}H NMR (500 MHz, dmso-D_6, 363 K): δ 8.68 (1H, d, *J* 1.9, *H*6'), 8.48 (1H, d, *J* 1.5, *H*2'), 8.10 (1H, app br s, *H*7), 7.92 (1H, app s, *H*4'), 7.76-7.85 (4H, m, *H*14, *H*15), 7.57 (1H, app t, *J* 7.8, *H*6), 7.37-7.48 (4H, m, *H*4, *Ph*), 7.26-7.35 (3H, m, *H*5, *Ph*), 5.98 (1H, s, *H*2), 3.79 (2H, app m, *H*10), 3.01 (1H, br s, *H*9), 2.72 (1H, br s, *H*9').

^{13}C NMR (126 MHz, dmso-D_6, 363 K): δ 169.2 (*C*=O), 167.9 (*C*=O), 151.6 (*C*6'), 146.7 (*C*2'), 142.2 (*C*7a), 139.2 (*C*3a), 137.2 (*C*4'), 135.8 (*C*3'), 134.7 (*C*14/*C*15), 132.1 (*C*13), 131.4 (*C*6), 129.9 (*Ph*), 129.5 (*Ph*), 126.2 (*C*4/*C*5/*Ph*), 126.1 (*C*4/*C*5/*Ph*), 126.0 (*C*4/*C*5/*Ph*), 123.4 (*C*14/*C*15), 120.7 (*C*5'), 118.9 (*C*N), 117.4 (*C*7), 71.0 (*C*2), 56.9 (*C*3), 33.9 (*C*10), 33.6 (*C*9).‡

‡ 1 peak obscured.

HRMS: $[C_{31}H_{22}O_3N_4{}^{79}Br]^+$ ($[M+H]^+$) requires 577.0870; found 577.0869.

IR: ν_{max}(film)/cm^{-1} 3049, 2248, 1704, 1675, 1389, 1221, 1172, 1110, 871, 732.

MP: 194-196 °C.

(2*RS*,3*RS*)-1-(3-(1,3-Dioxoisoindolin-2-yl)propanoyl)-3-phenyl-2-(5-((E)-7-(pyrrolidin-1-yl)hept-1-en-1-yl)pyridin-3-yl)indoline-3-carbonitrile **238**

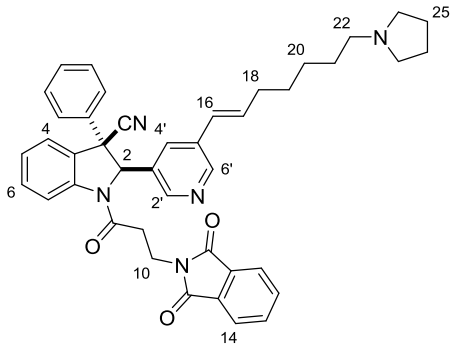

Indoline **238** was prepared according to general procedure 4, using indoline **237** (60 mg, 0.10 mmol), vinylstannane **57** (57 mg, 0.13 mmol), $Pd(PPh_3)_4$ (12 mg, 0.01 mmol) in NMP (2 mL). The reaction mixture was stirred at 85 °C for 2 h. Purification by flash pressure column chromatography (5.5% MeOH/CH_2Cl_2 + aq. NH_4OH) afforded indoline **238** was a colorless oil (54 mg, 0.08 mmol, 78%).

^{1}H NMR (500 MHz, C_6D_6, 348 K): δ 8.61 (1H, app s, *H*6'), 8.55 (1H, app s, *H*2'), 8.40 (1H, app br s, *H*7), 7.50 (1H, app s, *H*4'), 7.34-7.43 (2H, m, *H*14), 7.29 (2H, app d, *J* 7.7, *o-Ph*), 7.05-7.13 (2H, m, *H*4, *H*6), 6.99-7.05 (2H, m, *m-Ph*), 6.90-6.99 (3H, m, *H*15, *p-Ph*), 6.76 (1H, app t, *J* 7.7, *H*5), 3.74 (1H, ddd, *J* 14.1, 7.0, 7.0, *H*10), 3.65 (1H, ddd, *J* 14.1, 7.0, 7.0, *H*10'), 2.33-2.53 (8H, m, *H*22, *H*24, *H*9, *H*9'), 1.94 (1H, app q, *J* 6.7, *H*18), 1.64 (4H, m, *H*25), 1.48 (2H, m, *H*21), 1.24-1.39 (4H, m, *H*19, *H*20).

^{13}C NMR (126 MHz, C_6D_6, 348 K): δ 168.7 (*C*=O), 167.7 (*C*=O), 149.9 (*C*6'), 147.2 (*C*2'), 143.7 (*C*7a), 141.0 (*i-Ph*), 134.9 (*C*17), 134.7 (*C*3'/*C*5'), 133.8 (*C*3'/*C*5'), 133.7 (*C*15), 132.9 (*C*13), 131.2 (*C*6), 130.7 (*C*4'), 130.1 (*m-Ph*), 129.3 (*p*-Ph), 126.8 (*C*16), 126.3 (*C*4), 126.3 (*o-Ph*), 126.2 (*C*5), 123.3 (*C*14), 118.9 (*C*N), 118.0 (*C*7), 74.4 (*C*2), 58.3 (*C*3), 56.7 (*C*22), 54.7 (*C*24), 34.5 (*C*9/*C*10), 34.4 (*C*9/*C*10), 33.6 (*C*18), 29.6 (*C*19/*C*20/*C*21), 29.5 (*C*19/*C*20/*C*21), 27.8 (*C*19/*C*20/*C*21), 24.4 (*C*25).‡

‡ 1 peak obscured.

HRMS: $[C_{42}H_{42}O_3N_5]^+$ ($[M+H]^+$) requires 664.3282; found 664.3279.

IR: ν_{max}(film)/cm^{-1} 2933, 1709, 2436, 1642, 1381, 1282, 1198, 1122, 829, 722.

(2*RS*,3*RS*)-1-(3-Aminopropanoyl)-3-phenyl-2-(5-((E)-7-(pyrrolidin-1-yl)hept-1-en-1-yl)pyridin-3-yl)indoline-3-carbonitrile **239**

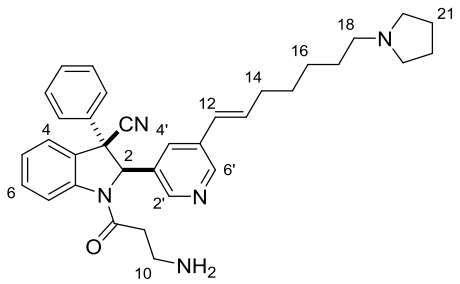

Hydrazine monohydrate (18 µL, 0.35 mmol) was added to a solution of indoline **238** (46 mg, 0.069 mmol) in MeOH (2mL) and stirred at 50 °C for 4 h. The mixture was filtered and concentrated. CH_2Cl_2 was added to the remaining residue, the resulting precipitate was removed by filtration, and the filtrate concentrated. Purification by flash pressure column chromatography (5.5% MeOH/CH_2Cl_2 + 0.5% aq. NH_4OH) afforded indoline **239** as a pale yellow oil (29 mg, 0.054 mmol, 78%).

^{1}H NMR (500 MHz, C_6D_6, 348 K): δ 8.66 (1H, app s, *H*6'), 8.51 (1H, app s, *H*2'), 8.44 (1H, app br s, *H*7), 7.45 (1H, app s, *H*4'), 7.27 (2H, app d, *J* 6.8, *o-Ph*), 7.14 (1H, app t, *J* 7.8, *H*6), 7.08 (1H, app d, *J* 7.8, *H*4), 6.94-7.05 (3H, m, *m-Ph*, *p-Ph*), 6.78 (1H, app t, *J* 7.6 *H*5), 5.95-6.10 (2H, m, *H*12, *H*13), 5.45 (1H, s, *H*2), 2.65 (1H, app sex, *J* 6.8, *H*10), 2.58 (1H, app sex, *J* 6.8, *H*10'), 2.43 (4H, m, *H*20), 2.38 (2H, t, *J* 7.2, *H*18), 1.83-2.05 (4H, m, *H*9, *H*9', *H*14), 1.65 (4H, m, *H*21), 1.48 (2H, app quin, *J* 6.8, *H*17), 1.23-1.39 (4H, m, *H*15, *H*16), 0.63 (3H, br s, NH_2, includes H_2O signal).

^{13}C NMR (126 MHz, C_6D_6, 348 K): δ 171.0 (*C*=O), 149.9 (*C*6'), 147.3 (*C*2'), 144.0 (*C*7a), 141.3, 135.1 (*C*13), 134.7, 134.1, 131.2 (*C*6), 130.7 (*C*4'), 130.2 (*m-Ph*/*p-Ph*), 129.3 (*m-Ph*/*p-Ph*), 126.8 (*C*12), 126.5 (*C*4), 126.3 (*o-Ph*), 126.0 (*C*5), 119.1 (*C*N), 118.0 (*C*7), 74.3 (*C*2), 58.3 (*C*3), 56.8 (*C*18), 54.7 (*C*20), 40.1 (*C*10), 38.4 (*C*9), 33.7 (*C*14), 29.6 (*C*15/*C*16/*C*17), 29.6 (*C*15/*C*16/*C*17), 27.9 (*C*15/*C*16/*C*17), 24.5 (*C*21).‡

‡ 1 peak obscured.

HRMS: $[C_{34}H_{40}ON_5]^+$ ($[M+H]^+$) requires 534.3227; found 534.3228.

IR: ν_{max} (film)/cm^{-1} 3345 (br, N-H), 3027, 2929, 1672 (C=O), 1598, 1479, 1391, 1276, 755.

N-(3-((2*RS*,3*RS*)-3-Cyano-3-phenyl-2-(5-((E)-7-(pyrrolidin-1-yl)hept-1-en-1-yl)pyridin-3-yl)indolin-1-yl)-3-oxopropyl)-3-(3-(pent-4-yn-1-yl)-3H-diazirin-3-yl)propanamide **240**

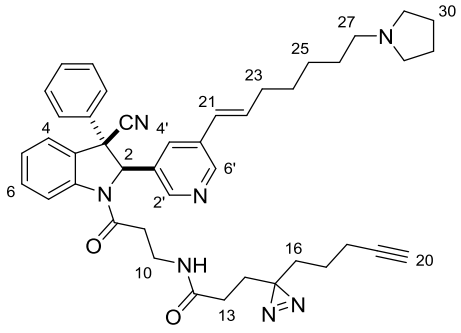

Indoline **240** was prepared according to a modified literature procedure.[145] 1-Hydroxybenzotriazole hydrate (8.5 mg, 0.047 mmol), *N*-(3-Dimethylaminopropyl)-*N*'-ethylcarbodiimide hydrochloride (9 mg, 0.05 mmol), and *N*,*N*-diisopropylethylamine (13 µL, 0.075 mmol) were added to a solution of indoline **239** (20 mg, 0.037 mmol) in DMF (0.6 mL). A solution of diazirine **233** (6.8 mg, 0.037 mmol) in DMF (0.4 mL) was added, and the reaction mixture was stirred at rt for 9 h. H_2O was added, and the mixture was extracted with EtOAc. The combined organic extracts were washed with brine, dried over Na_2SO_4, filtered, and concentrated. Purification by flash pressure column chromatography (5% MeOH/CH_2Cl_2 + 0.5% aq. NH_4OH) afforded indoline **240** as a pale yellow oil (17 mg, 0.024 mmol, 66%).

^{1}H NMR (500 MHz, C_6D_6, 348 K): δ 8.66 (1H, d, *J* 1.7, *H*6'), 8.52 (1H, d, *J* 1.8, *H*2'), 8.37 (1H, app br s, *H*7), 7.47 (1H, app s, *H*4'), 7.26 (2H, m, *o*-*Ph*), 7.15 (1H, obscured, *H*6), 7.09 (1H, app d, *J* 7.4, *H*4), 6.97-7.07 (3H, m, *m*-*Ph*, *p*-*Ph*), 6.79 (1H, app t, *J* 7.4, *H*5), 5.99-6.17 (2H, m, *H*21, *H*22), 5.47 (1H, s, *H*2), 5.26 (1H, s, N*H*), 3.18 (2H, app m, *H*10), 2.43 (4H, m, *H*29), 2.39 (2H, t, *J* 7.14, *H*27), 2.27 (1H, app m, *H*9), 2.02 (1H, app br s, *H*9'), 1.97 (2H, app br s, *H*23), 1.83 (2H, td, *J* 6.8, 2.6, *H*18), 1.74 (1H, t, *J* 2.6, *H*20), 1.65 (4H, m, *H*30), 1.41-1.54 (4H, m, *H*25, *H*26), 1.26-1.38 (6H, m, *H*13, *H*14, *H*24), 1.19 (2H, app quin, *J* 7.0, *H*16), 1.08 (2H, quin, *J* 7.2, *H*17).

^{13}C NMR (126 MHz, C_6D_6, 348 K): δ 170.8 (*C*=O), 170.6 (*C*=O), 149.9 (*C*6'), 147.1 (*C*2'), 143.6 (*C*7a), 141.0 (*i-Ph*), 135.2 (*C*22), 134.6 (*C*5'), 133.8 (*C*3'), 131.2 (*C*6), 130.9 (*C*4'), 130.2 (*m-Ph*), 129.4 (*p-Ph*), 126.7 (*C*21), 126.6 (*C*4), 126.3 (*o-Ph*), 126.3 (*C*5), 118.9 (*C*N), 117.7 (*C*7), 83.8 (*C*19), 74.2 (*C*2), 69.6 (*C*20), 58.1 (*C*3), 56.8 (*C*27), 54.7 (*C*29), 36.3 (*C*9), 35.5 (*C*10), 33.6 (*C*23), 32.5 (*C*16), 30.5, 29.6, 29.5, 29.0, 28.2 (*C*15), 27.9, 24.4 (*C*30), 23.4 (*C*17), 18.4 (*C*18).‡

‡ 1 peak obscured.

HRMS: $[C_{43}H_{50}O_2N_7]^+$ ([M+H]$^+$) requires 696.4021; found 696.4019.

IR: ν_{max} (film)/cm^{-1} 3298 (sharp, C-H), 2932, 2790, 1670, 1542, 1479, 1395, 756, 698.

Tert-butyl 2-oxopyrrolidine-1-carboxylate **249**

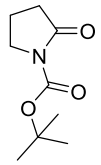

Pyrrolidinone **249** was prepared according to a literature procedure.[199] 2-Pyrrolidinone (4.0 g, 47 mmol) was dissolved in acetonitrile (38 mL) and cooled to 0 °C. A solution of di-*tert*-butyl dicarbonate (11.3 g, 51.7 mmol) in CH_3CN (16 mL) was added dropwise. *N*,*N*-dimethylaminopyridine (574 mg, 4.7 mmol) was added, and the mixture was allowed to warm to rt and stirred at rt for 1 h. The mixture was concentrated and the remaining residue was dissolved in EtOAc and washed with H_2O. The pH of the aqueous wash was adjusted to approx. 7 using HCl (aq., 1 M) and extracted with EtOAc. The combined organic extracts were washed with brine, dried over Na_2SO_4, filtered, and concentrated. Purification by flash pressure column chromatography (25% EtOAc/petroleum ether) afforded pyrrolidinone **249** as a pale yellow hygroscopic solid (7.96 g, 43 mmol, 91%). The spectral data matched those reported in the literature.

^{1}H NMR (400 MHz, $CDCl_3$): δ 3.74 (2H, t, *J* 7.2, *H*5), 2.51 (2H, t, *J* 8.1, *H*3), 1.99 (2H, app quin, *J* 7.6, *H*4), 1.52 (9H, C(C*H*$_3$)$_3$).

^{13}C NMR (101 MHz, $CDCl_3$): δ 173.3 (*C*=O), 150.1 (*C*=O), 82.6 (*C*(CH$_3$)$_3$), 46.4 (*C*5), 32.8 (*C*3), 27.9

(C(*C*H$_3$)$_3$), 17.3 (*C*4).

LCMS (ES$^+$): 208.2 ([M+Na]$^+$).

IR: ν_{max}(film)/cm^{-1} 2979, 1782, 1750, 1712, 1366, 1308, 1252, 1150, 1018, 778.

Phenyl 2-methylbenzoate **246**

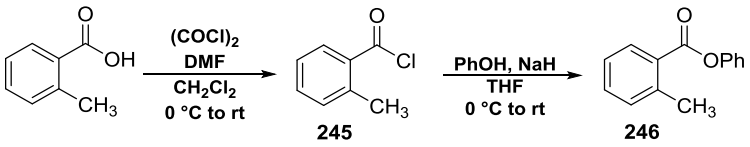

Ester **246** was prepared according to a literature procedure.[200] *o*-Toluic acid (5.0 g, 37 mmol) and DMF (3 drops) were dissolved in CH_2Cl_2 (75 mL) and cooled to 0 °C, and oxalyl chloride (6.2 mL, 73.4 mmol) was added dropwise. The solution was allowed to warm to rt, stirred for 4 h, and concentrated to afford acyl chloride **245** as a pale yellow oil (5.69 g, 36.8 mmol, quant.). Sodium hydride (60% dispersion in mineral oil, 700 mg, 17.5 mmol) was added to a solution of phenol (913 mg, 9.71 mmol) in THF (20 mL) at 0 °C and stirred for 30 min. A solution of acyl chloride **245** (1.5 g, 9.7 mmol) in THF (20 mL) was added dropwise, the mixture was allowed to warm to rt, and stirred for 30 min. H_2O (30 mL) was added, and the mixture was extracted with EtOAc. The combined organic extracts were washed with brine, dried over Na_2SO_4, filtered, and concentrated. Purification by flash pressure column chromatography (4% Et_2O/petroleum ether) afforded ester **246** as a colorless oil (1.97 g, 9.30 mmol, 96%). The spectral data matched those reported in the literature.

^{1}H NMR (400 MHz, $CDCl_3$): δ 8.20 (1H, app d, *J* 7.95, *H*6), 7.40-7.56 (3H, m, *H*4, *Ph*), 7.18-7.40 (5H, m, *H*3, *H*5, *Ph*), 2.71 (3H, s, C*H*$_3$).

^{13}C NMR (101 MHz, $CDCl_3$): δ 165.8 (*C*=O), 150.9 (*i-Ph*), 141.3 (*C*1/*C*2), 132.7 (*C*4/*Ph*), 131.9 (*C*3/*C*5/*Ph*), 131.1 (*C*6), 129.5 (*C*4/*Ph*), 128.5 (*C*1/*C*2), 125.9 (*C*3/*C*5/*Ph*), 125.8 (*C*3/*C*5/*Ph*), 121.8 (*C*3/*C*5/*Ph*), 21.9 (*C*H$_3$).

IR: ν_{max}(film)/cm^{-1} 3042, 1736 (C=O), 1488, 1290, 1242, 1190, 1043, 734, 688.

Perfluorophenyl 2-methylbenzoate **253**

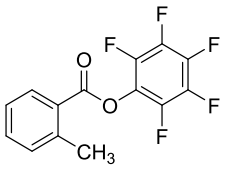

Pentafluorophenol (1.79 g, 9.70 mmol) was added to a solution of acyl chloride **245** (1.5 g, 9.7 mmol) and triethylamine (1.62 mL, 11.6 mmol) in CH_2Cl_2 (100 mL) and stirred at rt for 20 min. NH_4Cl (saturated aq., 100 mL) was added, and the mixture was extracted with CH_2Cl_2. The combined organic extracts were washed with brine, dried over Na_2SO_2, filtered and concentrated. Purification by flash pressure column chromatography (0.5% Et_2O/petroleum ether) afforded ester **253** as a colorless solid (2.73 g, 9.03 mmol, 93%).

^{1}H NMR (400 MHz, $CDCl_3$): δ 8.20 (1H, dd, *J* 8.2, 1.3, *H*6), 7.56 (1H, app td, *J* 7.6, 1.4, *H*4), 7.30-7.44 (2H, m, *H*3, *H*5), 2.68 (3H, s, C*H*$_3$).

^{13}C NMR (101 MHz, $CDCl_3$): δ 162.8 (*C*=O), 142.3, 133.9 (*C*4), 132.2 (*C*3/*C*5), 131.7 (*C*6), 126.2 (*C*3/*C*5), 125.9, 21.8 (*C*H$_3$).‡

^{19}F NMR (377 MHz, $CDCl_3$): δ -152.5 (m), -158.2 (app t, *J* 21.9), -162.5 (m).

‡ C_6F_5 not observed due to insufficient signal-to-noise ratio.

IR: ν_{max} (film)/cm^{-1} 1760 (C=O), 1518, 1228, 1028, 995, 733.

MP: 31-32 °C.

Phenyl 2-(bromomethyl)benzoate **247**

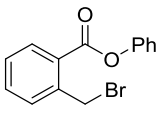

Benzyl bromide **247** was prepared according to a literature procedure.[201] *N*-bromosuccinimide (1.51 g, 8.48 mmol) and benzoyl peroxide (41 mg, 0.17 mmol) were added to a solution of ester **246** (1.8 g, 8.5 mmol) in CCl_4 (25 mL) at 0 °C. The mixture was allowed to warm to rt and stirred under

reflux for 3.5 h. The mixture was allowed to cool to rt over 14 h and filtered. The filtrate was washed with H_2O, then brine. The organic layer was dried over Na_2SO_4, filtered, and concentrated. Purification by flash pressure column chromatography (3% Et_2O/petroleum ether) afforded benzyl bromide **247** as a colorless solid (1.70 g, 5.84 mmol, 69%). The spectral data matched those reported in the literature.

^{1}H NMR (400 MHz, $CDCl_3$): δ 8.22 (1H, dd, *J* 7.8, 1.2, *H*6), 7.51-7.63 (2H, m, *H*3, *H*4), 7.42-7.51 (3H, m, *H*5, *Ph*), 7.23-7.35 (3H, m, *Ph*), 5.02 (2H, s, ArC*H*$_2$Br).

^{13}C NMR (101 MHz, $CDCl_3$): δ 165.0 (*C*=O), 150.6 (*i-Ph*), 139.9 (*C*1/*C*2), 133.1 (*C*3/*C*4), 131.8 (*C*6), 131.8 (*C*3/*C*4), 129.5 (*C*5/*Ph*), 128.7 (*C*5/*Ph*), 128.4 (*C*1/*C*2), 126.1 (*Ph*), 121.7 (*Ph*), 31.3 (Ar*C*H$_2$Br).

IR: ν_{max} (film)/cm^{-1} 1733 (C=O), 1486, 1250, 1189, 1161, 1054, 1043, 689.

MP: 42-44 °C (lit 50-51 °C).

Perfluorophenyl 2-(bromomethyl)benzoate **254**

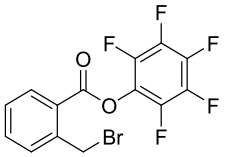

Benzyl bromide **254** was prepared according to a modified literature procedure.[201] *N*-bromosuccinimide (1.12 g, 6.30 mmol) and benzoyl peroxide (31 mg, 0.13 mmol) were added to a solution of ester **253** (2.4 g, 6.3 mmol) in CCl_4 (20 mL) at 0 °C. The mixture was allowed to warm to rt and stirred under reflux for 24 h. The mixture was allowed to cool to rt and filtered. The filtrate was washed with H_2O, then brine. The organic layer was dried over Na_2SO_4, filtered, and concentrated. Purification by flash pressure column chromatography (0.5% Et_2O/petroleum ether) afforded benzyl bromide **254** as a colorless solid (1.47 g, 3.86 mmol, 61%).

^{1}H NMR (400 MHz, $CDCl_3$): δ 8.26 (1H, dd, *J* 8.0, 1.4, *H*6), 7.67 (1H, app td, *J* 7.8, 1.4, *H*4), 7.59 (1H, dd, *J* 7.8, 1.4, *H*3), 7.52 (1H, app td, *J* 7.6, 1.4, *H*5), 4.95 (2H, s, ArC*H*$_2$Br).

^{13}C NMR (101 MHz, $CDCl_3$): δ 161.9 (*C*=O), 141.0 (*C*1/*C*2), 134.4 (*C*4), 132.3 (*C*6), 132.2 (*C*3), 128.9 (*C*5), 125.4 (*C*1/*C*2), 30.5 (Ar*C*H_2Br).‡

^{19}F NMR (377 MHz, $CDCl_3$): δ -152.1 (m), -157.6 (t, *J* 22.3), -162.1 (m).

‡ C_6F_5 peaks not observed due to insufficient signal-to-noise ratio.

HRMS (Cl^+): $[C_{14}H_{10}{}^{79}BrF_5O_2N]^+$ ($[M+NH_4]^+$) requires 397.9815; found 397.9809.

IR: ν_{max} (film)/cm^{-1} 1759 (C=O), 1516, 1233, 1030, 995, 760, 700.

MP: 82-84 °C.

Methyl 2-(bromomethyl)benzoate **256**

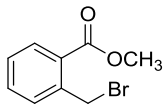

Benzyl bromide **256** was prepared according to a literature procedure.[201] *N*-bromosuccinimide (2.37 g, 13.3 mmol) and benzoyl peroxide (65 mg, 0.27 mmol) were added to a solution of methyl *o*-toluate (1.9 mL, 13 mmol) in CCl_4 (105 mL) at 0 °C. The mixture was allowed to warm to rt and stirred under reflux for 2.5 h. The mixture was allowed to cool to rt and filtered. The filtrate was washed with H_2O, then brine. The organic layer was dried over Na_2SO_4, filtered, and concentrated. Purification by flash pressure column chromatography (3% Et_2O/petroleum ether) afforded benzyl bromide **256** as a colorless solid (2.09 g, 9.12 mmol, 69%). The spectral data matched those reported in the literature.

^{1}H NMR (400 MHz, $CDCl_3$): δ 7.98 (1H, dd, *J* 7.7, 1.2, *H*6), 7.44-7.54 (2H, m, *H*3, *H*4), 7.38 (1H, app td, *J* 7.6, 1.9, *H*5), 4.97 (2H, s, Ar*CH*$_2$Br), 3.95 (3H, s, CO_2CH_3).

^{13}C NMR (101 MHz, $CDCl_3$): δ 167.0 (*C*=O), 139.2 (*C*1/*C*2), 132.5 (*C*3/*C*4), 131.6 (*C*3/*C*4), 131.3 (*C*6), 129.0 (*C*1/*C*2), 128.5 (*C*5), 52.3 (CO_2CH_3), 31.5 (Ar*C*H_2Br).

IR: ν_{max} (film)/cm^{-1} 1749 (C=O), 1434, 1294, 1076, 1046, 798, 761.

MP: 64-66 °C (lit 32-33 °C).

Tert-butyl 2-oxo-3-(2-(phenoxycarbonyl)benzyl)pyrrolidine-1-carboxylate **250**

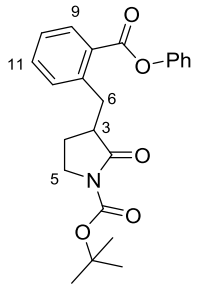

Pyrrolidinone **250** was prepared according to a modified literature procedure.[202] A solution of *N*,*N*-diisopropylamine (0.30 mL, 2.1 mmol) in THF (5 mL) was cooled to -78 °C, and ^{n}BuLi (2.4 M in hexane, 0.81 mL, 1.9 mmol) was added dropwise. The mixture was allowed to warm to 0 °C and stirred for 10 min before being re-cooled to -78 °C. A solution of pyrrolidinone **249** (300 mg, 1.62 mmol) in THF (5 mL) was added dropwise and stirred for 30 min. A solution of benzyl bromide **247** (519 mg, 1.78 mmol) in THF (5 mL) was added dropwise over 5 min and stirred at -70 °C to -75 °C for 2 h. The reaction mixture was diluted with Et_2O (20 mL), allowed to warm to 0 °C, and quenched with NH_4Cl (saturated aq., 30 mL). The mixture was extracted with Et_2O, and the combined organic extracts were washed with brine, dried over Na_2SO_4, filtered, and concentrated. Purification by flash pressure column chromatography (20% EtOAc/petroleum ether) afforded pyrrolidinone **250** as a colorless paste (287 mg, 0.73 mmol, 45%).

^{1}H NMR (400 MHz, $CDCl_3$): δ 8.16 (1H, dd, *J* 7.9, 1.4, *H*9), 7.53 (1H, app td, *J* 7.5, 1.4, *H*11), 7.34-7.48 (4H, m, *H*10, *H*12, *Ph*), 7.28 (1H, m, *Ph*), 7.19-7.24 (2H, m, *Ph*), 3.72 (1H, ddd, *J* 11.5, 8.2, 2.7, *H*5), 3.66 (1H, dd, *J* 13.3, 5.5, *H*6), 3.49 (1H, ddd, *J* 11.2, 10.4, 2.0, *H*5'), 3.14 (1H, dd, *J* 13.3, 8.5, *H*6'), 2.96 (1H, app m, *H*3), 2.01 (1H, app m, *H*4), 1.75 (1H, app m, *H*4'), 1.51 (9H, s, C(C*H*$_3$)$_3$).

^{13}C NMR (101 MHz, $CDCl_3$): δ 175.1 (*C*=O), 165.7 (*C*=O), 150.7 (*C*=O/*i*-*Ph*), 150.3 (*C*=O/*i*-*Ph*), 141.8 (*C*7/*C*8), 132.8 (*C*11), 132.1 (*C*10/*C*12/*Ph*), 131.3 (*C*9), 129.5 (*C*10/*C*12/*Ph*), 128.8 (*C*7/*C*8), 126.7 (*C*10/*C*12/*Ph*), 125.9 (*Ph*), 121.7 (*Ph*), 82.7 (*C*(CH$_3$)$_3$), 45.3 (*C*3), 44.4 (*C*5), 34.1 (*C*6), 28.0 (C(*C*H$_3$)$_3$),

24.0 (*C*4).

HRMS (ES$^+$): $C_{23}H_{25}O_5N^{23}Na$ ([M+Na]$^+$) requires 418.1630; found 418.1633.

IR: ν_{max} (film)/cm^{-1} 1782, 1755, 1714, 1601, 1518, 1313, 1231, 1148, 1028, 994.

Tert-butyl 3-(2-(methoxycarbonyl)benzyl)-2-oxopyrrolidine-1-carboxylate **257**

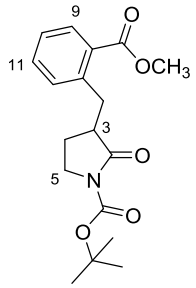

Pyrrolidinone **257** was prepared according to a modified literature procedure.[202] A solution of *N*,*N*-diisopropylamine (0.45 mL, 3.2 mmol) in THF (10 mL) was cooled to -78 °C, and ^{n}BuLi (2.4 M in hexane, 1.24 mL, 2.97 mmol) was added dropwise. The mixture was allowed to warm to 0 °C and stirred for 10 min before being re-cooled to -78 °C. A solution of pyrrolidinone **249** (500 mg, 2.70 mmol) in THF (10 mL) was added dropwise and stirred for 30 min. A solution of benyzl bromide **256** (618 mg, 2.70 mmol) in THF (10 mL) was added dropwise over 5 min and stirred at -70 °C to -75 °C for 1 h. The reaction mixture was diluted with Et_2O (40 mL), allowed to warm to 0 °C, and quenched with NH_4Cl (saturated aq., 50 mL). The mixture was extracted with Et_2O, and the combined organic extracts were washed with brine, dried over Na_2SO_4, filtered, and concentrated. Purification by flash pressure column chromatography (20% EtOAc/petroleum ether) afforded pyrrolidinone **257** as a colorless paste (636 mg, 1.91 mmol, 71%).

^{1}H NMR (400 MHz, $CDCl_3$): δ 7.90 (1H, dd, *J* 7.8, 1.3, *H*9), 7.44 (1H, app td, *J* 7.5, 1.4, *H*11), 7.28-7.34 (2H, *H*10, *H*12), 3.89 (3H, s, CO_2CH_3), 3.73 (1H, ddd, *J* 11.0, 8.4, 2.6, *H*5), 3.66 (1H, dd, *J* 12.7, 4.2, *H*6), 3.50 (1H, ddd, *J* 11.5, 10.2, 2.4, *H*5'), 2.90 (1H, dd, *J* 12.7, 9.2, *H*6'), 2.85 (1H, app m, *H*3), 1.97 (1H, app m, *H*4), 1.72 (1H, app m, *H*4'), 1.53 (9H, s, $C(CH_3)_3$).

^{13}C NMR (101 MHz, $CDCl_3$): δ 175.1 (*C*=O), 167.9 (*C*=O), 150.4 (*C*=O), 140.8 (*C*7/*C*8), 132.1 (*C*11),

131.6 (*C*10/*C*12), 130.8 (*C*9), 129.8 (*C*7/*C*8), 126.5 (*C*10/*C*12), 82.7 (*C*(CH_3)$_3$), 52.1 (CO_2CH_3), 45.4 (*C*3), 44.4 (*C*5), 34.3 (*C*6), 28.0 (C(*C*H_3)$_3$), 24.0 (*C*4).

HRMS (ES^+): $[C_{18}H_{23}O_5N^{23}Na]^+$ ([M+Na]$^+$) requires 356.1468; found 356.1466.

IR: ν_{max}(film)/cm^{-1} 2973, 1780, 1748, 1713, 1296, 1256, 1150, 1086, 945.

Benzyl 2-(hydroxymethyl)benzoate **259**

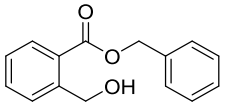

Ester **259** was prepared according to a literature procedure.[203] A suspension of phthalide (4.00 g, 29.8 mmol) was stirred in NaOH (aq., 1 M, 30 mL) at 100 °C for 1 h. The mixture was allowed to cool to rt and concentrated by creating an azeotropic mixture with toluene. The remaining solid residue was dissolved in DMF (20 mL), and benzyl bromide (3.55 mL, 29.8 mmol) was added. The mixture was stirred at rt for 2 h. H_2O (40 mL) was added, and the mixture was extracted with EtOAc. The combined organic extracts were washed with brine, dried over Na_2SO_4, filtered, and concentrated. Purification by flash pressure column chromatography (20% EtOAc/petroleum ether) afforded ester **259** as a colorless solid (5.33 g, 22.0 mmol, 74%, contains minor impurities). The spectral data matched those reported in the literature.

^{1}H NMR (400 MHz, $CDCl_3$): δ 8.07 (1H, dd, *J* 7.9, 1.2, *H*6), 7.55, (1H, app td, *J* 7.5, 1.4, *H*4), 7.45-7.50 (3H, m, *H*3, *Ph*), 7.34-7.45 (4H, m, *H*5, *Ph*), 5.39 (2H, s, Ar$CO_2C\mathit{H}_2$Ph), 4.81 (2H, s, Ar$C\mathit{H}_2$OH), 3.77 (1H, br s, O*H*).

^{13}C NMR (101 MHz, $CDCl_3$): δ 167.7 (*C*=O), 143.1, 135.5, 133.1 (*C*4), 131.2 (*C*6), 130.3 (*C*3/*Ph*), 128.7, 128.6 (*C*5/*Ph*), 128.4 (*C*3/*Ph*), 128.2 (*C*5/*Ph*), 127.8 (*C*5/*Ph*), 67.1 (Ar$CO_2C\mathit{H}_2$Ph), 64.7 (Ar$C\mathit{H}_2$OH).

IR: ν_{max}(film)/cm^{-1} 3264 (br, O-H), 1764 (C=O), 1258, 1024, 733, 697.

MP: 52-54 °C.

Benzyl 2-(bromomethyl)benzoate **260**

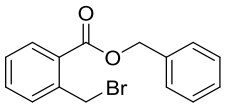

Triphenylphosphine (3.1 g, 12 mmol) was added to a solution of ester **259** (2.4 g, 9.9 mmol) and carbon tetrabromide (3.9 g, 12 mmol) in CH_2Cl_2 (100 mL) at 0 °C and stirred for 1 h. Ice-cooled hexane was added, the resulting suspension filtered, and the filtrate concentrated. Purification by flash pressure column chromatography (5% Et_2O/petroleum ether) afforded ester **260** as a yellow oil (2.66 g, 8.72 mmol, 88%).

^{1}H NMR (400 MHz, $CDCl_3$): δ 8.02 (1H, dd, *J* 7.8, 1.2, *H*6), 7.45-7.55 (4H, m, *H*4, *Ph*), 7.33-7.45 (4H, m, *H*3, *H*5, *Ph*), 5.41 (2H, s, $ArCO_2CH_2Ph$), 4.98 (2H, s, $ArCH_2Br$).

^{13}C NMR (101 MHz, $CDCl_3$): δ 166.3 (*C*=O), 139.3, 135.6, 132.6 (*C*4), 131.7 (*Ph*), 131.4 (*C*6), 129.0, 128.6 (*C*3/*C*5/*Ph*), 128.5 (*C*3/*C*5/*Ph*), 128.4 (*Ph*), 128.4 (*C*3/*C*5/*Ph*), 67.1 ($ArCO_2CH_2Ph$), 31.5 ($ArCH_2Br$).

IR: ν_{max} (film)/cm^{-1} 3033, 1765 (C=O), 1254, 1151, 1111, 756, 697.

Tert-butyl 3-(2-((benzyloxy)carbonyl)benzyl)-2-oxopyrrolidine-1-carboxylate **261**

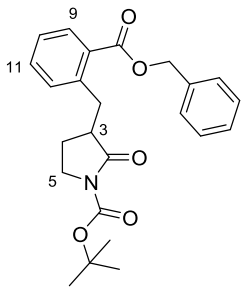

Pyrrolidinone **261** was prepared according to a modified literature procedure.[202] A solution of *N*,*N*-diisopropylamine (0.54 mL, 3.9 mmol) in THF (12 mL) was cooled to -78 °C, and ^{n}BuLi (2.4 M in hexane, 1.5 mL, 3.6 mmol) was added dropwise. The mixture was allowed to warm to 0 °C and stirred for 10 min before being re-cooled to -78 °C. A solution of pyrrolidinone **249** (600 mg,

3.2 mmol) in THF (12 mL) was added dropwise and stirred for 30 min. A solution of benzyl bromide **260** (990 mg, 3.2 mmol) in THF (12 mL) was added dropwise over 5 min and stirred at -70 °C to -75 °C for 1.5 h. The reaction mixture was diluted with Et_2O (40 mL), allowed to warm to 0 °C, and quenched with NH_4Cl (saturated aq., 50 mL). The mixture was extracted with Et_2O, and the combined organic extracts were washed with brine, dried over Na_2SO_4, filtered, and concentrated. Purification by flash pressure column chromatography (17% EtOAc/petroleum ether) afforded pyrrolidinone **261** as a colorless solid (557 mg, 1.36 mmol, 42%).

^{1}H NMR (400 MHz, $CDCl_3$): δ 7.94 (1H, dd, *J* 7.8, 1.3, *H*9), 7.42-7.49 (3H, m, *H*11, *Ph*), 7.28-7.41 (5H, m, *H*10, *H*12, *Ph*), 5.35 (2H, s, OC*H*$_2$Ph), 3.61-3.70 (2H, m, *H*5, *H*6), 3.43 (1H, ddd, *J* 10.8, 7.5, 2.1, *H*5'), 3.02 (1H, dd, *J* 13.4, 9.2, *H*6'), 2.87 (1H, app m, *H*3), 1.88 (1H, app m, *H*4), 1.66 (1H, app m, *H*4'), 1.55 (9H, s, C(C*H*$_3$)$_3$).

^{13}C NMR (101 MHz, $CDCl_3$): δ 175.1 (*C*=O), 167.2 (*C*=O), 150.4 (*C*=O), 140.9 (*C*7), 135.8 (*i-Ph*), 132.1 (*C*11), 131.7 (*C*12), 130.9 (*C*9), 129.9 (*C*8), 128.6 (*Ph*), 128.5 (*Ph*), 128.3 (*Ph*), 126.6 (*C*10), 82.7 (O*C*(CH$_3$)$_3$), 66.8 (O*C*H$_2$Ph), 45.4 (*C*3), 44.4 (*C*5), 34.1 (*C*6), 28.0 (C(*C*H$_3$)$_3$), 23.9 (*C*4).

MP: 87-88 °C.

HRMS (ES$^+$): $[C_{24}H_{27}O_5N^{23}Na]^+$ ([M+Na]$^+$) requires 432.1781; found 432.1778.

IR: ν_{max} (film)/cm^{-1} 2982, 1782, 1748, 1713, 1315, 1250, 1152, 752.

2-((1-(*Tert*-butoxycarbonyl)-2-oxopyrrolidin-3-yl)methyl)benzoic acid **258**

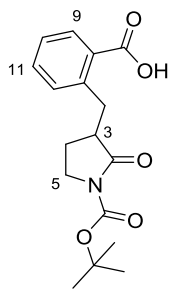

Pyrrolidinone **258** was prepared according to general procedure 3 using pyrrolidinone **261** (500 mg, 1.22 mmol) and Pd/C (degussa type, 50 mg) in THF (15 mL). The reaction mixture was stirred at rt

under a H_2 atmosphere for 5.5 h to afford pyrrolidinone **258** as a colorless solid (382 mg, 1.20 mmol, quant).

^{1}H NMR (500 MHz, $CDCl_3$): δ 8.07 (1H, dd, *J* 7.9, 1.3, *H*9), 7.50 (1H, app td, *J* 7.6, 1.4, *H*11), 7.31-7.39 (2H, m, *H*10, *H*12), 3.70-3.79 (2H, m, *H*5, *H*6), 3.52 (1H, ddd, *J* 10.9, 9.9, 2.8, *H*5'), 3.09 (1H, dd, *J* 13.4, 9.0, *H*6'), 2.99 (1H, app m, *H*3), 1.99 (1H, app m, *H*4), 1.75 (1H, app m, *H*4'), 1.54 (9H, s, $C(C\mathit{H}_3)_3$).ł

^{13}C NMR (126 MHz, $CDCl_3$): δ 175.4 (*C*=O), 171.9 (*C*=O), 150.4 (*C*=O), 141.8 (*C*7/*C*8), 133.0 (*C*11), 132.0 (*C*9), 131.8 (*C*10/*C*12), 128.6 (*C*7/*C*8), 126.7 (*C*10/*C*12), 82.8 ($OC(CH_3)_3$), 45.3 (*C*3), 44.4 (*C*5), 34.2 (*C*6), 28.0 ($C(CH_3)_3$), 24.1 (*C*4).

ł CO_2H peak is not observed.

HRMS (ES^+): $[C_{17}H_{21}O_5N^{23}Na]^+$ ([M+Na]$^+$) requires 342.1312; found 342.1310.

IR: ν_{max} (film)/cm^{-1} 3289, 1776, 1716, 1369, 1307, 1257, 1152, 947, 752.

MP: 105-108 °C.

Tert-butyl 2-oxo-3-(2-((perfluorophenoxy)carbonyl)benzyl)pyrrolidine-1-carboxylate **255**

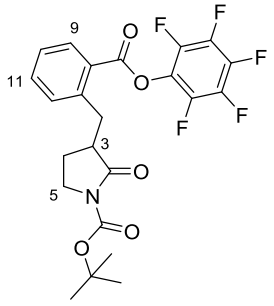

Pyrrolidinone **255** was prepared according to a modified literature procedure.[204] *N*,*N*-dicyclohexylcarbodiimide (155 mg, 0.75 mmol) was added to a solution of pyrroldidinone **258** (200 mg, 0.63 mmol) and pentafluorophenol (127 mg, 0.69 mmol) in THF (10 mL) and stirred at rt for 1 h. The reaction mixture was filtered and concentrated. Purification by flash pressure column chromatography (40% Et_2O/petroleum ether) afforded pyrrolidinone **255** as a colorless solid

(262 mg, 0.54 mmol, 86%).

^{1}H NMR (400 MHz, $CDCl_3$): δ 8.22 (1H, dd, *J* 7.9, 1.3, *H*9), 7.60 (1H, app td, *J* 7.6, 1.3, *H*11), 7.47 (1H, app d, *H*12), 7.42 (1H, app td, *J* 7.9, 1.3, *H*10), 3.74 (1H, ddd, *J* 10.8, 8.7, 2.4, *H*5), 3.66 (1H, dd, *J* 13.6, 5.4, *H*6), 3.51 (1H, ddd, *J* 11.1, 7.8, 2.1, *H*5'), 3.11 (1H, dd, *J* 13.5, 8.5, *H*6'), 2.90 (1H, app m, *H*3), 2.02 (1H, app m, *H*4), 1.72 (1H, app m, *H*4'), 1.52 (9H, s, C(CH_3)$_3$).

^{13}C NMR (101 MHz, $CDCl_3$): δ 174.9 (*C*=O), 162.7 (*C*=O), 150.3 (*C*=O), 143.1 (*C*7/*C*8), 134.1 (*C*11), 132.5 (*C*12), 131.9 (*C*9), 127.1 (*C*10), 125.9 (*C*7/*C*8), 82.8 (O*C*(CH$_3$)$_3$), 45.2 (*C*3), 44.3 (*C*5), 34.2 (*C*6), 28.0 (OC(*C*H$_3$)$_3$), 24.1 (*C*4).ł

^{19}F NMR (377 MHz, $CDCl_3$): δ -152.5 (m), -157.8 (t, *J* 21.8), -162.1 (m).

ł Peaks corresponding to C_6F_5 system obscured.

HRMS (ES$^+$): [$C_{23}H_{20}O_5NF_5{}^{23}Na$]$^+$ ([M+Na]$^+$) requires 508.1154; found 508.1151.

IR: ν_{max}(film)/cm^{-1} 2983, 1769, 1757, 1715, 1520, 1316, 1232, 1151, 1029, 995.

MP: 126-130 °C.

Tert-butyl 1,2'-dioxo-1,3-dihydrospiro[indene-2,3'-pyrrolidine]-1'-carboxylate **251**

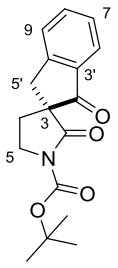

KO^{t}Bu (18 mg, 0.16 mmol) was added to a solution of pyrrolidinone **255** (40 mg, 0.082 mmol) in toluene (2 mL) and stirred at -10 °C for 2.5 h. NH_4Cl (saturated aq.) was added, and the mixture was extracted with EtOAc. The combined organic extracts were washed with brine, dried over Na_2SO_4, filtered, and concentrated. Purification by preparatory TLC (40% Et_2O/petroleum ether) afforded spiro-pyrrolidinone **251** as a colorless solid (12 mg, 0.040 mmol, 48%).

^{1}H NMR (500 MHz, $CDCl_3$): δ 7.74 (1H, app d, *J* 7.6, *H*6), 7.64 (1H, app t, *J* 7.6, *H*8), 7.50 (1H, app d, *J* 7.6, *H*9), 7.40 (1H, app t, *J* 7.6, *H*7), 4.15 (1H, app m, $H5_A$), 3.86 (1H, app td, *J* 9.8, 2.2, $H5_B$), 3.77 (1H, d, *J* 17.0, $H5'_A$), 3.01 (1H, d, *J* 17.0, $H5'_B$), 2.50 (1H, ddd, *J* 12.8, 7.7, 2.2, $H4_A$), 2.16 (1H, app m, $H4_B$), 1.54 (9H, s, $C(CH_3)_3$).

^{13}C NMR (126 MHz, $CDCl_3$): δ 203.0 (*C*2'), 171.8 (*C*2), 153.3 ($NCO_2{}^tBu$), 150.1 (*C*3'/*C*4'), 135.6 (*C*8), 134.4 (*C*3'/*C*4'), 127.9 (*C*7), 126.3 (*C*9), 124.8 (*C*6), 83.3 ($OC(CH_3)_3$), 60.5 (*C*3), 44.0 (*C*5), 37.6 (*C*5'), 28.7 (*C*4), 28.0 ($OC(CH_3)_3$).

HRMS (ES^+): $[C_{17}H_{19}O_4N^{23}Na]^+$ ([M+Na]$^+$) requires 324.1206; found 324.1206.

IR: ν_{max} (film)/cm^{-1} 1781, 1746, 1714, 1368, 1312, 1278, 1153, 960, 749.

MP: 74-76 °C.

1-Methylindolin-2-one **258**

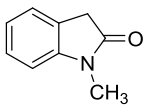

Oxindole **258** was prepared according to a literature procedure.[205] 1-Methylisatin (5.0 g, 31 mmol) was dissolved in hydrazine-hydrate (78-82%, 34 mL) and stirred at 95 °C for 2.5 h. The reaction mixture was allowed to cool to rt, ice-cooled H_2O (40 mL) was added, and the mixture was extracted with EtOAc. The combined organic extracts were washed with brine, dried over Na_2SO_4, filtered, and concentrated. Recrystallization from EtOAc/hexane afforded oxindole **258** as an orange solid (2.45 g, 16.6 mmol, 54%). The spectral data matched those reported in the literature.

^{1}H NMR (400 MHz, $CDCl_3$): δ 7.21-7.33 (2H, m), 7.04 (1H, app t, *J* 7.5), 6.82 (1H, app d, *J* 7.8), 3.52 (2H, s, $ArCH_2$), 3.21 (3H, s, CH_3).

^{13}C NMR (101 MHz, $CDCl_3$): δ 175.0 (*C*=O), 145.1, 127.8, 124.4, 124.2, 122.3, 108.0, 35.7 (CH_3), 26.1 ($ArCH_2$).

IR: ν_{max} (film)/cm^{-1} 1703 (C=O), 1614, 1470, 1347, 1124, 750.

Benzyl 2-formylbenzoate **259**

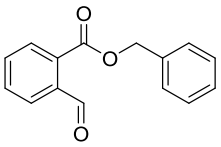

Ester **259** was prepared according to a literature procedure.[206] K_2CO_3 (1.1 g, 8.0 mmol) and benzyl bromide (0.80 mL, 6.7 mmol) were added to a solution of 2-formylbenzoic acid (1.0 g, 6.7 mmol) in *N*,*N*-DMF (6 mL). The reaction mixture was stirred at rt for 2.5 h, diluted with EtOAc, and washed three times with H_2O, then brine. The organic layer was dried over Na_2SO_4, filtered, and concentrated to afford ester **259** as a colorless liquid (1.6 g, 6.7 mmol, quant). The spectral data matched those reported in the literature.

^{1}H NMR (400 MHz, $CDCl_3$): δ 10.64 (1H, s C*H*O), 8.01 (1H, app m), 7.95 (1H, app m), 7.60-7.70 (2H, m), 7.45-7.50 (2H, m, *Ph*), 7.34-7.45 (3H, m, *Ph*), 5.43 (2H, s, OC*H*$_2$Ph).

^{13}C NMR (101 MHz, $CDCl_3$): δ 192.0 (*C*=O), 166.0 (*C*=O), 137.1, 135.2, 132.9, 132.4, 131.9, 130.4, 128.7 (*Ph*), 128.6, 128.4 (*Ph*), 128.4 (*Ph*), 67.2 (O*C*H$_2$Ph).

IR: ν_{max} (film)/cm^{-1} 3041, 1712, 1695, 1256, 1193, 1073, 1029, 747, 696.

2-((1-Methyl-2-oxoindolin-3-yl)methyl)benzoic acid **261**

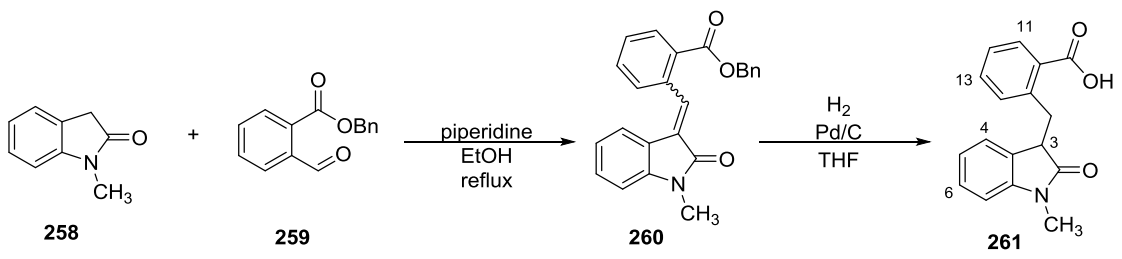

Oxindole **260** was prepared according to a modified literature procedure.[207] A solution of oxindole **258** (1.20 g, 8.15 mmol), ester **259** (2.15 g, 8.97 mmol), and piperidine (81 µL, 0.82 mmol) in EtOH

was stirred at reflux for 17 h. The mixture was allowed to cool to rt and concentrated. The remaining residue was dissolved in EtOAc and washed 3 times with $NaHCO_3$ (saturated aq.) and twice with HCl (aq., 1 M). The organic layer was washed with brine, dried over Na_2SO_4, filtered, and concentrated. Purification by flash pressure column chromatography (7% EtOAc/toluene) afforded oxindole **260** as an orange oil and as a 1:3 mixture of *E*/*Z* alkene isomers (1.70 g, 4.60 mmol, 56%).

Oxindole **261** was prepared according to general procedure 3, using oxindole **260** (1.6 g, 4.3 mmol) and Pd/C (degussa, 160 mg) in THF (45 mL). The reaction mixture was stirred at rt under a H_2 atmosphere for 3.5 h to afford oxindole **261** as a pale yellow oil (1.22 g, 4.33 mmol, quant).

^{1}H NMR (400 MHz, $CDCl_3$): δ 9.62 (1H, br s, CO_2H), 8.09 (1H, dd, *J* 7.8, 1.2, *H*11), 7.47 (1H, app td, *J* 7.5, 1.3, *H*13), 7.36 (1H, app td, *J* 7.5, 1.0, *H*12), 7.19-7.30 (2H, m, *H*5/*H*6, *H*14), 6.93 (1H, app t, *J* 7.5, *H*5/*H*6), 6.80 (1H, app d, *J* 7.8, *H*4/*H*7), 6.77 (1H, app d, *J* 7.4, *H*4/*H*7), 3.97 (1H, t, *J* 7.3, *H*3), 3.84 (1H, dd, *J* 13.3, 6.4, *H*8), 3.38 (1H, dd, *J* 13.3, 8.5, *H*8'), 3.20 (3H, s, CH_3).

^{13}C NMR (101 MHz, $CDCl_3$): δ 177.8 (*C*=O), 171.7 (*C*=O), 143.9, 140.4, 132.6 (*C*14), 132.4 (*C*13), 131.8 (*C*11), 129.3, 128.6, 127.9 (*C*5/*C*6), 127.0 (*C*12), 124.6 (*C*4/*C*7), 122.2 (*C*5/*C*6), 107.9 (*C*4/*C*7), 46.2 (*C*3), 35.4 (*C*8), 26.2 (CH_3).

HRMS (ES^+): $[C_{17}H_{15}O_3N^{23}Na]^+$ ($[M+Na]^+$) requires 304.0944; found 304.0941.

IR: ν_{max} (film)/cm^{-1} 3060, 1706, 1638, 1469, 1254, 1124, 1042, 746.

Perfluorophenyl 2-((1-methyl-2-oxoindolin-3-yl)methyl)benzoate **263**

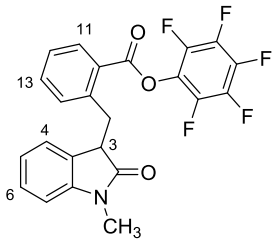

Oxindole **263** was prepared according to a modified literature procedure.[204] *N*,*N*-dicyclohexylcarbodiimide (244 mg, 1.19 mmol) was added to a solution of oxindole **261**

(278 mg, 0.99 mmol) and pentafluorophenol (183 mg, 0.99 mmol) in THF (12 mL) and stirred at rt for 45 min. The reaction mixture was filtered and concentrated. Purification by flash pressure column chromatography (15% EtOAc/petroleum ether) afforded oxindole **263** as a yellow paste (352 mg, 0.79 mmol, 80%).

^{1}H NMR (400 MHz, $CDCl_3$): δ 8.29 (1H, dd, *J* 8.0, 1.3, *H*11), 7.63 (1H, app td, *J* 7.6, 1.4, *H*13), 7.48 (1H, app td, *J* 7.8, 1.2, *H*12), 7.43 (1H, app d, *J* 7.7, *H*14), 7.26 (1H, app t, *J* 7.7, *H*5/*H*6), 6.94 (1H, app td, *J* 7.6, 0.9, *H*5/*H*6), 6.76-6.85 (2H, m, *H*4, *H*7), 3.69-3.85 (2H, m, *H*3, *H*8), 3.41 (1H, dd, *J* 13.0, 7.7, *H*8'), 3.21 (3H, s, CH_3).

^{13}C NMR (101 MHz, $CDCl_3$): δ 177.1 (*C*=O), 162.5 (*C*=O), 143.9, 142.5, 133.8 (*C*13), 133.1 (*C*14), 132.2 (*C*11), 128.3, 128.0 (*C*5/*C*6), 127.4 (*C*12), 126.0, 124.4 (*C*4/*C*7), 122.2 (*C*5/*C*6), 108.0 (*C*4/*C*7), 46.0 (*C*3), 35.5 (*C*8), 26.1 (*C*H_3).‡

^{19}F NMR (377 MHz, $CDCl_3$): δ -152.3 (m), -158. (t, *J* 22.0), -162.3 (m).

‡ C_6F_5 peaks not observed due to insufficient signal-to-noise ratio.

HRMS (ES^+): $[C_{23}H_{15}O_3NF_5]^+$ ($[M+H]^+$) requires 448.0967; found 448.0966.

IR: ν_{max}(film)/cm^{-1} 3081, 2947, 1709 (C=O), 1682 (C=O), 1611, 1470, 1377, 750.

1'-Methylspiro[indene-2,3'-indoline]-1,2'(3H)-dione **264**

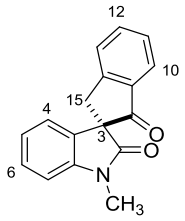

Racemic: K_2CO_3 (aq., 50% w/w, 56 µL, 0.40 mmol) was added to a suspension of oxindole **263** (36 mg, 0.080 mmol) and tetrabutylammonium bromide (2.6 mg, 0.88 mmol) in toluene (1.6 mL) and stirred at rt for 5 h. $NaHCO_3$ (saturated aq., 3 mL) was added, and the mixture was extracted with EtOAc. The combined organic extracts were washed with brine, dried over Na_2SO_4, filtered,

and concentrated. Purification by flash pressure column chromatography (40% Et_2O/petroleum ether) afforded oxindole **264** as a colorless solid (14 mg, 0.053 mmol, 66%).

Asymmetric: A suspension of oxindole **263** (250 mg, 0.56 mmol) and the catalyst (31 mg, 0.056 mmol) in *m*-xylene (22 mL) was stirred at 0 °C for 10 min. K_2CO_3 (aq., 50% w/w, 383 µL, 2.79 mmol) was added, and the reaction mixture was stirred at 0 °C for 48 h. NH_4Cl (saturated aq.) was added, and the mixture was extracted with EtOAc. The combined organic extracts were washed with brine, dried over Na_2SO_4, filtered, and concentrated. Purification by flash pressure column chromatography (40% Et_2O/petroleum ether) afforded oxindole **264** as a colorless solid (110 mg, 0.42 mmol, 76%, e.r. 95:5). The enantioenrichment could by augmented by recrystallization from 1:1 Et_2O/petroleum (e.r. > 98:2).

^{1}H NMR (400 MHz, $CDCl_3$): δ 7.82 (1H, app d, *J* 7.7, *H*10), 7.71 (1H, app td, *J* 7.7, 1.2, *H*12), 7.62 (1H, app d, *J* 7.7, *H*13), 7.47 (1H, app t, *J* 7.5, *H*11), 7.33 (1H, app td, *J* 7.8, 1.3, *H*5/*H*6), 7.01 (1H, app td, *J* 7.5, 1.0, *H*5/*H*6), 6.88-6.96 (2H, m, *H*4, *H*7), 3.83 (1H, d, *J* 17.2, *H*15), 3.45 (1H, d, *J* 17.2, *H*15'), 3.30 (3H, s, C*H*$_3$).

^{13}C NMR (101 MHz, $CDCl_3$): δ 199.8 (*C*=O), 174.9 (*C*=O), 153.8, 144.8, 135.6 (*C*12), 135.1, 130.2, 128.9 (*C*5/*C*6), 128.1 (*C*11), 126.5 (*C*13), 125.5 (*C*10), 122.9 (*C*5/*C*6), 122.0 (*C*4/*C*7), 108.6 (*C*4/*C*7), 63.0 (*C*3), 37.6 (*C*15), 26.8 (*C*H_3).

HRMS (ES^+): $[C_{17}H_{13}O_2N^{23}Na]^+$ ($[M+Na]^+$) requires 286.0839; found 286.0839.

IR: ν_{max} (film)/cm^{-1} 3045, 2891, 1722, 1697, 1609, 1468, 1346, 1275, 1088, 750.

MP: 178-180 °C.

$[\alpha]_D^{25.0}$ = -94 (*c* = 0.1, $CHCl_3$, e.r. 95:5).

Chiral HPLC: (Chiralpak ADH, 10% ^{i}PrOH, 90% hexane, 1.0 mL/min, λ = 254 nm, 20 µL injection) τ_D (minor) = 17.1 min, τ_D (major) = 22.9 min.

6.2.2 Biochemical Experimental Procedures

2-OG Competition

Solutions containing H3K36me2 peptide (20 μM), $Fe^{II}(NH_4)SO_4$ (20 μM), sodium-L-ascorbate (200 μM), and 2-OG (0.4 μM, 0.8 μM, 1.2 μM, 2.0 μM, 4.0 μM, 6.0 μM) in MES buffer (pH 7.0) were prepared in a deep 96-well plate (total volume per well = 600 μL). A solution of KDM2A in MES buffer (50 mM MES, 100 mM NaCl [pH 7.0]) was prepared (total volume = 12 mL) and divided equally into 3 falcon tubes, to which was added **(*S*,*S*)-108** (tube A: 0 nM, tube B: 500 nM, tube C: 1000 nM). After incubation at 0 °C for 45 min, 600 μL of solution A was added to each well, and the progress of demethylation was monitored *via* automated sampling using the RapidFire mass spectrometry platform (Agilent Technologies, Wakefield MA). The relative concentration of H3K36me1 was determined by integration of the extracted ion chromatogram corresponding to the H3K36me1 peptide using MassHunter software (Agilent Technologies). This procedure was repeated with solutions B and C using freshly-prepared 2-OG wells. Initial rates were determined by calculating the slope of the linear region of the reaction (see section 8.2 in the appendix for raw data and regression analysis).

Peptide Competition

Solutions containing 2-OG (20 μM), $Fe^{II}(NH_4)SO_4$ (20 μM), sodium-L-ascorbate (200 μM), and H3K36me2 peptide (2 μM, 4 μM, 10 μM, 20 μM, 32 μM, 80 μM) in MES buffer (pH 7.0) were prepared in a deep 96-well plate (total volume per well = 600 μL). A solution of KDM2A in MES buffer (50 mM MES, 100 mM NaCl [pH 7.0]) was prepared (total volume = 12 mL) and divided equally into 3 falcon tubes, to which was added **(*S*,*S*)-108** (tube A: 0 nM, tube B: 500 nM, tube C: 1000 nM). After incubation at 0 °C for 45 min, 600 μL of solution A was added to each well, and the progress of demethylation was monitored *via* automated sampling using the RapidFire mass spectrometry platform (Agilent Technologies, Wakefield MA). The relative concentration of H3K36me1 was determined by integration of the extracted ion chromatogram corresponding to

the H3K36me1 peptide using MassHunter software (Agilent Technologies). This procedure was repeated with solutions B and C using freshly-prepared peptide wells. Initial rates were determined by calculating the slope of the linear region of the reaction (see section 8.2 in the appendix for raw data and regression analysis).

Bio-layer Interferometry (BLI)

The following stock solutions were prepared using a freshly prepared HEPES buffer (25 mM HEPES, 50 mM NaCl, 0.5% glycerol [pH 7.5]).

1. Blank solution (1000 µL)

   -[$(NH_4)_2Fe^{II}(SO_4)_2 \cdot 6H_2O$] – 10 µM

2. Biotin control (500 µL)

   -D-Biotin – 10 µM

   -[$(NH_4)_2Fe^{II}(SO_4)_2 \cdot 6H_2O$] – 10 µM

3. **225** positive control (500 µL)

   -**225** – 10 µM

   -[$(NH_4)_2Fe^{II}(SO_4)_2 \cdot 6H_2O$] – 10 µM

4. **224** (500 µL)

   -**224** – 10 µM

   -[$(NH_4)_2Fe^{II}(SO_4)_2 \cdot 6H_2O$] – 10 µM

5. KDM2a solution (200 µL)

   -KDM2a – 5 µM

   -[$(NH_4)_2Fe^{II}(SO_4)_2 \cdot 6H_2O$] – 10 µM

   -2-oxoglutarate (2-OG) – 10 µM

Binding experiments were carried out using a FortéBio Octet Red96 instrument. The strepravidin-coated tips (FortéBio 18-5019) were initially left in the blank solution for 120 s to obtain a baseline measurement. The tips were subsequently transferred to the solutions containing the biotinylated

compounds and loaded for 300 s and then returned to the blank solution for a further 300 s. The tips were incubated in the KDM2a solution for 450 s and then returned to the blank solution.

Photoaffinity Labelling of KDM2A with 230 or 240

A solution containing the following components was prepared using MES buffer (50 mM MES, 100 mM NaCl [pH 7.0]) and incubated at 0 °C for 45 min.

-KDM2a – 1 μM

-**230** or **240** – 4 μM

-$Ni^{II}Cl_2$ – 50 μM

-2-OG – 10 μM

The solution was irradiated in 60 μL aliquots with 350 nm uv-light at 1-4 °C using a CaproBox™ (Caprotec, Berlin). Irradiation times longer than 5 min were carried out in 5 min pulses, separated by 2 min intervals to prevent sample warming. Samples were analyzed by liquid-chromatography/mass-spectrometry (see subsection 8.3.1 in the appendix for mass spectra corresponding to UV-activation of **230**.

7. REFERENCES

1. Kornberg, R. D.; Thomas, J. O., Chromatin structure. Oligomers of the histones. *Science* **1974,** *184* (4139), 865-8.
2. Kornberg, R. D., Chromatin structure. Repeating unit of histones and DNA. *Science* **1974,** *184* (4139), 868-71.
3. Felsenfeld, G., A brief history of epigenetics. *Cold Spring Harbor Perspect. Biol.* **2014,** *6* (1), 1-11.
4. Initial sequencing and analysis of the human genome. *Nature* **2001,** *409* (6822), 860-921.
5. Richmond, T. J.; Finch, J. T.; Rushton, B.; Rhodes, D.; Klug, A., Structure of the nucleosome core particle at 7 Å resolution. *Nature* **1984,** *311* (5986), 532-7.
6. Luger, K.; Mader, A. W.; Richmond, R. K.; Sargent, D. F.; Richmond, T. J., Crystal structure of the nucleosome core particle at 2.8 Å resolution. *Nature* **1997,** *389* (6648), 251-260.
7. Thoma, F.; Koller, T.; Klug, A., Involvement of histone H1 in the organization of the nucleosome and of the salt-dependent superstructures of chromatin. *J. Cell Biol.* **1979,** *83* (2, Pt. 1), 403-27.
8. Srahl, B. O.; Allis, C. D., The language of covalent histone modifications. *Nature* **2000,** *403* (6765), 41-45.
9. Wolffe, A. P.; Hayes, J. J., Chromatin disruption and modification. *Nucleic Acids Res.* **1999,** *27* (3), 711-720.
10. Tsunaka, Y.; Kajimura, N.; Tate, S.-i.; Morikawa, K., Alteration of the nucleosomal DNA path in the crystal structure of a human nucleosome core particle. *Nucleic Acids Res.* **2005,** *33* (10), 3424-3434.
11. Arrowsmith, C. H.; Bountra, C.; Fish, P. V.; Lee, K.; Schapira, M., Epigenetic protein families: a new frontier for drug discovery. *Nat. Rev. Drug Discovery* **2012,** *11* (5), 384-400.
12. Shahbazian, M. D.; Grunstein, M., Functions of site-specific histone acetylation and deacetylation. *Annu. Rev. Biochem.* **2007,** *76*, 75-100.
13. Black, J. C.; Van, R. C.; Whetstine, J. R., Histone Lysine Methylation Dynamics: Establishment, Regulation, and Biological Impact. *Mol. Cell* **2012,** *48* (4), 491-507.
14. Turner, B. M., Cellular memory and the histone code. *Cell* **2002,** *111* (3), 285-291.
15. Ruthenburg, A. J.; Li, H.; Patel, D. J.; Allis, C. D., Multivalent engagement of chromatin modifications by linked binding modules. *Nat. Rev. Mol. Cell Biol.* **2007,** *8* (12), 983-994.
16. Taverna, S. D.; Li, H.; Ruthenburg, A. J.; Allis, C. D.; Patel, D. J., How chromatin-binding modules interpret histone modifications: lessons from professional pocket pickers. *Nat. Struct. Mol. Biol.* **2007,** *14* (11), 1025-1040.
17. Nicol-Benoit, F.; le, G. P.; Michel, D., Drawing a Waddington landscape to capture dynamic epigenetics. *Biol. Cell* **2013,** *105* (12), 576-84.
18. Tollervey, J. R.; Lunyak, V. V., Epigenetics: judge, jury and executioner of stem cell fate. *Epigenetics* **2012,** *7* (8), 823-840.
19. Perino, M.; Veenstra, G. J. C., Chromatin Control of Developmental Dynamics and Plasticity. *Dev. Cell* **2016,** *38* (6), 610-620.
20. Sen, P.; Shah, P. P.; Nativio, R.; Berger, S. L., Epigenetic Mechanisms of Longevity and Aging. *Cell* **2016,** *166* (4), 822-839.
21. Fire, A.; Xu, S.; Montgomery, M. K.; Kostas, S. A.; Driver, S. E.; Mello, C. C., Potent and specific genetic interference by double-stranded RNA in Caenorhabditis elegans. *Nature***1998,** *391* (6669), 806-811.
22. Eissenberg, J. C.; James, T. C.; Foster-Hartnett, D. M.; Hartnett, T.; Ngan, V.; Elgin, S. C. R., Mutation in a heterochromatin-specific chromosomal protein is associated with suppression of position-effect variegation in Drosophila melanogaster. *Proc. Natl. Acad. Sci. U. S. A.* **1990,** *87* (24), 9923-7.
23. Frescas, D.; Guardavaccaro, D.; Kuchay, S. M.; Kato, H.; Poleshko, A.; Basrur, V.; Elenitoba-Johnson, K. S.; Katz, R. A.; Pagano, M., KDM2A represses transcription of centromeric satellite repeats and maintains the heterochromatic state. *Cell Cycle* **2008,** *7* (22), 3539-3547.

24. Arrowsmith, C. H.; Audia, J. E.; Austin, C.; Baell, J.; Bennett, J.; Blagg, J.; Bountra, C.; Brennan, P. E.; Brown, P. J.; Bunnage, M. E.; Buser-Doepner, C.; Campbell, R. M.; Carter, A. J.; Cohen, P.; Copeland, R. A.; Cravatt, B.; Dahlin, J. L.; Dhanak, D.; Edwards, A. M.; Frye, S. V.; Gray, N.; Grimshaw, C. E.; Hepworth, D.; Howe, T.; Huber, K. V. M.; Jin, J.; Knapp, S.; Kotz, J. D.; Kruger, R. G.; Lowe, D.; Mader, M. M.; Marsden, B.; Mueller-Fahrnow, A.; Muller, S.; O'Hagan, R. C.; Overington, J. P.; Owen, D. R.; Rosenberg, S. H.; Roth, B.; Ross, R.; Schapira, M.; Schreiber, S. L.; Shoichet, B.; Sundstrom, M.; Superti-Furga, G.; Taunton, J.; Toledo-Sherman, L.; Walpole, C.; Walters, M. A.; Willson, T. M.; Workman, P.; Young, R. N.; Zuercher, W. J., The promise and peril of chemical probes. *Nat. Chem. Biol.* **2015,** *11* (8), 536-541.

25. Cole, P. A., Chemical probes for histone-modifying enzymes. *Nat. Chem. Biol.* **2008,** *4* (10), 590-597.

26. Filippakopoulos, P.; Qi, J.; Picaud, S.; Shen, Y.; Smith, W. B.; Fedorov, O.; Morse, E. M.; Keates, T.; Hickman, T. T.; Felletar, I.; Philpott, M.; Munro, S.; McKeown, M. R.; Wang, Y.; Christie, A. L.; West, N.; Cameron, M. J.; Schwartz, B.; Heightman, T. D.; La Thangue, N.; French, C.; Wiest, O.; Kung, A. L.; Knapp, S.; Bradner, J. E., Selective inhibition of BET bromodomains. *Nature* **2010,** *468* (7327), 1067-1073.

27. Garnier, J.-M.; Sharp, P. P.; Burns, C. J., BET bromodomain inhibitors: a patent review. *Expert Opin. Ther. Pat.* **2014,** *24* (2), 185-199.

28. Walport, L. J.; Hopkinson, R. J.; Schofield, C. J., Mechanisms of human histone and nucleic acid demethylases. *Curr. Opin. Chem. Biol.* **2012,** *16* (5-6), 525-534.

29. Gaweska, H.; Fitzpatrick, P. F., Structures and Mechanism of the Monoamine Oxidase Family. *Biomolecular concepts* **2011,** *2* (5), 365-377.

30. Greer, E. L.; Shi, Y., Histone methylation: a dynamic mark in health, disease and inheritance. *Nat. Rev. Genet.* **2012,** *13* (5), 343-357.

31. Roach, P. L.; Clifton, I. J.; Fulop, V.; Harlos, K.; Barton, G. J.; Hajdu, J.; Andersson, I.; Schofield, C. J.; Baldwin, J. E., Crystal structure of isopenicillin N synthase is the first from a new structural family of enzymes. *Nature* **1995,** *375* (6533), 700-4.

32. Costas, M.; Mehn, M. P.; Jensen, M. P.; Que, L., Jr., Dioxygen Activation at Mononuclear Nonheme Iron Active Sites: Enzymes, Models, and Intermediates. *Chem. Rev.* **2004,** *104* (2), 939-986.

33. Clifton, I. J.; McDonough, M. A.; Ehrismann, D.; Kershaw, N. J.; Granatino, N.; Schofield, C. J., Structural studies on 2-oxoglutarate oxygenases and related double-stranded β-helix fold proteins. *J. Inorg. Biochem.* **2006,** *100* (4), 644-669.

34. Price, J. C.; Barr, E. W.; Glass, T. E.; Krebs, C.; Bollinger, J. M., Jr., Evidence for Hydrogen Abstraction from C1 of Taurine by the High-Spin Fe(IV) Intermediate Detected during Oxygen Activation by Taurine:α-Ketoglutarate Dioxygenase (TauD). *J. Am. Chem. Soc.* **2003,** *125* (43), 13008-13009.

35. Price, J. C.; Barr, E. W.; Tirupati, B.; Bollinger, J. M., Jr.; Krebs, C., The first direct characterization of a high-valent iron intermediate in the reaction of an α-ketoglutarate-dependent dioxygenase: A high-spin Fe(IV) complex in taurine/α-ketoglutarate dioxygenase (TauD) from Escherichia coli. *Biochemistry* **2003,** *42* (24), 7497-7508.

36. Hanauske-Abel, H. M.; Gunzler, V., A stereochemical concept for the catalytic mechanism of prolylhydroxylase: applicability to classification and design of inhibitors. *J. Theor. Biol.* **1982,** *94* (2), 421-55.

37. Walport, L. J.; Hopkinson, R. J.; Chowdhury, R.; Schiller, R.; Ge, W.; Kawamura, A.; Schofield, C. J., Arginine demethylation is catalysed by a subset of JmjC histone lysine demethylases. *Nat. Commun.* **2016,** *7*, 11974.

38. Cheng, Z.; Cheung, P.; Kuo, A. J.; Yukl, E. T.; Wilmot, C. M.; Gozani, O.; Patel, D. J., A molecular threading mechanism underlies Jumonji lysine demethylase KDM2A regulation of methylated H3K36. *Genes Dev.* **2014,** *28* (16), 1758-1771.

39. Hojfeldt, J. W.; Agger, K.; Helin, K., Histone lysine demethylases as targets for anticancer therapy. *Nat. Rev. Drug Discovery* **2013,** *12* (12), 917-930.

40. Binda, C.; Valente, S.; Romanenghi, M.; Pilotto, S.; Cirilli, R.; Karytinos, A.; Ciossani, G.; Botrugno, O. A.; Forneris, F.; Tardugno, M.; Edmondson, D. E.; Minucci, S.; Mattevi, A.; Mai, A., Biochemical, Structural, and Biological Evaluation of Tranylcypromine Derivatives as Inhibitors of Histone Demethylases LSD1 and LSD2. *J. Am. Chem. Soc.* **2010,** *132* (19), 6827-6833.

41. Binda, C.; Li, M.; Hubalek, F.; Restelli, N.; Edmondson, D. E.; Mattevi, A., Insights into the mode of inhibition of human mitochondrial monoamine oxidase B from high-resolution crystal structures. *Proc. Natl. Acad. Sci. U. S. A.* **2003,** *100* (17), 9750-9755.

42. Mimasu, S.; Umezawa, N.; Sato, S.; Higuchi, T.; Umehara, T.; Yokoyama, S., Structurally Designed trans-2-Phenylcyclopropylamine Derivatives Potently Inhibit Histone Demethylase LSD1/KDM1. *Biochemistry* **2010,** *49* (30), 6494-6503.

43. Rotili, D.; Tomassi, S.; Conte, M.; Benedetti, R.; Tortorici, M.; Ciossani, G.; Valente, S.; Marrocco, B.; Labella, D.; Novellino, E.; Mattevi, A.; Altucci, L.; Tumber, A.; Yapp, C.; King, O. N. F.; Hopkinson, R. J.; Kawamura, A.; Schofield, C. J.; Mai, A., Pan-Histone Demethylase Inhibitors Simultaneously Targeting Jumonji C and Lysine-Specific Demethylases Display High Anticancer Activities. *J. Med. Chem.* **2014,** *57* (1), 42-55.

44. Rose, N. R.; Ng, S. S.; Mecinovic, J.; Lienard, B. M. R.; Bello, S. H.; Sun, Z.; McDonough, M. A.; Oppermann, U.; Schofield, C. J., Inhibitor Scaffolds for 2-Oxoglutarate-Dependent Histone Lysine Demethylases. *J. Med. Chem.* **2008,** *51* (22), 7053-7056.

45. Rose, N. R.; Woon, E. C. Y.; Tumber, A.; Walport, L. J.; Chowdhury, R.; Li, X. S.; King, O. N. F.; Lejeune, C.; Ng, S. S.; Krojer, T.; Chan, M. C.; Rydzik, A. M.; Hopkinson, R. J.; Che, K. H.; Daniel, M.; Strain-Damerell, C.; Gileadi, C.; Kochan, G.; Leung, I. K. H.; Dunford, J.; Yeoh, K. K.; Ratcliffe, P. J.; Burgess-Brown, N.; von Delft, F.; Muller, S.; Marsden, B.; Brennan, P. E.; McDonough, M. A.; Oppermann, U.; Klose, R. J.; Schofield, C. J.; Kawamura, A., Plant Growth Regulator Daminozide Is a Selective Inhibitor of Human KDM2/7 Histone Demethylases. *J. Med. Chem.* **2012,** *55* (14), 6639-6643.

46. Hopkinson, R. J.; Tumber, A.; Yapp, C.; Chowdhury, R.; Aik, W.; Che, K. H.; Li, X. S.; Kristensen, J. B. L.; King, O. N. F.; Chan, M. C.; Yeoh, K. K.; Choi, H.; Walport, L. J.; Thinnes, C. C.; Bush, J. T.; Lejeune, C.; Rydzik, A. M.; Rose, N. R.; Bagg, E. A.; McDonough, M. A.; Krojer, T. J.; Yue, W. W.; Ng, S. S.; Olsen, L.; Brennan, P. E.; Oppermann, U.; Mueller, S.; Klose, R. J.; Ratcliffe, P. J.; Schofield, C. J.; Kawamura, A., 5-Carboxy-8-hydroxyquinoline is a broad spectrum 2-oxoglutarate oxygenase inhibitor which causes iron translocation. *Chem. Sci.* **2013,** *4* (8), 3110-3117.

47. Luo, X.-L.; Liu, Y.-X.; Kubicek, S.; Myllyharju, J.; Tumber, A.; Ng, S.; Che, K.-H.; Podoll, J.; Heightman, T. D.; Oppermann, U.; Schreiber, S. L.; Wang, X., A Selective Inhibitor and Probe of the Cellular Functions of Jumonji C Domain-Containing Histone Demethylases. *J. Am. Chem. Soc.* **2011,** *133* (24), 9451-9456.

48. Liang, Y.; Vogel, J. L.; Arbuckle, J. H.; Rai, G.; Jadhav, A.; Simeonov, A.; Maloney, D. J.; Kristie, T. M., Targeting the JMJD2 histone demethylases to epigenetically control herpesvirus infection and reactivation from latency. *Sci. Transl. Med.* **2013,** *5* (167), 167ra5, 11 pp.

49. Kruidenier, L.; Chung, C.-w.; Cheng, Z.; Liddle, J.; Che, K. H.; Joberty, G.; Bantscheff, M.; Bountra, C.; Bridges, A.; Diallo, H.; Eberhard, D.; Hutchinson, S.; Jones, E.; Katso, R.; Leveridge, M.; Mander, P. K.; Mosley, J.; Ramirez-Molina, C.; Rowland, P.; Schofield, C. J.; Sheppard, R. J.; Smith, J. E.; Swales, C.; Tanner, R.; Thomas, P.; Tumber, A.; Drewes, G.; Oppermann, U.; Patel, D. J.; Lee, K.; Wilson, D. M., A selective jumonji H3K27 demethylase inhibitor modulates the proinflammatory macrophage response. *Nature* **2012,** *488* (7411), 404-408.

50. Heinemann, B.; Nielsen, J. M.; Hudlebusch, H. R.; Lees, M. J.; Larsen, D. V.; Boesen, T.; Labelle, M.; Gerlach, L.-O.; Birk, P.; Helin, K., Inhibition of demethylases by GSK-J1/J4. *Nature* **2014,** *514* (7520), E1-E2.

51. Bavetsias, V.; Lanigan, R. M.; Ruda, G. F.; Atrash, B.; McLaughlin, M. G.; Tumber, A.; Mok, N. Y.; Le Bihan, Y.-V.; Dempster, S.; Boxall, K. J.; Jeganathan, F.; Hatch, S. B.; Savitsky, P.; Velupillai, S.; Krojer, T.; England, K. S.; Sejberg, J.; Thai, C.; Donovan, A.; Pal, A.; Scozzafava, G.; Bennett, J. M.; Kawamura, A.; Johansson, C.; Szykowska, A.; Gileadi, C.; Burgess-Brown, N. A.; von Delft, F.; Oppermann, U.; Walters, Z.; Shipley, J.; Raynaud, F. I.; Westaway, S. M.; Prinjha, R. K.; Fedorov, O.; Burke, R.; Schofield, C. J.; Westwood, I. M.; Bountra, C.; Muller, S.; van Montfort, R. L. M.; Brennan, P. E.; Blagg, J., 8-Substituted Pyrido[3,4-d]pyrimidin-4(3H)-one Derivatives As Potent, Cell Permeable, KDM4 (JMJD2) and KDM5 (JARID1) Histone Lysine Demethylase Inhibitors. *J. Med. Chem.* **2016,** *59* (4), 1388-1409.

52. Albrecht, B. K.; Gehling, V. S.; Harmange, J.-C.; Lai, T.; Liang, J.; Dragovich, P.; Ortwine, D.; Labadie, S.; Zhang, B.; Kiefer, J. Pyrazolopyrimidinecarbonitriles ad KDM5A demethylase inhibitors and their preparation. WO2015135094A1, 2015.

53. Lohse, B.; Nielsen, A. L.; Kristensen, J. B. L.; Helgstrand, C.; Cloos, P. A. C.; Olsen, L.; Gajhede, M.; Clausen, R. P.; Kristensen, J. L., Targeting histone lysine demethylases by truncating the histone 3 tail to obtain selective substrate-based inhibitors. *Angew. Chem., Int. Ed.* **2011,** *50* (39), 9100-9103, S9100/1-S9100/27.

54. Woon, E. C. Y.; Tumber, A.; Kawamura, A.; Hillringhaus, L.; Ge, W.; Rose, N. R.; Ma, J. H. Y.; Chan, M. C.; Walport, L. J.; Che, K. H.; Ng, S. S.; Marsden, B. D.; Oppermann, U.; McDonough, M. A.; Schofield, C. J., Linking of 2-Oxoglutarate and Substrate Binding Sites Enables Potent and Highly Selective Inhibition of JmjC Histone Demethylases. *Angew. Chem., Int. Ed.* **2012,** *51* (7), 1631-1634, S1631/1-S1631/32.

55. Leurs, U.; Lohse, B.; Rand, K. D.; Ming, S.; Riise, E. S.; Cole, P. A.; Kristensen, J. L.; Clausen, R. P., Substrate- and Cofactor-independent Inhibition of Histone Demethylase KDM4C. *ACS Chem. Biol.* **2014,** *9* (9), 2131-2138.

56. Tsukada, Y.-i.; Fang, J.; Erdjument-Bromage, H.; Warren, M. E.; Borchers, C. H.; Tempst, P.; Zhang, Y., Histone demethylation by a family of JmjC domain-containing proteins. *Nature* **2006,** *439* (7078), 811-816.

57. Blackledge, N. P.; Zhou, J. C.; Tolstorukov, M. Y.; Farcas, A. M.; Park, P. J.; Klose, R. J., CpG islands recruit a histone H3 lysine 36 demethylase. *Mol. Cell* **2010,** *38* (2), 179-190.

58. Zhou, J. C.; Blackledge, N. P.; Farcas, A. M.; Klose, R. J., Recognition of CpG island chromatin by KDM2A requires direct and specific interaction with linker DNA. *Mol. Cell. Biol.* **2012,** *32* (2), 479-489.

59. Lu, T.; Jackson, M. W.; Singhi, A. D.; Kandel, E. S.; Yang, M.; Zhang, Y.; Gudkov, A. V.; Stark, G. R., Validation-based insertional mutagenesis identifies lysine demethylase FBXL11 as a negative regulator of NFκB. *Proc. Natl. Acad. Sci. U. S. A.* **2009,** *106* (38), 16339-16344, S16339/1-S16339/8.

60. Wang, T.; Chen, K.; Zeng, X.; Yang, J.; Wu, Y.; Shi, X.; Qin, B.; Zeng, L.; Esteban, M. A.; Pan, G.; Pei, D., The Histone Demethylases Jhdm1a/1b Enhance Somatic Cell Reprogramming in a Vitamin-C-Dependent Manner. *Cell Stem Cell* **2011,** *9* (6), 575-587.

61. Kawakami, E.; Tokunaga, A.; Ozawa, M.; Sakamoto, R.; Yoshida, N., The histone demethylase Fbxl11/Kdm2a plays an essential role in embryonic development by repressing cell-cycle regulators. *Mech. Dev.* **2015,** *135*, 31-42.

62. Dalgliesh, G. L.; Furge, K.; Greenman, C.; Chen, L.; Bignell, G.; Butler, A.; Davies, H.; Edkins, S.; Hardy, C.; Latimer, C.; Teague, J.; Andrews, J.; Barthorpe, S.; Beare, D.; Buck, G.; Campbell, P. J.; Forbes, S.; Jia, M.; Jones, D.; Knott, H.; Kok, C. Y.; Lau, K. W.; Leroy, C.; Lin, M.-L.; McBride, D. J.; Maddison, M.; Maguire, S.; McLay, K.; Menzies, A.; Mironenko, T.; Mulderrig, L.; Mudie, L.; O'Meara, S.; Pleasance, E.; Rajasingham, A.; Shepherd, R.; Smith, R.; Stebbings, L.; Stephens, P.; Tang, G.; Tarpey, P. S.; Turrell, K.; Dykema, K. J.; Khoo, S. K.; Petillo, D.; Wondergem, B.; Anema, J.; Kahnoski, R. J.; Teh, B. T.; Stratton, M. R.; Futreal, P. A., Systematic sequencing of renal carcinoma reveals inactivation of histone modifying genes. *Nature* **2010,** *463* (7279), 360-363.

63. Kuo, A. J.; Cheung, P.; Chen, K.; Zee, B. M.; Kioi, M.; Lauring, J.; Xi, Y.; Park, B. H.; Shi, X.; Garcia, B. A.; Li, W.; Gozani, O., NSD2 Links Dimethylation of Histone H3 at Lysine 36 to Oncogenic Programming. *Mol. Cell* **2011,** *44* (4), 609-620.

64. Black, J. C.; Manning, A. L.; Van Rechem, C.; Kim, J.; Ladd, B.; Cho, J.; Pineda, C. M.; Murphy, N.; Daniels, D. L.; Montagna, C.; Lewis, P. W.; Glass, K.; Allis, C. D.; Dyson, N. J.; Getz, G.; Whetstine, J. R., KDM4A lysine demethylase induces site-specific copy gain and rereplication of regions amplified in tumors. *Cell* **2013,** *154* (3), 541-555.

65. Huang, Y.; Liu, Y.; Yu, L.; Chen, J.; Hou, J.; Cui, L.; Ma, D.; Lu, W., Histone demethylase KDM2A promotes tumor cell growth and migration in gastric cancer. *Tumor Biol.* **2015,** *36* (1), 271-278.

66. Dhar, S. S.; Alam, H.; Li, N.; Wagner, K. W.; Chung, J.; Ahn, Y. W.; Lee, M. G., Transcriptional Repression of Histone Deacetylase 3 by the Histone Demethylase KDM2A Is Coupled to Tumorigenicity of Lung Cancer Cells. *J. Biol. Chem.* **2014,** *289* (11), 7483-7496.

67. Xu, W.; Podoll, J. D.; Dong, X.; Tumber, A.; Oppermann, U.; Wang, X., Quantitative Analysis of Histone Demethylase Probes Using Fluorescence Polarization. *J. Med. Chem.* **2013,** *56* (12), 5198-5202.

68. England, K. S.; Tumber, A.; Krojer, T.; Scozzafava, G.; Ng, S. S.; Daniel, M.; Szykowska, A.; Che, K.; von Delft, F.; Burgess-Brown, N. A.; Kawamura, A.; Schofield, C. J.; Brennan, P. E., Optimisation of a

triazolopyridine based histone demethylase inhibitor yields a potent and selective KDM2A (FBXL11) inhibitor. *MedChemComm* **2014,** *5* (12), 1879-1886.

69. England, K. A potent and selective inhibitor of a histone demethylase. University of Oxford, Oxford, **2015**.

70. Chen, Y. K.; Nie, Z.; Stafford, J. A.; Veal, J. M. Histone demethylase inhibitors. WO2016044342A1, 2016.

71. Vedadi, M.; Barsyte-Lovejoy, D.; Liu, F.; Rival-Gervier, S.; Allali-Hassani, A.; Labrie, V.; Wigle, T. J.; DiMaggio, P. A.; Wasney, G. A.; Siarheyeva, A.; Dong, A.; Tempel, W.; Wang, S.-C.; Chen, X.; Chau, I.; Mangano, T. J.; Huang, X.-p.; Simpson, C. D.; Pattenden, S. G.; Norris, J. L.; Kireev, D. B.; Tripathy, A.; Edwards, A.; Roth, B. L.; Janzen, W. P.; Garcia, B. A.; Petronis, A.; Ellis, J.; Brown, P. J.; Frye, S. V.; Arrowsmith, C. H.; Jin, J., A chemical probe selectively inhibits G9a and GLP methyltransferase activity in cells. *Nat. Chem. Biol.* **2011,** *7* (8), 566-574.

72. Herold, J. M.; Wigle, T. J.; Norris, J. L.; Lam, R.; Korboukh, V. K.; Gao, C.; Ingerman, L. A.; Kireev, D. B.; Senisterra, G.; Vedadi, M.; Tripathy, A.; Brown, P. J.; Arrowsmith, C. H.; Jin, J.; Janzen, W. P.; Frye, S. V., Small-Molecule Ligands of Methyl-Lysine Binding Proteins. *J. Med. Chem.* **2011,** *54* (7), 2504-2511.

73. Maciver, E. E.; Thompson, S.; Smith, M. D., Catalytic asymmetric 6pi electrocyclization: enantioselective synthesis of functionalized indolines. *Angew. Chem., Int. Ed.* **2009,** *48* (52), 9979-82.

74. Sharma, K.; Wolstenhulme, J. R.; Painter, P. P.; Yeo, D.; Grande-Carmona, F.; Johnston, C. P.; Tantillo, D. J.; Smith, M. D., Cation-Controlled Enantioselective and Diastereoselective Synthesis of Indolines: An Autoinductive Phase-Transfer Initiated 5-endo-trig Process. *J. Am. Chem. Soc.* **2015,** *137* (41), 13414-13424.

75. Lamb, A. D.; Davey, P. D.; Driver, R. W.; Thompson, A. L.; Smith, M. D., Enantioselective Synthesis of 4- and 6-Azaindolines by a Cation-Directed Cyclization. *Org. Lett.* **2016,** *18* (20), 5372-5375.

76. Li, M.; Woods, P. A.; Smith, M. D., Cation-directed enantioselective synthesis of quaternary-substituted indolenines. *Chem. Sci.* **2013,** *4* (7), 2907-2911.

77. Wolstenhulme, J. R.; Cavell, A.; Gredicak, M.; Driver, R. W.; Smith, M. D., A cation-directed two-component cascade approach to enantioenriched pyrroloindolines. *Chem. Commun.* **2014,** *50* (88), 13585-13588.

78. Johnston, C. P.; Kothari, A.; Sergeieva, T.; Okovytyy, S. I.; Jackson, K. E.; Paton, R. S.; Smith, M. D., Catalytic enantioselective synthesis of indanes by a cation-directed 5-endo-trig cyclization. *Nat. Chem.* **2015,** *7* (2), 171-177.

79. Kawamura, A.; Tumber, A.; Rose, N. R.; King, O. N. F.; Daniel, M.; Oppermann, U.; Heightman, T. D.; Schofield, C., Development of homogeneous luminescence assays for histone demethylase catalysis and binding. *Anal. Biochem.* **2010,** *404* (1), 86-93.

80. Bonnett, R., Photosensitizers of the porphyrin and phthalocyanine series for photodynamic therapy. *Chem. Soc. Rev.* **1995,** *24* (1), 19-33.

81. Ullman, E. F.; Kirakossian, H.; Singh, S.; Wu, Z. P.; Irvin, B. R.; Pease, J. S.; Switchenko, A. C.; Irvine, J. D.; Dafforn, A.; et, a., Luminescent oxygen channeling immunoassay: measurement of particle binding kinetics by chemiluminescence. *Proc. Natl. Acad. Sci. U. S. A.* **1994,** *91* (12), 5426-30.

82. Wilkinson, F.; Helman, W. P.; Ross, A. B., Rate constants for the decay and reactions of the lowest electronically excited singlet state of molecular oxygen in solution. An expanded and revised compilation. *J. Phys. Chem. Ref. Data* **1995,** *24* (2), 663-1021.

83. Bosse, R.; Illy, C.; Chelsky, D., *Principles of AlphaScreen*. 2002.

84. Hutchinson, S. E.; Leveridge, M. V.; Heathcote, M. L.; Francis, P.; Williams, L.; Gee, M.; Munoz-Muriedas, J.; Leavens, B.; Shillings, A.; Jones, E.; Homes, P.; Baddeley, S.; Chung, C.-w.; Bridges, A.; Argyrou, A., Enabling lead discovery for histone lysine demethylases by high-throughput RapidFire mass spectrometry. *J. Biomol. Screening* **2012,** *17* (1), 39-48.

85. Brown, P. J.; Porter, J. SGC - Chemical Probes 2015.

86. Makosza, M.; Tomashewskij, A. A., Does Nitroarylation of Phenylacetonitrile Proceed as a Phase-Transfer Catalyzed Process? *J. Org. Chem.* **1995,** *60* (17), 5425-9.

87. MacMillan, K. S.; Nguyen, T.; Nguyen, T.; Hwang, I.; Boger, D. L., Total synthesis and evaluation of iso-duocarmycin SA and iso-yatakemycin. *J. Am. Chem. Soc.* **2009,** *131* (3), 1187-94.

88. Kosugi, M.; Shimizu, Y.; Migita, T., Alkylation, arylation, and vinylation of acyl chlorides by means of organotin compounds in the presence of catalytic amounts of tetrakis(triphenylphosphine)palladium(0). *Chem. Lett.* **1977,** (12), 1423-4.

89. Milstein, D.; Stille, J. K., A general, selective, and facile method for ketone synthesis from acid chlorides and organotin compounds catalyzed by palladium. *J. Am. Chem. Soc.* **1978,** *100* (11), 3636-8.

90. Darwish, A.; Lang, A.; Kim, T.; Chong, J. M., The Use of Phosphine Ligands to Control the Regiochemistry of Pd-Catalyzed Hydrostannations of 1-Alkynes: Synthesis of (E)-1-Tributylstannyl-1-alkenes. *Org. Lett.* **2008,** *10* (5), 861-864.

91. Appel, R., Tertiary phosphane/tetrachloromethane, a versatile reagent for chlorination, dehydration, and phosphorus-nitrogen linking. *Angew. Chem.* **1975,** *87* (24), 863-74.

92. Farina, V. F.; Krishnamurthy, V.; Scott, W. J., *Organic Reactions*. 1997; Vol. 50.

93. Berger, D. M.; Dutia, M.; Powell, D.; Floyd, M. B.; Torres, N.; Mallon, R.; Wojciechowicz, D.; Kim, S.; Feldberg, L.; Collins, K.; Chaudhary, I., 4-Anilino-7-alkenylquinoline-3-carbonitriles as potent MEK1 kinase inhibitors. *Bioorg. Med. Chem.* **2008,** *16* (20), 9202-9211.

94. Harrowven, D. C.; Curran, D. P.; Kostiuk, S. L.; Wallis-Guy, I. L.; Whiting, S.; Stenning, K. J.; Tang, B.; Packard, E.; Nanson, L., Potassium carbonate-silica: a highly effective stationary phase for the chromatographic removal of organotin impurities. *Chem. Commun.* **2010,** *46* (34), 6335-6337.

95. Sonogashira, K.; Tohda, Y.; Hagihara, N., Convenient synthesis of acetylenes. Catalytic substitutions of acetylenic hydrogen with bromo alkenes, iodo arenes, and bromopyridines. *Tetrahedron Lett.* **1975,** (50), 4467-70.

96. Lindlar, H., A new catalyst for selective hydrogenations. *Helv. Chim. Acta* **1952,** *35*, 446-50.

97. Takami, K.; Yorimitsu, H.; Oshima, K., Trans-Hydrometalation of Alkynes by a Combination of InCl3 and DIBAL-H: One-Pot Access to Functionalized (Z)-Alkenes. *Org. Lett.* **2002,** *4* (17), 2993-2995.

98. Chu, S.; Wallace, S.; Smith, M. D., A Cascade Strategy Enables a Total Synthesis of (-)-Gephyrotoxin. *Angew. Chem., Int. Ed.* **2014,** *53* (50), 13826-13829.

99. Rostovtsev, V. V.; Green, L. G.; Fokin, V. V.; Sharpless, K. B., A stepwise Huisgen cycloaddition process: copper(I)-catalyzed regioselective "ligation" of azides and terminal alkynes. *Angew. Chem., Int. Ed.* **2002,** *41* (14), 2596-2599.

100. Morales, S.; Guijarro, F. G.; Garcia Ruano, J. L.; Cid, M. B., A General Aminocatalytic Method for the Synthesis of Aldimines. *J. Am. Chem. Soc.* **2014,** *136* (3), 1082-1089.

101. Hanamoto, T.; Shimomoto, N.; Kikukawa, T.; Inanaga, J., Efficient synthesis of enantiomerically pure trans-2,5-bis(arylethynyl)pyrrolidines. A new entry into C2-symmetric chiral secondary amines. *Tetrahedron: Asymmetry* **1999,** *10* (15), 2951-2959.

102. Szostak, M.; Spain, M.; Parmar, D.; Procter, D. J., Selective reductive transformations using samarium diiodide-water. *Chem. Commun.* **2012,** *48* (3), 330-46.

103. Clark, P. G. K.; Vieira, L. C. C.; Tallant, C.; Fedorov, O.; Singleton, D. C.; Rogers, C. M.; Monteiro, O. P.; Bennett, J. M.; Baronio, R.; Mueller, S.; Daniels, D. L.; Mendez, J.; Knapp, S.; Brennan, P. E.; Dixon, D. J., LP99: Discovery and Synthesis of the First Selective BRD7/9 Bromodomain Inhibitor. *Angew. Chem., Int. Ed.* **2015,** *54* (21), 6217-6221.

104. Hay, D. A.; Fedorov, O.; Martin, S.; Singleton, D. C.; Tallant, C.; Wells, C.; Picaud, S.; Philpott, M.; Monteiro, O. P.; Rogers, C. M.; Conway, S. J.; Rooney, T. P. C.; Tumber, A.; Yapp, C.; Filippakopoulos, P.; Bunnage, M. E.; Muller, S.; Knapp, S.; Schofield, C. J.; Brennan, P. E., Discovery and Optimization of Small-Molecule Ligands for the CBP/p300 Bromodomains. *J. Am. Chem. Soc.* **2014,** *136* (26), 9308-9319.

105. Baldwin, J. E.; Thomas, R. C.; Kruse, L. I.; Silberman, L., Rules for ring closure: ring formation by conjugate addition of oxygen nucleophiles. *J. Org. Chem.* **1977,** *42* (24), 3846-52.

106. Ooi, T.; Maruoka, K., Recent advances in asymmetric phase-transfer catalysis. *Angew. Chem., Int. Ed.* **2007,** *46* (23), 4222-4266.

107. Ooi, T.; Kameda, M.; Maruoka, K., Molecular Design of a C2-Symmetric Chiral Phase-Transfer Catalyst for Practical Asymmetric Synthesis of α-Amino Acids. *J. Am. Chem. Soc.* **1999,** *121* (27), 6519-6520.

108. Lygo, B.; Allbutt, B.; James, S. R., Identification of a highly effective asymmetric phase-transfer catalyst derived from α-methylnaphthylamine. *Tetrahedron Lett.* **2003,** *44* (30), 5629-5632.

109. Gapp, B. V.; Konopka, T.; Penz, T.; Dalal, V.; Buerckstuemmer, T.; Bock, C.; Nijman, S. M. B., Parallel reverse genetic screening in mutant human cells using transcriptomics. *Mol. Syst. Biol.* **2016,** *12* (8).

110. Lipinski, C. A.; Lombardo, F.; Dominy, B. W.; Feeney, P. J., Experimental and computational approaches to estimate solubility and permeability in drug discovery and development settings. *Advanced Drug Delivery Reviews* **2001,** *46* (1–3), 3-26.

111. Molinspiration Cheminformatics. www.molinspiration.com.

112. Hughes, J. D.; Blagg, J.; Price, D. A.; Bailey, S.; DeCrescenzo, G. A.; Devraj, R. V.; Ellsworth, E.; Fobian, Y. M.; Gibbs, M. E.; Gilles, R. W.; Greene, N.; Huang, E.; Krieger-Burke, T.; Loesel, J.; Wager, T.; Whiteley, L.; Zhang, Y., Physiochemical drug properties associated with in vivo toxicological outcomes. *Bioorganic & Medicinal Chemistry Letters* **2008,** *18* (17), 4872-4875.

113. Kaiser, N.-F. K.; Hallberg, A.; Larhed, M., In Situ Generation of Carbon Monoxide from Solid Molybdenum Hexacarbonyl. A Convenient and Fast Route to Palladium-Catalyzed Carbonylation Reactions. *J. Comb. Chem.* **2002,** *4* (2), 109-111.

114. Krasovskiy, A.; Knochel, P., A LiCl-mediated Br/Mg exchange reaction for the preparation of functionalized aryl- and heteroarylmagnesium compounds from organic bromides. *Angew. Chem., Int. Ed.* **2004,** *43* (25), 3333-3336.

115. Bollini, M.; Domaoal, R. A.; Thakur, V. V.; Gallardo-Macias, R.; Spasov, K. A.; Anderson, K. S.; Jorgensen, W. L., Computationally-Guided Optimization of a Docking Hit to Yield Catechol Diethers as Potent Anti-HIV Agents. *J. Med. Chem.* **2011,** *54* (24), 8582-8591.

116. Han, Z.; Liu, P.; Gu, L.; Zhang, Y.; Li, H.; Chen, S.; Chai, J., Structural Basis for Histone Demethylation by JhDM1. *Frontier Science* **2007,** *1*, 52-67.

117. Berman, H. M.; Westbrook, J.; Feng, Z.; Gilliland, G.; Bhat, T. N.; Weissig, H.; Shindyalov, I. N.; Bourne, P. E., The Protein Data Bank. In *Nucleic Acids Research* **2000**, 28, 235-242.

118. Trott, O.; Olson, A. J., AutoDock Vina: Improving the speed and accuracy of docking with a new scoring function, efficient optimization, and multithreading. *J. Comput. Chem.* **2010,** *31* (2), 455-461.

119. Abagyan, R.; Totrov, M.; Kuznetsov, D., ICM - a new method for protein modeling and design: applications to docking and structure prediction from the distorted native conformation. *J. Comput. Chem.* **1994,** *15* (5), 488-506.

120. McClure, D. E.; Arison, B. H.; Baldwin, J. J., Mode of nucleophilic addition to epichlorohydrin and related species: chiral aryloxymethyloxiranes. *J. Am. Chem. Soc.* **1979,** *101* (13), 3666-8.

121. Urata, K.; Takaishi, N., The alkyl glycidyl ether as synthetic building blocks. *J. Am. Oil Chem. Soc.* **1994,** *71* (9), 1027-33.

122. Le Huerou, Y.; Doyon, J.; Gree, R. L., Stereocontrolled Synthesis of Key Advanced Intermediates toward Simplified Acetogenin Analogues. *J. Org. Chem.* **1999,** *64* (18), 6782-6790.

123. Soula, G., Tris(polyoxaalkyl)amines (trident), a new class of solid-liquid phase-transfer catalysts. *J. Org. Chem.* **1985,** *50* (20), 3717-21.

124. Ballesteros, P.; Claramunt, R. M.; Elguero, J., Study of the catalytic properties of tris(3,6-dioxaheptyl)amine (TDA-1) in heteroaromatic nucleophilic substitution of chloropyridines and their N-oxides. *Tetrahedron* **1987,** *43* (11), 2557-64.

125. Lamb, A. D. Asymmetric synthesis of heterocycles via cation-directed cyclizations and rearrangements. University of Oxford, Oxford, **2014**.

126. Shultz, M. D., Setting expectations in molecular optimizations: Strengths and limitations of commonly used composite parameters. *Bioorganic & Medicinal Chemistry Letters* **2013,** *23* (21), 5980-5991.

127. Leeson, P. D.; Springthorpe, B., The influence of drug-like concepts on decision-making in medicinal chemistry. *Nat. Rev. Drug Discov.* **2007,** *6* (11), 881-890.

128. Miyamoto, S.; Kollman, P. A., What determines the strength of noncovalent association of ligands to proteins in aqueous solution? *Proc. Natl. Acad. Sci. U. S. A.* **1993,** *90* (18), 8402-6.

129. Vankar, Y. D.; Rao, C. T., *J. Chem. Res.* **1985,** *232*.

130. Zhang, Z.; Ren, J.; Stammers, D. K.; Baldwin, J. E.; Harlos, K.; Schofield, C. J., Structural origins of the selectivity of the trifunctional oxygenase clavaminic acid synthase. *Nat. Struct. Biol.* **2000,** *7* (2), 127-133.

131. Zhou, J.; Kelly, W. L.; Bachmann, B. O.; Gunsior, M.; Townsend, C. A.; Solomon, E. I., Spectroscopic Studies of Substrate Interactions with Clavaminate Synthase 2, a Multifunctional α-KG-Dependent Non-Heme Iron Enzyme: Correlation with Mechanisms and Reactivities. *J. Am. Chem. Soc.* **2001,** *123* (30), 7388-7398.

132. Cleland, W. W., The kinetics of enzyme-catalyzed reactions with two or more substrates or products. I. Nomenclature and rate equations. *Biochim. Biophys. Acta, Spec. Sect. Enzymol. Subj.* **1963,** *67*, 104-37.

133. Yu, M.; Magalhaes, M. L. B.; Cook, P. F.; Blanchard, J. S., Bisubstrate Inhibition: Theory and Application to N-Acetyltransferases. *Biochemistry* **2006,** *45* (49), 14788-14794.

134. Korczynska, M.; Le, D. D.; Younger, N.; Gregori-Puigjane, E.; Tumber, A.; Krojer, T.; Velupillai, S.; Gileadi, C.; Nowak, R. P.; Iwasa, E.; Pollock, S. B.; Ortiz Torres, I.; Oppermann, U.; Shoichet, B. K.; Fujimori, D. G., Docking and Linking of Fragments To Discover Jumonji Histone Demethylase Inhibitors. *J. Med. Chem.* **2016,** *59* (4), 1580-1598.

135. Cascella, B.; Mirica, L. M., Kinetic Analysis of Iron-Dependent Histone Demethylases: α-Ketoglutarate Substrate Inhibition and Potential Relevance to the Regulation of Histone Demethylation in Cancer Cells. *Biochemistry* **2012,** *51* (44), 8699-8701.

136. Lineweaver, H.; Burk, D., The Determination of Enzyme Dissociation Constants. *J. Am. Chem. Soc.* **1934,** *56* (3), 658-666.

137. Pierce, M. M.; Raman, C. S.; Nall, B. T., Isothermal Titration Calorimetry of Protein-Protein Interactions. *Methods* **1999,** *19* (2), 213-221.

138. Dayne, D. BioLayer Interferometry (BLI) *FortéBio Interactions* [Online], 2012.

139. Boeri Erba, E.; Petosa, C., The emerging role of native mass spectrometry in characterizing the structure and dynamics of macromolecular complexes. *Protein Sci.* **2015,** *24* (8), 1176-1192.

140. Dubinsky, L.; Krom, B. P.; Meijler, M. M., Diazirine based photoaffinity labeling. *Bioorg. Med. Chem.* **2012,** *20* (2), 554-570.

141. Lenz, T.; Fischer, J. J.; Dreger, M., Probing small molecule-protein interactions: A new perspective for functional proteomics. *J. Proteomics* **2011,** *75* (1), 100-115.

142. Preston, G. W.; Wilson, A. J., Photo-induced covalent cross-linking for the analysis of biomolecular interactions. *Chem. Soc. Rev.* **2013,** *42* (8), 3289-3301.

143. Domling, A.; Ugi, I., Multicomponent reactions with isocyanides. *Angew. Chem., Int. Ed.* **2000,** *39* (18), 3168-3210.

144. Bush, J. T.; Walport, L. J.; McGouran, J. F.; Leung, I. K. H.; Berridge, G.; van Berkel, S. S.; Basak, A.; Kessler, B. M.; Schofield, C. J., The Ugi four-component reaction enables expedient synthesis and comparison of photoaffinity probes. *Chem. Sci.* **2013,** *4* (11), 4115-4120.

145. Dubinsky, L.; Jarosz, L. M.; Amara, N.; Krief, P.; Kravchenko, V. V.; Krom, B. P.; Meijler, M. M., Synthesis and validation of a probe to identify quorum sensing receptors. *Chem. Commun.* **2009,** (47), 7378-7380.

146. Pardin, C.; Roy, I.; Chica, R. A.; Bonneil, E.; Thibault, P.; Lubell, W. D.; Pelletier, J. N.; Keillor, J. W., Photolabeling of Tissue Transglutaminase Reveals the Binding Mode of Potent Cinnamoyl Inhibitors. *Biochemistry* **2009,** *48* (15), 3346-3353.

147. Ahad, A. M.; Jensen, S. M.; Jewett, J. C., A Traceless Staudinger Reagent To Deliver Diazirines. *Org. Lett.* **2013,** *15* (19), 5060-5063.

148. Hodgson, D. M.; Labande, A. H.; Pierard, F. Y. T. M.; Exposito Castro, M. A., The Scope of Catalytic Enantioselective Tandem Carbonyl Ylide Formation-Intramolecular [3 + 2] Cycloadditions. *J. Org. Chem.* **2003,** *68* (16), 6153-6159.

149. Del Mar, E. G.; Largman, C.; Brodrick, J. W.; Fassett, M.; Geokas, M. C., Substrate specificity of human pancreatic elastase 2. *Biochemistry* **1980,** *19* (3), 468-72.

150. Perez, J. M., Evidence for the participation of an isomerization pathway in diazirine phtolysis. Study of primary processes and energy partitioning. *J. Chem. Soc., Faraday Trans.* **1982,** *78* (12), 3509-18.

151. Wang, J.; Kubicki, J.; Peng, H.; Platz, M. S., Influence of solvent on carbene intersystem crossing rates. *J. Am. Chem. Soc.* **2008,** *130* (20), 6604-6609.

152. McGarrity, J. F.; Smyth, T., Hydrolysis of diazomethane-kinetics and mechanism. *J. Am. Chem. Soc.* **1980,** *102* (24), 7303-8.

153. Ziebell, M. R.; Nirthanan, S.; Husain, S. S.; Miller, K. W.; Cohen, J. B., Identification of binding sites in the nicotinic acetylcholine receptor for [3H]azietomidate, a photoactivatable general anesthetic. *J. Biol. Chem.* **2004,** *279* (17), 17640-17649.

154. Mix, K. A.; Raines, R. T., Optimized Diazo Scaffold for Protein Esterification. *Org. Lett.* **2015,** *17* (10), 2358-2361.

155. Brunner, J.; Senn, H.; Richards, F. M., 3-Trifluoromethyl-3-phenyldiazirine. A new carbene generating group for photolabeling reagents. *J. Biol. Chem.* **1980,** *255* (8), 3313-18.

156. Morley, A. D.; Pugliese, A.; Birchall, K.; Bower, J.; Brennan, P.; Brown, N.; Chapman, T.; Drysdale, M.; Gilbert, I. H.; Hoelder, S.; Jordan, A.; Ley, S. V.; Merritt, A.; Miller, D.; Swarbrick, M. E.; Wyatt, P. G., Fragment-based hit identification: thinking in 3D. *Drug Discovery Today* **2013,** *18* (23-24), 1221-7.

157. Besnard, J.; Jones, P. S.; Hopkins, A. L.; Pannifer, A. D., The Joint European Compound Library: boosting precompetitive research. *Drug Discov. Today* **2015,** *20* (2), 181-186.

158. Congreve, M.; Carr, R.; Murray, C.; Jhoti, H., A 'rule of three' for fragment-based lead discovery? *Drug Discov. Today* **2003,** *8* (19), 876-7.

159. Zartler, E. R.; Shapiro, M. J., *Fragment-Based Drug Discovery, A Practical Approach*. Wiley: 2008.

160. Hann, M. M.; Leach, A. R.; Harper, G., Molecular Complexity and Its Impact on the Probability of Finding Leads for Drug Discovery. *J. Chem. Inf. Comput. Sci.* **2001,** *41* (3), 856-864.

161. Davis, B. J.; Erlanson, D. A., Learning from our mistakes: The 'unknown knowns' in fragment screening. *Bioorg. Med. Chem. Lett.* **2013,** *23* (10), 2844-2852.

162. Park, C.-M.; Bruncko, M.; Adickes, J.; Bauch, J.; Ding, H.; Kunzer, A.; Marsh, K. C.; Nimmer, P.; Shoemaker, A. R.; Song, X.; Tahir, S. K.; Tse, C.; Wang, X.; Wendt, M. D.; Yang, X.; Zhang, H.; Fesik, S. W.; Rosenberg, S. H.; Elmore, S. W., Discovery of an Orally Bioavailable Small Molecule Inhibitor of Prosurvival B-Cell Lymphoma 2 Proteins. *J. Med. Chem.* **2008,** *51* (21), 6902-6915.

163. Cox, O. B.; Spencer, J.; Brennan, P. In *Design and utilisation of a poised fragment library in the search for inhibitors of PHIP(2), an atypical bromodomain*, American Chemical Society: 2016; pp MEDI-399.

164. House, H. O.; Auerbach, R. A.; Gall, M.; Peet, N. P., Chemistry of carbanions. XXII. C- vs. O-acylation of metal enolates. *J. Org. Chem.* **1973,** *38* (3), 514-22.

165. Zhong, M.; Brauman, J. I., Ambident Reactivity of Enolate Anions in the Gas Phase. Experimental Determination of Carbon vs Oxygen Acylation with CF3COCl. *J. Am. Chem. Soc.* **1996,** *118* (3), 636-41.

166. Breugst, M.; Zipse, H.; Guthrie, J. P.; Mayr, H., Marcus Analysis of Ambident Reactivity. *Angew. Chem., Int. Ed.* **2010,** *49* (30), 5165-5169, S5165/1-S5165/53.

167. Mermerian, A. H.; Fu, G. C., Catalytic Enantioselective Synthesis of Quaternary Stereocenters via Intermolecular C-Acylation of Silyl Ketene Acetals: Dual Activation of the Electrophile and the Nucleophile. *J. Am. Chem. Soc.* **2003,** *125* (14), 4050-4051.

168. Woods, P. A.; Morrill, L. C.; Bragg, R. A.; Smith, A. D., Isothiourea-Catalysed Asymmetric C-Acylation of Silyl Ketene Acetals. *Chem. - Eur. J.* **2011,** *17* (39), 11060-11067, S11060/1-S11060/73.

169. Birrell, J. A.; Desrosiers, J.-N.; Jacobsen, E. N., Enantioselective Acylation of Silyl Ketene Acetals through Fluoride Anion-Binding Catalysis. *J. Am. Chem. Soc.* **2011,** *133* (35), 13872-13875.

170. Hayashi, M.; Bachman, S.; Hashimoto, S.; Eichman, C. C.; Stoltz, B. M., Ni-Catalyzed Enantioselective C-Acylation of α-Substituted Lactams. *J. Am. Chem. Soc.* **2016,** *138* (29), 8997-9000.

171. Rahemtulla, B. F.; Clark, H. F.; Smith, M. D., Catalytic Enantioselective Synthesis of C1- and C2-Symmetric Spirobiindanones through Counterion-Directed Enolate C-Acylation. *Angew. Chem., Int. Ed.* **2016,** *55* (42), 13180-13183.

172. Maynard, G. D.; Le, T.-b. Preparation of substituted benzimidazolyl[1,4]diazepanes useful as histamine and tachykinin receptor antagonists. US20010034343A1, 2001.

173. Makosza, M., Two-phase reactions in the chemistry of carbanions and halocarbenes-useful tool in organic synthesis. *Pure Appl. Chem.* **1975,** *43* (3-4), 439-62.

174. Ma, B.; Parkinson, J. L.; Castle, S. L., Novel Cinchona alkaloid derived ammonium salts as catalysts for the asymmetric synthesis of β-hydroxy α-amino acids via aldol reactions. *Tetrahedron Lett.* **2007,** *48* (12), 2083-2086.

175. Shirakawa, S.; Yamamoto, K.; Kitamura, M.; Ooi, T.; Maruoka, K., Dramatic rate enhancement of asymmetric phase-transfer-catalyzed alkylations. *Angew. Chem., Int. Ed.* **2005,** *44* (4), 625-628.

176. Ball-Jones, N. R.; Badillo, J. J.; Franz, A. K., Strategies for the enantioselective synthesis of spirooxindoles. *Org. Biomol. Chem.* **2012,** *10* (27), 5165-81.

177. Pavlovska, T. L.; Redkin, R. G.; Lipson, V. V.; Atamanuk, D. V., Molecular diversity of spirooxindoles. Synthesis and biological activity. *Mol. Diversity* **2016,** *20* (1), 299-344.

178. Frost, J. R.; Huber, S. M.; Breitenlechner, S.; Bannwarth, C.; Bach, T., Enantiotopos-Selective C-H Oxygenation Catalyzed by a Supramolecular Ruthenium Complex. *Angew. Chem., Int. Ed.* **2015,** *54* (2), 691-695.

179. Wolff, L., Chemischen Institut der Universität Jena: Methode zum Ersatz des Sauerstoffatoms der Ketone und Aldehyde durch Wasserstoff. *Justus Liebigs Annalen der Chemie* **1912,** *394* (1), 86-108.

180. Knoevenagel, E., Condensation von Malonsäure mit aromatischen Aldehyden durch Ammoniak und Amine. *Berichte der deutschen chemischen Gesellschaft* **1898,** *31* (3), 2596-2619.

181. Motoyama, Y.; Aoki, M.; Takaoka, N.; Aoto, R.; Nagashima, H., Highly efficient synthesis of aldenamines from carboxamides by iridium-catalyzed silane-reduction/dehydration under mild conditions. *Chem. Commun.* **2009,** (12), 1574-1576.

182. Gregory, A. W.; Chambers, A.; Hawkins, A.; Jakubec, P.; Dixon, D. J., Iridium-Catalyzed Reductive Nitro-Mannich Cyclization. *Chem. - Eur. J.* **2015,** *21* (1), 111-114.

183. Huang, P.-Q.; Ou, W.; Han, F., Chemoselective reductive alkynylation of tertiary amides by Ir and Cu(I) bis-metal sequential catalysis. *Chem. Commun.* **2016,** *52* (80), 11967-11970.

184. Rana, S.; Natarajan, A., Face selective reduction of the exocyclic double bond in isatin derived spirocyclic lactones. *Org.Biomol. Chem.* **2013,** *11* (2), 244-247.

185. Bernasconi, C. F.; Kittredge, K. W., Carbanion stabilization by adjacent sulfur: polarizability, resonance, or negative hyperconjugation? experimental distinction based on intrinsic rate constants of proton transfer from (phenylthio)nitromethane and 1-nitro-2-phenylethane. *J. Org. Chem.* **1998,** *63* (6), 1944-1953.

186. Rhoads, S. J.; Decora, A. W., Effect of ring size on acidity and rate of C-alkylation of cyclic β-oxo esters. *Tetrahedron* **1963,** *19* (11), 1645-59.

187. Pangborn, A. B.; Giardello, M. A.; Grubbs, R. H.; Rosen, R. K.; Timmers, F. J., Safe and Convenient Procedure for Solvent Purification. *Organometallics* **1996,** *15* (5), 1518-1520.

188. Armarego, W. L. F.; Perrin, D. D., *Purification of Laboratory Chemicals*. 4 ed.; Butterworth Heinemann: Oxford, 1996.

189. Prasad, G.; Hanna, P. E.; Noland, W. E.; Venkatraman, S., 18-Crown-6 as a catalyst in the dialkylation of o-nitrophenacyl derivatives. *J. Org. Chem.* **1991,** *56* (25), 7188-90.

190. Felpin, F.-X.; Miqueu, K.; Sotiropoulos, J.-M.; Fouquet, E.; Ibarguren, O.; Laudien, J., Room-Temperature, Ligand- and Base-Free Heck Reactions of Aryl Diazonium Salts at Low Palladium Loading: Sustainable Preparation of Substituted Stilbene Derivatives. *Chem. – Eur. J.* **2010,** *16* (17), 5191-5204.

191. Caldarelli, S. A.; El Fangour, S.; Wein, S.; Tran van Ba, C.; Perigaud, C.; Pellet, A.; Vial, H. J.; Peyrottes, S., New Bis-thiazolium Analogues as Potential Antimalarial Agents: Design, Synthesis, and Biological Evaluation. *J. Med. Chem.* **2013,** *56* (2), 496-509.

192. Wei, Z.-L.; Petukhov, P. A.; Bizik, F.; Teixeira, J. C.; Mercola, M.; Volpe, E. A.; Glazer, R. I.; Willson, T. M.; Kozikowski, A. P., Isoxazolyl-serine-based agonists of peroxisome proliferator-activated receptor: design, synthesis, and effects on cardiomyocyte differentiation. *J. Am. Chem. Soc.* **2004,** *126* (51), 16714-16715.

193. Altendorfer, M.; Raja, A.; Sasse, F.; Irschik, H.; Menche, D., Modular synthesis of polyene side chain analogues of the potent macrolide antibiotic etnangien by a flexible coupling strategy based on hetero-bis-metallated alkenes. *Org. Biomol. Chem.* **2013,** *11* (13), 2116-2139.

194. Coombs, J. R.; Zhang, L.; Morken, J. P., Enantiomerically Enriched Tris(boronates): Readily Accessible Conjunctive Reagents for Asymmetric Synthesis. *J. Am. Chem. Soc.* **2014,** *136* (46), 16140-16143.

195. Mallia, C. J.; Englert, L.; Walter, G. C.; Baxendale, I. R., Thiazole formation through a modified Gewald reaction. *Beilstein J. Org. Chem.* **2015,** *11*, 875-883.

196. Kobayashi, S.; Horibe, M.; Saito, Y., Enantioselective synthesis of both diastereomers, including the α-alkoxy-β-hydroxy-β-methyl(phenyl) units, by chiral tin(II) Lewis acid-mediated asymmetric aldol reactions. *Tetrahedron* **1994,** *50* (32), 9629-42.

197. Jackson, R. F. W.; Wishart, N.; Wood, A.; James, K.; Wythes, M. J., Preparation of enantiomerically pure protected 4-oxo α-amino acids and 3-aryl α-amino acids from serine. *J. Org. Chem.* **1992,** *57* (12), 3397-404.

198. Tantama, M.; Lin, W.-C.; Licht, S., An Activity-Based Protein Profiling Probe for the Nicotinic Acetylcholine Receptor. *J. Am. Chem. Soc.* **2008,** *130* (47), 15766-15767.

199. Hansen, M. M.; Harkness, A. R.; Coffey, D. S.; Bordwell, F. G.; Zhao, Y., Substrate acidities and conversion times for reactions of amides with di-tert-butyl dicarbonate. *Tetrahedron Lett.* **1995,** *36* (49), 8949-52.

200. Myers, A. G.; Charest, M. G.; Lerner, C. D.; Brubacker, J. D.; Siegel, D. R. Synthesis of tetracyclines and analogs thereof. WO2005112945A2, 2005.

201. Roberts, R. S.; Sevilla Gomez, S.; Buil Albero, M. A. Preparation of new pyrazole derivatives as CRTH2 antagonists. WO2012069175A1, 2012.

202. Bi, B.; Maurer, K.; Moeller, K. D., Building Addressable Libraries: The Use of "Safety-Catch" Linkers on Microelectrode Arrays. *J. Am. Chem. Soc.* **2010,** *132* (49), 17405-17407.

203. Kim, K. S.; Kim, J. H.; Lee, Y. J.; Lee, Y. J.; Park, J., 2-(Hydroxycarbonyl)benzyl Glycosides: A Novel Type of Glycosyl Donor for Highly Efficient β-Mannopyranosylation and Oligosaccharide Synthesis by Latent-Active Glycosylation. *J. Am. Chem. Soc.* **2001,** *123* (35), 8477-8481.

204. Ward, D. E.; Vazquez, A.; Pedras, M. S. C., Probing host-selective phytotoxicity: synthesis and biological activity of phomalide, isophomalide, and dihydrophomalide. *J. Org. Chem.* **1999,** *64* (5), 1657-1666.

205. Pedras, M. S. C.; Jha, M., Concise Syntheses of the Cruciferous Phytoalexins Brassilexin, Sinalexin, Wasalexins, and Analogues: Expanding the Scope of the Vilsmeier Formylation. *J. Org. Chem.* **2005,** *70* (5), 1828-1834.

206. Ikeda, T.; Yamazaki, T.; Tsuchida, H. Preparation of [[[2,3-dihydrospiro[indene-1,4'-piperidin]-2-yl]oxy]acetyl]amino-linked 4-piperidinyl (biphenyl-2-yl)carbamates amino derivatives as neurokinin NK1, neurokinin NK2 and muscarine M3 receptor antagonists. WO2010106988A1, 2010.

207. Bouerat, L. M. E.; Fensholdt, J.; Nielsen, S. F.; Liang, X.; Havez, S. E.; Andersson, E. C.; Jensen, L.; Hansen, J. R. Preparation of indolinone derivatives as agents to prevent, treat and/or ameliorate multiple sclerosis. WO2005058309A1, 2005.

8. APPENDIX

8.1 Biochemical Assay Data

8.1.1 AlphaScreen Data

KDM2A

ID	SGC ID	mean pIC50	pIC50 SD	pIC50 SEM	n	pIC50 ± XX (n)
121	KDOOA011841a	5.753	0.249	0.176	2	5.8±0.18 (2)
122	KDOOA011842a	6.088	0.217	0.154	2	6.1±0.15 (2)
58	KDOOA011843a	6.408	0.359	0.179	4	6.4±0.18 (4)
59	KDOOA011844a	6.605	0.134	0.067	4	6.6±0.07 (4)

JARID1A

ID	SGC ID	n	pIC50	% Inhibition at 50 µM
107	KDOIN000004a	1	< 4.3	39.0
106	KDOIN000005a	1	< 4.3	30.9
108	KDOIN000003a	1	< 4.3	25.5
79	KDOIN000010a	1	< 4.3	20.0
(***R***,***R***)**-108**	KDOIN000014a	1	< 4.3	40.0
(***S***,***S***)**-108**	KDOIN000015a	1	< 4.3	-20.3
142	KDOIN000033a	1	< 4.3	46.6
143	KDOIN000034a	1	< 4.3	49.1
144	KDOIN000035a	1	< 4.3	47.5
136	KDOIN000040a	1	< 4.3	23.0

99	KDOIN000041a	1	< 4.3	36.7
102	KDOIN000042a	1	< 4.3	24.0
121	KDOOA011841a	1	< 4.3	39.5
59	KDOOA011844a	1	< 4.3	39.1
58	KDOOA011843a	1	< 4.3	35.3

JARID1B

ID	SGC ID	mean pIC50	pIC50 SD	pIC50 SEM	n	pIC50 ± XX (n)
(*S*,*S*)-108	KDOIN000015a	4.882	0.555	0.160	12	4.9±0.16 (12)
142	KDOIN000033a	5.019	0.548	0.158	12	5.0±0.16 (12)

JARID1C

ID	SGC ID	mean pIC50	pIC50 SD	pIC50 SEM	n	pIC50 ± XX (n)	% Inhibition at 100 µM
58	KDOOA011843a				1	< 4.0	29.3
59	KDOOA011844a				1	< 4.0	32.3
121	KDOOA011841a				1	< 4.0	46.7
122	KDOOA011842a	4.439	0.709	0.501	2	4.4±0.50 (2)	
(*S*,*S*)-108	KDOIN000015a	4.803	0.207	0.066	10	4.8±0.07 (10)	
142	KDOIN000033a	5.006	0.185	0.058	10	5±0.06 (10)	

JMJD1A

ID	SGC ID	mean pIC50	pIC50 SD	pIC50 SEM	n	pIC50 ± XX (n)	Mean % Inhibition at 100 µM (n)
(*S*,*S*)-108	KDOIN000015a				1	< 4.0	35.4 (1)
121	KDOOA011841a				1	< 4.0	21.1 (1)
122	KDOOA011842a				1	< 4.0	32.5 (1)

59	KDOOA011844a				2	< 4.0	15.1±9.5 (2)
58	KDOOA011843a				2	< 4.0	18.1±12 (2)
142	KDOIN000033a	5.00	0.457	0.323	2	5.0±0.32 (2)	

JMJD2A

ID	SGC ID	pIC50	pIC50 SD	mean pIC50	pIC50 SD	pIC50 SEM	n	pIC50 ± XX (n)	% Inhib. (μM) (n)
107	KDOIN000004a	< 4.7					1	< 4.7	10.2 (18.75) (1)
106	KDOIN000005a	< 4.7					1	< 4.7	-1.3 (18.75) (1)
108	KDOIN000003a	< 4.7					1	< 4.7	-1.1 (18.75) (1)
79	KDOIN000010a	< 4.7					1	< 4.7	-12.7 (18.75) (1)
(*R*,*R*)-108	KDOIN000014a	< 4.7					1	< 4.7	7.8 (18.75) (1)
(*S*,*S*)-108	KDOIN000015a	< 4.7					3	< 4.7	27.0±4.0 (10) (3)
129	KDOIN000021a	< 4.7					1	< 4.7	3.4 (18.75) (1)
128	KDOIN000022a	< 4.7					1	< 4.7	27.8 (18.75) (1)
141	KDOIN000032a	< 4.7					1	< 4.7	19.8 (18.75) (1)
142	KDOIN000033a	< 4.7					3	< 4.7	24.4±9.1 (10) (3)
143	KDOIN000034a	< 4.7					1	< 4.7	18.3 (18.75) (1)
144	KDOIN000035a	< 4.7					1	< 4.7	8.5 (18.75) (1)

135	KDOIN000036a	< 4.7					1	< 4.7	19.4 (18.75) (1)
136	KDOIN000040a	< 4.7					1	< 4.7	21.8 (18.75) (1)
99	KDOIN000041a	< 4.7					1	< 4.7	-9.59 (18.75) (1)
102	KDOIN000042a	< 4.7					1	< 4.7	-5.4 (18.75) (1)
159	KDOIN000044a	< 4.7					1	< 4.7	-5.9 (18.75) (1)
59	KDOOA011844a	< 4.7					1	< 4.7	18.8 (100) (1)
58	KDOOA011843a	< 4.7					1	< 4.7	14.7 (100) (1)
121	KDOOA011841a	4.14002	0.350	4.140	0.350	0.247	2	4.1±0.25 (2)	
122	KDOOA011842a	4.4130	0.220	4.413	0.220	0.156	2	4.4±0.16 (2)	

JMJD2C

ID	SGC ID	mean pIC50	pIC50 SD	pIC50 SEM	n	pIC50 ± XX (n)	% Inhib. (conc, µM)
58	KDOOA011843a				1	< 4.0	14.7 (100)
59	KDOOA011844a				1	< 4.0	18.8 (100)
(*S*,*S*)-108	KDOIN000015a				1	< 5.0	30.5 (10)
142	KDOIN000033a				1	< 5.0	32.3 (10)
121	KDOOA011841a	4.140	0.350	0.247	2	4.1±0.25 (2)	
122	KDOOA011842a	4.413	0.220	0.156	2	4.4±0.16 (2)	

JMJD2D

ID	SGC ID	pIC50	n	% Inhibition at 10 µM
(*S*,*S*)-108	KDOIN000015a	< 4.0	1	22.6
142	KDOIN000033a	< 4.0	1	14.4

JMJD3A

ID	SGC ID	pIC50	n	% Inhibition at 100 µM
59	KDOOA011844a	< 4.0	1	2.4
121	KDOOA011841a	< 4.0	1	24.6
122	KDOOA011842a	< 4.0	1	42.5
58	KDOOA011843a	< 4.0	1	3.3

8.1.2 RapidFire Data

KDM2A

ID	SGC ID	mean pIC50	pIC50 SD	pIC50 SEM	n	pIC50 ± xx (n)
159	KDOIN000044a	3.159207903	1.653338174	0.826669087	4	3.2±0.83 (4)
172	KDOIN000071a	4.802995272	0.11198334	0.079184179	2	4.8±0.08 (2)
170	KDOIN000070a	4.788078916	0.20249314	0.143184272	2	4.8±0.14 (2)
169	KDOIN000068a	4.835052627	0.245666789	0.173712652	2	4.8±0.17 (2)
168	KDOIN000067a	4.796967113	0.294834582	0.208479532	2	4.8±0.21 (2)
171	KDOIN000069a	4.876801925	0.191956773	0.135733936	2	4.9±0.14 (2)
165	KDOIN000064a	4.98254927	0.104978195	0.074230794	2	5.0±0.07 (2)
166	KDOIN000066a	4.986320303	0.167837859	0.118679288	2	5.0±0.12 (2)
167	KDOIN000065a	5.201004266	0.122901239	0.086904299	2	5.2±0.09 (2)
216	KDOIN000060a	5.199434697	0.198782731	0.099391365	4	5.2±0.1 (4)

79	KDOIN000010a	5.517841305	0.044179523	0.03123964	2	5.5±0.03 (2)
121	KDOOA011841a	5.532836034	0.062370939	0.044102914	2	5.5±0.04 (2)
135	KDOIN000036a	5.620875854	0.084538968	0.059778078	2	5.6±0.06 (2)
69	KDOIN000057a	5.639406586	0.148869744	0.105266805	2	5.6±0.11 (2)
193	KDOIN000061a	5.623970818	0.464913079	0.328743191	2	5.6±0.33 (2)
106	KDOIN000005a	5.761452402	0.104112061	0.052056031	4	5.8±0.05 (4)
70	KDOIN000056a	5.798602876	0.162325535	0.114781487	2	5.8±0.11 (2)
144	KDOIN000035a	5.916855857	0.083691595	0.059178894	2	5.9±0.06 (2)
207	KDOIN000074a	5.884389488	0.161597414	0.114266627	2	5.9±0.11 (2)
181	KDOIN000062a	5.881074247	0.382538799	0.270495778	2	5.9±0.27 (2)
122	KDOOA011842a	5.990549104	0.056914272	0.040244468	2	6.0±0.04 (2)
129	KDOIN000021a	6.016193358	0.066060921	0.046712125	2	6.0±0.05 (2)
135	KDOIN000034a	5.989700043	0.070204711	0.049642228	2	6.0±0.05 (2)
141	KDOIN000032a	5.988429556	0.084312169	0.059617707	2	6.0±0.06 (2)
128	KDOIN000022a	5.983384452	0.113844314	0.080500086	2	6.0±0.08 (2)
99	KDOIN000041a	5.995678626	0.205898437	0.145592181	2	6.0±0.15 (2)
(*R*,*R*)-102	KDOIN000042b	6.0736061	0.093035086	0.065785741	2	6.1±0.07 (2)
109	KDOIN000058a	6.076652344	0.092187907	0.065186694	2	6.1±0.07 (2)
107	KDOIN000004a	6.176531102	0.10165971	0.050829855	4	6.2±0.05 (4)
58	KDOOA011843a	6.340464093	0.191567908	0.135458966	2	6.3±0.14 (2)
(*R*,*R*)-108	KDOIN000014a	6.416461181	0.051240798	0.036232716	2	6.4±0.04 (2)
(*S*,*S*)-102	KDOIN000059a	6.40099076	0.086691835	0.061300385	2	6.4±0.06 (2)
196	KDOIN000073a	6.368150538	0.097423601	0.068888889	2	6.4±0.07 (2)
102	KDOIN000042a	6.537452271	0.121626441	0.086002881	2	6.5±0.09 (2)
136	KDOIN000040a	6.484788696	0.180009982	0.127286279	2	6.5±0.13 (2)
142	KDOIN000033a	6.61672335	0.096236075	0.068049182	2	6.6±0.07 (2)
108	KDOIN000003a	6.606371807	0.174002414	0.087001207	4	6.6±0.09 (4)
214	KDOIN000075a	6.708187313	0.066551488	0.047059008	2	6.7±0.05 (2)
59	KDOOA011844a	6.662341109	0.185727515	0.131329186	2	6.7±0.13 (2)

(*S*,*S*)-108	KDOIN000015a	6.798602876	0.040581384	0.028695372	2	6.8±0.03 (2)
213	KDOIN000072a	6.910094889	0.064486016	0.045598499	2	6.9±0.05 (2)

8.2 2-OG and Peptide Competition

8.2.1 Raw Data Graphs

2-OG Competition

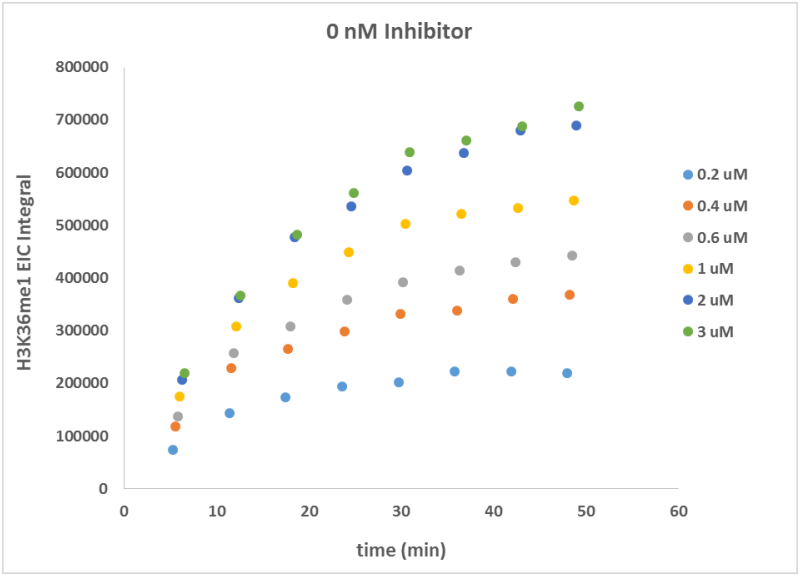

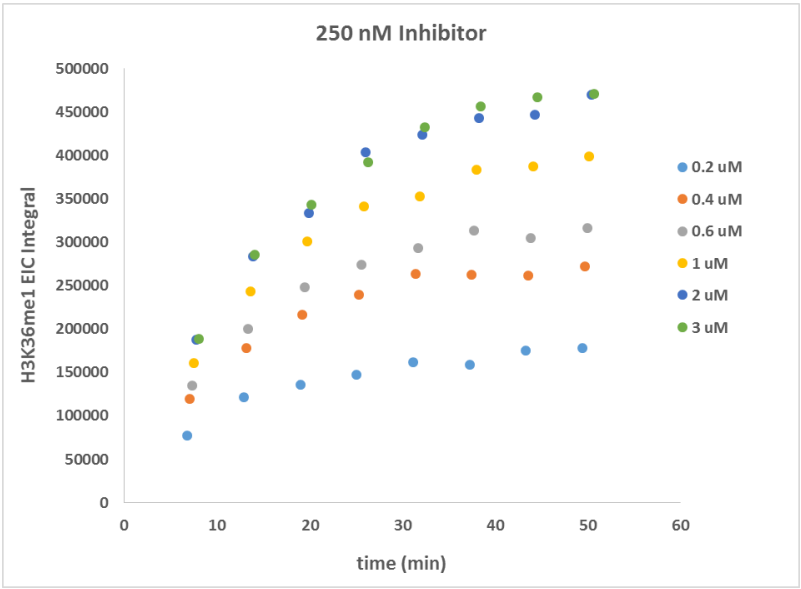

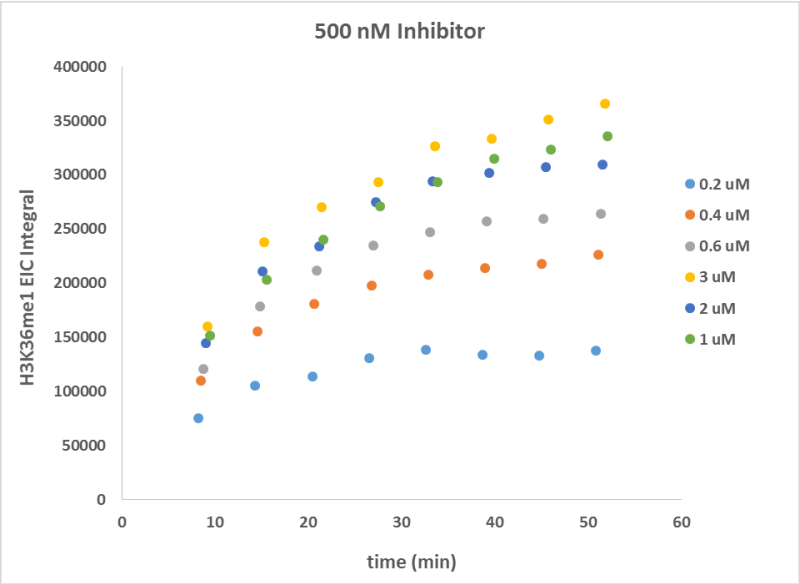

Peptide Competition

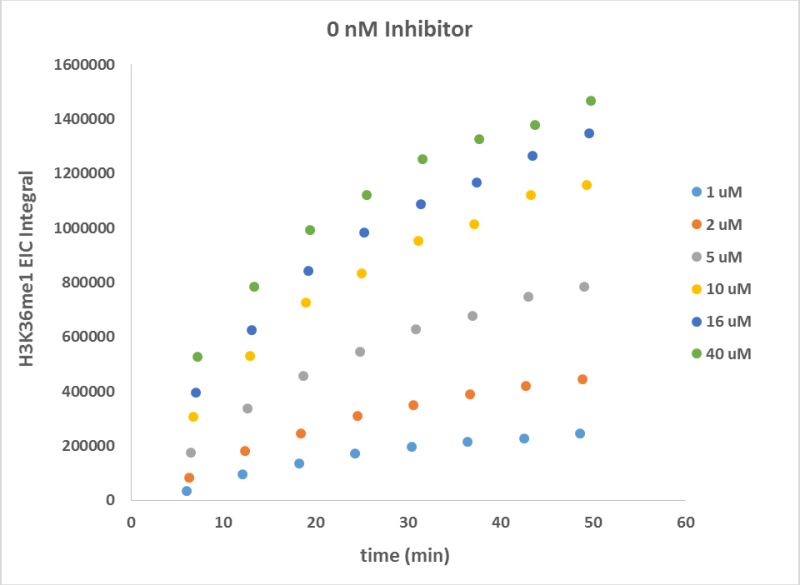

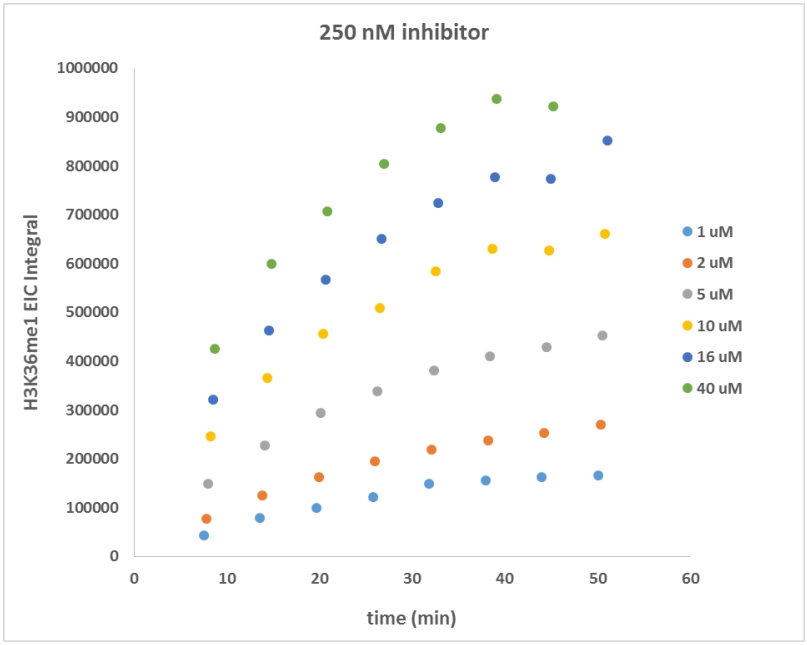
250 nM inhibitor
H3K36me1 EIC Integral
1000000
900000
800000
700000
600000
500000
400000
300000
200000
100000
0
0
10
20
30
40
50
60
time (min)
1 uM
2 uM
5 uM
10 uM
16 uM
40 uM

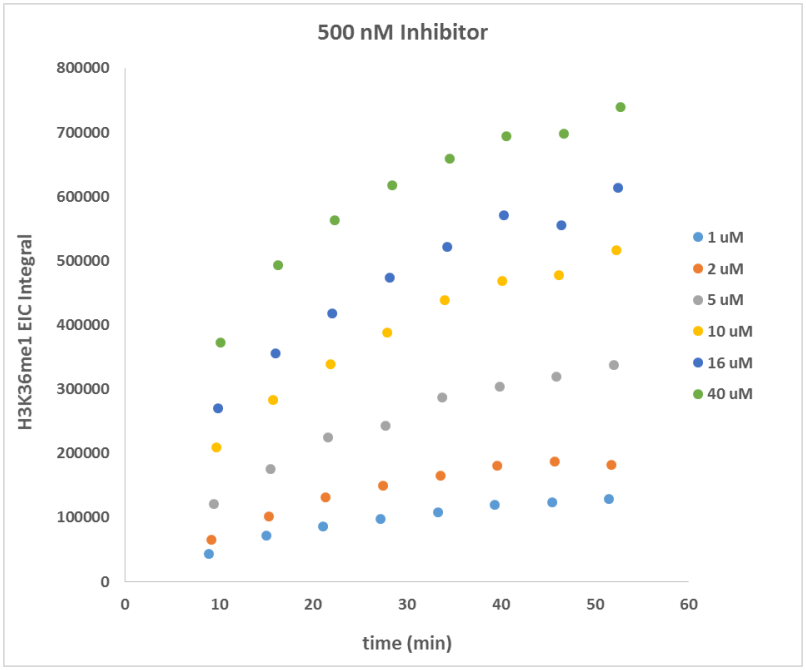
500 nM Inhibitor
H3K36me1 EIC Integral
800000
700000
600000
500000
400000
300000
200000
100000
0
0
10
20
30
40
50
60
time (min)
1 uM
2 uM
5 uM
10 uM
16 uM
40 uM

8.2.2 Regression Analysis

2-OG Competition Michaelis-Menten Plot

	[(*S*,*S*)-108] = 0 nM	[(*S*,*S*)-108] = 250 nM	[(*S*,*S*)-108] = 500 nM
Best-fit values			
Vmax	20743	13233	9020
Km	0.8909	0.6612	0.6372
Std. Error			
Vmax	976.2	228.7	326.1
Km	0.1045	0.03166	0.06468
95% CI (profile likelihood)			
Vmax	18318 to 23805	12618 to 13899	8183 to 10004
Km	0.6455 to 1.237	0.578 to 0.756	0.48 to 0.8431
Goodness of Fit			
Degrees of Freedom	4	4	4
R square	0.9911	0.9981	0.9915
Absolute Sum of Squares	981549	82554	176138
Sy.x	495.4	143.7	209.8
Constraints			
Km	Km > 0	Km > 0	Km > 0
Number of points			
# of X values	6	6	6
# Y values analyzed	6	6	6

2-OG Competition Lineweaver-Burk Plot

	[(*S*,*S*)-108] = 0 nM	[(*S*,*S*)-108] = 250 nM	[(*S*,*S*)-108] = 500 nM
Best-fit values ± SE			
Slope	3.895e-005 ± 3.466e-006	4.713e-005 ± 9.89e-007	7.454e-005 ± 2.244e-006
Y-intercept	5.421e-005 ± 8.417e-006	7.887e-005 ± 2.402e-006	0.0001064 ± 5.451e-006
X-intercept	-1.392	-1.673	-1.427
1/slope	25673	21216	13416
95% Confidence Intervals			
Slope	2.933e-005 to 4.857e-005	4.439e-005 to 4.988e-005	6.831e-005 to 8.077e-005
Y-intercept	3.085e-005 to 7.758e-005	7.22e-005 to 8.554e-005	9.125e-005 to 0.0001215
X-intercept	-2.542 to -0.6608	-1.91 to -1.46	-1.755 to -1.145
Goodness of Fit			
R square	0.9693	0.9982	0.9964
Sy.x	0.00001352	0.000003859	0.000008757
Is slope significantly non-zero?			
F	126.3	2271	1103
DFn, DFd	1, 4	1, 4	1, 4
P value	0.0004	<0.0001	<0.0001
Deviation from zero?	Significant	Significant	Significant
Equation	Y = 3.895e-005*X + 5.421e-005	Y = 4.713e-005*X + 7.887e-005	Y = 7.454e-005*X + 0.0001064
Data			
Number of X values	6	6	6
Maximum number of Y Replicates	1	1	1
Total number of values	6	6	6
Number of missing values	0	0	0

Peptide Competition Michaelis-Menten Plot

	[(*S*,*S*)-108] = 0 nM	[(*S*,*S*)-108] = 250 nM	[(*S*,*S*)-108] = 500 nM
Best-fit values			
Vmax	48724	26670	16719
Km	4.98	5.537	4.784
Std. Error			
Vmax	1840	704.3	920.8
Km	0.5982	0.4497	0.8488
95% CI (profile likelihood)			
Vmax	44045 to 54121	24806 to 28744	14295 to 19842
Km	3.589 to 6.868	4.408 to 6.936	2.777 to 8.14
Goodness of Fit			
Degrees of Freedom	4	4	4
R square	0.9914	0.996	0.9785
Absolute Sum of Squares	8297236	1082958	2168304
Sy.x	1440	520.3	736.3
Constraints			
Km	Km > 0	Km > 0	Km > 0
Number of points			
# of X values	6	6	6
# Y values analyzed	6	6	6

Peptide Competition Lineweaver-Burk Plot

	[(*S*,*S*)-108] = 0 nM	[(*S*,*S*)-108] = 250 nM	[(*S*,*S*)-108] = 500 nM
Best-fit values ± SE			
Slope	0.0001034 ± 2.457e-006	0.0001778 ± 7.781e-006	0.0002195 ± 8.41e-006
Y-intercept	2.087e-005 ± 1.146e-006	4.222e-005 ± 3.628e-006	6.85e-005 ± 3.922e-006
X-intercept	-0.2018	-0.2374	-0.312
1/slope	9667	5623	4555
95% Confidence Intervals			
Slope	9.662e-005 to 0.0001103	0.0001562 to 0.0001994	0.0001962 to 0.0002429
Y-intercept	1.769e-005 to 2.406e-005	3.215e-005 to 5.23e-005	5.761e-005 to 7.939e-005
X-intercept	-0.2451 to -0.163	-0.3257 to -0.1657	-0.396 to -0.2424
Goodness of Fit			
R square	0.9977	0.9924	0.9942
Sy.x	0.000002071	0.00000656	0.00000709
Is slope significantly non-zero?			
F	1773	522.4	681.5
DFn, DFd	1, 4	1, 4	1, 4
P value	<0.0001	<0.0001	<0.0001
Deviation from zero?	Significant	Significant	Significant
Equation	Y = 0.0001034*X + 2.087e-005	Y = 0.0001778*X + 4.222e-005	Y = 0.0002195*X + 6.85e-005
Data			
Number of X values	6	6	6
Maximum number of Y replicates	1	1	1
Total number of values	6	6	6
Number of missing values	0	0	0

8.3 Photoaffinity Labelling

8.3.1 Mass Spectra of UV-Activation of 230

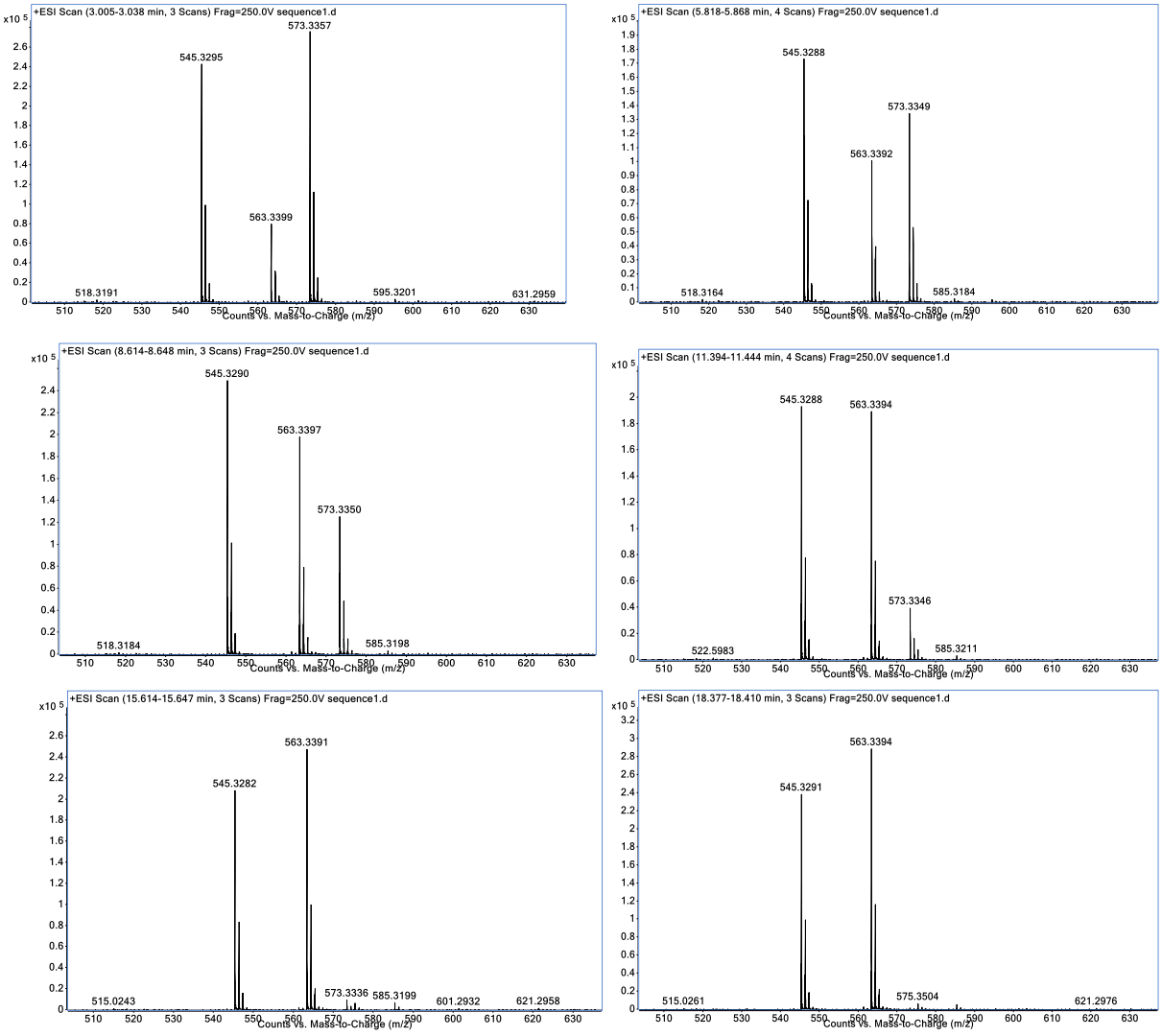

Progress of photoactivation of **230** (mw 572.33) by irradiation with UV-light (250 nm) for 1 min, 2 min, 3 min, 5 min, 10 min, 15 min.

8.3.2 Distribution of Photo-Crosslinked Residues on KDM2A

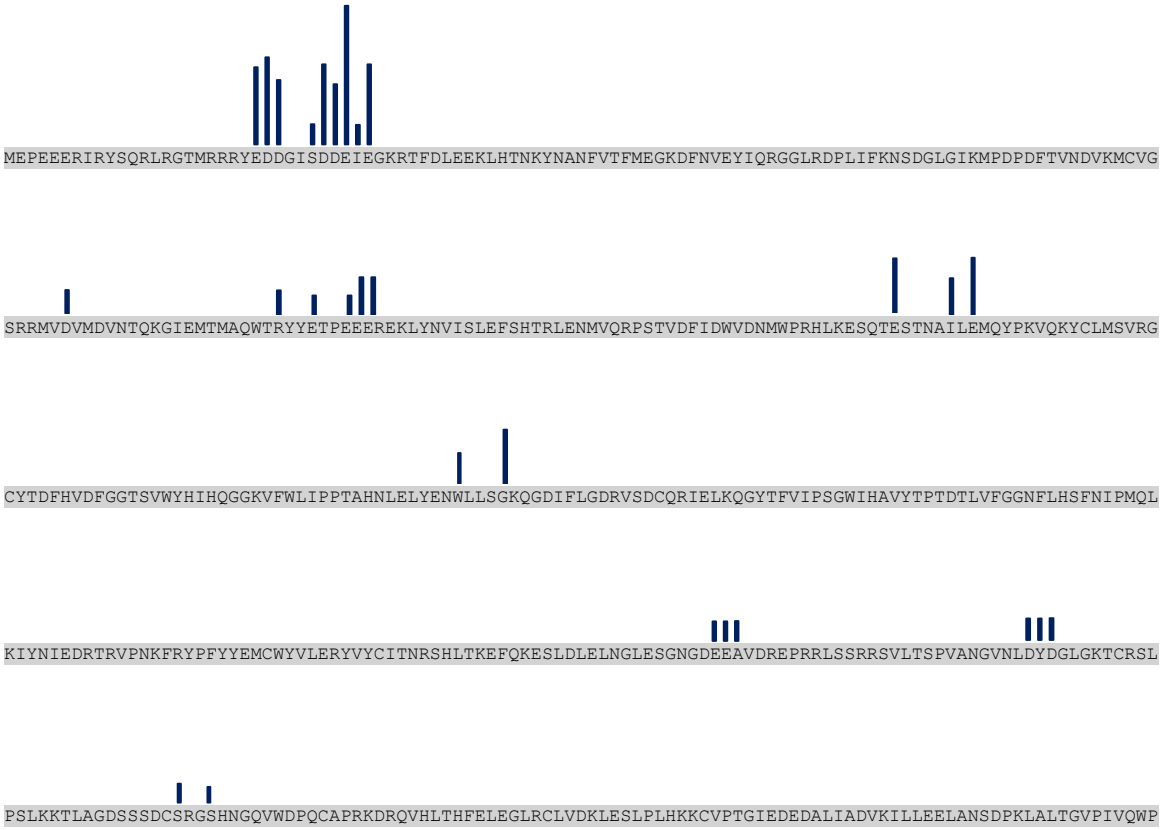

KDM2A sequence (residues 1-519): Blue bars indicate relative proportion of peptides that contain covalently-modified residue.

8.4 HPLC Traces and X-ray Crystallography

8.4.1 HPLC Traces

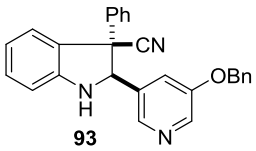

93

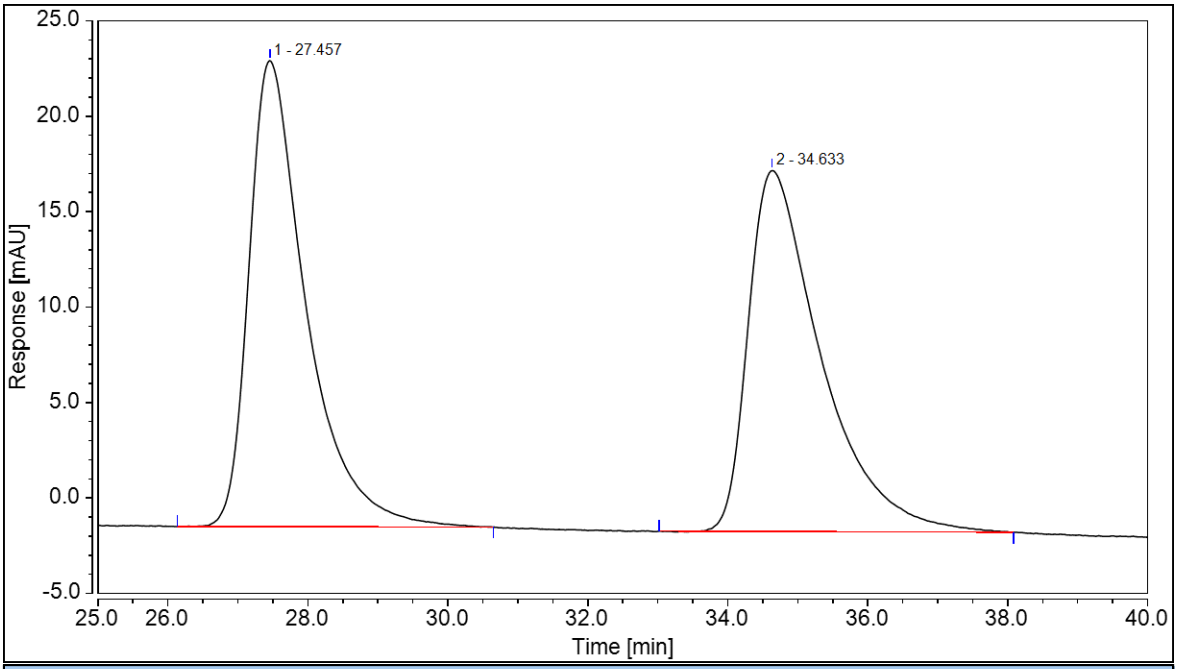

Integration Results

No.	Peak Name	Retention Time min	Area mAU*min	Height mAU	Relative Area %	Relative Height %	Amount
n.a.	Peak 1	n.a.	n.a.	n.a.	n.a.	n.a.	n.a.
1		27.457	23.060	24.426	50.37	56.36	n.a.
2		34.633	22.723	18.910	49.63	43.64	n.a.
Total:			**45.783**	**43.336**	**100.00**	**100.00**	

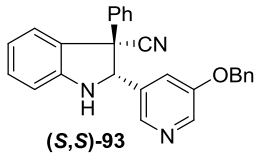

(*S*,*S*)-93

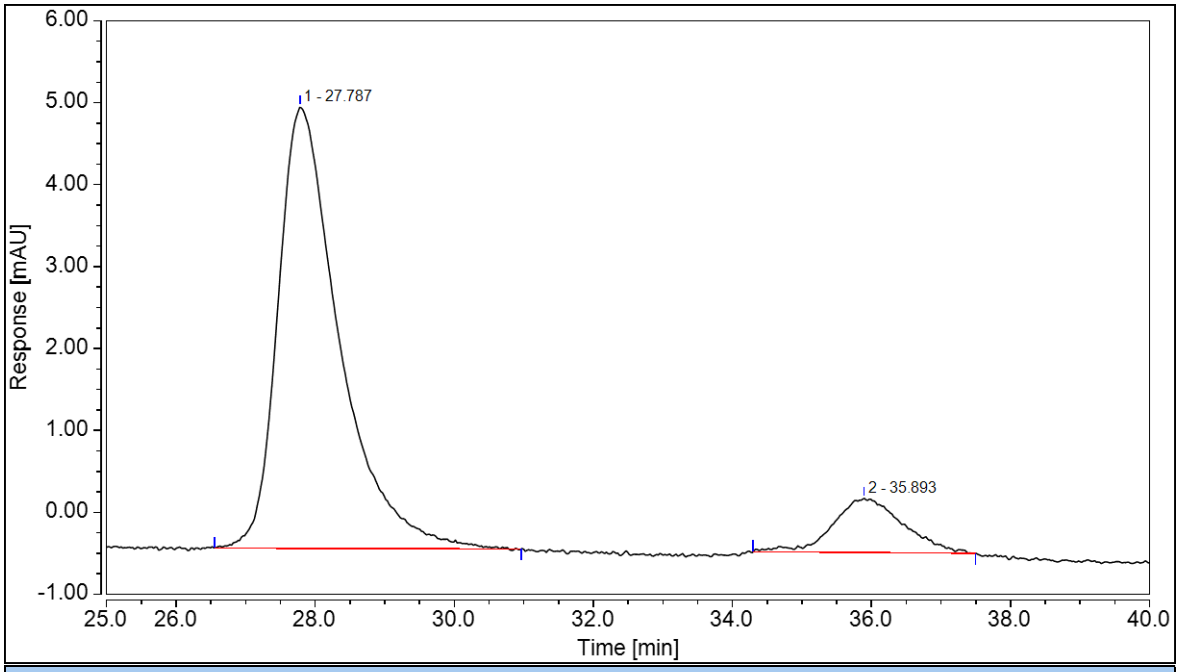

Integration Results

No.	Peak Name	Retention Time min	Area mAU*min	Height mAU	Relative Area %	Relative Height %	Amount
n.a.	Peak 1	n.a.	n.a.	n.a.	n.a.	n.a.	n.a.
1		27.787	5.507	5.390	87.68	89.06	n.a.
2		35.893	0.774	0.662	12.32	10.94	n.a.
Total:			**6.281**	**6.053**	**100.00**	**100.00**	

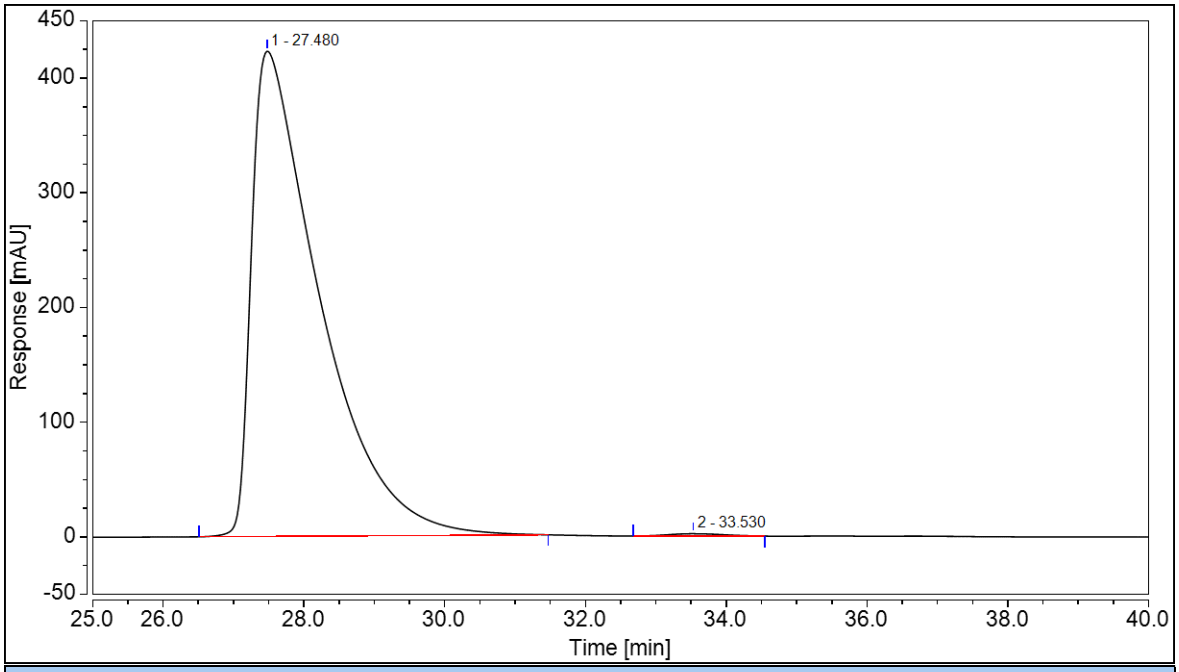

Integration Results

No.	Peak Name	Retention Time min	Area mAU*min	Height mAU	Relative Area %	Relative Height %	Amount
n.a.	Peak 1	n.a.	n.a.	n.a.	n.a.	n.a.	n.a.
1		27.480	474.103	423.118	99.61	99.51	n.a.
2		33.530	1.877	2.069	0.39	0.49	n.a.
Total:			**475.979**	**425.187**	**100.00**	**100.00**	

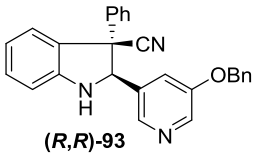

(*R*,*R*)-93

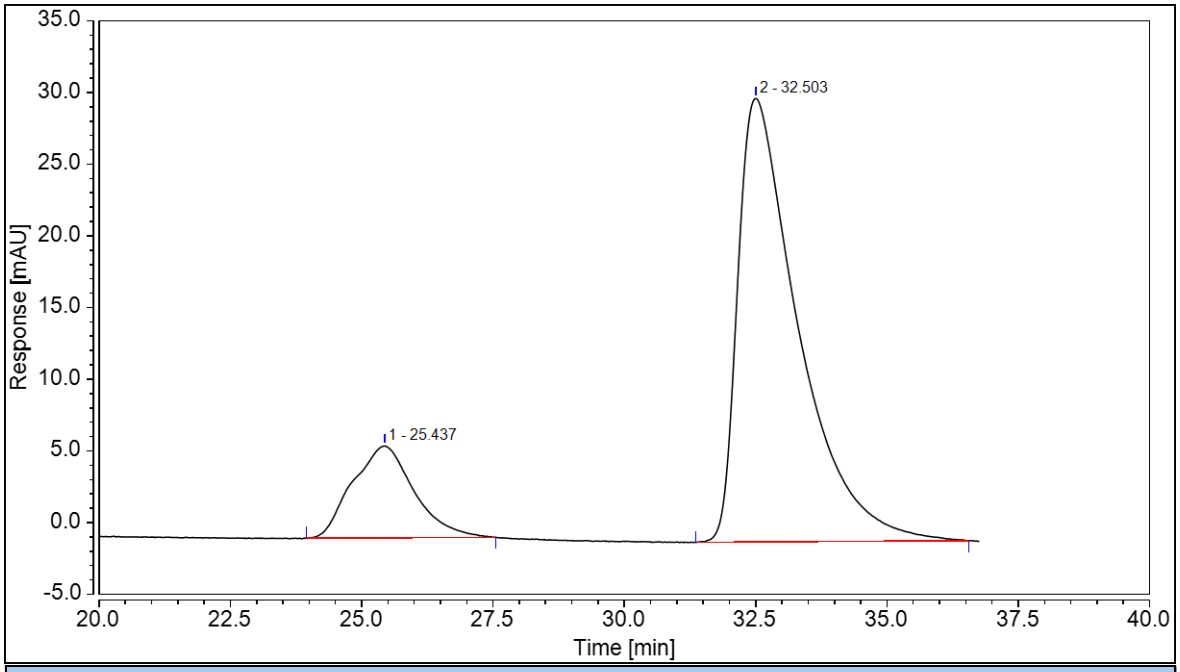

Integration Results

No.	Peak Name	Retention Time min	Area mAU*min	Height mAU	Relative Area %	Relative Height %	Amount
n.a.	Peak 1	n.a.	n.a.	n.a.	n.a.	n.a.	n.a.
1		25.437	8.708	6.418	17.41	17.18	n.a.
2		32.503	41.297	30.945	82.59	82.82	n.a.
Total:			**50.006**	**37.363**	**100.00**	**100.00**	

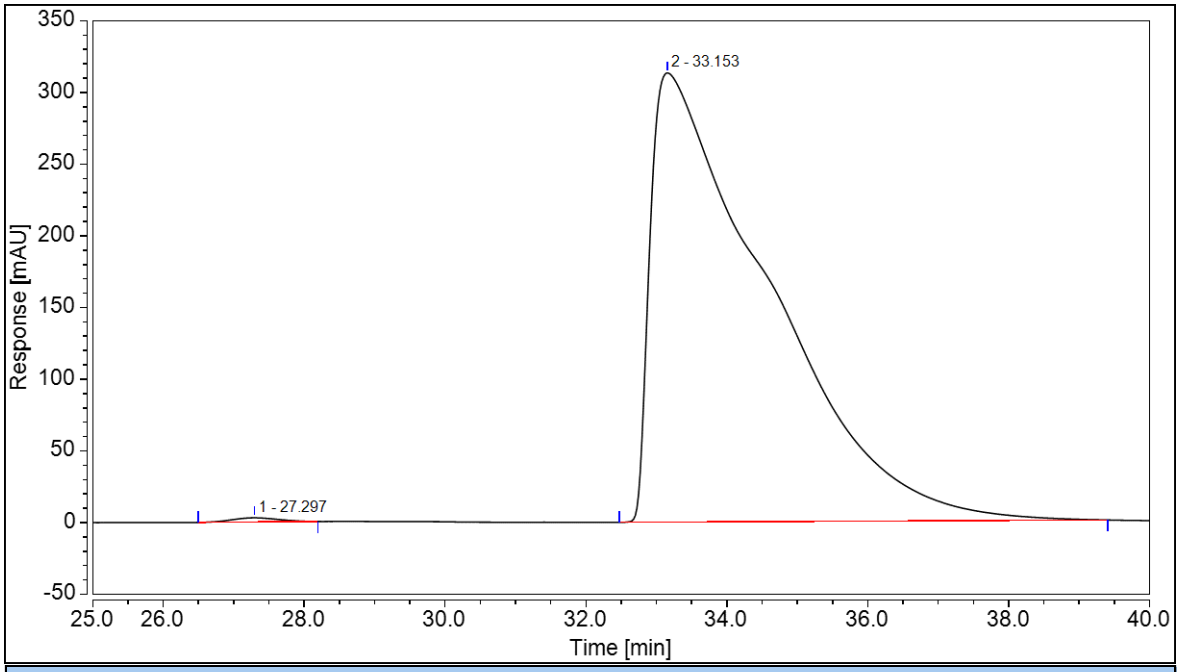

Integration Results

No.	Peak Name	Retention Time min	Area mAU*min	Height mAU	Relative Area %	Relative Height %	Amount
n.a.	Peak 1	n.a.	n.a.	n.a.	n.a.	n.a.	n.a.
1		27.297	2.224	2.924	0.36	0.92	n.a.
2		33.153	608.014	313.355	99.64	99.08	n.a.
Total:			**610.238**	**316.279**	**100.00**	**100.00**	

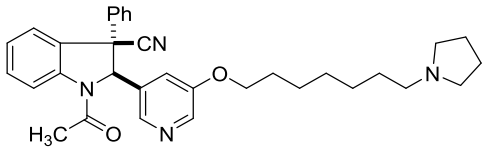

102

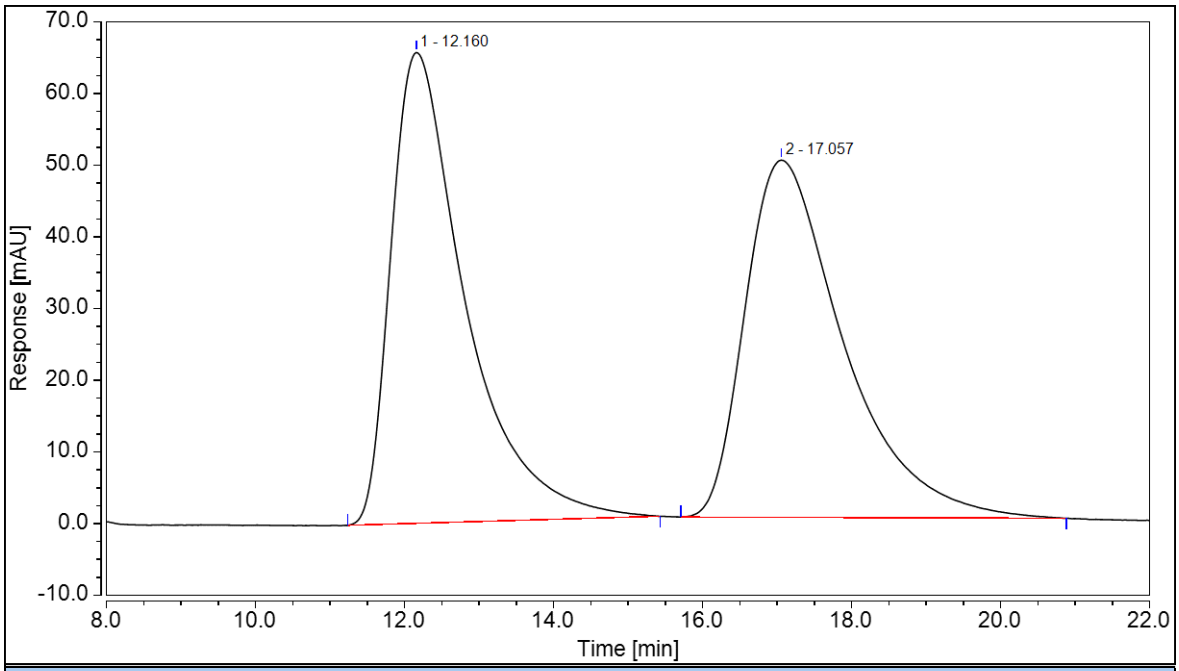

Integration Results

No.	Peak Name	Retention Time min	Area mAU*min	Height mAU	Relative Area %	Relative Height %	Amount
n.a.	Peak 1	n.a.	n.a.	n.a.	n.a.	n.a.	n.a.
1		12.160	75.775	65.695	49.85	56.86	n.a.
2		17.057	76.239	49.842	50.15	43.14	n.a.
Total:			**152.013**	**115.537**	**100.00**	**100.00**	

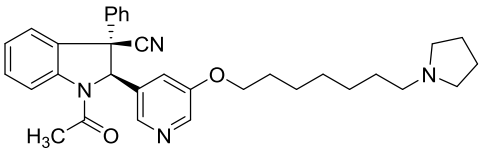

(*R*,*R*)-102

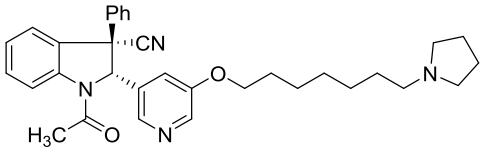

(*S*,*S*)-102

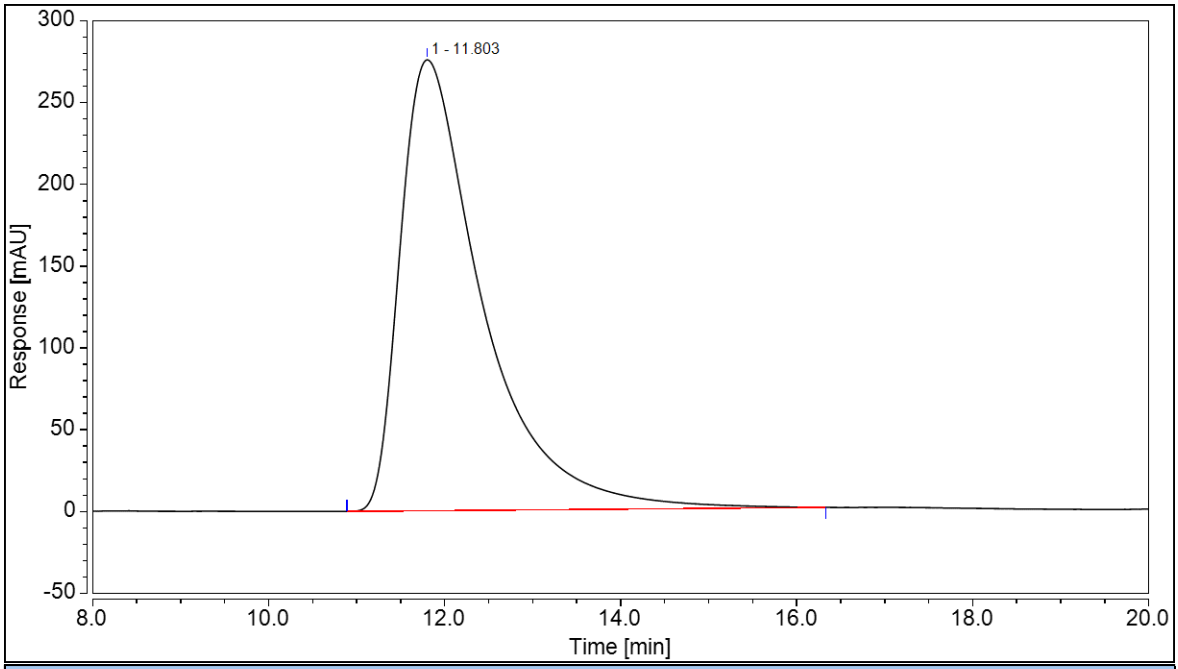

Integration Results

No.	Peak Name	Retention Time min	Area mAU*min	Height mAU	Relative Area %	Relative Height %	Amount
n.a.	Peak 1	n.a.	n.a.	n.a.	n.a.	n.a.	n.a.
1		11.803	299.556	275.728	100.00	100.00	n.a.
Total:			**299.556**	**275.728**	**100.00**	**100.00**	

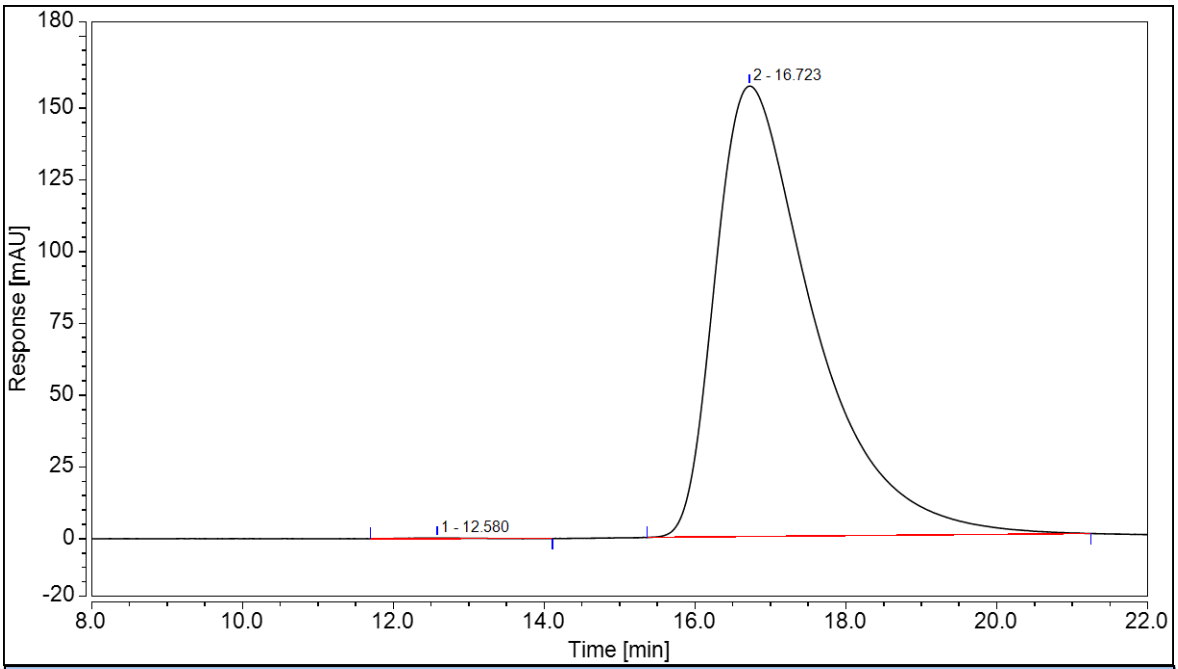

Integration Results

No.	Peak Name	Retention Time min	Area mAU*min	Height mAU	Relative Area %	Relative Height %	Amount
n.a.	Peak 1	n.a.	n.a.	n.a.	n.a.	n.a.	n.a.
1		12.580	0.207	0.245	0.09	0.16	n.a.
2		16.723	237.678	156.873	99.91	99.84	n.a.
Total:			**237.886**	**157.119**	**100.00**	**100.00**	

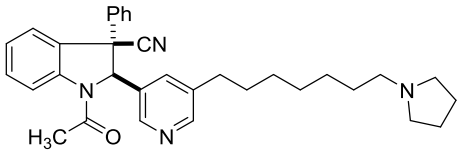

108

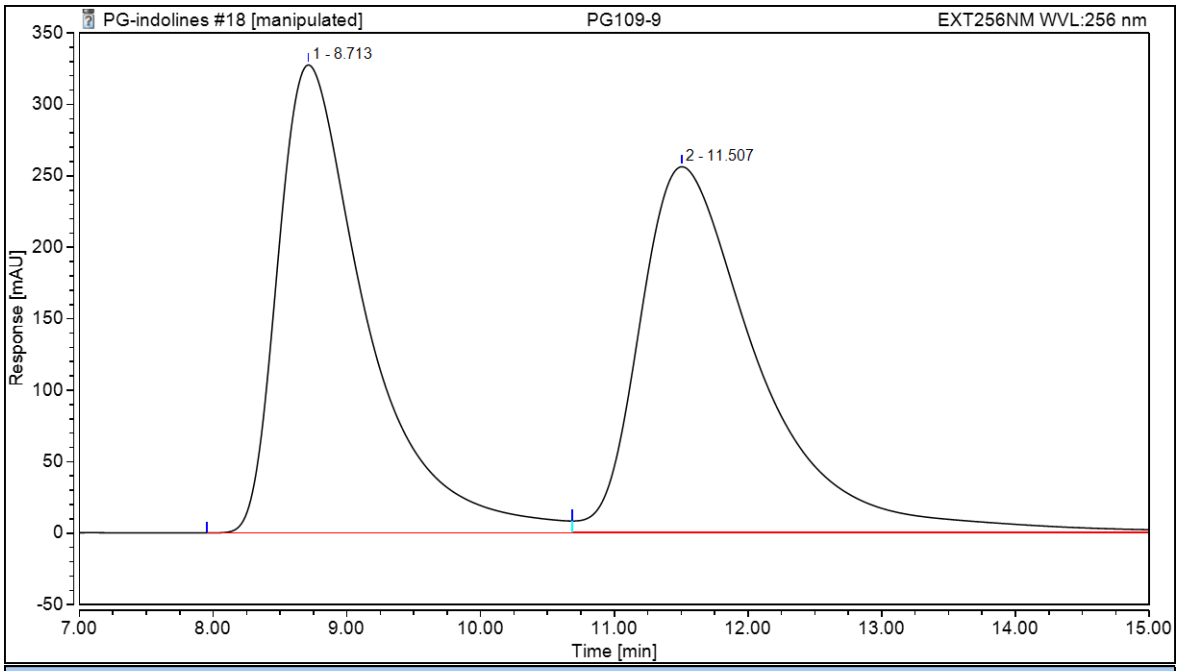

Integration Results

No.	Peak Name	Retention Time min	Area mAU*min	Height mAU	Relative Area %	Relative Height %	Amount
n.a.	Peak 1	n.a.	n.a.	n.a.	n.a.	n.a.	n.a.
1		8.713	252.388	327.471	48.69	56.12	n.a.
2		11.507	266.010	256.089	51.31	43.88	n.a.
Total:			**518.397**	**583.560**	**100.00**	**100.00**	

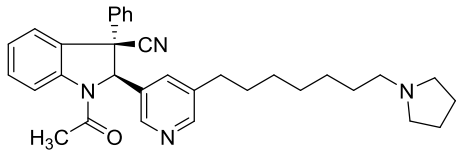

(*R*,*R*)-108

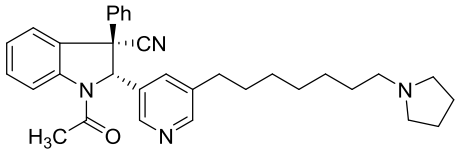

(*S*,*S*)-108

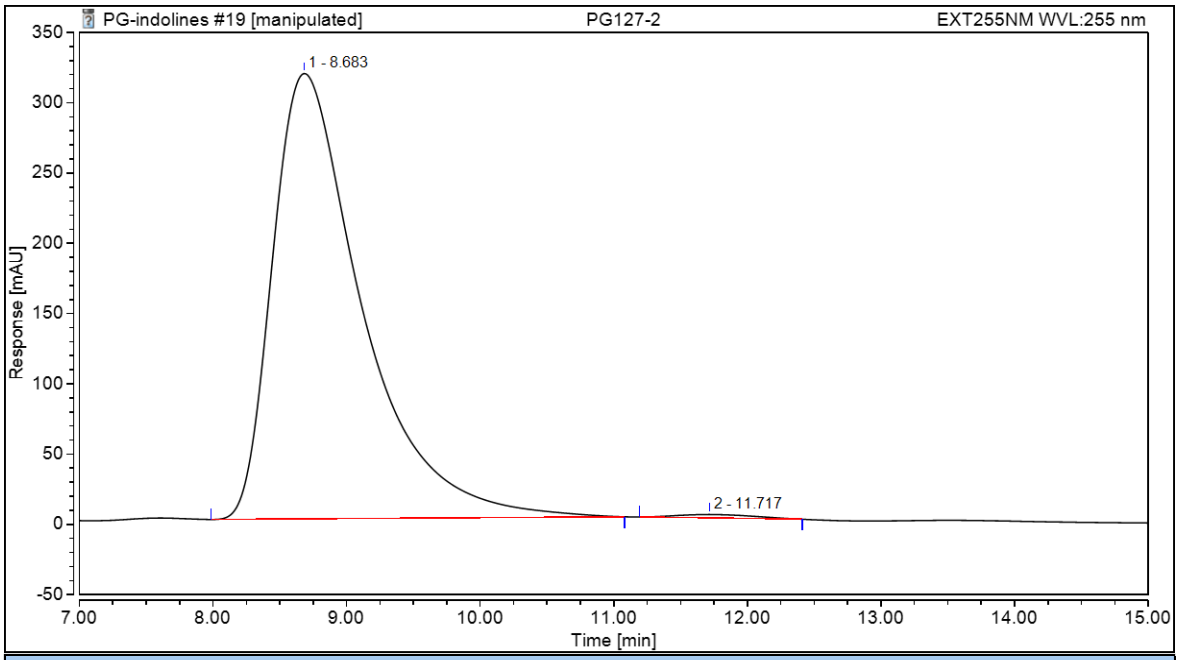

Integration Results

No.	Peak Name	Retention Time min	Area mAU*min	Height mAU	Relative Area %	Relative Height %	Amount
n.a.	Peak 1	n.a.	n.a.	n.a.	n.a.	n.a.	n.a.
1		8.683	246.252	316.982	99.33	99.24	n.a.
2		11.717	1.659	2.436	0.67	0.76	n.a.
Total:			**247.911**	**319.418**	**100.00**	**100.00**	

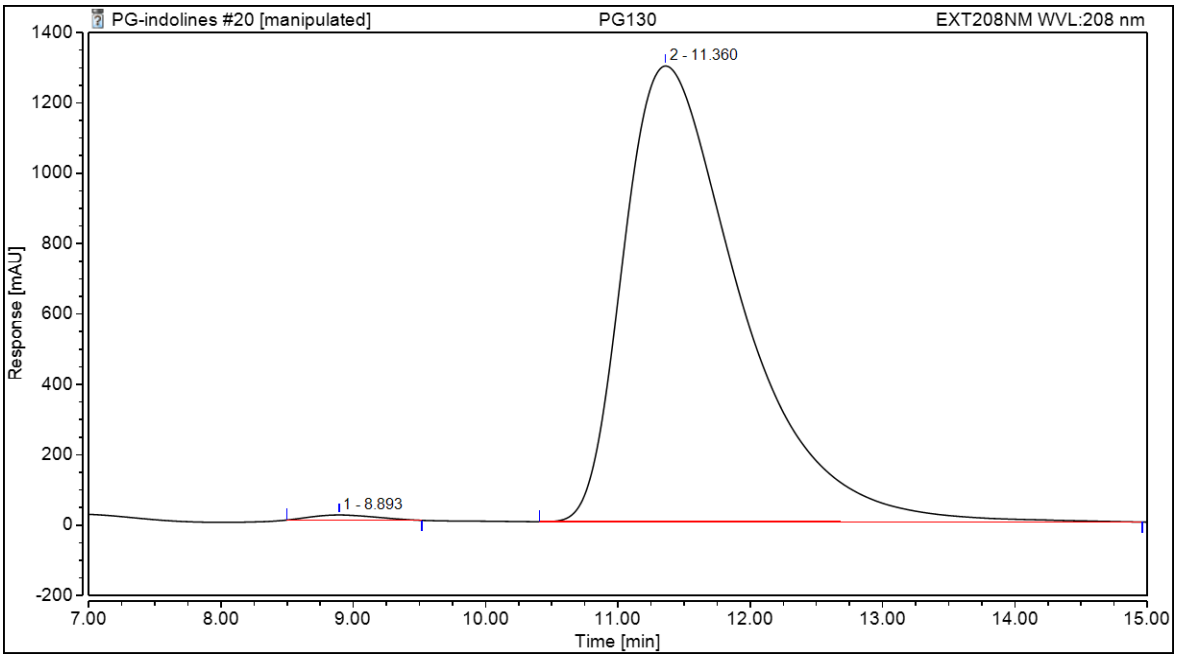

Integration Results

No.	Peak Name	Retention Time min	Area mAU*min	Height mAU	Relative Area %	Relative Height %	Amount
n.a.	Peak 1	n.a.	n.a.	n.a.	n.a.	n.a.	n.a.
1		8.893	8.271	14.658	0.62	1.12	n.a.
2		11.360	1328.356	1295.627	99.38	98.88	n.a.
Total:			**1336.627**	**1310.284**	**100.00**	**100.00**	

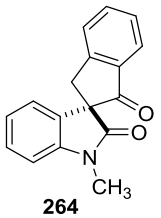

264

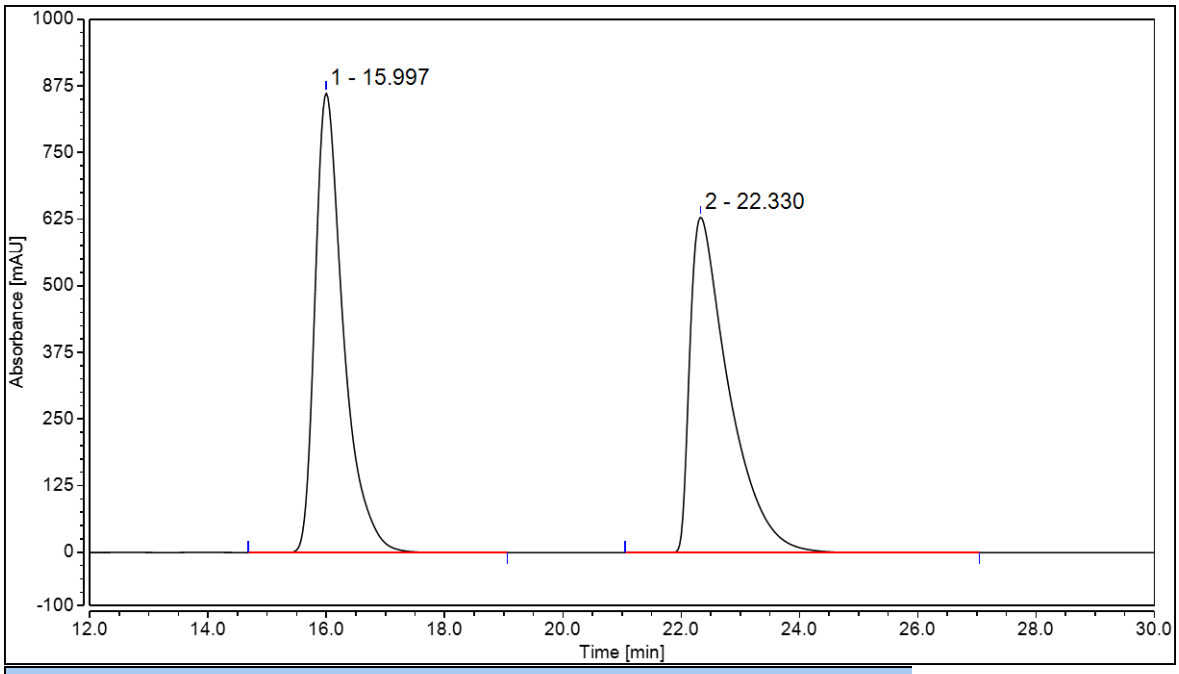

Integration Results

No.	Peak Name	Retention Time min	Area mAU*min	Height mAU	Relative Area %
1		15.997	478.460	862.367	49.96
2		22.330	479.317	629.402	50.04
Total:			**957.777**	**1491.769**	**100.00**

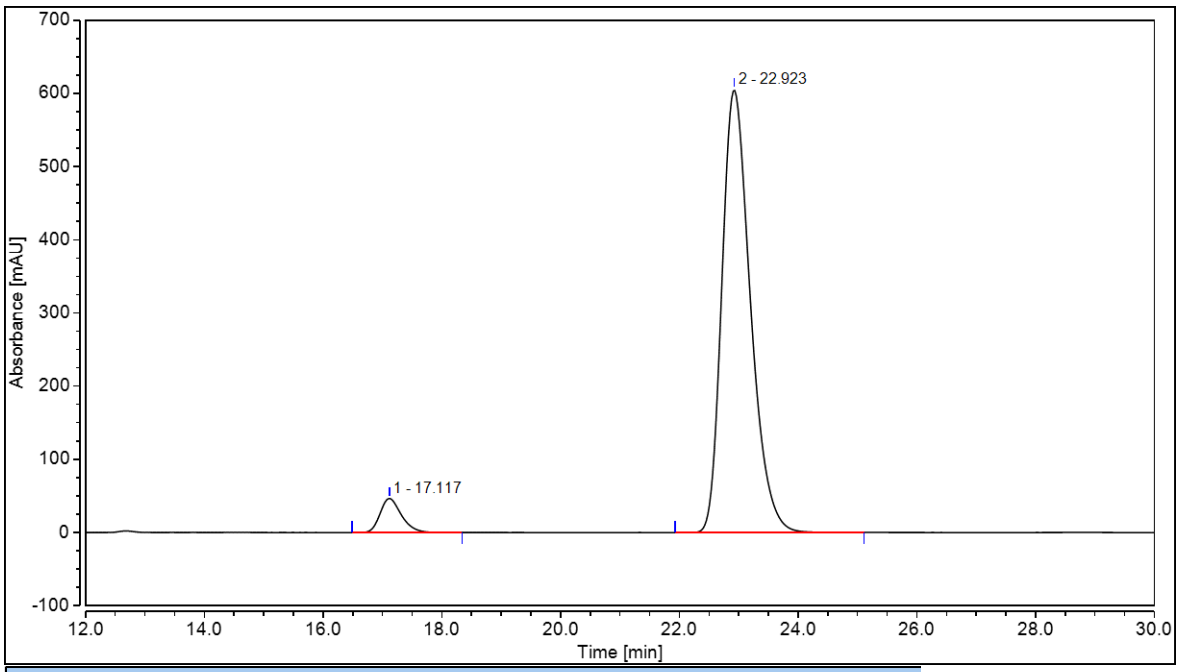

Integration Results

No.	Peak Name	Retention Time min	Area mAU*min	Height mAU	Relative Area %
1		17.117	19.397	46.630	5.45
2		22.923	336.434	604.983	94.55
Total:			**355.831**	**651.613**	**100.00**

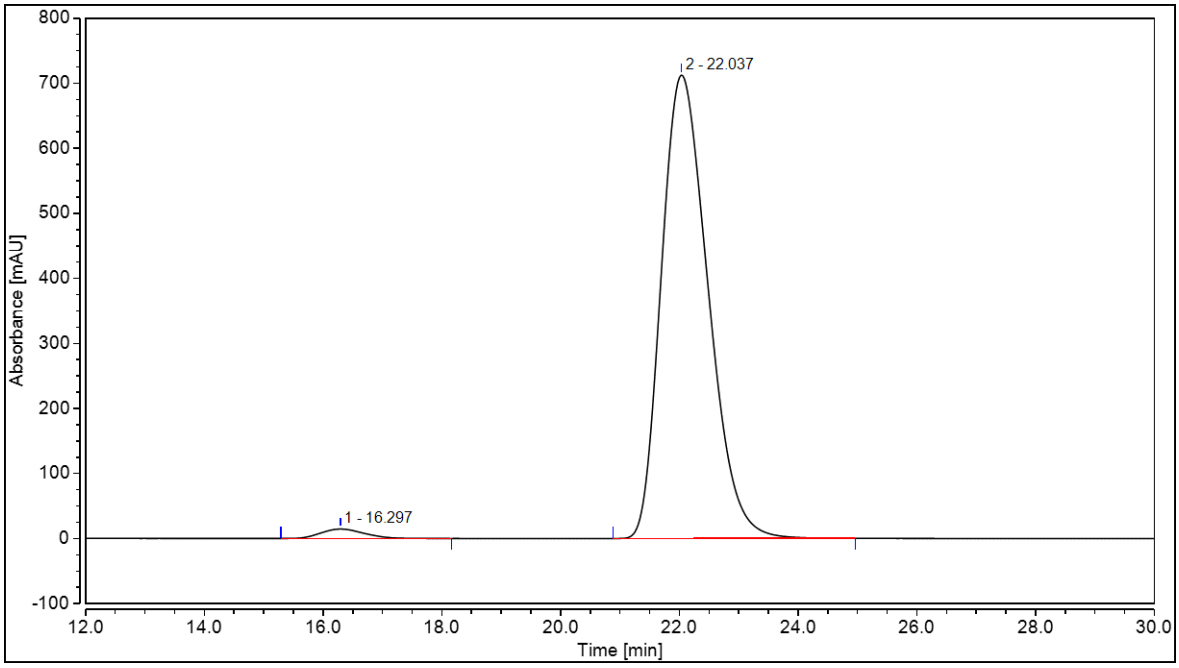

Integration Results

No.	Peak Name	Retention Time min	Area mAU*min	Height mAU	Relative Area %
1		16.297	12.322	14.532	1.87
2		22.037	646.396	712.571	98.13
Total:			**658.718**	**727.103**	**100.00**

8.4.2 X-ray Crystallography Data

X-ray Crystallographic Data and Structure Refinement for 77, 007JDJ14

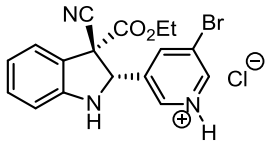

77

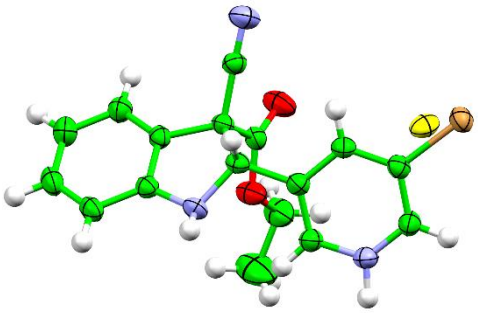

Identification code	007JDJ14	
Empirical formula	$C_{17}H_{15}BrClN_3O_2$	
Formula weight	408.68	
Temperature	150 K	
Wavelength	0.71073 Å	
Crystal system	Triclinic	
Space group	C 2/c	
Unit cell dimensions	a = 41.1184 Å	α = 90°
	b = 8.77720 Å	β = 113.8427°
	c = 22.7766 Å	γ = 90 °
Volume	7518.66 $Å^3$	
Z,Z’	Z: 16 Z': 0	
Density (calculated)	1.44 Mg m^{-3}	
Absorption coefficient	2.342 mm^{-1}	
F(000)	3296.0	
Crystal size	0.04 x 0.18 x 0.40 mm ^{3}	
Theta range for data collection	5.122° to 27.496°	
Reflections collected	15307	
Independent reflections	8581	
Absorption correction	Multi-scan	
Refinement method	Full-matrix least squares on F^2	
Goodness-of-fit on F^2	0.974	
Final R indices [I>2σ(I)]	R^1 = 0.0656, wR^2 = 0.1703	
R indices (all data)	R^1 = 0.0888, wR^2 = 0.1852	

X-ray Crystallographic Data and Structure Refinement for 100, 030JDJ15

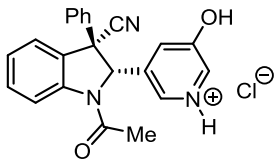

100

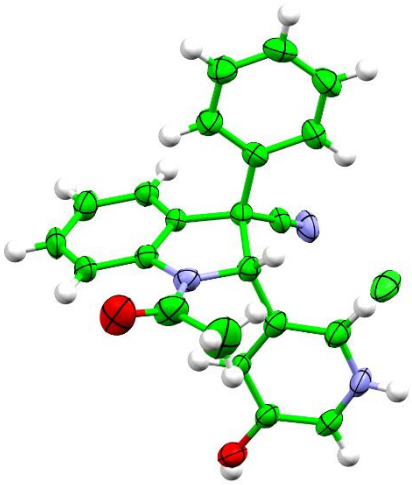

Identification code	030JDJ15	
Empirical formula	$C_{23}H_{21}ClN_3O_{2.5}$	
Formula weight	414.89	
Temperature	150 K	
Wavelength	1.54180 Å	
Crystal system	Triclinic	
Space group	P 1	
Unit cell dimensions	a = 8.6005 Å	α = 103.198°
	b = 8.7390 Å	β = 92.916°
	c = 15.6102 Å	γ = 98.395°
Volume	1125.70 $Å^3$	
Z,Z’	Z: 2 Z': 0	
Density (calculated)	1.22 Mg m^{-3}	
Absorption coefficient	1.706 mm^{-1}	
F(000)	434.0	
Crystal size	0.01 x 0.03 x 0.20 mm^3	
Theta range for data collection	5.218° to 75.980°	
Reflections collected	22875	
Independent reflections	8722	
Absorption correction	Multi-scan	
Refinement method	Full-matrix least squares on F^2	
Goodness-of-fit on F^2	0.996	
Final R indices [I>2σ(I)]	R^1 = 0.0753, wR^2 = 0.2132	
R indices (all data)	R^1 = 0.0800, wR^2 = 0.2208	

Crystallographic Information files

The crystallographic information files (.cif) for all X-ray structures in this thesis can be found in the attached CD.